Strategies and Tactics for the Synthesis of Polycyclic Alkaloids

Adel M. ElSohly

Submitted in partial fulfillment of the
requirements for the degree of
Doctor of Philosophy
In the Graduate School of Arts and Sciences

COLUMBIA UNIVERSITY

2012

ABSTRACT

Strategies and Tactics for the Synthesis of Polycyclic Alkaloids

Adel M. ElSohly

Chapter 1. The Myrmicarin Alkaloids: Isolation, Characterization, and Previous Synthetic Approaches

The myrmicarin family of oligomeric natural products comprises one of the most ornate collections of polycyclic alkaloids known. The structural characterization of their unique scaffolds was accomplished through elegant spectroscopic studies. Furthermore, the synthesis of these alkaloids has attracted the attention of the synthetic community, with several syntheses of the monomeric myrmicarins completed. Significant effort has been put forth toward the synthesis of the higher order structures, though no successful approach has been reported to date. These isolation and characterization studies as well as synthetic approaches toward the family are reviewed.

Chapter 2. The Evolution of Efficient, Enantioselective Total Syntheses of Monomeric Myrmicarin Alkaloids

In order to provide a family-level solution to the myrmicarin alkaloids, we adopted a strategy-level approach to their synthesis. Utilizing concepts from retrosynthetic analysis and diversity oriented synthesis, an enantioselective and highly streamlined synthesis of the monomeric myrmicarin alkaloids as well as potential dimerization precursors was established from a common intermediate with late stage diversification.

Chapter 3. Dimerization Studies Toward the Synthesis of Myrmicarin 430A

An alternative strategy for the synthesis of myrmicarin 430A is presented using a dienamine precursor. This approach allows for the stereoselective synthesis of the all *trans* stereotriad of the central cyclopentane moiety of myrmicarin 430A. Mechanistic aspects concerning the final bond closure are presented in light of quantum chemical calculations.

Chapter 4. An Introduction to the *Securinega* Alkaloids and NHC Catalysis

The *Securinega* alkaloids comprise a large family of tetracyclic alkaloids, many of which contain a conjugated butenolide moiety. While many distinct synthetic approaches have appeared for the synthesis of members of this family, only a relatively small number of approaches are applied to the synthesis of the butenolide portion of these natural products. The various synthetic endeavors to accessing this structural motif are presented.

NHC catalysis is a growing field of research for its ability to promote unusual chemical transformations. As this field of research is of relevance to our latter studies, a brief overview of modern NHC catalysis is presented.

Chapter 5. Development of an NHC-Catalyzed Cascade Reaction to Access the Core Architecture of the *Securinega* Alkaloids

In targeting the family of *Securinega* alkaloids, a retrosynthesis was devised that proposes a novel intramolecular cyclization approach of an ynal and ketone to deliver the

bridging butenolide moiety of these natural products. The development of this reaction and its application toward the synthesis of various *Securinega* alkaloids is presented.

TABLE OF CONTENTS

ACKNOWLEDGEMENTS

I have the insurmountable task of thanking all of the people who have made this Ph. D. possible, and what follows is my best attempt at doing so.

Prof. Scott Snyder for being a mentor and putting up with my crazy ideas for the past 5 years. You are also thanked for giving me creative freedom to explore chemistry.
The Snyder Group past and present members who have made this research group a joy to work in and for inspiring me to always push myself.

Dr. Ferenc Kontes is thanked for being the best collaborator I have ever worked with. Having you as a research partner and hood-mate enriched my Ph. D. experience in ways I cannot express. You are an invaluable mentor and a sincere friend.
Dr. Yunqing Lin is thanked for all of her moral support and for taking us to Dim Sum.
Dr. Daniel Wespe is thanked for being a great friend and a wonderful colleague. Egypt was a blast!
Alexandria Brucks and Nathan Wright are thanked for making this corner the coolest corner in the lab. Nate is specifically thanked for putting up with me as a hood mate for a year.
Wes and Aaron Sattler are thanked first and foremost for always being great friends and for being willing to discuss random chemistry with me. You are also thanked for X-ray chrystallographic expertise.
Profs. Jim Leighton and Tristan Lambert are thanked for serving on my committee and for discussions and suggestions about chemistry.

Dr. John Decatur and Dr. Yasuhiro Itagaki are thanked for immense support in providing expertise in spectroscopic analysis.

Carlos, Socky, Daisy, Dani, and Alix are thanked for all of their administrative assistance. I was once told I am an administrative nightmare, so I thank you all for your patience and helpfulness!
Robert and Chris for being really helpful whenever a chemical got lost in shipment.
Bill and Jay are thanked for making sure our labs were always up and running.

The National Science Foundation is thanked for a pre-doctoral fellowship.
The Paul and Daisy Soros Fellowship is thanked for funding and for being an overall awesome program.
Roche is thanked for an invitation to the Excellence in Chemistry Symposium.

My family for all of their love and support throughout my life. Your confidence in me is humbling, and I cannot express my gratitude enough.
My wife, Donia Elsherbeni cannot be thanked enough for everything she has put up with over the past 5 years. Your constant love and support have made this Ph.D. not only possible but enjoyable.
My daughter, Iris is thanked for being my shining reminder that there's more to life than research. Your smile instantly makes me forget bad days in lab.

General Introduction

The molecular scaffolds isolated from natural sources covers an expansive range of chemical space, often times exhibiting carbon skeletons that are completely unprecedented or that would appear too strained to exist. The challenges associated with the synthesis of these complex frameworks has pushed synthetic organic chemistry to its limits, requiring the development of new reactions, reagents, and strategies to provide solutions to access the desired targets. Furthermore, the tools developed during these endeavors have found broad-reaching application in various fields of study, such as materials science, chemical biology, and medicinal chemistry. With this background in mind, the work disclosed in this dissertation aims to address two major challenges in the synthesis of complex natural product motifs: new strategies and reactions to rapidly build molecular complexity. Specifically, the science disclosed in this dissertation encompasses two major projects that each focused on the synthesis of polycyclic alkaloids.

First, Chapters 1–3 address the development of a unique strategy to access the polycyclic frameworks of the myrmicarin family of alkaloids. Central to these studies is the development of an efficient strategy to access dimerization precursors that exhibit unprecedented reactivity to access key stereochemical features of myrmicarin 430A, a molecule containing a central cyclopentane core that is asymmetrically substituted on every carbon. Indeed, general methods for accessing these types of frameworks are completely absent in the literature. The second project, detailed in Chapters 4 and 5, is concerned with the development of a new reaction to access the strained, polycyclic framework of the *Securinega* alkaloids. Specifically, this new reaction provides the first example of a nucleophilic homoenolate derived from an ynal substrate, greatly expanding the scope of *N*-heterocyclic carbene mediated transformations.

CHAPTER 1

The Myrmicarin Alkaloids: Isolation, Characterization, and Previous Synthetic Approaches

1.1 Isolation and Structural Elucidation of the Myrmicarin Alkaloids

The myrmicarin family of acetate-derived oligomeric alkaloid natural products is comprised of monomeric, dimeric, and trimeric secondary metabolites (**1.1**–**1.8**, Figure

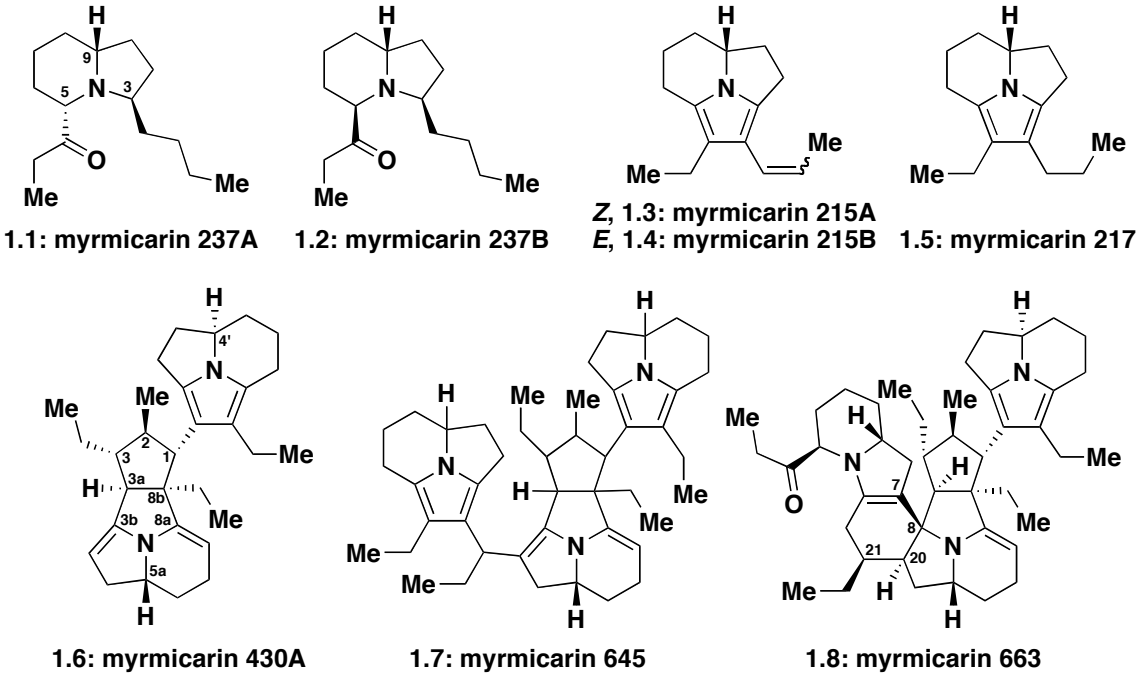

Figure 1.1 Structures of the myrmicarin alkaloids (**1.1**–**1.8**).

1.1) isolated from the poison gland secretion of various species of the *Myrmicaria* genus of African ants.[1] These ants are characterized by an unusually large poison secretion gland, and apart from monoterpene hydrocarbons, these secretions consist almost exclusively of the active alkaloid compounds that are used to subdue prey, biological activity of which is common for other indolizidine natural products. The hydrocarbon components of these secretions are responsible for acting as a surfactant to facilitate spreading of the viscous components. A summary of the isolation and structural determination efforts are presented below. Here, we note that the naming scheme adopted in the literature and throughout this work refers to the molecular mass of the alkaloid.

The simplest and most reduced monomeric congeners of this family are myrmicarins 237A/B (**1.1** and **1.2**), first isolated in 1995[1a] from *Myrmicaria eumenoides*. These alkaloids were found to undergo rapid equilibration at C5 at ambient temperatures, requiring detailed NMR experiments to be performed on fully equilibrated mixtures of the two alkaloids. The gross structures of **1.1** and **1.2** were elucidated on the basis of high-resolution mass-spectral and 2D-INADEQUATE NMR data. The relative and absolute configurations were established via synthesis as described in Section 1.2.1.

The tricyclic myrmicarins[1b] (**1.3**–**1.5**) as well as the higher-order oligomers **1.6** and **1.8** were subsequently obtained from *Myrmicaria opaciventris*. GC/MS analysis of fresh secretions from these ants showed a great deal of intraspecies variabilty in the composition of both the hydrocarbon and alkaloid constituents, with colonies from east Africa (Kenya) showing a large proportion of monomeric, C_{15} alkaloids (myrmicarins 215A/B and 217) and some dimeric, C_{30} alkaloids (myrmicarins 430A/B) while colonies from west Africa (Cameroon) exhibited an overwhelming fraction of trimeric, C_{45} alkaloids (myrmicarin 663) with only trace amounts of monomeric and dimeric compounds detected. Importantly, these crude extracts were shown to be highly air sensitive, with the trimeric alkaloids undergoing extensive decomposition, the dimeric alkaloids suffering complete decomposition, and the monomeric constituents exhibiting notable decomposition after exposure to air for only one hour at ambient temperature. Isolation of the monomeric components could be accomplished by column chromatography on neutral alumina, and catalytic reduction showed myrmicarins 215A/B to be unsaturated analogs of myrmicarin 217. Phase-sensitive 2D-NMR experiments

allowed for the structural assignment of these alkaloids as the first example of naturally occurring pyrrolo[2,1,5-*cd*]indolizidines.

Unfortunately, isolation of the major dimeric constituent, myrmicarin 430A[1c] (**1.6**), was precluded by its extreme sensitivity to air, silica, and alumina. Exposure of crude extracts to silica or alumina resulted in decomposition within minutes. The structure, therefore, was elucidated from NMR analysis of the crude poison gland secretion without any further purification, of which **1.6** constituted only ~5% of a mixture of compounds dominated by myrmicarins 215A/B and 217. Again, phase sensitive 2D-NMR experiments were required to elucidate the gross and relative configuration at all stereocenters except for that at C4' within this natural product. This final stereocenter's configuration can reasonably be inferred to be of the same configuration as C5a assuming that the monomeric counterparts are homochiral. Overall, this characterization tour de force is quite remarkable given the extent of signal overlap between the pyrroloindolizidine subunit of **1.6** and **1.3**–**1.5**. The structure of this heptacyclic natural product is exceedingly complex, bearing a central cyclopentane moiety that is asymmetrically substituted at every carbon, one of which is an all-carbon quaternary center. Furthermore, the presence of a single nitrogen atom within two enamine functional groups in a highly strained framework is likely the cause of the considerable oxidative instability exhibited by this alkaloid.

The major trimeric component, myrmicarin 663[1d] (**1.8**), was isolated from both *M. opaciventris* and *M. striata*. Although this compound was also found to be air sensitive, its increased overall stability relative to myrmicarin 430A allowed its isolation in high purity by either column chromatography on neutral alumina or acidic aqueous extraction

of the crude pentane-soluble extract. Apart from a few isolated signals downfield of 3.3 ppm in the 1D ^{1}H-NMR spectrum, a large amount of signal overlap was observed, particularly in the aliphatic region. Fortunately, 2D-NMR experiments allowed full assignment of the NMR spectrum and determination of the relative configuration of all stereocenters. Thus, the structure was determined to be as depicted in Figure 1.1. With twelve stereocenters—eight of which are contiguous—adorning a decacyclic framework, we believe myrmicarin 663 represents the most complex alkaloid isolated from an insect to date.

Unsurprisingly, these fascinating natural products have attracted the attention of the synthetic community. A number of total syntheses of the indolizidine and tricyclic, monomeric myrmicarins as well as dimerization efforts had been accomplished prior to the start of our work towards these natural products; a summary of these endeavors are provided in the next two sections.

1.2 Previous Total Syntheses of the Monomeric Myrmicarins

1.2.1 Francke's Racemic and Enantiospecific Syntheses of Myrmicarins 237A/B

As alluded to in the previous section, the relative and absolute configuration of myrmicarins 237A/B were assigned through synthesis in the course of Francke's isolation efforts. First, a racemic synthesis was developed[1a] to determine the relative configurations at C3 and C9 (c.f. **1.1**, Figure 1.1) since the remaining stereocenter at C5 was anticipated to be epimerizable. Francke's early studies (not depicted) demonstrated that indolizidines bearing a C3,C9-*cis* disposition with respect to the methine protons did not match their obtained spectra for myrmicarins 237A/B. Therefore, synthetic efforts

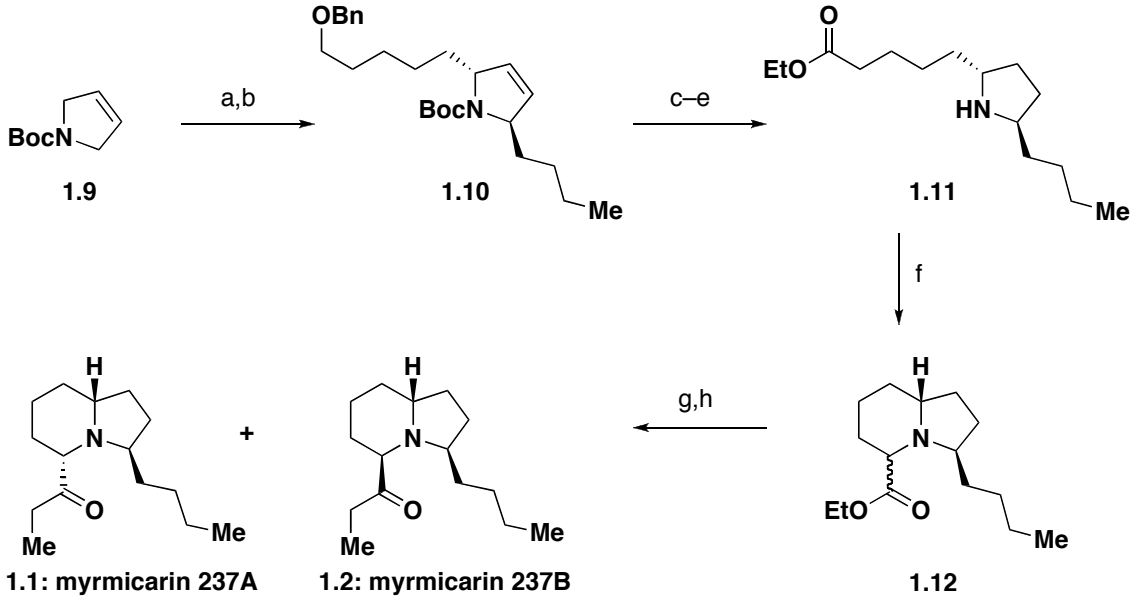

Scheme 1.1 Francke's racemic synthesis of myrmicarins 237A/B (**1.1**, **1.2**). *Reagents and Conditions:* a) LDA, THF, BnBr; –78 → 0 °C, (70%); b) LDA, THF, $BnO(CH_2)_5Br$, –78 → 0 °C (67%); c) H_2 (80 atm), Pd/C, H_2O, MeOH, 23 °C (88%); d) PDC, DMF, 35 °C (79%); e) HCl, EtOH, reflux (83%); f) LDA, THF, I_2, –78 → 0 °C; $NaHCO_3$ (65%); g) KOH, EtOH, 60 °C (89%); h) EtLi, Et_2O, 0 → 20 °C (61%); purification on Al_2O_3 (40% **1.1**, 26% **1.2**). LDA = lithium diisopropylamide, PDC = pyridinium dichromate.

shifted to the preparation of the C3,C9-*trans* series of compounds (Scheme 1.1). The requisite *trans* configuration was secured in short order by sequential alkylation of pyrroline **1.9**. A three-step sequence involving catalytic hydrogenation of the benzyl ether and alkene, alcohol oxidation to the carboxylic acid, and Fischer esterification/N-Boc deprotection afforded ester **1.11**. Alpha-iodination was followed by spontaneous intramolecular cyclization to give indolizidine **1.12**. The ethyl ketone moiety at C5 was then installed through a sponification of the ester and ethyllithium addition to the resultant carboxylic acid, completing the racemic total syntheses of myrmicarin 237A/B (**1.1** and **1.2**) and confirming the C3/C9-*trans* relative configuration.

Having established the relative configurations of myrmicarins 237A/B, Francke pursued the enantioselective synthesis[1a] of these natural products as depicted in Scheme

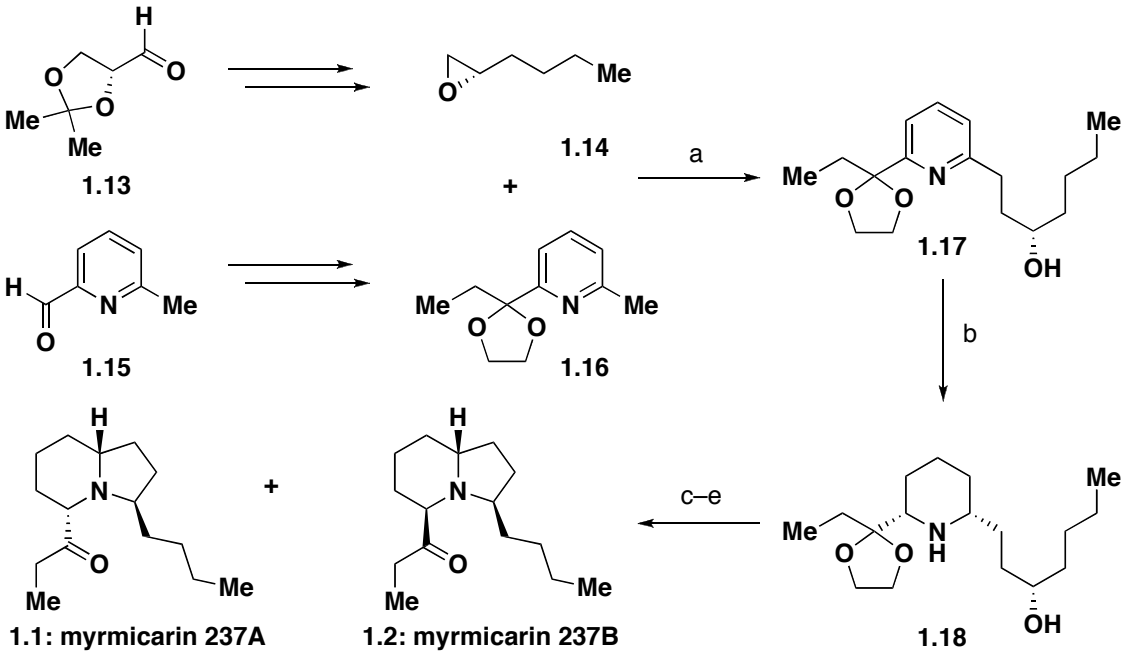

Scheme 1.2 Francke's enantiospecific synthesis of myrmicarins 237A/B (**1.1**, **1.2**). *Reagents and Conditions:* a) *n*-BuLi, **1.16**, DMPU, THF, –50 → 0 °C (86%); b) H_2 (50 atm), Pd/C, EtOH, 23 °C (99%, 3:2 dr) c) TsCl, DMAP, pyridine, –10 → 0 °C (56%); d) HCl, H_2O, Me_2CO, 57 °C (86% **1.1**, 98% ee); e) silica gel; purification on Al_2O_3 (42% **1.2**, 98% ee). DMPU = *N*,*N*′-dimethylpropylene urea, Ts = *p*-toluenesulfonyl, DMAP = 4-(dimethylamino)pyridine.

1.2. The absolute stereochemistry at C3 was secured via nucleophilic attack of lithiated methyl pyridine **1.16** onto homochiral epoxide **1.14**. Subsequent hydrogenation of pyridine **1.17** afforded a 3:2 mixture of diastereomers that could be separated following intramolecular cyclization to afford the indolizidine core. Ketal deprotection then afforded the natural products and assigned the absolute stereochemistry at C9 of these alkaloids to be (*R*). As a point of clarity, the C9 stereocenter has also been referred to as C8a in the literature. Importantly, this absolute configuration has served as the basis for the absolute configuration assignment for the tricyclic and higher order oligomeric members of the family.

1.2.2 Lhommet's Enantiospecific Synthesis of Myrmicarins 237A/B

In 1999, the Lhommet group[2] succeeded in accomplishing the second enantiospecific total synthesis of myrmicarin 237A/B. In their synthesis, the absolute chirality was established using chiral pool starting material (*S*)-pyroglutamic acid. From aldehyde **1.20** (Scheme 1.3), Horner–Wadsworth–Emmons olefination afforded

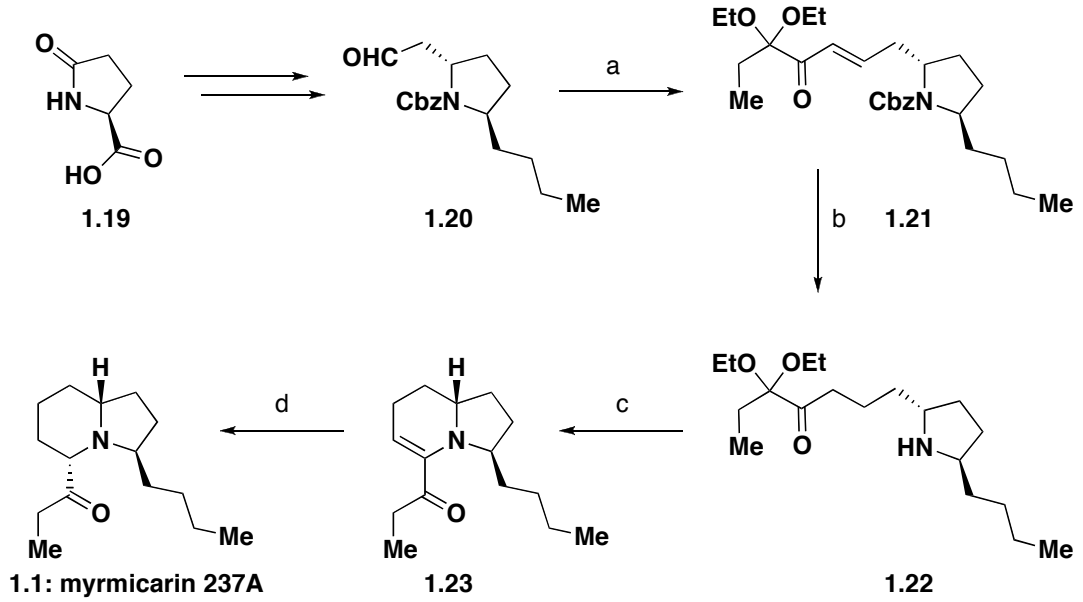

Scheme 1.3 Lhommet's enantiospecific synthesis of myrmicarin 237A (**1.1**). *Reagents and Conditions:* a) $(EtO)_2P(O)CH_2C(O)C(OEt)_2Et$, KHMDS, THF, 0 °C (85%); b) H_2 (1 atm), Pd/C, MeOH, r.t.; c) TFA, H_2O (98%, 2 steps); d) HCl, $NaBH_3CN$ (84%; 92:8 dr). KHMDS = potassium bis(trimethylsilyl)amide, TFA = trifluoroacetic acid.

unsaturated ketone **1.21**. Unfortunately, reduction of the alkene and Cbz protecting group was not accompanied by intramolecular cyclization onto the resultant ketone, a result that was rationalized to be due to the steric hindrance imparted by the ketal protecting group. The ketal group was therefore removed, and intramolecular condensation onto the 1,2-diketone proceeded smoothly to afford enamine **1.23**. Enamine reduction with HCl and $NaCNBH_3$ afforded myrmicarin 237A as the major product (92:8 d.r.). In total, this synthesis required 15 steps in its longest linear sequence and afforded the natural product in 8% overall yield.

1.2.3 Schröder's Racemic Synthesis of Myrmicarin 217

The first total synthesis of a tricyclic myrmicarin alkaloid was accomplished in 1998 by Schröder and Francke[3] with their successful approach to myrmicarin 217 outlined in Sheme 1.4. Their synthesis began with intermediate **1.17** from their previous work[2] toward myrmicarin 237A/B (see Scheme 1.2). Here, initial oxidation of the alcohol and ketalization of the resultant ketone allowed for diastereoselective reduction of the pyridine moiety to the 2,6-*cis*-disubstituted piperidine **1.24**. Then, deprotection of both

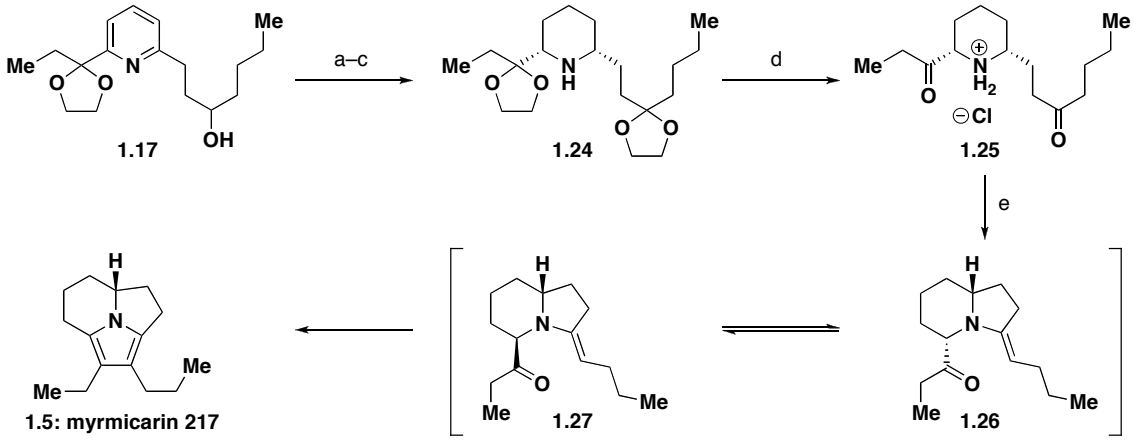

Scheme 1.4 Schröder's racemic synthesis of myrmicarin 217 (**1.5**). *Reagents and Conditions:* a) PDC, mol. sieves, CH_2Cl_2, 20 °C; b) *p*TSA, $(CH_2OH)_2$, Dean Stark (83%, 2 steps); c) H_2 (25 atm), Pd/C, EtOH, r.t. (97%); d) 1M HCl, 70 °C; e) C_6H_6, 40° C (53%, 2 steps). PDC = pyridinium dichromate, *p*TSA = *p*-toluene sulfonic acid.

ketals and basic work-up allowed for rapid intramolecular cyclization to afford the unsaturated indolizidine **1.26** that rapidly underwent epimerization at C5 *in situ*. In addition, a slower cyclocondensation reaction took place that afforded myrmicarin 217. Unfortunately, the mechanistic studies could not discern if one or both of the diastereomers (i.e. **1.26** and **1.27**) was competent in undergoing intramolecular pyrrole formation. Intriguingly, this work also demonstrated a strong preference for the unsaturation of enamine **1.26** to be exocyclic to the pyrrolidine ring.

1.2.4 Vallée's Enantiospecific Synthesis of Myrmicarin 217

The first non-racemic synthesis of myrmicarin 217 was secured by Vallée[4] in 2000. In their enantiospecific approach, glutamic acid was used as the chiral building block used to introduce the lone chiral center of **1.28** (c.f. Scheme 1.5). Overall, their sequence relied on iterative Friedel–Crafts acylations followed by exhaustive reduction to establish critical bonds and proper oxidation state. In particular, condensation of the diethyl diester of glutamic acid with 2,5-dimethoxytetrahydrofuran afforded pyrrole **1.28**; this material subsequently underwent intramolecular Friedel–Crafts acylation in the

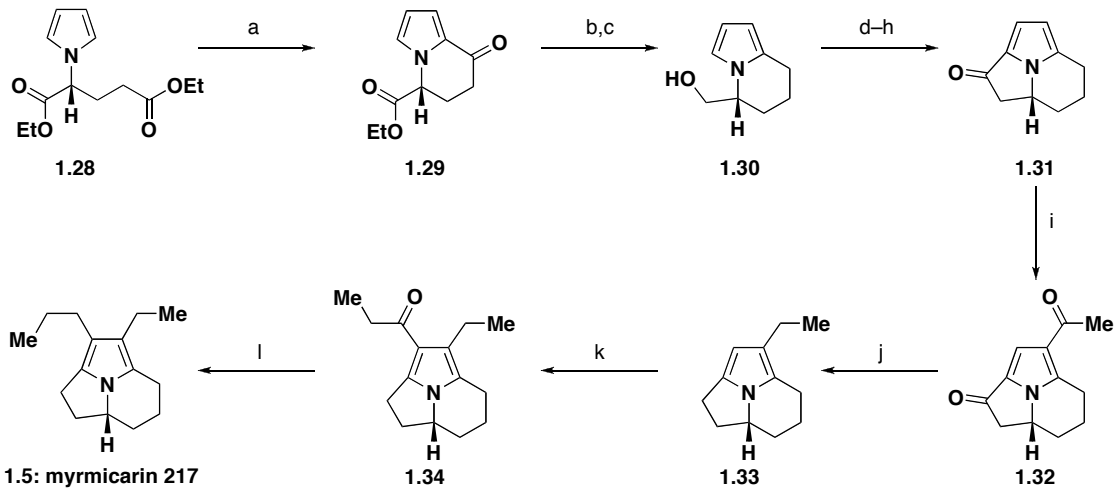

Scheme 1.5 Vallée's enantiospecific synthesis of myrmicarin 217 (**1.5**). *Reagents and Conditions:* a) BBr_3, CH_2Cl_2, 5 °C → r.t. (92%); b) $NaBH_3CN$, ZnI_2, CH_2Cl_2, 40 °C; c) $LiAlH_4$, THF, 0 °C → r.t. (72%, 2 steps); d) MsCl, pyridine, CH_2Cl_2, 0 °C; e) NaCN, DMF, 90 °C (90%, 2 steps); f) NaOH, H_2O, MeOH, 65 °C (90%); g) EtOC(O)Cl, Et_3N, THF, 0 °C; h) BF_3•OEt_2, CH_2Cl_2, 40 °C (57%, 2 steps); i) AcCl, $AlCl_3$, CH_2Cl_2, 40 °C (93%); j) $LiAlH_4$, THF, reflux (60%); k) $CH_3CH_2CONMe_2$, $POCl_3$, toluene, 90 °C (68%); l) $LiAlH_4$, 1,4,-dioxane, 100 °C (60%). Ms = methanesulfonyl, Ac = acyl.

presence of BBr_3 to afford keto-ester **1.29**. Reduction of the benzylic ketone and ester allowed for a one carbon homologation sequence with cyanide as nucleophile. Hydrolysis of the resultant nitrile and subsequent Friedel–Crafts acylation gave rise to pyrroloindolizidin-2-one **1.31**. Treatment of this intermediate with acyl chloride and

$AlCl_3$ afforded the regioselective C4-pyrrole acylation. Reduction of both ketones with $LiAlH_4$ afforded intermediate **1.33** that was subsequently treated with the Vilsmeier reagent derived from *N*,*N*-dimethylpropanamide to give oxidized myrmicarin 217 congener **1.34**. Reduction of the ketone to the corresponding methylene was again accomplished with $LiAlH_4$ to give the final natural product in 7.5% yield from pyrrole **1.28**.

1.2.5 Vallée's Enantiospecific Synthesis of Myrmicarins 215A/B

Subsequent to their disclosure of their total synthesis of myrmicarin 217, the Vallée group pursued a total synthesis of myrmicarin 215A/B.[5] Their strategy was predicated on the ability to regioselectively acylate pyrroloindolizidine **1.35** (Scheme 1.6). In practice, it was found that **1.35** could indeed be regioselectively acylated at C4 with Vilsmeier reagents using toluene as solvent. The observed selectivity was rationalized as a result of a preference for the resultant cation to reside in the six-membered ring as supported by theoretical calculations. The formylated product was then homologated by MeLi addition and reduction of the resultant alcohol, affording pyrrole **1.33**. Subsequent Vislmeier formylation afforded aldehyde **1.37** that underwent Wittig olefination to give myrmicarins A (**1.3**) and B (**1.4**) in a 4:1 ratio, completing the first total synthesis of the oxidzed tricyclic myrmicarins.

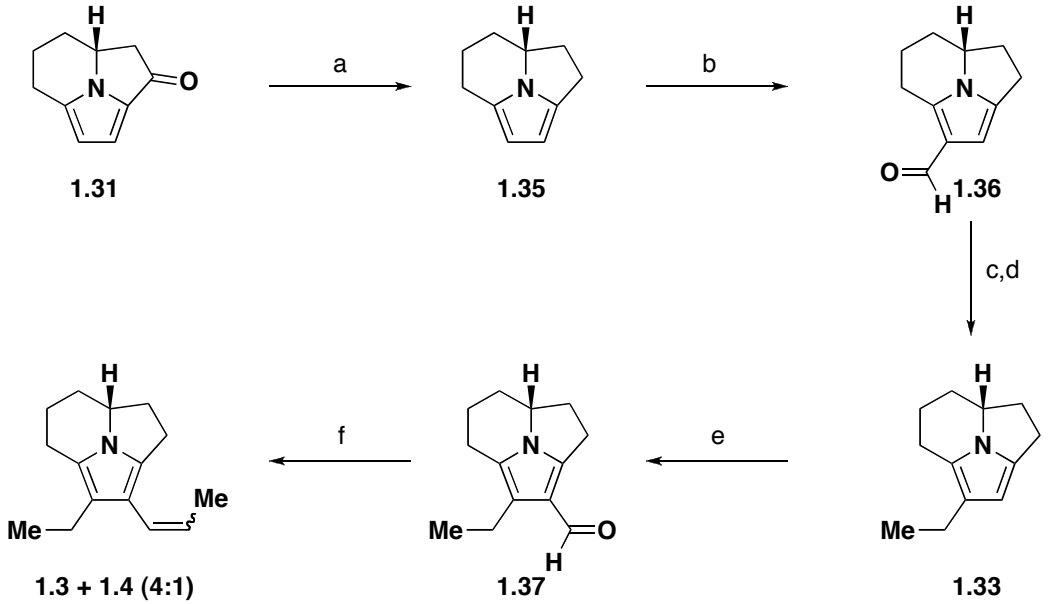

Scheme 1.6 Vallée's enantiospecific synthesis of myrmicarin 215A/B (**1.3**, **1.4**). *Reagents and Conditions:* a) $LiAlH_4$, 1,4-dioxane, 100 °C (86%); b) DMF, $POCl_3$, toluene, 83 °C (53%); c) MeLi, THF, 0 °C; d) $LiAlH_4$, 1,4,-dioxane, 88 °C (72%, 2 steps); e) DMF, $POCl_3$, CH_2Cl_2, 40 °C (80%); f) Ph_3PEtBr, NaH, THF, 65 °C (78%, 4:1 **1.3**:**1.4**).

1.2.6 Lazzaroni's Formal Enantiospecific Synthesis of Myrmicarin 217

In 2003, the Lazzaroni group disclosed a formal enantiospecific synthesis[6] of myrmicarin 217 by intercepting intermediate **1.30** from Vallée's synthesis[4] using a dehydrative cyclization, as summarized in Scheme 1.7. Subsequent alkene and ester reduction completed the formal total synthesis of myrmicarin 217.

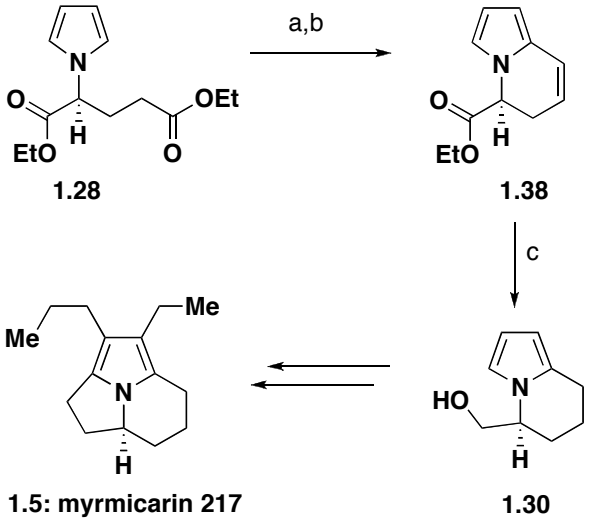

Scheme 1.7 Lazzaroni's enantiospecific formal synthesis of myrmicarin 217 (**1.5**). *Reagents and Conditions:* a) DIBAL-H, –78 °C (65%); b) DMSO, 100 °C (55%); c) $LiAlH_4$, THF, r.t. (85%). DIBAL-H = diisobutylaluminum hydride.

1.2.7 Movassaghi's Enantioselective Synthesis of the Tricyclic Myrmicarins

In 2005, the Movassaghi research group disclosed the first[7] of a series of works targeting the myrmicarin alkaloids. Their initial report detailed the first enantioselective total syntheses of the tricyclic alkaloids **1.3**–**1.5**. Ester **1.39** (see Scheme 1.8), obtained from a crossed Claisen reaction and *Z*-selective vinyl triflate formation, sets the stage for a palladium mediated *N*-vinylation with pyrrole **1.40**. This reaction was one that the authors previously reported in a separate disclosure[8] and, overall, was quite efficient, affording the desired product in excellent yield and on multigram scale (>15 gram scale reported to date). Next, enantioselective conjugate reduction of enoate **1.41** was accomplished in 89% yield and 85% ee using a complex derived from $Cu(OAc)_2$ and (*S*)-BINAP with PMHS as the hydride source. Friedel–Crafts cyclization and reduction of the resultant alkene smoothly afforded keto-ester **1.43**. The next required operation was the

chemoselective reduction of the *tert*-butyl ester in the presence of the ketone.

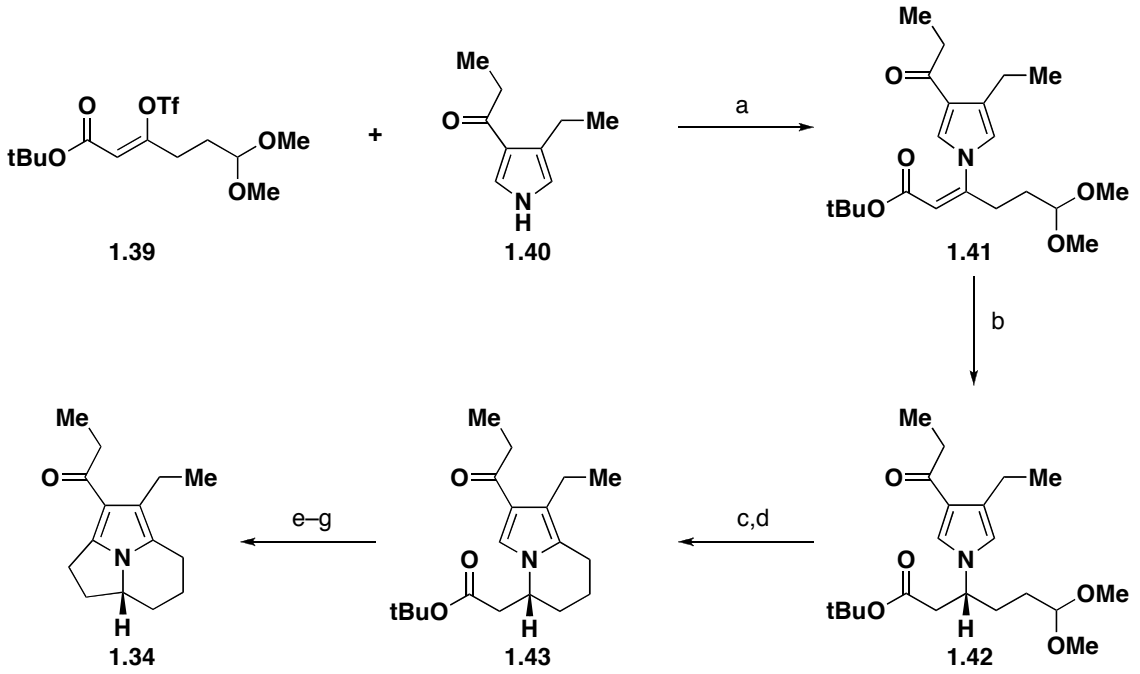

Scheme 1.8 Movassaghi's enantioselective synthesis of key intermediate **1.34**. *Reagents and Conditions:* a) Pd_2dba_3, XPhos, K_3PO_4, toluene, 60 °C (95%); b) 15% $Cu(OAc)_2 \cdot H_2O$, (*S*)-BINAP, PMHS, THF, *t*-BuOH, r.t. (89%, 85% ee); c) Me_2CO, H_2O, AcOH, 40 °C; d) H_2, Pd/C, EtOAc, r.t. (> 98%, 2 steps); e) Et_3N, TIPSOTf, THF, –78 → 0 °C; $LiAlH_4$; HCl, r.t. (87%); f) I_2, PPh_3, imidazole, CH_2Cl_2, 0 °C (82%); g) $AgBF_4$, CH_2Cl_2, C_6H_6, r.t. (80%). dba = dibenzylideneacetone, BINAP = 2,2'-Bis(diphenylphosphino)-1,1'-binaphthyl, PMHS = poly(methylhydrosiloxane), TIPSOTf = triisopropylsilyl trifluoromethanesulfonate.

This task was successfully achieved by a two-step, one pot protocol involving formation of the TIPS-ester and $LiAlH_4$-mediated reduction. The chemoselectivity of this reduction is likely due to strong resonance donation of the pyrrole nitrogen into the ketone in the form of a vinylogous amide. Ring closure to tricycle **1.34** was then completed through iodination of the primary alcohol and treatment with a silver salt. This intermediate could serve as a common building block to access all three myrmicarin alkaloids as demonstrated in Scheme 1.9. Before discussing these efforts, it is important to note that the ketone moiety in **1.34** imparted enhanced stability relative to the myrmicarins and that

this compound could be stored for long periods of time without detrimental degradation. Furthermore, this intermediate could be accessed on a multi-gram scale.

Efforts thus turned toward the tricyclic natural products, and myrmicarin 217 (**1.5)** was accessed from **1.34** through $LiAlH_4$ reduction of the benzylic ketone under forcing conditions. Myrmicarin 215A (**1.3**) was accessed via dehydration of ketone **1.34**

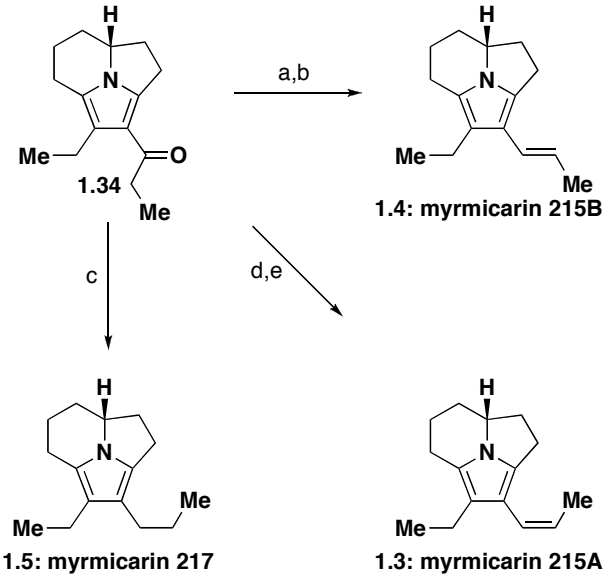

Scheme 1.9 Movassaghi's conversion of common intermediate **1.34** into the tricyclic myrmicarins (**1.3**–**1.5**). *Reagents and Conditions:* a) $LiAlH_4$, Et_2O, –78 → 0 °C (100%); b) HCl (aq), Et_2O, r.t. (61%); c) $LiAlH_4$, 1,4-dioxane, 100 °C (92%); d) 2-chloro-3-ethylbenzoxazolium tetrafluoroborate, Et_3N, CH_2Cl, r.t. (12% + 80% rsm); e) H_2, Lindlar cat., EtOAc, pyridine, r.t. (74%).

with 2-chloro-3-ethylbenzoxazolium tetrafluoroborate to the alkyne followed by Lindlar reduction to the *Z*-alkene. Unfortunately, this reaction had to be stopped prior to completion due to complications arising from long reaction times and competitive C6—C7 oxidation. Finally, myrmicarin 215B (**1.4**) was prepared by reduction of the benzylic ketone to the alcohol followed by an acidic work-up to promote dehydration. In total, this work constitutes the first highly stereoselective syntheses of the myrmicarin 215 alkene isomers.

1.2.8 Lhommet's Enantiospecific Formal Synthesis of the Tricyclic Myrmicarins

In 2010, Lhommet and co-workers reported an enantiospecific total synthesis of the tricyclic myrmicarins.[9] Homochiral pyrrolidine **1.44** (c.f. Scheme 1.10) was acetylated (to facilitate subsequent purification), hydrogenated to remove the chiral auxiliary, and subsequently re-protected as the corresponding Cbz carbamate. Installation

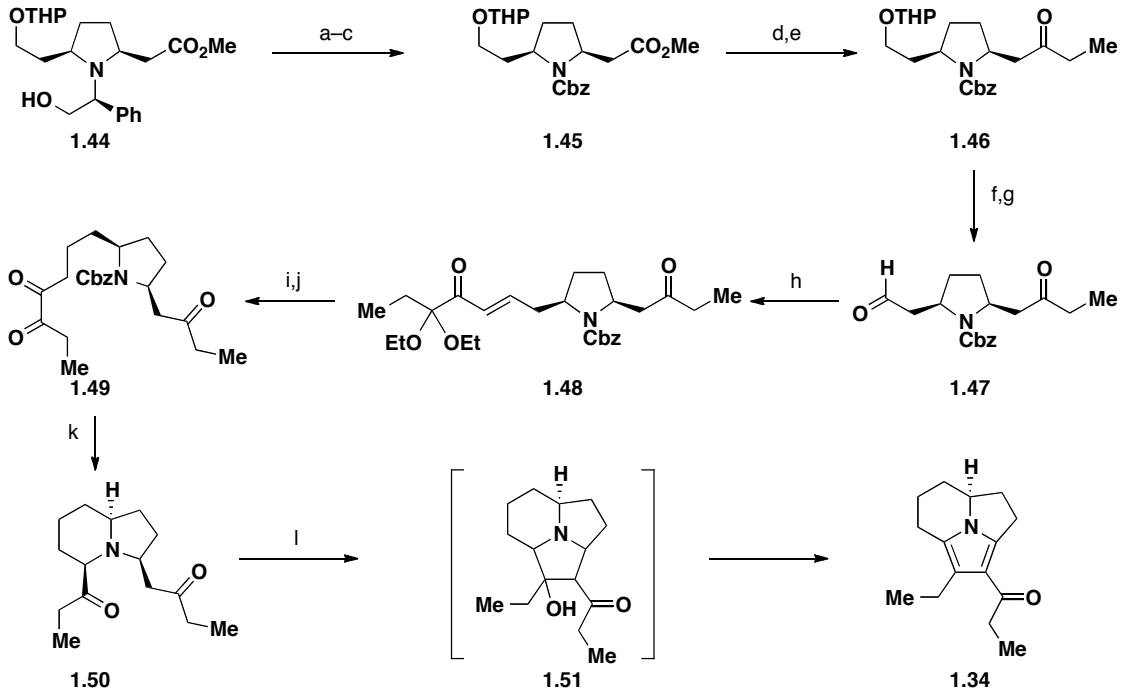

Scheme 1.10 Lhommet's enantiospecific formal synthesis of the tricyclic myrmicarins. *Reagents and Conditions:* a) AcCl, Et_3N, DMAP, CH_2Cl_2, r.t.; b) H_2 (1 atm), Pd/C, MeOH, r.t.; c) BnOC(O)Cl, K_2CO_3, CH_2Cl_2, 0 °C → r.t. (57%, 3 steps); d) (MeO)NHMe•HCl, *n*-BuLi, THF, –78 °C; **1.45**; e) EtMgBr, THF, –78 → 0 °C (65%, 2 steps); f) PPTS, EtOH, 50 °C (84%); g) $(COCl)_2$, DMSO; Et_3N, –60 °C → r.t. (91%); h) $(EtO)_2P(O)CH_2C(O)C(OEt)_2Et$, KHMDS, THF, 0 °C; **1.47**, 0 → 70 °C (89%); i) H_2 (1 atm), PtO_2, MeOH, r.t. (93%); j) 50% aq. TFA, $CHCl_3$, r.t. (99%); k) H_2 (1 atm), Pd/C, MeOH, r.t. (50%); l) LiOH•H_2O, EtOH, 80 °C (64%). Ac = acyl, DMAP = 4-(dimethylamino)pyridine, PPTS = pyridinium *p*-toluenesulfonate, KHMDS = potassium bis(trimethylsilyl)amide, TFA = trifluoroacetic acid.

of the ethyl ketone moiety was smoothly accomplished over two steps to afford **1.46**. Removal of the THP ether and subsequent Swern oxidation afforded aldehyde **1.47.** This intermediate was then subjected to Horner-Wadsworth-Emmons olefination, as in their previous work (see Section 1.2.2), to give unsaturated ketone **1.48**. Alkene reduction and

ketal deprotection then provided diketone **1.49** that, upon reductive removal of the Cbz protecting group, underwent intramolecular reductive amination to give **1.50** as a single diastereomer. Treatment of this diketone with LiOH•H_2O in refluxing EtOH smoothly transformed **1.50** into **1.34** *via* an intramolecular aldol condensation and *in situ* aromatization, intercepting Vallée and Movassaghi's intermediate and completing a formal synthesis of the tricyclic family members.

1.3 Movassaghi's Efforts Toward Myrmicarin 430A

1.3.1 Direct Dimerization of Myrmicarins 215A/B

With access to gram quantitites of myrmicarin 215B, the Movassaghi group began explorations[10] directed toward the total synthesis of myrmicarin 430A (**1.6**, Figure 1.1).

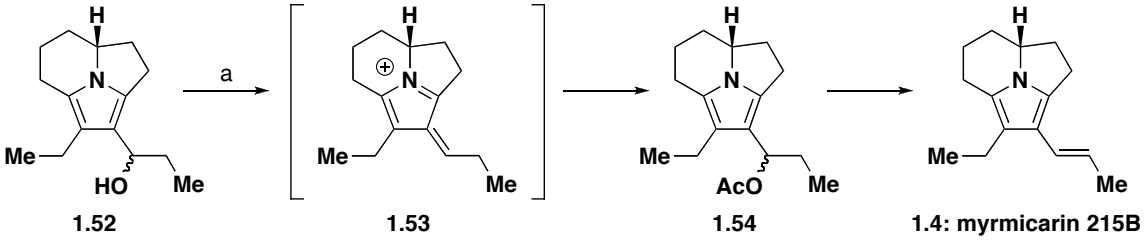

Scheme 1.11 Reactivity of alcohol **1.52** under weakly acidc conditions. *Reagents and Conditions:* a) AcOH, C_6D_6, 23 °C.

Following the authors' proposed biosynthetic hypothesis of direct dimerization of myrmicarin 215A/B through the intermediacy of an azafulvenium ion, a diasteromeric mixture of alcohols **1.52** was subjected to catalytic AcOH in benzene-d_6 and monitored by NMR as depicted in Scheme 1.11. This experiment demonstrated initial formation of acetate derivative **1.54**; this intermediate slowly underwent elimination to give myrmicarin 215B (**1.4**), providing circumstantial evidence of an azafulvenium intermediate **1.53**. When the same alcohols were treated with a slight excess of a stronger

acid (TFA), *in situ* NMR monitoring revealed rapid conversion to myrmicarin 215B and subsequent formation of a new iminium species that was found to be unstable to isolation

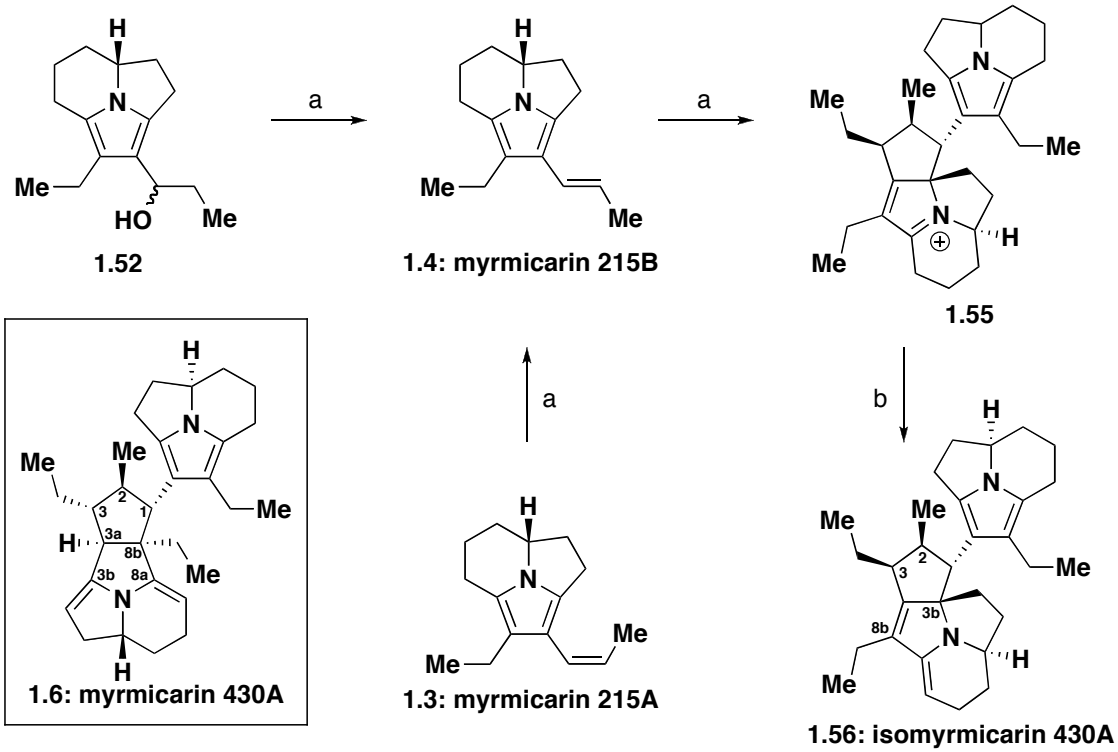

Scheme 1.12 Dimerizations of **1.52**, myrmicarin 215B (**1.4**), and myrmicarin 215A (**1.3**). *Reagents and Conditions:* a) TFA, C_6D_6, 23 °C; b) resin-bound BEMP, C_6D_6, 23 °C. TFA = trifluoroacetic acid, BEMP = 2-*tert*-butylimino-2-diethylamino-1,3-dimethylperhydro-1,3,2-diazaphosphorine.

(Scheme 1.12). Furthermore, the same dimeric material could be obtained from treatment of either myrmicarin 215B or 215A with a slight excess of TFA. Intriguingly, NMR monitoring of the dimerization of myrmicarin 215A revealed a small but constant amount of myrmicarin 215B throughout the course of the reaction, suggesting that alkene isomerization was slow compared to dimerization.

In order to provide an isolable intermediate for characterization, the putative iminium intermediate **1.55** was treated with resin-bound BEMP as a base to give an intermediate that was of sufficient purity to be fully characterized by 2D NMR studies, revealing compound **1.56** (isomyrmicarin 430A) as the sole product of the reaction. This

compound is epimeric at one stereocenter and regioisomeric about one bond to myrmicarin 430A (**1.6**, Scheme 1.12). In particular, the initial bond formation (C2—C3, c.f. **1.56**) results in the opposite stereochemistry at C3 required for myrmicarin 430A. This stereochemical outcome can be rationalized by attack of the nucleophile from the convex face of the presumed azafulvenium ion. Additionally, subsequent intramolecular nucleophilic attack of the pyrrole on the presumed azafulvenium intermediate occurred from C3b of the pyrrole where attack from C8b is required. Subsequent NMR experiments confirmed the structure of the iminium ion formed during the course of the dimerization to be **1.55**. Attempts to derivatize isomyrmicarin 430A for X-ray analysis were unsuccessful; however, catalytic reduction and alkene isomerization provided monoenamine **1.57** (see Scheme 1.13) that was sufficiently stable to isolation to be purified and stored under an inert atmosphere at low temperature without significant decomposition. Furthermore, the use of different acids, solvents, and/or additives either resulted in ring protonation of the pyrrole or formation of heptacyclic iminium **1.55**. Overall, the high diastereoselectivity observed in the course of these dimerizations suggests a strong bias for these materials to react as described above; however, it also inspires hope that the proper reagent or starting material could similarly provide an efficient and highly diastereoselective prepartion of myrmicarin 430A. Much effort has thus been expended toward altering this inherent reactivity.

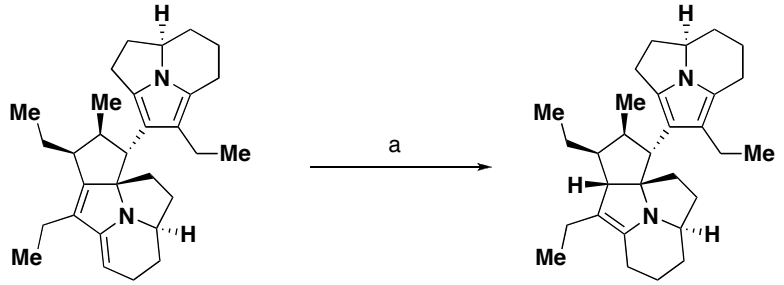

Scheme 1.13 Chemoselective reduction of isomyrmicarin 430A (**1.56**). *Reagents and Conditions:* a) H_2 (1 atm), Pd/C, C_6D_6, 23 °C (87% from **1.4**).

1.3.2 Explorations of a Concerted [6π$_a$+2π$_s$] Cycloaddition

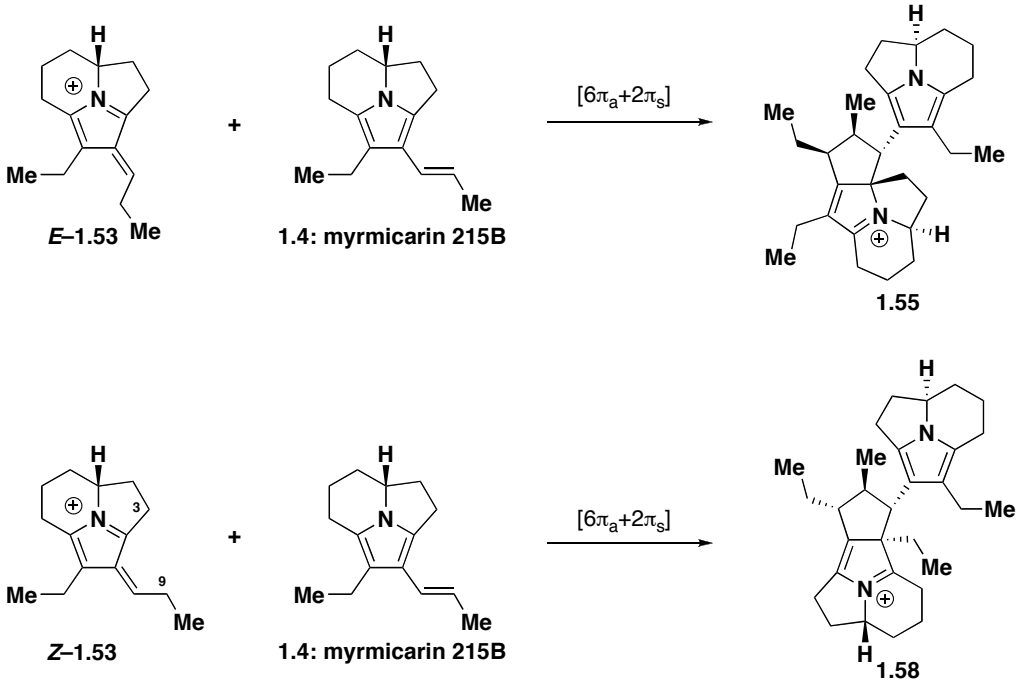

Figure 1.2 Proposed dimerization of *E*- and *Z*-**1.53** *via* a concerted [6π_a + 2π_s] cycloaddition.

An intriguing proposal was brought forth by Movassaghi and co-workers in 2007[11] wherein they suspected that the overall high levels of diasteroselectivity and relative insensitivity to the reagents used for dimerization could be a result of a concerted, thermally allowed [6π_a+2π_s] cycloaddition reaction of *E*-azafulvenium ion **1.53** depicted in Figure 1.2. Their preliminary calculations suggested that *Z*-**1.53** is more

stable by ~1.3 kcal/mol over its counterpart. However, it was hoped that the observed formation of isomyrmicarin 430A was a result of the less stable *E*-**1.53** undergoing rapid reaction to afford the observed product. This idea was particularly appealing given that

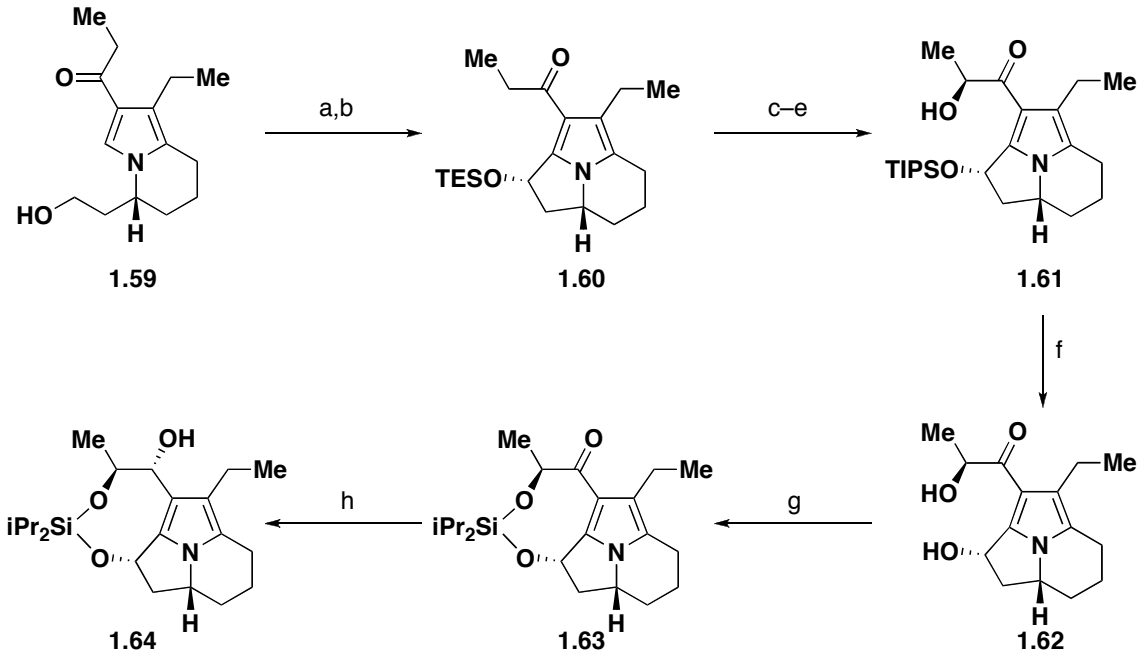

Scheme 1.14 Synthesis of conformationally restricted dimerization precursor **1.64**. *Reagents and Conditions:* a) IBX, DMSO, 23 °C (82%); b) TESOTf, 2,6-lutidine, C_6H_6, 23 °C; HCl, 23 °C; c) TBAF, THF, 0 °C (81%, 2 steps); d) TIPSOTf, 2,6-lutidine, CH_2Cl_2, –40 °C (82%); e) KHMDS, Davis oxaziridine, THF, –78 °C (90%, 5:1 dr); f) TBAF, THF, 23 °C (92%); g) *i*-Pr_2SiCl_2, DMAP, DMF, 23 °C (77%); h) $LiAlH_4$, Et_2O, –78 → 0 °C (77%, 6:1 dr). IBX = 2-iodoxybenzoic acid, TESOTf = triethylsilyl trifluoromethanesulfonate, TBAF = tetrabutylammonium fluoride, TIPSOTf = triisopropylsilyl trifluoromethanesulfonate, KHMDS = potassium bis(trimethylsilyl)amide, DMAP = 4-(dimethylamino)pyridine.

concerted cycloaddition with the corresponding *Z*-azafulvenium ion would give rise to the desired natural product. To test this hypothesis, the Movassaghi group set out to prepare a constrained dimerization precursor that could only access the *Z*-azafulvenium geometry by tethering C3 and C9 within the monomeric framework.

The requisite precursors were synthesized as shown in Scheme 1.14. Alcohol **1.59**, an intermediate from their previous route to the tricyclic myrmicarins, was oxidized with IBX to the corresponding aldehyde. This new motif was subsequently activated with

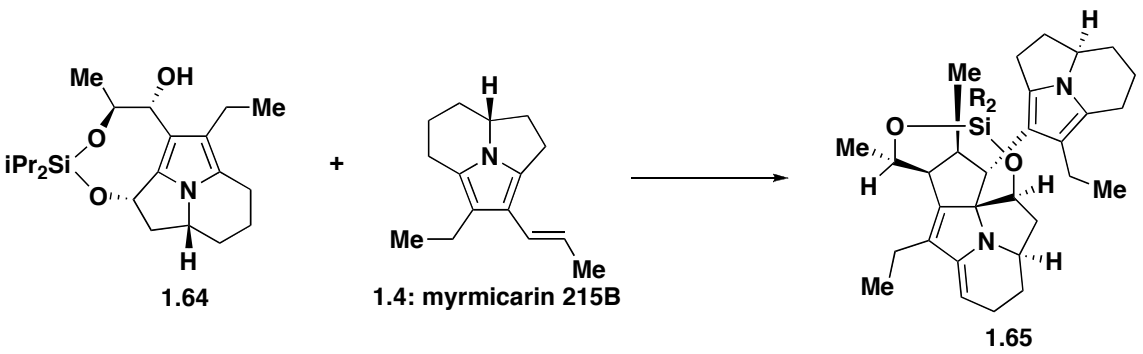

Scheme 1.15 Chemoselective heterodimerization of **1.64** and myrmicarin 215B (**1.4**). *Reagents and Conditions:* a) $Sc(OTf)_3$, MeCN-d_3, 23 °C (>90%, single diastereomer). OTf = trifluoromethanesulfonate.

TESOTf for intramolecular Friedel–Crafts reaction, furnishing protected alcohol **1.60**. Removal of the TES protecting group and re-protection as the TIPS ether allowed for a stereoselective (5:1 d.r.) oxidation of the potassium enolate with Davis oxaziridine to afford alcohol **1.61**. Removal of the TIPS protecting group and treatment with iPr_2SiCl_2 effectively tethered the alcohols at C3 and C9 to afford **1.63**. Reduction of the ketone afforded the C8 alcohol **1.64** poised for dehydrative dimerization. After some experimentation, $Sc(OTf)_3$ was found to be an excellent Lewis acid catalyst for the selective heterodimerization of **1.64** with myrmicarin 215B, affording compound **1.65** (Scheme 1.15) after workup and isolation. This molecule also displayed the same connectivities and stereochemistry observed in isomyrmicarin 430A (**1.56**).

Simple molecular models indicated that while the *E*-azafulvenium derived from **1.64** would be strained, it was not inaccessible. A similar analysis of the C9-epimer strongly suggested that *E*-azafulvenium ion would be prohibitively strained (see **1.69**, Scheme 1.16), and thus, this C9 epimer was pursued and accessed as depicted in Scheme 1.17. Mitsunobu reaction of **1.61** and saponification effecively inverted the C9 alcohol, and a similar sequence to that described above then led to alcohol **1.67**. $Sc(OTf)_3$-catalyzed heterodimerization thus afforded compound **1.68** (Scheme 1.18), again

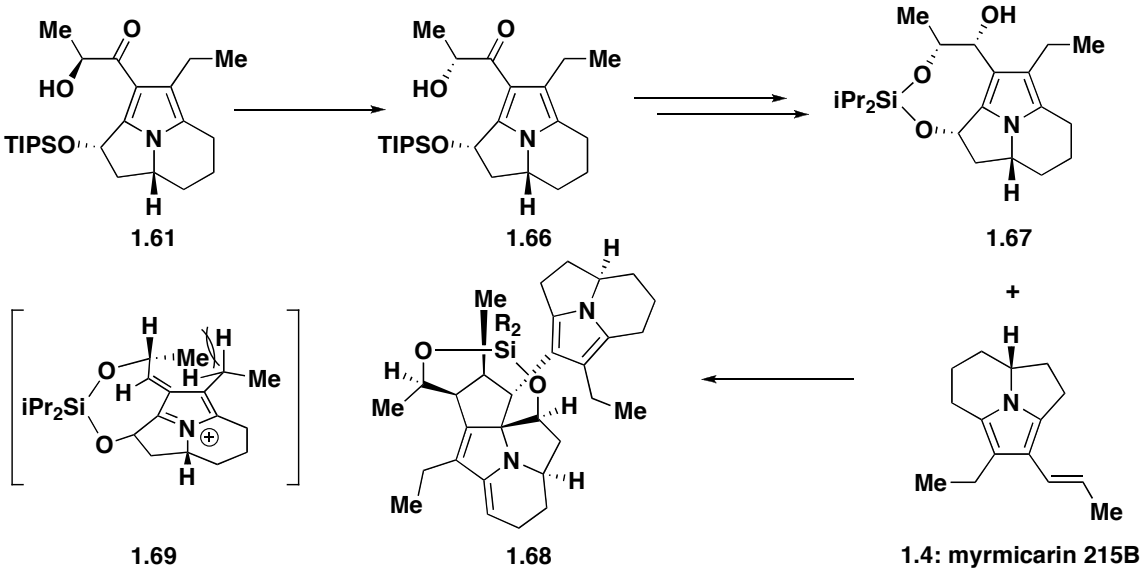

Scheme 1.16 Synthesis of conformationally restricted dimerization precursor **1.66** and selective heterodimerization with myrmicarin 215B (**1.4**). *Reagents and Conditions:* a) PPh_3, DEAD, *p*-NO_2-$C_6H_4CO_2H$, THF, 23 °C (61%, 72% brsm); b) LiOH, THF/H_2O, 50 °C (100%); c) $Sc(OTf)_3$, MeCN-d_3, 23 °C (>90%, single diastereomer). OTf = trifluoromethanesulfonate.

consistent with the isomyrmicarin 430A framework. Collectively, these experiments strongly suggest that the dimerizations are not concerted and likely involve a stepwise, ionic mechanism. As further support for this conclusion, the *Z*-azafulvenium derived from **1.61** would have been expected to produce the opposite stereochemistry at C3 than that which was observed.

1.3.3 Brönsted Acid-Promoted Reversible Dimerization

In order to gain a detailed mechanistic understanding of the Brönsted acid promoted dimerization of myrmicarin 215B, the Movassaghi group looked to the slow introduction of HCl through photoirradiation of methylene chloride solutions of myrmicarin 215B in hopes of observing intermediates en route to dimeric materials. Their efforts in this regard[12] are summarized in Scheme 1.19. In the event, irradiation of a

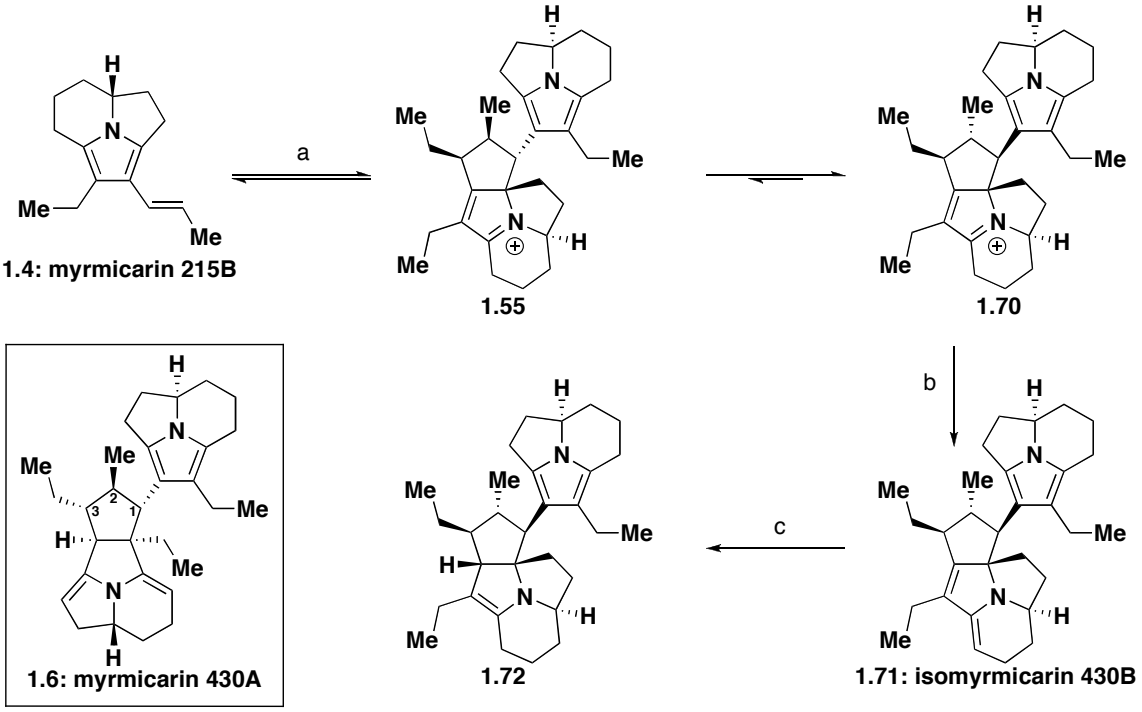

Scheme 1.17 Reversible dimerization of myrmicarin 215B (**1.4**). *Reagents and Conditions:* a) hν, CH_2Cl_2, 10 h, 23 °C; b) Et_3N, silica gel (66%, 2 steps); c) H_2, Pd/C, C_6H_6, 23 °C (40%).

methylene chloride-d_2 solution of myrmicarin 215B (**1.4)** with a medium pressure mercury lamp smoothly afforded iminium **1.55** (the precursor to isomyrmicarin 430A) after 2 h. Prolonged exposure, however, resulted in isomerization to a new iminium ion **1.70**. Filtration of the crude reaction mixture through Et_3N-deactivated silica gel afforded a new heptacyclic compound that was found to be exceedingly unstable but still allowed for 2D-NMR experiments to be performed. These experiments suggested that an isomerization to compound **1.71** (isomyrmicarin 430B) had occurred. The stereochemistry of this intemediate was corroborated by NOESY experiments on the reduced congener **1.72**, a molecule that exhibited greatly enhanced stability relative to its oxidized counterpart. While the connectivity of this heptacycle is identical to isomyrmicarin 430A, the stereochemical relationship around the central cyclopentane

core had been altered to *trans, trans* about the C1—C2, C2—C3 bonds; however, the stereochemical configuration at C3 remains epimeric to that of myrmicarin 430A.

Deuterium labeling experiments using methylene chloride-d_2/D_2O mixtures (7% v/v) indicated that the dimerization to form iminium **1.55** is reversible, with intermediates capable of converting back into myrmicarin monomers. These experiments suggest that the iminium ion leading to isomyrmicarin 430B is the thermodynamic product of this dimerization, likely due to the strain minimization imparted by the *trans, trans* configuration denoted above. Furthermore, isomyrmicarin 430B was not found to revert to tricyclic myrmicarins under identical conditions. The possibility was thus considered that the incorrect stereochemical disposition at C3 could be responsible for the regioisomeric C3b nucleophilic closure of the heptacycle. To test this hypothesis, compound **1.73** in Scheme 1.20 was prepared and treatmed with TFA followed by BEMP work-up. This reaction afforded **1.74**, suggesting that the incorrect stereochemical disposition at C3 alone was not responsible for the observed regioselectivity.

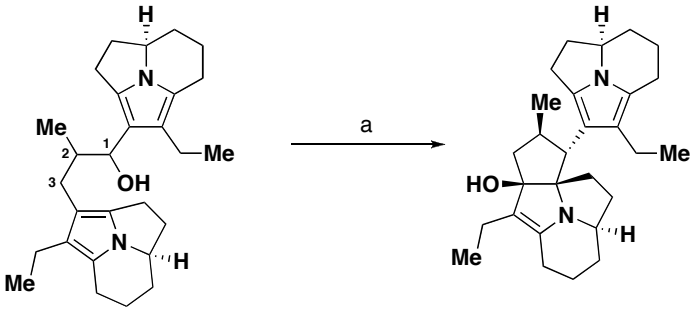

1.73 **1.74**

Scheme 1.18 Intramolecular cyclization of C3-nor-derivative **1.73**. *Reagents and Conditions:* a) TFA, C_6D_6 23 °C; BEMP (29%). TFA = trifluoroacetic acid, BEMP = 2-*tert*-butylimino-2-diethylamino-1,3-dimethylperhydro-1,3,2-diazaphosphorine.

1.4 Our General Strategy to Target the Entire Family of Myrmicarin Alkaloids

Before our work began towards these natural products, Movassaghi's total syntheses of the tricyclic myrmicarins[7] and initial dimerization studies[10] had already appeared in the literature (see Sections 1.2.7 and 1.3.1, respectively). Additionally, only three months after commencing our work, Movassaghi's concerted cycloaddition strategy[11] toward myrmicarin 430A (see Section 1.3.2) was reported. Having carefully studied these reports, we re-analyzed the entire family of natural products in hopes of identifying and proposing a dimerization precursor distinct from myrmicarin 215A/B. Indeed, while the mechanistic scenarios outlined by the Movassaghi group would provide rapid access to the natural products, a number of observations led to reservations regarding the viability of myrmicarin 215-type structures to afford the desired dimeric materials.

First, Movassaghi's preliminary calculations and subsequent experimental efforts suggested that the electrophilic azafulvenium ion likely resides and reacts through the *Z* olefin geometric isomer. Given this information and expected convex face/convex face approach of the nucleophile and electrophile to minimize sterics, the resultant C2—C3 bond would be expected to be epimeric to that of the natural isolate, a result that has been experimentally validated by the Movassaghi group. Second, the presence of only one chiral center far-removed from the site of reactivity suggested these structures would be difficult to functionalize in order to alter their inherent stereochemical bias during dimerization. Furthermore, should such functionalization be possible, we anticipated that the steps required for removal of these groups after successful preparation of a myrmicarin 430-like structure would prove exceedingly difficult, if not impossible.

Third, the natural isolate myrmicarin 663 (**1.8**) provided some evidence that myrmicarin 215-type structures may not be the biosynthetic precursors to oligomerization given that one third of its structure is inconsistent with direct oligomerization of a pyrroloindolizidine substructure. Inspired by this realization, we hoped that a molecule of general structure **1.75** (Figure 1.3) that blends the structural features of myrmicarin 237

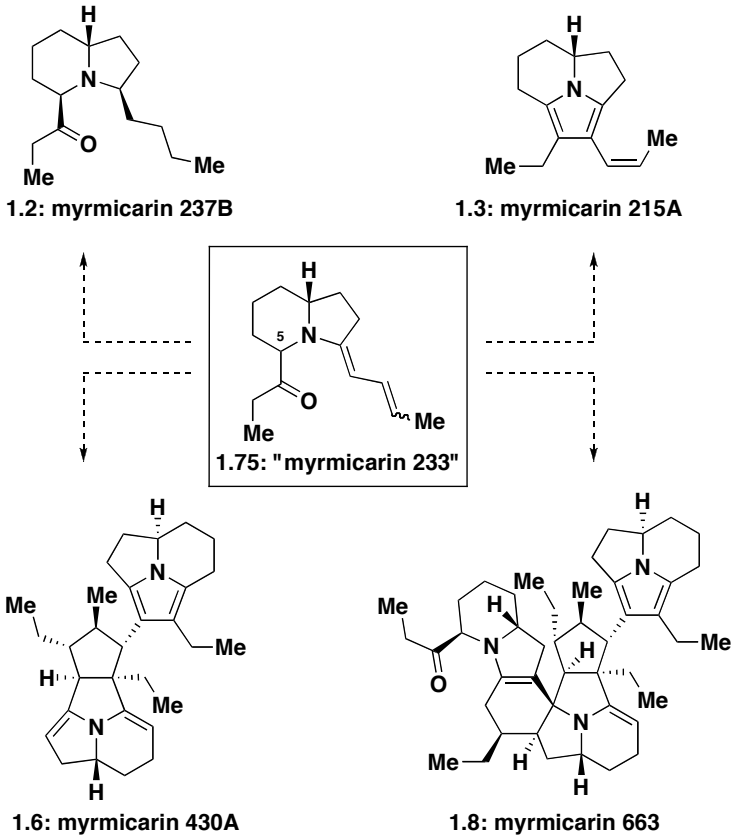

Figure 1.3 Our strategy to access the entire family of myrmicarin alkaloids from indolizidines of general structure **1.75**.

and the oxidation state of myrmicarin 215 might provide the necessary flexibility to afford the desired stereocontrol during dimerization. This idea was particularly appealing since the presence of an additional chiral center at C5 proximal to the site of reactivity could influence the facial presentations of the two monomers prior to dimerization.

Indeed, a similar biosynthetic hypothesis has been advanced by Francke and co-workers[1b]; however, their proposal indicated the presence of cross-conjugated dienamines that we anticipated would be difficult to access due to the strain imparted by placing three sp^2 atoms within the 5-membered ring. During the initial isolation of the tricyclic myrmicarins, GC/MS analysis provided circumstantial evidence for such "myrmicarin 233"-like structures, albeit in very low quantities. In the next few chapters of this thesis, we recount our synthetic efforts focused on this overall plan.

1.5 References

1. a) W. Francke, F. Schröder, F. Walter, V. Sinnwell, H. Baumann, M. Kaib, *Liebigs Ann.* **1995**, 965 – 977; b) F. Schröder, S. Franke, W. Francke, H. Baumann, M. Kaib, J. M. Pasteels, D. Daloze, *Tetrahedron* **1996**, *52*, 13539 – 13546; c) F. Schröder, V. Sinnwell, H. Baumann, M. Kaib, *Chem. Commun.* **1996**, 2139 – 2140; d) F. Schröder, V. Sinnwell, H. Baumann, M. Kaib, W. Francke, *Angew. Chem.* **1997**, *109*, 161 – 164; *Angew. Chem. Int. Ed. Engl.* **1997**, *36*, 77 – 80.

2. G. V. Thanh, J.-P. Celerier, G. Lhommet, *Tetrahedron Lett.* **1999**, *40*, 3713–3716.

3. F. Schröder, W. Francke, *Tetrahedron* **1998**, *54*, 5259–5264.

4. B. Sayah, N. Pelloux-Léon, Y. Valleé, *J. Org. Chem.* **2000**, *65*, 2824–2826.

5. B. Sayah, N. Pelloux-Léon, A. Milet, J. Pardillos-Guindet, Y. Valleé, *J. Org. Chem.* **2001**, *66*, 2522–2525.

6. R. Settambolo, G. Guazzelli, R. Lazzaroni, *Tetrahedron: Asym.* **2003**, *14*, 1447–1449.

7. M. Movassaghi, A. E. Ondurs, *Org. Lett.* **2005**, *7*, 4423–4426.

8. M. Movassaghi, A. E. Ondrus, *J. Org. Chem.* **2005**, *70*, 8638–8641.

9. M. Santarem, C. Vanucci-Bacqué, G. Lhommet, *Heterocycles* **2010**, *81*, 2523–2537.

10. A. Ondrus, M. Movassaghi, *Tetrahedron* **2006**, *62*, 5287–5297.

11. M. Movassaghi, A. E. Ondrus, B. Chen, *J. Org. Chem.* **2007**, *72*, 10065–10074.

12. A. E. Ondrus, M. Movassaghi, *Org. Lett.* **2009**, *11*, 2960–2963.

CHAPTER 2

The Evolution of Efficient, Enantioselective Total Syntheses of Monomeric Myrmicarin Alkaloids

2.1 First Generation Total Synthesis of Myrmicarin 217

In line with our proposed dimerization strategy, our focus was aimed at developing a short, efficient synthesis of the tricyclic myrmicarins (**2.1**–**2.3**, Figure 2.1) and molecules of general structure **2.4**. Initially, we sought to develop a novel approach

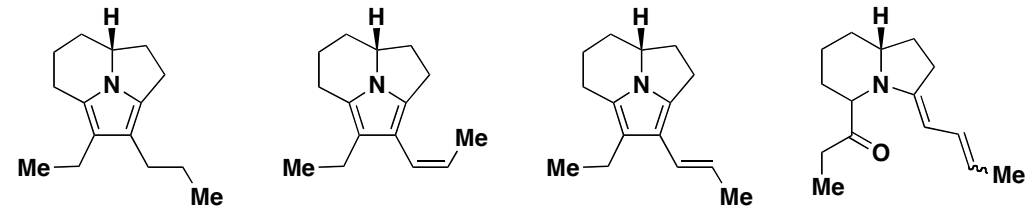

Figure 2.1 Structures of the tricyclic myrmicarins (**2.1**–**2.3**) and our proposed synthetic precursor (**2.4**) to access **2.2**, **2.3**, and dimeric materials.

to the indolizidine core, and several routes were aimed at achieving this goal. After much exploration, however, these efforts proved taxing and hampered our ability to focus on the main objective, namely developing a synthesis of myrmicarin 430A. The detail of these studies will not be detailed here, but to provide a sense of the approaches involved, we have summarized the results in Scheme 2.1 below.

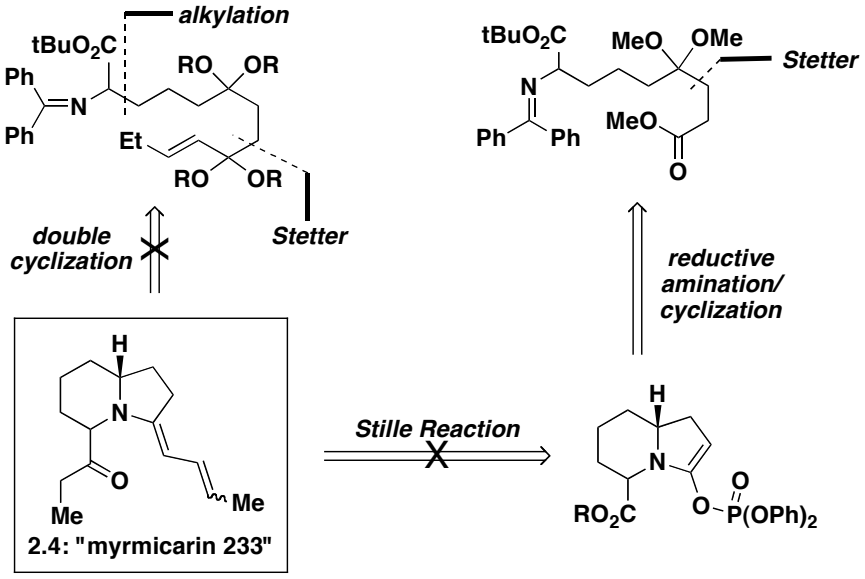

Scheme 2.1 Early approaches to dienamines of general structure **2.4**.

As our early efforts to develop a novel route to access the indolizidine core of the myrmicarin natural products proved fruitless, our attention turned next to known literature preparations of indolizidine natural products[1] in hopes of accessing appropriate materials to address our key goals and synthetic questions. After a survey of several known strategies to forge indolizidine skeletons, a recent report from the Ma group[2] attracted our attention. In their disclosure, Cu-propiolate nucleophiles were added to acylpyridinium salts both efficiently and enantioselectively, enabling a total synthesis of indolizidine alkaloids 167B and 223AB. The decision was made to follow this precedent as it was anticipated that dimerization studies would likely require access to enantioenriched monomeric starting materials (see Chapter 3) and, ultimately, it furnished material that could then be manipulated to our desired dienamine precursors.

Though we eventually desired access to dienamine compounds, we anticipated that access to the monoenamine counterpart (a known compound) would function as an excellent model system without the complication of considering alkene isomer geometries. Hence, we embarked on our first successful route to prepare myrmicarin 217 (**2.1**), as outlined in Schemes 2.2 and 2.3. Compound **2.11**, a known derivative from Ma's work, was accessed in short order over three steps. Pyridine dearomatization with methyl propiolate as nucleophile delivered the desired dienecarbamate **2.9** in 72% yield. At this point, the unoptimized, but commercially available ligand **2.8,** was used in our studies, and thus, the enantioselectivity of this reaction was not determined. Pd/C mediated reduction of the alkyne and partial reduction of the dienecarbamate afforded enecarbamate **2.10**. Sakurai-type allylation in the presence of TFA and allyltrimethylsilane afforded the 2,6-*cis* disubstituted piperidine **2.11** as a single

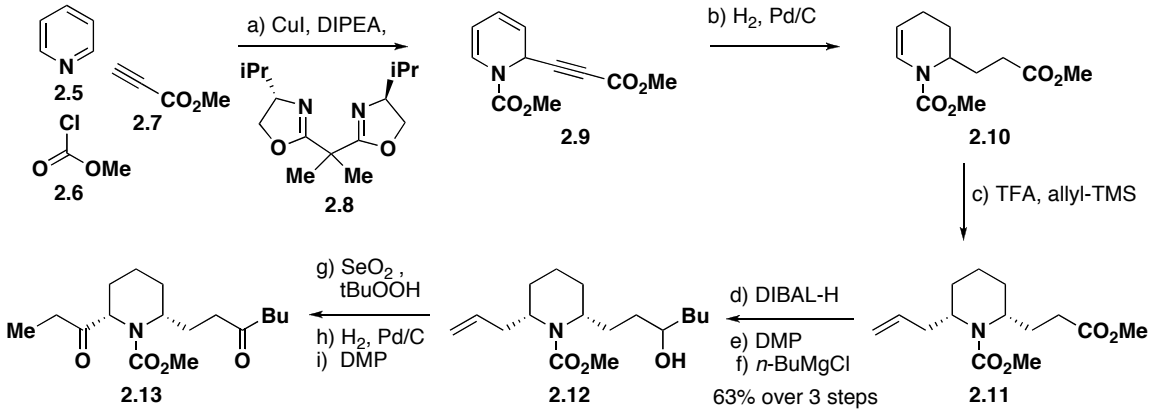

Scheme 2.2 Synthesis of key intermediate diketone **2.13**.

diastereomer in 74% yield over the two steps. The stereoselectivity of the latter reaction is a result of axial attack on the formed iminium ion from the half chair conformer that places the side chain axial (see Figure 2.2). This conformational preference of 2-substituted, carbamate-protected piperidines arises from an $A_{1,3}$-like interaction that exists when substitutents are equatorially oriented. From here, DIBAL-H reduction of

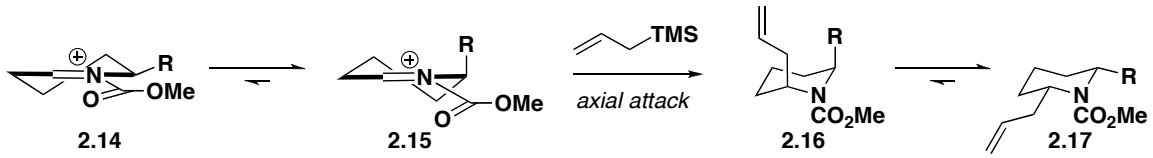

Figure 2.2 Rationale of stereochemistry observed in the Sakurai-type allylation.

ester **2.11** proved non-trivial, and ultimately an optimization of the conditions used during the quench proved necessary to achieve reproducibly high yields. For example, the use of NaOH or Rochelle's salt during the quench led to extensive intramolecular cyclization of the formed alcohol onto the methyl carbamate. Although stirring with CSA in MeOH at room temperature could recycle the material, this procedure proved cumbersome. Eventually, we found that quenching the reaction mixture with 1 M H_2SO_4 cleanly afforded the primary alcohol and effectively supressed the unwanted cyclization. Oxidation of the primary alcohol with Dess–Martin periodinane[3] furnished the desired

aldehyde. Subsequent Grignard addition with *n*-BuMgCl furnished secondary alcohol **2.12** in 62% yield from **2.11**.

Our next goal was the installation of the desired ketone onto the allyl side chain. Allylic oxidation[4] with catalytic SeO_2 and *t*-BuOOH in DCE at 70°C afforded a 1.2:1 mixture of ketone and allylic alcohol in a 42% combined yield. Despite several attempts to alter the product distribution and increase the yield by including protic additives[4] and changing catalyst/co-catalyst loadings, the above conditions proved optimal. Interestingly, the Pd-catalyzed allylic oxidation[5] of terminal allyl groups was completely unsuccessful in our hands; starting material was recovered unchanged in near quantitative yield. Furthermore, efforts to install the hydroxyl group at different stages of the synthesis either proved less efficient or unsuccessful. As such, the mixture of compounds was then taken forward together and hydrogenated over catalytic Pd/C. Subequent oxidation with Dess–Martin periodinane afforded diketone **2.13**.

Cyclization precursor **2.13** was then treated with TMSI in CH_2Cl_2 at 23 °C, effectively removing the methyl carbamate and affording enamine **2.18** after aqueous

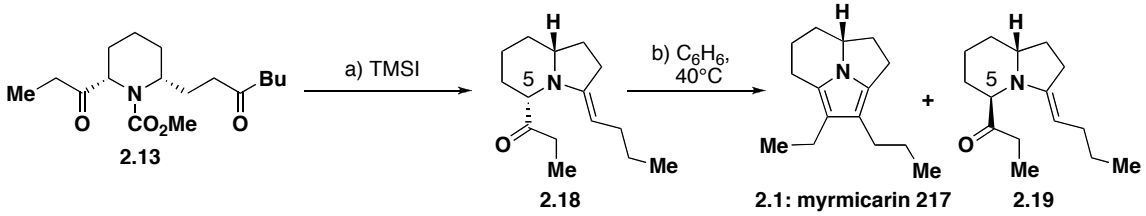

Scheme 2.3 Total synthesis of myrmicarin 217 (**2.1**).

workup. This compound was previously shown to cyclize to myrmicarin 217 (**2.1**) with heating to 40 °C in benzene,[6] a process that we were able to repeat, thus completing our first generation total synthesis of myrmicarin 217. It is worth recalling at this juncture that enamine **2.18** was also previously shown to be configurationally unstable at C5,

undergoing *in situ* epimerization to **2.19** during the heating required to effect cyclization.[6] What the literature report did not address, however, is whether one or both of the isomers were capable of undergoing cyclization, a point of import in our later studies that we will revisit in the next section. Nevertheless, this route provided an overall proof of concept, and myrmicarin 217 (**2.1**) was accessed in 6.6% yield over 10 steps.

2.2 Second Generation Synthesis of Myrmicarin 217

While we were pleased to have discovered that our first generation route could indeed provide access to the desired indolizidine core of the myrmicarins, the overall yield of the sequence was non-optimal. Furthermore, several of the reactions performed much more poorly on attempted scale-up. We therefore began to modify our route and initiate optimization studies. Ideally, we desired a route that would be capable of delivering large amounts of both C5 epimers of indolizidine substrates since dimerization studies were anticipated to require much experimentation to achieve, and our first generation route only afforded milligram quantities of **2.18**. The following additional observations were made in hopes of improving material throughput and route flexibility in anticipation of targeting myrmicarin 215A (**2.2**) and myrmicarin 215B (**2.3**):

1. The semi-reduction of dienecarbamate **2.9** proved tenuous on scale-up, and a large part of the material was lost to overreduced material that could not be separated from the desired enecarbamate.
2. The Sakurai allylation (**2.10** → **2.11**) required large excesses of nucleophile to reach full conversion and, more importantly, only provided access to the 2,6-*cis* diastereomeric series of compounds.

3. The SeO_2 mediated allylic oxidation of **2.12** gave a mixture of compounds and gave poor yields. In addition, the timing of this reaction would require alteration with myrmicarin 215 as a target.
4. Deprotection of the methyl carbamate within **2.13** required the use of TMSI, which would likely be incompatible with the proposed β,γ-unsaturated ketone precursor to myrmicarin 215.

With the above key considerations in mind, we embarked on the design of a new route. Careful evaluation revealed that the first three concerns could be alleviated by exploring an alternate method for the introduction of the ethyl ketone. In particular, we were drawn to the report of α-*N*-Boc deprotonations on piperidine scaffolds.[7] Importantly, this method is known to give rise to 2,6-*trans*-disubstituted piperidine scaffolds by virtue of the stabilizing interaction imparted by the *N*-Boc group in conjunction with the aforementioned axial conformation adopted by such systems. In the context of our synthesis, we hoped that quenching the formed lithiated piperidine with DMF would afford a 2,6-*trans* piperidine whose aldehyde could be subsequently epimerized to afford the thermodynamically more stable 2,6-*cis* stereoisomer. Furthermore, this method would require protection of the piperidine nitrogen as the corresponding *tert*-butyl carbamate. Balance was needed, however, in that we hoped that such a protecting group would be stable throughout the early stages of the synthesis but labile enough to undergo mild deprotection conditions at the end of the sequence.

The optimized route to racemic myrmicarin 217 is shown in Scheme 2.4. Initial Yamaguchi alkynylation[8] with Grignard **2.20** afforded dienecarbamate **2.22**. The use of benzyl chloroformate (**2.21)** instead of methyl chloroformate was anticipated to allow for

a protecting group switch during the subsequent reduction step. Pleasingly, protecting group exchange did indeed proceed smoothly during the exhaustive reduction, affording **2.24** in 80% yield over the two steps. Interestingly, the only major side product from this reaction was aromatized pyridine **2.23**, a compound that presumably arose from palladium-mediated olefin isomerization from the propargylic alcohol into the ring. This

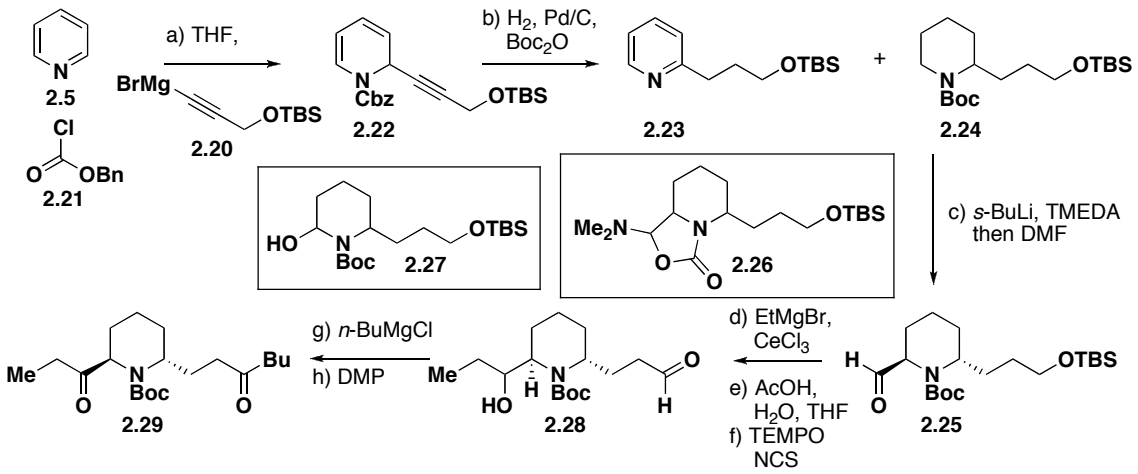

Scheme 2.4 Synthesis of diketone intermediate **2.29**.

type of product was never observed during the reduction of the ester counterpart, suggesting that conjugation to the ester likely prevented the corresponding olefin isomerization from occurring. A control experiment on the corresponding methyl carbamate of **2.22** did not lead to any detectable amounts of rearomatized products, suggesting that deprotection of the benzyl carbamate is a prerequisite for this isomerization.

Moving forward, silyl protected alcohol **2.24** was subjected to deprotonation conditions following literature precedent[9]; however, in our hands, the major product from the reaction was cyclic carbamate **2.26**, and this reaction required several rounds of optimization to achieve high yields of the desired aldehyde reproducibly. Two factors

were found to be particularly important to the success of this reaction. First, TMEDA had to be freshly distilled from KOH prior to use; the use of TMEDA that had been stored for longer than approximately 2 weeks resulted in a significant reduction in yield. Second, careful temperature control during the deprotonation step and subsequent nucleophilic addition were required. After initial addition of *s*-BuLi to a precooled solution of **2.24** and TMEDA in Et_2O at –78 °C, the reaction was warmed to –40 °C and maintained at that temperature for 1 h before being re-cooled to –78 °C. DMF could then be added and the reaction warmed again to –40 °C where the reaction was kept for an addition 1.5 h prior to quenching with saturated aqueous NH_4Cl. Furthermore, the quality of the *s*-BuLi used in the reaction proved important, as older bottles led to significant amounts of oxidized product **2.27**. With these optimizations in place, aldehyde **2.26** could be accessed efficiently (97% yield) and reliably even on scale-up.

Pressing forward, nucleophilic addition of ethylmagnesium bromide to a suspension of aldehyde **2.25** and $CeCl_3$ in THF[10] afforded the corresponding secondary alcohol in high yield. The presence of $CeCl_3$ prevented low conversion to the desired product due to competing α-deprotonation of the aldehyde. Deprotection of the primary alcohol with acetic acid and water in THF set the stage for a TEMPO-mediated selective primary alcohol oxidation[11] under phase transfer conditions, affording aldehyde **2.28** in high yield after silica gel chromatography. Treatment of aldehyde **2.28** with *n*-BuMgCl afforded the diol as an inconsequential mixture of diastereomers, and Dess-Martin oxidation afforded high yields of diketone **2.29**.

Deprotection of the *tert*-butyl carbamate in a 1:1 mixture of TFA and CH_2Cl_2 at 0 °C quickly led to full deprotection of the nitrogen (Scheme 2.5). Work-up with cold

aqueous NaOH then provided enamine **2.19**, the C5 epimer of **2.18**. To our surprise, this compound was completely stable to the cyclization conditions reported in reference 6, and furthermore, this compound was found to be configurationally stable, suggesting that

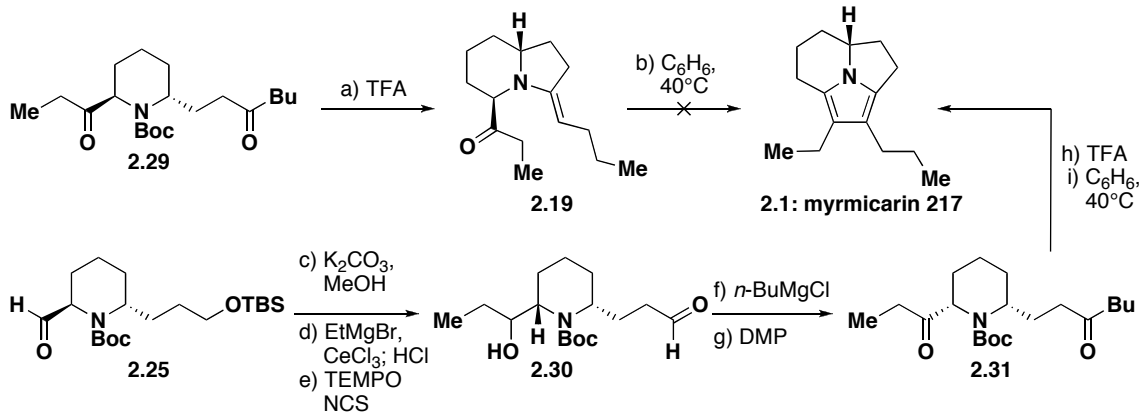

Scheme 2.5 Second generation total synthesis of myrmicarin 217 (**1**).

this isomer is thermodynamically more stable than **2.18** and that compound **2.18** is the diastereoisomer that undergoes cyclodehydration. Thus, we had our first experimental indication that the stereochemistry about C5 has a significant effect on the propensity of such intermediates to undergo cyclodehydration. This result also suggested that two different sets of conditions would be required to effect the desired cyclization of each epimer. At this point, we elected to leave such explorations for our studies toward myrmicarin 215A and myrmicarin 215B.

The observation that the 2,6-*cis* piperidine-derived diastereomer (**2.18**) underwent more facile cyclization to myrmicarin 217 prompted us to return to the preparation of the requisite 2,6-*cis* scaffold using our optimized protocol described above. After formylation, aldehyde **2.25** was subjected to epimerization with K_2CO_3 in MeOH at ambient temperature for 3 hours, affording a ~10:1 *cis*:*trans* ratio of isomers in 83% yield that could be separated by silica gel chromatography. Subsequent experiments revealed

that quenching this formylation reaction with methanol and adding solid potassium carbonate to the reaction mixture could effect the one pot conversion of **2.24** directly into the *cis* isomer. Intriguingly, this one pot process proved both cleaner and higher yielding (93%). The ethyl group was then introduced using the same procedure described above. At this juncture, we discovered that the subsequent TBS-deprotection step could be eliminated by quenching the Grignard addition with dilute HCl and stirring for 2 hours at ambient temperature. This one pot procedure afforded the corresponding diol in 89% yield. The same sequence of reactions described above then afforded diketone **2.31**. Deprotection with TFA afforded the cyclized product without incident and thus constituted a highly optimized sequence to racemic myrmicarin 217 (20% overall yield) requiring only 8 steps. Attention then turned to the more oxidized congeners of the family, namely myrmicarin 215A (**2.2**) and myrmicarin 215B (**2.3**).

2.3 Enantioselective Total Synthesis of Myrmicarins 215A and 215B

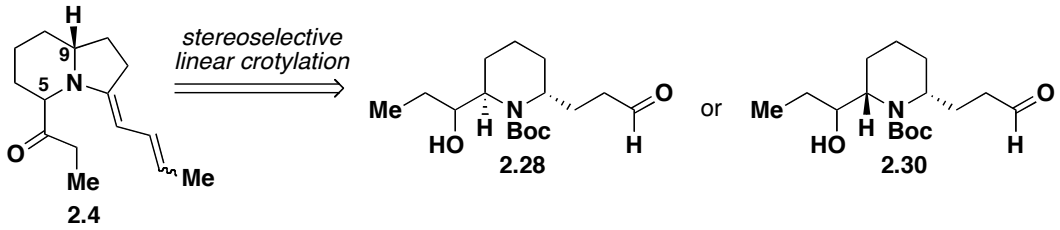

Figure 2.3 General strategy to access dienamines of general structure **2.4**.

As our ultimate goal in this project was to develop a synthesis of myrmicarin 430A,[12] access to the more oxidized dienamine precursors was required given that half of the target structure contains the tricyclic pyrroloindolizidine core of myrmicarin 215. Our target therefore became indolizidines of general structure **2.4** (Figure 2.3), compounds we hoped would be able to undergo dimerization in a stereoselective fashion. However, it

was unclear, *a priori*, which pair of C5 and alkene diastereomers would lead to the desired stereochemical outcome upon dimerization, a topic expanded upon in great detail in Chapter 3. Here, we hoped to use the same chemistry delineated in Section 2.2 to effect cyclodehydration of the 5,9-*cis*-keto-dienamine targets. Importantly, we had yet to develop a procedure for cyclodehydration of the corresponding 5,9-*trans* series of compounds, an issue we chose to address in the context of these oxidized targets, as the inability to convert **2.29** to myrmicarin 217 was inconsequential.

These molecules, however, provided an additional level of complexity in route design since the olefin geometry constituted a second stereodivergence. We thus adopted a diversity-oriented approach wherein our last stereodivergence would be made as close to the end of the sequence as possible. This goal was achieved by anticipating that aldehydes **2.28** and **2.30** could each undergo stereoselective linear crotylation to afford both *cis* and *trans* olefin isomers. Indeed, a large body of literature suggested that such transformations would be possible,[13] and furthermore, those reactions catalyzed by Lewis acids were particularly appealing since we anticipated that a simple switch in the Lewis acid source could afford the desired stereodivergence.

Our synthesis began with efforts to optimize the enantioselective pyridine aromatization reported by Ma[2] for our desired Cbz-protected substrate. Unfortunately, the reported procedure indicated that the reaction in the presence of benzyl carbamates *does not proceed*. Undeterred, we began to explore the ability of this reaction to afford product, even if the reaction gave poor enantioselectivites, with the hope that low enantioselectivities could be overcome through optimization.

A summary of our extensive optimization is summarized in Table 2.1. In our hands, following the exact literature procedure also led to no observed reaction. One

Table 2.1. Optimization of CuI catalyzed addition to Cbz-protected acyl pyridinium salts[a].

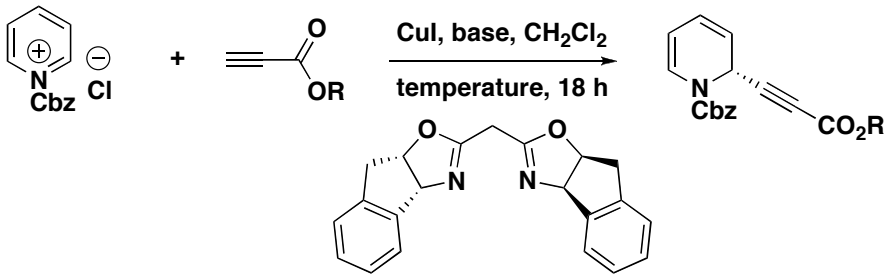

entry	R	base[b]	T (°C)	CuI source[c]	yield (%)	ee (%)
1	Me	DIPEA	–78	commercial	< 20	25[d]
2	Me	DIPEA	–78	commercial	65	43[e]
3	Me	DIPEA	–78→r.t.	commercial	65	65[e]
4	Me	DIPPA	–78→r.t.	purified	72	70[e]
5	Me	DIPPA	–78→–50	purified	75	73[e]
6	Et	DIPPA	–70	purified	49	80[e]
7	**Et**	**DIPPA**	**–65**	**purified**	**86**	**86[e]**
8	Et	DIPPA	–65	commercial	86	73[e]

[a]Standard conditions: CuI (0.1 equiv), Ligand (0.11 equiv), base (5 equiv), propiolate (5 equiv). [b]DIPEA = *i*-Pr_2NEt, DIPPA = *i*-Pr_2NPr-*n*. [c]Commercial source of CuI used as received or CuI purified before use. [d]Neat pyridine cooled before chloroformate addition. [e]Pyridine diluted with CH_2Cl_2 and cooled prior to chloroformate addition.

critical observation, however, was made. According to the reported procedure, benzyl chloroformate was added neat to pyridine with stirring at 23 °C, and immediate bubbling ensued. Although we had no direct evidence, we suspected that CO_2 was being liberated from the reaction mixture as a result of the reaction exotherm causing deprotection of the carbamate and subsequent formation of the benzyl pyridinium derivative (precipitate remained in the reaction mixture). To test this hypothesis, we cooled the pyridine to –20 °C prior to the addition of benzyl chloroformate, and pleasingly, this alteration did indeed afford some of the desired product but in very low yields (<20%) and enantioselectivity

(25% ee). During this experiment, the additional observation was made that the desired acylpyridinium that precipitated also caused ineffective stirring of the mixture. Hence, dilution of pyridine with a portion of CH_2Cl_2 and cooling to –40 °C prior to chloroformate addition allowed for a reliable and effective preparation of the necessary acylpyridinium derivative. Pleasingly, this alteration also afforded better yield (65%) and enantioselectivity (43% *ee*) of the reaction. Unfortunately, at –78 °C, the reaction mixture formed a very thick sludge that once again caused stirring to become erratic, and often, the reaction mixture would stop stirring altogether. Subsequent experiments showed a dependence of the stereoselectivity on the temperature of the reaction, with slow warming from –78 °C → 23 °C affording product in improved enantioselectivity (65% yield, 65% *ee*, entry 3). Exploration of the reaction temperature revealed that –65 °C proved optimal, affording the best balance of yield and enantioselectivity. Interestingly, the enantioselectivity of reactions carried out at –78 °C were lower than those obtained at –65 °C. We attribute this phenomenon to the fact that upon completion of the reaction, the crude mixture was directly evaporated and loaded onto silica gel. In the lower temperature reaction, we believe that incomplete reaction and sudden warming of the reaction mixture allowed the background reaction to take over, eroding the stereoselection. Further improvements in yield and enantioselectivity could be achieved by using ethyl propiolate as the nucleophile and diisopropylpropylamine as the tertiary amine base. While the CuI source used had little effect on yield, the enantioselectivity was highly dependent upon the quality of the CuI. Commercial sources of CuI when used as received resulted in enantioselectivities consistently between 60–70% *ee*, even when high purity sources were used (>99.99%). Surprisingly, purification of the commercial

sources of CuI according to Armarego and Chai[14] allowed for a dramatic increase in enantioselectivity, with results consistently above 80% *ee* under the optimized conditions. Even more surprising, the purified CuI could be stored for more than a year in a vial protected from light without any noticeable change in yield or enantioselectivity of the reaction. Thus, our optimized conditions were able to afford high yields and enantioselectivities of **2.32**, even on multi-gram scale. To date, the reaction has been carried out on up to 20 mmol scale without a significant reduction in yield or enantioselectivity (84% yield, 86% *ee*). We believe this reaction can find broad use to complement the reported procedure since the benzyl carbamate protecting group is much easier to deprotect than the methyl, ethyl, or isobutyl counterparts.

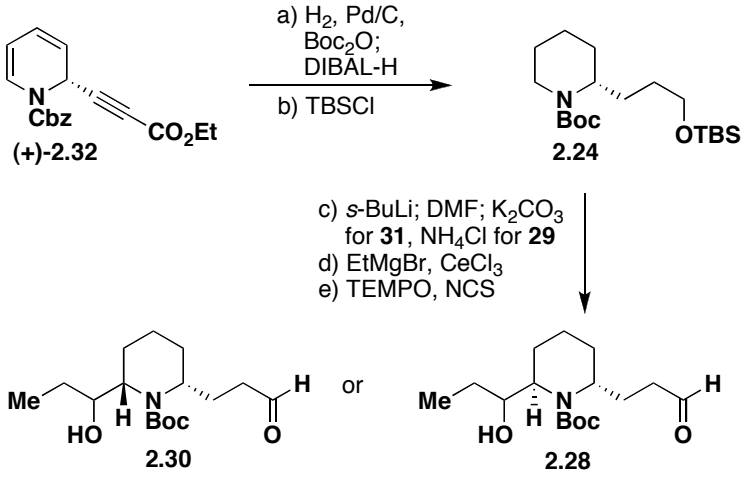

Scheme 2.6 Synthesis of enantioenriched **2.28** and **2.30**. *Reagents and Conditions:* a) H_2 , Pd/C, Boc_2O, EtOAc, 23 °C, 16 h (84%); b) DIBAL-H, THF, –78 °C, 45 min; 0 °C 15 min, (98%); c) TBSCl, imidazole, CH_2Cl_2, 25 °C, 12 h (98%); d) *s*-BuLi , TMEDA, Et_2O, –78 –40 °C, 1 h; DMF, –78 –40 °C, 1.5 h; NH_4Cl or K_2CO_3/MeOH, (90% for **2.30**, 97% for **2.28**); e) $CeCl_3$, EtMgBr, THF, –40 °C; HCl 3 h (92% for **2.30**, 89% for **2.28**); f) TEMPO, NCS, *n*-Bu_4NCl , NaBr, CH_2Cl_2, pH 8.6 aqueous buffer, 0 °C, 1.5 h (93% for **2.30**, 96% for **2.28**). Boc_2O = di-*tert*-butyldicarbonate, DIBAL-H = diisobutylaluminum hydride, TBS = tert-butyldimethylsilyl, DMF = N,N-dimethylformamide, TEMPO = 2,2,6,6-tetramethyl-1-piperidinyloxy free radical, NCS = N-chlorosuccinimide, TMEDA = N,N,N',N'-tetramethylethylenediamine.

Having developed a procedure to access large quantities of dienecarbamate **2.32** with good enantioselectivity, we proceeded to convert **2.32** into **2.24**, which proceeded largely without incident as depicted in Scheme 2.6. We do, however, make the following comment regarding the DIBAL-H reduction. As mentioned in Section 2.1, the use of basic conditions during the quench resulted in intramolecular cyclization, even in the presence of the Boc carbamate. Furthermore, the strongly acidic conditions used when the nitrogen was protected as the methyl carbamate were incompatibile with the Boc-protected piperidine. We therefore were forced to adopt a different protocol to quench the reaction. In particular, we found that sequential addition of hexanes and a saturated aqueous solution of $MgSO_4$ to the reaction mixture and stirring at room temperature caused precipitation of the aluminum salts that were effectively filtered off of the reaction mixture to afford very high yields of the desired alcohol. Subsequent silyl ether protection of the alcohol intercepted racemic **2.24**, and the chemistry delineated in Section 2.2 was followed to elaborate **2.24** to **2.28** and **2.30**, giving access to enantioenriched materials.

Linear crotylation studies were then undertaken. Following literature precent for *E*-selective linear crotylation, aldehyde **2.30** was treated with the crotylaluminum reagent (Scheme 2.7) derived from a 2:1 ratio of $AlCl_3$ and 2-butenylmagnesium chloride[15] at –78 °C with immediate warming of the reaction mixture to 0 °C. This procedure furnished crotylated material in near quantitative yield as an inseparable ~4:1 mixture of linear to branched crotylation products. At this stage, the complex mixture of diastereomers precluded determination of a *Z*/*E* ratio by crude ^{1}H-NMR analysis. Fortunately, the linear and branched regioisomers could be separated by column chromatography following

oxidation with Dess–Martin periodinane. NMR analysis of this purified material revealed the presence of essentially a single compound (>15:1 ratio). To our surprise, coupling constant decomposition of the complex resonance at δ = 5.66 ppm in the ^{1}H-NMR spectrum allowed a vicinal alkene coupling constant of 10.8 Hz to be determined,

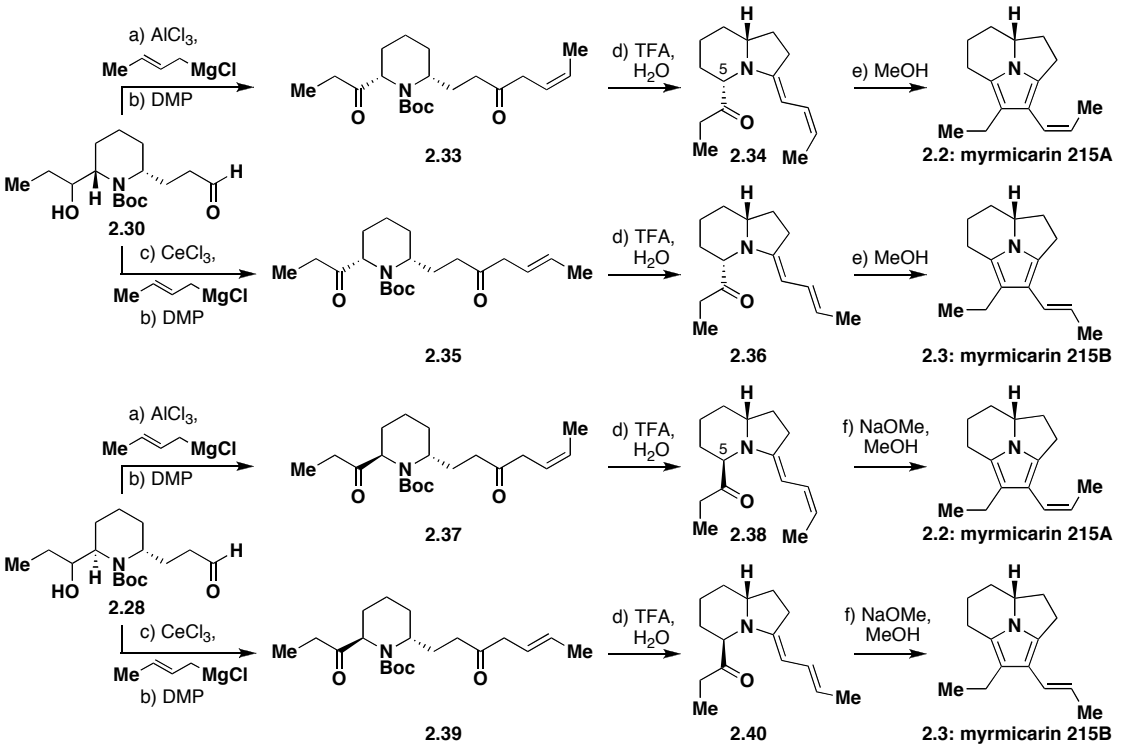

Scheme 2.7 Stereoselective total syntheses of myrmicarin 215A (**2.2**) and myrmicarin 215B (**2.3**). *Reagents and Conditions:* a) $AlCl_3$, 2-butenylmagnesium bromide, THF, –78 °C, 0 °C; b) DMP, CH_2Cl_2, 0 °C (>15:1 Z:E, 62% for **2.33**, 2 steps; >15:1 Z:E, 72% for **2.37**, 2 steps); c) $CeCl_3$, 2-butenylmagnesium bromide, THF, –78 to –40 °C [8:1 E:Z, 71% for **2.35** (2 steps, c and b); 8:1 E:Z, 66% for **2.39** (2 steps, c and b)]; d) TFA, H_2O, 0 °C (99%); e) degassed MeOH, 23 °C (99%); f) degassed MeOH, NaOMe, 50 °C (85%). DMP = Dess–Martin periodinane.

consistent with a *Z* alkene and contrary to the literature report. Interestingly, the original disclosure gives no mention of the method used to assign the olefin stereochemistry of the products, though GC was used to determine the ratio. When substrates used in the original disclosure were used, the *Z* diastereomer unvaryingly dominated the reaction mixture. We propose that the necessity of two equivalents of Lewis acid to achieve good yields and high stereoselectivity is a result of the Lewis acid functioning in a dual role:

one equivalent of $AlCl_3$ functions to activate the aldehyde and the second equivalent is involved in a transmetallation process that gives rise to a crotylaluminum reagent. The observed *Z*-selectivity can be explained through an open pre-transition state assembly as depicted in Figure 2.4 wherein the large dichloraluminum moiety points away from the

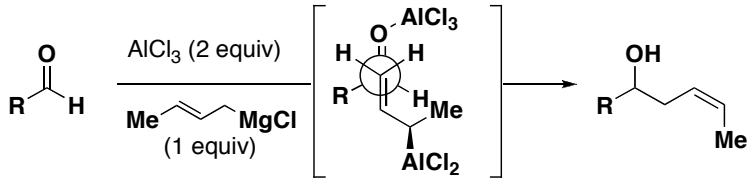

Figure 2.3 Proposed pre-transition state assembly leading to *Z*-olefins.

substrate, placing the methyl group on the side closer to the aldehyde proton. Such transition states have been proposed in the literature to account for the *Z*-selectivity observed in similar reactions.[13]

While pleased with our ability to reliably obtain large quantities of *Z*-alkene **2.33**, we still required a method to access the *E*-olefin diastereomer. Pleasingly, a switch of Lewis acid from $AlCl_3$ to $CeCl_3$[16] allowed for the smooth formation of the desired regioisomer (~6:1 linear to branched) with good alkene stereoselectivity (8:1 *E*:*Z*). Here, the observed *E*-selectivity is believed to originate from a closed, six-membered transition state that places the methyl group in a pseudoequatorial position. Pleasingly, application of the above two procedures to aldehyde **2.28** also afforded very similar results, securing stereoselective access to the desired four diastereomers **2.33**, **2.35**, **2.37**, and **2.39** primed for deprotection and cyclization.

Nitrogen deprotection with TFA/CH_2Cl_2 at 0 °C quickly consumed the starting material, and after a quench with cold, aqueous NaOH and extraction, NMR analysis of the crude reaction products revealed that in addition to nitrogen deprotection, the β,γ-

unsaturated ketone had isomerized to the thermodynamically more stable α,β-unsaturated ketone. To our surprise, this intermediate proved exceedingly recalcitrant to cyclization, preferring instead to undergo relatively rapid decomposition. Fortunately, deprotection conditions were identified following literature precedent[17] that could prevent the detrimental olefin isomerization from occurring. Deprotection of the diketones in a biphasic mixture of TFA, CH_2Cl_2, and H_2O (4:4:1) at 0 °C cleanly afforded dienamines **2.34**, **2.36**, **2.38**, and **2.40** in essentially quantitative yields after cold, aqueous NaOH workup.

In stark contrast to their monoenamine counterparts, these compounds were all configurationally stable even upon heating in benzene to reflux for several hours. Unfortunately, this heating procedure also failed to afford any traces of myrmicarin 215. Given the ease with which the *cis*-disposed diastereomer **2.18** underwent cyclization, we elected to pursue optimization studies with compound **2.36**. Initial deliberations led us to believe that the lack of species capable of assisting in proton transfer reactions in the reaction medium (anhydrous benzene) could be hampering the reaction, and thus the use of exogeneous base and acid additives were explored. Pleasingly, some conversion to myrmicarin 215 was observed (<10%); however, the conditions used also resulted in substantial olefin isomerization. Buffered conditions using pyrrolidine and AcOH did indeed provide higher yields (~15%), but the reaction conversions invariably plateaued at that value. At this point, we recognized that the desired reaction we wanted to achieve could be formally classified as a 5-(enol-*endo*)-*exo* trig cyclization (disfavored by Baldwin's Rules)[18] and constituted an intramolecular variant of a modification to the classic Knorr pyrrole synthesis.[19] Explorations of such reactions in the literature revealed

that these cyclizations are often carried out in polar, protic solvents. To our delight, simple dissolution of **2.36** in thoroughly degassed MeOH at room temperature for 1 h resulted in the quantitative conversion to myrmicarin 215B (**2.3**). Indeed, *Z*-olefin **2.34** could also be cleanly converted by the same procedure into myrmicarin 215A (**2.2**).

Unfortunately, dissolution in MeOH did not lead to any detectable conversion of compounds **2.38** or **2.40** to their pyrrole counterparts, providing further evidence that such 5,9-*trans* compounds were not capable of undergoing cyclization. After some experimentation, we found that exposure of either **2.38** or **2.40** to a solution of degassed sodium methoxide in methanol at 50 °C for 1 h followed by aqueous workup and column chromatography over basic alumina gave pyrroles **2.2** and **2.3**, respectively, each in 85% isolated yield. This process likely involves slow epimerization of the ketone followed by fast cyclodehydration. Overall, our total syntheses of myrmicarin 215A (**2.2**) and myrmicarin 215B (**2.3**) were completed in 10 steps in 33% and 38% overall yield, respectively. These total syntheses constitute the shortest and most efficient synthesis of these tricyclic myrmicarins to date.[20]

2.4 Conclusions and Remarks

All of the pyrrole containing natural products were found to be highly sensitive to air and prone to oxidation. Solutions of these compounds underwent substantial decomposition over a period of a few days even when stored frozen as a solution in benzene that had been degassed by the freeze-pump-thaw method. Pleasingly, the conditions used to cyclize dienamines **2.34** and **2.36** (i.e. dissolution in degassed MeOH) were also found to be effective in affording pyrrole products when monoenamine **2.18**

was used, thereby increasing the overall yield for our total synthesis of myrmicarin 217 (**2.1**). Furthermore, dieneamine **2.40** could be reduced diastereoselectively to myrmicarin 237B when exposed to catalytic Pd/C hydrogenation conditions in EtOAc.

The overall configurational stability of these dienamines was totally unexpected, but a plausible rationale for their stability is that the presence of the dienamine itself renders the nitrogen less basic than either its monoenamine counterpart or the fully reduced myrmicarin 237 structures. The inability to form stoichiometrically protonated species without the use of relatively strong acids (*vide infra*, Chapter 3) supports this assertion that these dienamines are indeed only weakly basic. The stability of this intermediate in an interrupted, intramolecular Knorr pyrrole synthesis also proved valuable as a mechanistic probe of the cyclocondensation step of this classic named reaction.[21] Finally, the ease with which compounds **2.18**, **2.34**, and **2.36** undergo cyclization leads us to propose that myrmicarin 217 (**2.1**), myrmicarin 215A (**2.2**), and myrmicarin 215B (**2.3**) are formed spontaneously under physiological conditions. As support for this proposal, we found that compounds **2.34** and **2.36** undergo cyclization in buffered aqueous solutions to afford their pyrrole counterparts. Thus, it appears that oxidation of the butyl side chain of myrmicarin 237A congeners leads to spontaneous cyclization, affording the tricyclic myrmicarin natural products.

Herein we have summarized our approach to prepare the tricyclic, monomeric myrmicarin alkaloids. These efforts allowed for large-scale access to the tricyclic myrmicarins and their oxidation-state equivalent dienamines. That conditions were identified that could both arrest and afford cyclization at will was critical in that it provided a strategy that would be of great advantage in later studies (*vide infra*, Chapter

3). Key to the overall success of our approach was a designed route that takes advantage of principles from diversity oriented synthesis to access the necessary stereodivergences from common intermediates, thereby streamlining the preparation of all of our dienamine substrates as well as myrmicarins 215A, 215B, and 217. Table 2.2 provides a direct comparison of the overall number of steps and efficiencies of our route to the tricyclic myrmicarin alkaloids versus those that have been previously reported.

Table 2.2 Comparison of efficiencies of reported total syntheses of the tricyclic myrmicarins.

Natural product	Synthesis	Steps	Yield
myrmicarin 217	Schröder, racemic	10	18.5%
	Vallée, enantiospecific[a]	12	7.5%
	Lazzaroni, formal enantispecific[a]	12	3.2%
	Movassaghi, enantioselective	10	21.1%
	Lhommet, formal enantiospecific[a]	13	6.3%
	our enantioselective	10	38–40%
myrmicarin 215	Vallée, enantiospecific[a]	14	6.8%
	Movassaghi, enantioselective	11 (M215A)	2.2%
		11 (M215B)	15.1%
	Lhommet, formal enantiospecific[a]	14 (M215A)	0.66%
		14 (M215B)	4.5%
	our enantioselective	10 (M215A)	33%
		10 (M215B)	38%

[a]Yields and step-count are based on the first intermediate presented.

2.5 References

1. a) J. P. Michael, *Nat. Prod. Rep.* **2003**, *20*, 458–475; b) J. P. Michael, *Nat.Prod. Rep.* **2004**, *21*, 625–649.
2. Z. Sun, S. Yu, Z. Ding, D. Ma, *J. Am. Chem. Soc.* **2007**, *129*, 9300–9301.
3. D. B. Dess, J. C. Martin, *J. Org. Chem.* **1983**, *48*, 4155–4156.
4. M. A. Umbreit, K. B. Sharpless, *J. Am. Chem. Soc.* **1977**, *99*, 5526–5528.
5. M. Chen, N. Prabagaran, N. Labenz, M. C. White, *J. Am. Chem. Soc.* **2005**, *127*, 6970–6971.
6. F. Schroder, W. Francke, *Tetrahedron* **1998**, *54*, 5259–5264.
7. P. Beak, W. K. Lee, *J. Org. Chem.* **1993**, *58*, 1109–1117.
8. R. Yamaguchi, Y. Nakazono, M. Kawanisi, *Tetrahedron Lett.* **1983**, *24*, 1801–1804.
9. S. Krishnan, J. T. Bagdanoff, D. C. Ebner, Y. K. Ramtohul, U. K. Tambar, B. M. Stoltz, *J. Am. Chem. Soc.* **2008**, *130*, 13745–13754.
10. T. Imamoto, N. Takiyama, K. Nakamura, T. Hatajima, Y. Kamiya, *J. Am. Chem. Soc.* **1989**, *111*, 4392–4398.
11. J. Einhorn, C. Einhorn, F. Ratajczak, J.-L. Pierre, *J. Org. Chem.* **1996**, *61*, 7452–7454.
12. F. Schröder, V. Sinnwell, H. Baumann, M. Kaib, *Chem. Commun.* **1996**, 2139–2140.
13. V. Fargeas, F. Zammattio, J.-M. Chrétien, M.-J. Bertrand, M. Paris, J.-P. Quintard, *Eur. J. Org. Chem.* **2008**, 1681–1688.
14. W. L. F. Armarego and C. L. L. Chai (2009) *Purification of Laboratory Chemicals, 6th ed.*, Butterworth-Heinemann, Boston:
15. Y. Yamamoto, K. Maruyama, *J. Org. Chem.* **1983**, *48*, 1564–1565.
16. S. Matsukawa, Y. Funabashi, T. Imamoto, *Tetrahedron Lett.* **2003**, *44*, 1007–1010.
17. A. S. Ripka, R. S. Bohacek, D. H. Rich, *Bioorg. Med. Chem. Lett.* **1998**, *8*, 357–

360.

18. a) J. E. Baldwin, L. I. Kruse, *J. Chem. Soc., Chem. Commun.* **1977**, *7*, 233–235. b) J. E. Baldwin, M. J. Lusch, *Tetrahedron* **1982**, *38*, 2939–2947.

19. a) L. Knorr, *Ber.* **1884**, *17*, 1635–1642; b) L. Knorr, *Liebigs Ann. Chem.* **1886**, *236*, 290–332.

20. S. A. Snyder, A. M. ElSohly, F. Kontes, *Angew. Chem. Int. Ed.* **2010**, *49*, 9693–9698.

21. S. A. Snyder, F. Kontes, A. M. ElSohly, *Heterocycles* **2012**, *84,* 265–274.

2.6 Experimental Section

General Procedures. All reactions were carried out under an argon atmosphere with dry solvents under anhydrous conditions, unless otherwise noted. Dry tetrahydrofuran (THF), toluene, benzene, diethyl ether (Et_2O) and methylene chloride (CH_2Cl_2) were obtained by passing commercially available pre-dried, oxygen-free formulations through activated alumina columns. Acetonitrile (MeCN) was dried and stored over 3 Å molecular sieves. Yields refer to chromatographically and spectroscopically (^1H and ^{13}C NMR) homogeneous materials, unless otherwise stated. Reagents were purchased at the highest commercial quality and used without further purification, unless otherwise stated. Reactions were magnetically stirred and monitored by thin-layer chromatography (TLC) carried out on 0.25 mm E. Merck silica gel plates (60F-254) using UV light as visualizing agent and cerium sulfate (CAM) or aqueous $KMnO_4$, and heat as developing agents. SiliCycle silica gel (60, academic grade, particle size 0.040–0.063 mm) was used for flash column chromatography. Where stated, Aldrich neutral alumina was used for flash chromatography. NMR spectra were recorded on Bruker DPX 300, Avance II 400, Avance III 400 and DMX 500 instruments and calibrated using residual undeuterated solvent as an internal reference ($CDCl_3$: 7.26 ppm for ^1H, 77.0 ppm for ^{13}C; C_6D_6: 7.16 ppm for ^1H, 128.06 for ^{13}C). The following abbreviations were used to explain the multiplicities: s = singlet, d = doublet, t = triplet, q = quartet, br = broad, app = apparent. IR spectra were recorded on a Perkin-Elmer 1000 series FT-IR spectrometer. High-resolution mass spectra (HRMS) were recorded in the Columbia University Mass Spectral Core facility on a JOEL HX110 mass spectrometer using FAB (fast atom bombardment) techniques.

Abbreviations. Ac = acetyl, Boc = *tert*-butyloxycarbonyl, Cbz = carboxybenzyl, DIBAL-H = diisobutylaluminum hydride, DIPEA = diisopropylethylamine, DIPPA = diisopropylpropylamine, DMF = *N,N*-dimethylformamide, TBS = *tert*-butyldimethylsilyl, TEMPO = 2,2,6,6-tetramethyl-1-pieridinyloxy free radical, TFA = trifluoroacetic acid, THF = tetrahydrofuran, TMEDA = *N,N,N',N'*-tetramethylethylenediamine.

Dienecarbamate 2.9. CuI (75 mg, 0.396 mmol, 0.1 equiv.) and ligand **2.8** were suspended in CH_2Cl_2 (6 mL) and cooled to –78 °C. To this suspension was added methyl propiolate (2.0 mL, 19.8 mmol, 5.0 equiv.) and DIPEA (3.4 mL, 19.8 mmol, 5.0 equiv.), and the mixture was stirred at this temperature for 30 min. In another flask, pyridine (0.32 mL, 3.96 mmol, 1.0 equiv.) was dissolved in CH_2Cl_2 (2 mL) and cooled to –20 °C and methyl chloroformate (1.5 mL, 19.8 mmol, 5.0 equiv.) was added dropwise. The suspension was warmed to ambient temperature and cooled again to –78 °C. The above copper suspension was transferred via syringe into the pyridinium suspension, and the reaction was stirred at –78 °C for 2 h and slowly warmed to 23 °C over 1.5 h. The reaction was directly concentrated and purified by flash chromatography (hexanes/EtOAc, 95:5→80:20) to afford 697 mg (80%) of diencarbamate **2.9**. **2.9**: ^{1}H NMR (300 MHz, $CDCl_3$, 1.5:1 mixture of rotamers) δ 6.81 (rotamer, d, J = 7.2 Hz, 0.4 H), 6.70 (rotamer, d, J = 7.8 Hz, 0.6 H), 6.05 (dd, J = 9.0, 5.7 Hz, 1 H), 5.78 (rotamer, d, J = 5.7 Hz, 0.6 H), 5.64 (d, J = 5.7 Hz, 0.4 H), 5.50–5.62 (m, 1 H), 5.30–5.49 (m, 1 H), 3.84 (s, 3 H), 3.75 (s, 3 H).

Enecarbamate 2.10. Diencarbamate **2.9** (697 mg, 3.15 mmol, 1.0 equiv.) was dissolved in 15 mL of MeOH, and Pd/C (10 wt%, 168 mg, 0.158 mmol, 0.05 equiv.) was added.

The flask was placed under an H_2 atmosphere (balloon), and the reaction vessel was purged 3 times with hydrogen. The reaction was then allowed to proceed under the hydrogen atmosphere for 3 h, and the mixture was filtered through celite and concentrated. In practice, the crude material was taken forward without any further purification, however, a small sample was purified to obtain spectral data. **2.10**: ^{1}H NMR (300 MHz, $CDCl_3$, 1.3:1 mixture of rotamers) δ 6.79 (rotamer, d, J = 8.1 Hz, 0.42 H), 6.64 (rotamer, d, J = 8.1 Hz, 0.55 H), 4.90–5.0 (rotamer, br m, 0.45 H), 4.82–4.89 (rotamer, br m, 0.56 H), 4.32–4.51 (rotamer, br m, 0.56 H), 4.22–4.32 (rotamer, br m, 0.45 H), 3.78 (s, 3 H), 3.67 (s, 3 H), 2.30–2.5 (m, 2 H), 2.00–2.12 (m, 2 H), 1.73–2.00 (m, 1 H), 1.65–1.73 (m, 3 H).

Allylated piperidine 2.11. The crude material from the preparation of **2.10** (assumed to be 3.15 mmol) was dissolved in CH_2Cl_2 (20 mL) and cooled to –20 °C. Allyltrimethylsilane (3.0 mL, 18.9 mmol, 6.0 equiv.) and TFA (0.96 mL, 12.6 mmol, 4.0 equiv.) were added and the reaction mixture was stirred at –20 °C for 2 h. Another 6.0 equiv. of allyltrimethylsilane and 4.0 equiv. of TFA were added, and stirring was continued at –20 °C for an additional 2 h. The reaction was warmed to 0 °C and quenched with saturated aqeous $NaHCO_3$. The aqueous layer was extracted with CH_2Cl_2, and the combined organic layers were washed with brine. The crude was purified on a silica gel flash column (hexanes/EtOAc, 9:1) to afford 600 mg (71% over 2 steps) of product. **2.11**: ^{1}H NMR (300 MHz, $CDCl_3$) δ 5.77 (ddt, J = 17.1, 10.2, 6.6 Hz, 1 H), 5.05 (d, J = 17.1 Hz), 5.04 (d, J = 10.2 Hz), 4.15–4.33 (m, 2 H), 3.68 (s, 3 H), 3.67 (s, 3 H), 2.25–2.40 (m, 4 H), 1.80–1.95 (m, 2 H), 1.41–1.70 (m, 6 H).

Alcohol 2.12. Piperidine **2.11** (450 mg, 1.67 mmol, 1.0 equiv.) was dissolved in 15 mL of THF and cooled to –78 °C. DIBAL-H (1.0 M in toluene, 4.2 mL, 4.2 mmol, 2.5 equiv.) was added dropwise, and the reaction was stirred at –78 °C for 1 h and warmed to 0 °C with an ice bath for 10 min. The reaction was carefully quenched by the addition of a 1.0 M aqueous H_2SO_4 solution, and the aqueous layer was extracted with EtOAc. The combined organic extracts were washed sequentially with aqueous $NaHCO_3$ and brine, dried ($MgSO_4$), filtered, and concentrated. The crude material was then dissolved in CH_2Cl_2 (15 mL), and DMP (885 mg, 1.67 mmol, 1.25 equiv.) was added. The reaction was stirred until complete consumption of the starting material was observed. The reaction mixture was concentrated, taken up in toluene to precipitate excess DMP, and filtered through celite. This crude material was then subjected to Grignard addition as in the synthesis of **2.29** with the following exception: 1.5 equivalents of Grignard and $CeCl_3$ were used in the reaction. The crude material after workup was purified on silica gel by flash column chromatography (hexanes/EtOAc, 80:20→50:50) afforded an inseparable mixture of product and starting aldehyde (~1:0.6 ratio). **2.12**: A good ^{1}H NMR spectrum of this compound could not be obtained since the remaining aldehyde could not be separated from this product.

Diketone 2.13. SeO_2 (6.7 mg, 0.060 mmol, 0.5 equiv.) and *t*-BuOOH (5.5 M in decane) were stirred at ambient temperature in 1,2-dichloroethane (0.7 mL) for 30 min. Alcohol **2.12** (35 mg, 0.12 mmol, 1 equiv.) was added as a solution in 0.3 mL of 1,2-dichloroethane, and the reaction mixture was heated to 70 °C for 3.5 h. The reaction was

poured into saturated aqueous $NaHCO_3$, diluted with H_2O, and extracted with EtOAc. The combined organic layers were washed with saturated aqueous Na_2SO_3, water, and brine. The crude material was purified on a small column to afford a mixture of allylic alcohol and α,β-unsaturated ketone. This mixture was subjected to hydrogenation with Pd/C in EtOAc at ambient temperature overnight. The reaction contents were filtered through celite and concentrated. The crude residue was dissolved in CH_2Cl_2 and DMP (76 mg) was added. After 2 h at room temperature, the reaction was quenched with saturated aqueous Na_2SO_3, and after extraction (CH_2Cl_2), drying ($MgSO_4$), filtration, and concentration, the crude material was purified by PTLC (hexanes/EtOAC, 7:3) to afford 12 mg (33% over 3 steps) of the desired diketone. **2.13**: ^{1}H NMR (400 MHz, $CDCl_3$) δ 4.72 (br s, 1 H), 4.21 (br s, 1 H), 3.70 (s, 3 H), 2.51–2.38 (m, 6 H), 2.23–2.14 (m, 1 H), 1.80–1.44 (m, 9 H), 1.36–1.28 (m, 2 H), 1.06 (t, *J* = 7.2 Hz, 3 H), 0.90 (t, *J* = 7.2 Hz, 3 H).

Silyl ether 2.24. From compound **2.32**: Dienecarbamate **2.32** (2.55 g, 8.19 mmol, 1.0 equiv) was dissolved in EtOAc (80 mL) and then Pd/C (10 wt %, 0.436 g, 0.410 mmol, 0.05 equiv) and Boc_2O (2.14 g, 9.83 mmol, 1.2 equiv) were added at 23 °C. The reaction vessel was then purged three times with H_2 gas and stirred under a H_2 atmosphere for 16 h at 23 °C. Upon completion, the reaction mixture was filtered through a pad of Celite and concentrated directly to afford the desired *N*-Boc-protected piperidine ester intermediate. [Note: the purity of **2.32** and the quality of the Pd reagent greatly affected the rate of the final reduction of an enecarbamate intermediate]. Taken forward without any additional purification, this newly formed intermediate was dissolved in THF (50

mL) and the resultant solution was cooled to –78 °C. DIBAL-H (1.0 M in toluene, 20.5 mL, 20.5 mmol, 2.5 equiv) was then added dropwise. After stirring for 45 min at –78 °C, the reaction contents were warmed to 0 °C and then stirred for an additional 15 min. Upon completion, the reaction mixture was poured into a stirred biphasic mixture of hexanes (300 mL) and saturated aqueous $MgSO_4$ (50 mL) at 0 °C, warmed to 23 °C, and stirred for an additional 1 h with solid $MgSO_4$ being added periodically to maintain a free-flowing suspension. This mixture was then filtered (washing with EtOAc), concentrated, and purified by flash column chromatography (silica gel, hexanes/EtOAc, 1:1) to afford the desired primary alcohol intermediate as a colorless liquid. [Note: quenching the reaction under basic conditions (NaOH or Rochelle's salt) resulted in cyclization of the alcohol onto the Boc group]. Finally, the newly formed alcohol was dissolved in CH_2Cl_2 (50 mL) and imidazole (0.781 g, 11.5 mmol, 1.4 equiv) and TBSCl (1.48 g, 9.83 mmol, 1.2 equiv) were added sequentially at 23 °C. The resultant reaction solution was stirred for 16 h at 23 °C. Upon completion, the reaction contents were poured into saturated aqueous $NaHCO_3$ (50 mL) and extracted with CH_2Cl_2 (2 × 30 mL). The combined organic layers were dried ($MgSO_4$), filtered, and concentrated. The resultant yellow residue was purified by flash column chromatography (silica gel, hexanes/EtOAc, 19:1) to afford the TBS-protected piperidine derivative **2.24** (2.34 g, 80% yield over 3 steps) as a colorless liquid. **2.24**: R_f = 0.38 (silica gel, hexanes/EtOAc, 4:1, CAM stain); $[\alpha]^{22}_D$ = +17.9° (at 86% *ee*, c = 1.02, CH_2Cl_2); IR (film) ν_{max} 2932, 2857, 1693, 1416, 1364, 1255, 1166, 1101, 836, 775 cm^{-1}; ^1H NMR (400 MHz, $CDCl_3$) δ 4.21 (br s, 1 H), 3.98 (br d, *J* = 10.0 Hz, 1 H), 3.63 (t, *J* = 5.4 Hz, 2 H), 2.76 (t, *J* = 12.6 Hz, 1 H), 1.78–1.68 (m, 1 H), 1.63–1.34 (m, 9 H), 1.46 (s, 9 H), 0.90 (s, 9 H), 0.06 (s, 6

H); ^{13}C NMR (100 MHz, $CDCl_3$) δ 155.1, 79.0, 62.9, 50.1, 38.5, 29.6, 28.6, 28.5, 25.9, 25.6, 19.0, 18.3, –5.3; HRMS (FAB) calc. for $C_{19}H_{39}NO_3Si^+$ [M+H$^+$] 358.2777, found 358.2766.

Aldehyde 2.25. TBS-protected piperidine derivative **2.24** (4.60 g, 12.9 mmol, 1.0 equiv) was dissolved in Et_2O (40 mL) and then TMEDA (2.43 mL, 16.2 mmol, 2.2 equiv) was added at 23 °C. The reaction contents were then cooled to –78 °C and *s*-BuLi (1.4 M in cyclohexane, 9.5 mL, 1.8 equiv) was added dropwise. The resultant pale yellow solution was allowed to warm to –40 °C over 1 h, then stirred at that temperature for an additional 1 h before cooling back to –78 °C. DMF (5.7 mL, 73.7 mmol, 10.0 equiv) was then added quickly in a single portion and the resultant solution was slowly warmed to –40 °C. After stirring for an additional 1.5 h at –40 °C, the reaction contents were quenched by the addition of saturated aqueous NH_4Cl (70 mL). The mixture was then allowed to warm to 23 °C and was extracted with Et_2O (2 × 50 mL). The combined organic layers were washed with brine (30 mL), dried ($MgSO_4$), filtered and concentrated to afford the crude product as a yellow oil. Purification of this material by flash column chromatography (silica gel, hexanes/EtOAc, 9:1) to afford the *trans*-piperidine aldehyde product (4.80 g, 97% yield) as a colorless oil. **2.25**: ^{1}H NMR (400 MHz, $CDCl_3$) δ 9.35 (d, J = 2.1 Hz, 1 H), 4.09 (br s, 1 H), 3.65–3.50 (m, 3 H), 1.80–1.70 (m, 1 H), 1.70–1.50 (m, 9 H), 1.48 (s, 9 H), 0.89 (s, 9 H), 0.046 (s, 6 H). [Note: careful control of reaction temperature after the addition of DMF is essential, as reaction temperatures above –40 °C led to large amounts of cyclic carbamate **2.26**.]

Cyclic carbamate 2.26. 2.26: ^{1}H NMR (300 MHz, $CDCl_3$) δ 4.79 (d, *J* = 3.9 Hz, 1 H), 3.97 (d, *J* = 7.2 Hz), 3.60 – 3.65 (m, 2 H), 3.46 (dt, *J* = 11.7 Hz, 3.9 Hz), 2.41 (s, 6 H), 1.20 – 1.85 (m, 10 H), 0.87 (s, 9 H), 0.024 (s, 3 H), 0.020 (s, 3 H).

Hydroxyaldehyde 2.28. Aldehyde **2.25** (0.266 g, 0.690 mmol, 1.0 equiv) was reacted with EtMgBr in the presence of $CeCl_3$ according to the procedure described in the preparation of compound **2.30** below, affording (0.185 g, 89% yield) as a 1.2:1 mixture of diastereomers about the secondary alcohol. This material (0.185 g, 0.614 mmol, 1.0 equiv) was oxidized using TEMPO as detailed in the preparation of compound **2.30** below, to afford the desired aldehyde **2.28** (0.176 g, 96% yield, 83% overall from **2.24**) as a 1.2:1 mixture of diastereomers about the secondary carbinol. **2.28**: R_f = 0.54 (silica gel, hexanes/EtOAc, 4:1, $KMnO_4$ stain); IR (film) ν_{max} 3401, 2934, 2873, 1724, 1668, 1429, 1392, 1366, 1252, 1167, 1116, 1073, 873 cm^{-1}; ^{1}H NMR (400 MHz, $CDCl_3$, integration of 1.0 per H for minor diastereomer, 1.2 per H for major diastereomer) δ 9.79 (app t, *J* = 1.2 Hz, 2 H), 4.13–4.04 (m, 2.2 H), 3.94 (ddd, *J* = 13.6, 6.0, 5.4 Hz, 1 H), 3.81 (ddd, *J* = 10.8, 5.4, 2.6 Hz, 1.2 H), 3.60 (ddd, *J* = 16.0, 5.4, 2.6 Hz, 1 H), 3.33 (td, *J* = 7.8, 4.4 Hz, 1 H), 3.04 (br d, *J* = 9.2 Hz, 1.2 H), 2.49–2.39 (m, 4.4 H), 2.11–1.99 (m, 2.2 H) 1.81–1.35 (m, 21 H), 1.44 (s, 9 H), 1.43 (s, 10.8 H). 0.99 (t, *J* = 7 Hz, 3 H), 0.97 (t, *J* = 7.2 Hz, 3.6 H); ^{13}C NMR (100 MHz, $CDCl_3$) δ 201.7, 201.6, 157.2, 156.5, 80.5, 80.3, 74.2, 72.9, 57.7, 57.3, 54.4, 53.5, 41.1, 40.8, 28.4, 27.8, 27.7, 26.6, 25.1, 24.5, 23.3, 19.6, 17.7, 10.9, 10.2; HRMS (FAB) calc. for $C_{16}H_{30}NO_4^+$ [M+H$^+$] 300.2175, found 300.2162.

Diketone 2.29. Anhydrous $CeCl_3$ (370 mg, 1.5 mmol, 3.0 equiv) was suspended in THF (8 mL). The resultant white slurry was stirred at 23 °C for 2 h, cooled to 0 °C, and a solution of **2.28** (150 mg, 0.5 mmol, 1.0 equiv) in THF (1 mL) was added via syringe. This mixture was stirred at 0 °C for 30 minutes, cooled to –40 °C, and then *n*-BuMgCl (2.0 M in Et_2O, 0.75 mL, 1.5 mmol, 3.0 equiv) was added dropwise via syringe. The resultant reaction mixture was slowly warmed to 0 °C and quenched with 1.0 M aqueous HCl. The aqueous layers were extracted with Et_2O, and the combined organic extracts were dried ($MgSO_4$), filtered, and concentrated. The crude material was subjected to DMP (636 mg, 1.5 mmol, 3.0 equiv.) oxidation. Upon completion of the reaction, a saturated solution of Na_2SO_3 was added, and the reaction was diluted with EtOAc. After vigorous stirring, both layers became clear, and the reaction mixture was transferred to a separatory funnel where the aqueous layer was extracted with CH_2Cl_2. The combined organics were washed once with saturated aqueous $NaHCO_3$, dried ($MgSO_4$), filtered, and concentrated. The crude material was purified on silica gel by flash chromatography (hexanes/EtOAc, 95:5) to afford 123 mg (70%) of diketone **2.29**. **2.29**: ^{1}H NMR (400 MHz, $CDCl_3$) δ 4.07 (br s, 1 H), 3.83 (br s, 1 H), 2.45 – 2.59 (m, 5 H), 1.89 – 2.00 (m, 2 H), 1.65 – 1.82 (m, 3 H), 1.49 – 1.65 (m, 6 H), 1.42 (s, 9 H), 1.28 – 1.39 (m, 2 H), 1.08 (t, J = 7.2 Hz), 0.91 (t, J = 7.2 Hz).

Hydroxyaldehyde 2.30. TBS-protected piperidine derivative **2.24** (2.64 g, 7.37 mmol, 1.0 equiv) was dissolved in Et_2O (40 mL) and then TMEDA (2.43 mL, 16.2 mmol, 2.2 equiv) was added at 23 °C. The reaction contents were then cooled to –78 °C and *s*-BuLi (1.4 M in cyclohexane, 9.5 mL, 1.8 equiv) was added dropwise. The resultant pale

yellow solution was allowed to warm to –40 °C over 1 h, then stirred at that temperature for an additional 1 h before cooling back to –78 °C. DMF (5.7 mL, 73.7 mmol, 10.0 equiv) was then added quickly in a single portion and the resultant solution was slowly warmed to –40 °C. After stirring for an additional 1.5 h at –40 °C, the reaction contents were quenched by the addition of MeOH (50 mL) and warmed to 23 °C. Excess K_2CO_3 was then added, and the reaction was stirred at 23 °C for 2 h. Upon completion, the reaction contents were poured into saturated aqueous NH_4Cl (100 mL) and extracted with CH_2Cl_2 (3 × 50 mL). The combined organic extracts were dried ($MgSO_4$), filtered, and concentrated to afford a crude yellow oil. This material was purified by flash column chromatography (silica gel, hexanes/EtOAc, 19:1) to afford the desired *cis*-piperidine aldehyde product (2.31 g, 81% yield) as a colorless oil along with some mixed *cis*- and *trans*-piperidine material (0.270 g, 10% yield). The mixed fractions were recycled by resubjecting to K_2CO_3 (excess) in MeOH (6 mL) for 2 h at 23 °C. Work-up and purification as above afforded a second batch of *cis*-piperidine product (0.246 g, 91% yield for this step), which was combined with the product from above (2.56 g overall, 90% yield). [Note: careful control of reaction temperature is essential, as reaction temperatures above –40 °C led to large amounts of cyclization of the resultant alkoxide onto the neighboring Boc group.] Next, anhydrous $CeCl_3$ (3.33 g, 13.5 mmol, 1.3 equiv) was suspended in THF (50 mL). The resultant white slurry was stirred at 23 °C for 2 h, cooled to 0 °C, and a solution of *cis*-piperidine aldehyde (3.99 g, 10.3 mmol, 1.0 equiv) in THF (10 mL) was added via cannula. This mixture was stirred at 0 °C for 30 minutes, cooled to –40 °C, and then EtMgBr (3.0 M in Et_2O, 4.5 mL, 13.5 mmol, 1.3 equiv) was added dropwise via syringe. The resultant reaction mixture was slowly warmed to 0 °C

and quenched with 1.0 M aqueous HCl (20.6 mL, 20.6 mmol, 2.0 equiv). The mixture was diluted with water (12 mL) and MeOH (12 mL) and was stirred at 23 °C for an additional 3 hours. The reaction contents were then extracted with CH_2Cl_2 (2 × 60 mL). The combined organic extracts were dried ($MgSO_4$), filtered, and concentrated to afford the crude product as a thick oil. Purification of this material by flash column chromatography (silica gel, hexanes/EtOAc, 7:3→1:1) afforded the desired diol (2.87 g, 92% yield) as a thick colorless oil. Finally, a portion of this diol (0.681 g, 2.26 mmol, 1.0 equiv) was dissolved in a 1:1 mixture of CH_2Cl_2 (20 mL) and aqueous pH 8.6 buffer ($NaHCO_3/K_2CO_3$, 20 mL) at 23 °C. The resultant biphasic mixture was then cooled to 0 °C and then NaBr (0.233 g, 2.26 mmol, 1.0 equiv), *n*-Bu_4NCl (0.031 g, 0.113 mmol, 0.05 equiv) and TEMPO (0.018 g, 0.113 mmol, 0.05 equiv) were added sequentially. Solid NCS (0.302 g, 2.26 mmol, 1.0 equiv) was then added in three equal portions, 15 min apart, to the vigorously stirred biphasic mixture. The bright resultant yellow reaction was stirred at 0 °C for an additional 1 h (to give a total of 1.5 h of stir time). Upon completion, the reaction contents were poured into water (40 mL) and extracted with CH_2Cl_2 (2 × 30 mL). The combined organic extracts were dried ($MgSO_4$), filtered, and concentrated. The resultant crude product was then purified by flash column chromatography (silica gel, hexanes/EtOAc, 4:1→3:2) to afford aldehyde **2.30** as a colorless oil (0.629 g, 93% yield, 77% overall from **2.24**). **2.30**: R_f = 0.52 (silica gel, hexanes/EtOAc, 4:1, $KMnO_4$ stain); IR (film) ν_{max} 3414, 2934, 2874, 1723, 1660, 1455, 1408, 1366, 1321, 1172, 1069, 975 cm^{-1}; ^1H NMR (400 MHz, $CDCl_3$) δ 9.77 (s, 1 H), 4.17 (br dd, *J* = 13.6, 6.4 Hz, 1 H), 3.99 (td, *J* = 7.2, 2.4 Hz, 1 H), 3.60 (br s, 1 H), 2.46 (ddd, *J* = 17.6, 14.2, 7.4 Hz, 2 H), 2.05–2.01 (m, 1 H), 1.92 (dq, *J* = 14.0, 7.2 Hz, 1 H),

1.80–1.31 (m, 9 H), 1.44 (s, 9 H), 0.98 (t, J = 7.4 Hz, 3 H); ^{13}C NMR (100 MHz, $CDCl_3$) δ 202.0, 155.8, 79.7, 74.5, 54.7, 49.7, 41.6, 28.4, 28.2, 27.4, 27.0, 23.8, 15.3, 10.6; HRMS (FAB) calc. for $C_{16}H_{30}NO_4^+$ [M+H$^+$] 300.2175, found 300.2172.

Diketone 2.31. This compound was prepared following the same procedure used to prepare compound **2.29**, delivering **2.31** in 72% yield. **2.31**: ^{1}H NMR (300 MHz, $CDCl_3$) δ 4.65 (br s, 1 H), 4.12 – 4.22 (br m, 1 H), 2.39 – 2.60 (m, 6 H), 2.11 – 2.20 (m, 1 H), 1.40 – 1.71 (m, 9 H), 1.45 (s, 9 H), 1.25 – 1.38 (m, 2 H), 1.05 (t, J = 7.2 Hz), 0.89 (t, J = 7.2 Hz).

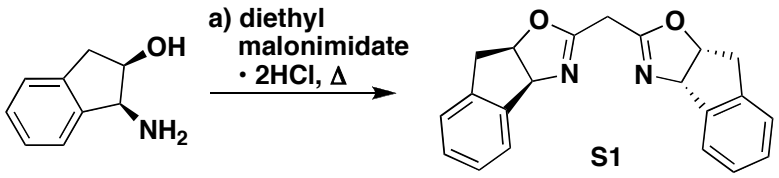

Scheme S1. Synthesis of ligand **S1** and key intermediate **10**: (a) (1*S*,2*R*)-(–)-*cis*-1-amino-2-indanol (2.1 equiv), diethyl malonimidate dihydrochloride (1.0 equiv), CH_2Cl_2, 40 °C, 48 h (81%).

Ligand S1. (1*S*,2*R*)-(–)-*cis*-1-Amino-2-indanol (1.08 g, 7.24 mmol, 2.1 equiv) and diethyl malonimidate dihydrochloride (0.80 g, 3.46 mmol, 1.0 equiv) were taken up in CH_2Cl_2 (80 mL), and the resulting suspension was refluxed for 16 h. Upon completion, the reaction contents were poured into water (160 mL) and extracted with CH_2Cl_2 (4 × 40 mL). The combined organic layers were dried ($MgSO_4$), filtered, and concentrated. The resultant crude product was recrystallized from *i*-PrOH (100 mL). The mother liquor was concentrated, and a second recrystallization was performed with *i*-PrOH (30 mL) to provide ligand **S1** (0.853 g from first crop, 0.071 g from second crop, 81% yield overall) as thin white needles. **S1**: ^{1}H NMR (400 MHz, $CDCl_3$) δ 7.47–7.45 (m, 2 H), 7.27–7.22

(m, 6 H), 5.57 (d, *J* = 8.0 Hz, 2 H), 5.34 (ddd, *J* = 8.0, 7.0, 1.8 Hz, 2 H), 3.39 (dd, *J* = 18.0, 7.2 Hz, 2 H), 3.26 (s, 2 H), 3.16 (dd, *J* = 18.0, 1.2 Hz, 2 H).

Dienecarbamate 2.32. To a stirred solution of ligand **S1** (0.094 g, 0.285 mmol, 0.12 equiv) in CH_2Cl_2 (3.0 mL) at 23 °C was added CuI (0.047 g, 0.248 mmol, 0.1 equiv) and the resultant suspension was stirred at 23 °C for 5 min during which time the suspension turned pink/purple. This suspension was then cooled to –78 °C and stirred for 10 min. Ethyl propiolate (1.25 mL, 12.4 mmol, 5.0 equiv) was added dropwise as a neat liquid followed by freshly distilled diisopropylpropylamine (2.27 mL, 12.4 mmol, 5.0 equiv). The resultant peach colored suspension was stirred at –78 °C for 45 min. In a separate flask, a solution of pyridine (0.2 mL, 2.48 mmol, 1.0 equiv) in CH_2Cl_2 (2.0 mL) was cooled to –40 °C and benzyl chloroformate (1.75 mL, 12.4 mmol, 5.0 equiv) was added dropwise with vigorous stirring. The resultant thick, white slurry was warmed to 0 °C and stirred for 20 min before cooling to –78 °C. To this suspension was then added the above Cu-complex solution via cannula and the resulting green suspension was stirred at –65 °C for 14 h. Upon completion, the reaction contents were quenched at –65 °C with saturated aqueous $NaHCO_3$ (15 mL) and then warmed to 0 °C, at which point the reaction mixture turned dark red. The reaction mixture was then extracted with CH_2Cl_2 (3 × 10 mL), and the combined organic extracts were dried ($MgSO_4$), filtered, and concentrated. The resultant dark red oil was purified by flash column chromatography (silica gel, hexanes/EtOAc, 19:1) to afford compound **2.32** (0.650 g, 84% yield) as a yellow oil. **2.32:** R_f = 0.40 (silica gel, hexanes/EtOAc, 4:1, CAM stain); $[\alpha]^{22}_D$ = +510.0° (at 85% *ee*, *c* = 0.18, CH_2Cl_2); IR (film) ν_{max} 1705, 1386, 1325, 1234, 1103, 998, 976, 716, 696 cm^{-1};

^{1}H NMR (400 MHz, $CDCl_3$) δ 7.46–7.34 (m, 5 H), 6.86 and 6.76 (rotamers, d, *J* = 7.6 Hz, 1 H), 6.06 (dd, *J* = 9.2, 5.6 Hz, 1 H), 5.82 and 5.72 (rotamers, d, *J* = 5.4 Hz, 1 H), 5.60 and 5.54 (rotamers, t, *J* = 6.8 Hz, 1 H), 5.41 and 5.36 (rotamers, t, *J* = 6.4 Hz, 1 H), 5.35–5.22 (m, 2 H), 4.23 (q, *J* = 7.0 Hz, 2 H), 1.32 (t, *J* = 7.0 Hz, 3 H); ^{13}C NMR (100 MHz, $CDCl_3$) δ 153.2, 153.0, 152.7, 135.4, 128.6, 128.5, 128.3, 128.1, 125.4, 124.8, 124.0, 123.7, 116..4, 115.9, 105.5, 105.4, 83.8, 74.9, 68.6, 68.4, 62.1, 43.9, 43.4, 14.0; HRMS (FAB) calc. for $C_{18}H_{17}NO_4^+$ [M^+] 311.1158, found 311.1170; HPLC (Daicel Chiralpak AD-H 250 × 4.6 mm, hexanes/*i*-PrOH, 9:1, UV detector at 300 nm) $t_{R,minor}$ = 9.8 min, $t_{R,major}$ = 10.5 min, ee = 85%. [Note: this reaction has been performed on up to 24.8 mmol scale without loss of enantioselectivity or yield. In order to obtain both high yield and high enantioselectivity, the purity of the CuI utilized (purified according to W. L. F. Armarego, D. D. Perrin, *Purification of Laboratory Chemicals*, **1998**, 4th ed.) as well as careful control of reaction temperature proved crucial. Compound **2.32** turns brown upon extended exposure to air (>15 min) and should be used immediately in the next reaction]. The absolute configuration of this compound was determined by conversion to myrmicarin 217 (**2.1**) whose absolute configuration was established in a previous enantiospecific synthesis (see Chapter 1).

***Cis*-alkene 2.33.** A solution of 2-butenylmagnesium chloride (0.5 M in THF, 9.56 mL, 4.78 mmol, 3.0 equiv) was diluted with dry THF (7.5 mL) and cooled to –78 °C. A solution of $AlCl_3$ (2.0 M in Et_2O, freshly prepared before use, 5.75 mL, 11.5 mmol, 6.0 equiv) was then added dropwise at –78 °C, leading to the formation of a white precipitate. After stirring for 10 min at –78 °C, a solution of aldehyde **2.30** (573 mg, 1.91

mmol, 1.0 equiv) in THF (2.5 mL) was added dropwise, and after 5 min of additional stirring, the reaction contents were immediately warmed to 0 °C by exchanging the dry ice/acetone bath with one made from ice and water. After stirring for 1 h at 0 °C, the reaction was quenched with saturated aqueous NH_4Cl (10 mL) and extracted with Et_2O (3 × 10 mL). The combined organic layers were dried ($MgSO_4$), filtered, and concentrated to afford the desired intermediate, which was carried forward without additional purification. [Note: slow warming from –78 °C leads to diminished *E*/*Z* selectivity.] The crude product from above was dissolved in CH_2Cl_2 (8 mL) and cooled to –10 °C. Dess–Martin periodinane (2.43 g, 5.73 mmol, 3.0 equiv) was then added in a single portion and the reaction contents were allowed to warm slowly to 0 °C over 1.5 h. Upon completion, the reaction mixture was quenched at 0 °C by first diluting with EtOAc (10 mL) and then adding saturated aqueous Na_2SO_3 (15 mL). After stirring vigorously at 23 °C for 15 minutes, the reaction contents were then extracted with EtOAc (3 × 10 mL). The combined organic layers were washed sequentially with saturated aqueous $NaHCO_3$ (10 mL) and brine (10 mL), dried ($MgSO_4$), and concentrated. The crude residue was carefully purified by flash column chromatography (silica gel, Et_2O/hexanes, 1:9→3:19), affording *cis*-alkene **2.33** (0.416 g, >15:1 *Z*/*E* ratio, 62% yield over 2 steps) as a colorless oil. **2.33:** R_f = 0.21 (silica gel, hexanes/EtOAc, 4:1, $KMnO_4$ stain); $[\alpha]^{22}_D$ = –45.6° (*c* = 0.525, CH_2Cl_2); IR (film) ν_{max} 2974, 2939, 1716, 1684, 1455, 1400, 1366, 1325, 1254, 1172, 1078, 874 cm^{-1}; ^1H NMR (400 MHz, $CDCl_3$) δ 5.66 (dqt, *J* = 10.8, 6.4, 1.6 Hz, 1 H), 5.58 (dtq, *J* = 10.8, 6.8, 1.6 Hz, 1 H), 4.65 (br s, 1 H), 4.17 (m, 1 H), 3.19 (d, *J* = 7.2 Hz, 2 H), 2.62–2.38 (m, 4 H), 2.16–2.08 (m, 1 H), 1.75 (dtd, *J* = 14.0, 8.4, 6.0 Hz, 1 H), 1.70–1.42 (m, 6 H), 1.62 (dd, *J* = 6.8, 1.2 Hz, 3 H), 1.45 (s, 9 H), 1.05 (t, 7.2 Hz, 3 H);

^{13}C NMR (100 MHz, $CDCl_3$) δ 210.5, 208.5, 155.6, 127.5, 122.1, 80.1, 77.2, 59.0, 50.0, 41.3, 39.8, 31.8, 28.4, 27.8, 24.6, 15.9, 13.0, 7.9; HRMS (FAB) calc. for $C_{20}H_{34}NO_4^+$ [M+H$^+$] 352.2488, found 352.2489.

***Trans*-alkene 2.35.** A suspension of pre-dried $CeCl_3$ (1.85 g, 7.51 mmol, 3.0 equiv) in dry THF (40 mL) was cooled to 0 °C and a solution of 2-butenylmagnesium chloride (0.5 M in THF, 15.0 mL, 7.51 mmol, 3.0 equiv) was added dropwise via syringe. The resulting intense orange-red solution was stirred for 30 min at 0 °C and then was cooled to –78 °C. A solution of aldehyde **2.30** (0.75 g, 2.50 mmol, 1.0 equiv) in THF (10 mL) was then added dropwise, and the resultant pale orange solution was allowed to warm to –40 °C over the course of 45 min. The reaction contents were then stirred at –40 °C for an additional 3 h and quenched by the addition of 10% aqueous AcOH (15 mL). The resultant biphasic mixture was warmed to 23 °C and extracted with Et_2O (3 × 10 mL). The combined organic layers were dried ($MgSO_4$), filtered, and concentrated. The crude product was used directly in the next reaction without any additional purification. [Note: proper drying of $CeCl_3$ is extremely important for the success of this reaction. The intense orange-red color is an indication that the desired crotylcerium reagent has been formed. When cooled to –78 °C, the suspension turns brown if the crotylcerium reagent has not been formed, which leads exclusively to the branched crotylation product]. Next, the crude product from above was dissolved in CH_2Cl_2 (20 mL) and cooled to –10 °C. Dess–Martin periodinane (3.18 g, 7.51 mmol, 3.0 equiv) was then added in a single portion and the reaction contents were allowed to warm slowly to 0 °C over 1.5 h. Upon completion, the reaction mixture was quenched at 0 °C by first diluting with EtOAc (10

mL) and then adding saturated aqueous Na_2SO_3 (15 mL). After stirring vigorously at 23 °C for 15 minutes, the reaction contents were then extracted with EtOAc (3 × 10 mL). The combined organic layers were washed sequentially with saturated aqueous $NaHCO_3$ (10 mL) and brine (10 mL), dried ($MgSO_4$), and concentrated. The resultant crude residue was purified by flash column chromatography (silica gel, Et_2O/hexanes, 1:9→3:19) to afford *trans*-alkene **2.35** (0.620 g, 8:1 *E*/*Z* ratio, 71% yield over 2 steps) as a colorless oil. **2.35**: R_f = 0.21 (silica gel, hexanes/EtOAc, 4:1, $KMnO_4$ stain); $[\alpha]^{22}_D$ = –38.6° (*c* = 0.20, CH_2Cl_2); IR (film) ν_{max} 2974, 2939, 1716, 1684, 1400, 1366, 1254, 1172, 1078, 874 cm^{-1}; ^1H NMR (400 MHz, $CDCl_3$) δ 5.59–5.48 (m, 2 H), 4.65 (br s, 1 H), 4.16 (m, 1 H), 3.10 (d, 2.8 Hz, 2 H), 2.61–2.38 (m, 4 H), 2.16–2.08 (m, 1 H), 1.74 (dtd, *J* = 14.4, 8.8, 6.0 Hz, 1 H), 1.68 (dd, *J* = 3.6, 1.2 Hz, 3 H), 1.67–1.42 (m, 6 H), 1.45 (s, 9 H), 1.05 (t, 7.2 Hz, 3 H); ^{13}C NMR (100 MHz, $CDCl_3$) δ 210.6, 209.1, 155.6, 129.5, 123.2, 80.1, 77.2, 59.0, 50.0, 46.7, 39.7, 31.8, 28.4, 27.8, 24.5, 18.0, 15.9, 7.9; HRMS (FAB) calc. for $C_{20}H_{34}NO_4^+$ [M+H^+] 352.2488, found 352.2483.

***Cis*-alkene 2.37.** This compound was prepared following the same general procedure described for **2.33** above, ultimately affording *cis*-alkene **2.37** (0.270 g, >15:1 *Z*/*E* ratio, 72% over 2 steps) as a colorless oil. **2.37:** R_f = 0.21 (silica gel, hexanes/EtOAc, 4:1, $KMnO_4$ stain); $[\alpha]^{22}_D$ = +18.7° (*c* = 1.07, CH_2Cl_2); IR (film) ν_{max} 2975, 2937, 1716, 1686, 1393, 1365, 1304, 1253 1166, 1119 cm^{-1}; ^1H NMR (400 MHz, $CDCl_3$) δ 5.68 (dqt, *J* = 10.8, 6.8, 1.6 Hz, 1 H), 5.57 (dtq, *J* = 10.8, 6.8, 1.6 Hz, 1 H), 4.07 (br s, 1 H), 3.83 (br s, 1 H), 3.18 (d, *J* = 6.8 Hz, 2 H), 2.57–2.45 (m, 3 H), 2.37 (dq, *J* = 17.2, 7.2 Hz, 1 H), 1.96–1.88 (m, 2 H), 1.80–1.46 (m, 6 H) 1.63 (dd, *J* = 6.8, 1.6 Hz, 3 H), 1.41 (s, 9 H), 1.07

(t, J = 7.2 Hz, 3 H); ^{13}C NMR (100 MHz, $CDCl_3$) δ 208.5, 208.2, 155.9, 127.8, 121.8, 80.8, 77.2, 60.0, 52.3, 41.5, 39.3, 31.3, 28.2, 26.1, 24.4, 16.7, 13.0, 8.0; HRMS (FAB) calc. for $C_{20}H_{34}NO_4^+$ [M+H$^+$] 352.2488, found 352.2506.

***Trans*-alkene 2.39.** This compound was prepared following the same general procedure as described for **2.36** above, ultimately affording *trans*-alkene **2.39** (0.244 g, ~8:1 *E*/*Z* ratio, 66% yield over 2 steps) as a colorless oil. **2.39:** R_f = 0.21 (silica gel, hexanes/EtOAc, 4:1, $KMnO_4$ stain); $[\alpha]^{22}_D$ = +14.2° (c = 1.16, CH_2Cl_2); IR (film) ν_{max} 2924, 2853, 1712, 1689, 1681, 1452, 1392, 1365, 1306, 1252, 1163, 1067 cm^{-1}; ^{1}H NMR (400 MHz, $CDCl_3$) δ 5.53 (m, 2 H), 4.05 (br s, 1 H), 3.81 (br s, 1 H), 3.08 (d, J = 5.6 Hz, 2 H), 2.48 (m, 3 H), 2.36 (dq, J = 17.2, 7.2 Hz, 1 H), 1.97–1.85 (m, 2 H), 1.77–1.45 (m, 6 H) 1.68 (d, J = 4.8 Hz, 3 H), 1.40 (s, 9 H), 1.06 (t, J = 7.2 Hz, 3 H); ^{13}C NMR (100 MHz, $CDCl_3$) δ 208.7, 208.4, 155.9, 129.8, 122.9, 80.7, 77.2, 60.0, 52.3, 46.8, 39.1, 31.3, 28.2, 26.1, 24.4, 18.0, 16.7, 8.0; HRMS (FAB) calc. for $C_{20}H_{34}NO_4^+$ [M+H$^+$] 352.2488, found 352.2476.

General Procedure for *N*-Boc Deprotection. To a solution of the *N*-Boc starting material (0.085 mmol, 1.0 equiv) in CH_2Cl_2 (0.40 mL) was added water (0.10 mL) at 0 °C and the resultant biphasic mixture was stirred vigorously for 5 min before TFA (0.40 mL) was added dropwise. The resultant mixture was stirred vigorously at 0 °C for 1 h and then was diluted with CH_2Cl_2 (5 mL). The reaction contents were then poured into a separatory funnel containing an ice-cold 1 M NaOH / 0.5 M K_2CO_3 solution (7 mL) and was shaken vigorously for 20 sec. The resultant layers were separated and the aqueous

layer was extracted with CH_2Cl_2 (2 × 5 mL). The combined organic layers were then dried (Na_2SO_4), filtered, and concentrated to afford the mono- or dienamine products as light yellow to orange oils. [Note: vigorous shaking of the separatory funnel is necessary to ensure complete deprotonation of the amine. When not shaken vigorously enough, the resultant products exhibit reduced *E*/*Z* ratios. The use of saturated $NaHCO_3$ in this operation led to poor mass recoveries, even following multiple extractions. The crude cyclized products were found to be unstable to isolation on neutral or basic alumina or Et_3N-deactivated silica gel].

Dienamine 2.34: (99%), pale yellow oil, >15:1 *Z*/*E* ratio; $[\alpha]^{22}_D$ = +88.8° (*c* = 0.335, CH_2Cl_2); IR (film) ν_{max} 2936, 2855, 1711, 1642, 1605, 1456, 1388, 1338, 1257, 1225, 1200, 1148, 1076, 940, 830, 713 cm^{-1}; ^1H NMR (400 MHz, C_6D_6) δ 6.12 (tq, *J* = 10.4, 1.6 Hz, 1 H), 5.25 (dq, *J* = 10.4, 6.8 Hz, 1 H), 5.2 (d, *J* = 11.2 Hz, 1 H), 3.30 (dd, *J* = 11.2, 4.4 Hz, 1 H), 2.56 (dq, *J* = 18.0, 7.2 Hz, 1 H), 2.42–2.30 (m, 2 H, including dq, *J* = 18.0, 7.2 Hz, 1 H), 2.22–2.09 (m, 2 H), 1.74 (dd, 6.8, 1.6 Hz, 3 H), 1.59–1.34 (m, 4 H), 1.19–1.07 (m, 5 H, includes td, *J* = 7.6, 0.4 Hz, 1 H), 0.93–0.85 (m, 2 H); ^{13}C NMR (100 MHz, C_6D_6) δ 212.6, 148.6, 127.0, 117.4, 93.6, 67.2, 61.6, 30.6, 28.9, 28.3, 27.9, 26.7, 23.1, 13.3, 8.3; HRMS (FAB) calc. for $C_{15}H_{24}NO^+$ [M+H$^+$] 234.1858, found 234.1869.

Dienamine 2.36: (99%), pale yellow oil, 8:1 *E*/*Z* ratio; $[\alpha]^{22}_D$ = +94.5° (*c* = 0.480, CH_2Cl_2); IR (film) ν_{max} 2935, 2855, 1710, 1652, 1619, 1455, 1376, 1309, 1270, 1104 cm^{-1}; ^1H NMR (400 MHz, C_6D_6) δ 6.10 (ddq, *J* = 14.8, 12.0, 1.6 Hz, 1 H), 5.32 (dq, *J* = 14.8 Hz, 6.8 Hz, 1 H), 5.04 (d, *J* = 10.4 Hz, 1 H), 3.29 (dd, *J* = 11.6, 4.4 Hz, 1 H), 2.58 (dq, *J*

= 18.4 Hz, 7.6 Hz, 1 H), 2.45–2.32 (m, 2 H, including dq, *J* =18.4, 7.6 Hz, 1 H), 2.19–2.10 (m, 2 H), 1.71 (dd, *J* = 6.8, 1.6 Hz, 3 H), 1.59–1.45 (m, 2 H), 1.41–1.34 (m, 2 H), 1.16–1.08 (m, 5 H, includes t, *J* = 7.2 Hz, 3 H), 0.92–0.85 (m, 2 H); ^{13}C NMR (100 MHz, C_6D_6) δ 212.7, 147.0, 129.1, 120.4, 98.0, 67.2, 61.6, 30.6, 28.9, 28.3, 28.1, 26.6, 23.1, 18.6, 8.3; HRMS (FAB) calc. for $C_{15}H_{24}NO^+$ [M+H$^+$] 234.1858, found 234.1849.

Dienamine 2.38: (99%), orange oil, 8:1 *Z*/*E* ratio; $[\alpha]^{22}_D$ = +165.5° (*c* = 0.565, CH_2Cl_2); IR (film) ν_{max} 2934, 2862, 1712, 1634, 1603, 1456, 1395, 1260, 1198, 1150, 1114 cm^{-1}; ^{1}H NMR (400 MHz, C_6D_6) δ 6.29 (tq, *J* = 11.2, 2.0 Hz, 1 H), 5.24 (dq, *J* = 11.2, 6.8 Hz, 1 H), 5.05 (d, *J* = 11.2 Hz, 1 H), 3.94 (d, *J* = 5.2 Hz, 1 H), 3.29 (dddd, *J* = 11.2, 8.4, 5.6, 3.2 Hz, 1 H), 2.49 (ddt, *J* = 16.0, 9.2, 2.4 Hz, 1 H), 2.26 (dtd, *J* = 16.0, 9.2, 1.6 Hz, 1 H), 2.12 (dq, *J* = 18.0, 7.2 Hz, 1 H), 1.98 (dq, 18.0, 7.2 Hz, 1 H), 1.84 (dd, *J* = 6.8, 1.6 Hz, 3 H), 1.82–1.78 (m, 1 H), 1.58 (dddd, *J* = 11.6, 9.2, 6.0, 2.4 Hz, 1 H), 1.43–1.12 (m, 4 H), 1.09–0.97 (m, 1 H), 0.94 (t, *J* = 7.2 Hz, 3 H), 0.77 (tdd, *J* = 16.0, 12.4, 3.6 Hz, 1 H); ^{13}C NMR (100 MHz, C_6D_6) δ 210.3, 149.0, 128.0 (obtained from HSQC), 113.3, 87.2, 59.6, 58.7, 33.6, 32.1, 29.5, 27.7, 25.1, 20.8, 13.4, 7.8; HRMS (FAB) calc. for $C_{15}H_{24}NO^+$ [M+H$^+$] 234.1858, found 234.1865.

Dienamine 2.40: (99%), orange oil, 5:1 *E*/*Z* ratio; IR (film) ν_{max} 2934, 2863, 1712, 1649, 1579, 1456, 1395, 1376, 1271 cm^{-1}; ^{1}H NMR (400 MHz, C_6D_6) δ 6.26 (ddq, *J* = 14.8, 10.4, 1.6 Hz, 1 H), 5.38 (dq, *J* = 14.8, 6.8 Hz, 1 H), 4.87 (d, *J* = 10.4 Hz, 1 H), 3.83 (d, *J* = 5.6 Hz, 1 H), 3.25 (dddd, *J* = 11.2, 8.0, 6.0, 3.2 Hz, 1 H), 2.47 (ddt, *J* = 16.0, 8.8, 2.0 Hz, 1 H), 2.25 (dtd, *J* = 15.6, 9.6, 1.2 Hz, 1 H), 2.11 (dq, *J* = 18.0, 7.2 Hz, 1 H), 1.95 (dq,

J = 18.0, 7.2 Hz, 1 H), 1.87 (dd, *J* = 6.8, 1.6 Hz, 3 H), 1.83–1.77 (m, 1 H), 1.58 (dddd, *J* = 11.6, 9.2, 6.0, 2.4 Hz, 1 H), 1.44–1.37 (m, 1 H), 1.35–1.10 (m, 4 H), 1.09–0.98 (m, 1 H), 0.92 (t, *J* = 7.2 Hz, 3 H), 0.77 (tdd, *J* = 16.0, 12.4, 3.2 Hz, 1 H); ^{13}C NMR (100 MHz, C_6D_6) δ 210.5, 147.3, 130.4, 116.2, 91.4, 59.7, 58.5, 33.5, 32.1, 29.6, 27.6, 25.2, 20.9, 18.8, 7.8; HRMS (FAB) calc. for $C_{15}H_{24}NO^+$ [M+H$^+$] 234.1858, found 234.1849.

(+)-Myrmicarin 217 (2.1). Compound **2.31** was deprotected according to the general *N*-Boc deprotection procedure. The crude product was then dissolved in MeOH that had been sparged with argon for at least 20 min, and after 1 h at 23 °C, the solvent was removed, affording the natural product in 99% over the 2 steps. **2.1**: $[\alpha]^{22}_D$ = +66.1° (at 84% *ee*, c = 0.260, CH_2Cl_2); IR (film) ν_{max} 2956, 2926, 2850, 1456, 1436, 1320, 1260, 1077, 1017, 799 cm^{-1}; ^{1}H NMR (400 MHz, C_6D_6) δ 3.33 (tdd, *J* = 10.8, 5.2, 3.6 Hz, 1 H), 2.67–2.53 (m, 7 H), 2.44 (ddd, *J* = 16.0, 11.6, 6.4 Hz, 1 H), 2.01 (dtd, *J* = 11.6, 5.2, 1.6 Hz, 1 H), 1.82–1.69 (m, 3 H), 1.64–1.53 (m, 2 H), 1.48–1.35 (m, 1 H), 1.30 (t, *J* = 7.6 Hz, 3 H), 1.07 (t, *J* = 7.2 Hz, 3 H), 0.88 (tdd, *J* = 13.6, 11.2, 2.8 Hz, 1 H); ^{13}C NMR (100 MHz, C_6D_6) δ 127.5, 121.3, 118.1, 113.8, 55.0, 37.3, 30.2, 28.2, 25.1 (2 C), 23.0, 20.8, 18.9, 16.6, 14.6; HRMS (FAB) calc. for $C_{15}H_{22}N^+$ [M-H]$^+$ 216.1752, found 216.1753. All spectroscopic data for this synthetic material matched those reported by Francke *et al.*[1]

(–)-Myrmicarin 215A (2.2). Freshly prepared **2.34** (0.020 g, 0.085 mmol, 1.0 equiv) was dissolved in degassed MeOH (1 mL, sparged with Ar for at least 20 min) at 23 °C, and after standing for 1 h, the solvent was removed to afford myrmicarin 215A (**2.2**,

0.019 g, 99% yield) as a white crystalline solid (0.019 g, 99% yield). Alternatively, freshly prepared **2.38** (0.020 g, 0.085 mmol, 1.0 equiv) was dissolved in degassed MeOH (1 mL) and NaOMe (0.046 g, 0.85 mmol, 10 equiv) was added at 23 °C. The resultant mixture was then stirred at 50 °C for 1 h, cooled to 23 °C, diluted with water (5 mL), and poured into a separatory funnel containing CH_2Cl_2 (5 mL). The aqueous layer was extracted with CH_2Cl_2 (3 × 5 mL), and the combined organic layers were dried (Na_2SO_4), filtered, and concentrated. The resultant crude residue was purified with a short plug of neutral alumina (Et_2O/pentane, 1:9) to afford myrmicarin 215A (**2.2**, 0.016 g, 85% yield) as a crystalline solid. **1**: $[\alpha]^{22}_D$ = –25.7° (*c* = 0.280, CH_2Cl_2); IR (film) ν_{max} 2926, 2850, 1638, 1442, 1321, 1198, 960 cm^{-1}; ^1H NMR (400 MHz, C_6D_6) δ 6.65 (dd, *J* = 11.2, 1.6 Hz, 1 H), 5.63 (dq, *J* = 11.2, 6.8 Hz, 1 H), 3.33 (tdd, *J* = 10.4, 5.2, 3.6 Hz, 1 H), 2.68–2.54 (m, 3 H), 2.49 (dd, *J* = 14.8, 8.0 Hz, 1 H), 2.39 (ddd, *J* = 18.8, 12.0, 7.2 Hz, 1 H), 1.97 (dt, *J* = 12.0, 6.0 Hz, 1 H), 1.89 (dd, *J* = 7.2, 1.6 Hz, 3 H), 1.73–1.65 (m, 1 H), 1.58–1.47 (m, 2 H), 1.43–1.31 (m, 2 H), 1.29 (t, *J* = 7.6 Hz, 3 H), 0.83 (tdd, *J* = 13.6, 10.8, 3.2 Hz, 1 H); ^{13}C NMR (100 MHz, C_6D_6) δ 128.9, 124.4, 122.0, 120.5, 119.1, 112.5, 55.3, 37.5, 30.1, 27.3, 22.6, 20.6, 19.0, 16.4, 15.5; HRMS (FAB) calc. for $C_{15}H_{21}N^+$ [M^+] 215.1674, found 215.1673. All spectroscopic data for this synthetic material matched those reported by Francke *et al.*[1]

(+)-Myrmicarin 215B (2.3). This compound was prepared via the methods described for the synthesis of **2.2** from either **2.36** (99% yield) or **2.40** (85% yield). **2.3**: $[\alpha]^{22}_D$ = +28.2° (*c* = 0.440, CH_2Cl_2); IR (film) ν_{max} 2925, 2850, 1653, 1430, 1321, 959 cm^{-1}; ^1H NMR (400 MHz, C_6D_6) δ 6.65 (dd, *J* = 15.6, 1.6 Hz, 1 H), 5.88 (dq, *J* = 15.6, 6.4 Hz, 1

H), 3.26 (tdd, *J* = 10.4, 5.2, 3.6 Hz, 1 H), 2.70–2.51 (m, 4 H), 2.37 (ddd, *J* = 16.0, 12.0, 6.8 Hz, 1 H), 1.99–1.91 (m, 1 H), 1.93 (dd, *J* = 6.8, 1.6 Hz, 3 H), 1.73–1.65 (m, 1 H), 1.57–1.45 (m, 2 H), 1.42–1.27 (m, 1 H), 1.31 (t, *J* = 7.6 Hz, 3 H), 0.83 (tdd, *J* = 13.2, 10.8, 2.4 Hz, 1 H); ^{13}C NMR (100 MHz, C_6D_6) δ 128.2, 125.7, 121.1, 118.9, 118.4, 113.6, 55.0, 36.8, 29.9, 25.9, 22.8, 20.5, 19.2, 18.9, 16.6; HRMS (FAB) calc. for $C_{15}H_{21}N^+$ [M^+] 215.1674, found 215.1682. All spectroscopic data for this synthetic material matched those reported by Francke *et al.*[1]

References

1. F. Schröder, S. Franke, W. Francke, H. Baumann, M. Kaib, J. M. Pasteels, D. Daloze, *Tetrahedron* **1996**, *52,* 13539–13546

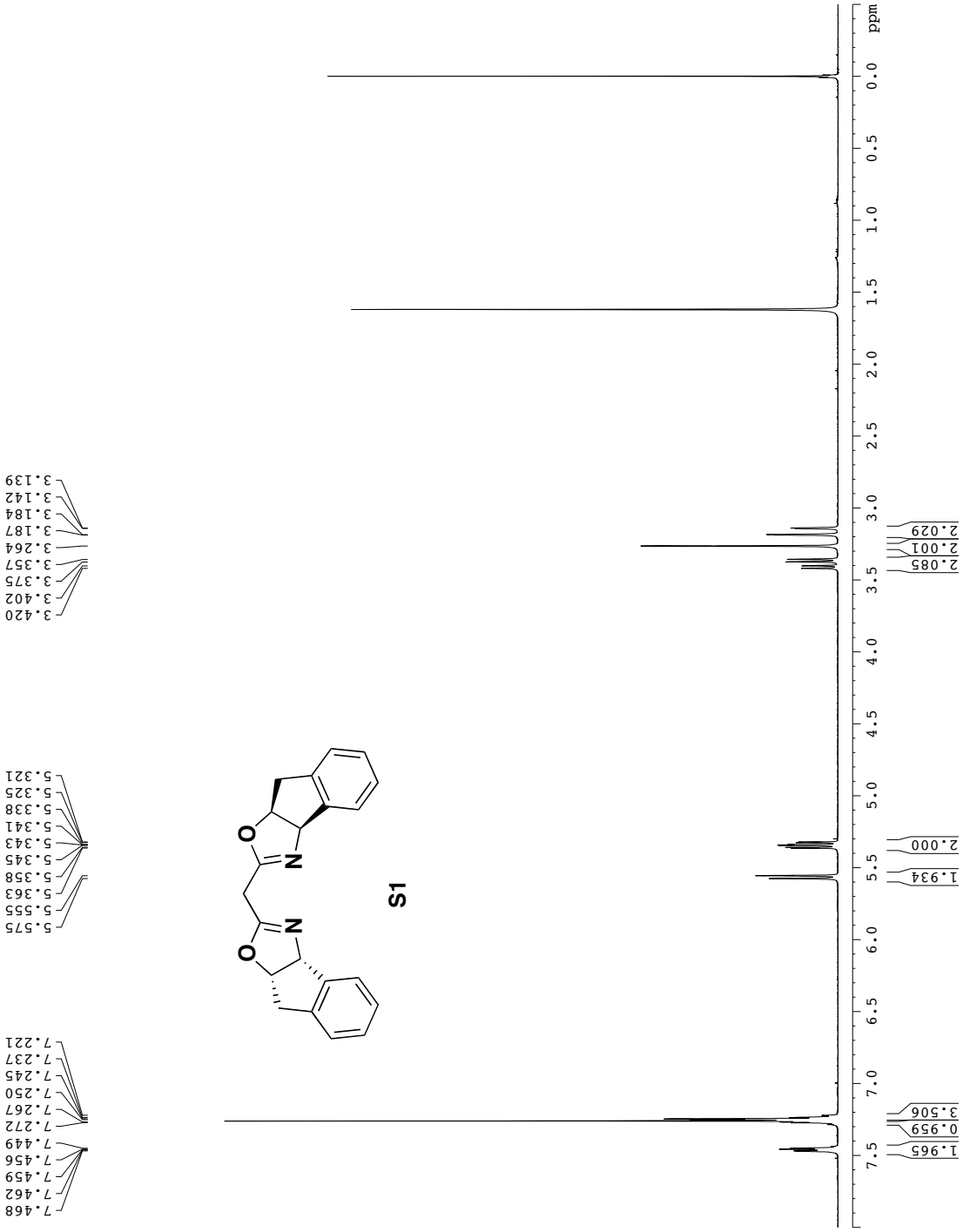
7.468
7.462
7.459
7.456
7.449
7.272
7.267
7.250
7.245
7.237
7.221
5.575
5.555
5.363
5.358
5.345
5.343
5.341
5.338
5.325
5.321
3.420
3.402
3.375
3.357
3.264
3.187
3.184
3.142
3.139
S1
1.965
0.959
3.506
2.000
1.934
2.085
2.001
2.029
ppm

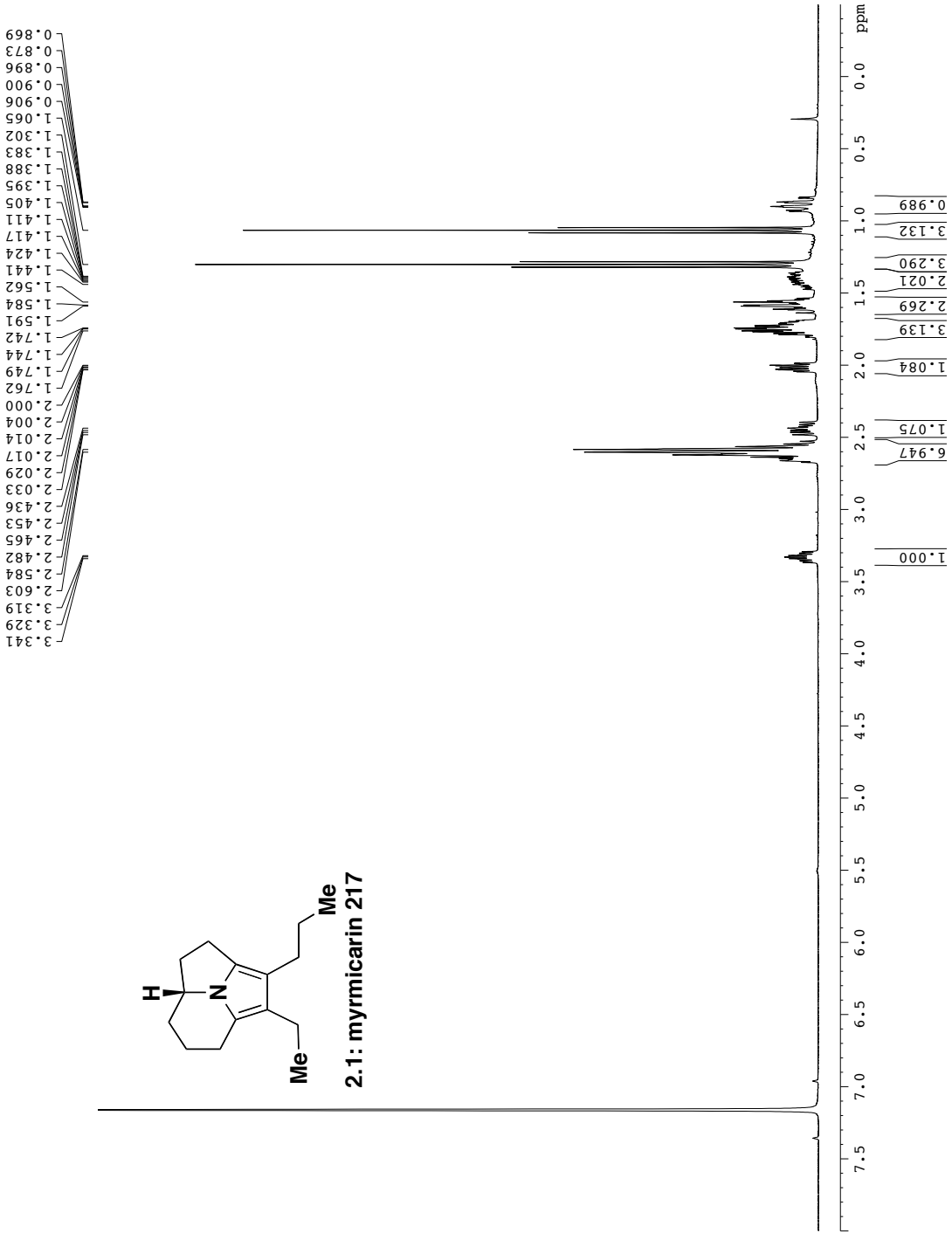
H
N
Me
Me
2.1: myrmicarin 217
ppm
0.0
0.5
1.0
1.5
2.0
2.5
3.0
3.5
4.0
4.5
5.0
5.5
6.0
6.5
7.0
7.5
0.989
3.132
3.290
2.021
2.269
3.139
1.084
1.075
6.947
1.000
0.869
0.873
0.896
0.900
0.906
1.065
1.302
1.383
1.388
1.395
1.405
1.411
1.417
1.424
1.441
1.562
1.584
1.591
1.742
1.744
1.749
1.762
2.000
2.004
2.014
2.017
2.029
2.033
2.436
2.453
2.465
2.482
2.584
2.603
3.319
3.329
3.341

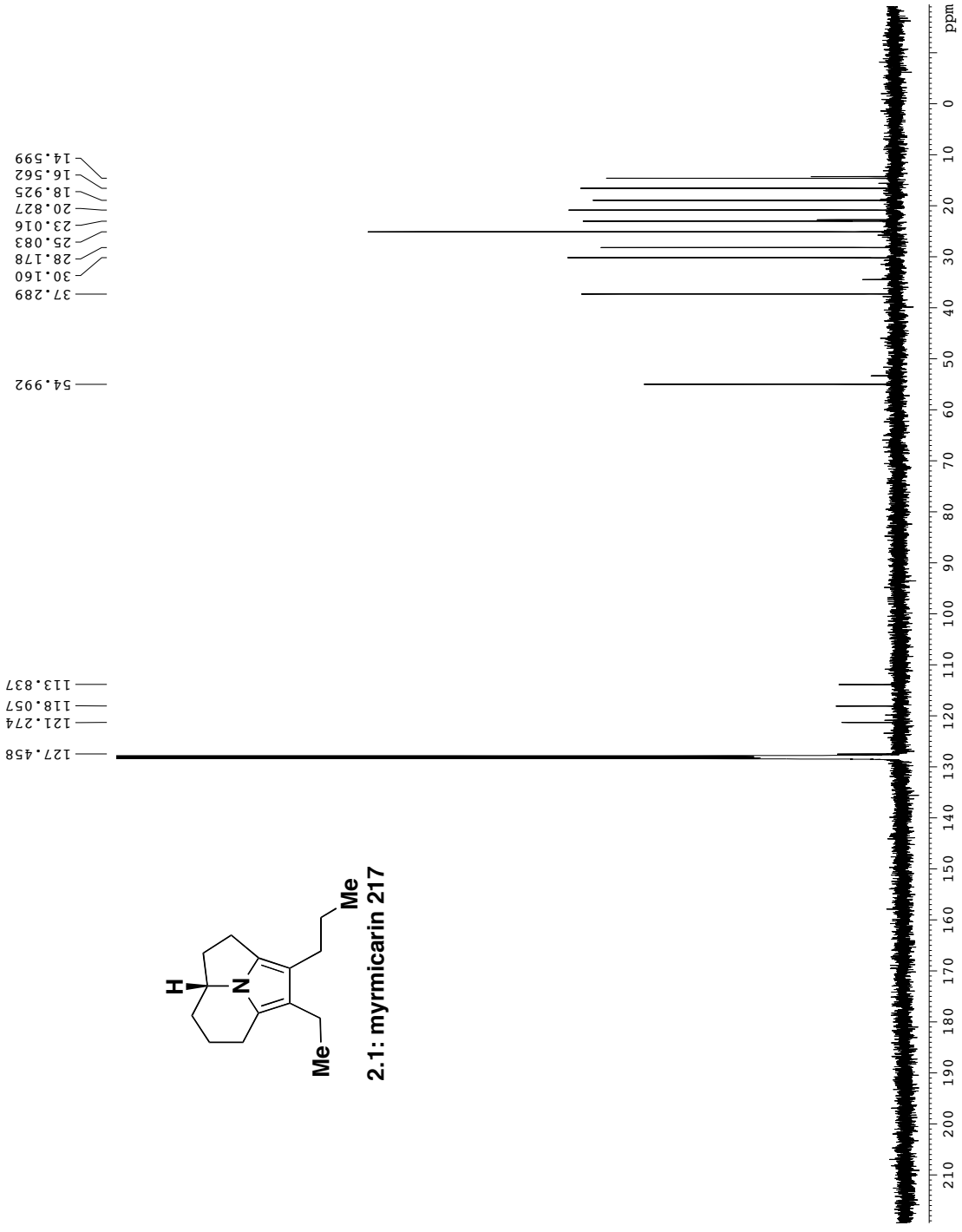
127.458
121.274
118.057
113.837
54.992
37.289
30.160
28.178
25.083
23.016
20.827
18.925
16.562
14.599
ppm
0
10
20
30
40
50
60
70
80
90
100
110
120
130
140
150
160
170
180
190
200
210
H
N
Me
Me
2.1: myrmicarin 217

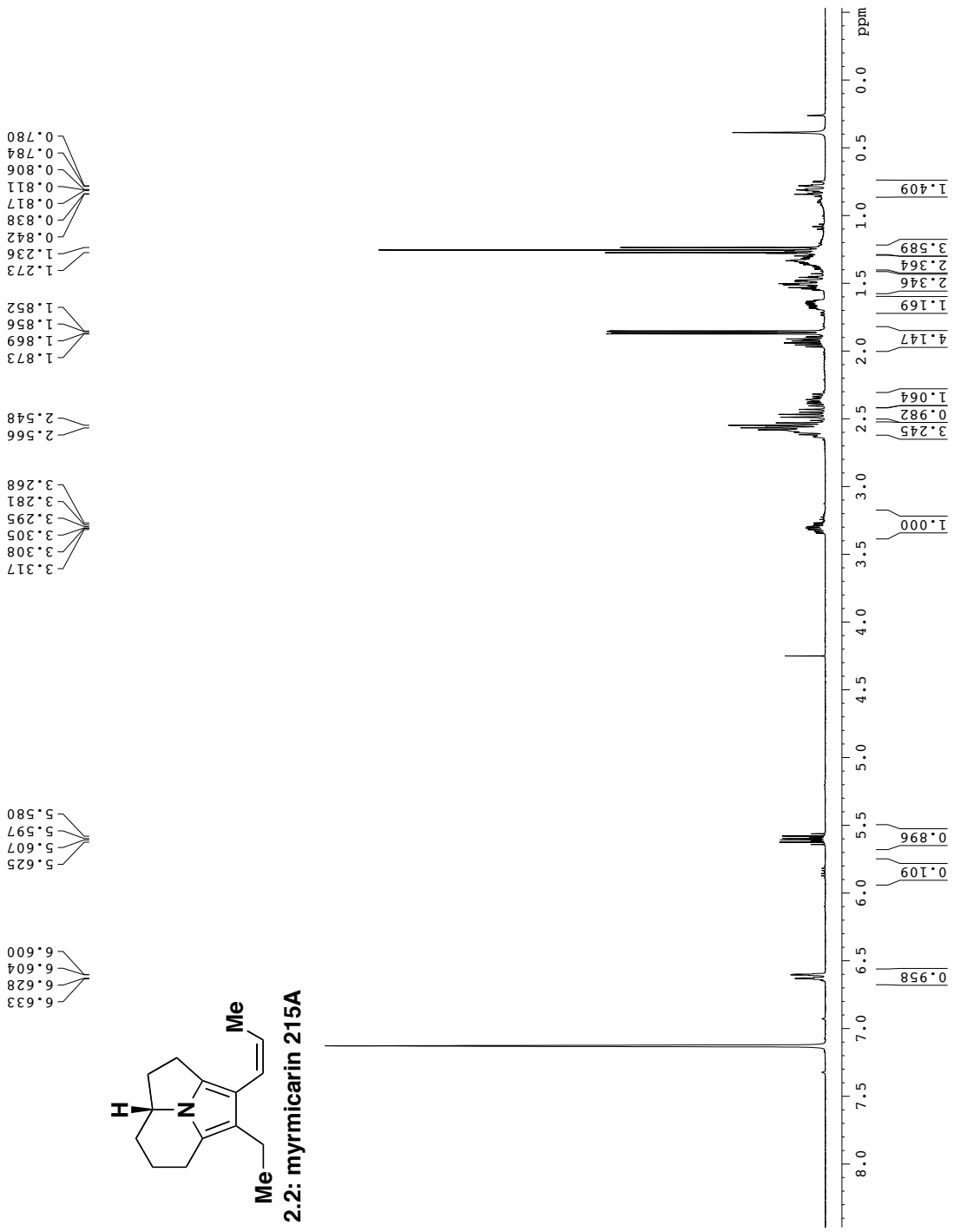
2.2: myrmicarin 215A
Me
Me
H
N
6.633
6.628
6.604
6.600
5.625
5.607
5.597
5.580
3.317
3.308
3.305
3.295
3.281
3.268
2.566
2.548
1.873
1.869
1.856
1.852
1.273
1.236
0.842
0.838
0.817
0.811
0.806
0.784
0.780
0.958
0.896
0.109
1.000
3.245
0.982
1.064
4.147
1.169
2.346
2.364
3.589
1.409
ppm

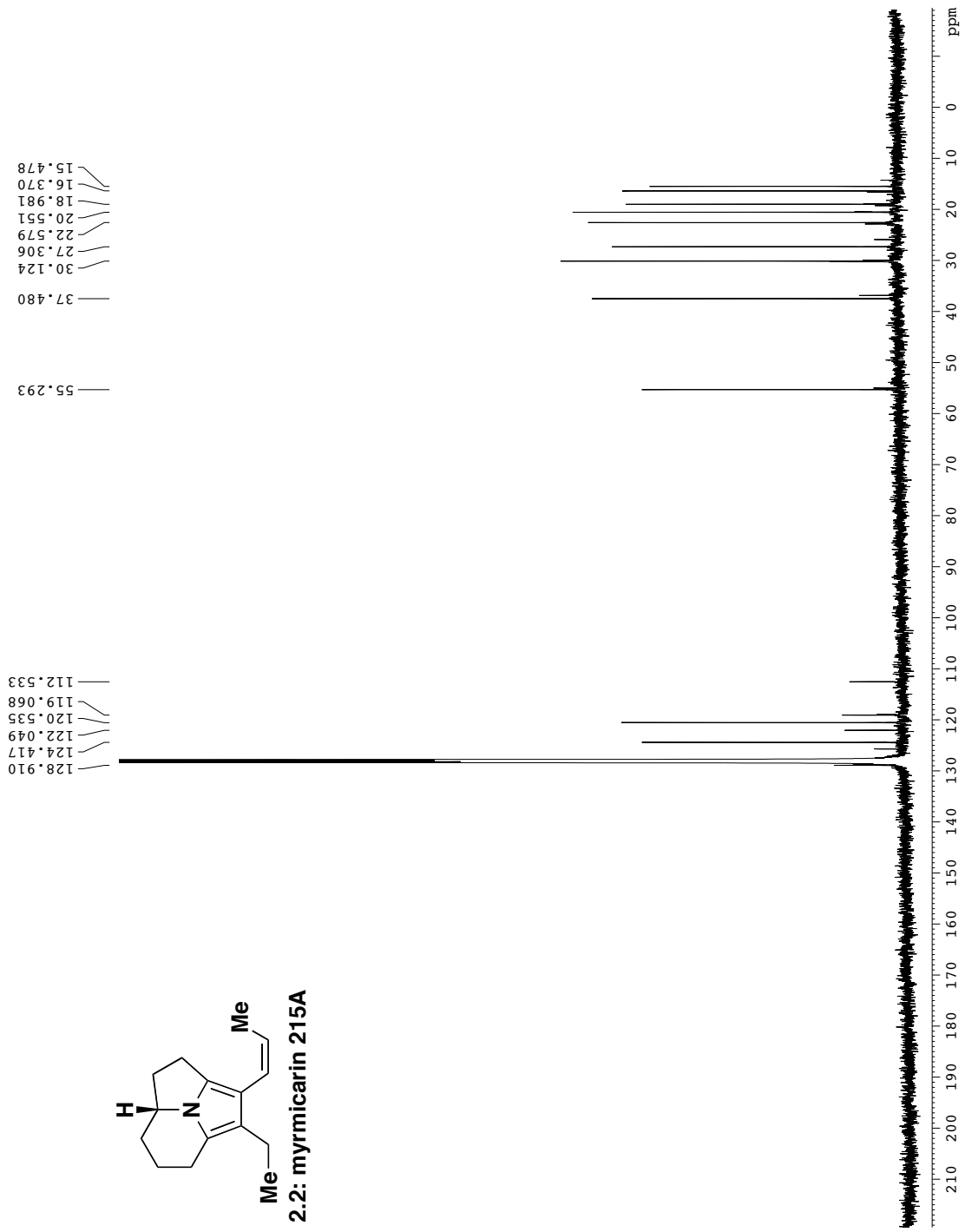

2.2: myrmicarin 215A

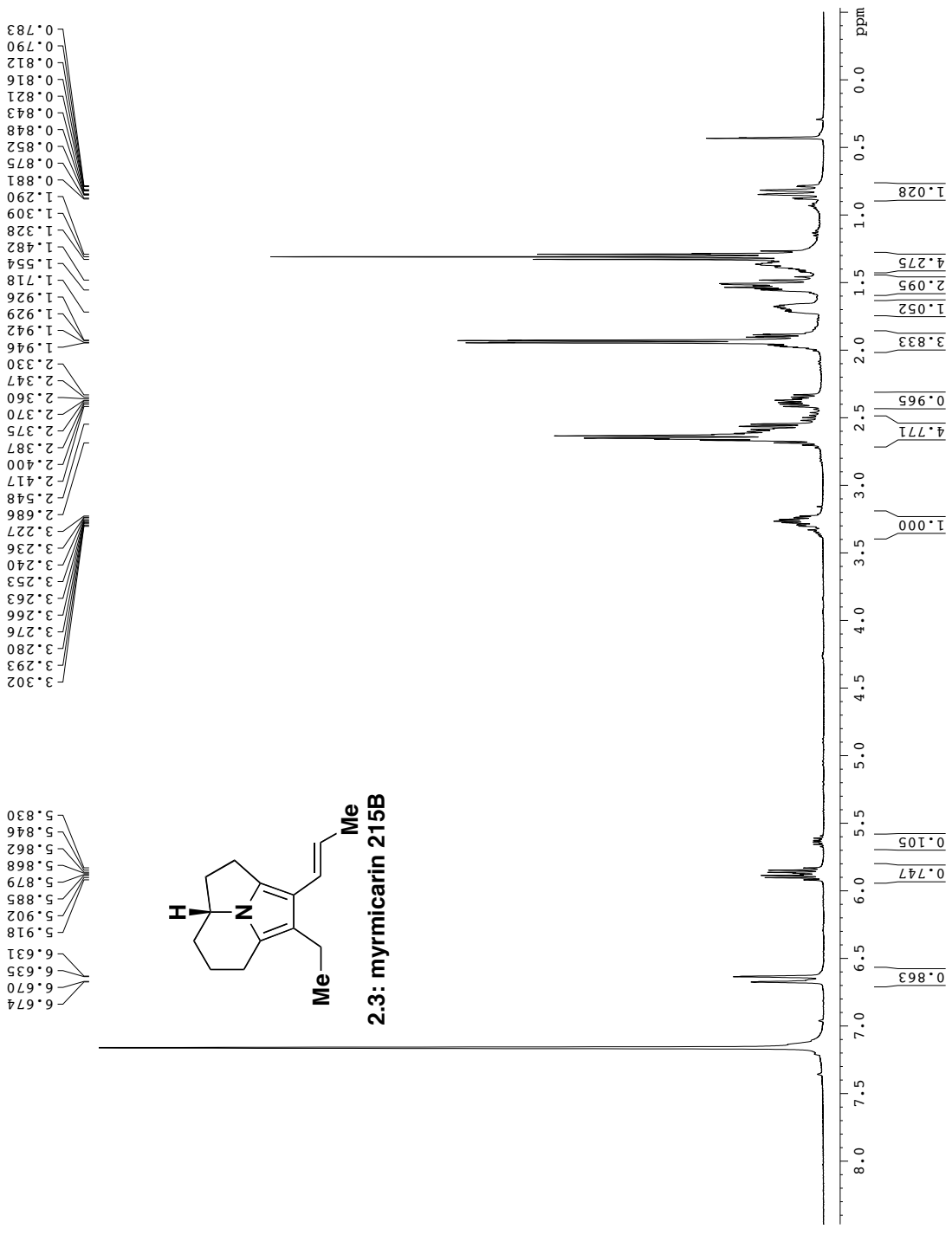
2.3: myrmicarin 215B
Me
Me
H
N
ppm
0.0
0.5
1.0
1.5
2.0
2.5
3.0
3.5
4.0
4.5
5.0
5.5
6.0
6.5
7.0
7.5
8.0
1.028
4.275
2.095
1.052
3.833
0.965
4.771
1.000
0.105
0.747
0.863
6.674
6.670
6.635
6.631
5.918
5.902
5.885
5.879
5.868
5.862
5.846
5.830
3.302
3.293
3.280
3.276
3.266
3.263
3.253
3.240
3.236
3.227
2.686
2.548
2.417
2.400
2.387
2.375
2.370
2.360
2.347
2.330
1.946
1.942
1.929
1.926
1.718
1.554
1.482
1.328
1.309
1.290
0.881
0.875
0.852
0.848
0.843
0.821
0.816
0.812
0.790
0.783

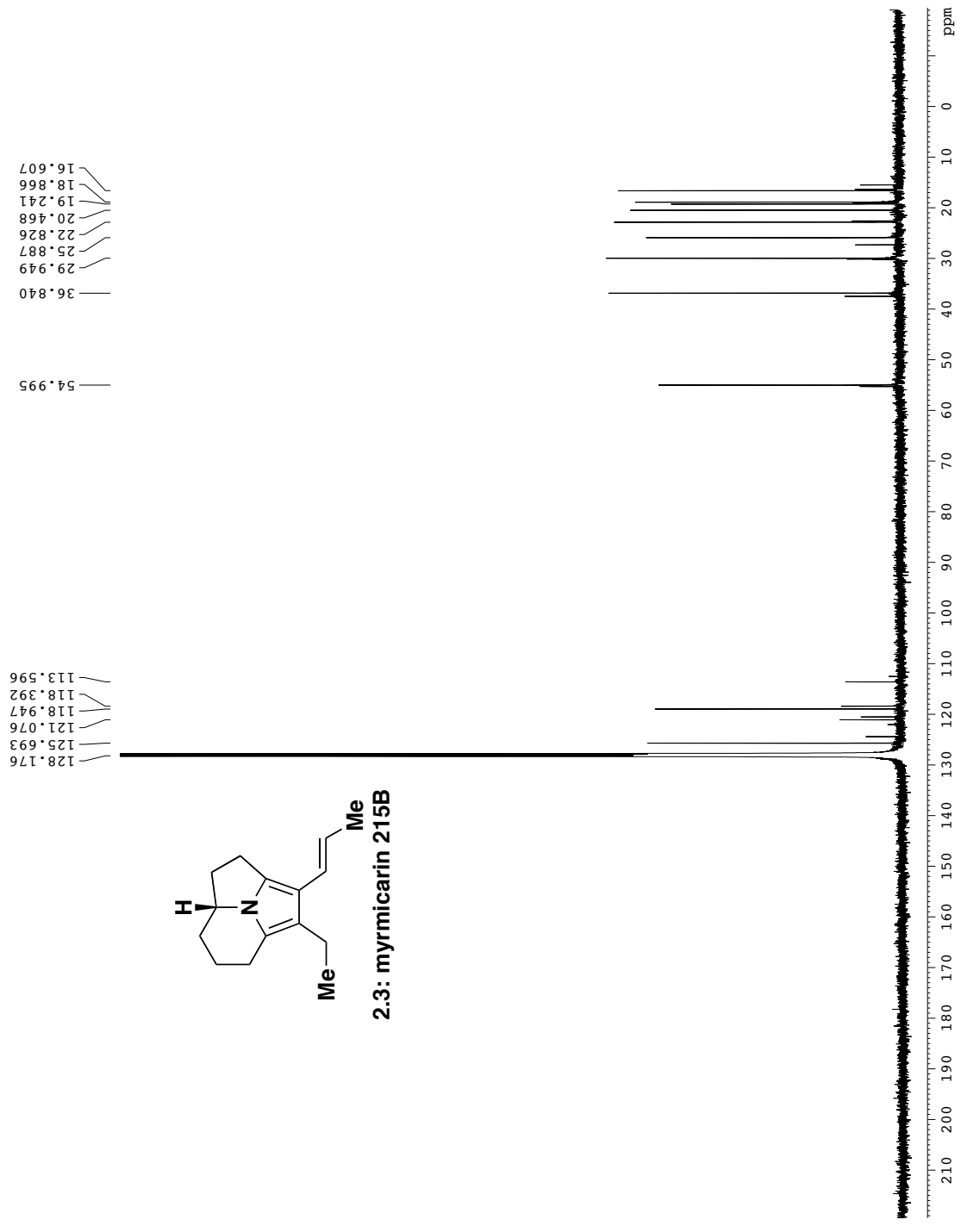
128.176
125.693
121.076
118.947
118.392
113.596
54.995
36.840
29.949
25.887
22.826
20.468
19.241
18.866
16.607
ppm
0
10
20
30
40
50
60
70
80
90
100
110
120
130
140
150
160
170
180
190
200
210
H
N
Me
Me
2.3: myrmicarin 215B

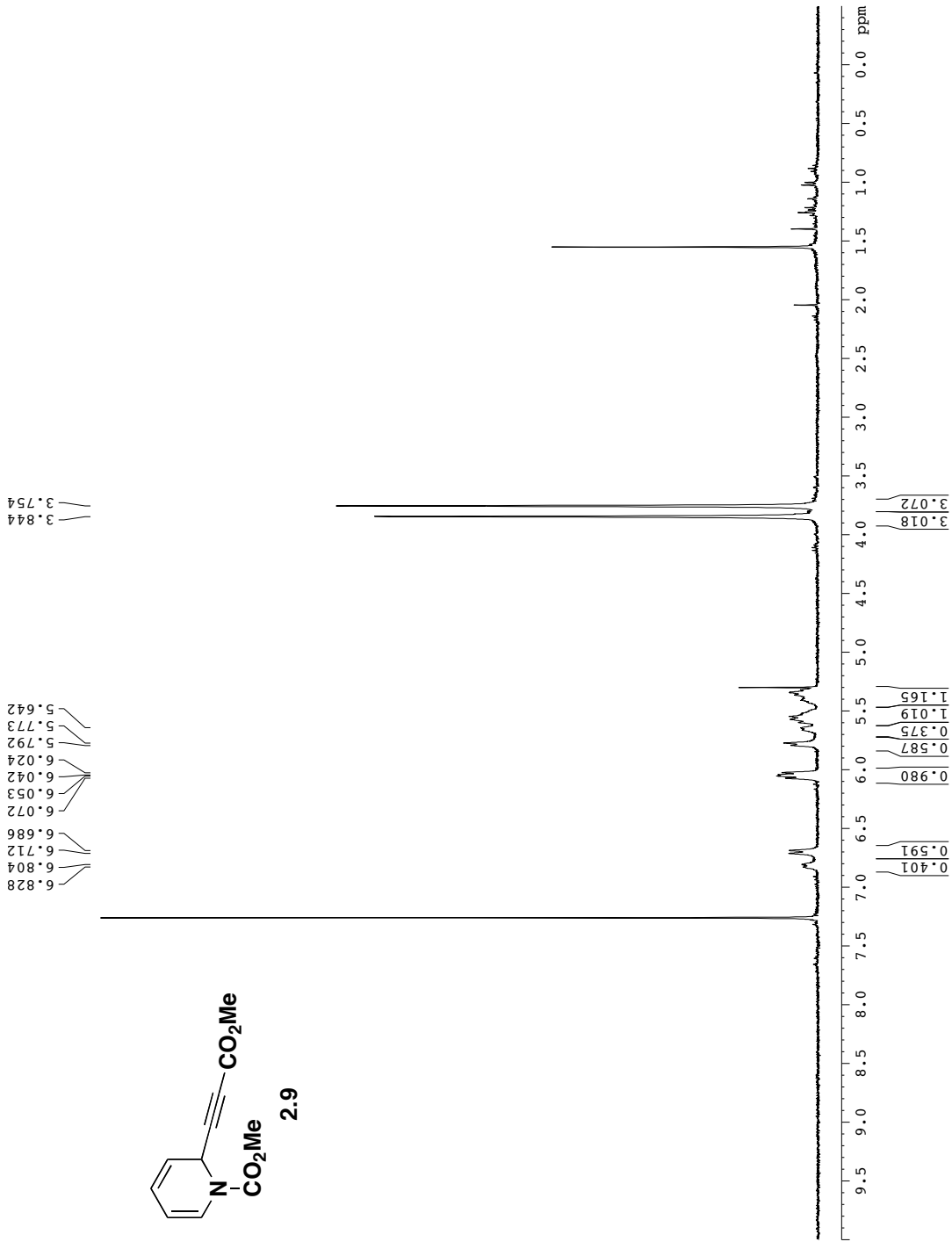
CO2Me
CO2Me
N
2.9
6.828
6.804
6.712
6.686
6.072
6.053
6.042
6.024
5.792
5.773
5.642
3.844
3.754
0.401
0.591
0.980
0.587
0.375
1.019
1.165
3.018
3.072
ppm

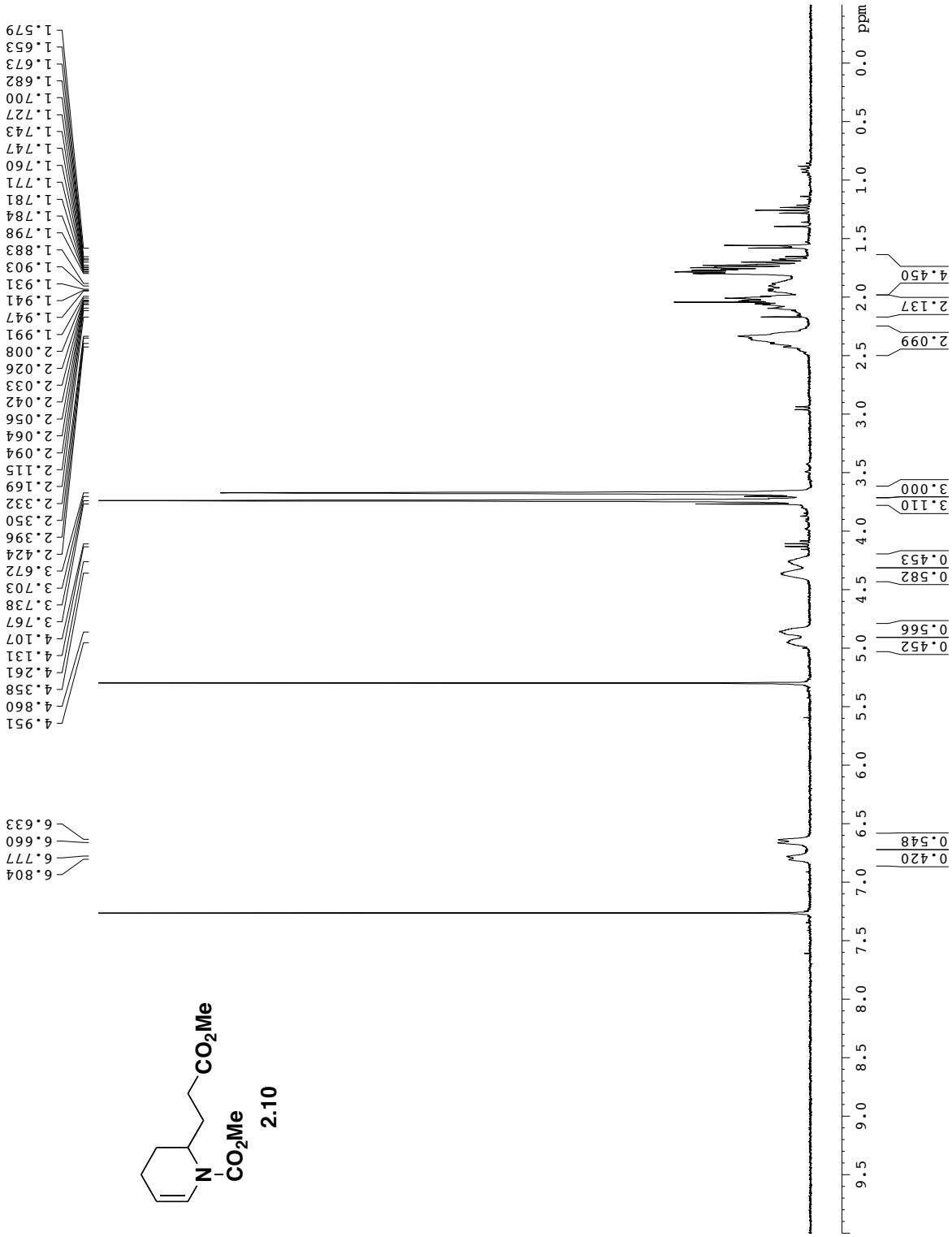
CO2Me
N
CO2Me
2.10
ppm
0.0
0.5
1.0
1.5
2.0
2.5
3.0
3.5
4.0
4.5
5.0
5.5
6.0
6.5
7.0
7.5
8.0
8.5
9.0
9.5
0.420
0.548
0.452
0.566
0.582
0.453
3.110
3.000
2.099
2.137
4.450
6.804
6.777
6.660
6.633
4.951
4.860
4.358
4.261
4.131
4.107
3.767
3.738
3.703
3.672
2.424
2.396
2.350
2.332
2.169
2.115
2.094
2.064
2.056
2.042
2.033
2.026
2.008
1.991
1.947
1.941
1.931
1.903
1.883
1.798
1.784
1.781
1.771
1.760
1.747
1.743
1.727
1.700
1.682
1.673
1.653
1.579

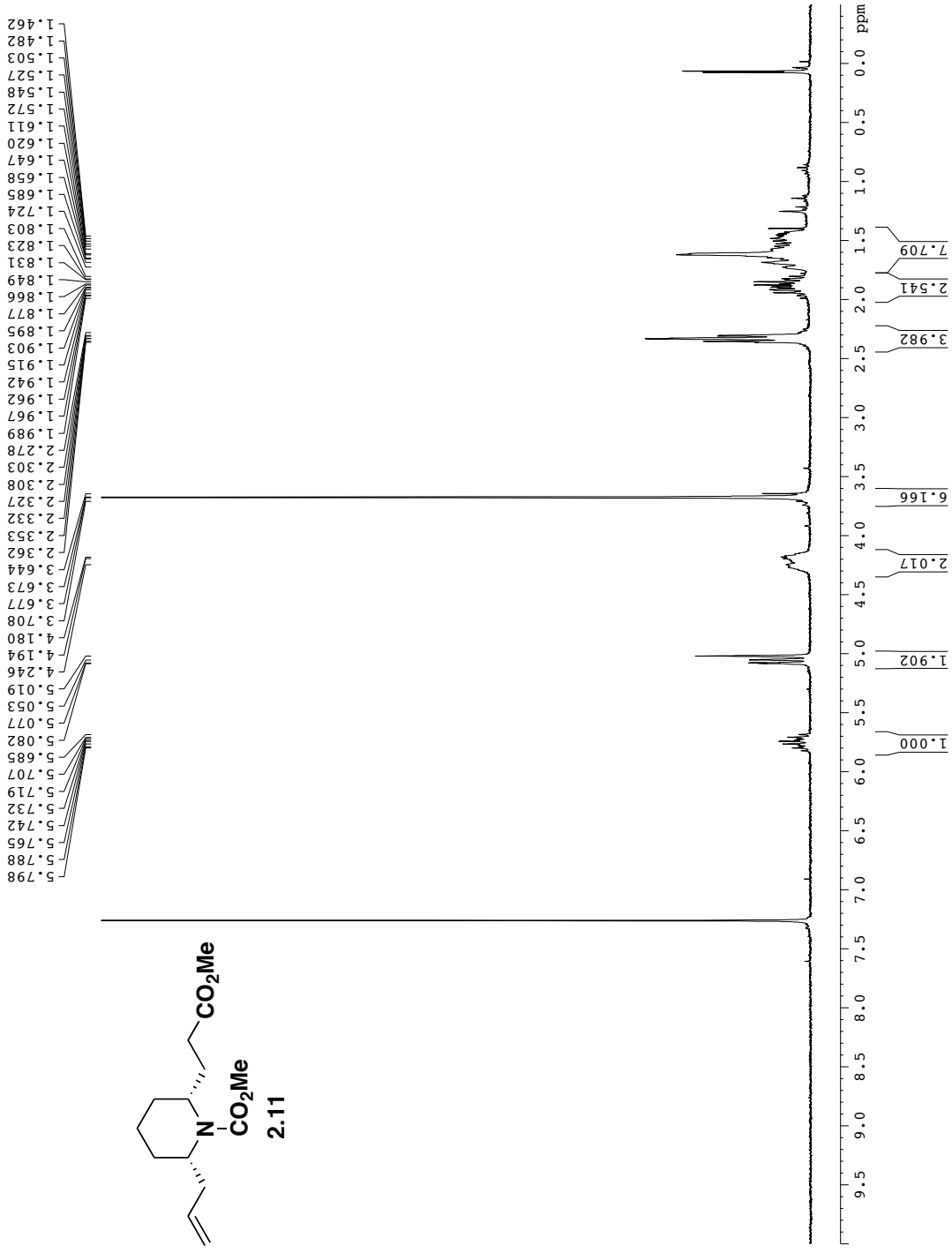
CO2Me
N
CO2Me
2.11
ppm
0.0
0.5
1.0
1.5
2.0
2.5
3.0
3.5
4.0
4.5
5.0
5.5
6.0
6.5
7.0
7.5
8.0
8.5
9.0
9.5
1.000
1.902
2.017
6.166
3.982
2.541
7.709

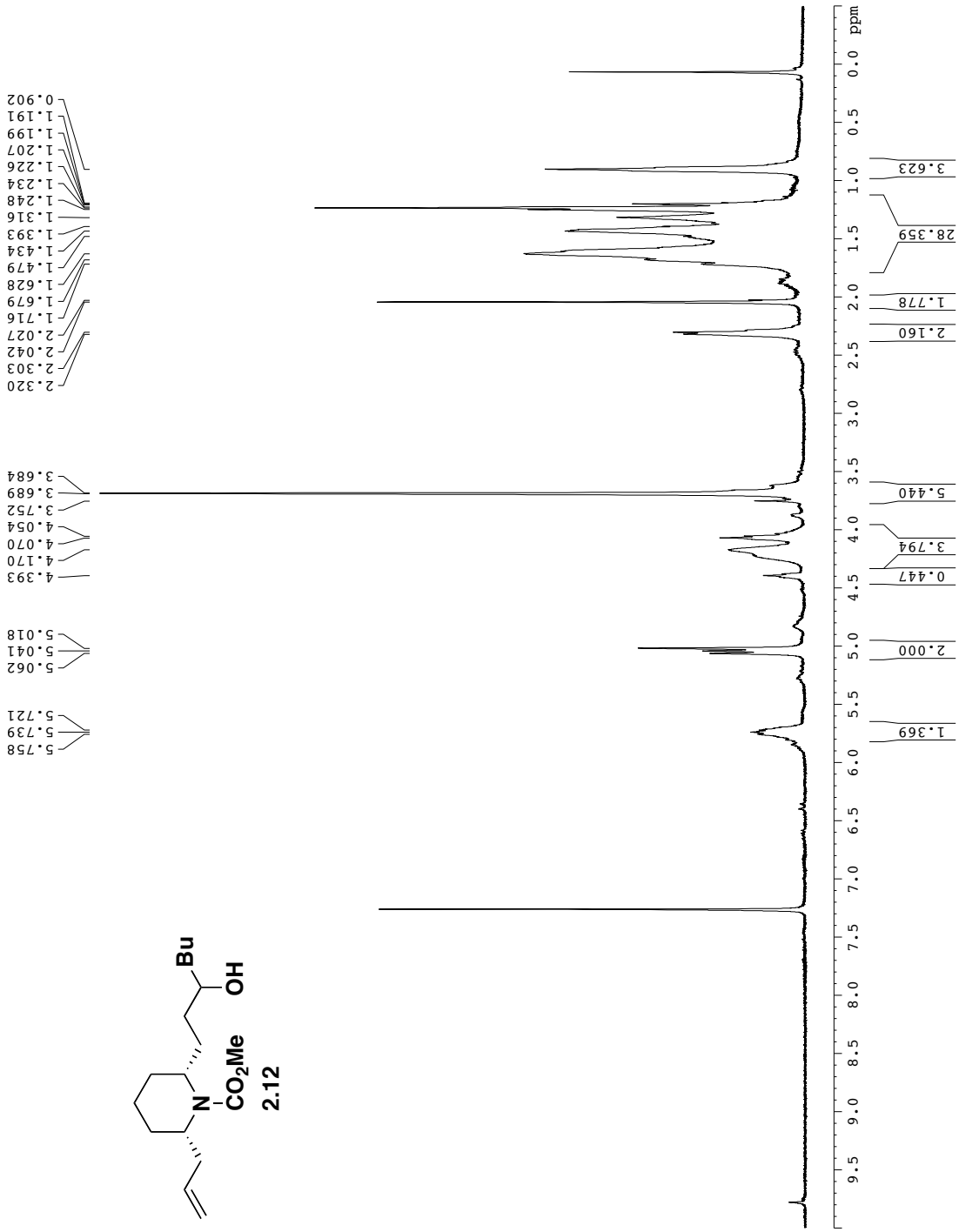
Bu
OH
N
CO2Me
2.12
ppm
0.0
0.5
1.0
1.5
2.0
2.5
3.0
3.5
4.0
4.5
5.0
5.5
6.0
6.5
7.0
7.5
8.0
8.5
9.0
9.5
1.369
2.000
0.447
3.794
5.440
2.160
1.778
28.359
3.623
5.758
5.739
5.721
5.062
5.041
5.018
4.393
4.170
4.070
4.054
3.752
3.689
3.684
2.320
2.303
2.042
2.027
1.716
1.679
1.628
1.479
1.434
1.393
1.316
1.248
1.234
1.226
1.207
1.199
1.191
0.902

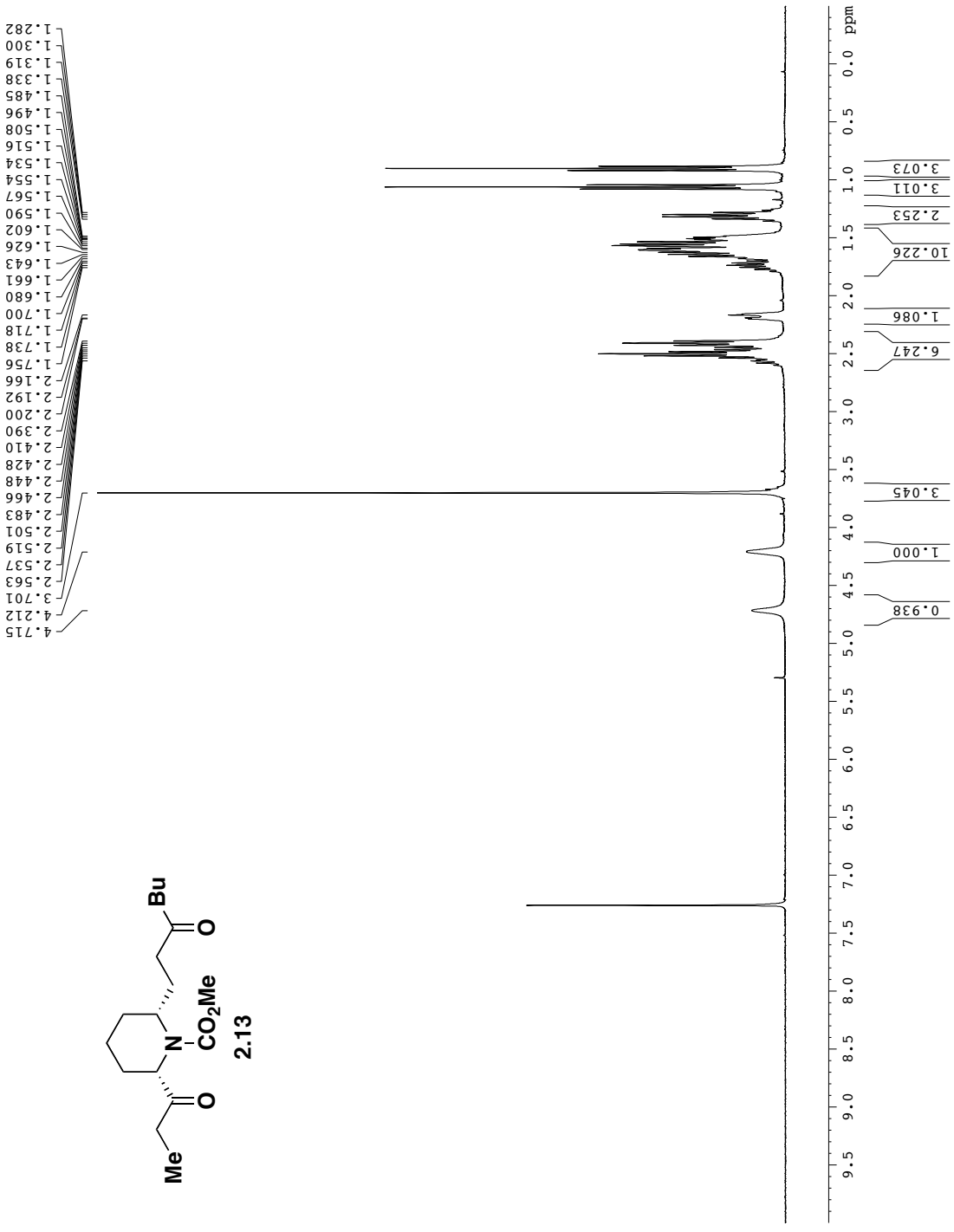
Bu
O
Me
O
N
CO2Me
2.13
ppm
0.938
1.000
3.045
6.247
1.086
10.226
2.253
3.011
3.073

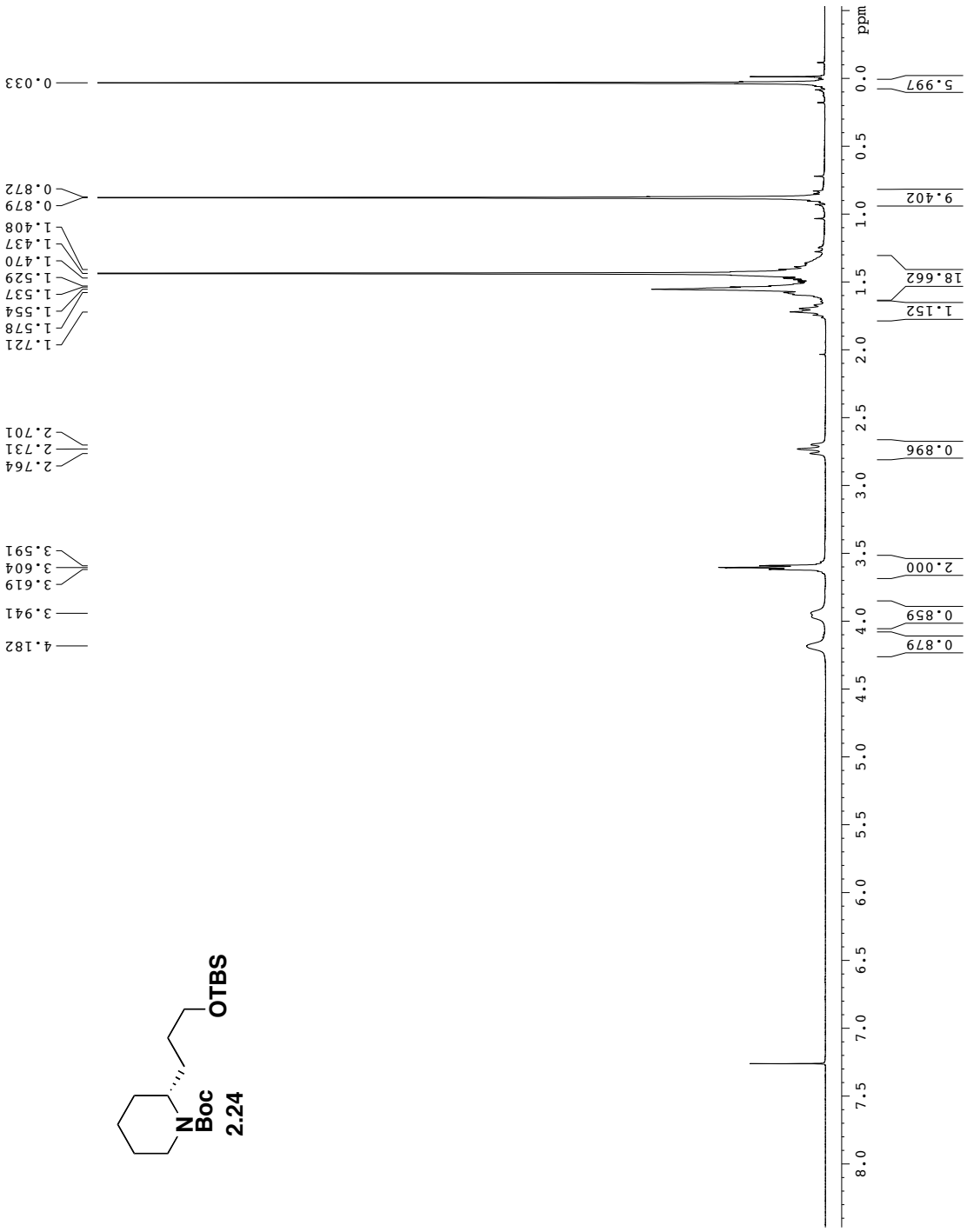
OTBS
N
Boc
2.24
ppm
0.0
0.5
1.0
1.5
2.0
2.5
3.0
3.5
4.0
4.5
5.0
5.5
6.0
6.5
7.0
7.5
8.0
5.997
9.402
18.662
1.152
0.896
2.000
0.859
0.879
0.033
0.872
0.879
1.408
1.437
1.470
1.529
1.537
1.554
1.578
1.721
2.701
2.731
2.764
3.591
3.604
3.619
3.941
4.182

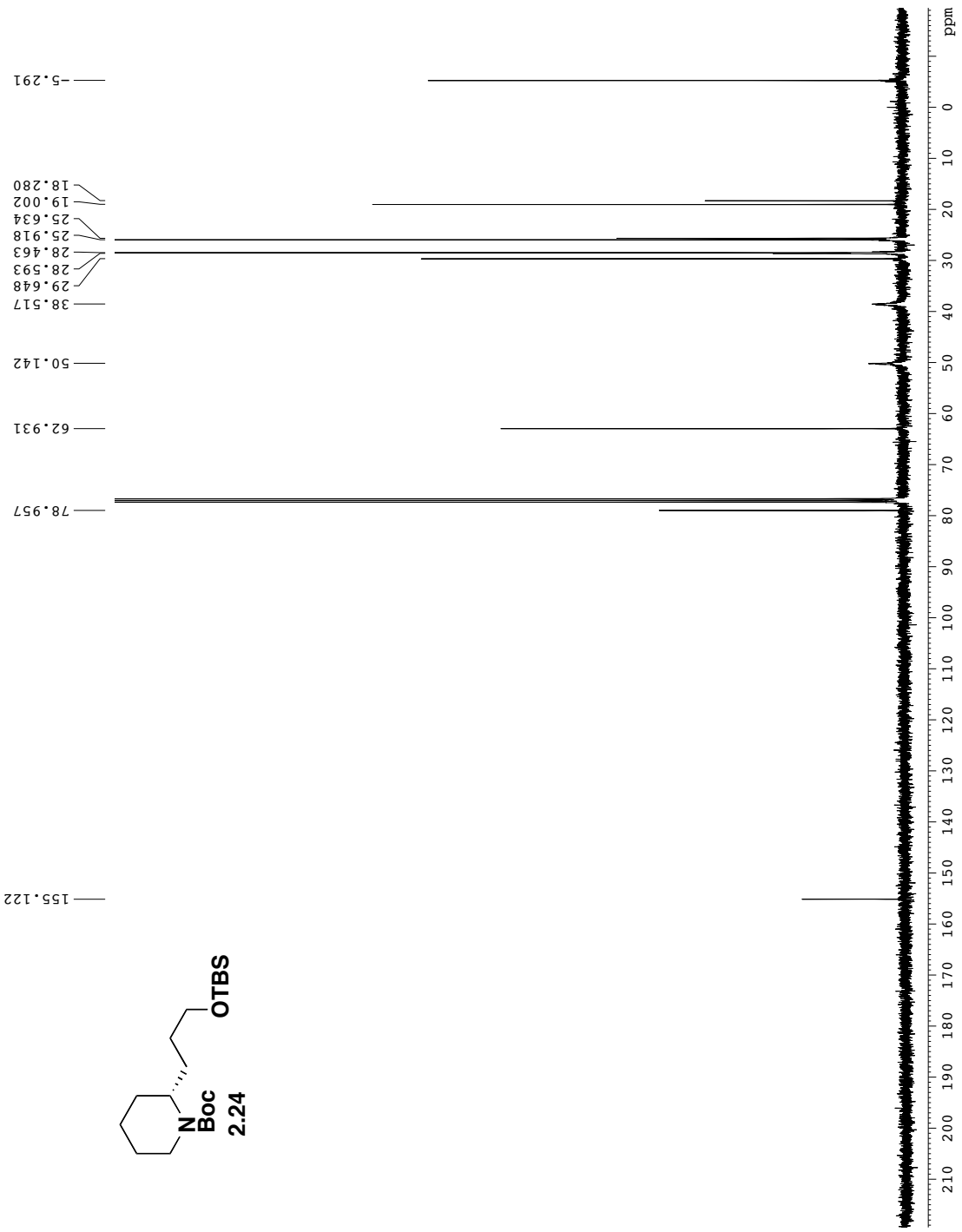
155.122
78.957
62.931
50.142
38.517
29.648
28.593
28.463
25.918
25.634
19.002
18.280
-5.291
ppm
0
10
20
30
40
50
60
70
80
90
100
110
120
130
140
150
160
170
180
190
200
210
N
Boc
OTBS
2.24

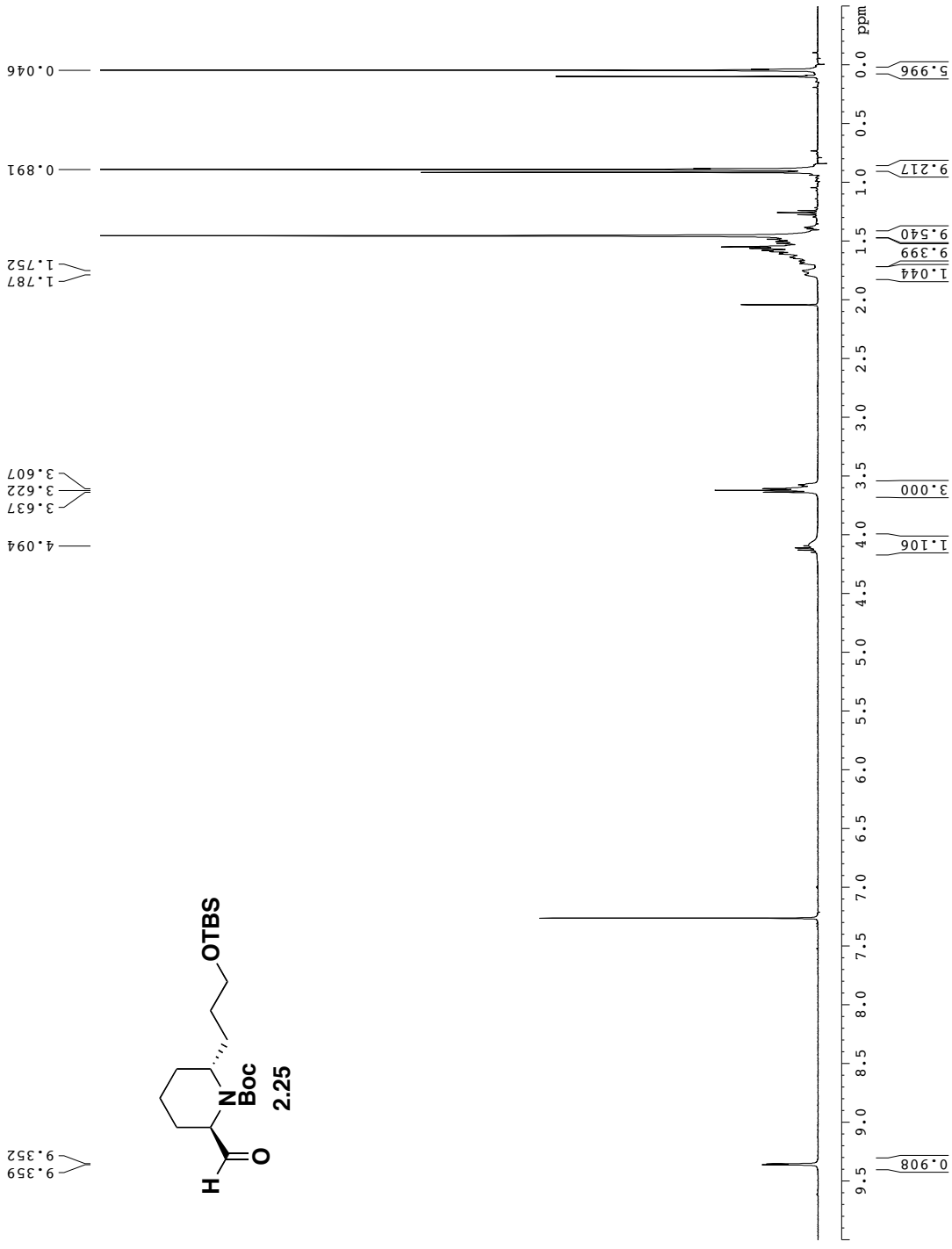
OTBS
N
Boc
O
H
2.25
ppm
0.0
0.5
1.0
1.5
2.0
2.5
3.0
3.5
4.0
4.5
5.0
5.5
6.0
6.5
7.0
7.5
8.0
8.5
9.0
9.5
5.996
9.217
9.540
9.399
1.044
3.000
1.106
0.908
0.046
0.891
1.787
1.752
3.637
3.622
3.607
4.094
9.359
9.352

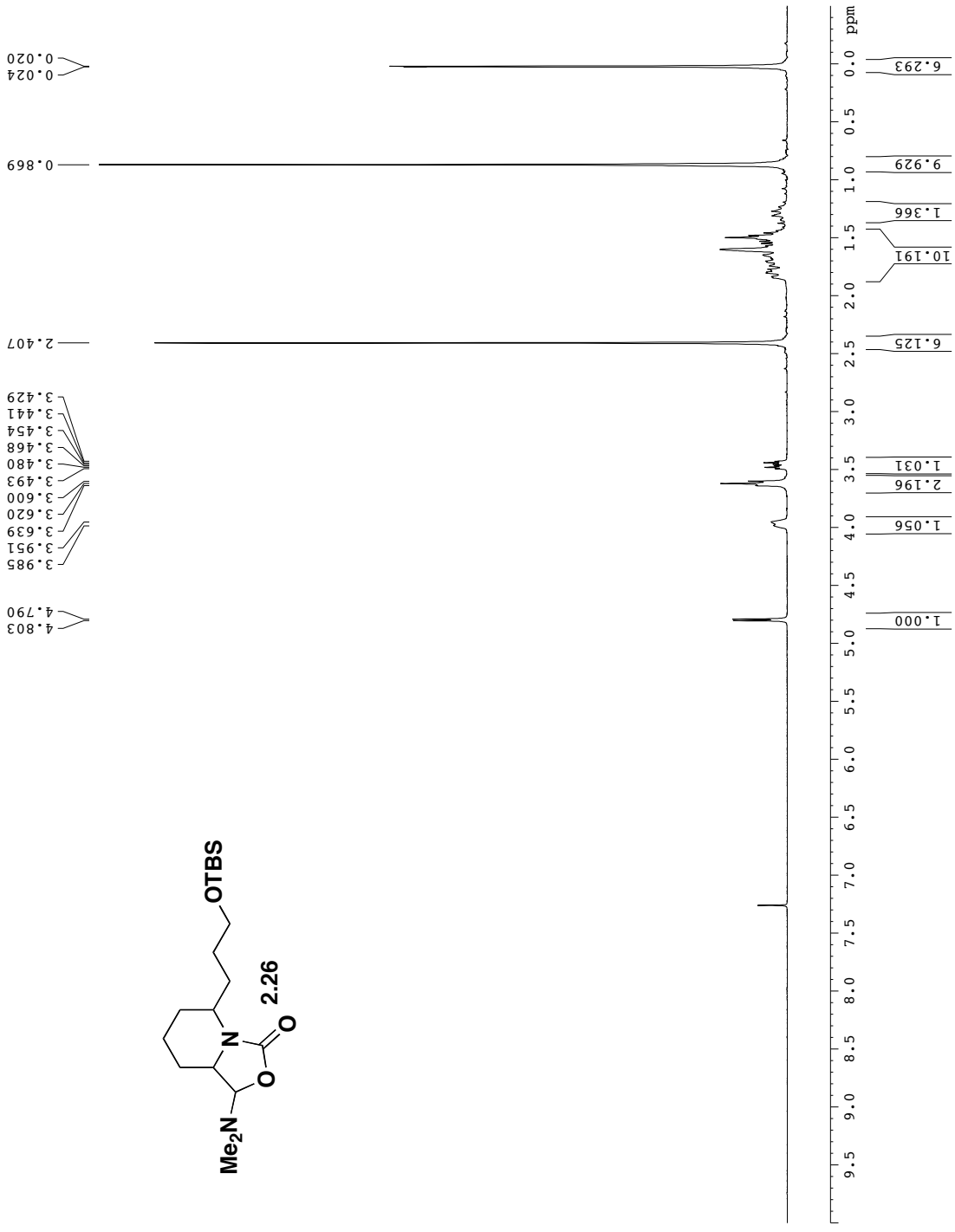
OTBS
N
O
O
2.26
Me2N
0.020
0.024
0.869
2.407
3.429
3.441
3.454
3.468
3.480
3.493
3.600
3.620
3.639
3.951
3.985
4.790
4.803
6.293
9.929
1.366
10.191
6.125
1.031
2.196
1.056
1.000
ppm

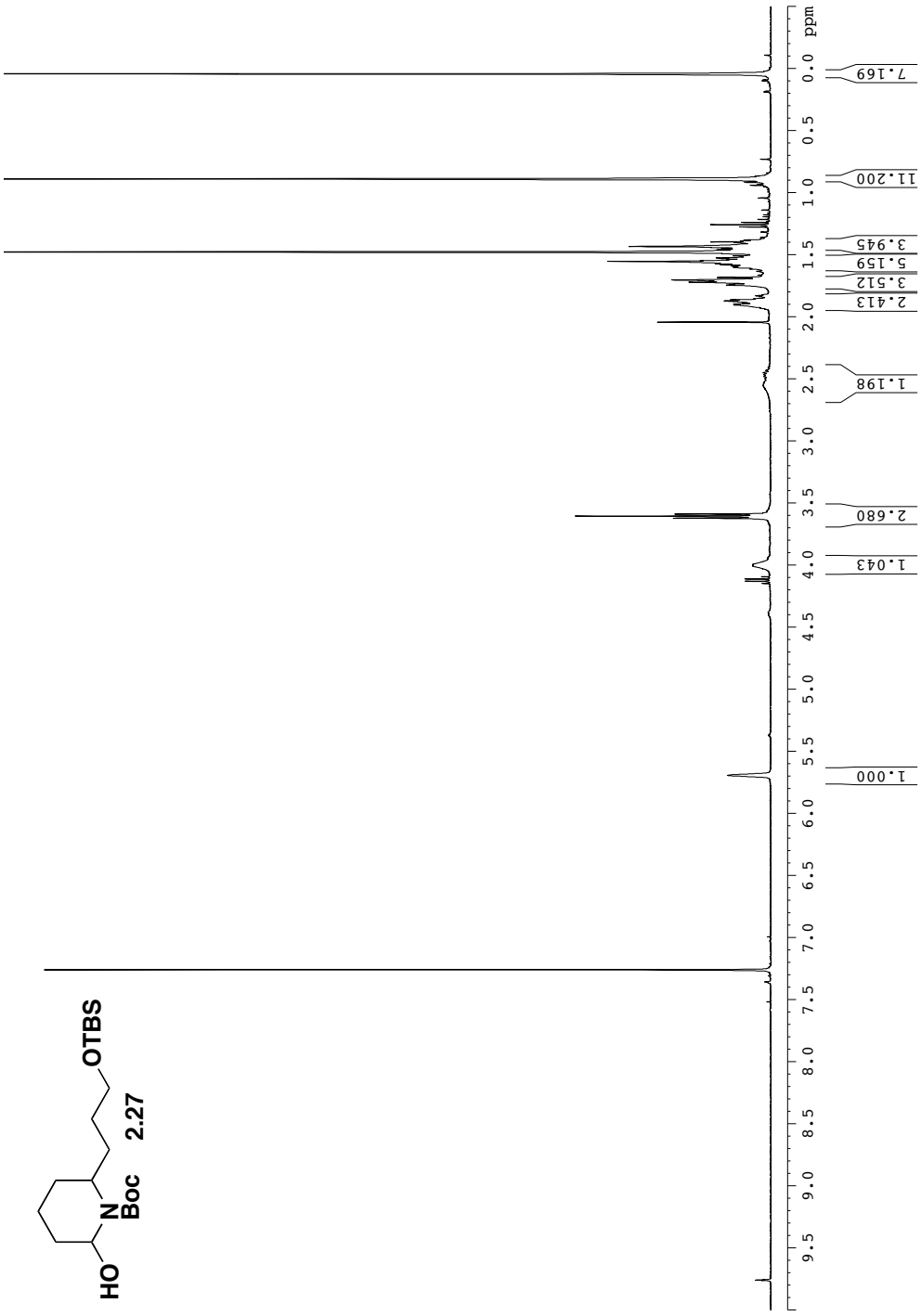
OTBS
2.27
Boc
N
HO
ppm
7.169
11.200
3.945
5.159
3.512
2.413
1.198
2.680
1.043
1.000

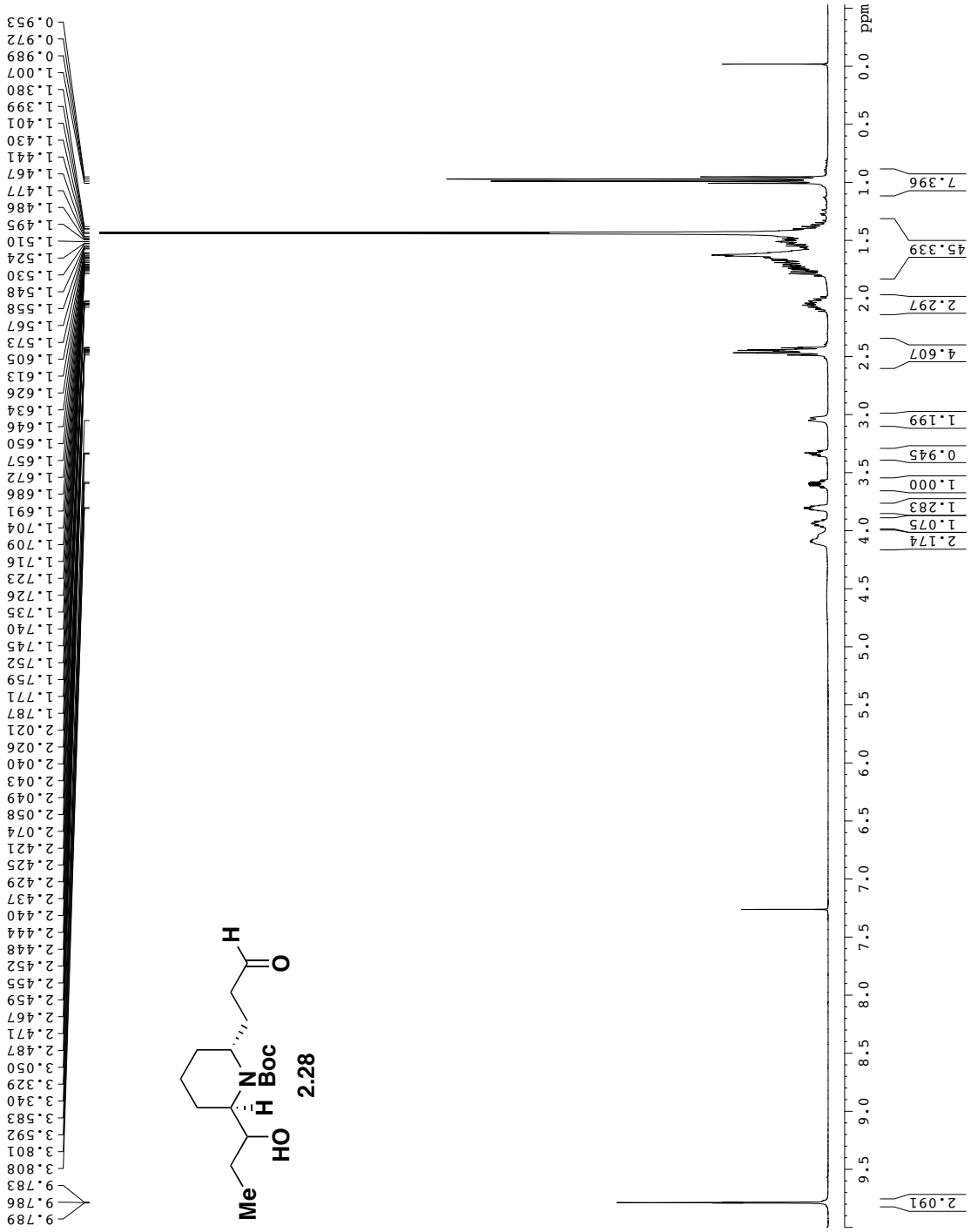
Me
HO
H
N
Boc
O
H
2.28
ppm
2.091
7.396
45.339
2.297
4.607
1.199
0.945
1.000
1.283
1.075
2.174

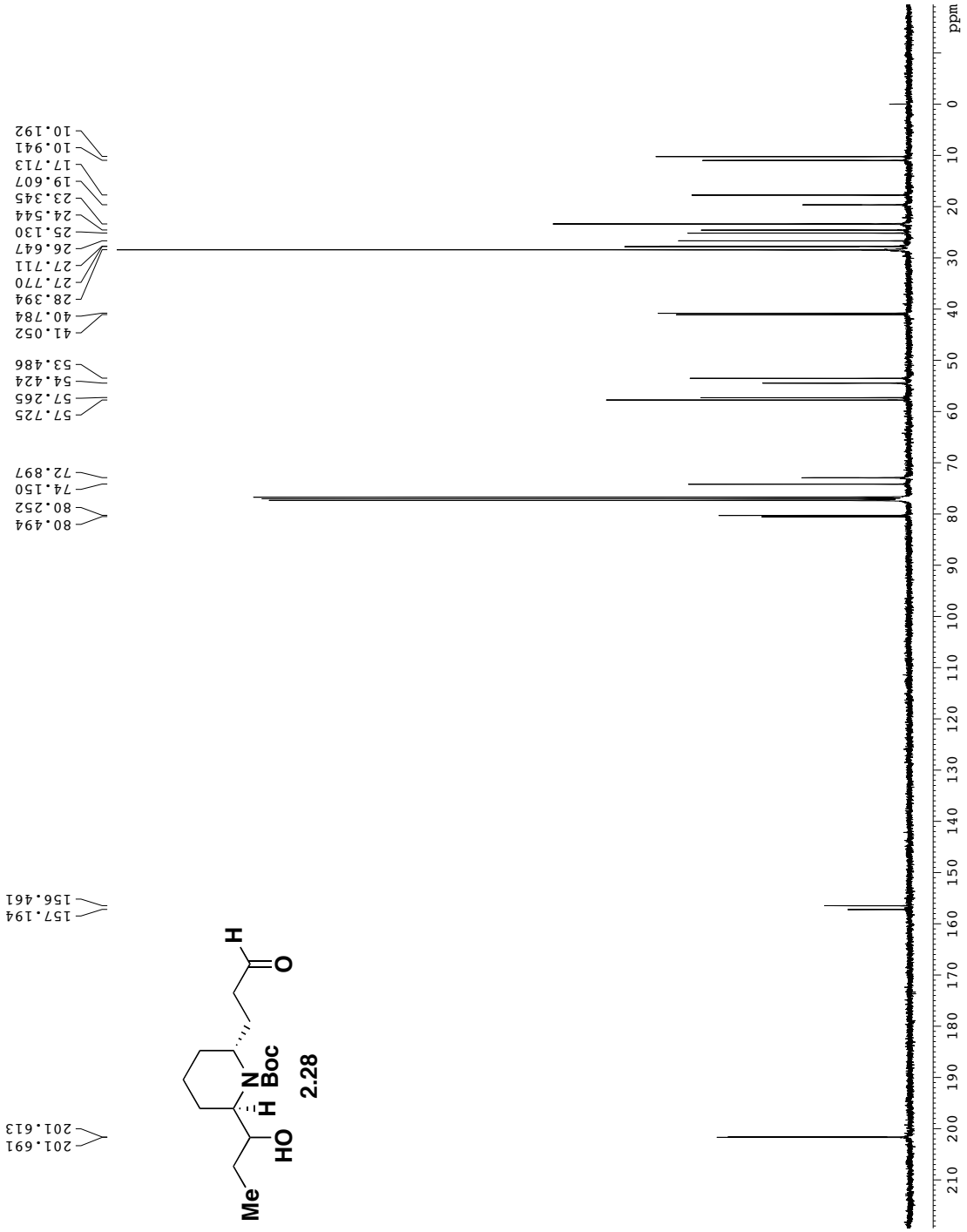
201.691
201.613
157.194
156.461
80.494
80.252
74.150
72.897
57.725
57.265
54.424
53.486
41.052
40.784
28.394
27.770
27.711
26.647
25.130
24.544
23.345
19.607
17.713
10.941
10.192
Me
HO
H
N
Boc
2.28
O
H
ppm

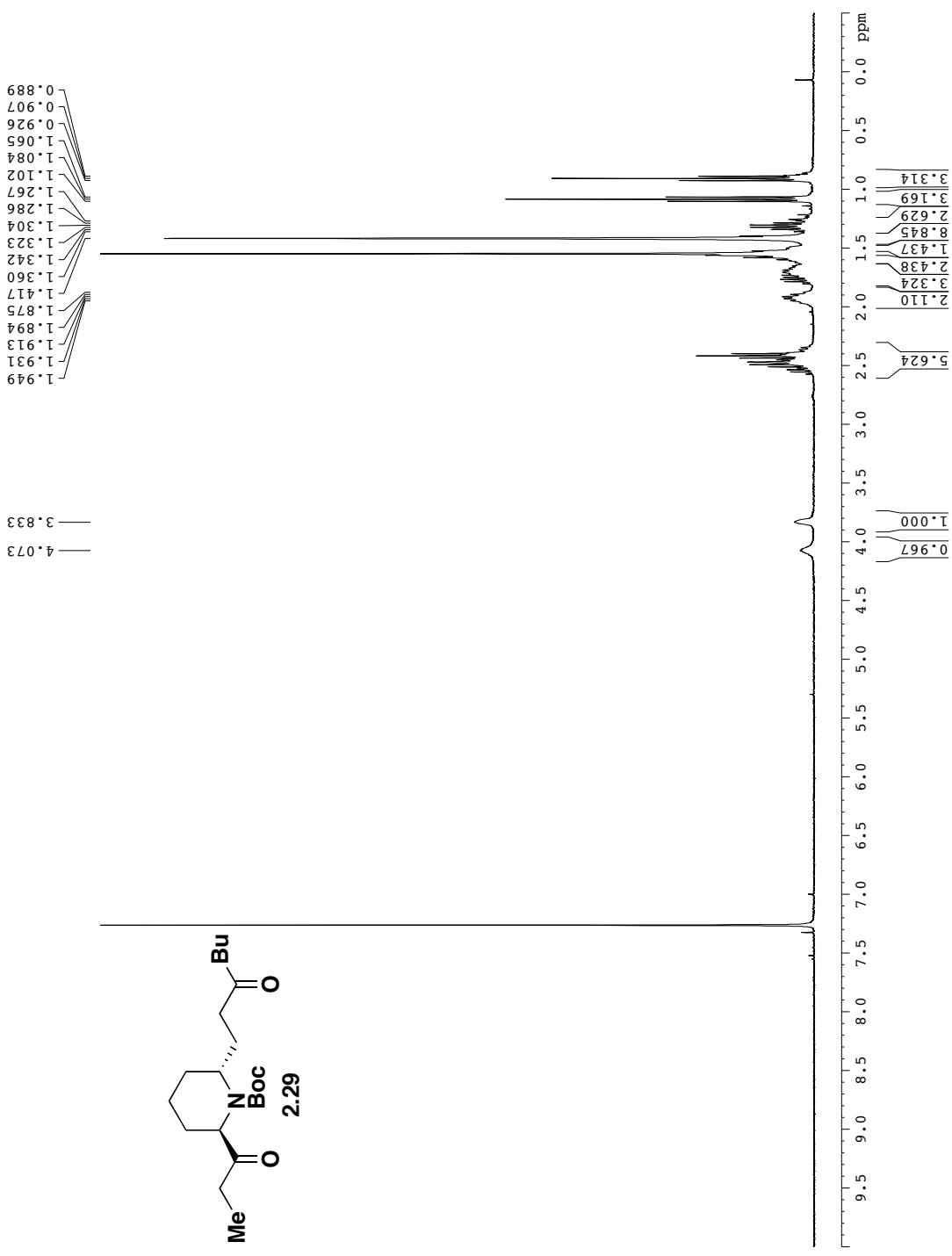
Bu
O
N
Boc
O
Me
2.29
ppm
0.0
0.5
1.0
1.5
2.0
2.5
3.0
3.5
4.0
4.5
5.0
5.5
6.0
6.5
7.0
7.5
8.0
8.5
9.0
9.5
0.967
1.000
5.624
2.110
3.324
2.438
1.437
8.845
2.629
3.169
3.314
4.073
3.833
1.949
1.931
1.913
1.894
1.875
1.417
1.360
1.342
1.323
1.304
1.286
1.267
1.102
1.084
1.065
0.926
0.907
0.889

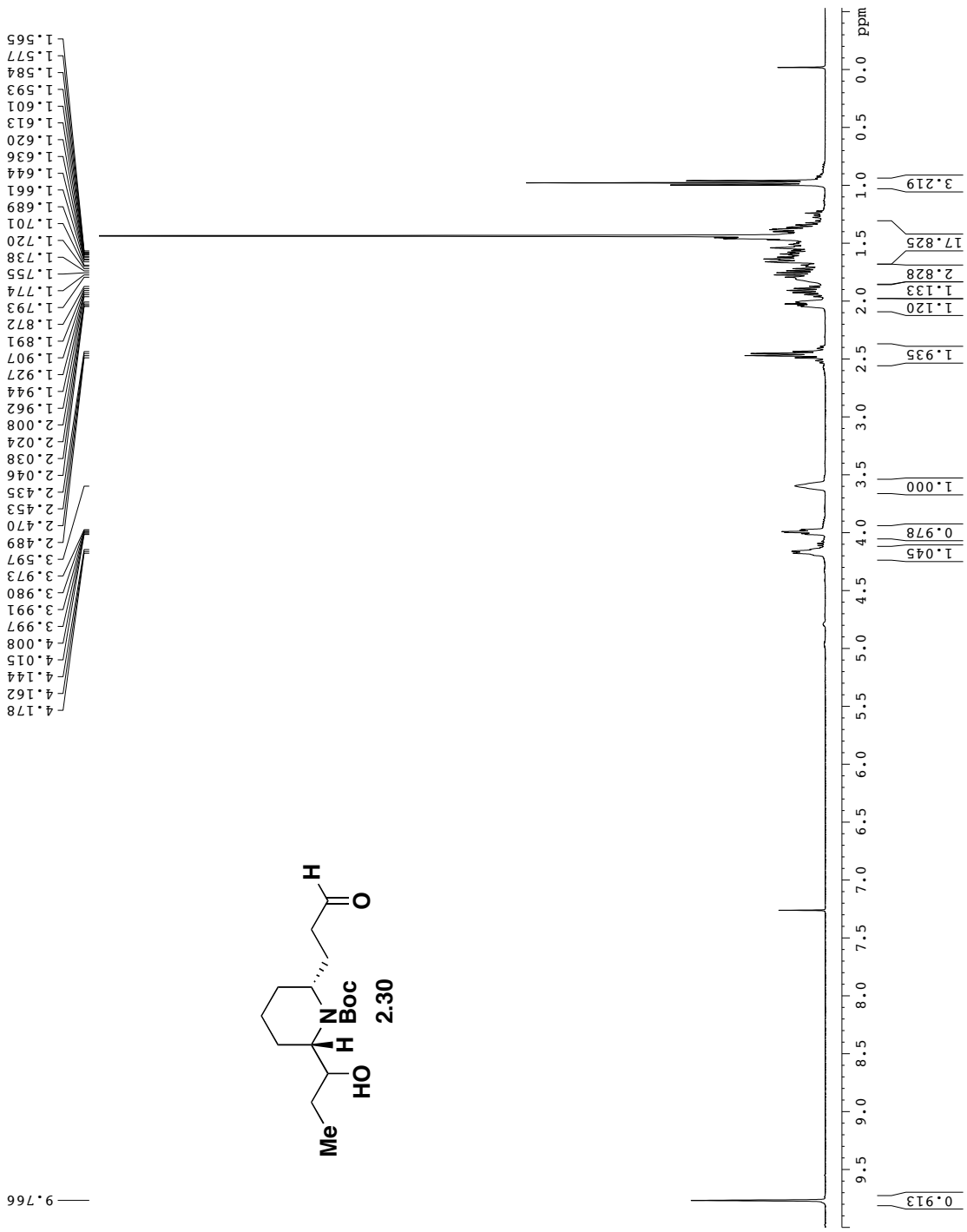
Me
HO
H
N
Boc
2.30
O
H
ppm
0.913
3.219
17.825
2.828
1.133
1.120
1.935
1.000
0.978
1.045

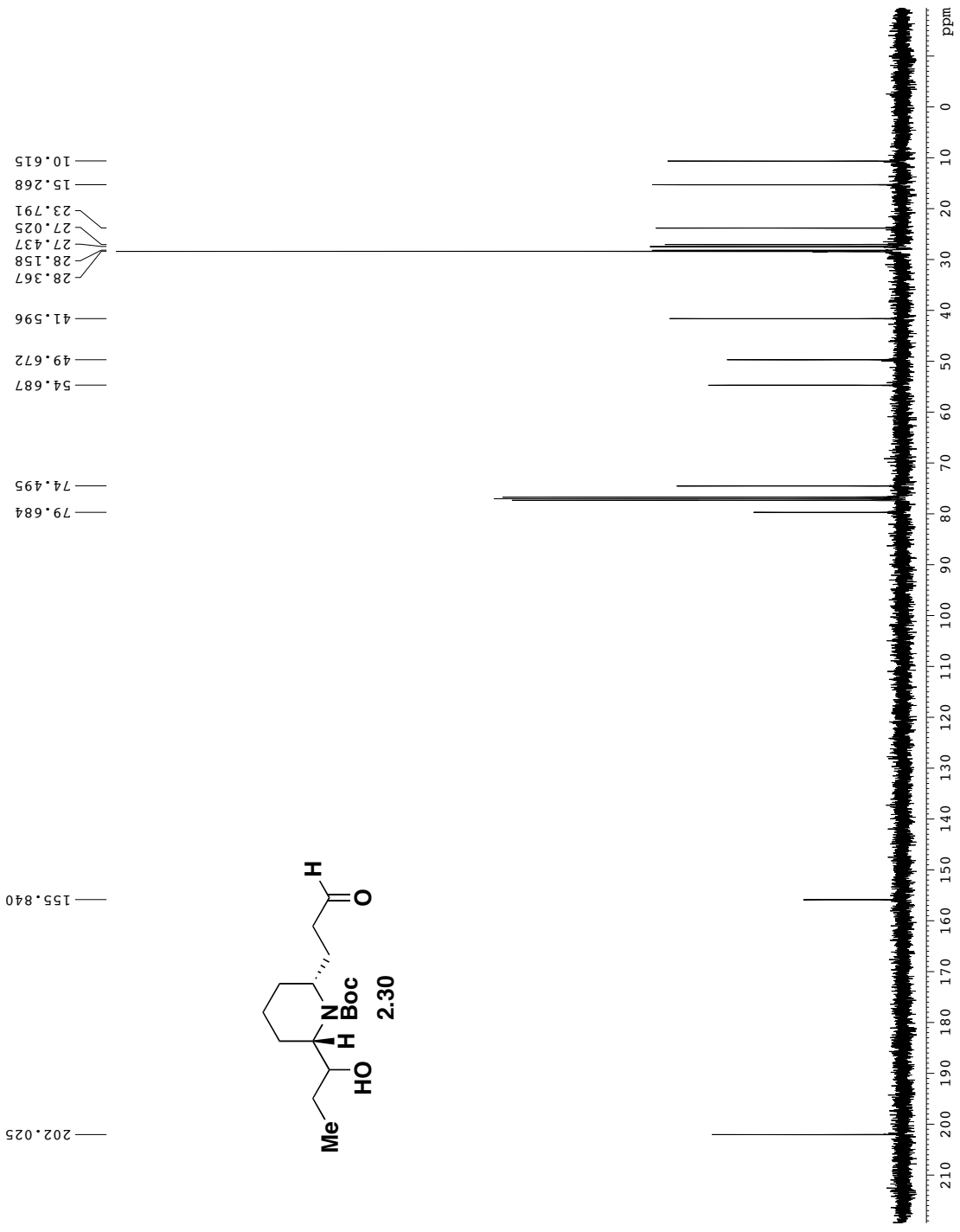
202.025
155.840
79.684
74.495
54.687
49.672
41.596
28.367
28.158
27.437
27.025
23.791
15.268
10.615
Me
HO
H
N
Boc
2.30
H
O
ppm

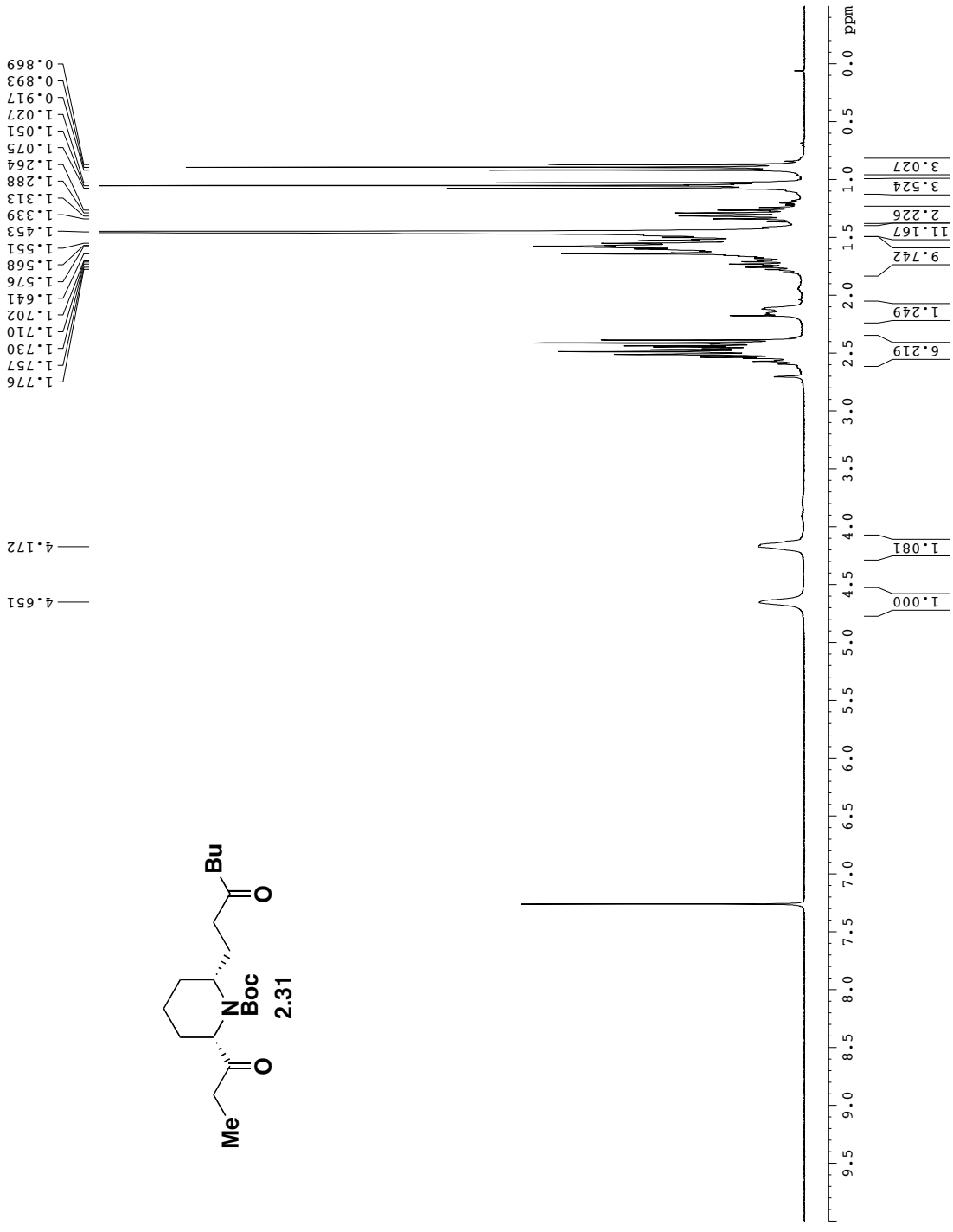
Bu
O
N
Boc
O
Me
2.31
ppm
0.0
0.5
1.0
1.5
2.0
2.5
3.0
3.5
4.0
4.5
5.0
5.5
6.0
6.5
7.0
7.5
8.0
8.5
9.0
9.5
1.000
1.081
6.219
1.249
9.742
11.167
2.226
3.524
3.027
4.651
4.172
1.776
1.757
1.730
1.710
1.702
1.641
1.576
1.568
1.551
1.453
1.339
1.313
1.288
1.264
1.075
1.051
1.027
0.917
0.893
0.869

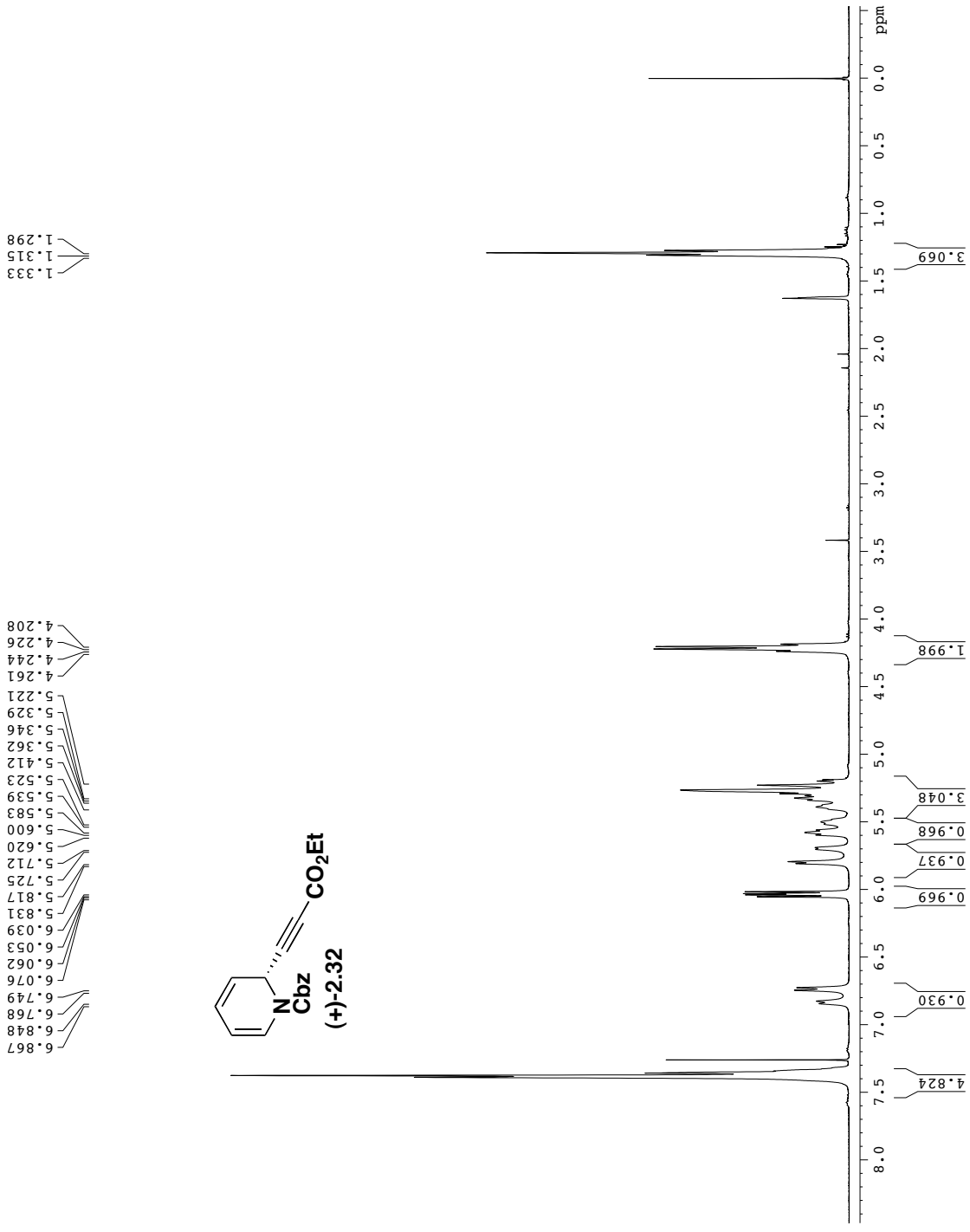
ppm
8.0
7.5
7.0
6.5
6.0
5.5
5.0
4.5
4.0
3.5
3.0
2.5
2.0
1.5
1.0
0.5
0.0
4.824
0.930
0.969
0.937
0.968
3.048
1.998
3.069
6.867
6.848
6.768
6.749
6.076
6.062
6.053
6.039
5.831
5.817
5.725
5.712
5.620
5.600
5.583
5.539
5.523
5.412
5.362
5.346
5.329
5.221
4.261
4.244
4.226
4.208
1.333
1.315
1.298
N
Cbz
CO2Et
(+)-2.32

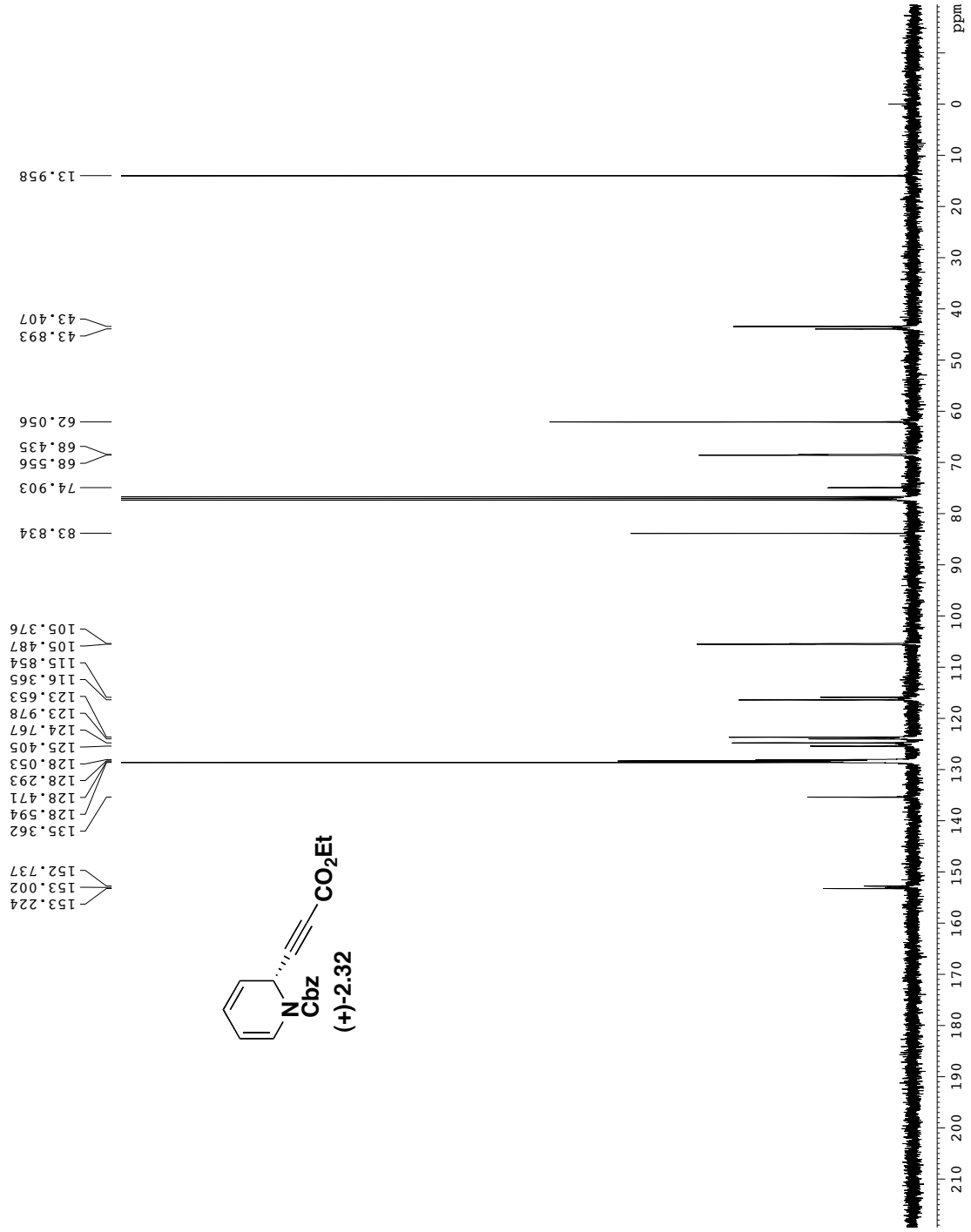
13.958
43.893
43.407
62.056
68.556
68.435
74.903
83.834
105.376
105.487
115.854
116.365
123.653
123.978
124.767
125.405
128.053
128.293
128.471
128.594
135.362
152.737
153.002
153.224
CO2Et
N
Cbz
(+)-2.32
ppm

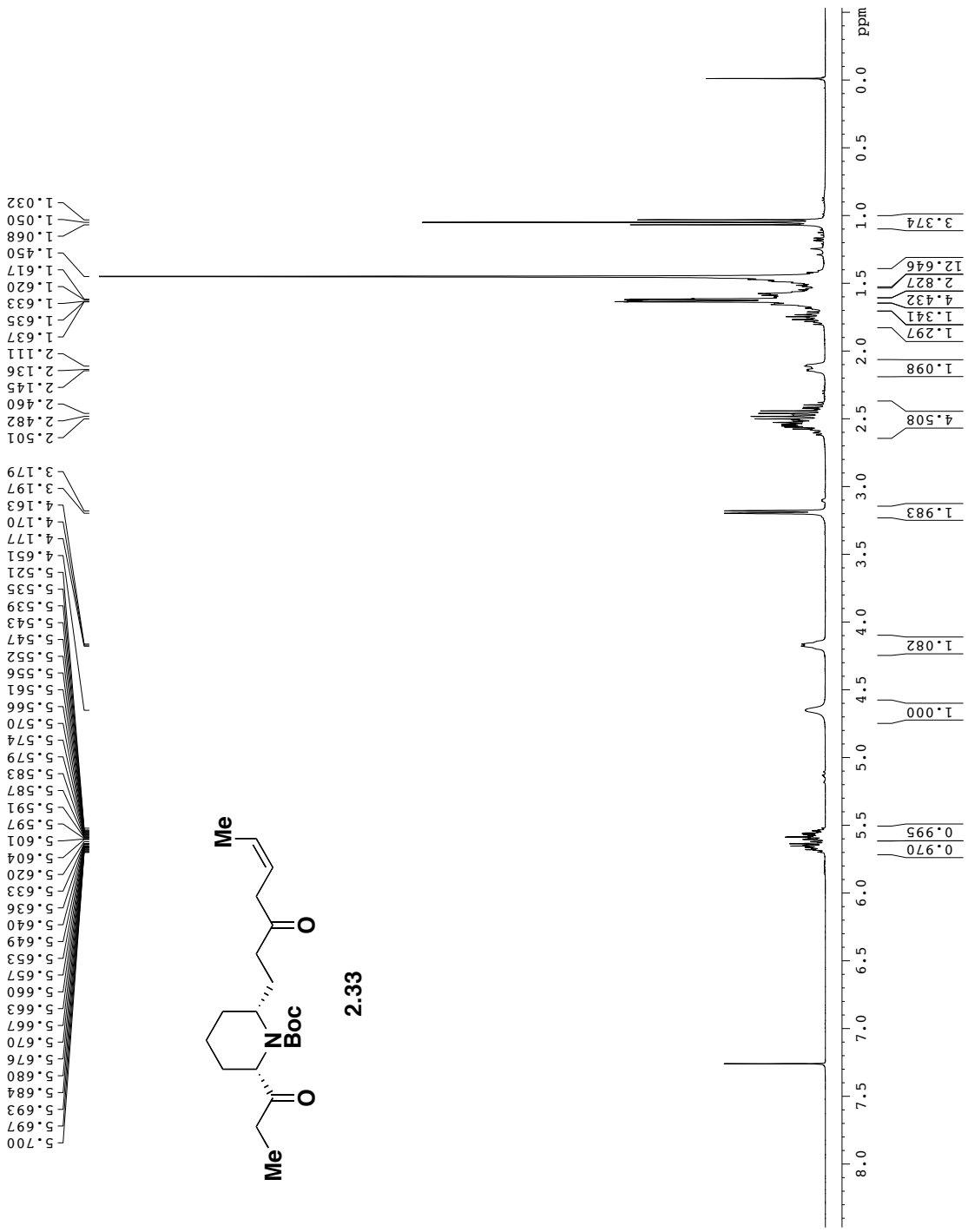
Me
O
N
Boc
O
Me
2.33
ppm
0.0
0.5
1.0
1.5
2.0
2.5
3.0
3.5
4.0
4.5
5.0
5.5
6.0
6.5
7.0
7.5
8.0
0.970
0.995
1.000
1.082
1.983
4.508
1.098
1.297
1.341
4.432
2.827
12.646
3.374
5.700
5.697
5.693
5.684
5.680
5.676
5.670
5.667
5.663
5.660
5.657
5.653
5.649
5.640
5.636
5.633
5.620
5.604
5.601
5.597
5.591
5.587
5.583
5.579
5.574
5.570
5.566
5.561
5.556
5.552
5.547
5.543
5.539
5.535
5.521
4.651
4.177
4.170
4.163
3.197
3.179
2.501
2.482
2.460
2.145
2.136
2.111
1.637
1.635
1.633
1.620
1.617
1.450
1.068
1.050
1.032

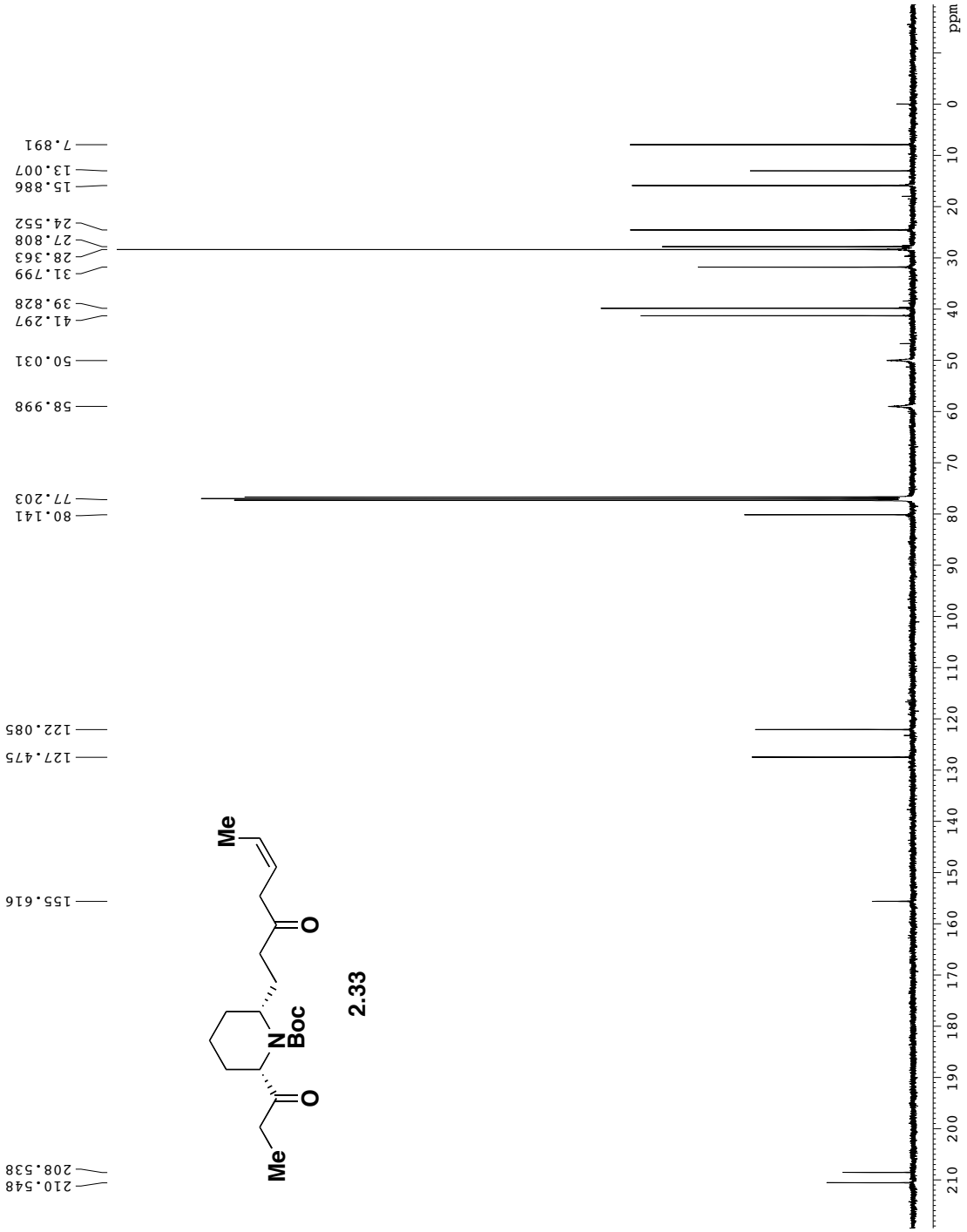
Me
O
N
Boc
O
Me
2.33
210.548
208.538
155.616
127.475
122.085
80.141
77.203
58.998
50.031
41.297
39.828
31.799
28.363
27.808
24.552
15.886
13.007
7.891
ppm

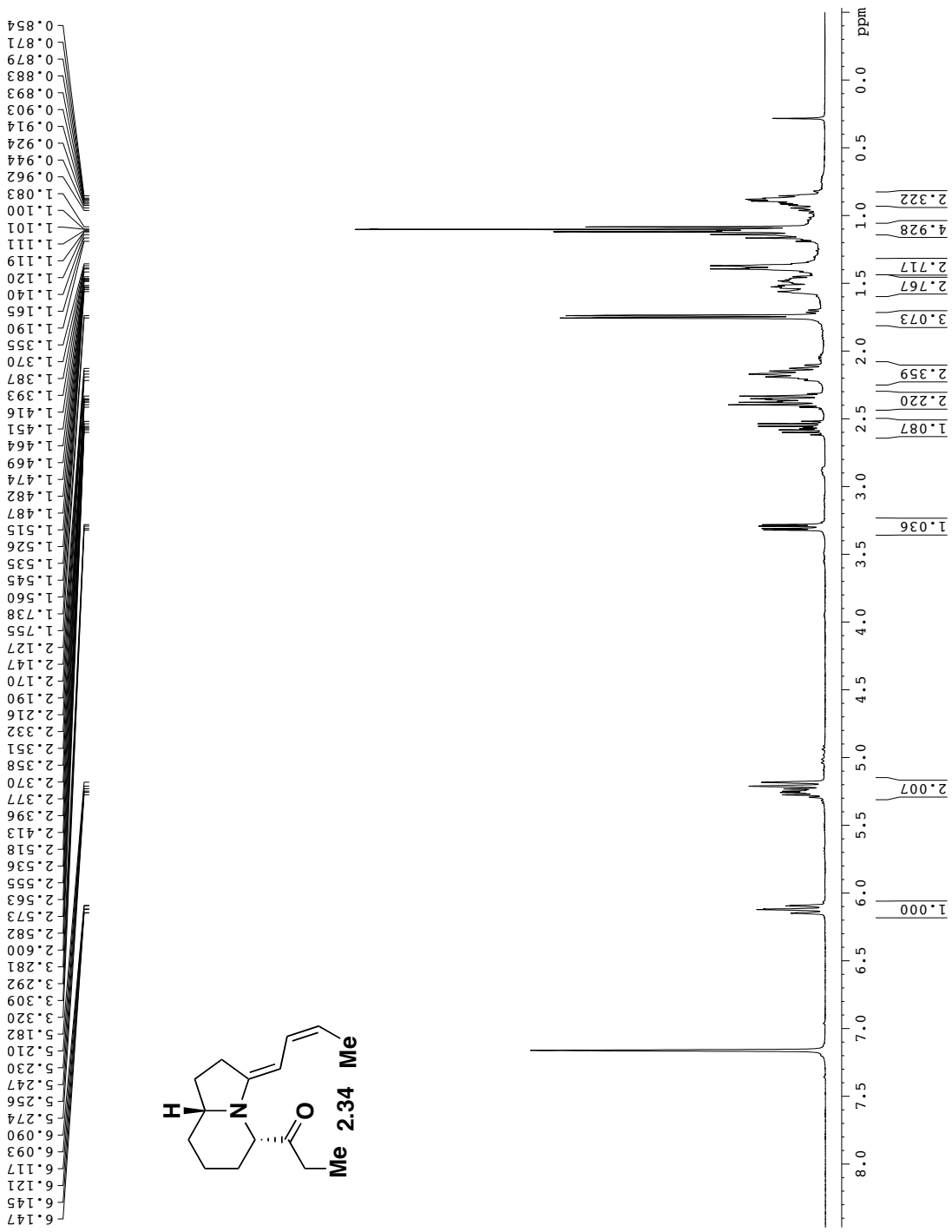
ppm
0.0
0.5
1.0
1.5
2.0
2.5
3.0
3.5
4.0
4.5
5.0
5.5
6.0
6.5
7.0
7.5
8.0
1.000
2.007
1.036
1.087
2.220
2.359
3.073
2.767
2.717
4.928
2.322
H
N
O
Me
2.34
Me

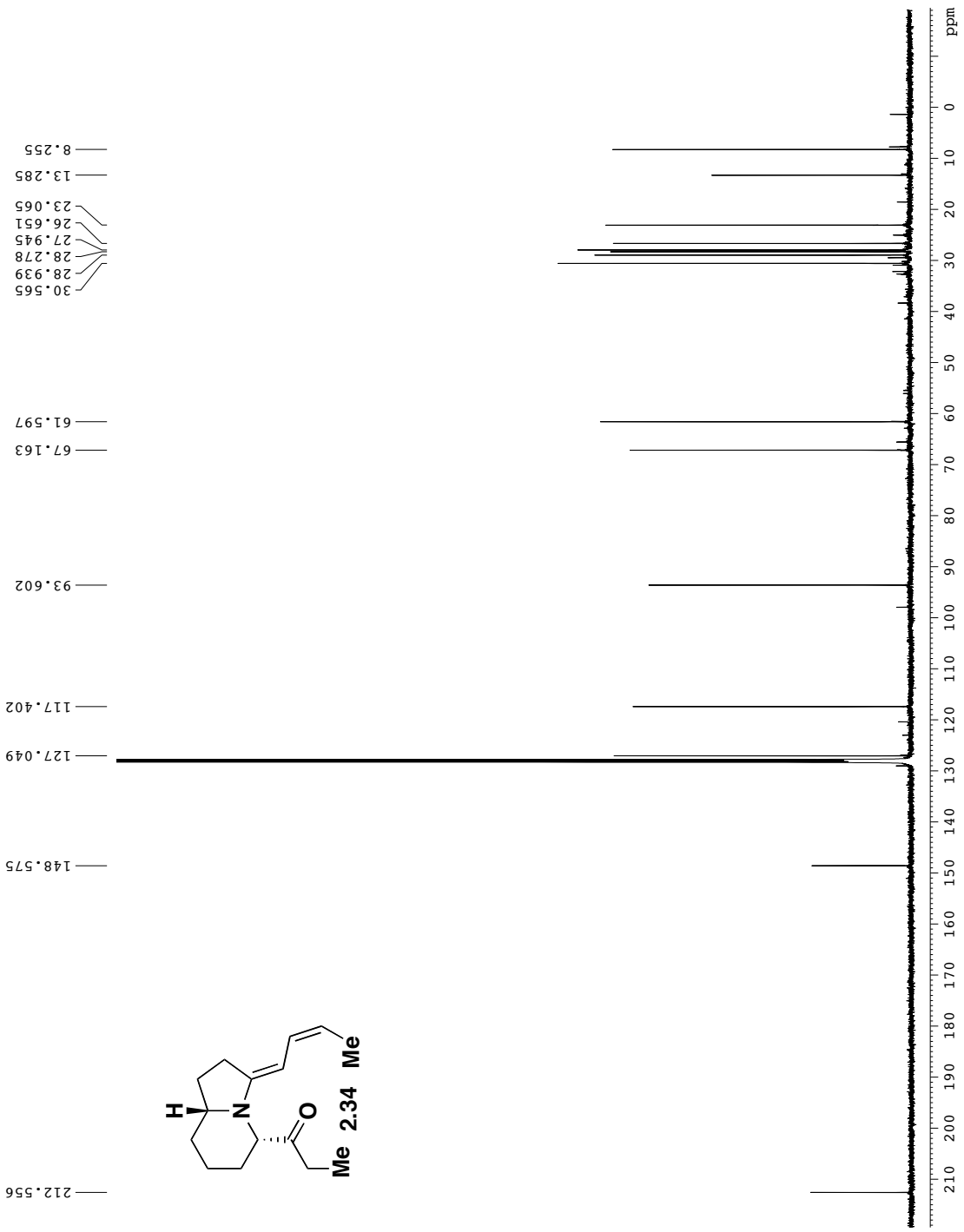
212.556
148.575
127.049
117.402
93.602
67.163
61.597
30.565
28.939
28.278
27.945
26.651
23.065
13.285
8.255
ppm
0
10
20
30
40
50
60
70
80
90
100
110
120
130
140
150
160
170
180
190
200
210
H
N
O
Me
2.34
Me

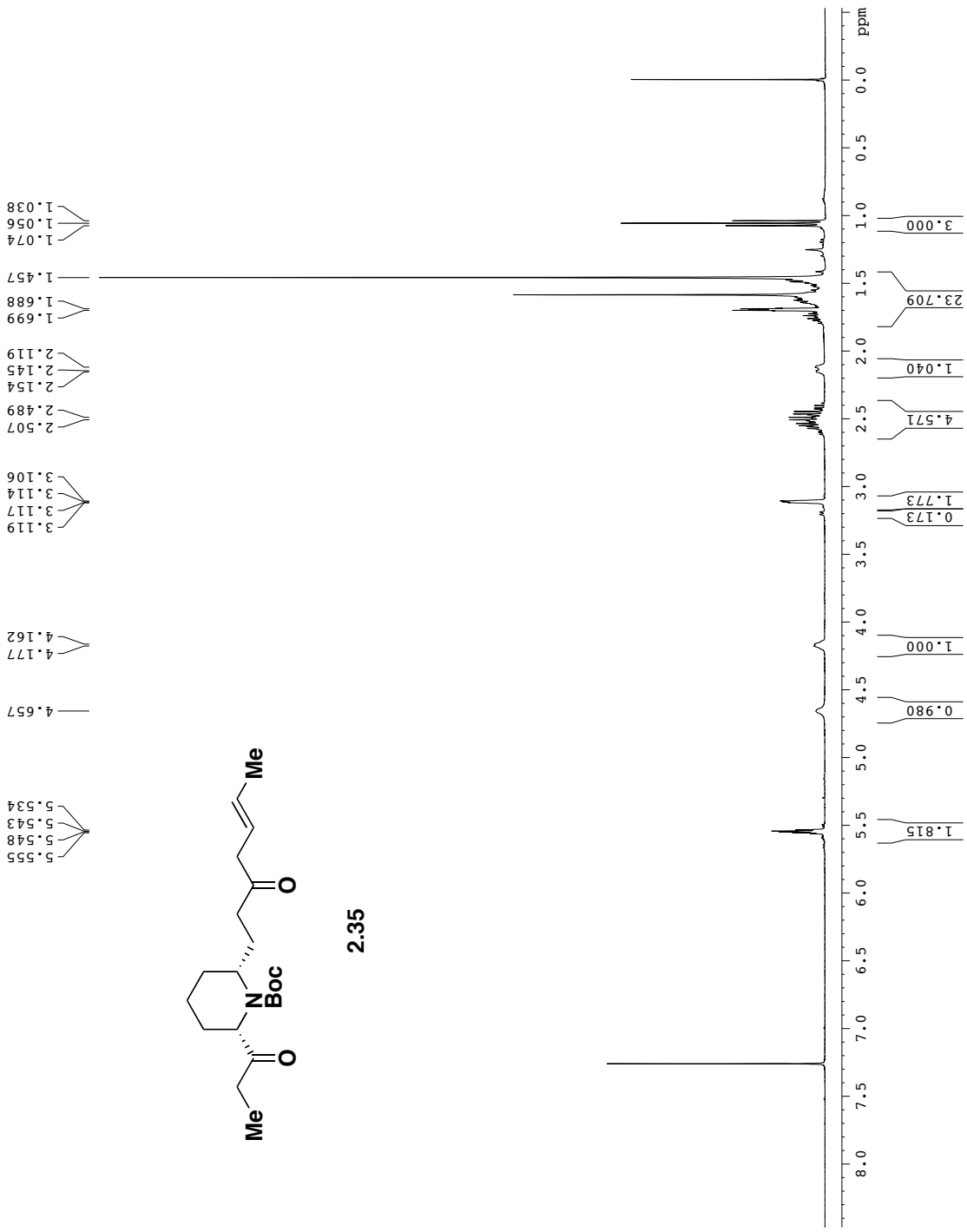
Me
O
N
Boc
O
Me
2.35
5.555
5.548
5.543
5.534
4.657
4.177
4.162
3.119
3.117
3.114
3.106
2.507
2.489
2.154
2.145
2.119
1.699
1.688
1.457
1.074
1.056
1.038
ppm
0.0
0.5
1.0
1.5
2.0
2.5
3.0
3.5
4.0
4.5
5.0
5.5
6.0
6.5
7.0
7.5
8.0
1.815
0.980
1.000
0.173
1.773
4.571
1.040
23.709
3.000

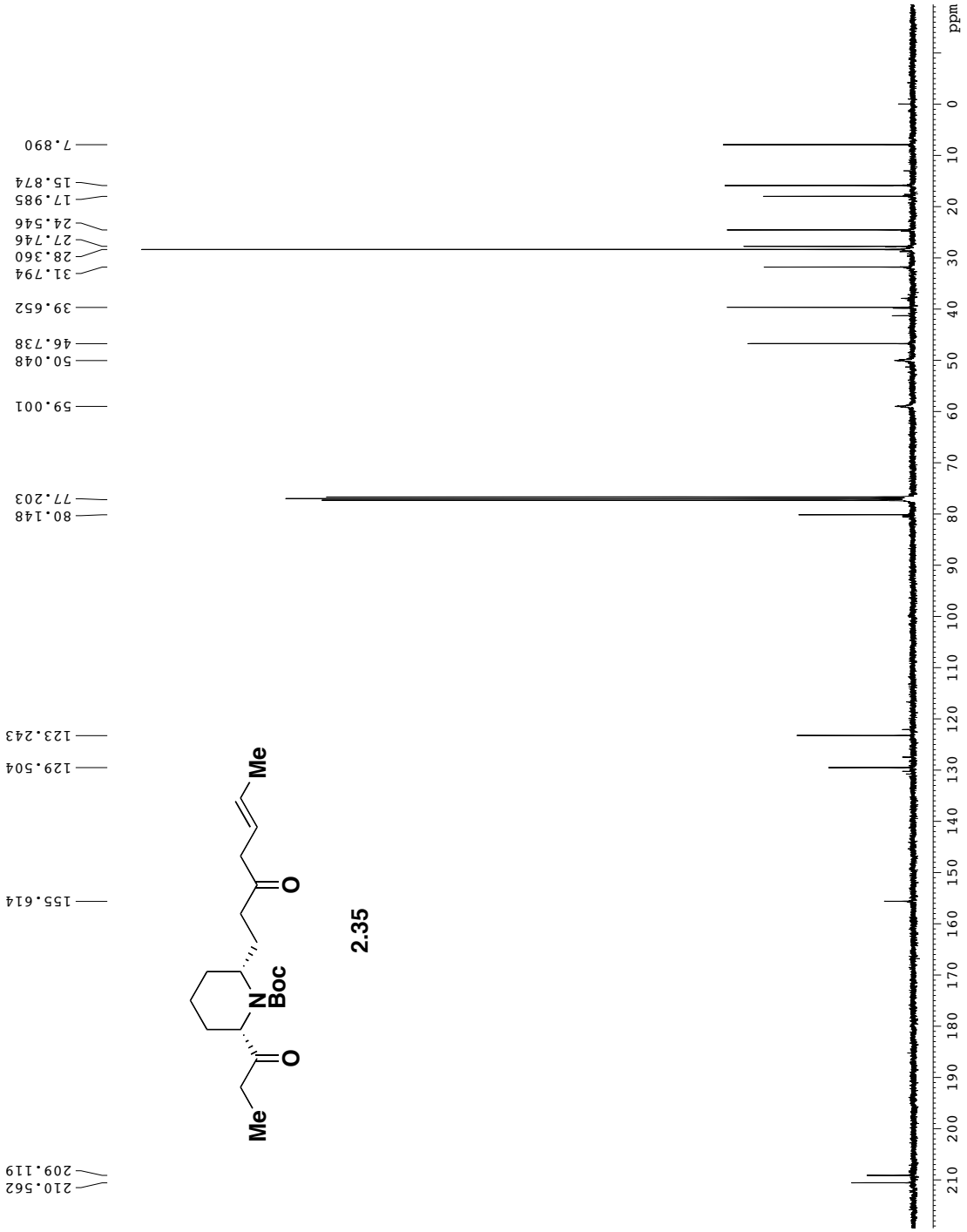
ppm
0
10
20
30
40
50
60
70
80
90
100
110
120
130
140
150
160
170
180
190
200
210
7.890
15.874
17.985
24.546
27.746
28.360
31.794
39.652
46.738
50.048
59.001
77.203
80.148
123.243
129.504
155.614
209.119
210.562
Me
O
N
Boc
O
Me
2.35

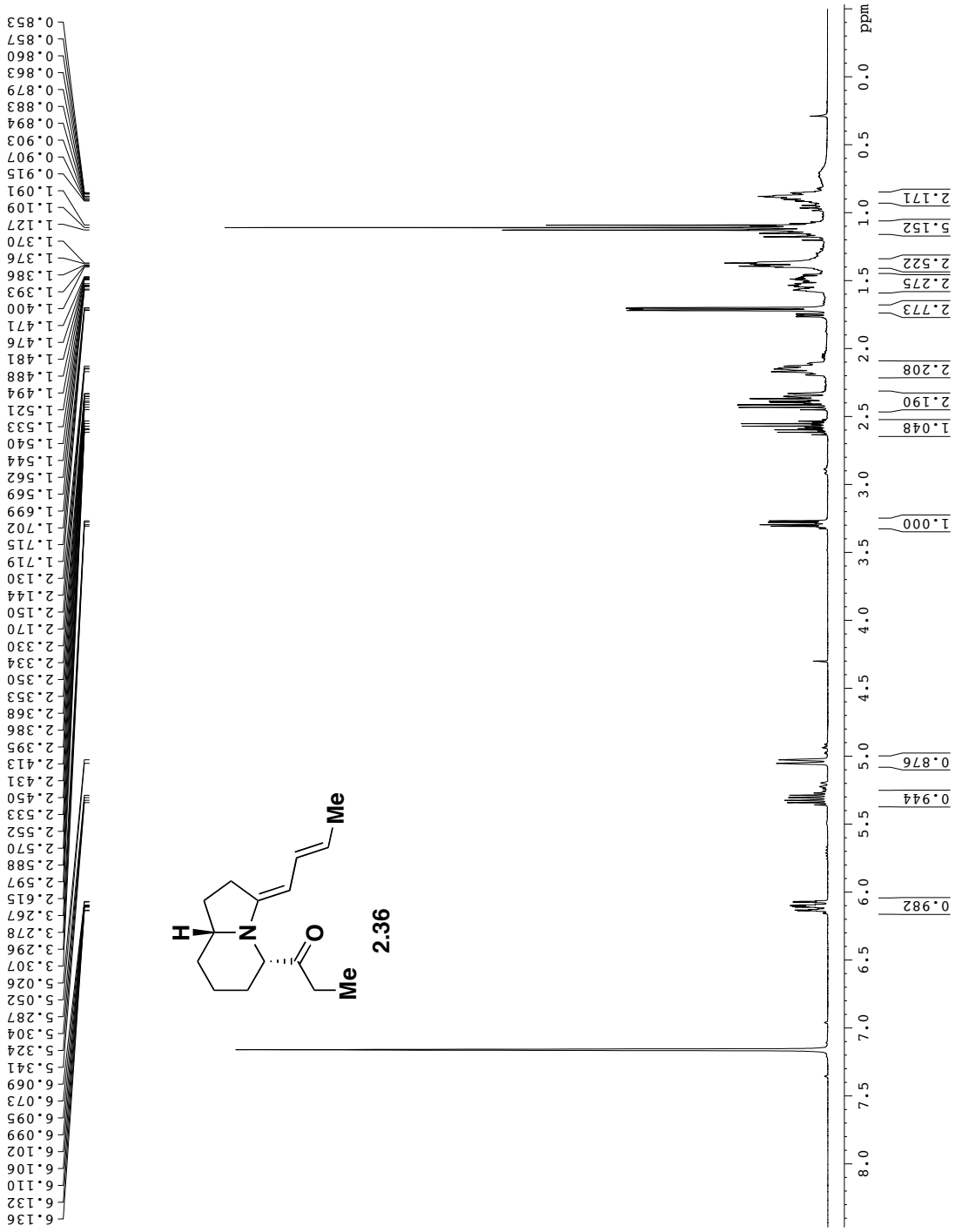
H
N
O
Me
Me
2.36
ppm
0.982
0.944
0.876
1.000
1.048
2.190
2.208
2.773
2.275
2.522
5.152
2.171

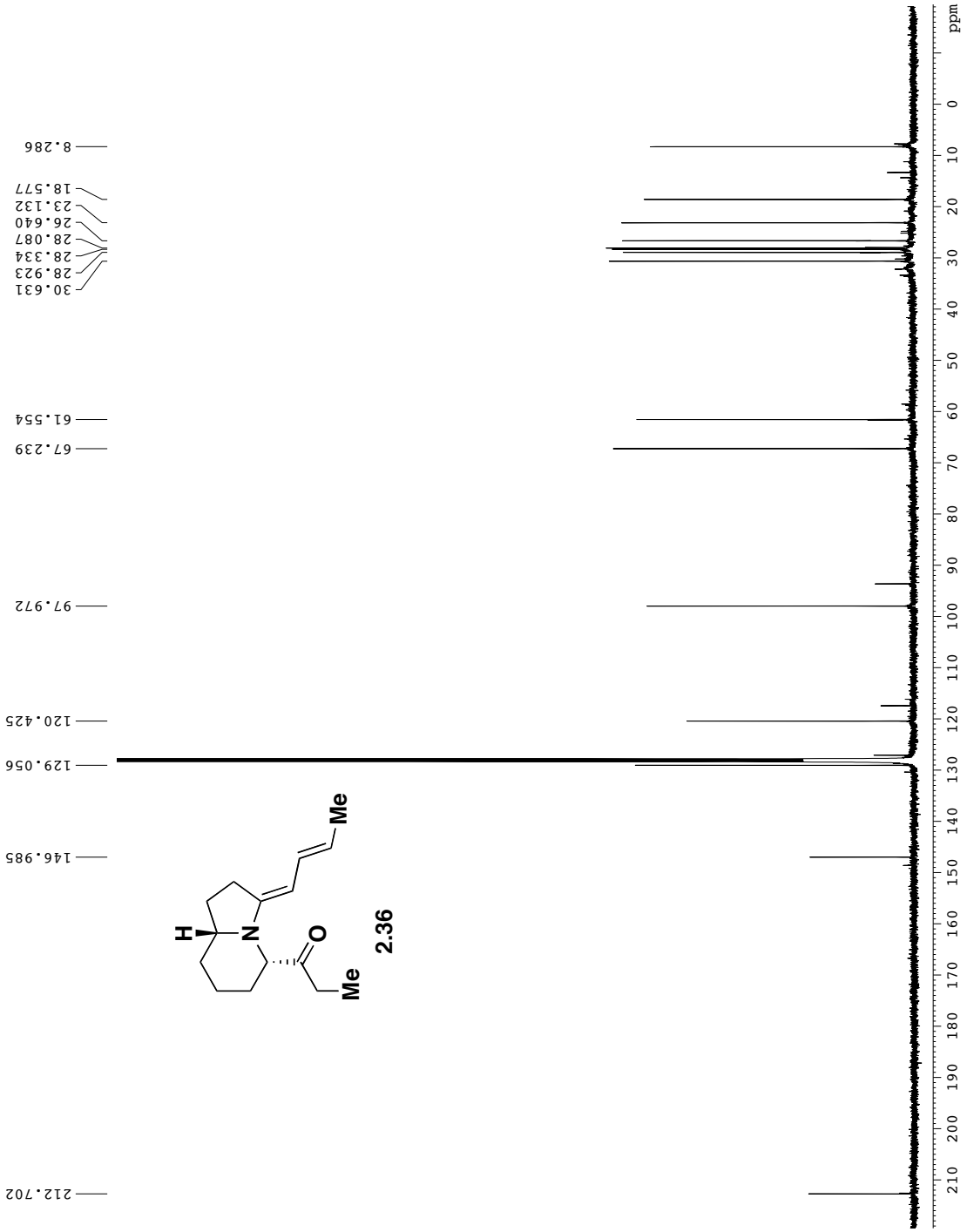
212.702
146.985
129.056
120.425
97.972
67.239
61.554
30.631
28.923
28.334
28.087
26.640
23.132
18.577
8.286
ppm
0
10
20
30
40
50
60
70
80
90
100
110
120
130
140
150
160
170
180
190
200
210
H
N
O
Me
Me
2.36

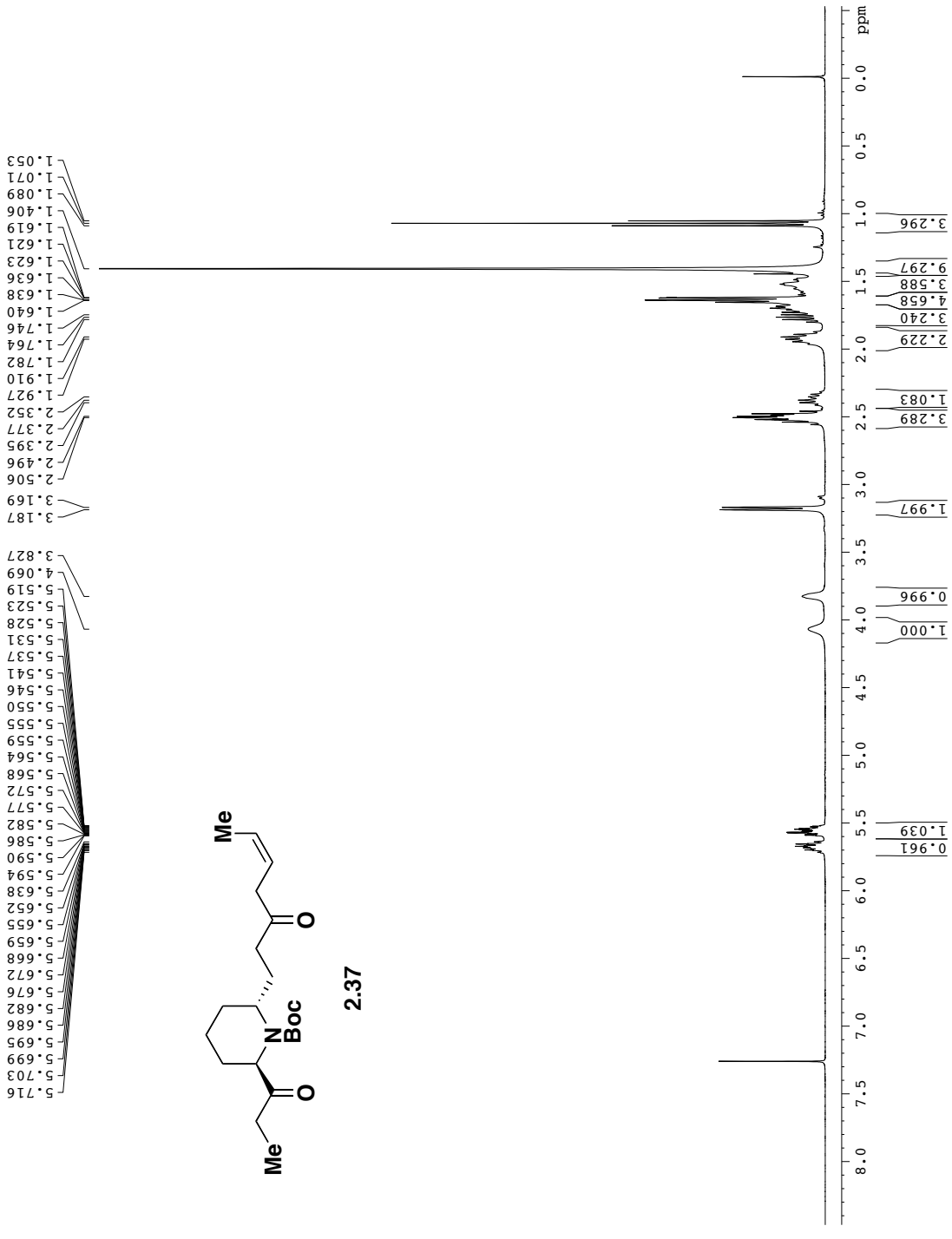
Me
O
N
Boc
O
Me
2.37
ppm
0.0
0.5
1.0
1.5
2.0
2.5
3.0
3.5
4.0
4.5
5.0
5.5
6.0
6.5
7.0
7.5
8.0
3.296
9.297
3.588
4.658
3.240
2.229
3.289
1.083
1.997
0.996
1.000
0.961
1.039

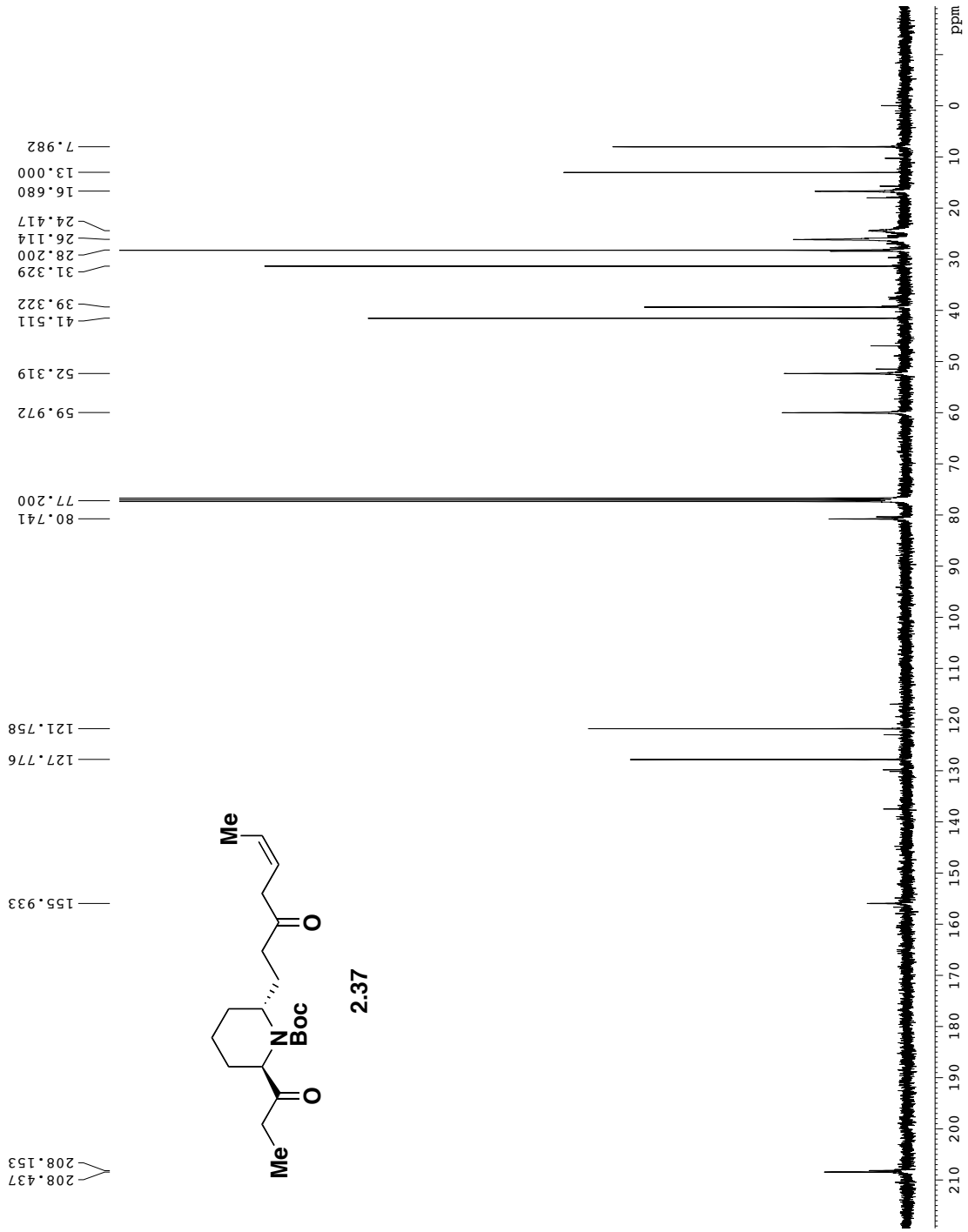
208.437
208.153
155.933
127.776
121.758
80.741
77.200
59.972
52.319
41.511
39.322
31.329
28.200
26.114
24.417
16.680
13.000
7.982
Me
O
N
Boc
O
Me
2.37
ppm

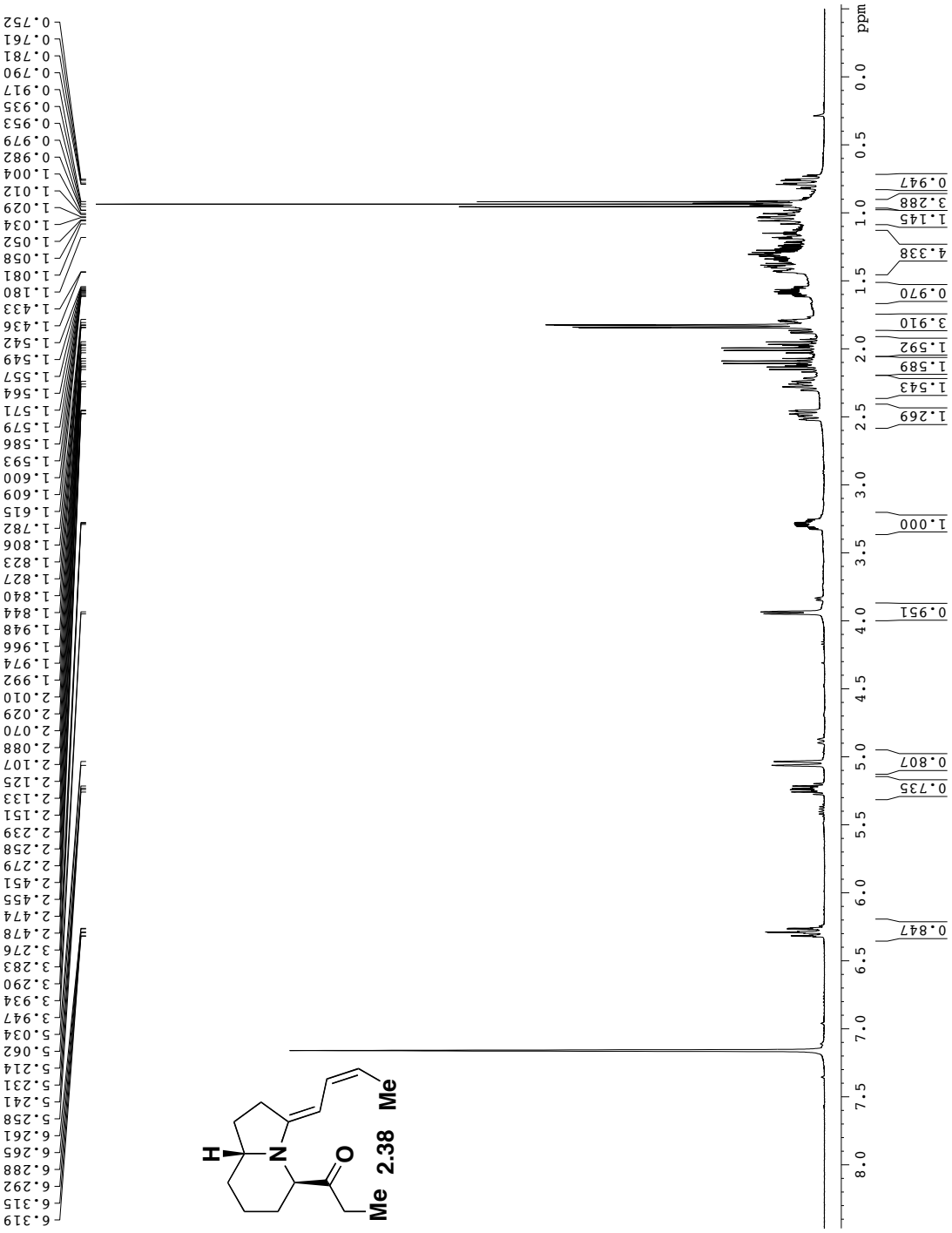
ppm
0.847
0.735
0.807
0.951
1.000
1.269
1.543
1.589
1.592
3.910
0.970
4.338
1.145
3.288
0.947
H
N
O
Me
2.38
Me

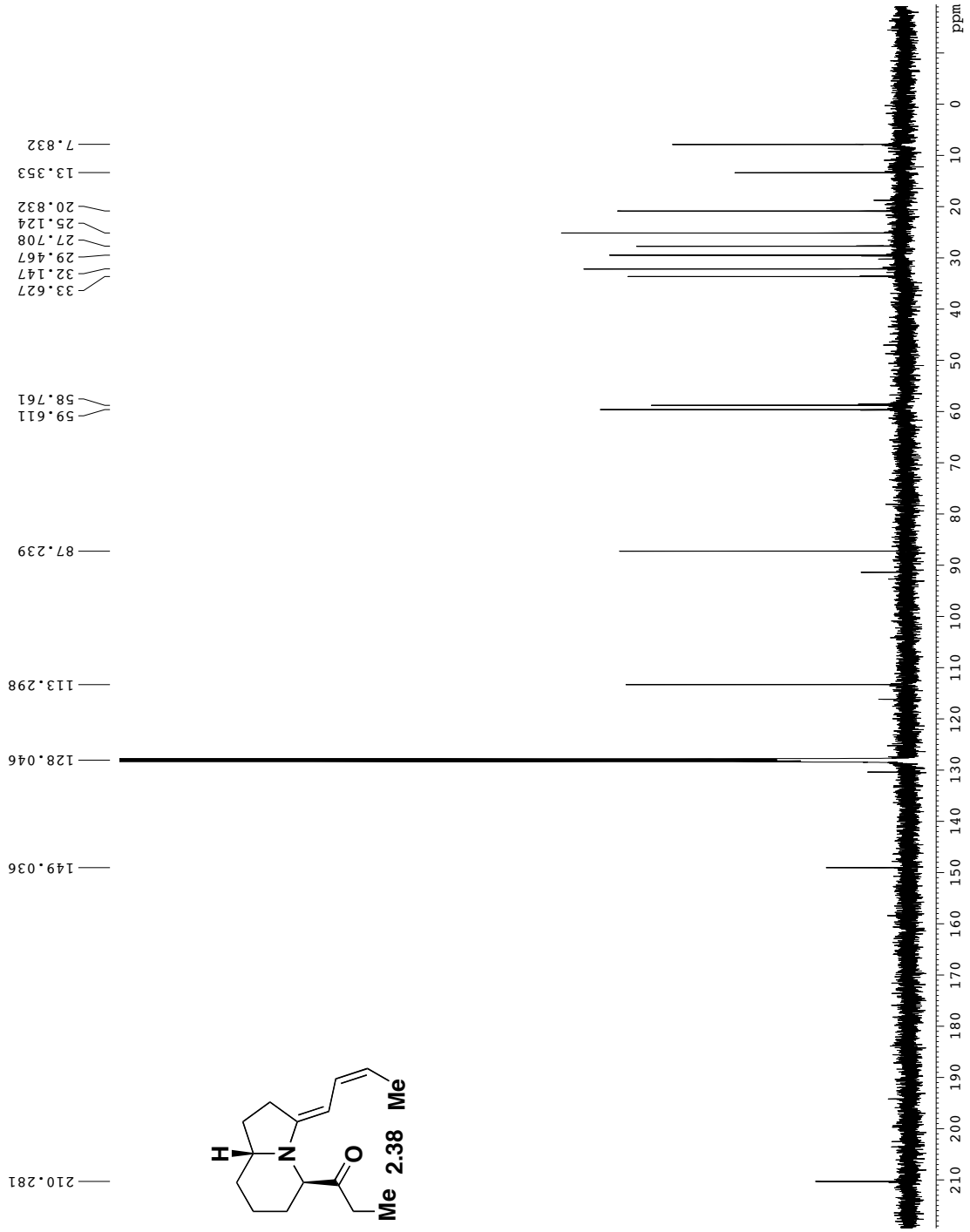
210.281
149.036
128.046
113.298
87.239
59.611
58.761
33.627
32.147
29.467
27.708
25.124
20.832
13.353
7.832
ppm
0
10
20
30
40
50
60
70
80
90
100
110
120
130
140
150
160
170
180
190
200
210
H
N
O
Me
2.38
Me

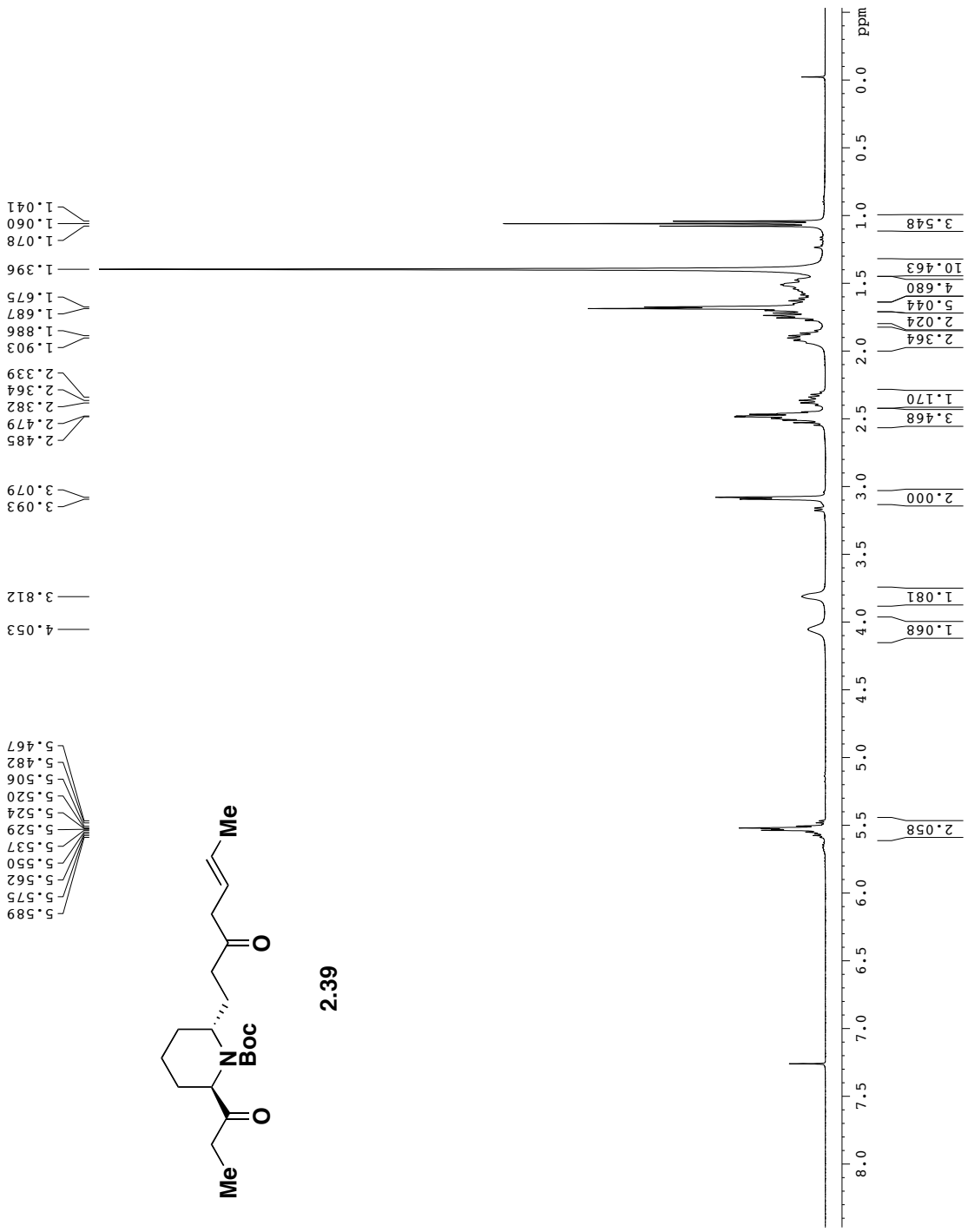
Me
O
N
Boc
O
Me
2.39
ppm
0.0
0.5
1.0
1.5
2.0
2.5
3.0
3.5
4.0
4.5
5.0
5.5
6.0
6.5
7.0
7.5
8.0
3.548
10.463
4.680
5.044
2.024
2.364
1.170
3.468
2.000
1.081
1.068
2.058
1.396
1.041
1.060
1.078
1.675
1.687
1.886
1.903
2.339
2.364
2.382
2.479
2.485
3.079
3.093
3.812
4.053
5.467
5.482
5.506
5.520
5.524
5.529
5.537
5.550
5.562
5.575
5.589

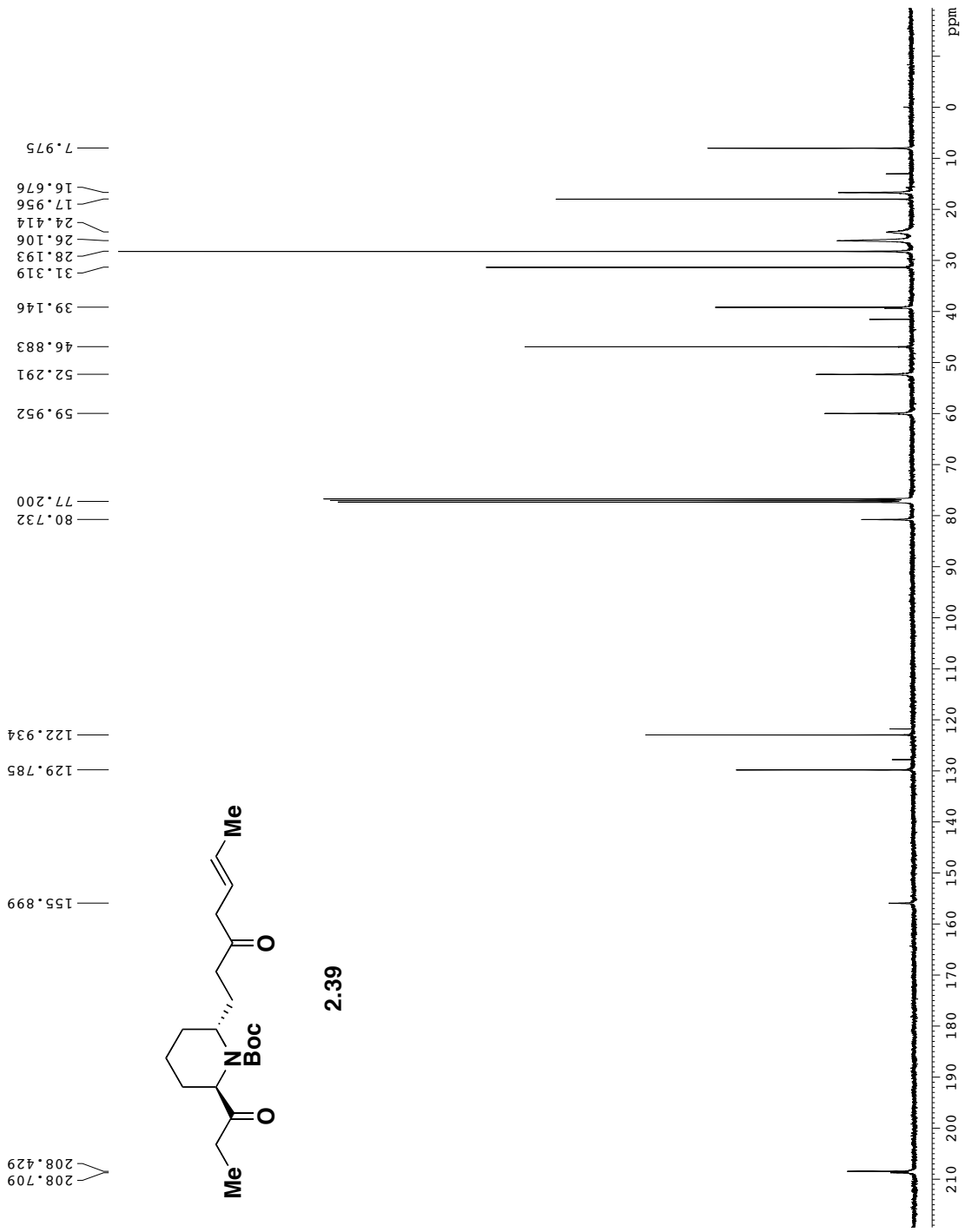
208.709
208.429
155.899
129.785
122.934
80.732
77.200
59.952
52.291
46.883
39.146
31.319
28.193
26.106
24.414
17.956
16.676
7.975
Me
N
Boc
O
O
Me
2.39
ppm

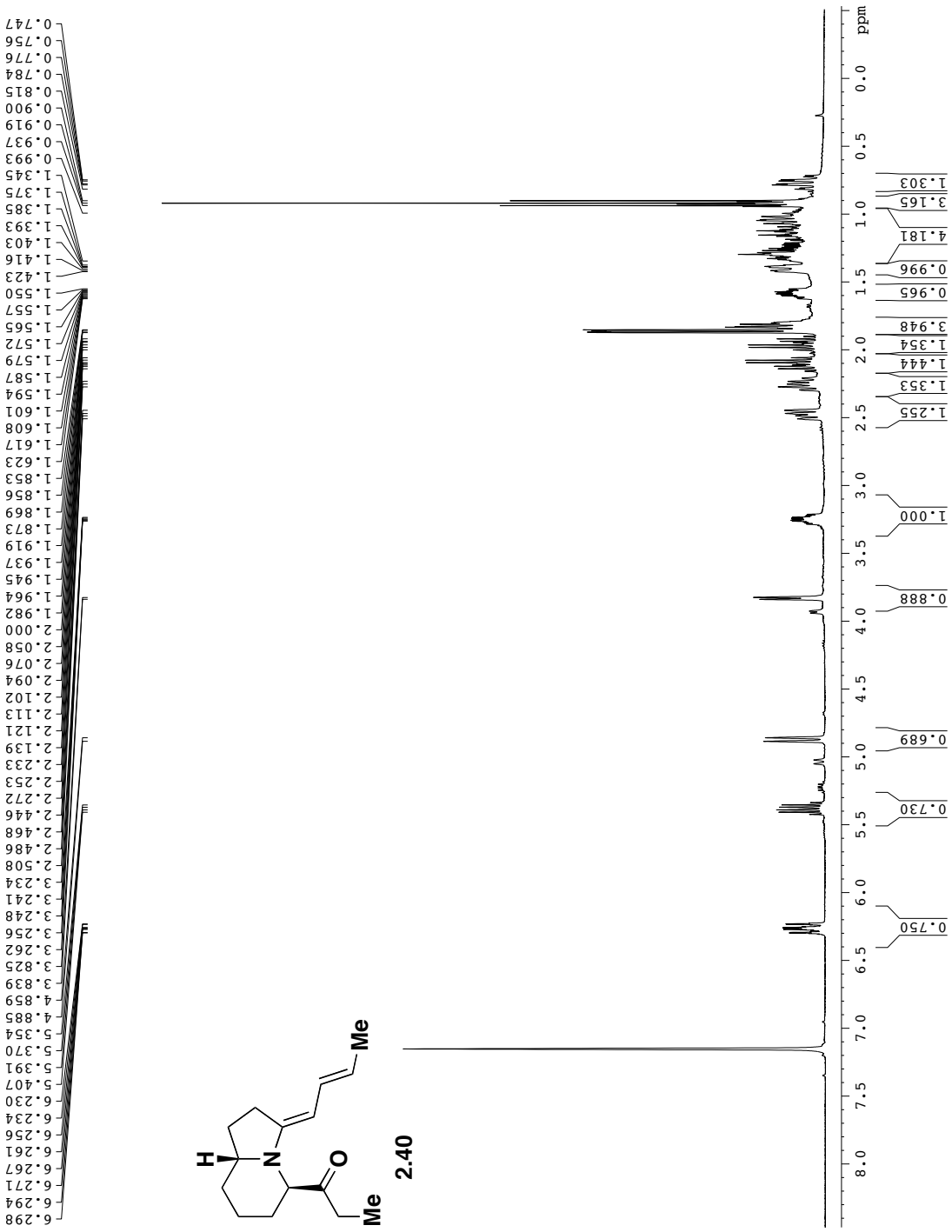
Me
H
N
O
Me
2.40
ppm
0.750
0.730
0.689
0.888
1.000
1.255
1.353
1.444
1.354
3.948
0.965
0.996
4.181
3.165
1.303

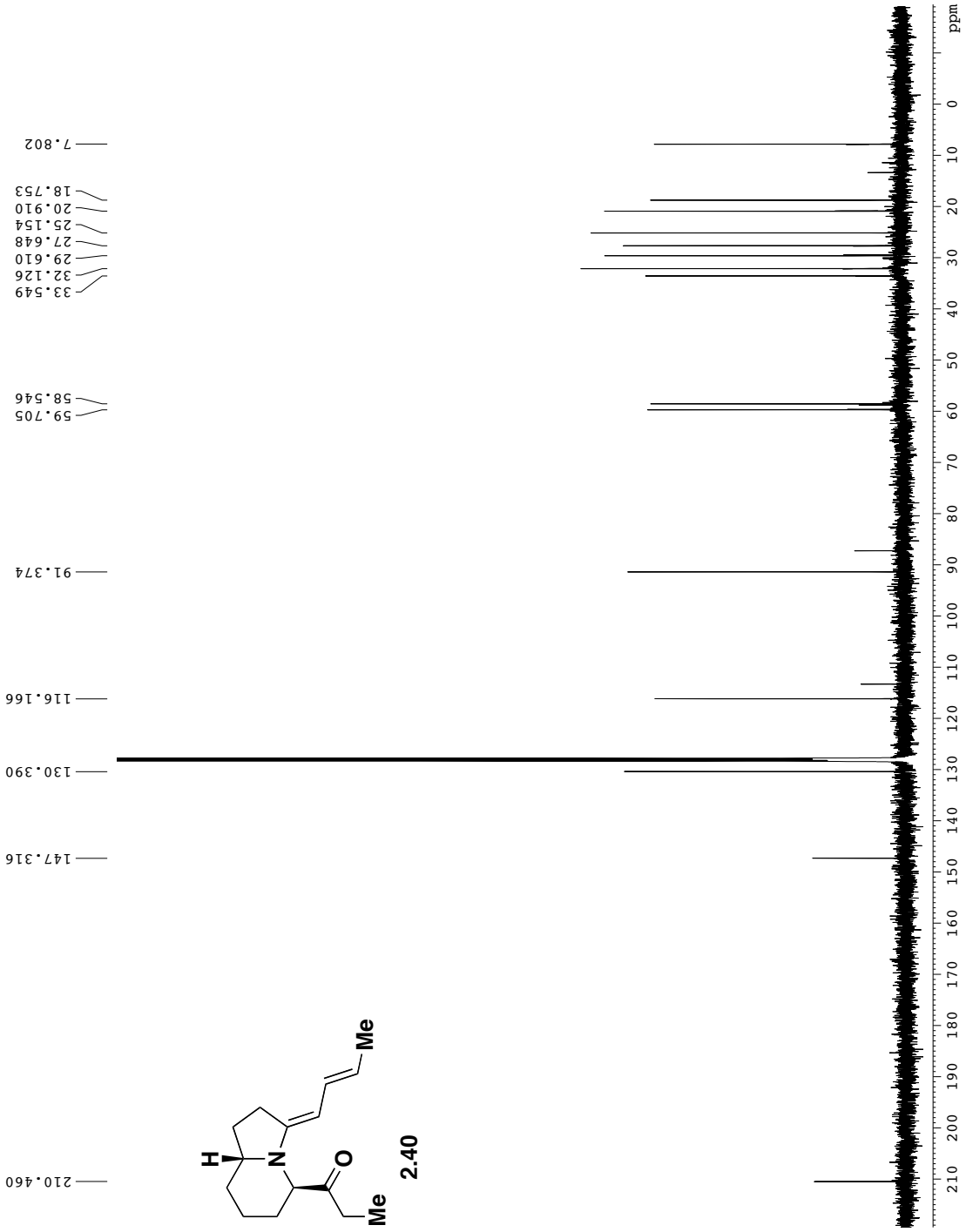
7.802
18.753
20.910
25.154
27.648
29.610
32.126
33.549
58.546
59.705
91.374
116.166
130.390
147.316
210.460
Me
H
N
O
Me
2.40
ppm

CHAPTER 3

Dimerization Studies Toward the Synthesis of Myrmicarin 430A

3.1 Initial Efforts to Effect a Direct, Biomimetic Dimerization

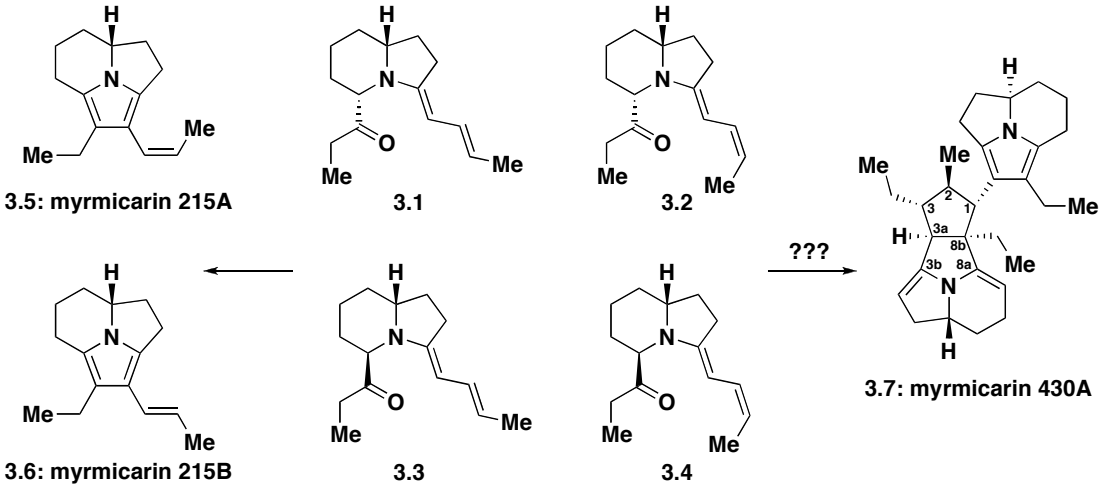

Figure 3.1 Dienamines **3.1**–**3.4** as synthetic precursors to the tricyclic myrmicarins **3.5** and **3.6** and proposed precursors for dimerization to myrmicarin 430A.

Inspired by the ease with which dienamines **3.1** and **3.2** (Figure 3.1) underwent cyclization in protic solvents to afford myrmicarins 215A (**3.5**) and B (**3.6**) (*vide supra*, Section 2.3), respectively, we similarly hoped that biomimetic conditions could be identified to directly afford myrmicarin 430A (**3.7**) from the same types of starting materials, i.e. **3.1**–**3.4**. Here, we anticipated that the increased basicity of the dienamines relative to myrmicarin 215B (**3.6**) would allow for milder conditions for dimerization. In this vein, dienamines **3.1**–**3.4** were dissolved in aqueous buffers of pH 4.5, 7.0, and 8.6. Unfortunately, these experiments only led to various degrees of alkene isomerization and/or cyclization to myrmicarin 215-type structures, highlighting the potential of such intermediates to be biomimetic precursors to the tricyclic myrmicarins.

Our strategy thus shifted to treatment of each of our dienamines with protic acid sources, such as acetic, chloroacetic, and trichloroacetic acid. Unfortunately, these experiments only afforded alkene isomerization products, regardless of the solvent used. These results were quite intriguing, given that the mechanistic pathway outlined in Figure

3.2 required to isomerize the olefin likely involved protonation at the γ-position followed by bond rotation and subsequent loss of proton. Thus, we hypothesized that the desired extended iminium **3.8**[1] was likely an intermediate en route to isomerization but either was not present in sufficient concentration to undergo dimerization or was not a competent electrophile for the dienamine. In order to address this issue, *in situ* NMR studies of these reactions were undertaken. In all cases, these experiments only indicated the presence of the alkene isomers with no traces of protonated products detectable at ambient temperature, suggesting the desired iminium ion was a fleeting intermediate under these conditions and did not build up to any appreciable extent. Furthermore, increasing the concentration of either the starting material or the acid source did not alter the reaction outcome.

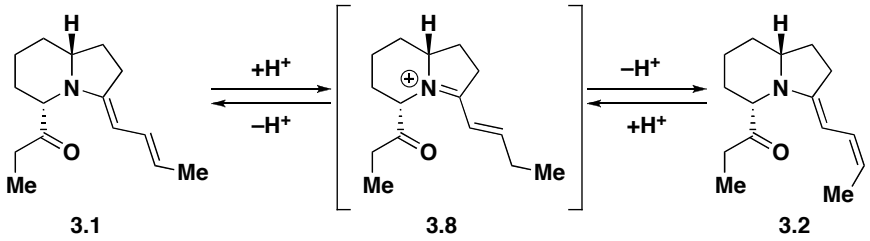

Figure 3.2 Acid catalyzed alkene isomerization of dienamine **3.1**.

3.2 A Controlled, Stepwise Dimerization Approach

Our inability to isolate or detect any traces of dimeric materials from our biomimetic dimerization studies led us to pursue a controlled, even if stepwise, approach toward myrmicarin 430A (**3.7**). Here, we were confident we could take advantage of the discovery that the choice of solvent could both prevent and promote cyclodehydration of dienamines **3.1**–**3.4**. Unfortunately, as alluded to in Chapter 2, at the outset of our work, it was unclear which combination of C5 epimers and alkene isomers would give rise to

the desired stereochemistry during C2—C3 bond (myrmicarin 430A numbering) formation during dimerization. Therefore, we required a method to generate our electrophilic species prior to addition of a nucleophile for a controlled homo- and/or heterodimerization to take place. In particular, we envisioned that γ-selective stoichiometric protonation of the dienamine could allow for introduction of a subsequent nucleophile. Once again, we hoped to take advantage of the increased basicity of the dienamine moiety relative to the myrmicarin vinyl pyrrole[2] to produce a stable

Table 3.1 Effect of acid source on regioselectivity of dienamine protonation.

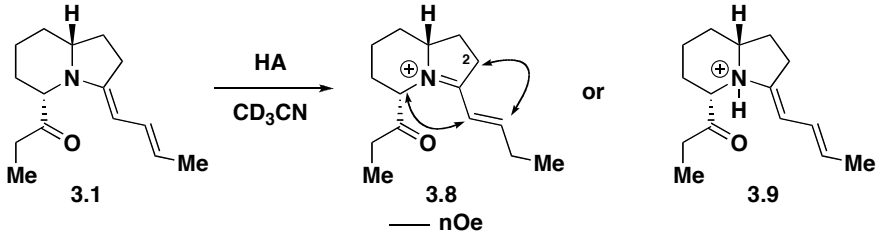

acid	pKa	result
CH_3CO_2H	4.75	alkene isomerization
$ClCH_2CO_2H$	2.81	alkene isomerization
Cl_2CHCO_2H	1.30	alkene isomerization
CF_3CO_2H	–0.26	**3.8** exclusively
$MeSO_3H$	–0.60	**3.9** exclusively

intermediate to allow for such reactivity. Although our previous studies outlined in Section 3.1 did not provide evidence of the desired iminium intermediates as stable species, we remained confident that a protic acid source could be identified that would be capable of delivering the desired electrophilic species and facilitating dimerization. Indeed, circumstantial evidence from low-resolution mass spectral analysis of these dienamines using APCI in the positive ionization mode consistently showed large peaks indicating the presence of dimeric species.

We began by adding a solution of dienamine **3.1** to a stoichiometric amount of a series of protic acids in MeCN-d_3 and monitoring the mixture by NMR. Our results revealed an interesting trend that appeared to be pK_a dependent (see Table 3.1). While weaker acids ($pK_a > 1.0$) only led to alkene isomerization, much stronger acids, such as CH_3SO_3H, led exclusively to nitrogen protonated compound **3.9** with no sign of alkene isomerization. When TFA was used, however, a completely regioselective and quantitative γ-protonation of the dienamine occurred, resulting in extended iminium **3.8**. This method proved general to all four dienamine diastereomers **3.1**–**3.4**. Furthermore, these salts were found to be stable for at least 1 day in deuterated acetonitrile at –20 °C without any detectable level of decomposition.

At this juncture, we undertook 2D-NOESY studies of iminium **3.8** in hopes of obtaining a detailed picture of its solution-state conformation. Key correlations depicted on the structure in Table 3.1 revealed that **3.8** exists essentially as drawn with an *E* alkene and the iminium arranged in an *s*-trans configuration. These results were propitious, as this electrophile occupied the opposite conformation of the presumed *Z*-azafulvenium, and thus approach of a nucleophile from the top face (with respect to our typical depiction) would deliver the desired stereochemistry at C3 as indicated in Figure 3.3. Our attention now turned to achieving dimerizations, the highlights of which are presented in Scheme 3.1. In our first experiments, enantioenriched dienamine **3.1** [the use of racemic material gave rise to substantial amounts of products from (*R*) + (*S*) dimerizations] was added to 0.5 equivalents of TFA in MeCN-d_3 at room temperature, and the reaction was monitored by ^{1}H NMR. Although the reaction mixture appeared quite complex, after 30 minutes at ambient temperature, all **3.8** had been consumed. The reaction was thus

quenched with cold, aqueous NaOH. Crude NMR analysis of this mixture showed alkene signals that suggested the presence of a new product that was tentatively assigned as **3.13**. This crude mixture was, however, quite complex, presumably due to the potential presence of diastereomers about the C2—C3 bond as well as ethyl ketone epimers in each

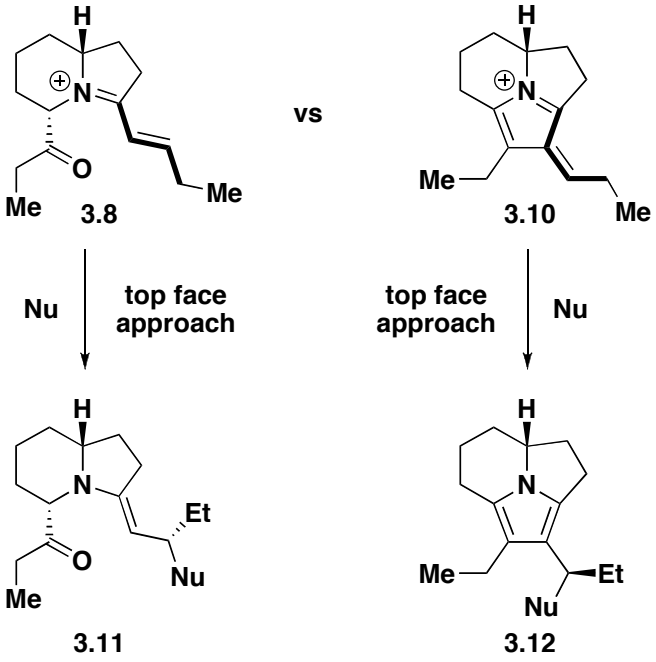

Figure 3.3 Predicted stereochemical outcome of nucleophilic addition to iminium **3.8** and azafulvenium **3.10**.

component of the proposed dimeric material. In addition, the presence of C1—C2 alkene stereoisomers was also possible. Thus, we rationalized that cyclodehydration of the crude reaction mixture could allow the convergence of any C5 epimers within the mixture to the same cyclodehydrated product. In practice, this proved a reliable method, and dissolution of the crude mixture in thoroughly degassed methanol at room temperature for 3 hours effected complete cyclodehydration by ^{1}H-NMR analysis. Subsequent

purification of this reaction mixture over neutral alumina afforded hexacycle **3.14** as an inseparable 2:1 mixture of diastereomers based on integration of the resolved resonances at δ = 3.60 and 3.56. 2D-NOESY experiments on the mixture revealed that both diastereomers observed correlations from the above resolved resonances to the single

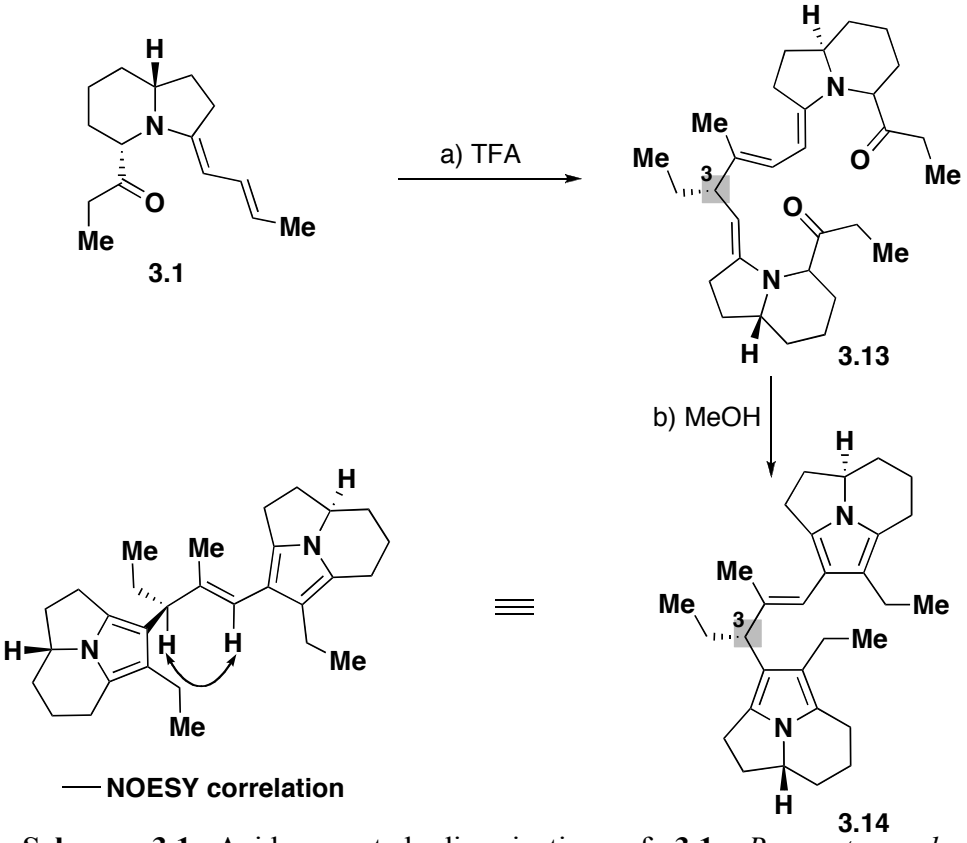

Scheme 3.1 Acid-promoted dimerization of **3.1**. *Reagents and Conditions:* a) TFA (0.5 equiv.), MeCN, r.t., 30 min.; b) degassed MeOH, r.t., 3 h (2:1 d.r., 54% over 2 steps). TFA = trifluoroacetic acid.

alkene resonance at δ = 6.67, suggesting that these compounds were diastereomeric at C3 and occupy an $A_{1,3}$-minimized structure as shown in Scheme 3.1. The minor component of this mixture was assigned as C3-*epi*-**3.14** in accordance with the data reported by Movassaghi and Ondrus,[3] and this product is consistent with nucleophilic attack from the concave face of the electrophile. The major component, however, was assigned as

hexacycle **3.14**, and for the first time, a dimerization that afforded the desired stereochemistry at C3 was achieved.

Table 3.2 Optimization of reaction conditions for the dimerization of dienamines **3.1**–**3.4**.

Electrophile	Nucleophile	Solvent	*T* (°C)	d.r.[a]
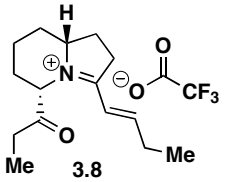 **3.8**	**3.1**	MeCN	23	2:1
	3.2	MeCN	23	1:1.2
	3.3	MeCN	23	1.3:1
	3.4	MeCN	23	1:1
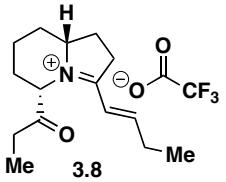 **3.8**	**3.1**	MeCN	0	2:1
	3.1	MeCN	–20 → 0	2:1
	3.1	DMF	23	1:1
	3.1	DMSO	23	2:1
	3.1	$MeNO_2$	23	2:1
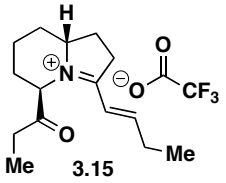 **3.15**	**3.1**	MeCN	23	1:1.5
	3.3	MeCN	23	1:1.2
	3.4	MeCN	23	1:1.2

[a] All diastereomeric ratios (d.r.) were determined after basic workup followed by bis-cyclodehydration in MeOH and are expressed as the ratio of hexacycle **3.14** to its C3b ethyl group epimer.

Pleased with the ability to not only achieve dimerizations but also access the desired C3 stereochemistry, we began optimizations and explorations directed at improving the diastereomeric ratio at C3 during these dimerizations. The results of these studies are summarized in Table 3.2. First, the d.r. of the reaction appeared to be temperature independent, as dimerizations performed at 0 °C and 23 °C gave identical results. Furthermore, the solvent used in the reaction had little effect on the observed ratio, with MeCN, DMSO, and $MeNO_2$ affording essentially identical results, and thus subsequent experiments were performed in MeCN. Here, we note that non-polar solvents

such as benzene and CH_2Cl_2 were not explored due to their inability to cleanly afford the desired iminium ions; addition of the dienamines to TFA in these solvents led to extensive decomposition with only traces of the desired iminium observed. Thus, our next approach was to examine the effect of the alkene geometry of the nucleophile used during the dimerization. When *cis*-alkene **3.2** was introduced to electrophile **3.8**, a 1:1.2 ratio of **3.14**:C3-*epi*-**3.14** was obtained after cyclodehydration. When C5 epimers **3.3** and **3.4** were used as nucleophile, the d.r. was 1.3:1 and 1:1, respectively. Unfortunately, the use of electrophile **3.15** consistently favored the undesired epimer, with the diastereomeric ratio varying between 1:1.2–1:1.5. The use of myrmicarin 215 as the nucleophilic component with either **3.8** or **3.15** as electrophile resulted in essentially no reaction, presumably a result of the ensuing azafulvenium ion being less stable than either of the iminium ions. Thus, our original conditions using dienamine **3.1** for homodimerization (2:1 d.r.) in a 54% isolated yield over the two steps proved optimal. Interestingly, the use of *i*-PrOH as solvent for the cyclodehydration step allowed for a slow enough overall rate of cyclodehydration that a kinetic resolution of the two diastereomers could be achieved resulting in a 5:1 d.r. favoring the desired product, albeit in greatly reduced yield (12% over 2 steps).

The overall modest diastereoselectivites observed in the above dimerizations are in stark contrast to the direct dimerizations of myrmicarin 215 reported by Movassaghi and co-workers[3,4] wherein single diastereomers were isolated (see Section 1.3). In our work, the reduced diastereoselectivity observed can likely be attributed to two main factors: increased flexibility of the nucleophilic side chain and reduced steric congestion around the electrophilic center. Particularly intriguing is the reversal of selectivity

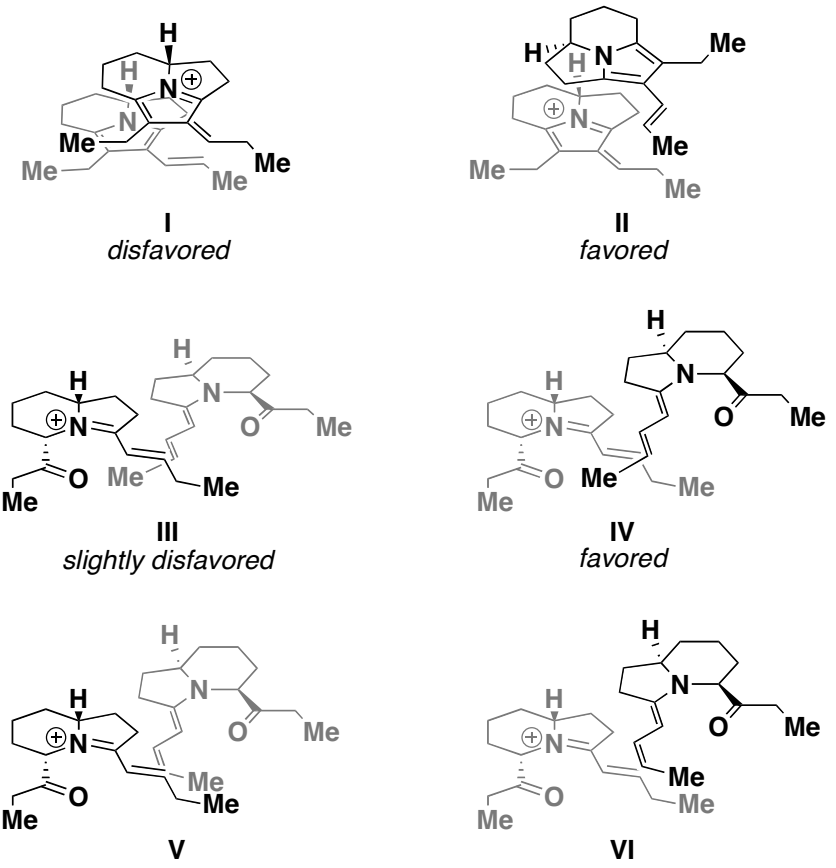

Figure 3.4 Pre-transition state dimerization assemblies of myrmicarin 215B (**3.6**) and dienamines **3.1** and **3.2**.

observed when *cis* alkene isomer **3.2** is used as nucleophile. Figure 3.4 depicts the most important pre-transition state assemblies that can be envisaged during these dimerizations. In all cases, the Seebach model[5] (i.e. the preference of nucleophilic π-bonds to attack electrophilic π-bonds *via* a gauche relationship) has been used to construct the depicted models. When myrmicarin 215 is used for dimerization, the increased rigidity of the framework and pseudo-*s*-cis conformation of the pyrrole π-bond and alkene make nucleophilic addition from the bottom face (assembly **I**) disfavored due to steric arguments. When dienamine **3.1** is used, however, its approach from the bottom face of the electrophile is much less congested, and the nucleophilic component can react placing the majority of the steric bulk distal to the site of reactivity, and hence, the minor interaction of the methyl group with the ethyl ketone makes assembly **III** only slightly

disfavored compared to **IV**. Furthermore, DFT calculations suggest that the nitrogen in dienamine **3.1** is notably pyramidalized (24.8° out of planarity), and the lone pair is oriented such that the indolizidine adopts a 5/6-*trans* ring junction, and thus, no clear convex or concave face is readily discernible. The use of *cis*-alkene nucleophile **3.2**, however, does not contain the unfavorable interaction described above (see **V** and **VI**), and thus, there exists essentially no preference for facial selectivity. The unfavorable diastereoselectivites observed when electrophile **3.15** is used are rationalized to be a result of increased steric encumbrance due to the presence of the C5-ethyl ketone disfavoring attack from the top face of the electrophile.

3.3 Total Synthesis of Isomyrmicarin 430C

With a reliable preparation of hexacycle **3.14** developed, the final synthetic transformation was anticipated to be electrophilic activation of the C1—C2 alkene followed by nucleophilic attack from C8b of the pyrrole to forge the final carbon-carbon bond of the natural product. While Movassaghi's previous results[3] indicated that the presence of the incorrect stereochemistry at C3 was not alone responsible for C3b attack over C8b attack of the pyrrole (see Section 1.3.3), we hoped that having the correct stereochemical disposition at C3 would provide a biasing factor that favored C1—C8b bond formation. Unfortunately, the mixture of hexacycle **3.14** and its C3 epimer were inseparable by standard flash chromatographic procedures. We thus turned to reverse-phase HPLC techniques. After some experimentation, conditions were identified that could separate the diastereomers, providing access to diastereomerically pure samples of

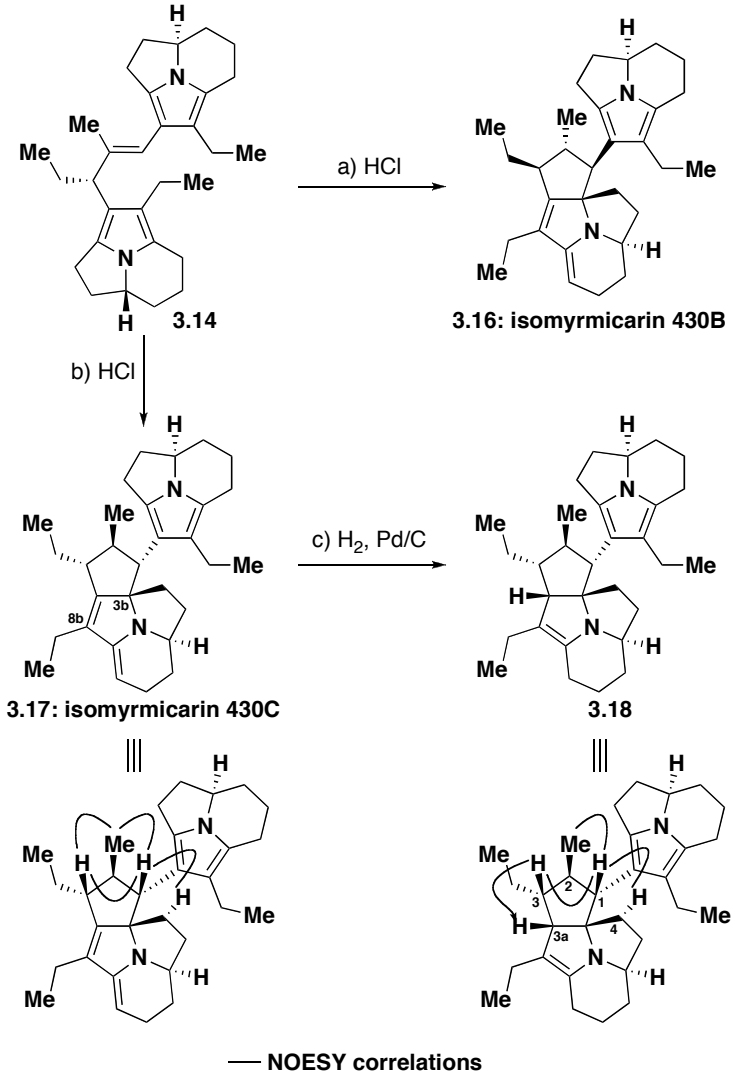

Scheme 3.2 Total synthesis of isomyrmicarin 430C (**3.71**). *Reagents and Conditions:* a) HCl (1.0M, Et_2O, 20 equiv.), CH_2Cl_2, r.t., 90 min.; b) HCl (1.0M, Et_2O, 20 equiv.), CH_2Cl_2, r.t., 45 min. (60%); c) H_2, Pd/C, C_6H_6, r.t., 45 min. (40%).

3.14 as a white solid. Unfortunately, the air sensitivity of this compound precluded the ability to obtain X-ray quality crystals to confirm the stereochemical assignment.

As Movassaghi had previously demonstrated that UV irradiation of a CH_2Cl_2 chloride solution of C3-*epi*-**3.14** quickly gave rise to isomyrmicarin 430B[3] (**3.16**, Scheme 3.2), we elected to use this precedent in the context of hexacycle **3.14**. Surprisingly, mercury lamp irradiation of a CH_2Cl_2 solution of **3.14** for several hours gave rise to isomyrmicarin 430B (**3.16**). Undeterred, we explored the use of different protic acid

sources, including $MeSO_3H$, *p*-TsOH, HBF_4, and HBr. All of these acid sources resulted in pyrrole ring protonated species that were subsequently unreactive and were only quenched following basic aqueous work up. This result was also independent of the solvent used (CH_2Cl_2, THF, $MeNO_2$, benzene). We thus returned to HCl as a protic acid source. We hypothesized that the puzzling outcome observed under irradiation conditions was a result of slow generation of HCl allowing time for a reversible process to take place prior to reaction completion. We therefore surmised that rapid introduction of HCl into the reaction mixture would attenuate any reversibility while still facilitating protonation of the C1—C2 alkene to promote intramolecular cyclization. In this vein, canula transfer of gaseous HCl generated from NaCl and concentrated H_2SO_4 to a CH_2Cl_2 solution of hexacycle **3.14** rapidly afforded a new heptacyclic iminium ion. This procedure, however, proved quite cumbersome and unpredictable, and ring protonated species were often observed. We thus chose to use ether solutions of hydrochloric acid to provide accurate, controlled amounts of acid to the reaction mixture, a procedure that proved both more convenient and reproducible. Under optimized conditions, 20 equivalents of a 1.0 M HCl solution in ether were added quickly to a stirred solution of the hexacycle in CH_2Cl_2. After 45 minutes, the reaction contents were quenched by the addition of resin-bound BEMP with 20 minutes of continued stirring. Concentration afforded a crude heptacyclic product that could then be purified on Et_3N-deactivated silica gel to afford a single heptacyclic compound whose diagnostic dd at $\delta = 4.74$ ppm in the ^{1}H-NMR spectrum was reminiscent of the isomyrmicarins but did not match the data reported for either isomyrmicarin 430A[4] or 430B.[3] In our hands, this new compound proved much more prone to decomposition than isomyrmicarin 430B. Indeed, thoroughly

degassed benzene solutions of this compound underwent extensive decomposition in less than 4 hours at room temperature. Although we were able to obtain stereochemical information from NOESY experiments, we were unable to obtain ^{13}C-NMR data on this compound as new peaks began to appear during acquisition. Detailed structural characterization therefore required derivatization to a more stable compound.

Following the procedure developed by Movassaghi and Ondrus,[4] the crude heptacyclic product could be hydrogenated with Pd/C in benzene to afford monoenamine **3.18** (Scheme 3.2) that was substantially more stable, and we were thus able to perform extensive structural analysis on this reduced compound. A full battery of 2D-NMR experiments supported the same gross structure of the isomyrmicarins, and 2D-NOESY experiments allowed the stereochemical assignment of this new compound to be determined. In particular, strong nOe correlations between the C1 and C3 methines and the C1 methine and C2 methyl allowed assignment of a *trans*, *trans* C1—C2, C2—C3 configuration to be established. The bridgehead stereochemistry was assigned from C3a—C1 as well as C4—C1 correlations. Thus, we assigned the structure of heptacyclic dienamine **3.17**, which we term isomyrmicarin 430C, as depicted in Scheme 3.2. Overall, isomyrmicarin 430C bears the correct top half of the central cyclopetane moiety as the natural isolate myrmicarin 430A (c.f. **3.7**, Figure 3.1) but is again regioisomeric to the natural product. Interestingly, HCl proved to be the only electrophilic species capable of affording any activation of the C1—C2 alkene. The use of other protic (TFA, $MeSO_3H$, pTSA, CSA, TfOH, and HBr) or Lewis acids [In(III), Au(I) including Au(I)/AgOTf, Pd(II), Hg(II), or BF_3•Et_2O] proved completely ineffective. Indeed, only Pd(II) and Hg(II) sources afforded any reaction, albeit through oxidation of one of the six membered

rings in hexacycle **3.14**; due to extensive signal overlap, the exact determination of which ring was oxidized proved unachievable.

As the preferred C2/C5 alkylation of pyrroles is widely accepted to be a kinetic outcome, efforts were made to isomerize[6] isomyrmicarin 430C to myrmicarin 430A through the use of strong protic acids and/or temperature elevation. These experiments led to either decomposition or recovered starting material following work up. While these results could not rule out the possibility that the desired isomerization had occurred and that the resultant myrmicarin 430A had undergone decomposition, the lack of any trace of the natural isolates in the crude NMR spectra and the collective results from both our work and the reports of Movassaghi and co-workers led us to believe that the observed cyclizations were not only kinetically, but also thermodynamically, more favorable. This hypothesis was examined through computational studies as described in Section 3.4.2.

First, however, a final word concerning the HCl-promoted cyclization of hexacycle **3.14** is in order. As mentioned above, we hypothesized that the extended reaction time required to achieve full conversion of hexacycle **3.14** under slow generation of HCl allowed for some type of equilibration process to occur that epimerized the C3 chiral center. Subsequently, we found that extended reaction times with HCl in Et_2O also afforded the same isomerization. Careful monitoring demonstrated that reaction times of even 1 hour (as opposed to 45 minutes) afforded substantial amounts of isomyrmicarin 430B, a molecule whose stereocenters at C1, C2, and C3 are all epimerized relative to isomyrmicarin 430C. Three possible mechanistic scenarios are proposed, two of which invoke an overall retrodimerization to monomeric species while the last involves intramolecular isomerizations. In the first case (Figure 3.5, path a), simple

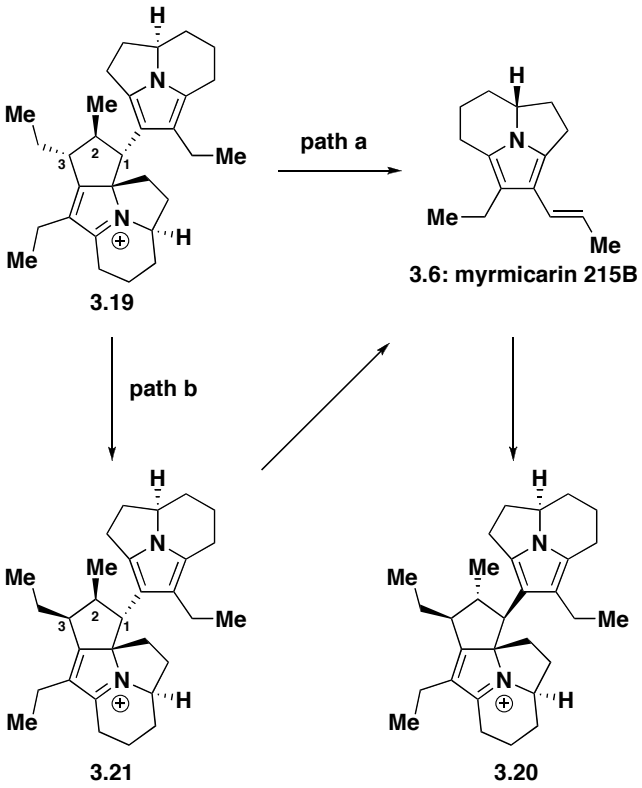

Figure 3.5 Isomerization mechanisms involving retro-dimerization to myrmicarin 215B for the conversion of **3.19** to **3.20**.

retrodimerization of **3.19** to myrmicarin 215-type structures and re-dimerization affords the thermodynamically more stable isomyrmicarin 430B skeleton **3.20** as previously reported.[3] Intriguingly, isomyrmicarin 430B, another C1—C2, C2—C3 *trans*, *trans* congener, has been shown to be recalcitrant to reversion. We thus proposed a second possibility (path b) wherein initial epimerization at C3 occurs, affording iminium **3.21**, the protonated congener of isomyrmicarin 430A (a compound that has been previously shown to revert to monomeric species). This proposal is supported circumstantially by the overall geometry occupied by iminium **3.19** whose C3 methine is well-aligned with the extended iminium ion for a deprotonation/reprotonation sequence to occur. However,

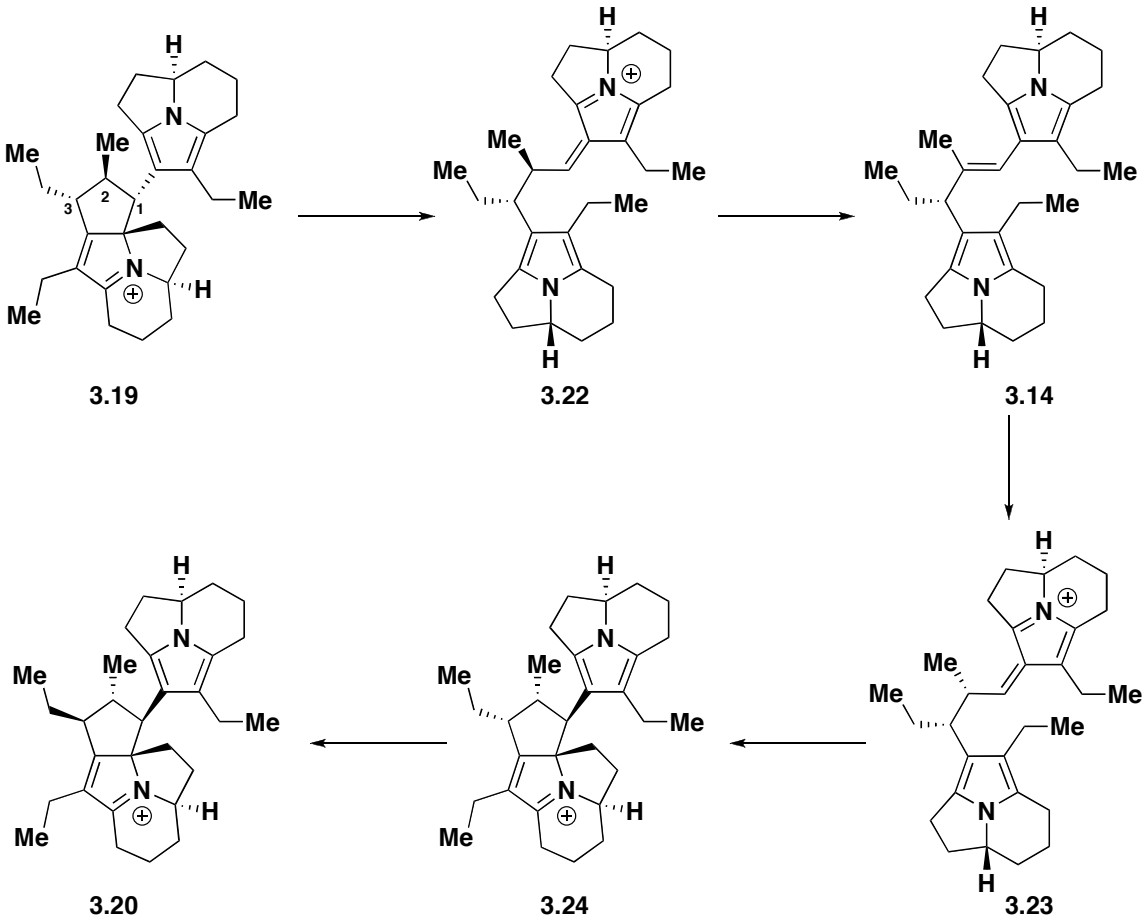

Figure 3.6 Intramolecular isomerization mechanism for the conversion of **3.19** to **3.20**.

the above two mechanisms are somewhat problematic in that the reported reversible dimerization required extended reaction times to undergo conversion to isomyrmicarin 430B; our reaction reached complete conversion in 1.5 h. As a final proposal, retro-Friedel-Crafts reaction to afford azafulvenium **3.22** (Figure 3.6) followed by deprotonation and reprotonation from the opposite face of the C1—C2 alkene gives azafulvenium **3.23** that undergoes intramolecular cyclization to **3.24**, effectively epimerizing the C1 and C2 stereocenters. Finally, an intramolecular epimerization of C3 through a deprotonation/reprotonation sequence as described above furnishes the isomyrmicarin 430B framework. Notably, any protonation at C3 from the bottom face

would place the newly formed C-H bond out of alignment with the π system, essentially rendering the epimerization irreversible.

3.4 Computational Studies

As alluded to earlier, our collective observations and the synthetic community's consistent inability to forge the requisite C1—C3b bond of myrmicarin 430A prompted us to initiate a series of computational studies aimed at addressing two key issues. First, we sought to provide computational evidence either for or against the proposed structure of myrmicarin 430A, as this compound was never isolated in a pure form[7] (see Section 1.1), and second, we hoped to gain insight into the mechanism by which the final bond formation occurred in our own work in order to shed light on the possibility of forging the correct C1—C3b bond under acidic conditions.

3.4.1 NMR Predictions of Myrmicarin 430A and Related Structures

The use of NMR prediction for structure elucidation has been an underutilized tool in synthetic organic chemistry laboratories. Recent studies have demonstrated that the use of quantum chemical calculations for not only ^{13}C-NMR predictions[8] but also ^{1}H—^{1}H coupling constants[9] can be a powerful tool in the proposal and structural revision of natural products. The recent rise in computing power has allowed these types of computations to become routine,[10] and we hoped that this technique would not only answer questions with regard to myrmicarin 430A but also provide predictive power capable of assisting in our own structure elucidation studies. Before undertaking NMR prediction studies on myrmicarin 430A itself, we recognized the need to validate a

particular method on a known, fully characterized substrate. In particular, the reported data from Movassaghi and Ondrus for isomyrmicarin 430B seemed an ideal testing ground for the types of functionality present in the natural isolate. Furthermore, we anticipated that the highly rigid framework of these molecules would lend themselves well to quantum-chemical NMR prediction without the need for Boltzmann weighting of various conformational isomers from Monte Carlo simulations.

To begin our studies, initial geometries for isomyrmicarin 430B were obtained from simple MMFF minimizations. Structures were refined using the B3LYP density functional[11] in conjunction with a small, split-valence double-ζ basis set (3-21G), and finally, in anticipation of the need for higher level optimized structures for our later studies (*vide infra*), the structures were further refined using B3LYP with the larger 6-31G(*d*) basis set. With optimized structures in hand, NMR shielding tensors were then computed using the mPW1PW91 density functional[12] with the 6-31G(*d*,*p*) basis set. Here, the larger basis set that incorporates *p*-polarization functions on hydrogen is necessary to obtain more accurate predictions of ^{1}H-NMR shielding constants. Furthermore, this combination of density functional and basis set has previously been shown to give good accuracy in predicting ^{13}C shifts.[8] Although ^{1}H-NMR shifts were computed, the highly condensed nature of these chemical shifts over a small chemical shift range made the use of ^{13}C-NMR shifts both more practical and more diagnostic. In addition, ^{13}C shifts tend to be relatively insensitive to solvent effects, a factor that effectively reduces the computational costs of the calculations.

The results of our validation experiments are summarized in Figure 3.7 wherein the calculated ^{13}C-NMR shifts of isomyrmicarin 430B are plotted against the

experimentally determined ^{13}C-NMR shifts of both isomyrmicarin 430B and isomyrmicarin 430A. Importantly, this method shows an excellent correlation of the experimental and calculated shifts for isomyrmicarin 430B while demonstrating a markedly lower correlation with isomyrmicarin 430A. Specifically, the mean absolute error for the correct structure is on the order of 2.7 ppm while that of the incorrect structure (i.e. isomyrmicarin 430A) is 4.6 ppm.

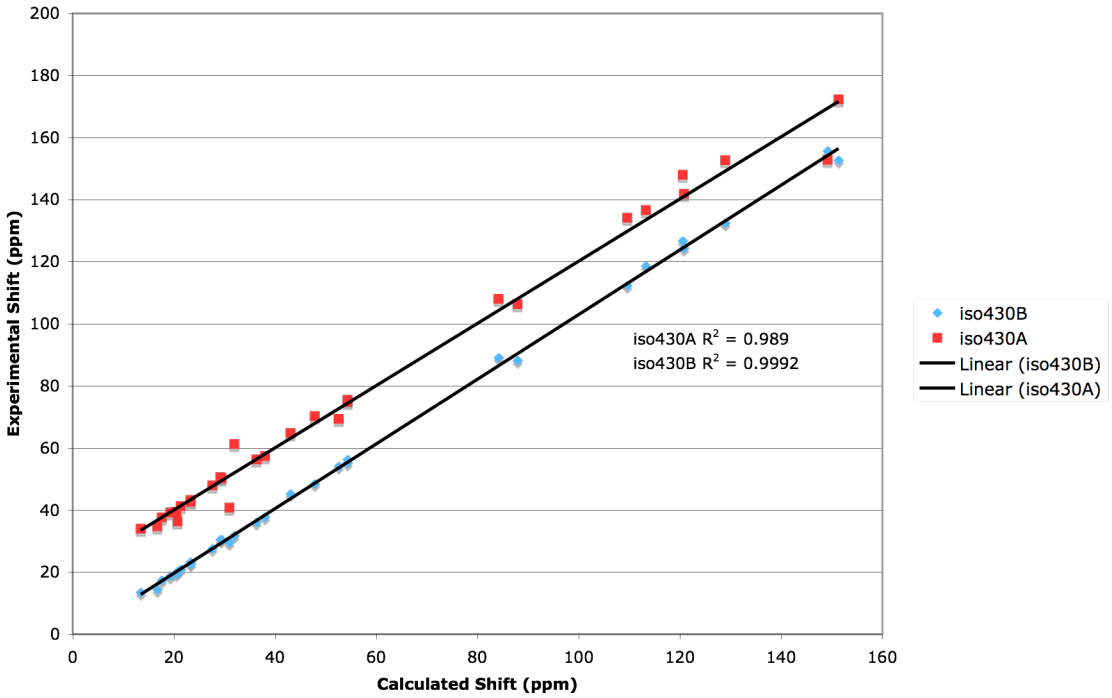

Figure 3.7 Validation studies of computed ^{13}C-NMR shifts.

With a validated method in place, NMR prediction studies were performed on myrmicarin 430A, and an excellent correlation was observed as demonstrated in Figure 3.8. Although the maximum deviation from the predicted value was relatively high (just under 8 ppm), this particular resonance corresponded to a freely rotatable carbon, and thus a somewhat larger deviation is to be expected. Pleasingly, however, the average deviation was less than 2.6 ppm. Interestingly, this method also proved capable of

providing relatively accurate predictions of the ^{1}H-NMR chemical shifts, particularly of the diagnostic enamine protons. Thus, the high correlation observed between our NMR predictions and the experimentally-derived ^{13}C-NMR shifts strongly suggest that the reported structure of myrmicarin 430A was correctly deduced.

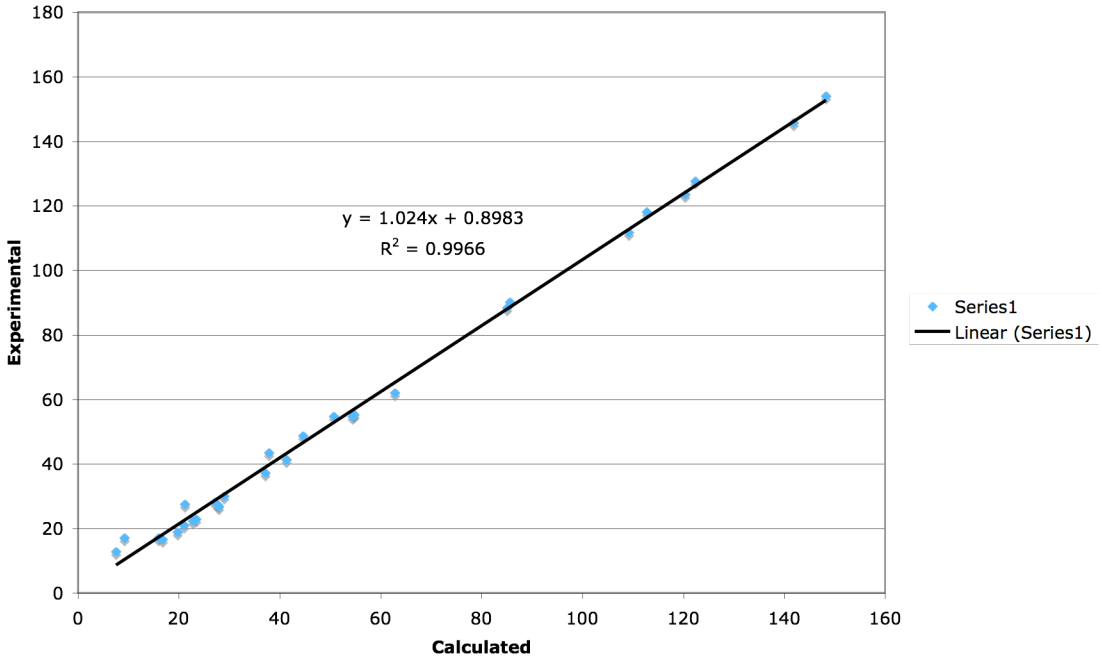

Figure 3.8 Computed versus experimental ^{13}C shifts for myrmicarin 430A.

In the course of our synthetic efforts, the structure of enamine **3.18** was proposed on the basis of NOESY data, and given the above excellent correlations to the experimentally-derived shifts, we elected to provide further computational evidence for our structural assignment. Due to limited sample quantitites, a full assignment was not possible for this structure, therefore, a different method for direct comparison analysis was needed. Here, we chose to perform a simple ascending numerical sort of the experimental and calculated NMR shifts, and a linear regression analysis of this pairing was made. In addition, the analogous comparison with available experimental data for

isomyrmicarins 430A and 430B was carried out. It was clear *a priori* that such a pairing would naturally lend to good correlations to all of these structures since the data points necessarily followed a positive, increasing trend; however, we hoped that such a pairing of the data would still prove capable of discerning between the above structures.

The results of this analysis are presented in Figure 3.9 where the data for isomyrmicarins 430A and 430B have been vertically shifted for clarity. As expected,

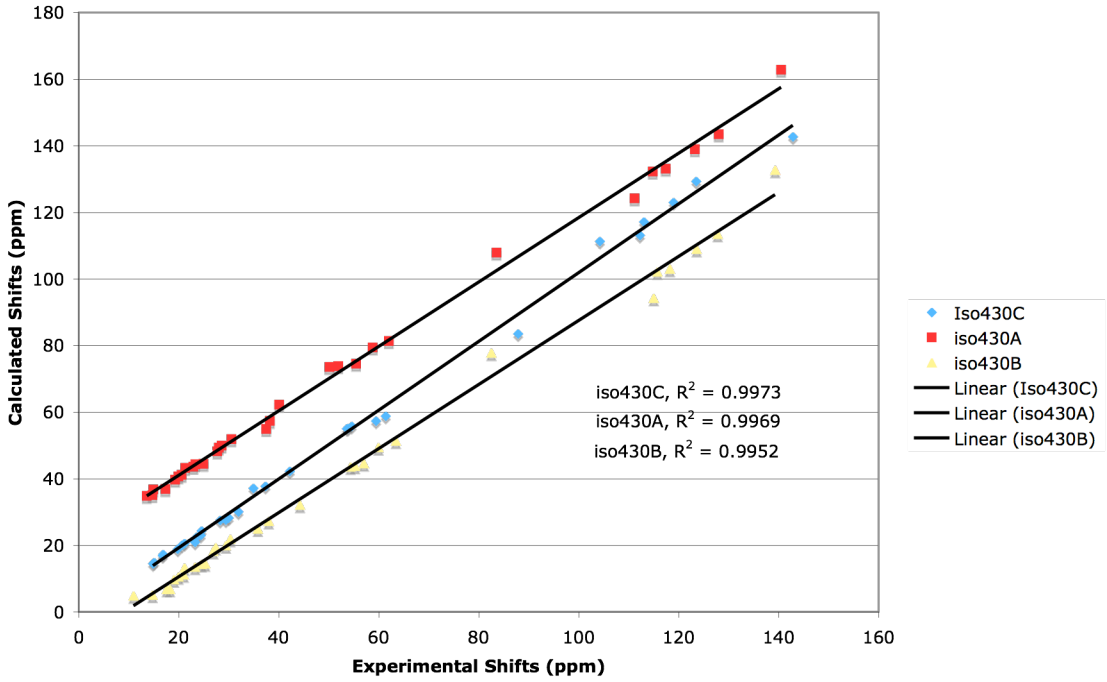

Figure 3.9 Comparison of ordered ^{13}C shifts in reduced isomyrmicarins.

least squares regression analysis indicates a high correlation to all three structures; however the best correlation was found with our proposed structure. Furthermore, isomyrmicarin 430A, the 3-*epi* isomer of isomyrmicarin 430C, showed the next best correlation while isomyrmicarin 430B showed the poorest correlation. Overall, these results bolster our proposed stereochemical assignment. With our computational NMR studies completed, our focus turned to the mechanism of the final bond formation.

3.4.2 Computational Exploration of the Final C1—C3b/C8b Bond Formation

Intrigued by the possibility that the consistent formation of isomyrmicarin 430-type structures is a result of both a thermodynamic and kinetic preference for C3b attack of the pyrrole within **3.22** onto its presumed azafulvenium, we set out to explore the potential energy surface of this final bond closure with quantum chemical methods. As a simplification, we chose to assume that protonation of hexacycle **3.14** occurs from the desired face, giving rise to azafulvenium **3.22**, which served as the starting point for our explorations. In particular, we recognized the need for rotation about the C3—C3a bond prior to competing cyclization from either the C3b or C8b carbon. Two local minima were identified corresponding to these rotameric structures (**3.22a** and **3.22b**, respectively). Next, the transition states corresponding to cyclization from C3b (**3.25**) and C8b (**3.26**) were located and optimized, and their structures were confirmed to be transition states through vibrational frequency analysis. Although IRC calculations could, in principle, definitively demonstrate that these transition states linked both the starting materials and the products, they were not persued due to their high computational cost. Evidence, however, could be garnered that the located structures are the desired transition states through animation of the vibrational modes corresponding to the single imaginary eigenvalue. Finally, the two cyclized iminium intermediates were located, and a potential energy surface of Gibbs free energies was constructed (Figure 3.10) from data derived from the above structures.

Several features of the potential energy surface are of interest. Intriguingly, rotamer **3.22b** (the precursor to myrmicarin 430A) is thermodynamically more stable than its counterpart, and the overall difference in structure is relatively small, with the

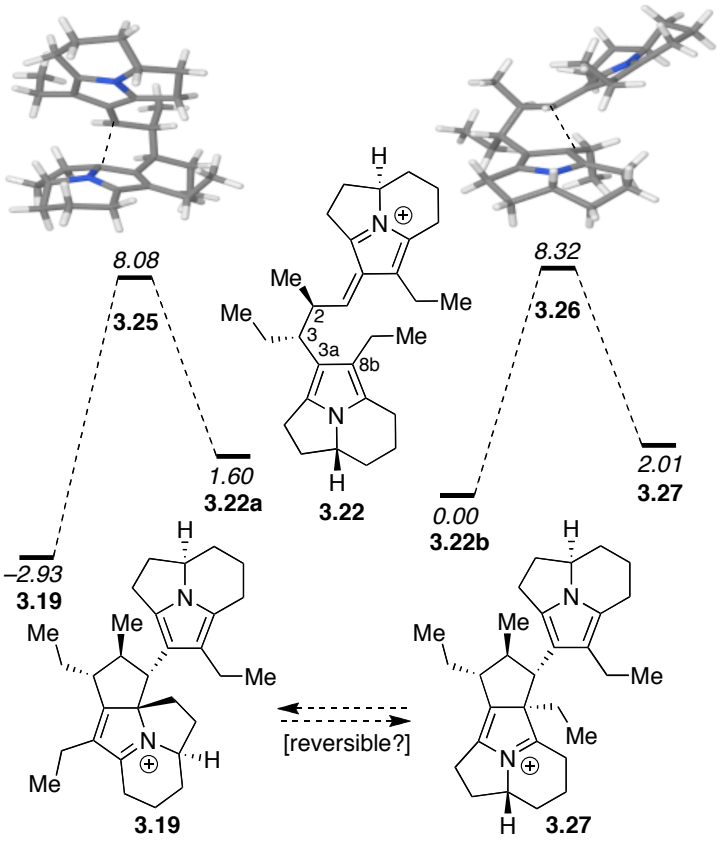

Figure 3.10. Potential energy surface of second bond formation. All values represent ΔG in kcal/mol.

major difference derived from the torsional angle defined by C2/C3/C3a/C8b (84° for **3.22a** and 69° for **3.22b**). The transition state energies also imply that the respective barriers to cyclization are essentially isoenergetic. The most striking feature, however, is the difference in energy between the heptacyclic iminium ion products, where **3.19** is calculated to be 4.94 kcal/mol more stable. Furthermore, the cyclization of **3.22b** leading to the deisred iminium **3.27** is endothermic by ~2 kcal/mol. The use of a larger basis set or inclusion of solvent effects does not change the conclusions drawn from this study. Hence, it appears that cyclization to form **3.27** from azafulvenium **3.22** is highly unlikely. Unfortunately, the final piece of data, namely the barrier to rotation about the C3—C3a bond, necessary to discount the ability of such structures to form the desired C1—C8b

bond proved elusive as we were unable to locate the transition state linking the two rotameric structures. Circumstantially, however, the overall small change in the geometry suggests that the barrier to this rotation is likely small relative to the barrier to cyclization.

The results obtained herein have some implications for the biosynthesis of myrmicarin 430A. Specifically, these calculations strongly suggest that either azafulvenium ion **3.22** is not a biosynthetic intermediate or that enzyme participation plays a large role in governing the regiochemistry of this final bond formation. Indeed, given the ease with which the general isomyrmicarin framework has been accessed from both myrmicarin 215 and "myrmicarin 233" congeners, it is quite remarkable that such structures are not natural isolates. The possibility of enzyme participation in either preventing rotation about the C3—C3a bond and/or coupling the alkylation event to an irreversible deprotonation is quite appealing in light of additional computational results. In particular, calculations suggest that isomyrmicarin 430C and myrmicarin 430A are essentially isoenergetic. Furthermore, the immediate product following deprotonation of heptacyclic iminium **3.27**, namely the proposed structure of myrmicarin 430B, has been shown to convert to myrmicarin 430A in C_6D_6, and our calculations indicate that this isomerization is thermodynamically favored, presumably due to strain release from the isomerization of the C3a—C3b alkene in myrmicarin 430B. Additionally, the newly isomerized alkene is both sterically more accessible and likely more nucleophilic, as suggested by the existence of myrmicarins 645 and 663. These factors, when combined, provide some rationale for the lack of evidence for any isomerization of myrmicarin 430A to an isomyrmicarin framework.

3.5 References

1. a) For an early review of the reactivity of dienamines and conjugated iminium ions, see: P. W. Hickmott, *Tetrahedron* **1984**, *40*, 2989–3051; b) For an example of a proton-initiated dienamine dimerization, see: G. Maas, R. Rahm, *Z. Naturforsch* **2005**, *60b*, 673–676; c) For an example of regioselective γ-amination of a catalytically generated dienamine, see: S. Bertelsen, M. Marigo, S. Brandes, P. Dinér, K. A. Jørgensen, *J. Am. Chem. Soc.* **2006**, *128*, 12973–12980; d) For an example of γ-alkylation of a dienamine with methyl vinyl ketone, see: P. W. Hickmott, R. Simpson, *J. Chem. Soc., Perkin Trans. 1*, **1992**, 357–363; e) For a recent review on dienamines/conjugated iminium ions in catalysis, see: D. B. Ramachary, Y. V. Reddy, *Eur. J. Org. Chem.* **2012**, 865–887.

2. For a review on the chemistry of C-vinylpyrroles, see: B. A. Trofimov, L. N. Sobenina, A. P. Demenev, A. I. Mikhaleva, *Chem. Rev.* **2004**, *104*, 2481–2506.

3. A. E. Ondrus, M. Movassaghi, *Org. Lett.* **2009**, *11*, 2960–2963.

4. A. E. Ondrus, M. Movassaghi, *Tetrahedron* **2006**, *62*, 5287–5297.

5. D. Seebach, J. Golinski, *Helv. Chim. Acta* **1981**, *64*, 1413–1423.

6. a) M. H. Palmer, D. S. Letich, C. W. Greenhalgh, *Tetrahedron* **1978**, *34*, 1015–1021; b) J. R. Carson, N. M. Davis, *J. Org. Chem.* **1981**, *46*, 839–843; c) For a review on the challenges of regioselective synthesis of highly substituted pyrroles, see: C. Schmuck, D. Rupprecht, *Synthesis* **2007**, 3095–3110.

7. F. Schröder, V. Sinnwell, H. Baumann, M. Kaib, *Chem. Commun.* **1996**, 2139–2140.

8. S. R. Rychnovsky, *Org. Lett.* **2006**, *8,* 2895–2898.

9. G. Saielli, K. C. Nicolaou, A. Ortiz, H. Zhang, A. Bagno, *J. Am. Chem. Soc.* **2011**, *133***,** 6072–6077.

10. a) For an excellent review of the quantum-chemical prediction of NMR shifts, see: M. W. Lodewyk, M. R. Siebert, D. J. Tantillo, *Chem. Rev.* **2012**, *112*, 1839–1862; b) For a review on the calculation of coupling constants, see: T. Bally, P. R. Rablen, *J. Org. Chem.* **2011**, *76*, 4818.

11. a) C. Lee, W. Yang, R. G. Parr, *Phys. Rev. B* **1988**, *37*, 785–789; b) A. D. Becke *J. Chem. Phys.* **1993**, *98*, 5648–5652.

12. P. Cimino, L. Gomez-Paloma, D. Duca, R. Riccio, G. Bifulco, *Magn. Reson. Chem.* **2004**, *42*, S26–S33.

3.6 Experimental Section

General Procedures. All reactions were carried out under an argon atmosphere with dry solvents under anhydrous conditions, unless otherwise noted. Dry tetrahydrofuran (THF), toluene, benzene, diethyl ether (Et_2O) and methylene chloride (CH_2Cl_2) were obtained by passing commercially available pre-dried, oxygen-free formulations through activated alumina columns. Acetonitrile (MeCN) was dried and stored over 3 Å molecular sieves. Yields refer to chromatographically and spectroscopically (^1H and ^{13}C NMR) homogeneous materials, unless otherwise stated. Reagents were purchased at the highest commercial quality and used without further purification, unless otherwise stated. Reactions were magnetically stirred and monitored by thin-layer chromatography (TLC) carried out on 0.25 mm E. Merck silica gel plates (60F-254) using UV light as visualizing agent and cerium sulfate (CAM) or aqueous $KMnO_4$, and heat as developing agents. SiliCycle silica gel (60, academic grade, particle size 0.040–0.063 mm) was used for flash column chromatography. Where stated, Aldrich neutral alumina was used for flash chromatography. NMR spectra were recorded on Bruker DPX 300, Avance II 400, Avance III 400 and DMX 500 instruments and calibrated using residual undeuterated solvent as an internal reference ($CDCl_3$: 7.26 ppm for ^1H, 77.0 ppm for ^{13}C; C_6D_6: 7.16 ppm for ^1H, 128.06 for ^{13}C; CD_3CN: 1.94 for ^1H). The following abbreviations were used to explain the multiplicities: s = singlet, d = doublet, t = triplet, q = quartet, br = broad, app = apparent. IR spectra were recorded on a Perkin-Elmer 1000 series FT-IR spectrometer. High-resolution mass spectra (HRMS) were recorded in the Columbia University Mass Spectral Core facility on a JOEL HX110 mass spectrometer using FAB (fast atom bombardment) techniques.

Abbreviations. BEMP = 2-*tert*-butylimino-2-diethylamino-1,3-dimethyl-perhydro-1,3,2-diazaphosphorine

Iminium ion 3.8. A solution of freshly prepared dienamine **3.1** (0.005 g, 0.021 mmol, 1.0 equiv) in CD_3CN (0.2 mL) was added dropwise to a solution of TFA (1.6 μL, 0.021 mmol, 1.0 equiv) in CD_3CN (0.1 mL) dropwise under argon with stirring. The transfer was quantitated with CD_3CN washes (2 × 0.1 mL), affording a pale yellow solution. ^1H NMR analysis showed exclusive conversion to compound **3.8**. [Note: These protonated species were found to be stable for >24 h as anhydrous solutions in CD_3CN at –20 °C. Attempts to isolate these salts via concentration of the solution resulted in complete decomposition of the materials]. **3.8**: ^1H NMR (300 MHz, CD_3CN) δ 7.36 (dt, J = 15.6, 6.3 Hz, 1 H), 6.18 (d, J = 15.6 Hz, 1 H), 5.14 (br s, 1 H), 4.38 (br m, 1 H), 3.46 (dd, J = 18.9, 9.6 Hz, 1 H), 3.12 (m, 1 H), 2.70 (q, 7.2 Hz, 2 H), 2.52–2.37 (m, 4 H), 2.29–2.17 (m, 1 H), 2.14–2.03 (m 1 H), 1.92–1.65 (m, 2 H), 1.62–1.46 (m, 1 H), 1.44–1.27 (m, 1 H), 1.08 (t, J = 7.2 Hz, 3 H), 1.07 (t, J = 7.2 Hz, 3 H).

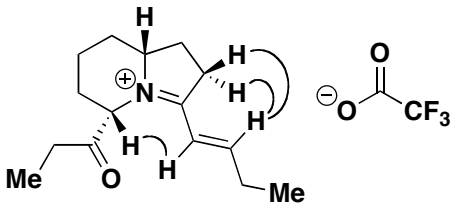

3.8

—— NOESY correlations

Ammonium ion 3.9. A solution of freshly prepared dienamine **3.1** (0.005 g, 0.021 mmol, 1.0 equiv) in CD_3CN (0.2 mL) was added dropwise to a solution of $MeSO_3H$ (1.4 μL, 0.021 mmol, 1.0 equiv) in CD_3CN (0.1 mL) dropwise under argon with stirring. The transfer was completed with 2 × 0.1 mL washes of CD_3CN, affording a pale yellow

solution. ^{1}H NMR analysis showed exclusive conversion to compound **3.9**. **3.9**: ^{1}H NMR (400 MHz, CD_3CN) δ 5.76 (dqt, *J* = 15.2, 6.8, 2.0 Hz, 1 H), 5.37 (dtq, *J* = 15.2, 6.8, 2.0 Hz, 1 H), 5.13 (br m, 1 H), 3.31–2.99 (m, 4 H), 2.69 (qd, *J* = 7.2, 2.8 Hz, 2 H), 2.48–2.39 (m, 2 H), 2.29–2.18 (m, 1 H), 2.12–2.03 (m, 1 H), 1.91–1.79 (m, 1 H), 1.71 (dq, *J* = 6.4, 1.6 Hz, 3 H), 1.59–1.47 (m, 1 H), 1.44–1.32 (m, 1 H), 1.10–1.01 (m, 1 H), 1.07 (t, *J* = 7.2 Hz, 3 H).

Hexacyclic alkene 3.14. A solution of freshly prepared dienamine **3.1** (53 mg, 0.227 mmol, 1.0 equiv) in CH_3CN (0.6 mL) was added dropwise to a solution of TFA (8.8 μL, 0.114 mmol, 0.5 equiv) in CH_3CN (0.2 mL) at 23 °C. The resulting yellow solution was stirred for 30 min at 23 °C. Upon completion, the reaction contents were diluted with CH_2Cl_2 (10 mL) and poured into ice-cold aqueous 1 M NaOH (10 mL). The layers were separated and the aqueous layer was extracted once more with CH_2Cl_2 (10 mL). The combined organic layers were then dried (Na_2SO_4) and concentrated to afford dimer **3.13** as a thick orange oil. Taken forward without any additional purification, this newly formed intermediate was immediately taken up in degassed MeOH (1 mL) and stirred for 3 h at 23 °C. The reaction contents were then concentrated directly, and the resultant residue was purified through a plug of neutral alumina (pentane/Et_2O, 9:1, 20 mL) to afford hexacycle **3.14** as a colorless oil that slowly formed a white solid upon standing under high vacuum; this material was a 2:1 mixture of diastereomers based on ^{1}H NMR analysis. This diastereomeric mixture was then further purified via semi-preparative HPLC (Shimadzu Epic C18 5μ 250 × 9.6 mm, water/MeCN, 40% for 5 min, 40%→0% over 30 min, 0% for 25 min, UV detector at 280 nm) $t_{R,\ minor}$ = 47 min, $t_{R,\ major}$ = 48 min)

to afford pure hexacycle **3.14**. Alternatively, crude dimer **3.13** was taken up in degassed *i*-PrOH (1 mL) and the reaction mixture was stirred for 4.5 h at 23 °C. **3.14** was then isolated, as detailed above, as a 5:1 mixture of diastereomers resulting through kinetic resolution. [Note: this compound was stored for several days in degassed benzene under an Ar atmosphere at –20 °C with minimal decomposition]. **3.14:** IR (film) ν_{max} 2955, 2923, 2849, 1456, 1420, 1321, 1082, 1018, 801 cm^{-1}; ^1H NMR (400 MHz, C_6D_6) δ 6.67 (s, 1 H), 3.56 (app t, *J* = 7.6 Hz, 1 H), 3.39–3.29 (m, 2 H), 2.93–2.85 (m, 2 H), 2.78–2.61 (m, 7 H), 2.50 (dd, *J* = 14.4, 8.0 Hz, 1 H), 2.50–2.39 (m, 2 H), 2.18–2.04 (m, 3 H), 1.99–1.95 (m, 1 H), 1.94 (d, *J* = 0.8 Hz, 3 H), 1.76–1.70 (m, 3 H), 1.61–1.49 (m, 3 H), 1.41–1.33 (m, 2 H), 1.42 (t, *J* = 7.6 Hz, 3 H), 1.39 (t, *J* = 7.6 Hz, 3 H), 1.22 (t, *J* = 7.6 Hz, 3 H), 0.98–0.81 (m, 2 H); ^{13}C NMR (100 MHz, C_6D_6) δ 136.6, 128.7, 126.9, 122.1, 122.0, 118.7, 118.7, 118.2, 116.6, 113.8, 55.2, 54.9, 49.3, 37.5, 37.4, 30.2, 30.0, 27.6, 27.3, 26.8, 23.0, 22.7, 20.8, 20.7, 19.2, 19.0, 16.5, 16.5, 16.0, 13.6; HRMS (FAB) calc. for $C_{30}H_{42}N_2^+$ [M^+] 430.3348, found 430.3326.

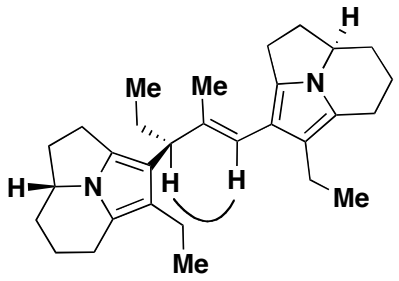

3.14

— NOESY correlations

Heptacyclic dienamine 3.17. Hexacycle **3.14** (5.0 mg, 0.012 mmol, 1.0 equiv) was dissolved in CH_2Cl_2 (1.0 mL), and a solution of HCl (1.0 M in Et_2O, 0.232 mL, 20.0 equiv) was added quickly. The initially bright yellow solution slowly became darker while stirring at 23 °C for 45 min. The reaction contents were then quenched by the

addition of 240 mg of resin-bound BEMP and stirred for 20 min. The reaction mixture was then filtered and concentrated to afford crude heptacyclic dienamine **3.17** as a brown oil, which was carried forward without further purification. Pure samples could be obtained after purification on Et_3N-deactivated silica gel (Et_3N/hexanes, 0.6%→2.5%), affording **3.17** (3.0 mg, 60% yield) as a pale yellow oil. **3.17**: IR (film) ν_{max} 2957, 2928, 2854, 1650, 1453, 1321, 1168, 1089, 960 cm^{-1}; ^1H NMR (400 MHz, C_6D_6) δ 4.74 (dd, *J* = 7.1, 3.1 Hz, 1 H), 3.41–3.31 (m, 1 H), 3.17–3.09 (m, 1 H), 3.02–2.92 (m, 1 H), 2.79–2.40 [m, 7 H, including 2.51 (d, *J* = 8.5 Hz, 1 H)], 2.32 (ddd, *J* = 15.2, 7.6, 1.4 Hz, 1 H), 2.20–1.89 (m, 6 H), 1.81–1.60 (m, 8 H), 1.42–0.82 [m, 16 H, including 1.39 (t, *J* = 7.5 Hz, 3 H), 1.30 (t, *J* = 7.4 Hz, 3 H), 1.13 (d, *J* = 7.4 Hz, 3 H)]; LRMS (APCI) calc. for $C_{30}H_{43}N_2^+$ [M+H$^+$] 431.34, found 431.36. [Note: this compound was found to be extremely sensitive, and extensive decomposition was observed within hours after isolation in degassed benzene].

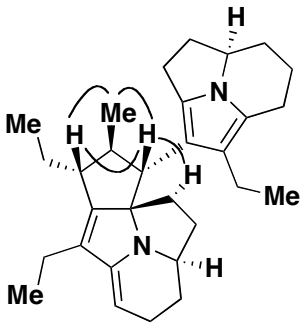

3.17
— NOESY correlations

Heptacyclic enamine 3.18. Crude heptacyclic dienamine **3.17** (5.0 mg, 0.012 mmol, 1.0 equiv) was dissolved in degassed benzene (0.4 mL) at 23 °C, and Pd/C (10 wt %, 0.010 g, 0.009 mmol, 0.8 equiv) was then added. The reaction was then purged with H_2 three times and was stirred under an H_2 atmosphere at 23 °C for 45 min. The reaction contents

were then filtered through a pad of Celite, concentrated, and purified on a short plug of Et_3N-deactivated silica gel (1.25% Et_3N in hexanes) to afford enamine **3.18** (1.2 mg, 24% yield over 2 steps) as a yellow oil. **3.18:** IR (film) ν_{max} 2955, 2924, 2851, 1647, 1458, 1376, 1320 cm^{-1}; HRMS (FAB) calc. for $C_{30}H_{45}N_2^+$ [M+H$^+$] 433.3583, found 433.3591. ^{1}H NMR (400 MHz, C_6D_6) δ 3.58–3.48 (m, 1 H), 3.24 (d, *J* = 8.0 Hz, 1 H), 3.07 (ddd, *J* = 15.3, 11.0, 6.3 Hz, 1 H), 2.87 (dd, *J* = 15.2, 7.8 Hz, 1 H), 2.72–2.61 (m, 4 H), 2.52–2.31 [m, 4 H, including 2.47 (d, *J* = 11.6 Hz, 1 H)], 2.20–2.06 (m, 6 H), 1.95–1.75 (m, 2 H), 1.75–1.44 (m, 6 H), 1.42–1.17 [m, 7 H, including 1.34 (t, *J* = 7.6 Hz, 3 H)], 1.16–0.80 [m, 11 H, including 1.13 (t, *J* = 7.1 Hz, 3 H), 1.10 (t, *J* = 7.4 Hz, 3 H), 1.04 (d, *J* = 6.5 Hz, 3 H)]; ^{13}C NMR (100 MHz, C_6D_6) δ 142.7, 129.3, 123.0, 117.2, 113.2, 111.3, 83.6, 58.8, 57.4, 55.8, 55.2, 55.1, 42.2, 37.7, 37.1, 30.1, 28.3, 27.6, 27.5, 24.4, 23.0, 22.5, 21.0, 20.6, 20.1, 18.9, 17.3, 16.9, 14.8, 14.5. The complete list of peaks in the carbon spectrum was obtained with the aid of an HMBC spectrum.

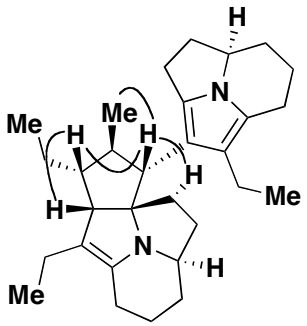

3.18
— NOESY correlations

Computational Details. Initial geometries from PM3 semi-empirical calculations were performed using the GAMESS program package.[1] Geometries were then further refined at the B3LYP/6-31G(d) level of theory using a medium integration grid using the

Schrödinger[2] suite of quantum chemical programs. Geometries were considered converged when maximum Cartesian gradients fell below 4.5×10^{-4} hartree/Bohr. In order to ensure that a larger basis set did not affect the conclusions drawn from these calculations, single point energy computations were undertaken on the structures obtained from the aforementioned geometry optimizations using Pople's 6-311+G(d,p) split-valence triple-ζ basis set, and solvent effects were also computed with this basis set using a Poisson-Boltzmann model with dichloromethane as the solvent[3,4] (dielectric constant = 8.93, probe radius = 2.33). To ensure that the obtained geometries were stationary points, analytic frequency calculations were undertaken, and thermodynamic parameters were obtained from those calculations. The Gibbs energies obtained therein were used to construct the potential energy surface plot within Figure 3.10 of the main text, as neither the use of a larger basis set nor the inclusion of solvation effects alters the conclusions drawn from this study. Electronic energies and Cartesian coordinates are reported below for myrmicarin 430A (**3.7**), myrmicarin 430B (proposed structure[5]), isomyrmicarin 430B, and all compounds in Figure 3.10.

Computed Equilibrium Geometries

Myrmicarin 430A (3.7)
E(SCF) = -1277.980077

C	-3.3282815377	-4.5317094523	-0.1913236491
C	-3.1101132923	-3.6806404270	0.8903044319
C	-3.8373904183	-2.4605363242	0.5983267165
C	-4.4504028945	-2.6126401151	-0.6418533561
N	-4.1068049219	-3.8555738901	-1.0848143990
C	-4.4254325270	-4.5580431252	-2.3115201722
C	-4.2178303672	-6.0199336488	-1.8480303971
C	-3.1008926772	-5.9185982425	-0.7529068621
C	-5.7815750112	-4.0414772104	-2.7967768213
C	-5.7322117038	-2.4941922318	-2.8247576587
C	-5.4862549163	-1.8549483026	-1.4321846171
C	-2.3072430423	-3.9375267719	2.1419729427
C	-2.4524712491	-5.3479602773	2.7665553392
C	-3.8690360979	-5.6819287180	3.2341958878
C	-1.4018158635	-5.3239530559	3.8938720140

C	-4.0063960494	-1.2637067718	1.5007846354
C	-5.1643238966	-1.4045567992	2.5073289192
C	-1.0852284066	-6.6614910028	4.5887505380
C	-0.6531618031	-7.8163884758	3.6755890330
C	-0.1748068140	-4.6251038409	3.2446614944
C	0.5416391232	-3.6548974626	4.1395265088
N	0.0659481514	-2.3738628339	3.8238125443
C	-0.3231064693	-2.2983941256	2.4842715305
C	-0.7355331823	-3.7130750880	2.0665701459
C	-0.1537505241	-4.1086205301	0.6922955453
C	1.3728147872	-4.0323933607	0.5617943032
C	1.5252288276	-3.6204345937	5.0484200382
C	1.8284743858	-2.1734384061	5.4176386512
C	0.8546116009	-1.3375494489	4.5130215424
C	-0.2186075585	-1.1508720560	1.7906870167
C	0.4650848784	0.0462351854	2.4229122035
C	1.5012490324	-0.4089185257	3.4747132539
H	-3.6706566775	-4.3127445776	-3.0787288972
H	-3.9464985421	-6.6890827374	-2.6704765965
H	-5.1434653751	-6.3942691935	-1.3944017109
H	-2.1061281871	-6.0263143275	-1.2102524248
H	-3.1948959067	-6.7144196775	-0.0071840777
H	-6.0094348047	-4.4315408468	-3.7958295438
H	-6.5738413566	-4.3857466848	-2.1177505397
H	-4.9307506128	-2.1884397094	-3.5118077708
H	-6.6653461606	-2.0982107538	-3.2412697053
H	-5.2049342392	-0.8018195938	-1.5604084455
H	-6.4364098872	-1.8441479479	-0.8762883453
H	-2.6671834913	-3.2355873324	2.9057936846
H	-2.1473935266	-6.0927036047	2.0167732154
H	-3.9298878023	-6.6961371011	3.6474408875
H	-4.5806685027	-5.6114266168	2.4051450658
H	-4.1970628760	-4.9839577816	4.0158176377
H	-1.7896451831	-4.6488893317	4.6714160650
H	-3.0737661645	-1.0698863142	2.0430124407
H	-4.1828453756	-0.3717134556	0.8840365335
H	-5.2535038355	-0.5105151342	3.1372867708
H	-6.1202799101	-1.5513184960	1.9904996671
H	-5.0127295058	-2.2677256504	3.1656411060
H	-0.3008854481	-6.4779837620	5.3364737175
H	-1.9691495126	-6.9765973040	5.1596991411
H	-0.4067693391	-8.7030115013	4.2708115908
H	-1.4475109974	-8.1021469631	2.9766351399
H	0.2345359377	-7.5664625991	3.0825757193
H	0.5163472480	-5.3789727126	2.8561877404
H	-0.4808757110	-5.1319048799	0.4632221331
H	-0.6116729307	-3.4718850547	-0.0725147886
H	1.6820561575	-4.3382522632	-0.4447990614
H	1.7318798043	-3.0122607683	0.7289913038
H	1.8865426042	-4.6884734870	1.2742971109
H	2.0504882980	-4.4725714545	5.4612295558
H	1.6436640937	-1.9619594869	6.4792354291
H	2.8804025919	-1.9102772887	5.2308638934
H	0.1758944104	-0.7427760623	5.1376051248
H	-0.5577712570	-1.0962358163	0.7613514241
H	-0.2580803125	0.7330988121	2.8920516188
H	0.9733699738	0.6349916649	1.6486202301
H	1.9491569766	0.4532260558	3.9832504079
H	2.3117380617	-0.9493196477	2.9679319003

Myrmicarin 430B (proposed structure)
E(SCF) = -1277.971197

C	-1.1862072137	-0.4102159583	2.7072133697
C	-1.4074554705	-1.1912004562	1.5739512108
C	-0.7030254287	-2.4386952193	1.7991115248
C	-0.0848629340	-2.3657216044	3.0434006414
N	-0.3825454041	-1.1319104945	3.5422509182
C	-0.0158741183	-0.4899994480	4.7884992377
C	-1.1535328426	0.5521624597	4.9034108266
C	-1.5181117937	0.8852062234	3.4168344030
C	0.1832959420	-1.5918772832	5.8311708572
C	1.1459079452	-2.6511646665	5.2424562333
C	0.6012260729	-3.3422980687	3.9644194818
C	-2.2140044180	-0.8711042890	0.3392162619
C	-0.6953053180	-3.6494417522	0.8997833306
C	-1.9101559224	-4.5780001270	1.0888834385
C	-3.5605121885	-0.1089816874	0.5944378444
C	-3.9822708736	0.5456342426	-0.7776599512
C	-4.3585783784	2.0418341690	-0.6751462953
C	-5.6135218589	2.3238409551	0.1587679251
C	-2.7854957655	0.2538584422	-1.6479612227
C	-2.6543134847	-0.3731417270	-2.8352416986
N	-1.4377786545	-1.0437718650	-2.9040890446
C	-0.6278851002	-0.7872787150	-1.8068039325
C	-1.5234695118	-0.0335644400	-0.8096344202
C	-0.8016860042	1.2174433518	-0.2521292987
C	-0.3942149949	2.2552178617	-1.3024708939
C	-3.3318614754	-0.5910908522	-4.1644921467
C	-2.1031057980	-0.7941306121	-5.1126432217
C	-1.0218230546	-1.4744585386	-4.2266175055
C	0.6926385641	-1.0485915196	-1.8767883048
C	1.2875707085	-1.5417223916	-3.1856447957
C	0.4543574272	-1.0933401118	-4.4162999847
C	-4.6330956117	-1.0220626623	1.1955134225
H	0.9451298068	0.0374073342	4.6589564326
H	-2.0186765627	0.0956054153	5.3994480497
H	-0.8595329205	1.4365887568	5.4771197987
H	-2.5659429677	1.1845548736	3.3197510163
H	-0.9116862023	1.7272405423	3.0519027777
H	-0.7851832581	-2.0500198886	6.0752279810
H	0.5963000529	-1.1773620930	6.7584639530
H	1.3674956701	-3.4153561009	5.9961258153
H	2.0998137222	-2.1569848100	5.0108317155
H	-0.1121659005	-4.1253277278	4.2643153068
H	1.4216943141	-3.8667994643	3.4578998657
H	-2.4846595494	-1.8248895894	-0.1313701211
H	0.2198860840	-4.2274405894	1.0857297699
H	-0.6375460683	-3.3336411998	-0.1485059754
H	-2.8483503119	-4.0504640895	0.8823307461
H	-1.9640907471	-4.9500293688	2.1189843398
H	-1.8549649859	-5.4449459286	0.4181786491
H	-3.3687621129	0.7014227128	1.3084545981
H	-4.8652462543	0.0186194241	-1.1679552493
H	-4.5105680507	2.4249891006	-1.6933279132
H	-3.5096593944	2.6054417490	-0.2656208757
H	-5.4853753573	2.0208238486	1.2046338885
H	-6.4824384389	1.7829658446	-0.2375656541
H	-5.8581843011	3.3927354784	0.1539695499
H	-1.4506272463	1.6977473863	0.4894632589
H	0.0838327959	0.8799173456	0.3008157989
H	0.3191145011	1.8331149905	-2.0178168468
H	-1.2653199934	2.6090332294	-1.8654577058
H	0.0796020750	3.1222006080	-0.8261549354
H	-3.9592983752	-1.4934692660	-4.1493237640

H	-3.9647919310	0.2465162177	-4.4691910158
H	-1.7359651727	0.1855400149	-5.4422362503
H	-2.3483969162	-1.3782804252	-6.0049232302
H	-1.1143294414	-2.5706992754	-4.3028753229
H	1.3430414694	-0.8693833787	-1.0273947908
H	2.3097510548	-1.1566378125	-3.2954395338
H	1.3842861351	-2.6391436738	-3.1963822750
H	0.5295535560	-0.0033048916	-4.5228111120
H	0.8530050148	-1.5434970517	-5.3329728110
H	-4.8935403000	-1.8285748919	0.4972970018
H	-4.2775882893	-1.4855423456	2.1231224602
H	-5.5533768132	-0.4710548200	1.4227741432

isomyrmicarin 430B

E(SCF) = -1277.984209

C	-4.0111098942	0.3223225416	3.1851388222
C	-2.6599775779	0.4155836933	2.8597927070
C	-2.3156246732	-0.8213229318	2.1890982506
C	-3.4584236981	-1.6140740356	2.1385233993
N	-4.4425727374	-0.9017262992	2.7592985929
C	-5.8433028197	-1.1992195297	2.9836873567
C	-6.4043366511	0.2329329513	3.1570860444
C	-5.2092190227	1.0423726689	3.7653314989
C	-6.3023168731	-2.1150831865	1.8468041063
C	-5.3130387746	-3.3019574740	1.7511022358
C	-3.8560095183	-2.8792251514	1.4215771981
C	-1.6962933028	1.5460603321	3.1110036322
C	-0.9637422435	-1.2005693697	1.6364648466
C	-0.0669308790	-1.9370377684	2.6501766369
C	-1.9174518487	2.3538483697	4.4312081468
C	-1.0865964002	3.6824265959	4.2674934096
C	-1.8624904016	4.9656828137	4.6472045525
C	-2.2650924478	5.0501374380	6.1234284066
C	-0.6845886864	3.6374727962	2.8173220390
C	-1.5461251224	2.6775750256	2.0352733866
N	-0.7284606274	2.4006600103	0.8452791294
C	0.3142728287	3.3507443794	0.7805177287
C	0.4141289160	3.9797534577	2.1151264046
C	1.5649744509	4.8434251983	2.5523299953
C	1.4393462387	6.3123514084	2.1042788259
C	-2.8692619053	3.2050475874	1.4185406351
C	-3.0078219001	2.4131391094	0.0992058317
C	-1.5467549447	2.1198616978	-0.3555706430
C	0.9925782137	3.5970980715	-0.3591841723
C	0.4791539535	2.9772746337	-1.6362638396
C	-1.0636941977	2.9265339080	-1.5734156519
C	-1.5589382395	1.5472608964	5.6820405702
H	-5.9540550004	-1.7485357341	3.9344411718
H	-6.6615978547	0.6454844652	2.1739810482
H	-7.3007956761	0.2619935061	3.7841908674
H	-5.2642884509	2.1014269647	3.4961470198
H	-5.2323766784	0.9926517982	4.8645090189
H	-6.3186402056	-1.5526826694	0.9030437581
H	-7.3184532883	-2.4834499032	2.0308849998
H	-5.6577792492	-4.0169201679	0.9955817476
H	-5.3265179767	-3.8356299841	2.7116394566
H	-3.7669780452	-2.7228051226	0.3357307900
H	-3.1794384677	-3.7100734131	1.6581259894
H	-0.6905580631	1.1107331177	3.1783404993
H	-0.4419810220	-0.3034489755	1.2827389569
H	-1.0981395136	-1.8423431797	0.7544616319
H	-0.5419095243	-2.8624857673	2.9968440259

H	0.1216542650	-1.3150506458	3.5329157912
H	0.9024049468	-2.1965196711	2.2065301811
H	-2.9796510456	2.6286247861	4.4923938017
H	-0.1912198271	3.6370108201	4.9055231088
H	-2.7585817288	5.0423606361	4.0158682817
H	-1.2390219001	5.8335943691	4.3942482306
H	-1.3876256245	4.9837398582	6.7787439122
H	-2.9519753817	4.2442010195	6.4060411590
H	-2.7680668045	6.0004179064	6.3370963831
H	1.6454747663	4.8104436637	3.6466189718
H	2.4991187220	4.4246304879	2.1567022517
H	1.3563766297	6.3873618241	1.0150955583
H	0.5465143949	6.7761922636	2.5384091594
H	2.3138079796	6.8926151065	2.4214878804
H	-3.7377488983	3.0808862762	2.0715339540
H	-2.7565023976	4.2760565891	1.2108808738
H	-3.5667964288	2.9700367199	-0.6614055420
H	-3.5385940960	1.4739905978	0.2807936128
H	-1.4479800575	1.0533561994	-0.5951370914
H	1.7995080874	4.3214702897	-0.3795339148
H	0.8728257438	1.9592402555	-1.7942065925
H	0.7983486985	3.5658456852	-2.5047931411
H	-1.4872417861	2.4792332060	-2.4812082612
H	-1.4408508832	3.9559625853	-1.5105590868
H	-1.7528258432	2.1141776435	6.5999169393
H	-2.1393205782	0.6189125281	5.7268713958
H	-0.4952849701	1.2755238809	5.6774092795

3.17: isomyrmicarin 430C

E(SCF) = -1277.979562

C	0.1511195677	2.2327931821	-1.2701077352
C	-0.7570316226	1.9803721513	-0.0533594633
N	0.0173847849	1.5475434592	1.1330622894
C	1.4225264231	1.4871602048	1.0711018693
C	2.0823296144	1.2325353304	-0.0785047532
C	1.2852448550	1.1895956640	-1.3595211458
C	1.9415284300	1.7965072158	2.4244899980
C	0.9165985327	2.2902527365	3.1547077410
C	-0.3582938448	2.2985016487	2.3375746463
C	-1.4356871591	1.6814607986	3.3250657172
C	-0.6665663056	1.4978024232	4.6807150404
C	0.5618180185	2.4634258739	4.6097428240
C	-1.5363441287	3.2365631443	0.4420059031
C	-0.8031715862	3.6590755905	1.7315873715
C	-2.1641042890	0.4479757798	2.8625804165
C	-1.6277440577	-0.8168314709	2.6448117119
N	-2.6485632953	-1.6207107759	2.2349078889
C	-3.8444548645	-0.9674439739	2.1885030092
C	-3.5801144199	0.3469922670	2.5683644018
C	-2.2907758276	-2.9891069499	1.9176840742
C	-0.9662852618	-3.1151996659	2.7095426225
C	-0.3774635579	-1.6629507353	2.6997130401
C	-3.5132871690	-3.8583096793	2.2197847165
C	-4.7359437079	-3.2391273574	1.4976310528
C	-5.0813254982	-1.8007428366	1.9698731562
C	-4.6218393322	1.4306044492	2.6976887623
C	-5.2549601808	1.5464191284	4.0970389394
C	-1.5638917876	1.6851236959	5.9039260057
C	1.6379797039	2.1991385208	5.6731659514
C	2.5858505893	3.3823180520	5.9072126839
C	3.3795855740	1.5323840652	2.7895138759
C	3.7043429634	0.0376868097	2.9677579361

H	-2.0723325123	-3.0668970559	0.8387324782
H	-1.1843742440	-3.4177387241	3.7411539100
H	-0.2853437484	-3.8534963619	2.2748321654
H	0.2590937047	-1.5009003093	1.8192035254
H	0.2470741658	-1.4729867430	3.5781490536
H	-3.6851316314	-3.8921728426	3.3045036377
H	-3.3535580365	-4.8875308950	1.8771209159
H	-5.6145996898	-3.8801358749	1.6326579061
H	-4.5243912389	-3.2252999022	0.4192788766
H	-5.6504248126	-1.8666705200	2.9096597702
H	-5.7608437339	-1.3350275364	1.2440324488
H	-2.1872559152	2.4624386267	3.4943992707
H	-4.1896575364	2.4027530968	2.4254080402
H	-5.4201852339	1.2488314515	1.9652066681
H	-4.5003469021	1.7841049025	4.8545901121
H	-6.0191416009	2.3334868457	4.1225003175
H	-5.7308492134	0.6035783598	4.3905809050
H	-0.2601451638	0.4778651660	4.7029293049
H	0.1761248323	3.4871489647	4.7629730074
H	1.1421685068	1.9662242990	6.6243254196
H	2.2061371554	1.2998307718	5.4038710614
H	3.0819629336	3.7004312795	4.9835576748
H	2.0370584084	4.2486975193	6.2961726404
H	3.3643264219	3.1286015466	6.6360651215
H	3.6473445913	2.0756513753	3.6992030344
H	4.0202288309	1.9382778201	1.9939555830
H	3.4503688532	-0.5261693539	2.0648174253
H	4.7713321308	-0.1068308850	3.1745458347
H	3.1366672042	-0.3920095362	3.8014842395
H	-1.4244010942	4.2628770659	2.4017286922
H	0.0916456218	4.2445790970	1.4851683787
H	-2.5757549802	2.9711810811	0.6645953719
H	-1.5564785553	4.0325920847	-0.3107005692
H	-1.4661650173	1.1823733916	-0.3048582909
H	3.1656909879	1.1830791860	-0.0987358086
H	0.8522393527	0.1925209516	-1.5460154220
H	1.9270105202	1.4092610016	-2.2212339066
H	0.6077802205	3.2277385854	-1.1877954037
H	-0.4668315617	2.2333093211	-2.1766098347
H	-1.9669437932	2.7058727545	5.9457659919
H	-1.0275559504	1.4995225080	6.8418550517
H	-2.4101250374	0.9901581218	5.8658049655

Compound 3.18

E(SCF) = -1279.202202

C	-5.4985803080	-1.3683327664	2.0863491284
C	-4.1380683966	-0.7328977958	2.2183433329
N	-3.0453509555	-1.5341217762	2.0645838081
C	-2.9245047267	-2.9250457505	1.6723029005
C	-4.2244928925	-3.6278009647	2.0713457060
C	-5.4128634366	-2.8080406952	1.5126941226
C	-3.6573125528	0.4924335743	2.6747353109
C	-2.2177636208	0.3865461954	2.8074216709
C	-1.8861558543	-0.9111158993	2.4292225631
C	-1.5682672974	-3.2810185381	2.3298168902
C	-0.7746191617	-1.9303901507	2.3380462108
C	-1.3003245695	1.4610700520	3.3371660299
C	-0.3774610735	2.2087113420	2.3275419461
C	0.7845428269	2.8265217433	3.1920073918
C	0.5796783685	2.2413271128	4.6422636763
C	-0.3200922693	1.0041088591	4.4400958100
N	0.3045709453	1.2760818721	1.3806675182

C	1.6759006940	1.6149785573	1.3910972121
C	2.0248517071	2.4586246423	2.3873800263
C	2.5722536009	1.0349640462	0.3231268550
C	1.7904132740	0.5896053720	-0.9314776151
C	0.5488052106	1.4672732343	-1.1059355068
C	-0.4110195323	1.2515631855	0.0712801704
C	-1.0975105371	3.1924524980	1.3854327170
C	-1.5232417125	2.3302324604	0.1856329745
C	3.3818047176	3.1157163402	2.5242217205
C	4.5434634876	2.2518406494	3.0509549107
C	-1.0139932505	0.5003560103	5.7066139083
C	1.8295035493	1.9639751343	5.4877137720
C	2.5027959959	3.2142128774	6.0667191050
C	-4.5223550970	1.6735372901	3.0403440444
C	-4.9469799012	1.7063432465	4.5209087891
H	-2.8233006786	-2.9883863570	0.5755476049
H	-1.7398960407	-3.6114262488	3.3616381888
H	-1.0429466729	-4.0822987654	1.8004939765
H	-0.1841538622	-1.8151353855	1.4182314718
H	-0.0681699761	-1.8802315885	3.1715351223
H	-4.2879833247	-3.6949320956	3.1662285668
H	-4.2496227556	-4.6498425838	1.6750711678
H	-6.3556569075	-3.3296216948	1.7131977773
H	-5.3118020554	-2.7589112445	0.4194308635
H	-5.9784500187	-1.4110017165	3.0760965376
H	-6.1688785257	-0.7673026386	1.4578556339
H	-1.9326511422	2.2393971455	3.7911805229
H	-4.0047059789	2.6109046333	2.7983543112
H	-5.4254489936	1.6665514270	2.4149278224
H	-4.0736608401	1.7490724884	5.1813159104
H	-5.5776505903	2.5785810514	4.7342828452
H	-5.5138086915	0.8060464563	4.7854811609
H	0.3010640361	0.1954311843	4.0284950970
H	-0.0295981251	2.9792140295	5.1912633537
H	1.5459449191	1.3165112340	6.3281265272
H	2.5436957549	1.3848194248	4.8915590681
H	2.8207978669	3.9126231656	5.2858161311
H	1.8147812373	3.7539987712	6.7295737231
H	3.3893284639	2.9502788970	6.6560067351
H	3.2836010092	4.0035190109	3.1612109103
H	3.6877607979	3.5033937588	1.5394271793
H	4.6758843056	1.3533085131	2.4384715709
H	5.4843193082	2.8156283028	3.0224343296
H	4.3808796961	1.9282341692	4.0828757863
H	-1.9365886906	3.7080609671	1.8656650624
H	-0.3796579784	3.9584321437	1.0638725525
H	-2.4896790201	1.8562623490	0.3786676907
H	-1.6158147138	2.9127669065	-0.7382342277
H	-0.8711901284	0.2621654231	-0.0472740727
H	3.3125570901	1.7976243199	0.0481705418
H	1.4738669977	-0.4573798476	-0.8289479087
H	2.4394063673	0.6349255710	-1.8138610751
H	0.8469595004	2.5248651810	-1.1611278229
H	0.0236512818	1.2343792255	-2.0407185776
H	-1.6003039545	1.3015331854	6.1769458852
H	-0.2977687008	0.1341126161	6.4512670232
H	-1.7001333494	-0.3207654572	5.4725977326
H	0.6915530904	3.9205955740	3.2495025279
H	3.1485039548	0.1903724488	0.7250397940

Compound 3.22a

E(SCF) = -1278.400309 Gibbs Energy = -1277.783449

C	-1.8123542833	-2.3270548217	-3.8814073335
C	-2.9408806214	-3.0356029246	-3.0891871486
N	-2.1504979709	-3.8510297974	-2.1729817581
C	-0.8519662820	-3.4753836463	-2.0185328388
C	-0.6035642570	-2.2635688402	-2.8871684519
C	-0.2036994077	-4.4767795501	-1.2880443048
C	-1.1916539070	-5.5119930774	-1.0549988482
C	-2.3849936210	-5.0858395427	-1.6407295863
C	-3.9298284958	-3.9615981262	-3.8008802608
C	-4.6566701385	-4.8190230350	-2.7409646242
C	-3.7042153003	-5.7495296107	-1.9450650388
C	1.2567717094	-4.3641451548	-0.8694275932
C	2.1064803149	-5.6382391386	-1.0512959274
C	2.1068910789	-6.1722441974	-2.4878496133
C	-1.0464413245	-6.8767640218	-0.4214569426
C	-1.0904573261	-6.9112954543	1.1158478308
C	1.3394584613	-3.7945651219	0.5805832906
C	2.7544639476	-3.3030172578	0.9795268219
C	0.3931275773	-2.6352889298	0.6881309206
C	-0.3957610484	-2.2780972363	1.7507360064
C	-1.2302314188	-1.0564775025	1.8573031308
C	-1.8280977282	-1.0776293732	3.0857241374
N	-1.4166561380	-2.2629442578	3.7121300683
C	-0.5662914996	-2.9796088517	3.0041858133
C	-1.7664748059	-2.8007881253	5.0318779142
C	-2.0756431294	-1.6156444825	5.9467513176
C	-3.1246558155	-0.7190031981	5.2482307513
C	-2.6275198540	-0.1048688236	3.9133550578
C	-0.1071955591	-4.1568380197	3.8237302953
C	-0.5611274379	-3.7427792185	5.2650263103
C	-1.3354479051	0.0335904671	0.8276049811
C	-0.1516343931	1.0214830472	0.8428913304
H	-2.6839820229	-3.3946492228	4.9078164786
H	0.2469556749	-3.1957881052	5.7632618683
H	-0.8201033853	-4.6047330373	5.8835489557
H	0.9700497172	-4.3286215965	3.7555662146
H	-0.6029537331	-5.0777383336	3.4897655195
H	-1.1566576324	-1.0513957298	6.1542614894
H	-2.4628352709	-1.9755012989	6.9052400665
H	-3.4221331204	0.0942697830	5.9165763846
H	-4.0279791821	-1.3151306266	5.0638531950
H	-1.9914352841	0.7636713523	4.1332105155
H	-3.4788398866	0.2820559965	3.3420535209
H	0.4207466388	-1.9395615126	-0.1473393971
H	-1.4265804396	-0.4146140517	-0.1695354914
H	-2.2675674232	0.5861123036	0.9931010176
H	-0.0686704347	1.5225752815	1.8130114899
H	0.7997703966	0.5141124175	0.6491016284
H	-0.2867059034	1.7909888428	0.0757857909
H	1.0344862525	-4.5802665567	1.2798171361
H	1.7020872353	-3.5947479662	-1.5209663683
H	1.7616711800	-6.4191292519	-0.3621064071
H	3.1406455058	-5.4163074731	-0.7616925455
H	2.4985830298	-5.4230154916	-3.1867076228
H	1.0989641317	-6.4407097770	-2.8190306258
H	2.7396769753	-7.0623665570	-2.5687919904
H	-1.8614371963	-7.5080135097	-0.7960233477
H	-0.1257557054	-7.3637897316	-0.7626208016
H	-0.2247171690	-6.3985243777	1.5511271057
H	-1.9990686147	-6.4254651296	1.4916880161
H	-1.0795016596	-7.9435428844	1.4840743113
H	-0.6199408072	-1.3172383233	-2.3251328373

H	0.3570572106	-2.3023803955	-3.4104870028
H	-2.1109477902	-1.3412389315	-4.2489898760
H	-1.5367797200	-2.9411105110	-4.7463403045
H	-3.5113576372	-2.2936775274	-2.5083674059
H	-4.2080581178	-6.0887226592	-1.0311067004
H	-3.5128639875	-6.6577631452	-2.5338491273
H	-5.4312090650	-5.4278672447	-3.2182437591
H	-5.1769050283	-4.1460552613	-2.0457131567
H	-3.3899085095	-4.6057318590	-4.5080445878
H	-4.6528920814	-3.3749309972	-4.3779110582
H	3.4640446564	-4.1350253360	0.9639069673
H	2.7606732605	-2.8752401587	1.9876775730
H	3.1169722830	-2.5367738113	0.2846034834

Compound 3.22b

E(SCF) = -1278.402608 Gibbs Energy = -1277.785993

C	-0.0189628786	-1.0061612046	1.8500618961
C	-0.0443606287	-2.4249843286	1.5632857315
C	-1.4382144106	-2.8634131282	1.8181073628
C	-2.1404493144	-1.7660571627	2.2290039681
N	-1.2316906983	-0.6948607362	2.2571303650
C	-1.4395578578	0.7060041945	2.6419388766
C	-0.2471459915	1.3679890467	1.9110546610
C	0.8318418810	0.2360199619	1.8177647457
C	-2.8940667251	1.0599092682	2.3304800832
C	-3.8057333920	0.0034810544	2.9981773096
C	-3.5932644092	-1.4371751090	2.4611532909
C	0.9859967186	-3.1982175008	1.1038389669
C	-1.9693758575	-4.2559309075	1.6244299165
C	-1.6125969688	-5.2147795893	2.7776370793
C	2.3579345776	-2.7613348758	0.6956479951
C	3.3862275119	-3.7848078016	1.2653737397
C	4.8488305228	-3.3514633551	1.0198282235
C	5.8729034896	-4.4089536701	1.4457196719
C	3.0619947509	-4.1118435010	2.7158985343
C	2.6398783208	-5.3697249353	3.1494738184
N	2.4603448620	-5.2985724411	4.4951133350
C	2.7935529742	-4.0710834686	4.9934353681
C	3.1595369481	-3.2829716844	3.9031646046
C	3.6420731208	-1.8553581522	4.0236124345
C	5.1087613740	-1.7163655105	4.4757179530
C	2.4804449811	-6.8122076273	2.7273325595
C	2.6632741258	-7.5653762778	4.0894731490
C	2.1715114957	-6.5617662951	5.1636445761
C	2.8665347986	-3.9153644300	6.4916744248
C	2.3861515989	-5.1892127643	7.2378320660
C	2.8169553215	-6.5058664338	6.5500965954
C	2.3826224915	-2.6485883909	-0.8500418391
H	-1.2910747513	0.7683439659	3.7299631906
H	-0.5508334909	1.6711497857	0.9030734909
H	0.1215938135	2.2522635401	2.4350652874
H	1.4410690646	0.3120565504	0.9133394263
H	1.5203925982	0.2543681100	2.6735477304
H	-3.0515199065	1.0822308709	1.2440151825
H	-3.1255933457	2.0576993936	2.7166010428
H	-3.6245494905	0.0203305634	4.0809738912
H	-4.8556022085	0.2761243089	2.8569430542
H	-4.1266155524	-1.5478396131	1.5067058436
H	-4.0497287134	-2.1570461296	3.1488414033
H	0.7655681548	-4.2496320823	0.9226812252
H	-3.0590694482	-4.2084008814	1.5173389210
H	-1.5928665410	-4.6656752471	0.6782776190

H	-0.5283429305	-5.2918182134	2.9142331440
H	-2.0422251709	-4.8658540416	3.7221412792
H	-2.0061075465	-6.2160972746	2.5742657288
H	2.5704982787	-1.7742222686	1.1178691074
H	3.2304989328	-4.7156206600	0.6974712941
H	5.0481378791	-2.4114273056	1.5485237611
H	4.9879736452	-3.1392974462	-0.0473381847
H	5.7250076581	-5.3462407754	0.8953029819
H	5.7980042795	-4.6321042621	2.5147308731
H	6.8922110602	-4.0642711017	1.2418489095
H	3.0064055100	-1.3172347160	4.7419536959
H	3.5207100663	-1.3321486539	3.0672640264
H	5.7903707013	-2.2058535352	3.7723888339
H	5.2634781991	-2.1768111177	5.4571624549
H	5.3981462376	-0.6618301873	4.5521864580
H	1.4882350860	-7.0227059044	2.3015643293
H	3.2194433772	-7.1288220003	1.9845974790
H	2.1225737235	-8.5153499570	4.1239055221
H	3.7273853473	-7.7749565004	4.2481597484
H	1.0816749747	-6.6602050247	5.2907357343
H	3.9077750347	-3.7081997136	6.7758754913
H	2.2877583261	-3.0484775837	6.8377798756
H	1.2900959111	-5.1797194169	7.3115941408
H	2.7646000336	-5.1620398060	8.2648286178
H	3.9102336796	-6.5477294022	6.4525162559
H	2.5072109608	-7.3673995533	7.1515730940
H	3.3590535336	-2.2909289327	-1.1884874937
H	1.6235680291	-1.9472121101	-1.2127374996
H	2.1975803149	-3.6214524387	-1.3196002985

Compound 3.25

E(SCF) = -1278.39282 Gibbs Energy = -1277.773113

C	-1.9408946579	-2.1352381252	-3.1989947037
C	-2.9074852987	-2.7196619573	-2.1383134041
N	-2.0181493756	-3.6643716521	-1.4468711061
C	-0.6613953194	-3.3745893278	-1.5425634854
C	-0.5107445647	-2.2660779186	-2.5827989040
C	0.0171272533	-4.6161191452	-1.2983406921
C	-0.9565028585	-5.5981252024	-1.0296979185
C	-2.2215344883	-4.9664579082	-1.1768315697
C	-4.1498418219	-3.4726921064	-2.6241166907
C	-4.6585399593	-4.4165972015	-1.5176151778
C	-3.6202455301	-5.5106704249	-1.1788245650
C	1.4919681993	-4.5083006151	-0.9722884250
C	2.3357397655	-5.7888901357	-0.9724945773
C	2.4772664261	-6.4241284819	-2.3610994533
C	-0.8103435702	-7.0638189711	-0.6914711282
C	-0.8063730835	-7.3929380462	0.8114824631
C	1.4327782299	-3.7643444131	0.3935717104
C	2.7631945414	-3.1489586173	0.8576050127
C	0.3622896604	-2.6757722967	0.2720562510
C	-0.5105390948	-2.3239201542	1.3328447968
C	-1.2364166090	-1.0532552158	1.4596784518
C	-1.9414514306	-1.0942929637	2.6407117933
N	-1.6923459363	-2.3317340448	3.2056726978
C	-0.8375572667	-3.0786171482	2.4944793502
C	-2.1568401129	-2.9077927196	4.4666062873
C	-2.4284316240	-1.7542453608	5.4329385944
C	-3.3466684408	-0.7291039442	4.7280357750
C	-2.7069291543	-0.0918978830	3.4671161456
C	-0.5318210867	-4.3289660924	3.2891813174
C	-1.0356747886	-3.9417548336	4.7203975456

C	-1.1418601721	0.1431093840	0.5493721595
C	0.1112108010	1.0087060939	0.7876475002
H	-3.1060412254	-3.4310645831	4.2735334353
H	-0.2206469710	-3.4708644375	5.2815557615
H	-1.3838667415	-4.8069381208	5.2899128796
H	0.5296498942	-4.5908045166	3.2905751740
H	-1.0770405783	-5.1975314434	2.8986655917
H	-1.4809054712	-1.2846475389	5.7295021050
H	-2.9074685440	-2.1298054190	6.3431588702
H	-3.6196475535	0.0685179766	5.4257091562
H	-4.2826633025	-1.2320968885	4.4503567005
H	-2.0165092416	0.7038795381	3.7805577580
H	-3.4819522642	0.4026142518	2.8691982915
H	0.6784550118	-1.8397757156	-0.3464768728
H	-1.1682607140	-0.1745664638	-0.5000073811
H	-2.0343806341	0.7647760075	0.6903958756
H	0.1345498670	1.3874014450	1.8149993324
H	1.0323918850	0.4372125664	0.6275262201
H	0.1242450839	1.8689450977	0.1095095016
H	1.1033614739	-4.4980341488	1.1370808251
H	1.9411188927	-3.8174519104	-1.7046777376
H	1.9201598872	-6.5132485023	-0.2616494347
H	3.3357822192	-5.5405049547	-0.5973484616
H	2.9715995125	-5.7374044569	-3.0580766022
H	1.5048104542	-6.6868289488	-2.7932494766
H	3.0797227509	-7.3368876931	-2.3135018445
H	-1.6390505062	-7.6080679215	-1.1632330455
H	0.0978947327	-7.4623018469	-1.1514538934
H	0.0453237209	-6.9285281280	1.3208787496
H	-1.7236887083	-7.0419519980	1.2991505042
H	-0.7394375090	-8.4749202070	0.9675907267
H	-0.1878870465	-1.3146997127	-2.1463734493
H	0.2314265068	-2.5291070214	-3.3431277242
H	-2.1885883454	-1.1038423072	-3.4648547172
H	-2.0063803592	-2.7377824208	-4.1116773672
H	-3.2056495860	-1.9457346429	-1.4181323175
H	-3.8573473937	-5.9780103049	-0.2142512959
H	-3.6705775901	-6.3213772853	-1.9194909229
H	-5.5948774200	-4.8917800334	-1.8252713660
H	-4.8853461964	-3.8301388094	-0.6176000834
H	-3.9006068762	-4.0531872353	-3.5227887458
H	-4.9267112955	-2.7560347117	-2.9093168508
H	3.5238282593	-3.9230547672	1.0020192156
H	2.6427419552	-2.6207323004	1.8093309538
H	3.1471498018	-2.4339942774	0.1200152241

Compound 3.19

E(SCF) = -1278.411939 Gibbs Energy = -1277.790663

C	-2.1992772586	-1.9689966466	-2.3590323183
C	-3.0534257197	-2.9428875173	-1.4949635520
N	-2.0335294307	-3.9241211638	-1.0526970077
C	-0.6450284801	-3.4774112005	-1.2331721730
C	-0.8386467712	-2.6866749380	-2.5578859821
C	0.1050577743	-4.7762853237	-1.2449577609
C	-0.7732041103	-5.8251026543	-1.1568338515
C	-2.1070979834	-5.2351225303	-1.1312526225
C	-4.1951439370	-3.6832877115	-2.1978051379
C	-4.6022912049	-4.9218204789	-1.3831434706
C	-3.4303413281	-5.9194576739	-1.2723847092
C	1.5475283916	-4.5187852096	-0.9133088967
C	2.4703768624	-5.7089338471	-0.6209687211
C	2.9821250427	-6.4256180790	-1.8771707547

C	-0.5447225455	-7.3134846240	-1.0673288954
C	-0.7060363660	-7.8891832724	0.3526132286
C	1.3257456912	-3.5373479692	0.2944233278
C	2.5478543801	-2.7013821468	0.6689252038
C	0.0829651596	-2.6519774620	-0.0852462992
C	-0.7421738094	-2.1827113607	1.0806715061
C	-1.0829111110	-0.8006838694	1.3599347486
C	-1.7905044555	-0.7772502826	2.5592572528
N	-1.8979270213	-2.0741726314	2.9647181710
C	-1.2668754903	-2.9425513268	2.1275966937
C	-2.4770783151	-2.6546374714	4.1684591020
C	-2.3877790948	-1.6017383836	5.2748393682
C	-2.9918122600	-0.2811598655	4.7400854637
C	-2.2340478204	0.3000962952	3.5166833232
C	-1.3530734440	-4.3192351388	2.7503846050
C	-1.6839807697	-3.9812723807	4.2431175251
C	-0.6665395054	0.4268141405	0.5857906639
C	0.6743913691	1.0359025894	1.0387031031
H	-3.5409741608	-2.8746401324	3.9832240302
H	-0.7506111892	-3.8191862831	4.7944154681
H	-2.2408171875	-4.7778118522	4.7444744559
H	-0.4325774086	-4.9048004207	2.6647907856
H	-2.1575062258	-4.9275957479	2.3085668581
H	-1.3382133667	-1.4559241585	5.5638501237
H	-2.9321212131	-1.9338199562	6.1655619658
H	-3.0093440874	0.4702942970	5.5359548434
H	-4.0394595449	-0.4663080223	4.4664344633
H	-1.3488156684	0.8462029460	3.8720957307
H	-2.8640186725	1.0473394602	3.0181467206
H	0.4706500610	-1.7609528568	-0.5899787106
H	-0.6061870483	0.2029357046	-0.4883436702
H	-1.4491368698	1.1904743494	0.6795938437
H	0.6400192453	1.3139894235	2.0976600065
H	1.4988816019	0.3253585193	0.9119897228
H	0.9121662414	1.9365677497	0.4610914266
H	1.0490985517	-4.1578187689	1.1549076830
H	1.9887438775	-3.9277196499	-1.7331801503
H	1.9627053612	-6.4142325950	0.0488067787
H	3.3354054636	-5.3366560147	-0.0600257120
H	3.5922237267	-5.7521112158	-2.4899961664
H	2.1660044514	-6.7921332663	-2.5110566308
H	3.6063909014	-7.2841407494	-1.6090110322
H	-1.2498039836	-7.8201322596	-1.7401590311
H	0.4510091643	-7.5516155926	-1.4467190007
H	0.0226871779	-7.4522863583	1.0433443230
H	-1.7056597270	-7.7006150439	0.7609561662
H	-0.5524138407	-8.9726865859	0.3399137414
H	-0.0145319135	-1.9965867876	-2.7522992062
H	-0.8942132522	-3.3912454307	-3.3961334380
H	-2.0625165415	-1.0240922012	-1.8270025604
H	-2.6841767595	-1.7437397218	-3.3131945401
H	-3.4258278603	-2.4377872646	-0.5979835956
H	-3.5726070835	-6.6117041658	-0.4325220750
H	-3.3703238612	-6.5567302387	-2.1659453461
H	-5.4576356679	-5.4236023343	-1.8444942844
H	-4.9217102744	-4.6112260730	-0.3805699112
H	-3.8778756291	-3.9833871296	-3.2064310245
H	-5.0427946659	-3.0015887205	-2.3184228099
H	3.3855320176	-3.3252396738	0.9969091846
H	2.3009511837	-2.0236691925	1.4931523617
H	2.8898061021	-2.0949380260	-0.1791630582

Compound 3.26

E(SCF) = -1278.392392 Gibbs Energy = -1277.772739

C	0.8309230642	-3.1293487094	3.9850397483
C	-0.0822040203	-2.2577710035	3.1607157218
N	-0.6429946882	-1.1556931095	3.7798748413
C	-0.4063100052	-0.5908027448	5.1076756857
C	0.0420977736	-1.7313857398	6.0221097740
C	1.2149042953	-2.4724794704	5.3375606858
C	-0.6776187376	-2.3547399222	1.9225758778
C	-1.6618029952	-1.2719033439	1.8203253375
C	-1.5905009571	-0.5570119213	3.0466056495
C	-1.7405871402	0.1605033285	5.3252704886
C	-2.2154363085	0.5381907448	3.8812588323
C	-2.5052463907	-1.0318798897	0.7058120728
C	-3.7951596151	-0.2121046627	0.8022933659
C	-4.9311070527	-1.1242292052	1.3074576955
C	-0.4321671440	-3.4358611979	0.9047044535
C	-1.4306813858	-4.6074886429	0.9858214320
C	-4.1112139354	0.4540102617	-0.5859145544
C	-4.5517428510	1.9326699112	-0.5001449934
C	-5.8846608520	2.1557907608	0.2223711546
C	-2.8577815373	0.2205730367	-1.3893126443
C	-1.5371075678	0.2751449806	-0.7298993227
C	-0.6393804406	-0.4274686407	-1.6031894083
N	-1.3781704117	-0.8879915964	-2.6139247282
C	-2.7096123271	-0.5167060976	-2.5334859995
C	0.8550861091	-0.5498501623	-1.6993957453
C	1.2930180098	-1.4719299478	-2.8698488622
C	0.4284795912	-1.3194796220	-4.1453892800
C	-1.0201483299	-1.6681531106	-3.7985288565
C	-3.4088460796	-1.0636551308	-3.7539896705
C	-2.2059187920	-1.3110490678	-4.7288048907
C	-1.0196963256	1.3809044430	0.1712586367
C	-0.6320007508	2.6642880171	-0.5841770414
H	0.4170512685	0.1352512332	5.0266002338
H	-2.4718150057	-0.5124104123	5.7871591909
H	-1.6285172108	1.0349015179	5.9707385200
H	-3.3055859959	0.5693690003	3.8066663703
H	-1.8429796747	1.5299271313	3.5900637887
H	-0.7963864090	-2.4168812531	6.2037921326
H	0.3592350765	-1.3351332542	6.9922801988
H	1.6078330757	-3.2455388029	6.0049008467
H	2.0320524341	-1.7563667301	5.1773780645
H	0.3214007095	-4.0827025848	4.1828661976
H	1.7405600690	-3.3851385881	3.4287229385
H	-2.5638261609	-1.8533636571	-0.0035536089
H	0.5849425165	-3.8253266597	1.0358362825
H	-0.4612990457	-3.0061285843	-0.1057045462
H	-2.4613301905	-4.2678304790	0.8328227326
H	-1.3866734236	-5.0917883875	1.9670581037
H	-1.2059371790	-5.3641566898	0.2258466415
H	-3.6481193711	0.5857501651	1.5374660601
H	-4.9311396424	-0.1024780837	-1.0588043564
H	-4.6303553002	2.3167514644	-1.5252300446
H	-3.7648635494	2.5251239612	-0.0154738451
H	-5.8355473657	1.8687870853	1.2790990429
H	-6.6922249471	1.5789011053	-0.2442887598
H	-6.1701509009	3.2121509431	0.1859854813
H	-1.7690227038	1.6322757392	0.9272593997
H	-0.1523518936	0.9987577442	0.7248139660
H	0.1592868785	2.4817613359	-1.3195707608
H	-1.4914835370	3.0819632421	-1.1187127031

H	-0.2657385980	3.4248013865	0.1142137779
H	-3.9348005572	-2.0046932536	-3.5418232162
H	-4.1420451164	-0.3702538484	-4.1740343136
H	-1.9802582867	-0.3893477064	-5.2770828108
H	-2.4116353596	-2.0985975266	-5.4576541607
H	-1.0756936703	-2.7345833372	-3.5332829761
H	1.2770369086	-0.9123537957	-0.7538929814
H	1.2742860318	0.4569293284	-1.8439779684
H	2.3423523027	-1.2688020492	-3.1050559683
H	1.2468138577	-2.5185613789	-2.5403080023
H	0.4797449360	-0.2914313910	-4.5262543353
H	0.8026067599	-1.9806486775	-4.9334241099
H	-5.1055285310	-1.9542188625	0.6123636500
H	-4.7005212190	-1.5496558093	2.2895205267
H	-5.8644592563	-0.5586267207	1.3904882810

Compound 3.27

E(SCF) = -1278.404143 Gibbs Energy = -1277.782794

C	-1.1407783858	-0.3948653420	2.6717393015
C	-1.4390607241	-1.1729453775	1.5511045942
C	-0.7251657997	-2.4273706911	1.7164517815
C	-0.0304826671	-2.3607112052	2.9195919800
N	-0.2889176835	-1.1259734191	3.4400126961
C	0.1205929249	-0.5131052051	4.6969494156
C	-1.0190568505	0.5164488734	4.8833077677
C	-1.4546552695	0.8811849171	3.4237111858
C	0.3597608253	-1.6398442231	5.7033226453
C	1.3014402039	-2.6825554362	5.0564948681
C	0.7086080823	-3.3485595302	3.7870966849
C	-2.2984725518	-0.8471632564	0.3724323173
C	-0.8135390704	-3.6477393192	0.8331104503
C	-2.0227962561	-4.5533865834	1.1375126303
C	-3.6414500170	-0.0770410690	0.6201519530
C	-4.0871450071	0.4999909454	-0.7813217942
C	-4.5229037963	1.9848690440	-0.7687826602
C	-5.7830216105	2.2531987003	0.0597137444
C	-2.8745452367	0.2184538883	-1.6275736074
C	-2.6658359743	-0.3319060816	-2.8422926441
N	-1.3478673114	-0.8621737202	-2.8352467711
C	-0.6939872392	-0.6867702245	-1.7214749332
C	-1.6174276374	0.0372487790	-0.7907353282
C	-0.9549929711	1.3242263696	-0.2268636991
C	-0.5544070597	2.3655461187	-1.2788025473
C	-3.2357912304	-0.6024756158	-4.2111753803
C	-1.9448864413	-0.8151100408	-5.0728373212
C	-0.9411806281	-1.4846768426	-4.1037339020
C	0.7551063538	-1.0403650351	-1.6509729601
C	1.2432311747	-1.7922508508	-2.9176447587
C	0.5733411396	-1.3062549048	-4.2266027383
C	-4.6937574921	-0.9683749774	1.2832355240
H	1.0720901718	0.0191102118	4.5379872519
H	-1.8575935194	0.0434190545	5.4073731415
H	-0.7065971318	1.3906607764	5.4608486961
H	-2.5095882701	1.1679656604	3.3784822960
H	-0.8729845841	1.7370783190	3.0521627285
H	-0.5978838018	-2.1039444829	5.9757856137
H	0.8066107926	-1.2438900318	6.6216784131
H	1.5494552511	-3.4631228750	5.7829646810
H	2.2468186613	-2.1851870458	4.8007545794
H	0.0131672767	-4.1428846999	4.0936918155
H	1.5090506276	-3.8517118686	3.2304569578
H	-2.5704219490	-1.7911854341	-0.1152264609

H	0.1057380093	-4.2375017642	0.9418192731
H	-0.8510506339	-3.3552339064	-0.2272061916
H	-2.9681224484	-4.0138205208	1.0082042754
H	-1.9898184374	-4.9097174218	2.1726105015
H	-2.0377578444	-5.4294608046	0.4784528233
H	-3.4405994642	0.7697428730	1.2866036480
H	-4.9322434642	-0.0880112751	-1.1632989292
H	-4.6991636822	2.2998076526	-1.8055977165
H	-3.6981506210	2.6066771885	-0.3977706935
H	-5.6318220076	2.0264919573	1.1209075160
H	-6.6287632518	1.6524199868	-0.2949890370
H	-6.0708095349	3.3069338340	-0.0125454628
H	-1.6462266261	1.7815013082	0.4857757031
H	-0.0833899676	1.0105982957	0.3591345937
H	0.1791242240	1.9776625061	-1.9956345264
H	-1.4207788887	2.7176141361	-1.8482126491
H	-0.1005547023	3.2348956537	-0.7923508178
H	-3.8577785446	-1.5074344349	-4.2163961041
H	-3.8514969960	0.2195611868	-4.5825726356
H	-1.5534496660	0.1536868346	-5.4032223552
H	-2.1297790444	-1.4269796221	-5.9583615570
H	-1.1762608861	-2.5552220296	-4.0241796625
H	0.9478593308	-1.6189674011	-0.7386340316
H	1.3122824382	-0.1008194858	-1.5180642787
H	2.3291517605	-1.6866340008	-2.9946611046
H	1.0445070391	-2.8643111806	-2.7960444805
H	0.8061336952	-0.2499248397	-4.4143096509
H	0.9529771912	-1.8803446906	-5.0772739742
H	-4.9501067881	-1.8202809355	0.6409349885
H	-4.3244035495	-1.3642065035	2.2347744766
H	-5.6161776268	-0.4133309639	1.4828634382

References

1. M. W. Schmidt, K. K. Baldridge, J. A. Boatz, S. T. Elbert, M. S. Gordon, J. H. Jensen, S. Koseki, N. Matsunaga, K. A. Nguyen, S. J. Su, T. L. Windus, M. Dupuis, J. A. Montgomery, *J. Comput. Chem.* **1983**, *14*, 1347 – 1363.

2. Jaguar, version 7.6, Schrödinger, LLC, New York, NY, **2009**.

3. D. J. Tannor, B. Marten, R. Murphy, R. A. Friesner, D. Sitkoff, A. Nicholls, M. Rinalda, W. A. Goddard III, B. Honig, *J. Am. Chem. Soc.* **1994**, *116*, 11875 – 11882.

4. J. Simons, P. Jorgensen, H. Taylor, J. Ozment, *J. Phys. Chem.* **1983**, *87*, 2745 – 2753.

5. F. Schröder, Ph.D. Thesis, University of Hamburg (Germany), **1996**.

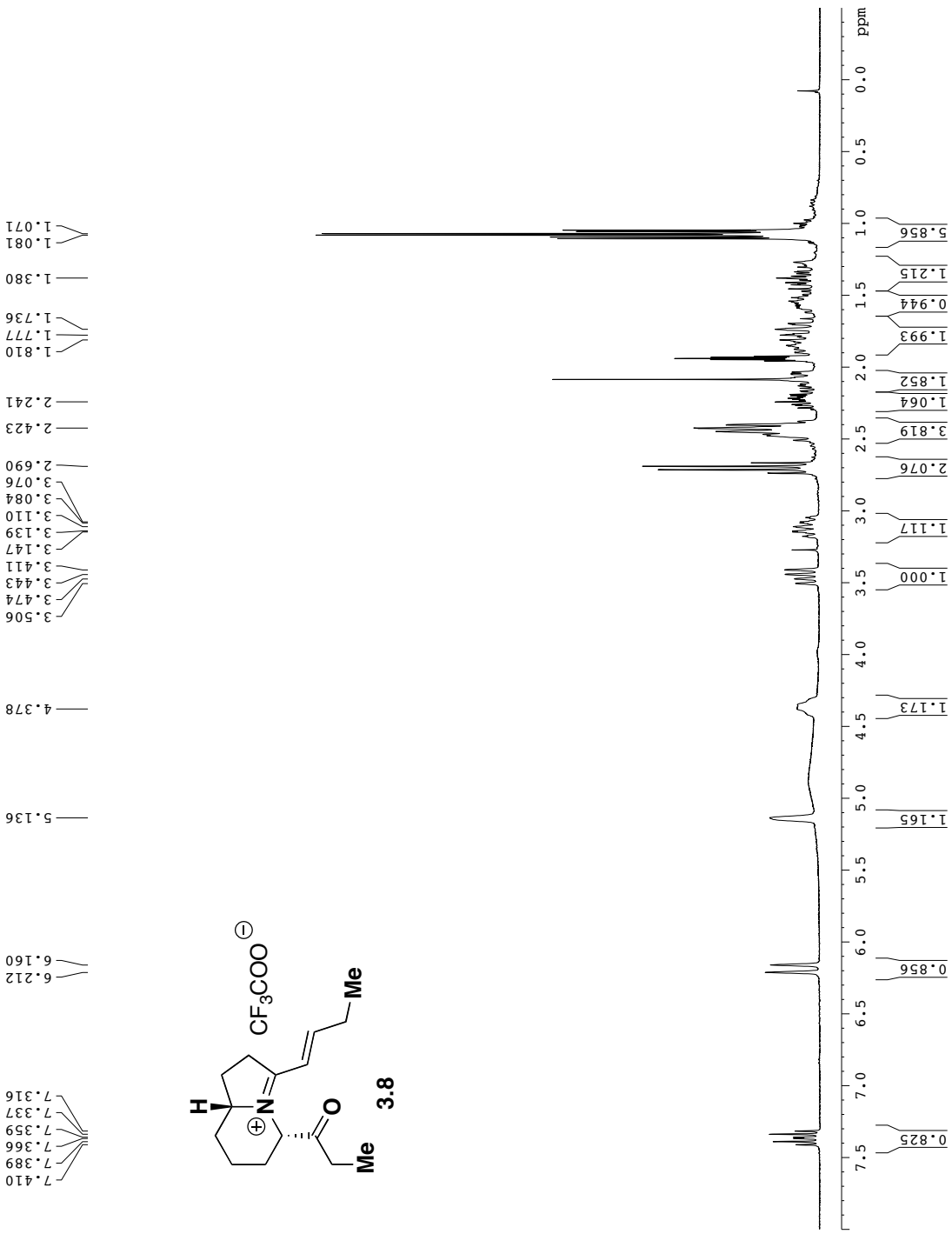
7.410
7.389
7.366
7.359
7.337
7.316
6.212
6.160
5.136
4.378
3.506
3.474
3.443
3.411
3.147
3.139
3.110
3.084
3.076
2.690
2.423
2.241
1.810
1.777
1.736
1.380
1.081
1.071
CF3COO
Me
Me
O
H
N
3.8
ppm
0.825
0.856
1.165
1.173
1.000
1.117
2.076
3.819
1.064
1.852
1.993
0.944
1.215
5.856

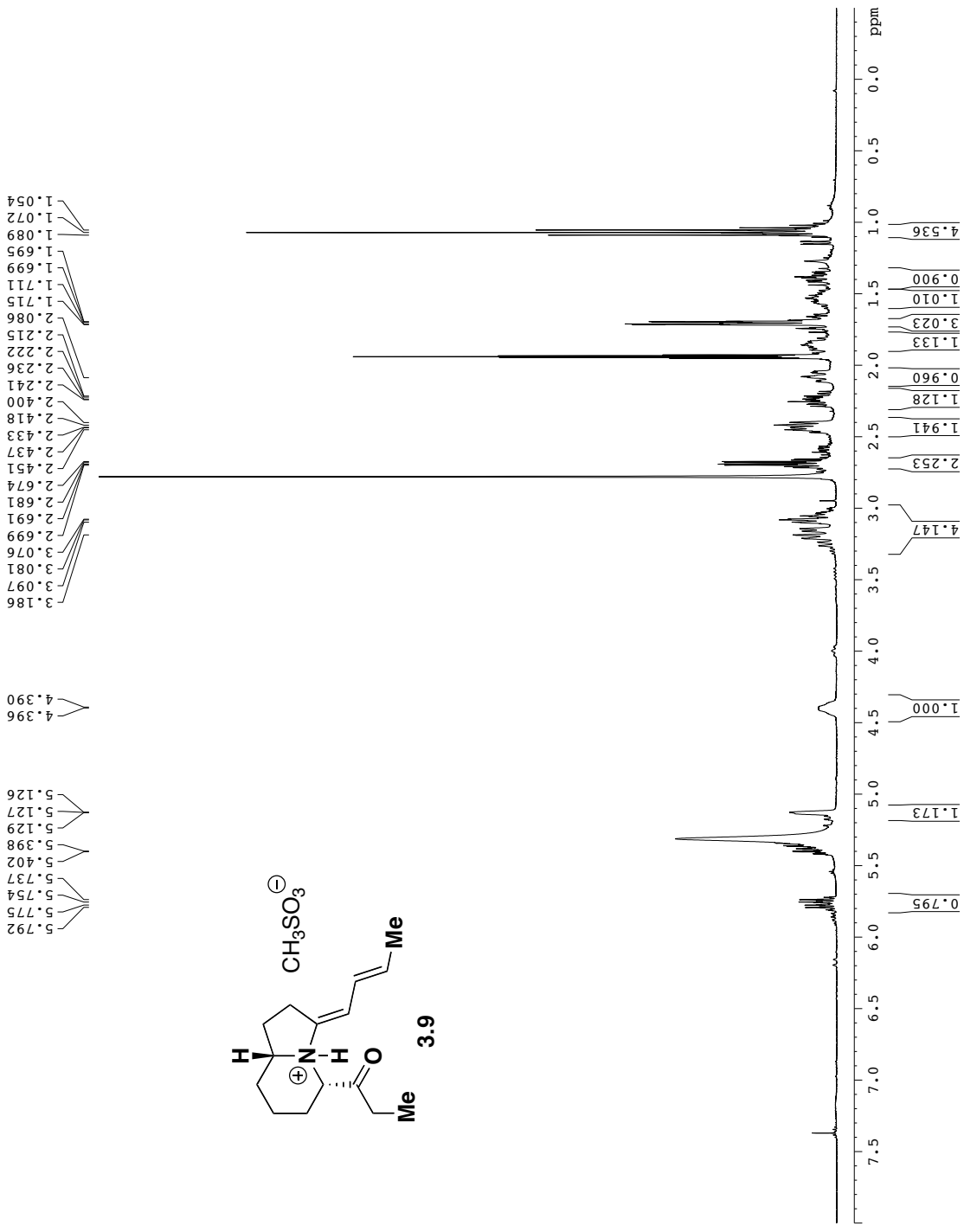
ppm
0.0
0.5
1.0
1.5
2.0
2.5
3.0
3.5
4.0
4.5
5.0
5.5
6.0
6.5
7.0
7.5
4.536
0.900
1.010
3.023
1.133
0.960
1.128
1.941
2.253
4.147
1.000
1.173
0.795
1.054
1.072
1.089
1.695
1.699
1.711
1.715
2.086
2.215
2.222
2.236
2.241
2.400
2.418
2.433
2.437
2.451
2.674
2.681
2.691
2.699
3.076
3.081
3.097
3.186
4.396
4.390
5.126
5.127
5.129
5.398
5.402
5.737
5.754
5.775
5.792
CH3SO3
Me
H
N
H
O
Me
3.9

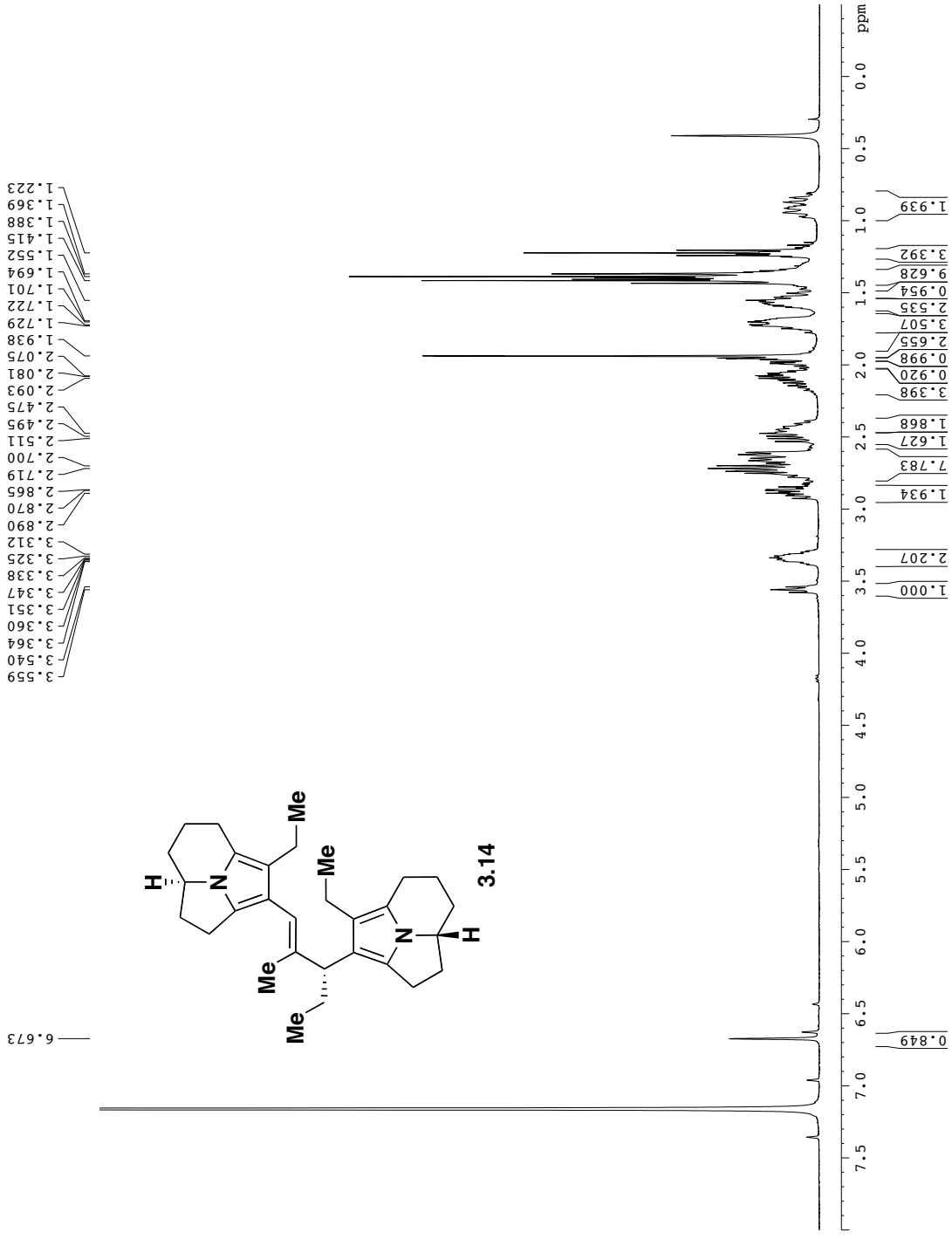
3.14
Me
Me
Me
Me
H
N
N
H
ppm
0.0
0.5
1.0
1.5
2.0
2.5
3.0
3.5
4.0
4.5
5.0
5.5
6.0
6.5
7.0
7.5
1.939
3.392
9.628
0.954
2.535
3.507
2.655
0.998
0.920
3.398
1.868
1.627
7.783
1.934
2.207
1.000
0.849
6.673
3.559
3.540
3.364
3.360
3.351
3.347
3.338
3.325
3.312
2.890
2.870
2.865
2.719
2.700
2.511
2.495
2.475
2.093
2.081
2.075
1.938
1.729
1.722
1.701
1.694
1.552
1.415
1.388
1.369
1.223

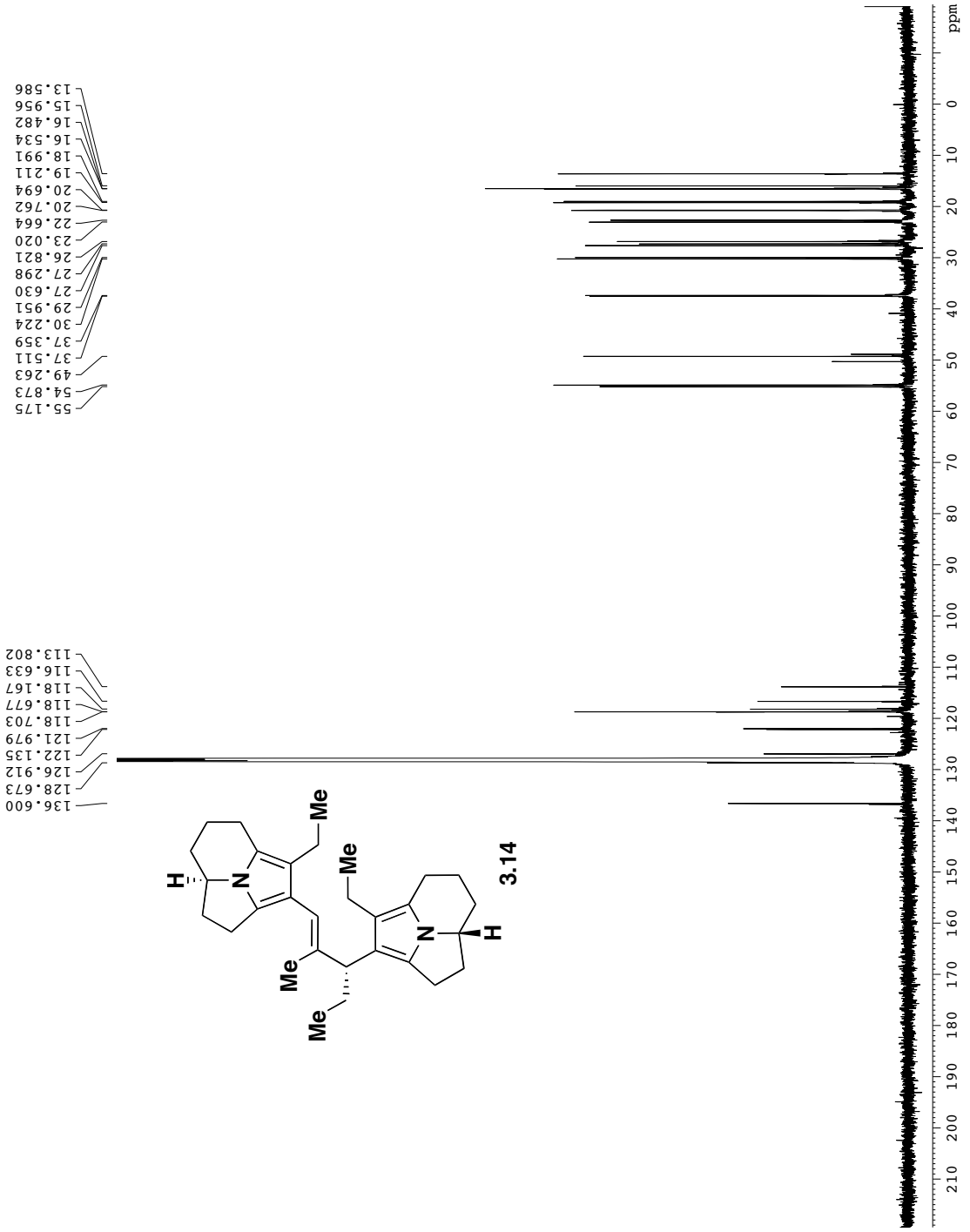
136.600
128.673
126.912
122.135
121.979
118.703
118.677
118.167
116.633
113.802
55.175
54.873
49.263
37.511
37.359
30.224
29.951
27.630
27.298
26.821
23.020
22.664
20.762
20.694
19.211
18.991
16.534
16.482
15.956
13.586
ppm
0
10
20
30
40
50
60
70
80
90
100
110
120
130
140
150
160
170
180
190
200
210
H
N
Me
Me
Me
Me
N
H
3.14

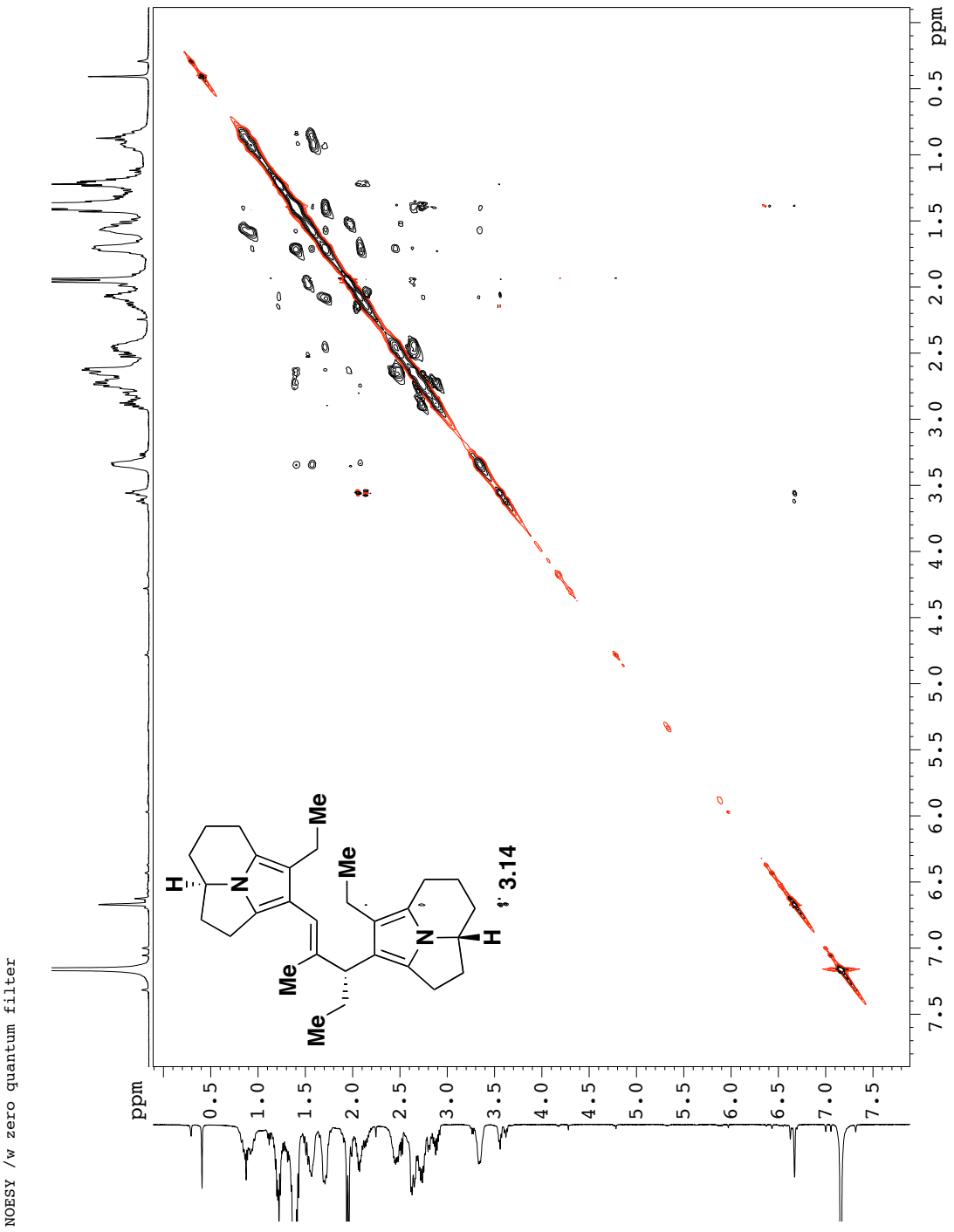
NOESY /w zero quantum filter
ppm
7.5 7.0 6.5 6.0 5.5 5.0 4.5 4.0 3.5 3.0 2.5 2.0 1.5 1.0 0.5 ppm
Me
Me
Me
Me
H
N
N
H
3.14

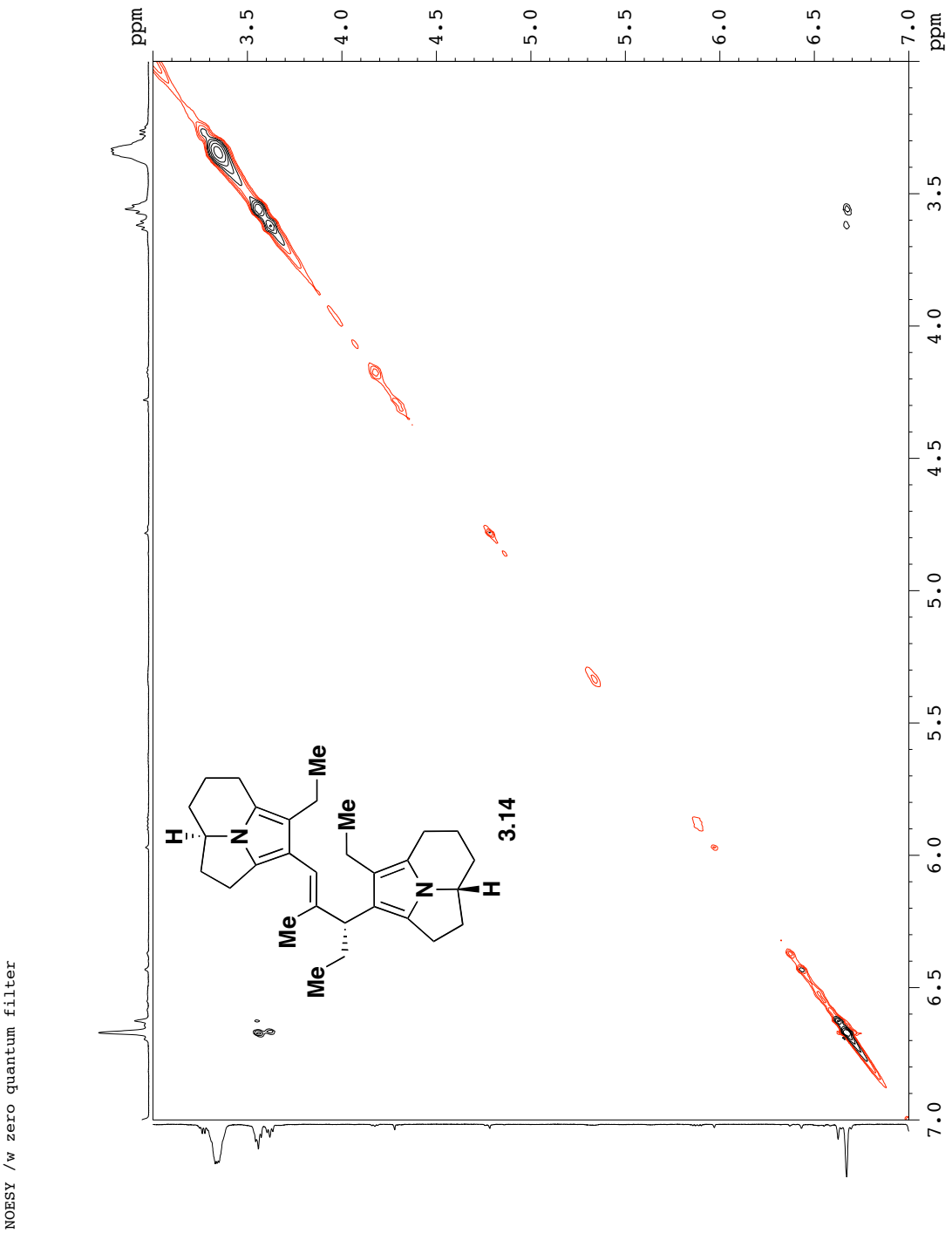
NOESY /w zero quantum filter
ppm
3.5
4.0
4.5
5.0
5.5
6.0
6.5
7.0
Me
Me
Me
Me
H
N
N
H
3.14

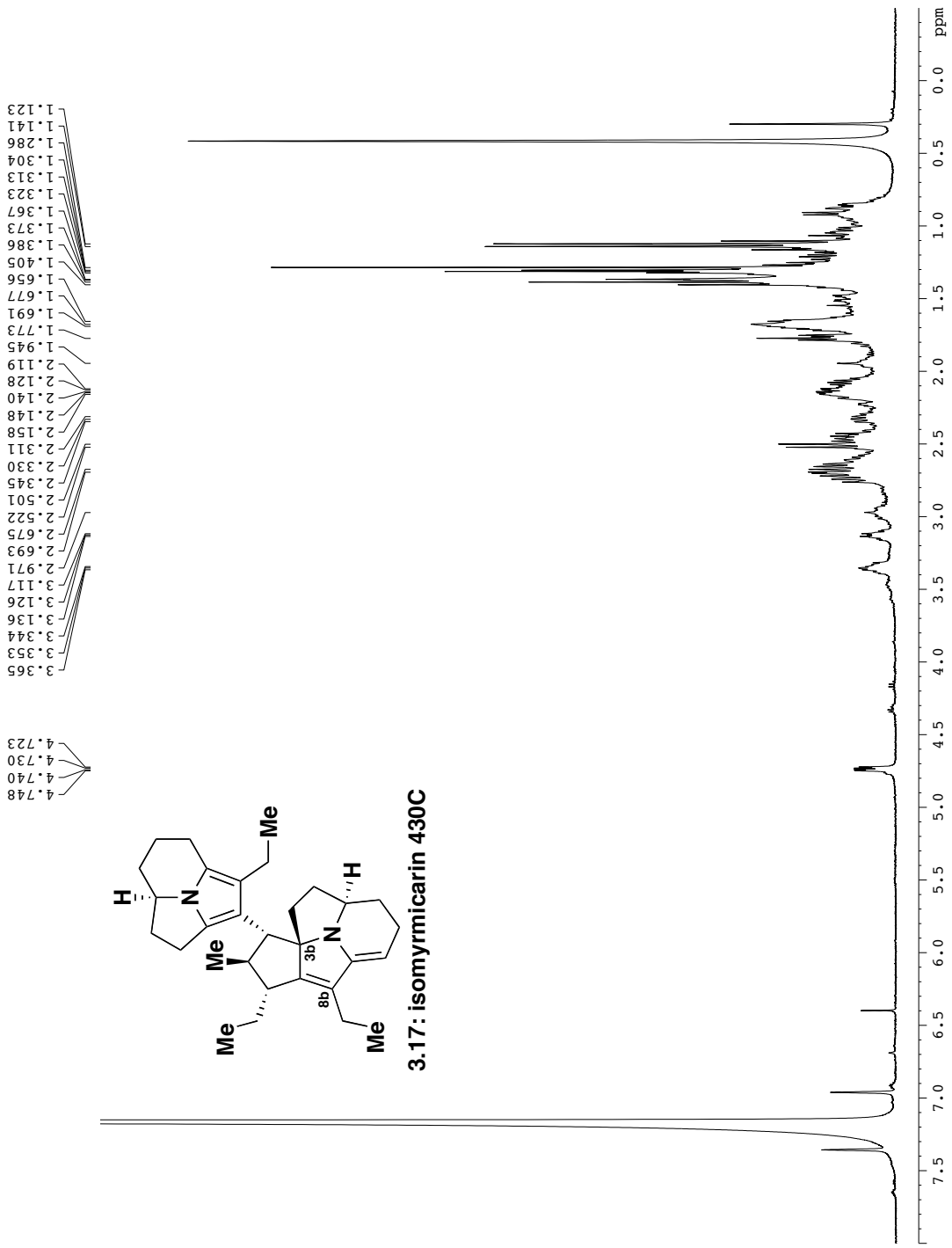
4.748
4.740
4.730
4.723
3.365
3.353
3.344
3.136
3.126
3.117
2.971
2.693
2.675
2.522
2.501
2.345
2.330
2.311
2.158
2.148
2.140
2.128
2.119
1.945
1.773
1.691
1.677
1.656
1.405
1.386
1.373
1.367
1.323
1.313
1.304
1.286
1.141
1.123
7.5
7.0
6.5
6.0
5.5
5.0
4.5
4.0
3.5
3.0
2.5
2.0
1.5
1.0
0.5
0.0
ppm
H
N
Me
Me
3b
8b
N
H
Me
Me
3.17: isomyrmicarin 430C

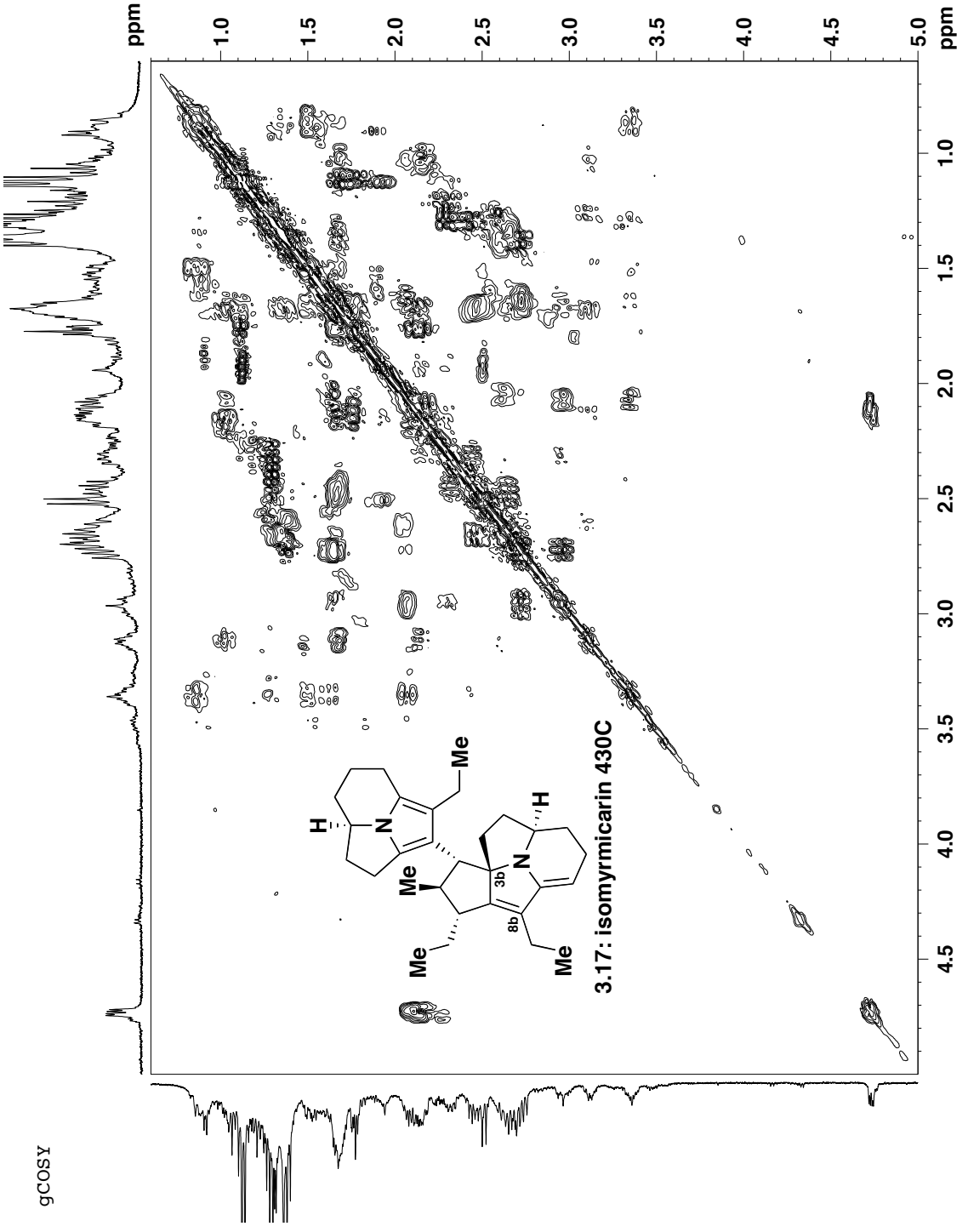
gCOSY
ppm
1.0
1.5
2.0
2.5
3.0
3.5
4.0
4.5
5.0
H
N
Me
Me
Me
Me
3b
8b
N
H
3.17: isomyrmicarin 430C

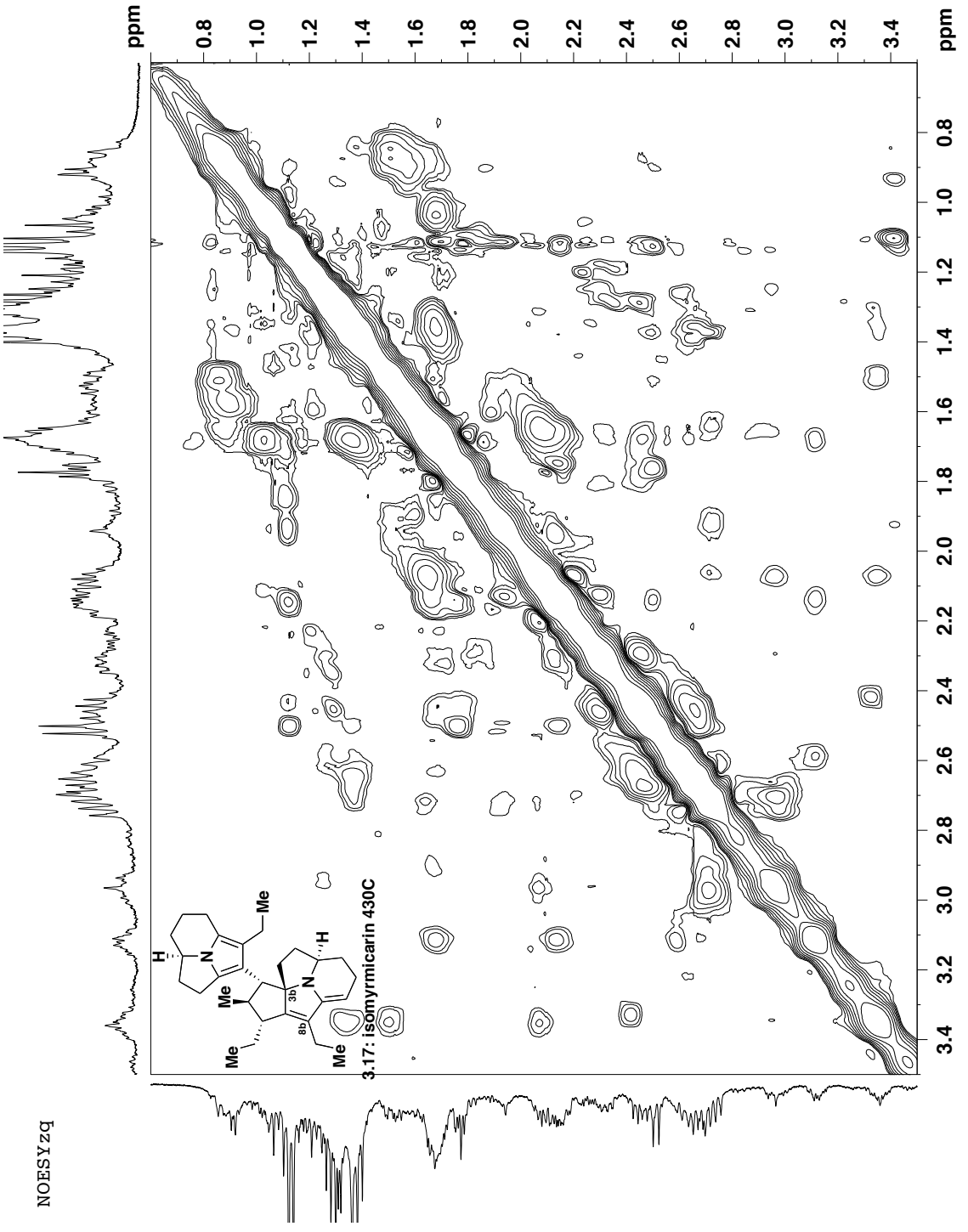
NOESYzq
ppm
0.8
1.0
1.2
1.4
1.6
1.8
2.0
2.2
2.4
2.6
2.8
3.0
3.2
3.4
3.17: isomyrmicarin 430C
Me
Me
Me
Me
H
H
N
N
3b
8b

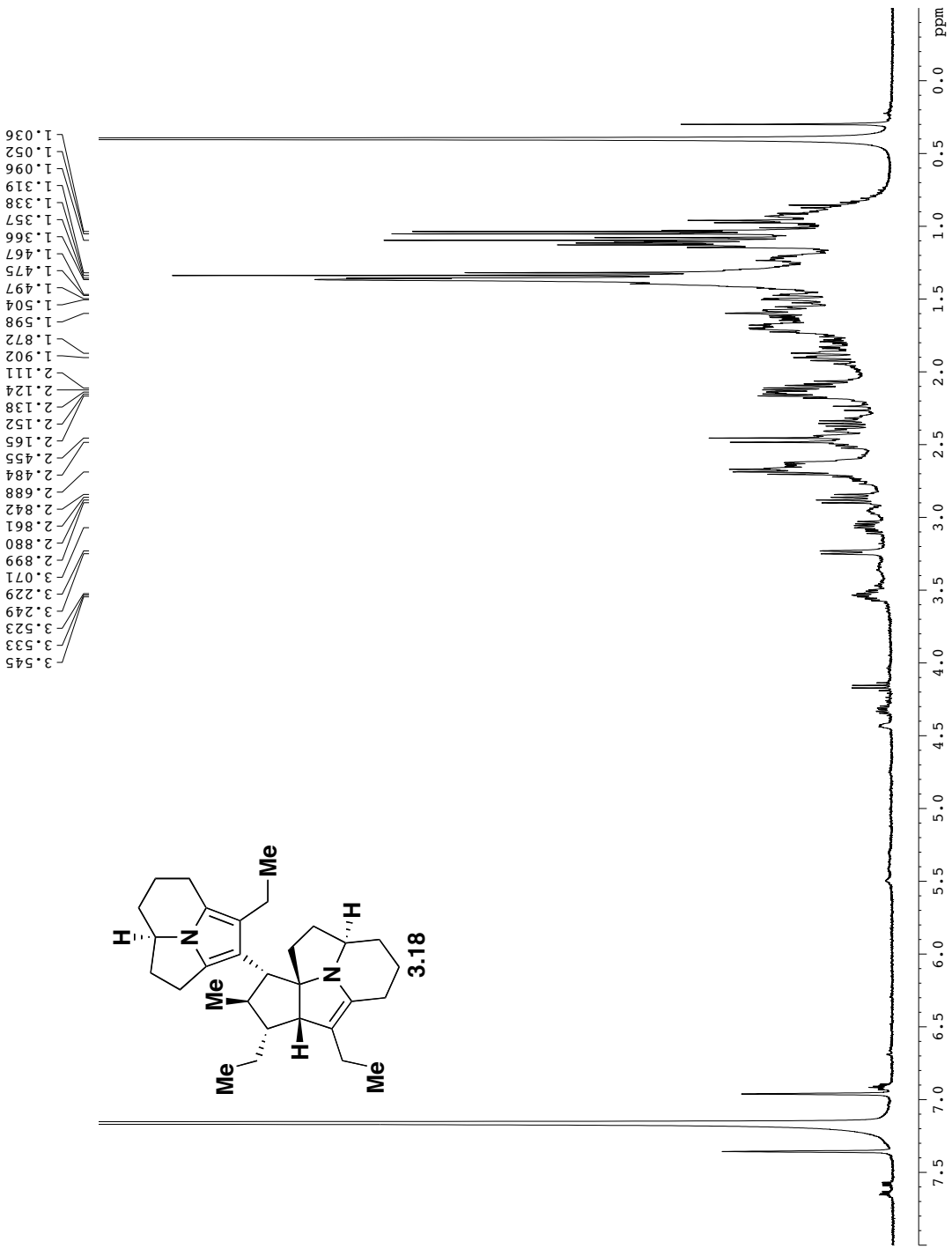
3.545
3.533
3.523
3.249
3.229
3.071
2.899
2.880
2.861
2.842
2.688
2.484
2.455
2.165
2.152
2.138
2.124
2.111
1.902
1.872
1.598
1.504
1.497
1.475
1.467
1.366
1.357
1.338
1.319
1.096
1.052
1.036
7.5
7.0
6.5
6.0
5.5
5.0
4.5
4.0
3.5
3.0
2.5
2.0
1.5
1.0
0.5
0.0
ppm
H
N
Me
Me
H
N
H
Me
Me
3.18

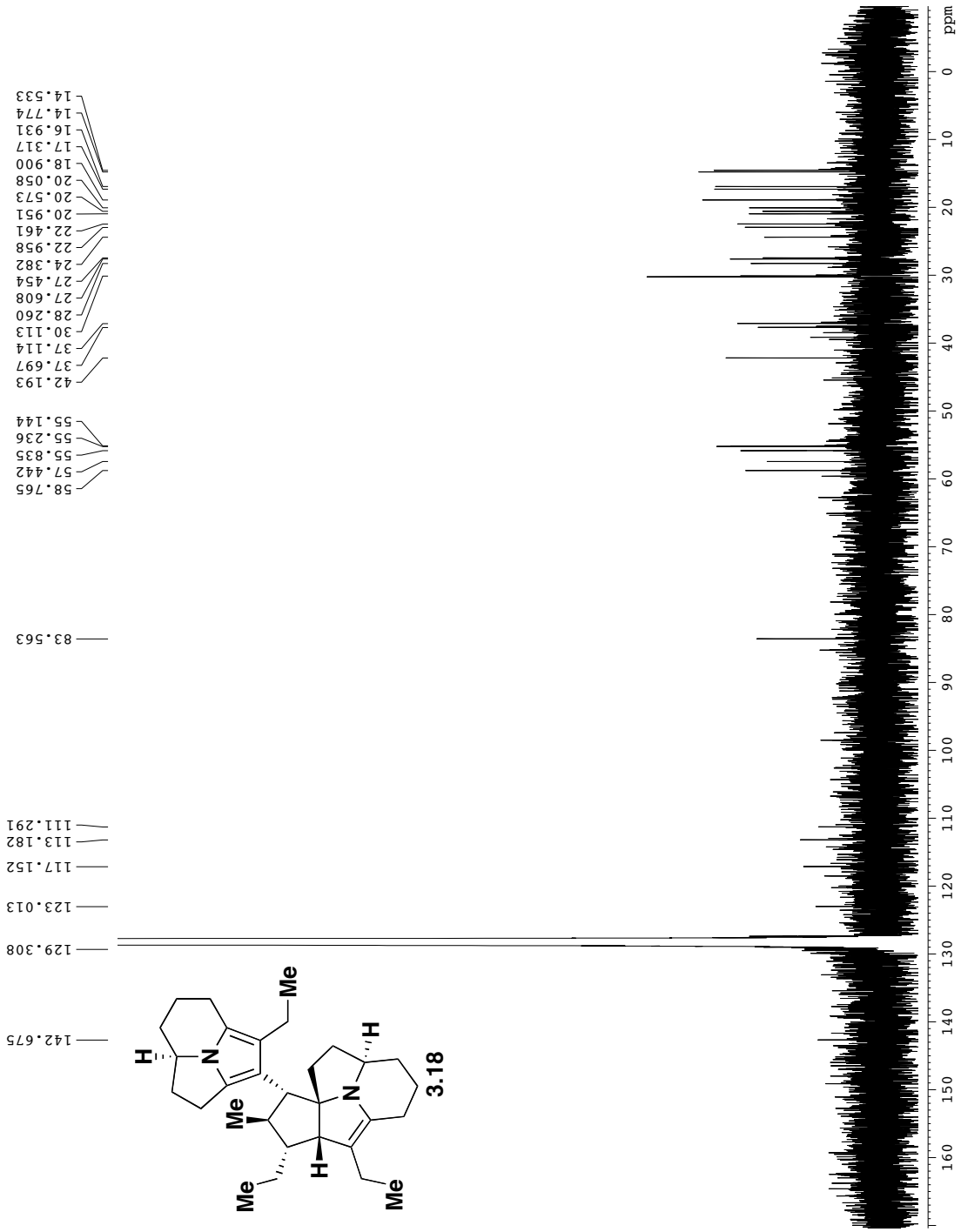
142.675
129.308
123.013
117.152
113.182
111.291
83.563
58.765
57.442
55.835
55.236
55.144
42.193
37.697
37.114
30.113
28.260
27.608
27.454
24.382
22.958
22.461
20.951
20.573
20.058
18.900
17.317
16.931
14.774
14.533
ppm
0
10
20
30
40
50
60
70
80
90
100
110
120
130
140
150
160
Me
Me
Me
Me
H
H
N
N
3.18

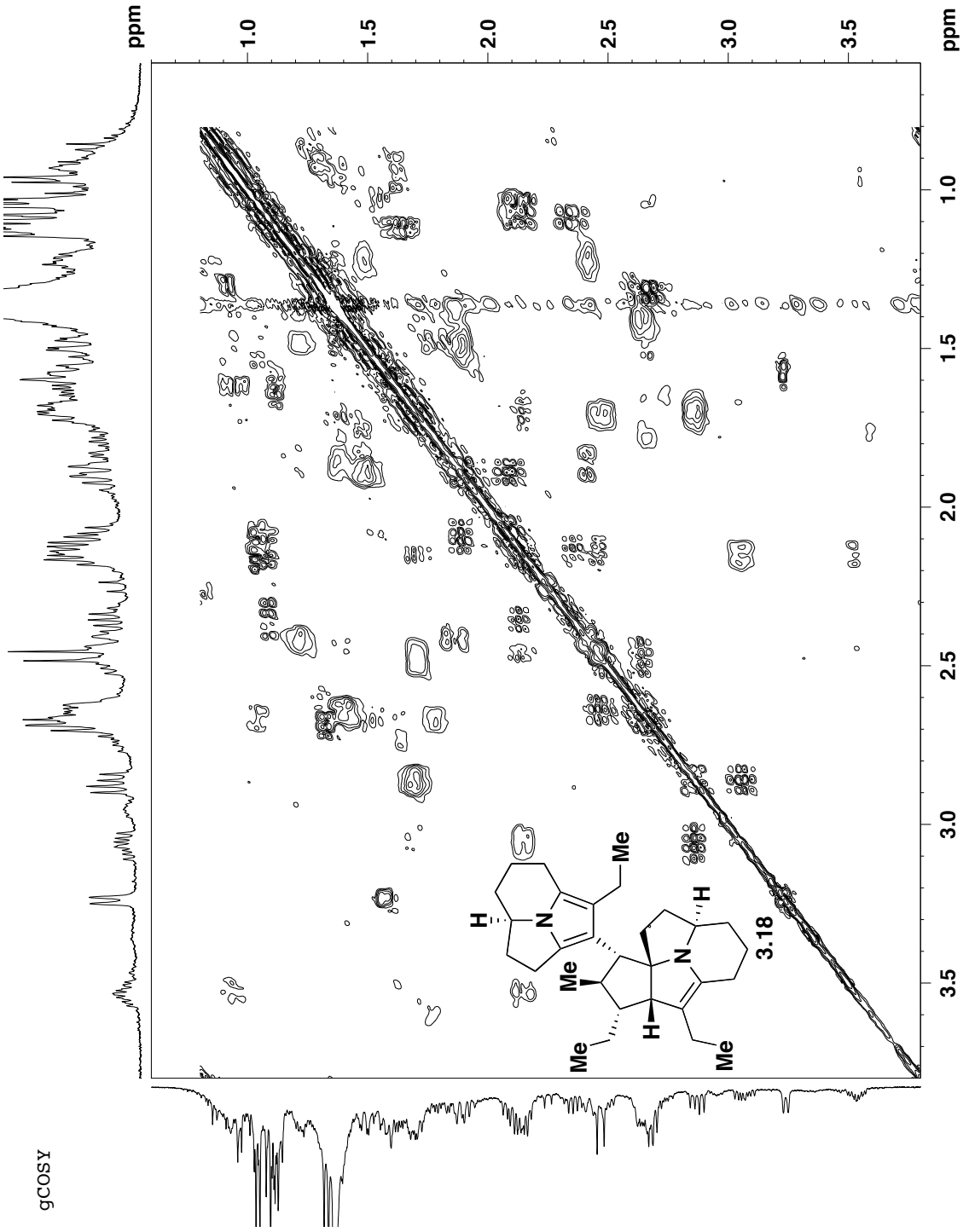
gCOSY
ppm
1.0
1.5
2.0
2.5
3.0
3.5
Me
H
N
Me
Me
H
N
H
Me
3.18

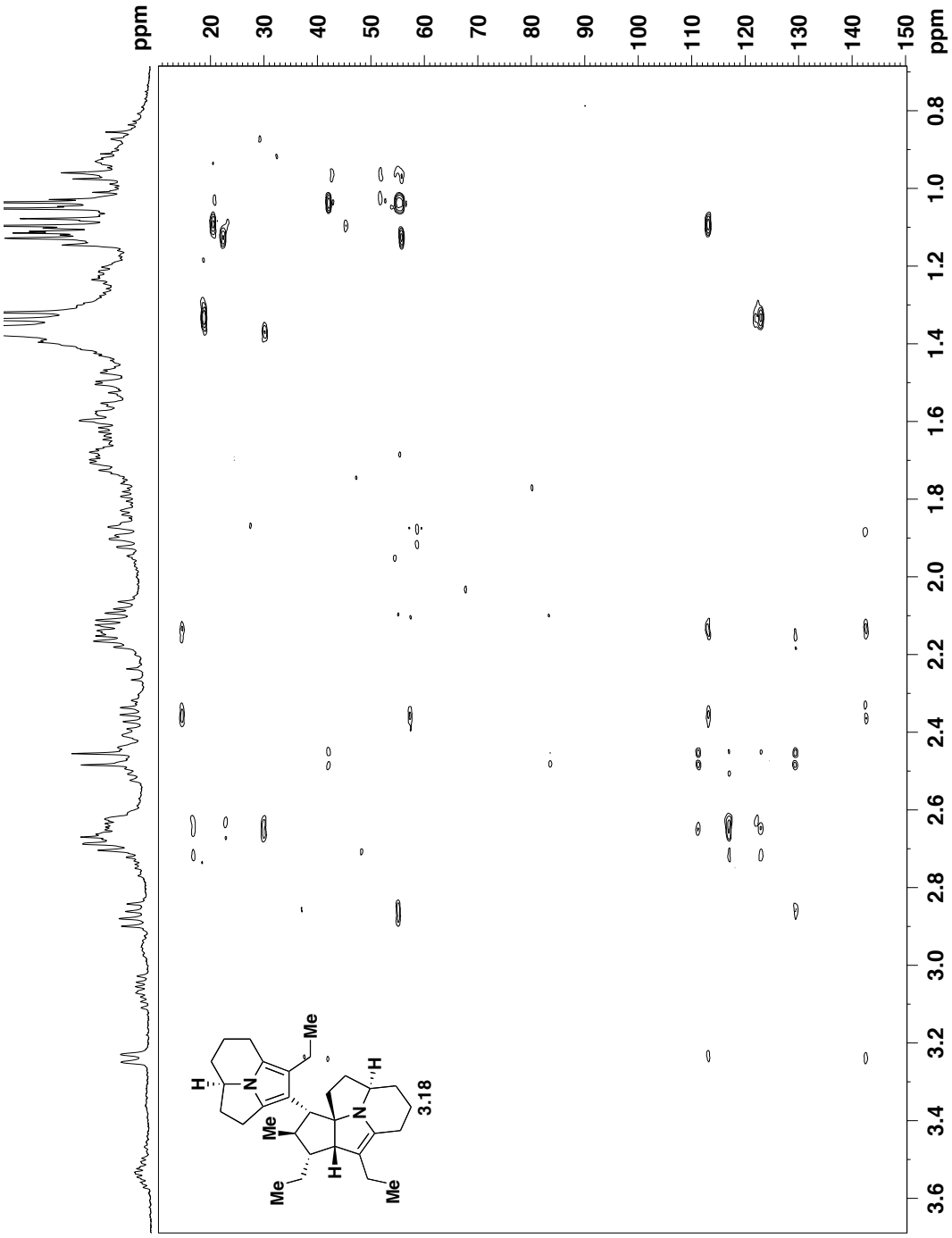
ppm
20
30
40
50
60
70
80
90
100
110
120
130
140
150
ppm
0.8
1.0
1.2
1.4
1.6
1.8
2.0
2.2
2.4
2.6
2.8
3.0
3.2
3.4
3.6
Me
Me
Me
Me
H
H
N
N
3.18

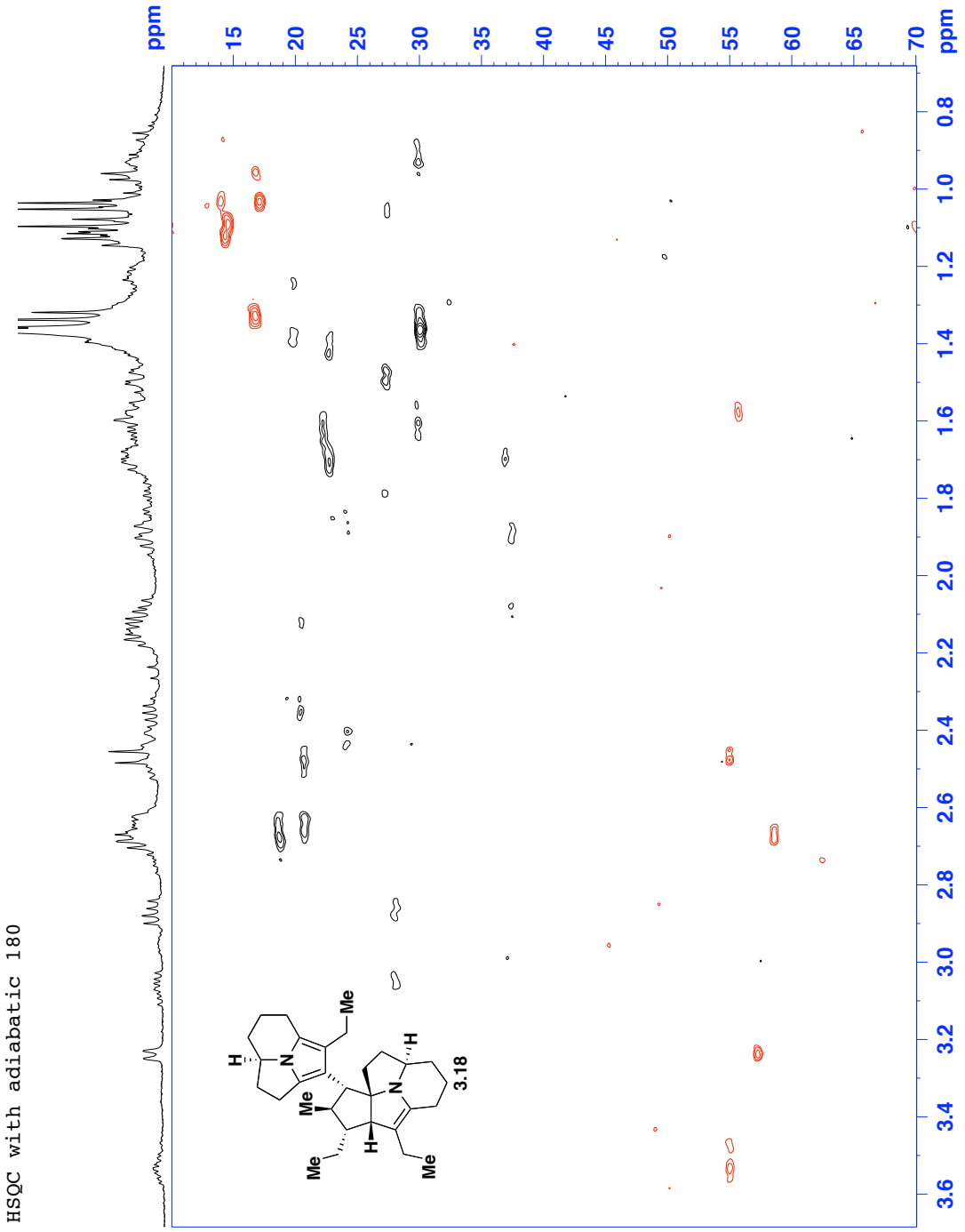
HSQC with adiabatic 180
ppm
15
20
25
30
35
40
45
50
55
60
65
70
ppm
0.8
1.0
1.2
1.4
1.6
1.8
2.0
2.2
2.4
2.6
2.8
3.0
3.2
3.4
3.6
H
N
Me
Me
H
Me
N
H
Me
3.18

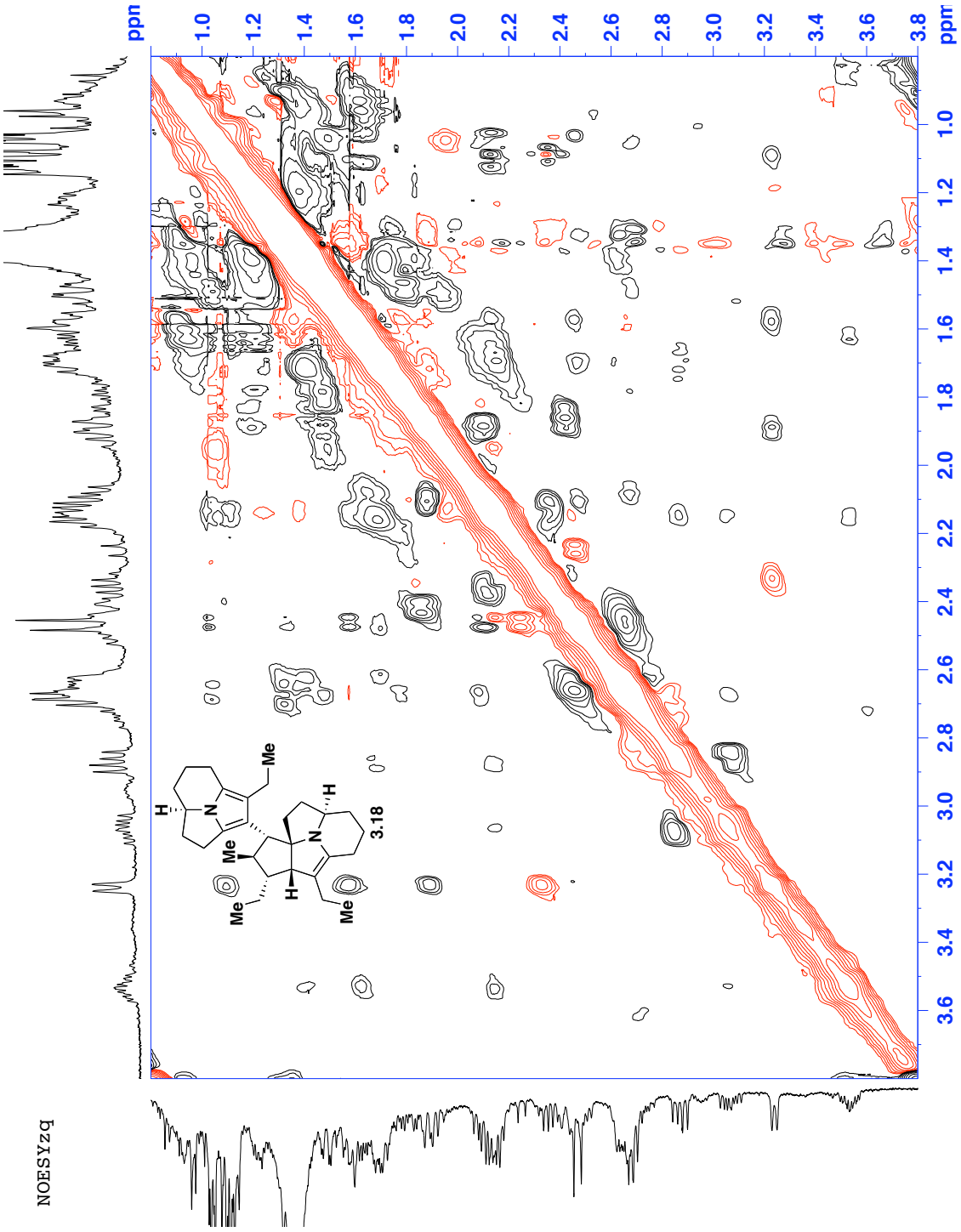
NOESYzq
ppm
1.0
1.2
1.4
1.6
1.8
2.0
2.2
2.4
2.6
2.8
3.0
3.2
3.4
3.6
3.8
Me
H
N
Me
H
N
Me
Me
H
3.18

CHAPTER 4

An Introduction to the *Securinega* Alkaloids and NHC Catalysis

The previous chapters have been devoted to an approach toward the myrmicarin alkaloids whose key development was predicated on a strategy-level solution to access the entire family of natural products. In the following chapters, attention will shift from strategy-level analysis of a family of natural products to tactic-level development of a reaction capable of forging the polycyclic core structures of the *Securinega* alkaloids from simpler starting materials.

4.1 A Brief Overview of the *Securinega* Alkaloids

Plants of the Euphorbiaceae family are sources of several families of natural products, including the *Daphniphyllum* and *Securinega* alkaloids.[1] The latter collection of polycyclic alkaloids has interesting biological activity[2], including GABA antagonism. In particular, several studies have focused on the biological properties of the most abundant member of the *Securinega* alkaloids, namely securinine. Structurally, the Securinega alkaloids are generally characterized by a bridged, tetracyclic substructure bearing an α,β,γ,δ-unsaturated lactone motif. Dozens of members of this family of alkaloids have been isolated, and a recent insurgence of novel structural motifs within this family has appeared in the literature. Though not exhaustively inclusive, we classify these alkaloids into 4 distinct structural classes as described in the following sections to provide a sense of the family's structural diversity. Intriguingly, these natural products are typically isolated as a single antipode from nature, although different organisms can produce the opposite enantiomer.[3]

4.1.1 Securinine-Type Alkaloids

The flagship member of the *Securinega* alkaoids, securinine (**4.1**, Figure 4.1) was first isolated in 1956, and its structure was initially elucidated by degradation studies and

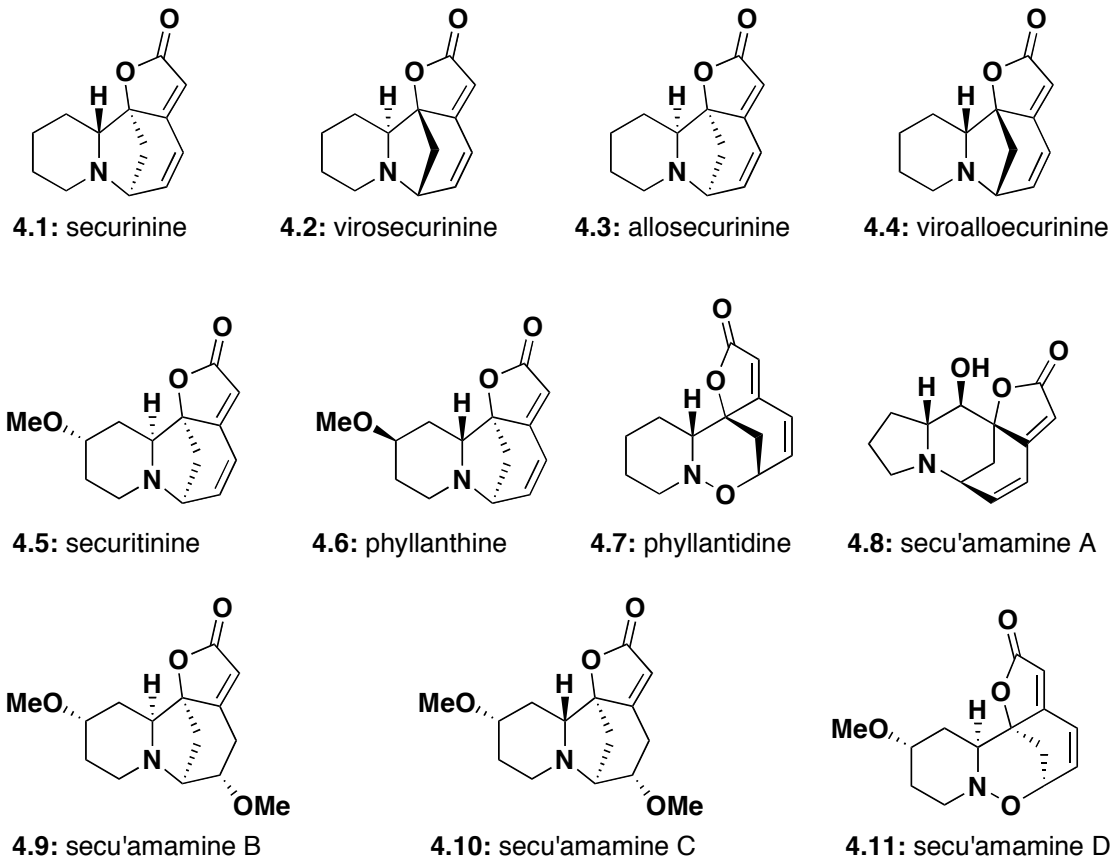

Figure 4.1 Structures of various securinine-type alkaloids **4.1**–**4.11**.

later confirmed by X-ray crystallographic methods.[4] This alkaloid is by far the most abundant of the *Securinega* alkaloids, and the indolizidine core is common to these congeners. In particular, it has been shown that the piperidine scaffold of these natural products is derived from lysine[5], while the bridged butenolide is derived from tyrosine.[5] The proposed biosynthesis of securinine highlighting these same studies is delineated in Figure 4.2. Other members of this family include virosecurinine (**4.2**), allosecurinine

(**4.3**) (also known as phyllochrysine) viroallosecurinine (**4.4**), securitinine (**4.5**), phyllanthine (**4.6**), and phyllantidine (**4.7**).[1]

In 2003, the novel indolizidine-bearing *Securinega* alkaloid secu'amamine A[6] (**4.8**) was isolated. Recent studies by Magnus and co-workers[7] provided an intriguing biogenetic relationship between this alkaloid and allosecurinine (**4.3**) through an

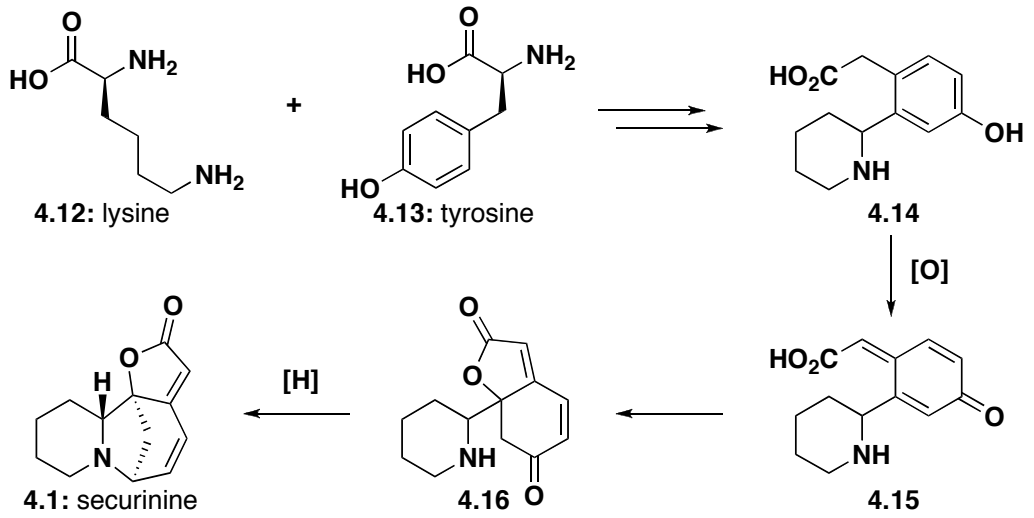

Figure 4.2 Proposed biosynthesis of securinine (**4.1**) from lysine and tyrosine.

aziridinium intermediate. Model systems of a simplified indolizidine core provided some evidence for such a relationship. Recently, secu'amamines B–D[8] (**4.9–4.11**) were isolated, and their structures were found to be consistent with the securinine indolizidine core structure as well.

4.1.2 Norsecurinine-Type Alkaloids

Norsecurinine (**4.17**, Figure 4.3), the lower homolog of securinine, was originally isolated in 1963[9], and after considerable efforts, its structure was elucidated. Its framework is characterized by an ornithine-derived pyrrolizidine core. Unlike the indolizidine-containing *Securinega* alkaloids, norsecurinine readily polymerizes upon

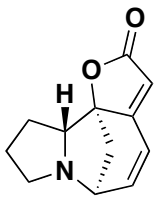

4.17: norsecurinine

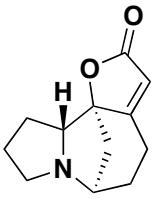

4.18: dihydronorsecurinine

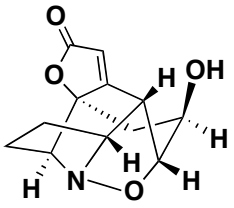

4.19: virosaine A

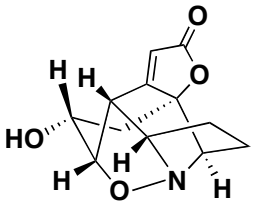

4.20: virosaine B

Figure 4.3 Structures of representative norsecurinine-type alkaloids **4.17**–**4.20**.

concentration from solution. Fortunately, purification as the hydrochloride salt, followed by free-basing, provided semi-stable solutions of pure compound that could be used for spectroscopic studies. Indeed, the later isolation and characterization of the flueggenines, which are norsecurinine dimers (see Figure 6, Section 4.1.4), provides evidence of the ease with which this alkaloid undergoes self-reaction. Other structures of this general motif include dihydronorsecurinine (**4.18**) and the very recently reported virosaines[10] (**4.19** and **4.20**). These latter alkaloids are pseudoenantiomers, and a proposed biosynthesis involving an intramolecular nitrone [3+2] cycloaddition has been advanced.

4.1.3 Neosecurinane- and Neonorsecurinane-Type Alkaloids

Securinol A (**4.22**, Figure 4.4) was first isolated in 1965, and five years later, its originally proposed structure was reported (**4.21**) to be a C-ring hydroxylated securinine-type alkaloid.[11] This structure, however, was revised in 1991 through X-ray crystallographic analysis of its hydrobromide salt, and the new structural framework was

designated as a neosecurinane skeleton.[12] The corresponding lower homologs, bubbialine (**4.23**) and epibubbialine (**4.24**), represent structures with a neonorsecurinane skeleton,

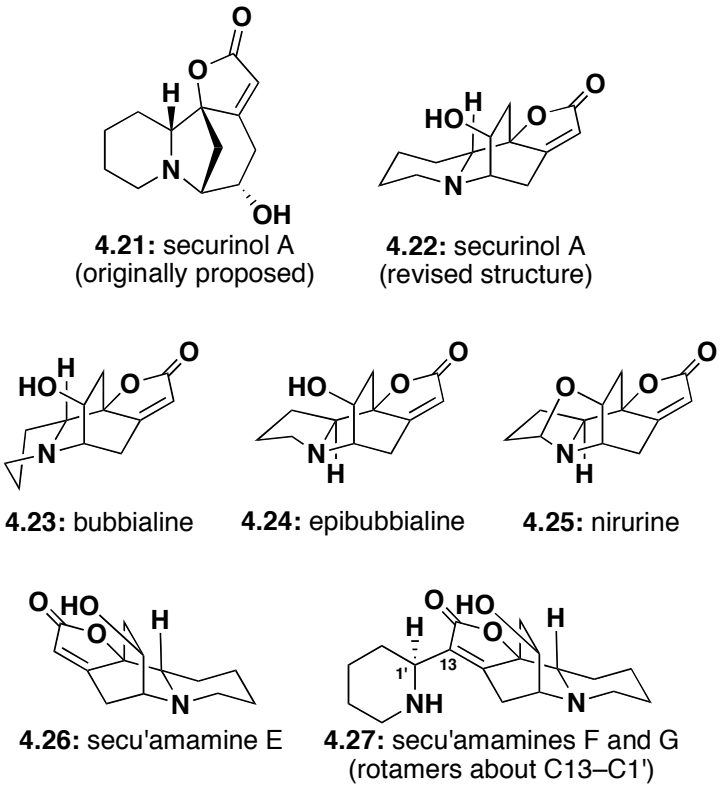

Figure 4.4 Representative structures of neosecurinane- and neonorsecurinane-type alkaloids.

and a clear relationship of this alkaloid with nirurine (**4.25**) can be envisaged upon inspection of their molecular architectures. Overall, these families of alkaloids contain a central [2.2.2] bicycle and are believed to derive from the union of either lysine or ornithine with dopamine subunits as outlined in Figure 4.5. Recently, three new neosecurinane alkaloids, namely secu'amamines E–G[13] were isolated (**4.26** and **4.27**). Secu'amamines F and G (**4.27**) bear an additional piperidine ring system that is rotationally restricted, giving rise to the separable rotameric species.

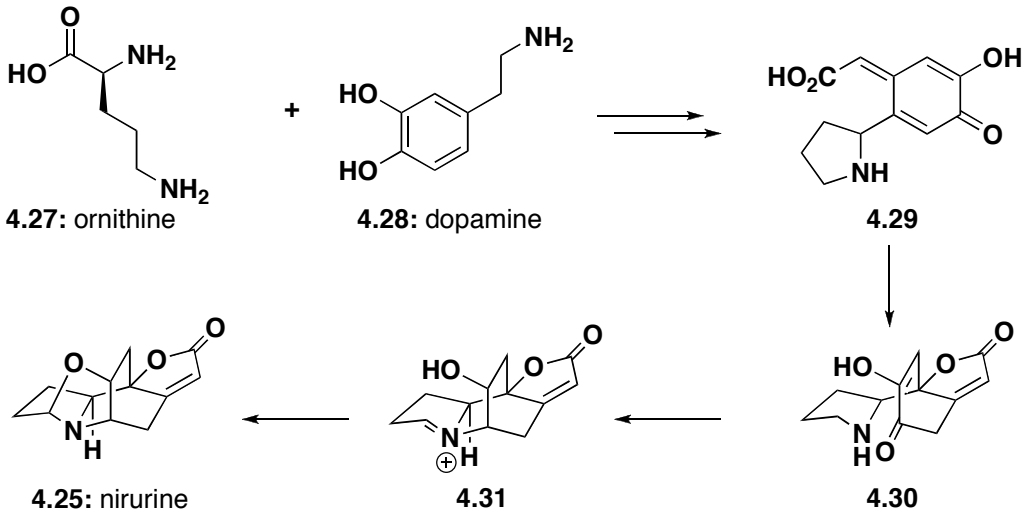

Figure 4.5 Proposed biosynthesis of nirurine (**4.25**) from ornithine and dopamine.

4.1.4 Dimeric Securinega *Alkaloids*

Four dimeric *Securinega* alkaloids are currently known in the literature (see Figure 4.6), flueggenines A and B[14] (**4.32** and **4.33**, norsecurinine homodimers) and

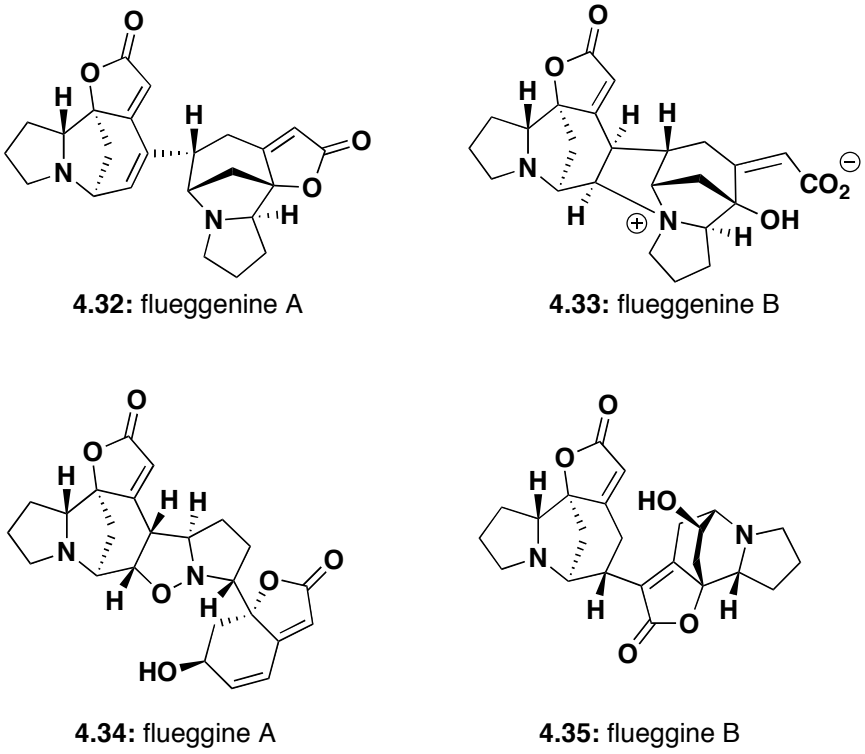

Figure 4.6 Dimeric *Securinega* alkaloids.

flueggines A (**4.34**, a norsecurinine homodimer) and B[15] (**4.35**, a dihydronorsecurinine/bubbialine heterodimer). Due to the reactive nature of the norsecurinine framekwork, it is somewhat unsurprising that dimeric species bearing these subunits are known while the more stable securinine framework has yet to be identified in a dimeric contex. The flueggenines are likely derived from a vinylogous Baylis–Hillman-type reaction, while flueggine A is anticipated to be the product of an intermolecular nitrone [3+2] cycloaddition.

4.2 Total Syntheses of Various *Securinega* Alkaloids

With their compact, polycyclic framework, the *Securinega* alkaloids have attracted much attention from the synthetic community. Though a detailed recounting of all of the previous syntheses is beyond the intended scope of this work, the following sections aim to summarize the various synthetic approaches that have successfully delivered the bridging, and highly intriguing, unsaturated butenolide core of these natural products.

4.2.1 Horii's Racemic Synthesis of Securinine

The first total synthesis of a *Securinega* alkaloid was accomplished by Horii and co-workers in 1966.[16] In their synthesis, intermediate **4.36** (c.f. Scheme 4.1) was oxidized by a two-step bromination/elimination sequence to give enone **4.37**. This intermediate underwent smooth 1,2-addition of ethoxyacetylide, and subsequent sulfuric acid quench frunished lactone **4.38**. Protecting group exchange, bromination, and intramolecular

cyclization furnished racemic securinine (i.e. securinine and virosecurinine), albeit in low yields (3.8% over 4 steps).

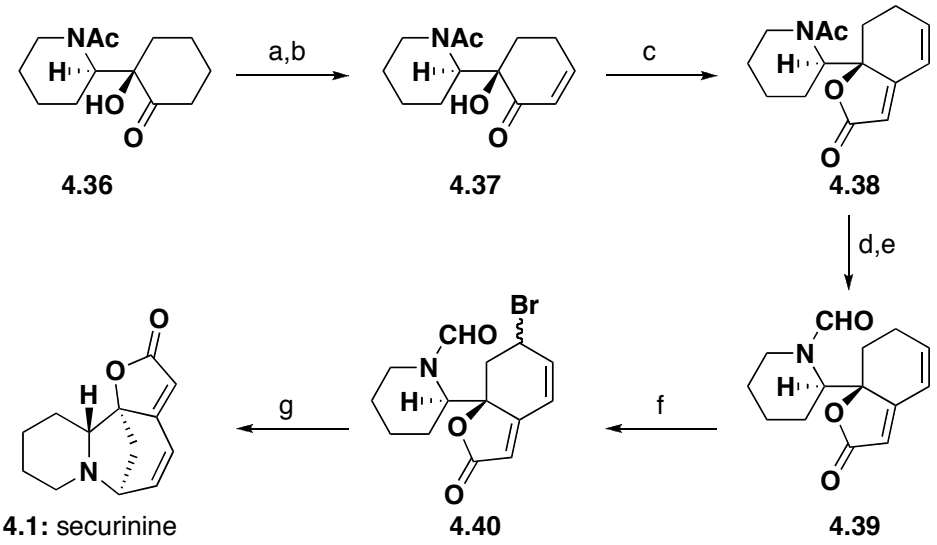

Scheme 4.1 Horii's racemic synthesis of securinine (**4.1**). *Reagents and Conditions:* a) Br_2, HBr, AcOH (75%); b) LiBr, Li_2CO_3, DMF, 120 °C (71%); c) EtOCCLi, Et_2O, –30 °C, then 15% H_2SO_4, heat; d) conc. HCl, 130 °C; e) HCO_2H, Ac_2O, heat (76%); f) NBS, CCl_4, benzoyl peroxide (66%); g) 20% HCl, heat, then NH_4OH (7.5%). NBS = *N*-bromosuccinimide.

4.2.2 Heathcock's Racemic Synthesis of Norsecurinine

Almost two decades passed before the second report of a total synthesis of a *Securinega* alkaloid was reported in the literature: Heathcock and co-workers' racemic synthesis of norsecurinine,[17] which is outlined in Scheme 4.2. Although (*S*)-proline was used as the starting material that was elaborated to intermediate **4.41**, a previous Wittig olefination en route racemized the chiral center. From here, simultaneous *N*-Boc deprotection, ketal deprotection, and alkene isomerization with HCl in AcOH afforded aza-Michael product **4.42** after basic work-up. Intramolecular aldol reaction with concomitant TMS protection of the resultant alcohol gave rise to keto-ester **4.43** in 57%

over 2 steps. Reduction/mesylation followed by treatment with lithium benzenethiolate afforded rearranged tricycle **4.44** that, fortunately, could be converted to alkene **4.45** upon oxidation and elimination. α-Selenation of the ester and lactonization under acidic conditions set the stage for *m*-CPBA-mediated selenoxide elimination to afford the desired natural product in moderate yield (28%) over the final 3 operations. Overall, this synthesis required that the majority of its synthetic manipulations focus on preparing the bridging butenolide motif, but the key concept worth noting is that the selenoxide elimination to establish unsaturation along the bridging butenolide became a strategy that several other groups would rely on in subsequent syntheses (*vide infra*).

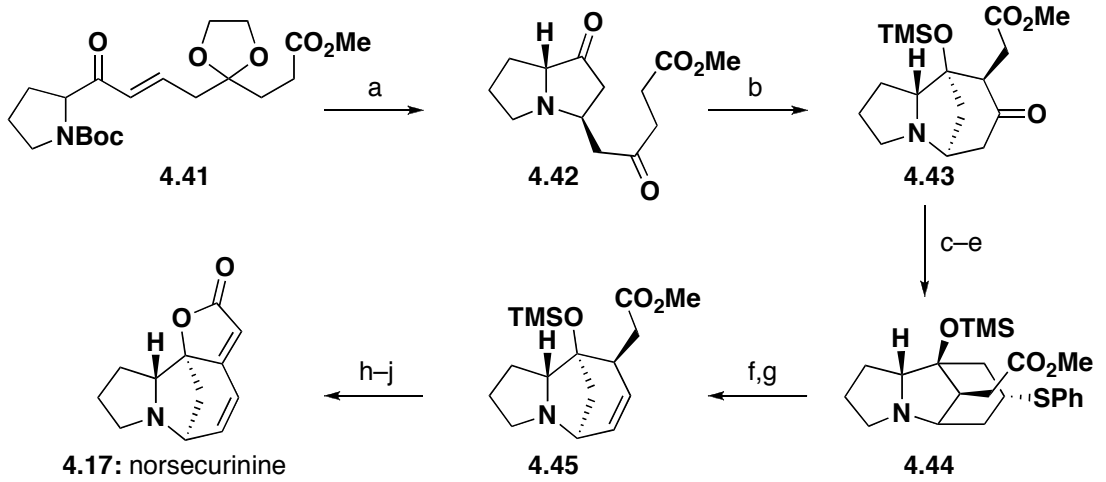

Scheme 4.2 Heathcock's racemic synthesis of norsecurinine (**4.17**). *Reagents and Conditions:* a) HCl, AcOH; b) *N*-Li-imidazole, *N*-TMS-imidazole (57%, 2 steps); c) catechol borane (67%); d) MsCl, Et_3N (90%); e) PhSLi, DMF, 100 °C (80%); f) *m*-CPBA (94%); g) toluene, heat (41%); h) LiHMDS, $(PhSe)_2$ (71%); i) *p*TSA, C_6H_6, reflux; j) *m*-CPBA, MeOH, –78 °C (40%). NBS = *N*-bromosuccinimide. TMS = trimethylsilyl, Ms = methanesulfonyl, *m*-CPBA = *meta*-chloroperbenzoic acid, LiHMDS = lithiu bis(trimethylsilyl)amide, *p*TSA = *p*-toluene sulfonic acid.

4.2.3 Jacobi's Enantiospecific Synthesis of (+) and (–)-Norsecurinine

In 1989, Jacobi utilized a Diels–Alder strategy[18] involving an oxazole diene to form the core carbon skeleton of the butenolide ring system in a concise fashion. In

particular, ynone **4.46** (a 2:1 mixture of diastereomers) underwent intramolecular Diels–Alder reaction with the pendant oxazole and retro-[4+2] reaction to expell a molecule of acetonitrile to give a separable 2:1 mixture of furan **4.47** and its undesired C7-epimer as

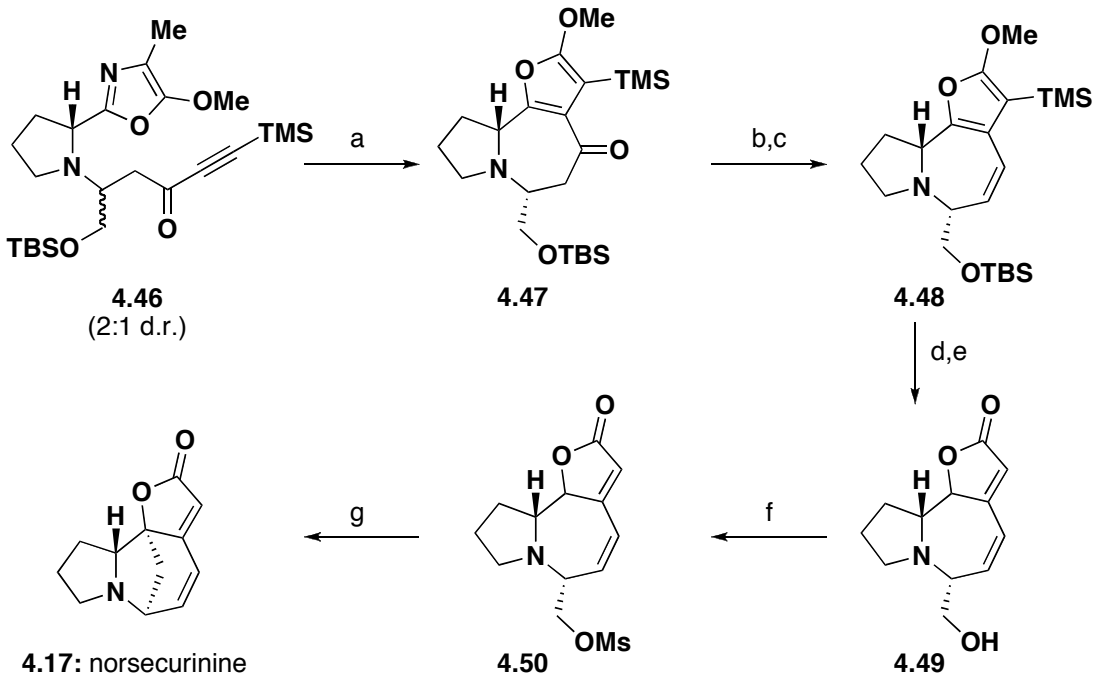

4.46 (2:1 d.r.) **4.47** **4.48** **4.49** **4.50** **4.17:** norsecurinine

Scheme 4.3 Jacobi's enantiospecific synthesis of norsecurinine (**4.17**). *Reagents and Conditions:* a) mesitylene, heat (46%, 2:1 d.r.); b) $NaBH_4$, EtOH, 25 °C (86%); c) Martin's sulfurane, CH_2Cl_2, –48 °C (63%); d) TBAF, THF, 0 °C (80%); e) NaI, $TiCl_4$, CH_2Cl_2, MeCN, 0 °C (73%); f) MsCl, Et_3N, CH_2Cl_2, 0 °C (98%); g) KHMDS, THF, –78 → 25 °C (69%).

delineated in Scheme 4.3. Fortunately, the latter compound underwent epimerization in the presence of Na_2CO_3 in MeOH to afford a 1:1 mixture of C7 epimers. Ketone reduction with $NaBH_4$ followed by elimination of the resultant alcohol with Martin's sulfurane afforded alkene **4.48**. Then, fluoride-induced removal of the silyl groups, unveiling of the butenolide with NaI and $TiCl_4$, and mesylation of the primary alcohol set the stage for the final, and critical, C–C bond formation. Pleasingly treatment of lactone **4.50** with KHMDS in THF at –78 °C followed by slow warming to ambient temperature

smoothly afforded norsecurinine (**4.17**) in 69% yield. Notably, the use of (*R*)-proline afforded enantiomerically pure norsecurinine since no racemization of the proline sterecenter was observed in the course of these studies.

4.2.4 Weinreb's Enantiospecific Syntheses of Norsecurinine, Dihydronorsecurinine, and Phyllanthine

In 2000, the Weinreb group disclosed a clever approach to the synthesis of three *Securinega* alkaloids from a common bicyclic intermediate.[19] In their analysis of this collection of natural products, they envisioned that compound **4.51** could be selectively functionalized α to the nitrogen with various groups that could later undergo annulation to afford several natural products.

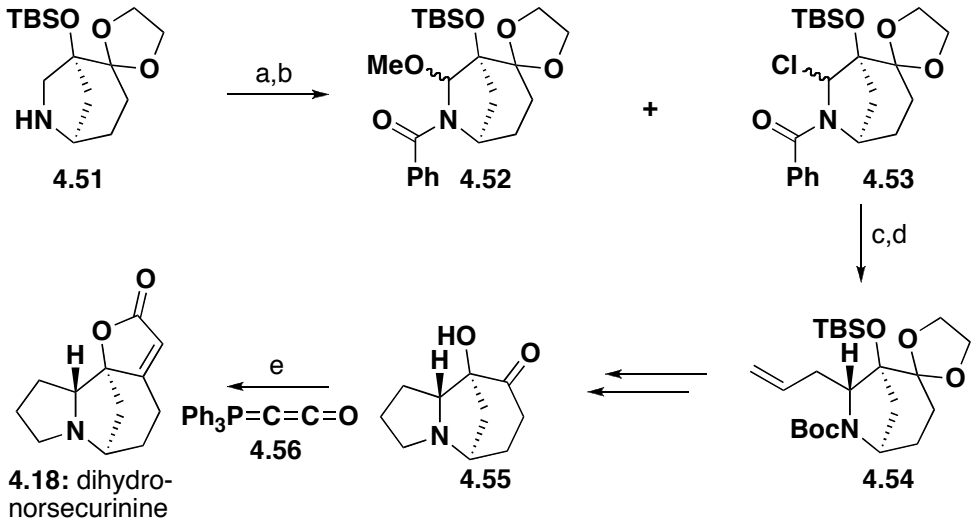

Scheme 4.4 Weinreb's enantiospecific synthesis of dihydronorsecurinine (**4.18**). *Reagents and Conditions:* a) isatonic anhydride, DMAP, MeCN, 25 °C (87%); b) $NaNO_2$, HCl, CuCl (100 mol %), MeOH, 25 °C (30% **4.52**, 26% **4.53**); c) allylmagnesium bromide, BF_3•OEt_2, THF, –78 → 0 °C; d) Boc_2O, Et_3N, CH_2Cl_2, reflux (68% from **4.52**/**4.53**); e) **4.56**, 12 kbar, toluene/CH_2Cl_2 (1:1), 25 °C (89%). DMAP = 4-(dimethylamino)pyridine, Boc = *tert*-butoxycarbonyl.

In targeting dihydronorsecurinine, intermediate **4.51** (Scheme. 4.4) was elaborated to allylated derivative **4.54** in 4 steps: nitrogen functionalization and oxidation using

methodology previously reported by their lab[20] facilitated subsequent nucleophilic addition and protecting group removal through the use of excess allylmagnesium bromide in the presence of BF_3•OEt_2. Reprotection as the Boc carbamate then afforded the desired intermediate **4.54**. From here, standard functional group manipulations afforded tricycle **4.55**, primed for installation of the butenolide. In a key operation, treatment of keto-alcohol **4.55** with the Bestmann ylide **4.56** under high pressure effectively delivered dihydronorsecurinine. Intermediate **4.55** also proved useful in accessing the oxidized congener norsecurinine (**4.17**) as outlined in Scheme 4.5. α-Selenation of the ketone and conversion of the alcohol to the corresponding phosphonate ester allowed a high-yielding (95%) intramolecular butenolide formation in the presence of K_2CO_3 (the Bestmann ylide was unsuccessful on this framework). Selenoxide elimination then delivered norsecurinine.

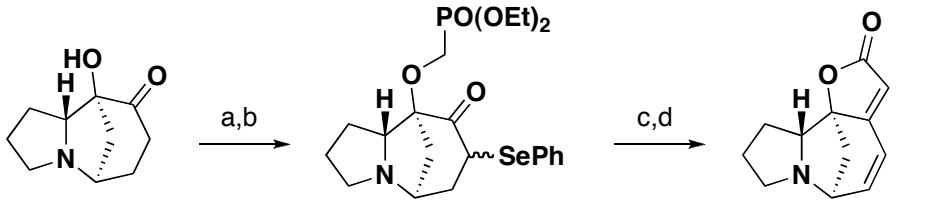

4.55 **4.56** **4.17:** norsecurinine

Scheme 4.5 Weinreb's enantiospecific synthesis of norsecurinine (**4.17**). *Reagents and Conditions:* a) PhSeCl, Et_3N, EtOAc, reflux (60%); b) $(EtO)_2POCH_2CO_2H$, CMC, CH_2Cl_2 (88%); c) K_2CO_3, 18-C-6, toluene, 0 °C (95%); d) DMDO, acetone, CH_2Cl_2, –78 °C (39%). CMC = 1-cyclohexyl-3-(2-morpholinoethyl)-carbodiimide metho-*p*-toluenesulfonate, DMDO = dimethyl dioxirane.

Finally, returning to key intermediate **4.51**, Weinreb and co-workers targeted phyllanthine, where they envisioned the desired six-membered ring resulting from a hetero-Diels–Alder reaction. To access the desired imine dienophile, intermediate **4.41** was oxidized with iodosobenzene (see Scheme 4.6), and the desired hetero-Diels–Alder reaction was performed in the presence of Danishefsky's diene to afford vinylogous

amide **4.57** in 84% yield. Reduction with L-selectride, methyl ether formation, and ketal deprotection furnished ketone **4.58**. A two-step net oxidation to the enone with concomitant TBS-deprotection furnished keto-alcohol **4.59** in good yield over 2 steps (49%). This intermediate was then elaborated using the chemistry described above to reach phyllanthine.

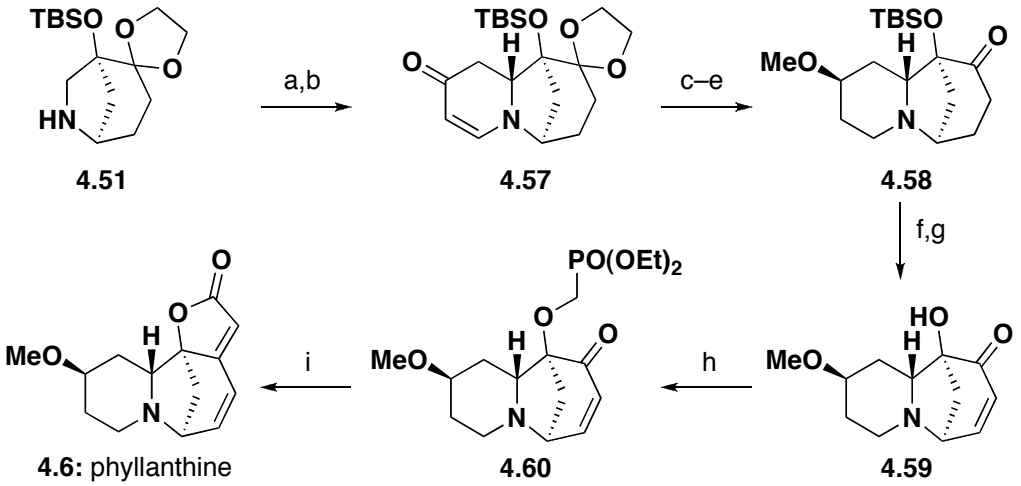

Scheme 4.6 Weinreb's enantiospecific synthesis of phyllanthine (**4.6**). *Reagents and Conditions:* a) PhIO, CH_2Cl_2, 25 °C (87%); b) Danishefsky's diene, $Yb(OTf)_3$, MeCN, 0 → 25 °C (84%); c) L-selectride, THF, –78 °C (85%); d) NaH, MeI, THF, 0 → 25 °C (87%); e) 3 M HCl, reflux (78%); f) $(PhSe)_2$, SeO_2, MsOH, CH_2Cl_2 (58%); g) NaI, MeCN, BF_3•OEt_2, 0 °C (84%); h) $(EtO)_2POCH_2CO_2H$, DCC, THF, 0 → 25 °C (67%); i) K_2CO_3, 18-C-6, toluene, 0 → 25 °C (84%). OTf = trifluoromethanesulfonate, DCC = *N,N′*-dicyclohexylcarbodiimide.

At a strategic level, these syntheses demonstrated a key disconnection of the butenolide as an intramolecular olefination retron that would be used in many subsequent syntheses, constituting a critical insight into the synthesis of this family as a whole.

4.2.5 Honda's Formal Synthesis of Racemic Securinine

Also in 2000, the Honda[21] group disclosed an intriguing formal synthesis of securinine that intersected with Horii's intermediate **4.38** (c.f. Scheme 4.1). In their

approach, sorbate ester **4.61** (Scheme 4.7) was subjected to deconjugative enolate protonation and intramolecular Diels–Alder reaction to afford compound **4.62**, an intermediate that contained all of the requisite carbon atoms of the natural product. In order to reduce the pyridine ring system, however, the alkene in **4.62** required protection, which was efficiently accomplished in the form of oxidation and acetonide protection in 96% yield over 2 steps. Unfortunately, the pyridine reduction proved to be only partially stereoselective (3:2 in favor of the desired isomer), though the major isomer could be processed successfully to acetamide **4.64**. This compound was then subjected to a Corey–Winter-like olefination and α-selenation of the lactone; selenoxide elimination then furnished Horii's intermediate (**4.38**), completing the formal synthesis.

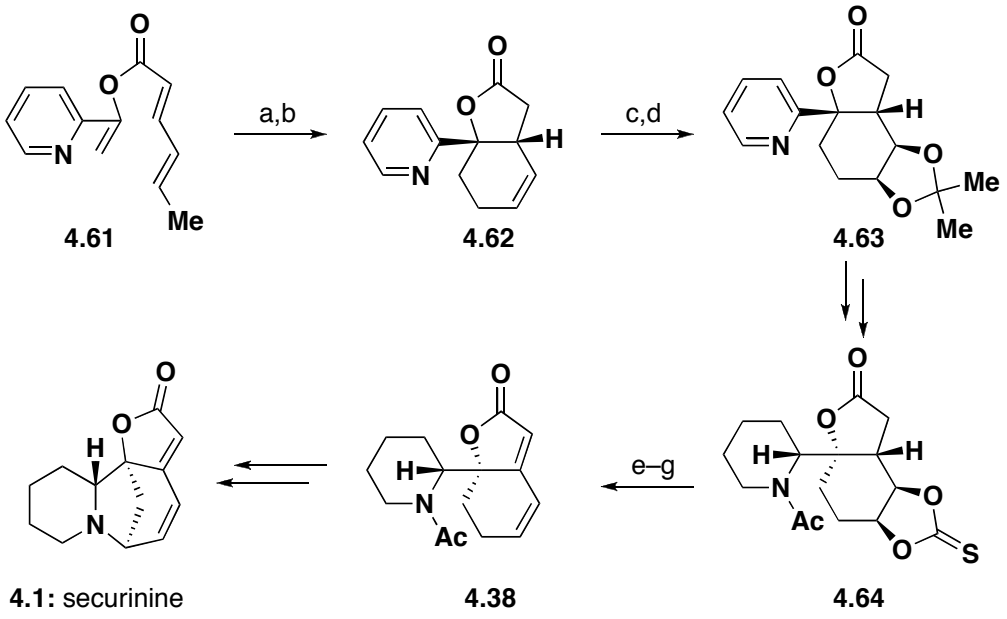

Scheme 4.7 Honda's racemic formal synthesis of securinine (**4.1**). *Reagents and Conditions:* a) LiHMDS, THF, HMPA, –78 °C, then AcOH (>42%); b) toluene, 180 °C (70%); c) OsO_4, NMO, *t*-BuOH, H_2O, 25 °C; d) 2,2-dimethoxypropane, CSA, DMF, 25 °C (96%, 2 steps); e) $Ni(COD)_2$, DMF, 60 °C (>80%); f) LDA, PhSeCl, THF, –78 °C; g) 30% H_2O_2, pyridine, CH_2Cl_2, 0 °C (40%, 2 steps). HMPA = hexamethylphosphoramide, NMO = 4-methylmorpholine *N*-oxide, CSA = camphor sulfonic acid, COD = 1,5-cyclooctadiene, LDA = lithium diisopropylamide.

4.2.6 Liras' Synthesis of Racemic Securinine

A year later, in 2001, Liras and co-workers[22] disclosed a concise total synthesis of racemic securinine. Here, a vinylogous Mukaiyama–Mannich raction of protected hydroxyfuran **4.66** with α-ethoxycarbamate **4.65** as depicted in Scheme 4.8 furnished the desired product as the major diastereomer in good yield (>57%). Conjugate addition of the lithium anion of allylphenylsulfoxide to the butenolide was accomplished

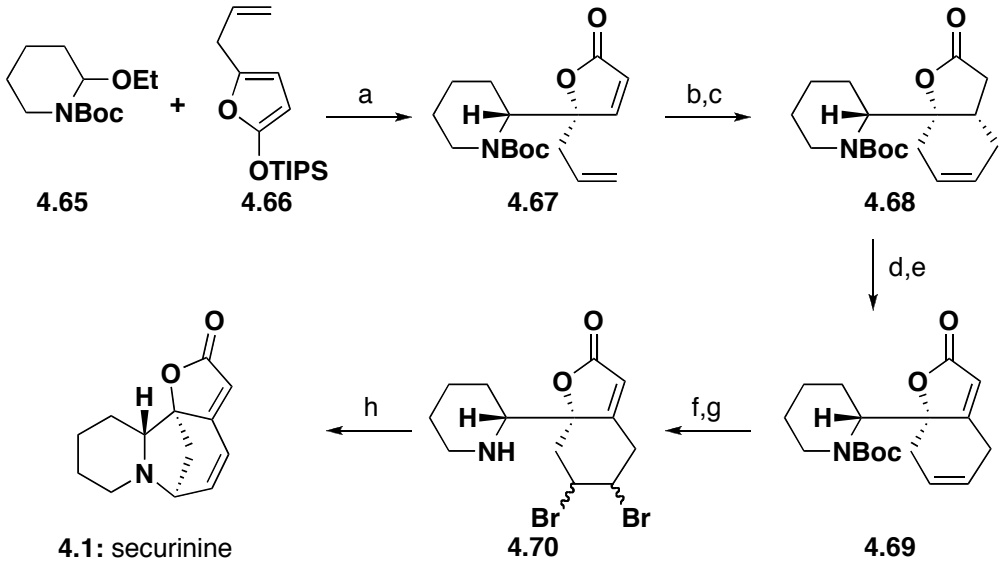

Scheme 4.8 Liras' racemic synthesis of securinine (**4.1**). *Reagents and Conditions:* a) TIPSOTf, heptane, –78 °C (57%); b) CH_2=$CHCH_2SOPh$, LiHMDS, THF, –78 °C (71%); c) Grubbs I, $ClCH_2CH_2Cl$, 70 °C (79%); d) LiHMDS, PhSeBr, THF, –78 → 25 °C; e) H_2O_2, CH_2Cl_2, 0 °C (43%, 2 steps); f) TFA, CH_2Cl_2; g) Br_2, $CHCl_3$, –10 → 25 °C; h) K_2CO_3, DMF, 70 °C (78%, 3 steps). TFA = trifluoroacetic acid.

diastereoselectively, and subsequent ring-closing metathesis with the 1st generation Grubbs metathesis initiator afforded alkene **4.68**. Two-step selenation/selenoxide elimination re-established the butenolide. *N*-Boc deprotection and alkene bromination afforded dibromide intermediate **4.70** that was eliminated to the conjugated butenolide

and ring closed with the nitrogen to afford racemic securinine. This work provided the first of several examples of ring-closing metathesis as a bond forming reaction within the unsaturated butenolide moiety.

4.2.7 Honda's Enantiospecific Synthesis of Securinine and Viroallosecurinine

Returning in 2004 to establish a novel total synthesis of securinine and viroallosecurinine, Honda and co-workers[23] demonstrated the second example of ring-closing metathesis in the context of the *Securinega* alkaloids (see Schemes 4.9 and 4.10).

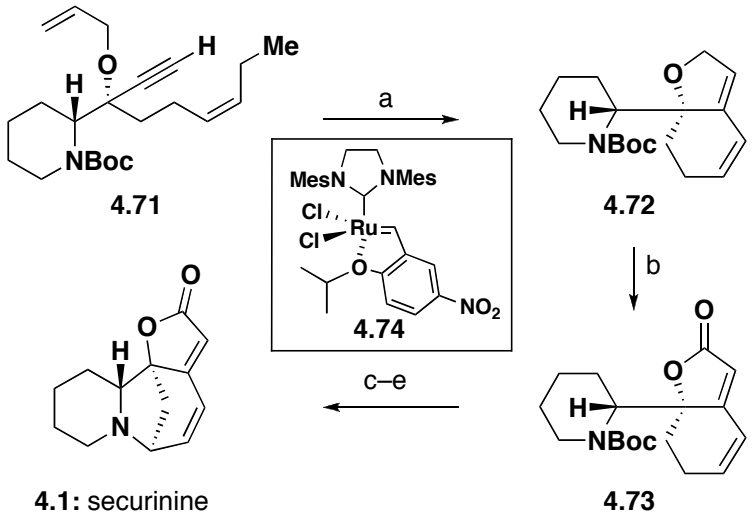

Scheme 4.9 Honda's enantiospecific synthesis of securinine (**4.1**). *Reagents and Conditions:* a) **4.74**, CH_2Cl_2, 25 °C (74%); b) CrO_3, 3,5-dimethylpyrazole, CH_2Cl_2, –20 °C (77%); c) NBS, AIBN, CCl_4, reflux; d) TFA, CH_2Cl_2, 25 °C; e) K_2CO_3, THF (45%, 3 steps). NBS = *N*-bromosuccinimide, AIBN = 2,2'-azobis(2-methylpropionitrile).

In thess studies, dieneyne **4.71** (derived from enantiomerically pure pipecolic acid) was subjected to a tandem ring-closing metathesis reaction in the presence of activated metathesis initiator **4.74** in 74%. The carbonyl of the butenolide was then efficiently installed with a CrO_3/3,5-dimethylpyrazole allylic oxidation (the Salmond protocol).

From here, the general Horii approach (see Section 4.2.1) was followed to access securinine (**4.1**). Worthy of note, however, is the substantially improved yield (45% over 3 steps) relative to the Horii procedure, likely a reflection of the more labile Boc protecting group as compared to the formamide from the Horii synthesis. In targeting viroallosecurinine, ketone **4.74** (an intermediate from their above approach to securinine) was first *N*-Boc deprotected to facilitate a chelation-controlled diastereoselective addition of the acetylide to the ketone, giving the opposite stereochemistry at the alcohol stereocenter. Reprotection of the amine and use of the same chemistry delineated above furnished viroallosecurinine (**4.4**).

4.2.8 The Alibés/de March Enantiospecific Synthesis of Securinine and Allonorsecurinine

Another enantiospecific synthesis of securinine starting from enantiopure pipecolic acid appeared in 2004 also involving a ring-closing metathesis strategy to establish the carbon framework of the butenolide. In this synthesis, Alibés, de March, and co-workers[24] elaborated ketone **4.76** (Scheme 4.11) to enoate **4.77** in 57% over 2 steps, a compound primed for ring-closing metathesis, which smoothly afforded the desired butenolide in 78% in the next step. Ketal deprotection followed by Stork–Wittig olefination afforded the *Z*-vinyl iodide **4.79** poised for intramolecular Heck reaction onto the butenolide. Application of similar conditions reported by Honda as described in Section 4.2.7 afforded the natural product (**4.1**). Similarly, the same strategy using proline as the starting material afforded allonorsecurinine (a non-natural compound) in 11 steps.

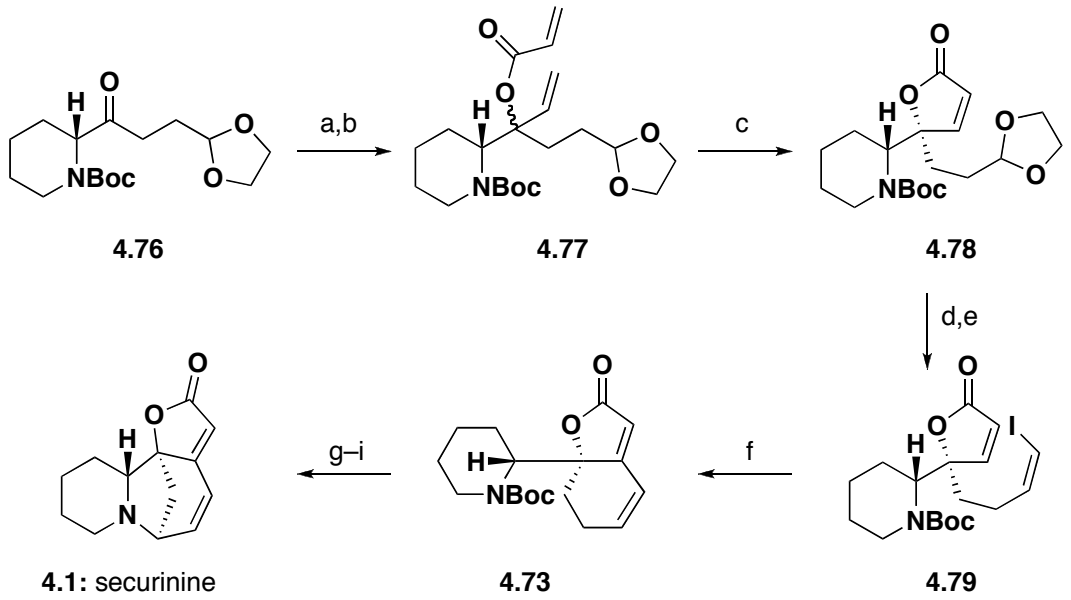

Scheme 4.11 The Alibés/de March enantiospecific synthesis of securinine (**4.1**). *Reagents and Conditions:* a) vinylmagnesium bromide, THF, –40 → 25 °C; b) acroloyl chloride, THF, 25 °C (57%, 2 steps); c) Grubbs II, CH_2Cl_2, reflux (78%); d) DDQ, MeCN, H_2O, 25 °C; e) Stork ylide, THF, –78 °C (28%, 2 steps); f) $PdCl_2(PPh_3)_2$, DMF, 90 °C (78%); g) NBS, CCl_4, reflux; h) TFA, $CHCl_3$, 25 °C; i) K_2CO_3, 25 °C (53%, 2 steps). DDQ = 2,3-Dichloro-5,6-dicyano-1,4-benzoquinone.

4.2.9 Figuerdo's Enantioselective Synthesis of Norsecurinine

The first enantioselective entry into the *Securinega* family of natural products was accomplished in 2005 by the Figuerdo and co-workers.[25] Here, the chiral center in intermediate **4.80** depicted in Scheme 4.12 was established by enantioselective epoxide ring opening using a method developed by the Trost group. This enantioenriched material (>98% *ee*) was then reduced and subjected to vinylogous Mukaiyama–Mannich reaction of its corresponding acyliminium species, successfully providing the desired adduct in 51% yield after crystallization. Ring-closing metathesis then afforded the diene in excellent yield (>98%), and the lactam was chemoselectively reduced with AlH_3. A final deprotection of the silyl ether provided the key intermediate from Jacobi's route (Section 4.2.3) that was then processed to the natural product (**4.17**).

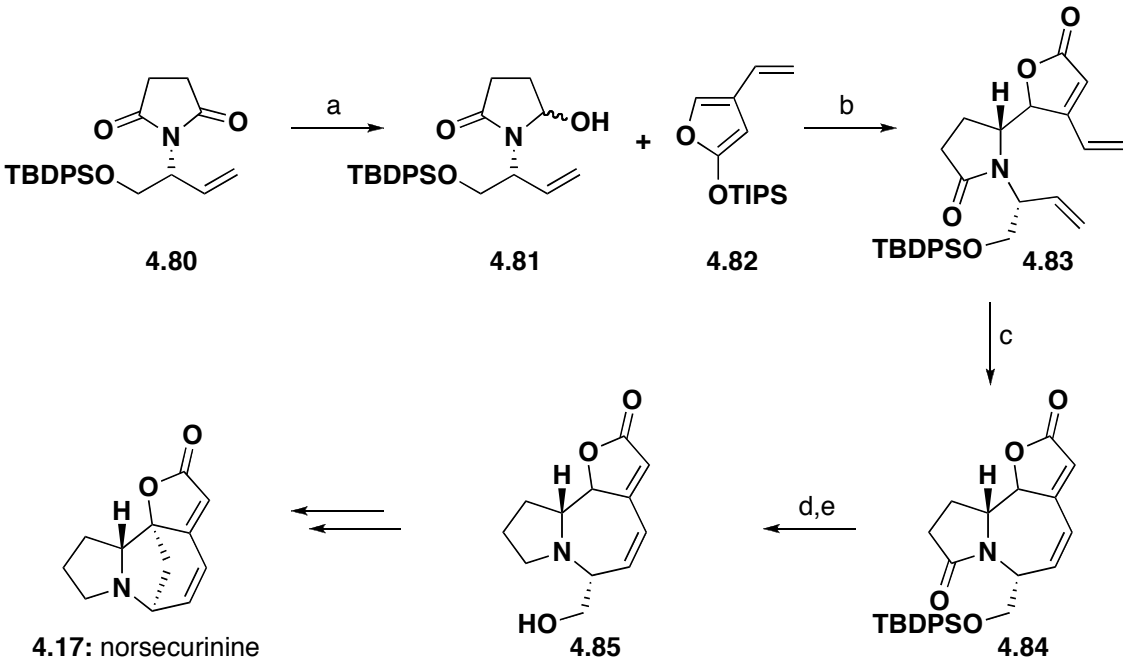

Scheme 4.12 Figuerdo's enantioselective synthesis of norsecurinine (**4.1**). *Reagents and Conditions:* a) $LiBEt_3H$, THF, –78 °C (87%); b) $BF_3{\bullet}OEt_2$, Et_2O (51%); c) Grubbs II, CH_2Cl_2, 25 °C (>98%); d) AlH_3, THF, 0 °C (57%); e) $HF{\bullet}Et_3N$, THF, 25 °C (94%).

4.2.10 Kerr's Enantiospecific Synthesis of Phyllantidine

In 2006, Kerr and co-workers[26] devised a creative approach outlined in Scheme 4.13 to the oxazine-containing *Securinega* alkaloid phyllantidine (**4.7**). This unique motif was established with good overall stereocontrol using a so-called "homo-1,3-dipolar cycloaddition" developed in their laboratory. In the event, a 3-component coupling of hydroxylamine **4.86**, aldehyde **4.87**, and homochiral vinyl cyclopropane diester **4.88** smoothly delivered the target 1,2-oxazine **4.89** in very good yield (86%) and high diastereoselectivity (12:1 *cis*/*trans*). Krapcho decarboxylation and α-hydroxylation of the resultant ester afforded alcohol **4.90** as the major product (3:1 d.r.). Processing of the ester to the aldehyde then allowed for nucleophilic addition of vinylmagnesium bromide, and subsequent oxidation of the resultant alcohol afforded intermediate **4.91**. This diene underwent facile ring-closing metathesis to establish the cyclic enone, and the procedure

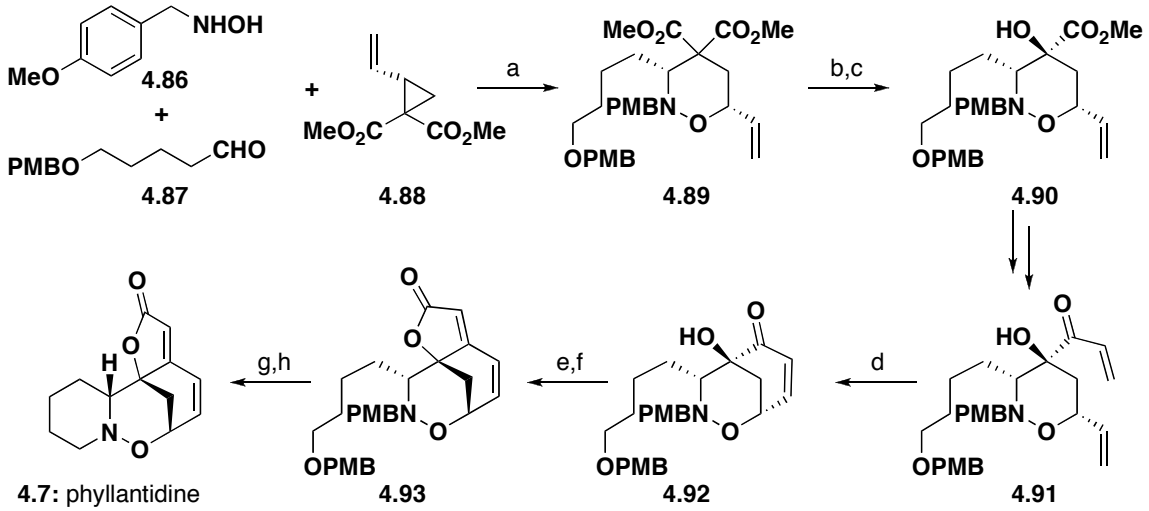

Scheme 4.13 Kerr's enantiospecific synthesis of phyllantidine (**4.7**). *Reagents and Conditions:* a) $Yb(OTf)_3$, toluene, reflux (86%); b) LiCl, DMSO, H_2O, 160 °C (85%); c) KHMDS, Davis oxaziridine, THF, –78 °C (80%); d) Grubbs II, CH_2Cl_2, reflux (74%); e) $(EtO)_2POCH_2CO_2H$, DCC, CH_2Cl_2 (71%); f) K_2CO_3, 18-C-6 (100%); g) DDQ, CH_2Cl_2 (98%); h) PPh_3, DIAD, toluene (98%). DIAD = diisopropyl azodicarboxylate.

developed by the Weinreb group was used secure butenolide **4.93** in 71% over 2 steps from α-hydroxy enone **4.92**. Final ring closure was accomplished *via* an intramolecular Mitsunobu reaction, delivering phyllantidine (**4.7**).

4.2.11 Kerr's Enantiospecific Synthesis of Allosecurinine

Two years after their reported synthesis of phyllantidine, the Kerr group then expanded upon their dipolar cycloaddition methodology, demonstrating that the intramolecular variant of the reaction could deliver pyrroloisoxazolidines as well. In practice, this reaction proved amenable to a total synthesis[27] of allosecurinine (**4.3**) as shown in Scheme 4.14. Treatment of homochiral hydroxylamine cyclopropane diester **4.94** with aldehyde **4.87** in the presence of $Yb(OTf)_3$ furnished the pyrroloisoxazolidine **4.95** in excellent yield (88%). Reductive cleave of the N–O bond and protection of the nitrogen as the corresponding Boc carbamate delivered alcohol **4.96**. Krapcho decarboxylation and alcohol elimination afforded alkene **4.97** in 81% over the 3

operations. This new material was processed similarly to their phyllantidine synthesis, installing the bridged butenolide system and completing allosecurinine (**4.3**).

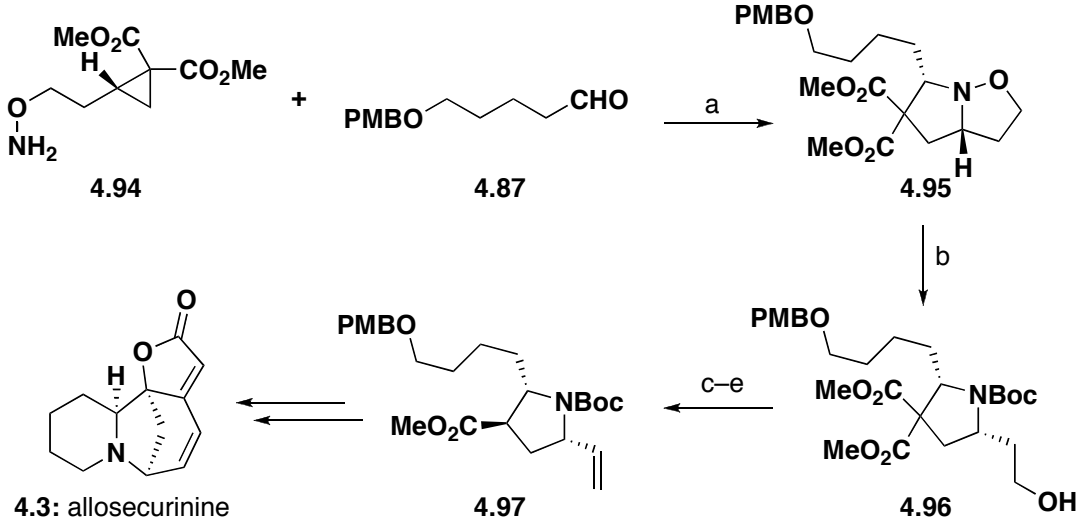

Scheme 4.14 Kerr's enantiospecific synthesis of allosecurinine (**4.3**). *Reagents and Conditions:* a) $Yb(OTf)_3$, CH_2Cl_2 (88%); b) $Pd(OH)_2$, Boc_2O, H_2, MeOH (85%); c) NaCN, H_2O, DMSO, 140 °C; d) $TMSCHN_2$, C_6H_6, MeOH; e) PBu_3, *o*-nitrobenzeneselenocyanate, THF, then H_2O_2, THF (81%, 3 steps).

4.2.12 The Busqué/de March Enantiospecific Synthesis of Allosecurinine and Viroallosecurinine

In 2008, Busqué, de March, and co-workers[28] employed the natural product menisdaurilide (shown as its silyl ether **4.99** in Scheme 4.15) in an intermolecular vinylogous Mukaiyama–Mannich reaction of its corresponding hydroxyfuran with iminium precursor **4.98**. Standard functional group manipulations of the silyl ether delivered the corresponding mesylate. Deprotection of the nitrogen allowed for facile intramolecular cyclization to deliver allosecurinine (**4.3**). Similarly, use of the opposite antipode of menisdaurilide afforded viroallosecurinine (**4.4**).

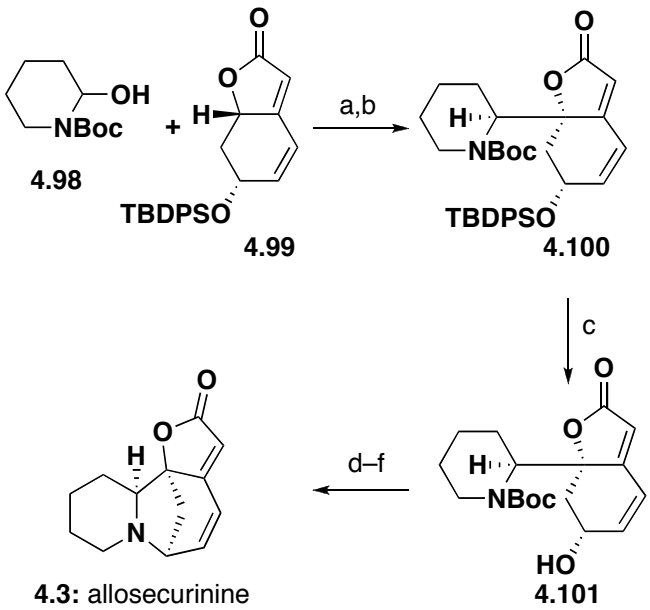

Scheme 4.15 The Busqué/de March enantiospecific synthesis of allosecurinine (**4.3**). *Reagents and Conditions:* a) TIPSOTf, Et_3N, Et_2O, 0 °C; b) *n*-Bu_2BOTf, –78 °C (76%); c) 3HF•Et_3N, THF, 25 °C (90%); d) MsCl, Et_3N, CH_2Cl_2, 0 °C; e) TFA, CH_2Cl_2, 25 °C; f) K_2CO_3, 25 °C (69%, 3 steps).

4.2.13 Weinreb's Enantiospecific Synthesis of Secu'amamine A

The first total synthesis of a rearranged securinine-type alkaloid was accomplished in 2008 by the Weinreb group,[29] a summary of which is provided in Scheme 4.16. Removal of the *N*-Boc protecting group of proline-derived substrate **4.102** and subsequent treatment with teriary amine base provided the kinetic aza-Michael product **4.103** as the major diastereomer of the reaction. Indeed, treatment of this product with basic alumina caused complete epimerization at the newly-formed stereocenter, indicating that the initially formed product is produced under kinetic control. Oxidative cleavage of the exocyclic methylene furnished the corresponding ketone. Intramolecular aldol/lactonization afforded the desired butyrolactone **4.104** and an uncyclized hydroxy ester (not shown) in a 6:1 ratio and 47% over the 2 steps. The latter compound could be recycled in high yield to the desired lactone. Palladium-mediated reduction of the ketone

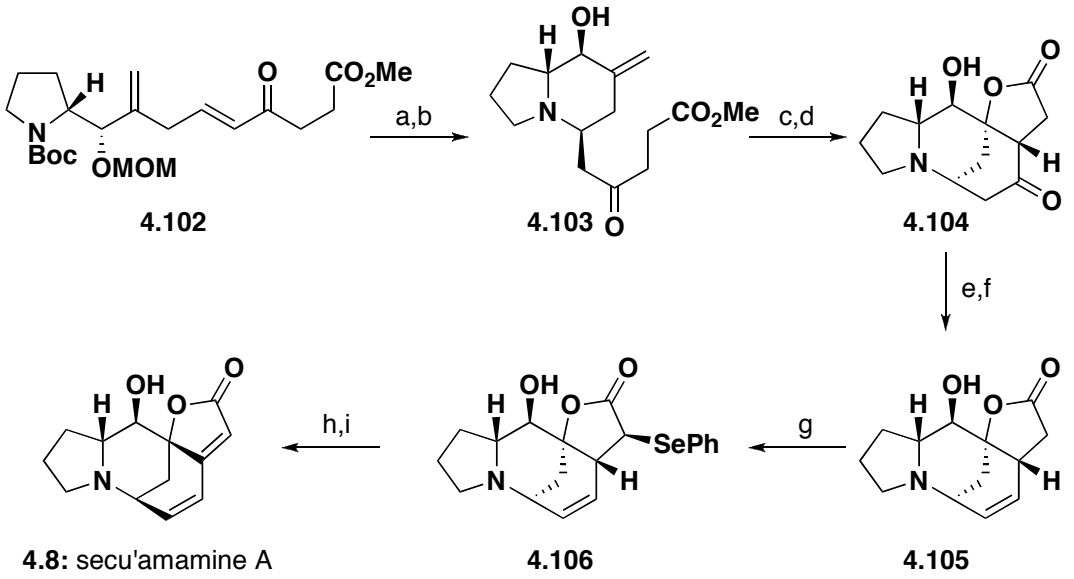

Scheme 4.16 Weinreb's enantiospecific synthesis of secu'amamine A (**4.8**). *Reagents and Conditions:* a) TFA, CH_2Cl_2; b) DIPEA, CH_2Cl_2, –78 °C (70%, 2 steps); c) OsO_4, NMO, $NaIO_4$, H_2O, THF (63%); d) NaOMe, MeOH, 25 °C (75%); e) KHMDS, $PhNTf_2$, THF (85%); f) $Pd(OAc)_2$, PPh_3, HCO_2H, DIPEA, DMF (95%); g) LDA, PhSeCl, THF (86%); h) $NaIO_4$, $NaHCO_3$, THF, H_2O (84%); i) HCl, MeOH, 60 °C (93%). DIPEA = Diisopropylethylamine.

via the corresponding enol triflate afforded the alkene in 81% overall. Finally, selenation/selenoxide elimination delivered the butenolide, and deprotection of the MOM ether delivered the final natural product.

4.2.14 Thadani's Enantiospecific Synthesis of Securinine

Thadani and co-workers reported a new strategy to access the securinine framework in 2009.[30] Overall, their approach relied on two different ring closing metathesis reactions and an intramolecular Heck reaction as delineated in Scheme 4.17. In particular, diene **4.107** (derived from *trans*-4-hydroxy-L-proline) was subjected to ring-closing metathesis with the 1st generation Grubbs initiator; alkene reduction was then accomplished with a standard Pd/C-mediated catalytic hydrogenation. Ester reduction to the aldehyde and olefination with the Stork ylide afforded the desired *cis*-

vinyl iodide **4.109** in 80% over the 2 steps. Unveiling of the secondary alcohol and oxidation to the ketone set the stage for a one-pot Grignard addition/acylation protocol. Then, a second ring closing metathesis delivered the butenolide with a final Heck reaction furnishing the desired natural product **4.1** in 64% for the final 2 transformations.

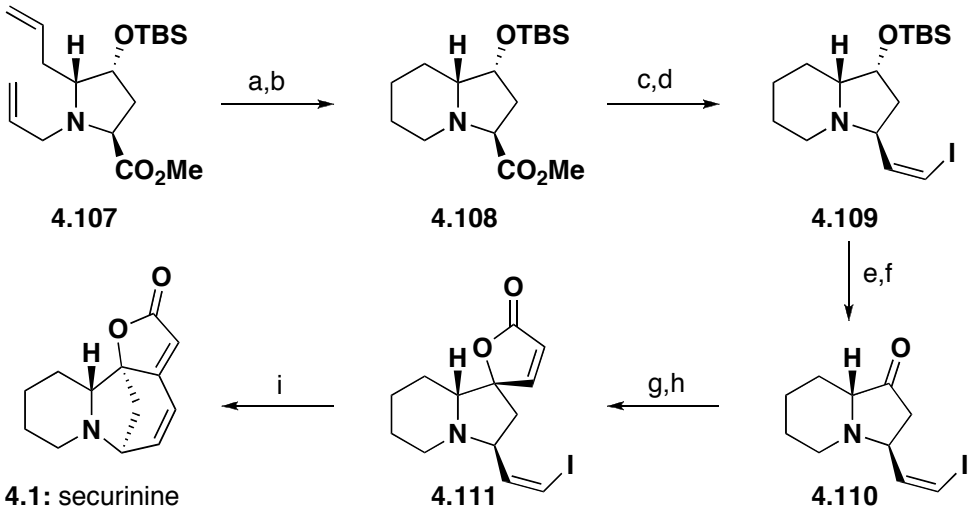

Scheme 4.17 Thadani's enantiospecific synthesis of securinine (**4.1**). *Reagents and Conditions:* a) Grubbs I, CH_2Cl_2, reflux (>93%); b) H_2, Pd/C, EtOAc (100%); c) DIBAL-H, toluene, –78 °C; d) Stork ylide, THF, –78 → –10 °C (80%, 2 steps); e) TBAF, THF, H_2O, 0 °C (79%); f) Swern oxidation (94%); g) vinylmagnesium bromide, THF, –20 °C, then acroloyl chloride, –78 → 25 °C (80%); h) Grubbs II, CH_2Cl_2, 60 °C (78%); i) Hermann-Beller catalyst, TBAB, NaOAc, DMA, 80 °C (82%). DIBAL-H = diisobutylaluminum hydride, TBAF = tetrabutylammonium fluoride, TBAB = tetrabutylammonium bromide.

4.2.15 Wood's Enantioselective Synthesis of Norsecurinine and Allonorsecurinine

In 2010, the second enantioselective total synthesis of norsecurinine **4.17** was accomplished by the Wood group.[31] Their key step involved an enantioselective tandem O–H insertion/Claisen rearrangement (see Scheme **4.18**) to access intermediate **4.114** from **4.14**. Azide displacement and Staudinger reduction afforded the pyrroline that was non-selectively reduced with $NaBH_4$ in EtOH and *N*-Boc protected (transformations not explicity shown) to give a diastereomeric mixture of pyrrolidines in a 1.4:1 ratio favoring

the drawn stereoisomer **4.115**. Oxidation of the primary alcohol delivered the corresponding aldehyde **4.115**, a motif that was then allylated and subjected to ring-closing metathesis conditions to deliver alkene **4.116** that was subsequently brominated. Oxidation of the secondary alcohol under Swern conditions was accompanied by concomitant bromide elimination to deliver enone **4.117**. TFA-mediated *N*-Boc deprotection/intramolecular cyclization afforded tricycle material that was processed using Weinreb's protocol to deliver the final natural product (**4.17**). Similarly, the pyrrolidine epimer was capable of affording the non-natural allonorsecurinine.

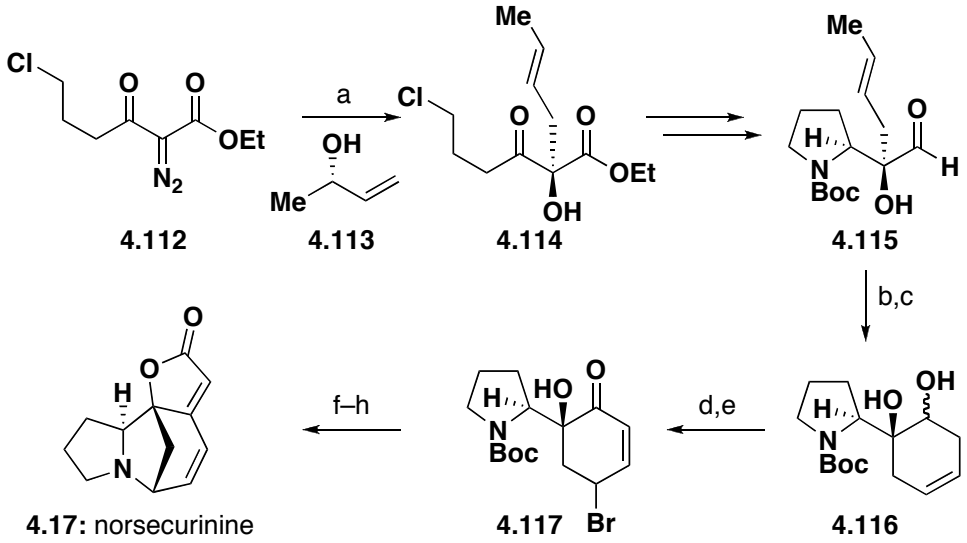

Scheme 4.18 Wood's enantiospecific synthesis of norsecurinine (**4.17**). *Reagents and Conditions:* a) $Rh_2(OAc)_4$, **4.113**, toluene, reflux, then BF_3•OEt_2, toluene, 25 °C (90% *ee*, 63% yield, 2 steps); b) allylmagnesium bromide, THF, 25 °C (72%); c) Grubb's II, CH_2Cl_2, reflux (87%); d) Br_2, CH_2Cl_2, 0 °C (95%); e) Swern oxidation (75%); f) TFA, CH_2Cl_2, reflux, then Et_3N, 25 °C; g) $(EtO)_2POCH_2CO_2H$, DCC, CH_2Cl_2; h) NaH, THF, 0 → 25 °C (38%, 3 steps).

4.3 A Brief Introduction to NHC Catalysis

The use of *N*-heterocyclic carbenes (NHCs) in inorganic chemistry and in organocatalysis has been an extremely fruitful field of research. The fact that several excellent reviews of NHC catalysis have appeared in the literature in recent years is a

testament to their growing use in catalysis.[32] For our purposes, a brief introduction to this field will prove useful in framing our own work toward the *Securinega* alkaloids, as will be described in the next chapter.

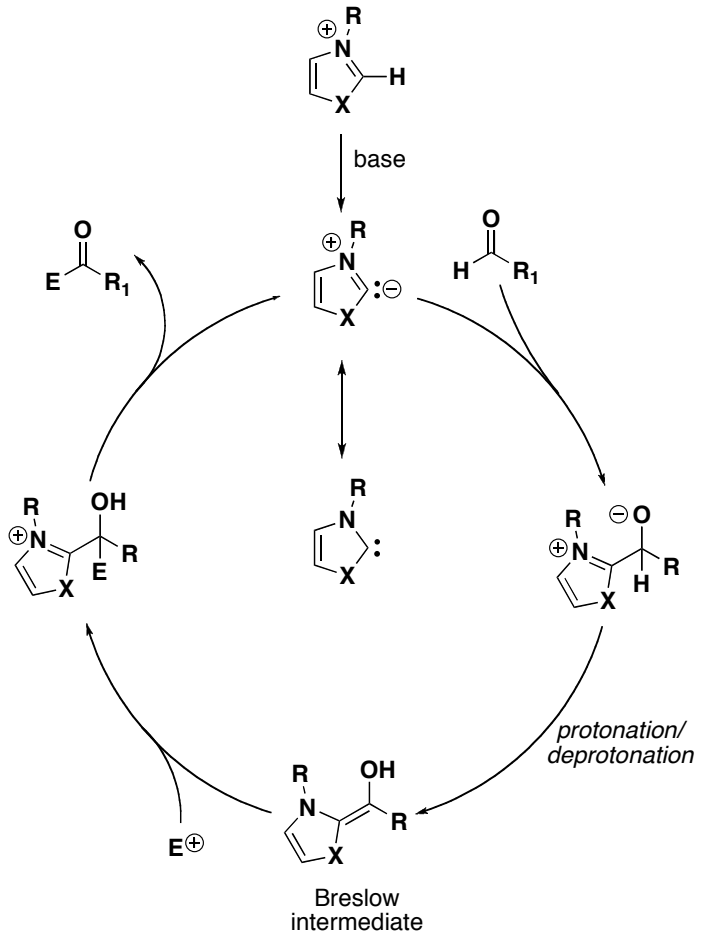

Figure 4.7 Catalytic cycle for NHC-catalyzed acyl anion generation from aldehydes.

The first literature report proposing an NHC as a structural unit in catalysis is attributed to Prof. Ronald Breslow in his landmark paper[33] detailing the mechanistic role of thiamine pyrophosphate (also known as vitamin B_1 or TPP) in the classic benzoin condensation. A general catalytic cycle for acyl anion generation from aldehydes is presented in Figure 4.7. Mechanistically, the reaction of the NHC with an aldehyde results in the formation of what is now termed the "Breslow intermediate." This

condensation effectively reverses the polarity of the acyl carbon, transforming a previously electrophilic center into a nucleophilic center *via* an acyl anion equivalent. This unusual reactivity has been exploited in various contexts, with the Stetter reaction[34] being one of the earliest reactions developed to take advantage of an NHC in catalysis. This reaction employs the acyl anion as the nucleophilic component in a Michael addition reaction to afford synthetically useful 1,4-dicarbonyl compounds.

While thiazolium catalysts formed the core of early NHC precatalysts, recent studies have overwhelmingly adopted the imidazolium and triazolium motifs depicted in Figure 4.8. These scaffolds have allowed for the preparation of chiral NHC precursors,

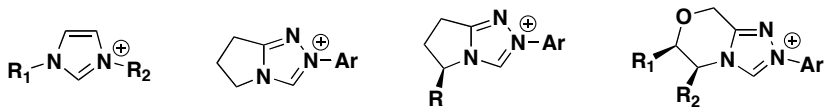

Figure 4.8 Common structural motifs in modern NHC catalysis.

depicted in a general sense in triazolium catalysts **4.120** and **4.121**, that have facilitated the development of catalytic, enantioselective transformations. For example, the Rovis group has performed extensive research in developing asymmetric Stetter reactions,[35] and in the intramolecular context, this reaction has proven both efficient and highly enantioselective.[35c,e] In the intermolecular context, however, a generally applicable enantioselective Stetter reaction remains elusive, and much current research has been devoted to this problem.

Beyond the generation of acyl anion equivalents, NHCs have found broad use in intramolecular redox transfer reactions,[36] some of which are depicted in Figure 4.9. For example, α,β-epoxy, α-chloro, and α,β-unsaturated aldehydes have been shown to be competent substrates in redox transfer reactions that formally oxidize the aldehyde to the

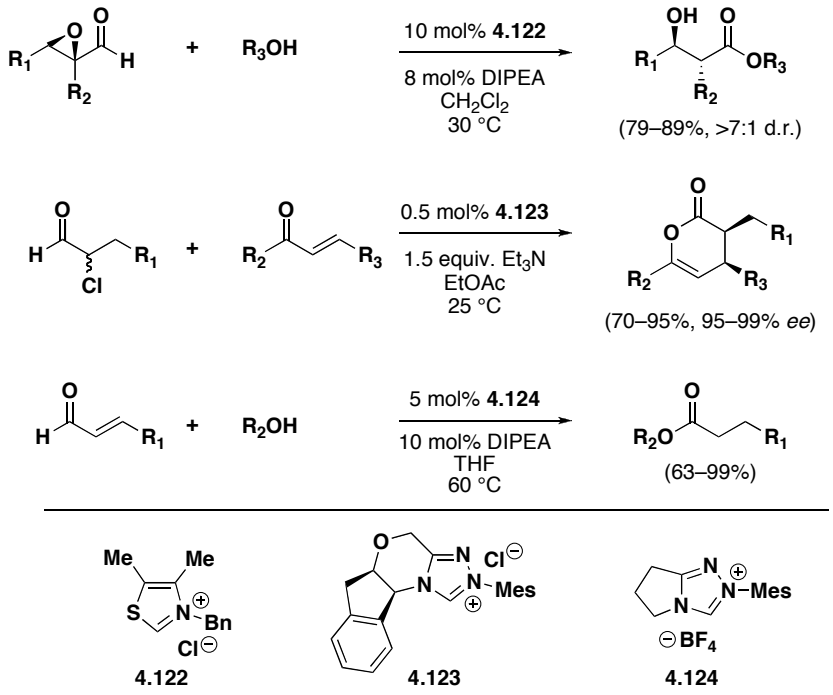

Figure 4.9 NHC-catalyzed redox transfer reactions of α-functionalized aldehydes.

acid/ester oxidation state while reducing the adjacent functional group. As an extension of this protocol, catalytic generation of homoenolate equivalents[37] (see Figure 4.10) have also appeared in the literature, allowing for the synthesis of diverse molecular scaffolds. In particular, the use of aldehydes and sulfonyl imines as electrophiles for homoenolates has greatly expanded the scope of such reactions, and very recently an enantioselective

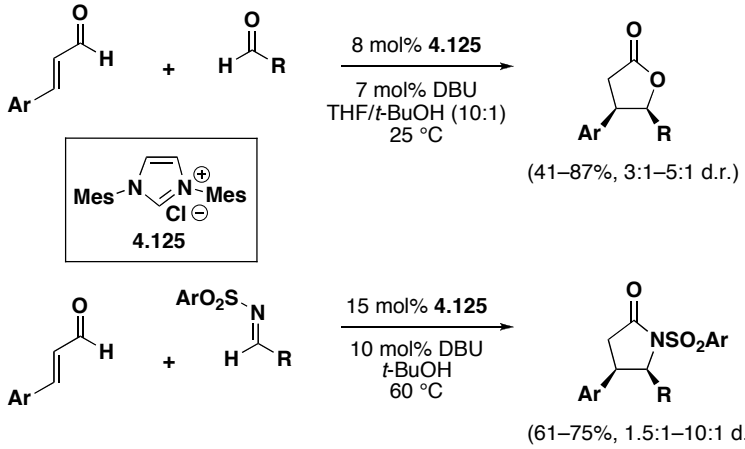

Figure 4.10 NHC-catalyzed generation of homoenolate quivalents from enals.

Claisen[38] reaction from a catalytically generated unsaturated acyl azolium intermediate has been realized. Finally, the development of cooperative NHC/Lewis acid catalysis[32i] has opened the door to previously poorly or completely unreactive electrophilic substrates, such as 1,2-keto-esters, often generating products with diastereoselectivities either opposite to or exceeding those reactions performed in the absence of Lewis acid. Figure 4.11 below provides some recent examples of NHC/Lewis acid cooperative catalysis for some relevant transformations.

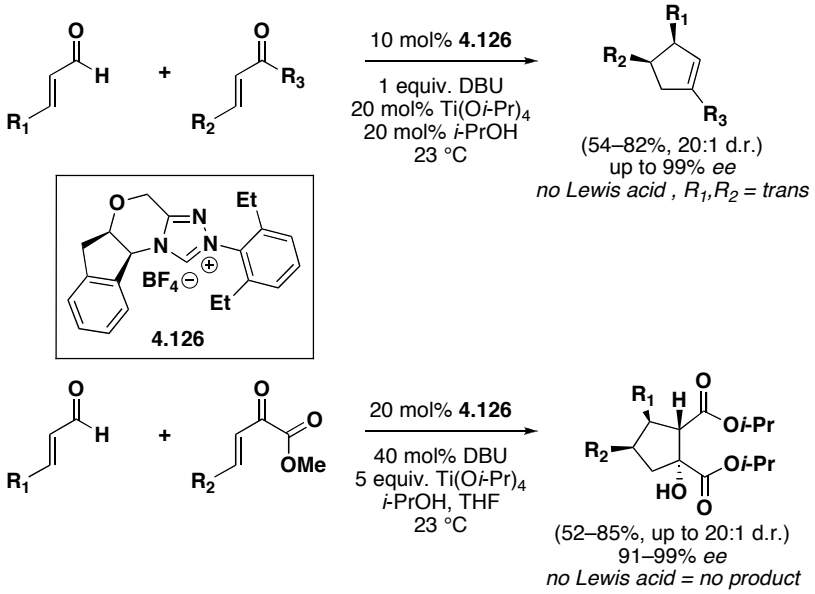

Figure 4.11 Recent examples of NHC/Lewis acid-mediated cooperative catalysis.

4.4 References

1. For a summary of the early isolations of various *Securinega* alkaloids, see: V. Snieckus, "The Securinega Alkaloids" in *The Alkaloids*, ed. R. H. F. Manske, 1975, vol. 14, pp. 425–506.

2. For an early review of the biological activities of these alkaloids, see: a) J. A. Beutler, A. N. Brubaker, *Drugs Fut.* **1987**, *12*, 957–976; For studies of the GABA activity of securinine, see: a) D. Rognan, T. Boulanger, R. Hoffmann, D. P. Vercauteren, J.-M. Andre, F. Durant, C.-G. Wermuth, *J. Med. Chem.* **1992**, *35*, 1969–1977; b) E. Galvez-Ruano, M. H. Aprison, D. H. Robertson, K. B. Lipkowitz, *J. Neursoci. Res.* **1995**, *42*, 666–673; For studies of other various biological activities, see: a) H. Weenen, M. H. H. Nkunya, D. H. Bray, L. B. Mwasumbi, L. S. Kinabo, V. A. Kilimali, J. B. Wijnberg, *Planta Med.* **1990**, *56*, 371–373; b) J. L. Mensah, I. Lagarde, C. Ceschin, G. Michael, J. Gleye, I. Fouraste, *J. Ethnopharmacol.* **1990**, *28*, 129–133; c) H. Tatematsu, M. Mori, T.-H. Yang, J.-J. Chang, T. T.-Y. Lee, K.-H. Lee, *J. Pharm. Sci.* **1991**, *80*, 325–327; d) N. Z. Dong, Z. L. Gu, W. H. Chou, C. Y. Kwok, *Acta Pharmacol. Sinica* **1999**, *20*, 267–270.

3. For an interesting review on enantiomeric natural products, see: J. M. Finefield, D. H. Sherman, M. Kreitman, R. M. Williams, *Angew.Chem. Int. Ed.* **2012**, *51*, 4802–4836.

4. S. Imado, M. Shiro, Z. Horii, *Chem. Pharm. Bull.* **1965**, *13*, 643–651 and references cited therein.

5. a) R. J. Parry, *Tetrahedron Lett.* **1974**, *15*, 307–310; b) R. J. Parry, *Bioorg. Chem.* **1978**, *7*, 277–288.

6. A. Ohsaki, H. Ishiyama, K. yoneda, J. Kobayashi, *Tetrahedron Lett.* **2003**, *44*, 3097–3099.

7. P. Magnus, A. I. Padilla, *Org. Lett.* **2006**, *8*, 3569–3571.

8. A. Ohsaki, Y. Kobayashi, K. Yoneda, A. Kishida, H. Ishiyama, *J. Nat.Prod.* **2007**, *70*, 2003–2005.

9. a) G. O. Iketubosin, D. W. Mathieson, *J. Pharm. Pharmacol.* **1963**, *15*, 810–815; b) S. Saito, T. Tanaka, K. Kodera, H. Nakai, N. Sugimoto, Z. Horii, M. Ikeda, Y. Tamura, *Chem. Pharm. Bull.* **1965**, *13*, 786–796.

10. B.-X. Zhao, Y. Wang, D.-M. Zhang, X.-J. Huang, L.-L. Bai, Y. Yan, J.-M. Chen, T.-Bu Lu, Y.-T. Wang, Q.-W. Zhang, W.-C. Ye, *Org. Lett.* **2012**, *14*, 3096–3099.

11. a) Z. Horii, M. Ikeda, Y. Tamura, S. Saito, K. Kodera, T. Iwamoto, *Chem. Pharm. Bull.* **1965**, *13*, 1307–1311; b) Z. Horii, M. Yamauchi, M. Ikeda, T. Momose, *Chem. Pharm. Bull.* **1970**, *18*, 2009–2012.

12. D. Arbain, A. A. Birbeck, L. T. Byrne, M. V. Sargent, B. W. Skelton, A. H. White, *J. Chem. Soc., perkin Trans. 1* **1991**, 1863–1869.

13. A. Ohsaki, T. Nagaoka, K. Yoneda, A. Kishida, *Tetrahedron Lett.* **2009**, *50*, 6965–6967.

14. L.-S. Gan, C.-Q. Fan, S.-P. Yang, Y. Wu, L.-P. Lin, J. Ding, J.-M. Yue, *Org. Lett.* **2006**, *8*, 2285–2288.

15. B.-X. Zhao, Y. Wang, D.-M. Zhang, R.-W. Jiang, G.-C. Wang, J.-M. Shi, X.-J. Huang, W.-M. Chen, C.-T. Che, W.-C. Ye, *Org. Lett.*, **2011**, *13*, 3888–3891.

16. S. Saito, H. Yoshikawa, Y. Sato, H. Nakai, N. Sugimoto, Z. Horii, M. Hanaoka, Y. Tamura, *Chem. Pharm. Bull.* **1966**, *14*, 313–314.

17. C. H. Heathcock, T. W. von Geldern, *Heterocycles* **1987**, *25*, 75–78.

18. a) P. A. Jacobi, C. A. Blum, R. W. DeSimone, U. E. S. Udong, *Tetrahedron Lett.* **1989**, *30*, 7173–7176; b) P. A. Jacobi, C. A. Blum, R. W. DeSimone, U. E. S. Dong, *J. Org. Chem.* **1991**, *113*, 5384–5392.

19. a) G. Han, M. G. LaPorte, J. J. Folmer, K. M. Werner, S. M. Weinreb, *Angew. Chem. Int. Ed.* **2000**, *39*, 237–240; b) G. Han, M. G. LaPorte J. J. Folmer, K. M. Werner, S. M. Weinreb, *J. Org. Chem.* **2000**, *65*, 6293–6306.

20. G. Han, M. G. LaPorte, M. C. McIntosh, S. M. Weinreb, *J. Org. Chem.* **1996**, *61*, 9483–9493.

21. a) T. Honda, H. Namiki, M. Kudoh, N. Wantanabe, H. Nagase, H. Mizutani, *Tetrahedron Lett.* **2000**, *41*, 5927–5930; b) T. Honda, H. Namiki, M. Kudoh, H. Nagase, H. Mizutani, *Heterocycles* **2003**, *59*, 169–187.

22. S. Liras, J. E. Davoren, J. bordner, *Org. Lett.* **2001**, *3*, 703–706.

23. a) T. Honda, H. Namiki, K. Kaneda, H. Mizutani, *Org. Lett.* **2004**, *6*, 87–89; b) T. Honda, H. Namiki, N. Watanabe, H. Mizutani, *Tetrahedron Lett.* **2004**, *45*, 5211–5213.

24. R. Alibés, M. Ballbe, F. Busqué, P. De March, L. Elias, M. Figueredo, J. Font, *Org. Lett.* **2004**, *6*, 1813–1816.

25. R. Alibés, P. Bayon, P. De March, M. Figueredo, J. Font, E. Garcia-Garcia, D. Gonzalez-Galvez, *Org. Lett.* **2005**, *7*, 5107–5109.

26. C. A. Carson, M. A. Kerr, *Angew. Chem. Int. Ed.* **2006***, 45*, 6560–6563.

27. A. B. Leduc, M. A. Kerr, *Angew. Chem. Int. Ed.* **2008**, *47*, 7945–7948.

28. F. Busqué, M. Canto, P. De March, M. Figueredo, J. Font, *Tetrahedron: Asym.* **2003**, *14*, 2021–2032.

29. P. Liu, S. Hong, S. M. Weinreb, *J. Am. Chem. Soc.* **2008**, *130*, 7562–7563.

30. B. Dhudshia, B. F. T. Cooper, C. L. B. Macdonald, A. N. Thadani, *Chem. Commun.* **2009**, 463–465.

31. M. R. Medeiros, J. L. Wood, *Tetrahedron* **2010**, *66*, 4701–4709.

32. a) A. T. Biju, N. Kuhl, F. Glorius, *Acc. Chem. Res.* **2011**, *44*, 1182–1195; b) P.-C. Chiang, J. W. Bode, N.-Heterocyclic Carbenes: From Laboratory Curiosities to Efficient Synthetic Tools; In *RSC Catalysis series*; S. Díez-González, Ed.; Royal Society of Chemistry: Cambridge, 2010; pp 339-445; c) C. D. Campbell, K. B. Ling, A. D. Smith, N-Heterocyclic Carbenes in Organocatalysis; In *N-Heterocyclic Carbenes in Transition Metal Catalysis and Organocatalysis, Catalysis by Metal Complexes*; C. S. J. Cazin, Ed.; Springer:Dortrecht, 2011; Vol. *32*, pp 263–297; d) J. L. Moore, T. Rovis, *Top. Curr. Chem.* **2009**, *291*, 77–144; e) E. M. Phillips, A. Chan, K. A. Scheidt, *Aldrichimica Acta* **2009**, *42*, 55–66; f) V. Nair, S. Vellalath, B. P. Babu, *Chem. Soc. Rev.* **2008**, *37*, 2691–2698; g) D. Enders, O. Niemeier, A. Henseler, *Chem. Rev.* **2007**, *107*, 5606–5655; h) N. Marion, S. Díez-González, S. P. Nolan, *Angew. Chem. Int. Ed.* **2007**, *46*, 2988–3000; i) D. T. Cohen, K. A. Scheidt, *Chem. Sci.* **2012**, *3*, 53–57.

33. R. Breslow, *J. Am. Chem. Soc.* **1958**, *80*, 3719–3726.

34. For an early review of the development of the Stetter reaction, see: H. Stetter, *Angew. Chem. Int. Ed.*, **1976**, *15*, 639–647.

35. a) D. A. DiRocco, K. M. Oberg, D. M. Dalton, T. Rovis, *J. Am. Chem. Soc.* **2009**, *131*, 10872–10874; b) Q. Liu, T. Rovis, *Org. Lett.* **2009**, *11*, 2856–2859; c) J. Read de Alaniz, T. Rovis, *Syn. Lett.* **2009**, 1189–1207; d) Q. Liu, S. Perrault, T. Rovis *J. Am. Chem. Soc.* **2008**, *130*, 14066–14067; e) J. Read de Alaniz, M. S. Kerr, J. L. Moore, T. Rovis, *J. Org. Chem.* **2008**, *73*, 2033–2040.

36. a) K. Y.-K. Chow, J. W. Bode, *J. Am. Chem. Soc.* **2004**, *126*, 8126–8127; b) M. He, G. Uc, J. W. Bode, *J. Am. Chem. Soc.* **2006**, *128*, 15088–15089;

37. a) S. S. Sohn, E. L. Rosen, J. W. Bode, *J. Am. Chem. Soc.* **2004**, *126*, 14370–14371; b) M. He, J. W. Bode, *Org. Lett.* **2005**, *7*, 3131–3134; c) M. Rommel, T. Fukuzumi, J. W. Bode, *J. Am. Chem. Soc.* **2008**, *130*, 17266–17267.

38. J. Kaeobamrun, J. Mahatthananchai, P. Zheng, J. W. Bode, *J. Am. Chem. Soc.* **2010**, *132*, 8810–8812

CHAPTER 5

Development of an NHC-Catalyzed Cascade Reaction to Access the Core Architecture of the *Securinega* Alkaloids

5.1 Retrosynthetic Analysis of Secu'amamine A

As detailed in the previous chapter, the majority of approaches to the unsaturated, bridging butenolide core of the *Securinega* alkaloids utilized a relatively narrow, albeit creative, range of strategies, and furthermore, the installation of this moiety generally required several steps that involved redox adjustments. In this regard, we hoped to provide a retrosynthetic analysis of this domain that would provide rapid access to this

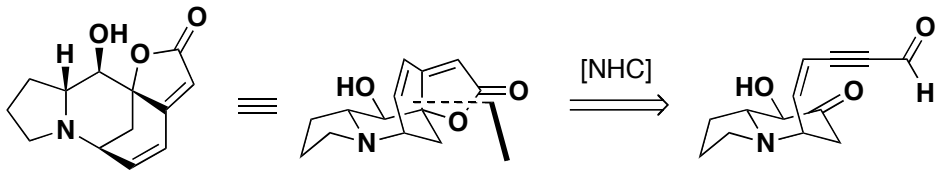

5.1: secu'amamine A **5.2**

Figure 5.1 Retrosynthetic analysis of secu'amamine A (**5.1**).

complex structural motif from simpler, acyclic precursors. Specifically, we chose secu'amamine A[1] as our target natural product for retrosynthesis given that only a single report detailing its synthesis[2] had appeared in the literature (see Section 4.2.13). Careful examination of the carbon framework within **5.1** (redrawn for clarity) suggested that the entire bridging butenolide motif could potentially be accessed from linear enynal precursor **5.2** *via* an intramolecular NHC-catalyzed homoenolate addition onto the lone ketone followed by lactonization (a formal [3+2] addition of an ynal and ketone).

This idea was particularly appealing in that such a direct preparation of this scaffold would clearly obviate the need for multiple functional group interconversions, allowing for a highly streamlined approach. Furthermore, such a retrosynthesis had the potential to provide a general approach to a large number of the *Securinega* alkaloids. While attractive in conception, it certainly was not clear at the outset of our work that such an approach could prove successful. Indeed, in the large body of literature

concerning NHC-derived homoenolates, to the best of our knowledge, not a single example of an ynal participating as a nucleophile in a homoenolate setting has been reported. Furthermore, the few examples utilizing ynals as substrates[3] clearly

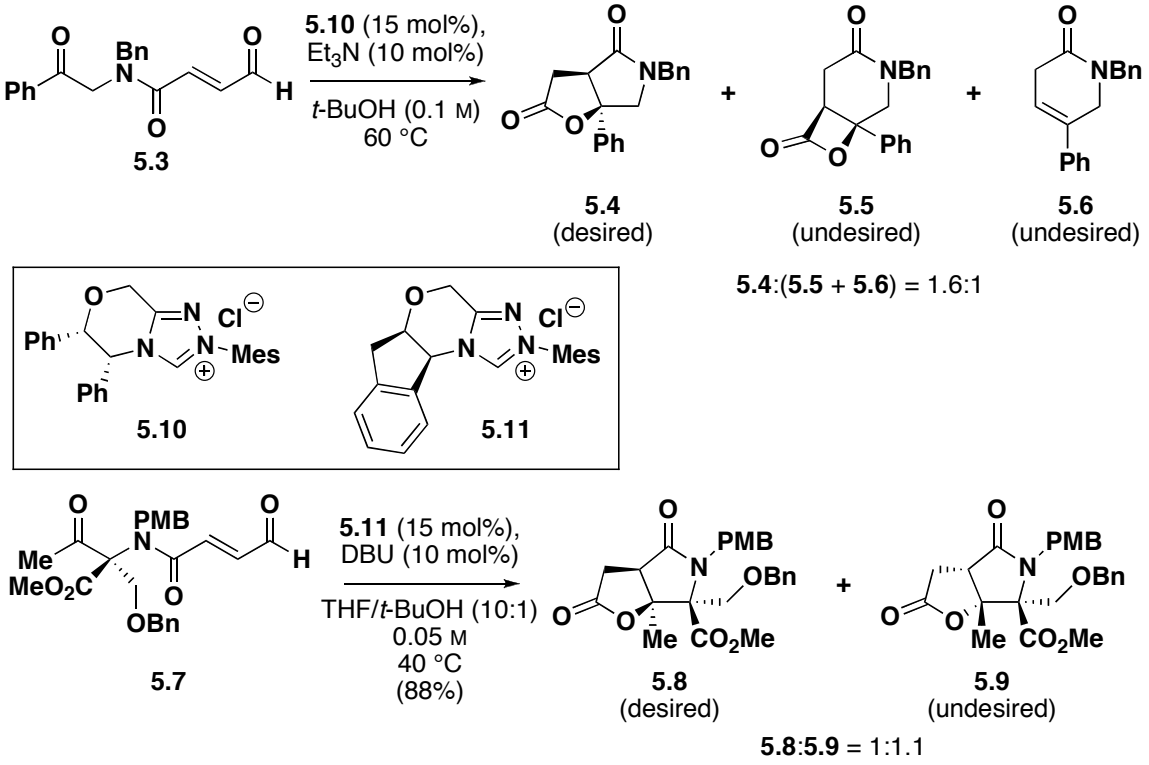

Scheme 5.1 Bode's intramolecular lactonization of enal-derived homoenolates. Product ratios, not isolated yields, were determined in the top reaction.

demonstrated a facile redox transfer reaction through protonation of their derived homoenolates. Additionally, only one report detailing enal-derived homoenolates as nucleophiles toward an unactivated ketone under NHC catalysis is known,[4] and only moderate success was achieved since good yields were only realized when non-enolizable ketones, such as **5.7**, were used (see Scheme 5.1). In our particular case, concerns were also raised by the potential sensitivity of such an ynal motif and its propensity to undergo intramolecular Michael addition from an enol/enolate derived from the ketone. Finally, the presence of additional conjugation to the ynal could potentially

introduce complications through homo-homoenolate reactivity. Even with the above concerns, we felt that if successful, the overall approach had the potential to dramatically increase the substrate scope of NHC homoenolate cataysis, providing access to formal hetero-Pauson–Khand[5] products, and thus we began a model study to test the feasibility of the idea.

5.2 Initial Studies to Access the [3.3.1] Bicyclic Framework of Secu'amamine A

As we hoped to target secu'amamine A, we chose compound **5.17** as a model for the piperidine ring-containing portion of the secu'amamine A indolizidine core. After some initial explorations, an efficient synthesis of the necessary test compound was realized as depicted in Scheme 5.2. First, *N*-Boc-4-piperidone was reduced with $NaBH_4$, and the resultant alcohol was protected with as the corresponding TBS ether. Piperidine lithiation with *s*-BuLi/TMEDA[6] allowed a formylation using DMF as the electrophile to afford aldehyde **5.13** as an inconsequential mixture of diastereomers. Stork–Wittig[7] olefination of this intermediate then provided *Z*-vinyl iodide **5.14** in good yield and excellent stereoselectivity (>20:1 *Z*:*E*). Sonogashira coupling of the iodide with propargyl alcohol afforded enynol **5.15** in good yields; pleasingly, no isomerization of the olefin was observed. Fluoride-mediated desilylation then provided diol **5.16**. Oxidation of the diol with 2.5 equivalents of Dess–Martin periodinane cleanly delivered the key step precursor keto-aldehyde **5.17** in quantitative yield. Intriguingly, the yield and mass recovery of product from this oxidation was highly dependent upon the reducing agent used during the quench. For example, use of Na_2SO_3 as the reductant led to extremely low crude mass recoveries (<10%), even after repeated extraction of the aqueous layer.

Control experiments demonstrated that decomposition was not occurring during the course of the reaction since simple solvent removal and NMR analysis of the crude material showed excellent conversion to product. Unfortunately, direct purification of the un-quenched material was only moderately successful since the product was also found to be relatively unstable to silica gel. A method, however, was required to remove the excess DMP and I(III) byproducts as these species were anticipated to be detrimental to the next reaction where they could function to oxidize the anticipated Breslow intermediate to the corresponding acylazolium. After some exploration of sacrifical reductants, we found that $Na_2S_2O_3$ proved capable of effecting the desired reduction without decomposing the product. Reproducibly high yields (>90%) were achieved by

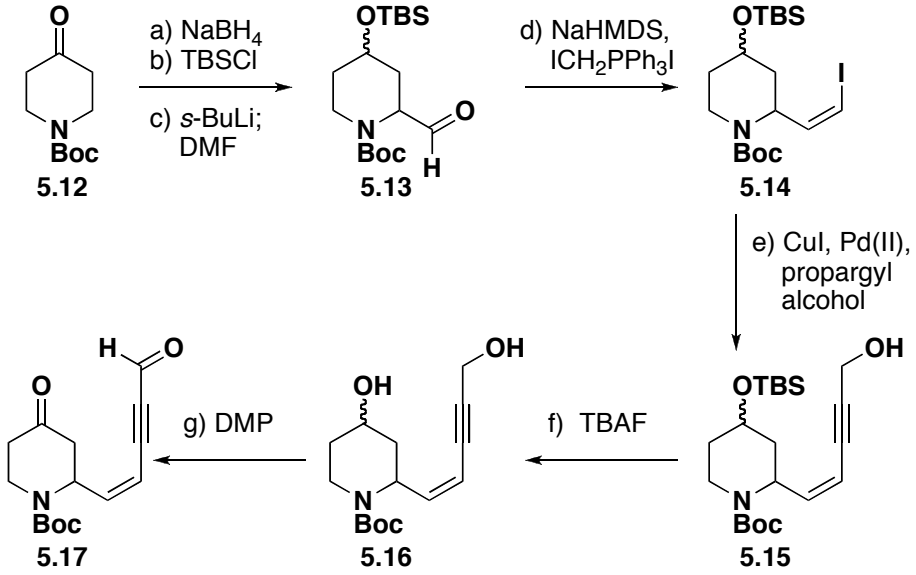

Scheme 5.2 Synthesis of cyclization precursor **5.17**. *Reagents and Conditions:* a) $NaBH_4$, MeOH, 0 °C; b) TBSCl, imidazole, CH_2Cl_2, 23 °C (99%, 2 steps); c) *s*-BuLi, TMEDA, Et_2O, –78 → –40 °C; DMF, –78 → –40 °C (85%); d) NaHMDS, ICH_2PPh_3I, THF/HMPA (10:1), –78 → –40 °C (85%); e) CuI (14 mol%), $PdCl_2(NCPh)_2$ (7 mol%), propargyl alcohol (3 equiv.) THF/piperidine (2:1), 23 °C (89%); f) TBAF, THF, 23 °C (85%); g) Dess–Martin periodinane, CH_2Cl_2, 23 °C (>95%). TBS = *tert*-butyldimethylsilyl, TMEDA = *N*,*N*,*N*′,*N*′-tetramethyl ethylenediamine, NaHMDS = sodium bis(trimethylsilyl)amide, HMPA = hexamethylphosphoramide, TBAF = tetrabutylamonium fluoride.

this method, and the crude material is exceedingly pure, obivating the need for purification.

With access to pure material, we began our first exploration of the desired, key NHC-catalyzed reaction. After an analysis of the literature, we elected to utilize conditions similar to those employed by Bode and co-workers[3a] in their enantioselective NHC-catalyzed Coates–Claisen reaction of ynal substrates **5.18** and Kojic acids **5.19**

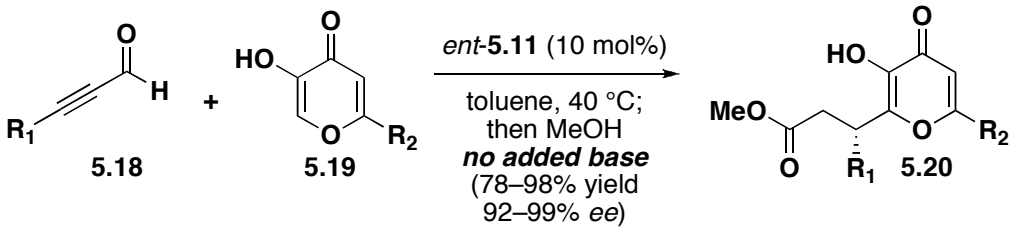

Scheme 5.3 Bode's enantioselective Claisen reaction of ynals **5.18** in the absence of additional base.

since they seemed an ideal fit for our purposes. In their report (summarized in Scheme 5.3), the authors found that their desired reaction could be promoted without the need of an exogeneous base; some experimental evidence suggested that the chloride counterion was capable of producing small amounts of reactive free carbene in solution. With our concerns that our substrate might be highly susceptible to intramolecular Michael additions (a result confirmed by later control experiments in the presence of Et_3N), we elected to follow the Bode precedent in our initial experiment with triazolium catalyst **5.21** (Scheme 5.4) on the basis of its ease of preparation[8] and precedent for the use of a similar NHC precatalysts on ynal substrates. In the event, keto-aldehyde **5.17** and an excess of NHC precursor **5.21** were dissolved in $CDCl_3$, heated to 50 °C overnight, and directly subjected to NMR analysis of the reaction mixture. The NMR spectrum suggested that essentially no reaction had occurred, with the starting material observed

without decomposition. Careful inspection of the ^{1}H-NMR spectrum, however, revealed the presence of a very minor component (<5%) exhibiting a new doublet at 6.79 ppm, in excellent agreement with the reported data for secu'amamine A. The reaction mixture was directly purified by PTLC, and pleasingly, ^{1}H-NMR analysis of the pure material indicated that the desired reaction had indeed taken place, validating our approach and providing the first example of an ynal-derived nucleophilic homoenolate.

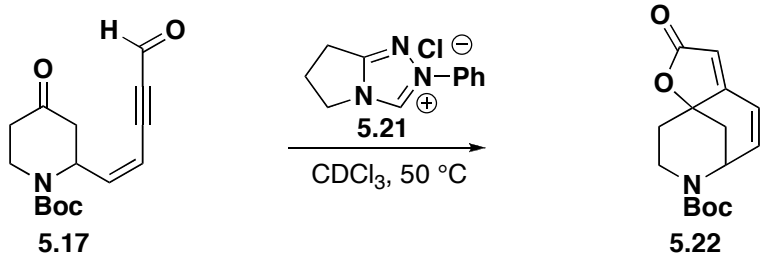

Scheme 5.4 Initial successful NHC-promoted cyclization of **5.17**.

5.3 Adaptation to a [3.2.1] Bicyclic Framework

Pleased with this initial result despite the low conversion, we then decided to explore the applicability of this reaction to the pyrrolidine lower homolog, as most of the natural products within the *Securinega* family display the bridging butenolide within a [3.2.1] bicyclic framework as opposed to the secu'amamine A [3.3.1] substructure. If successful, we would then explore reaction optimization. For these studies, *N*-Boc-*trans*-4-hydroxy-L-proline (**5.23**, Scheme 5.5) was used as the starting material. Aldehyde **5.24** was accessed from this commercially available compound in 4 standard steps. Methylation of the acid with $TMSCHN_2$ and protection of the alcohol as the TBS ether allowed for DIBAL-H reduction of the ester to the alcohol. Parikh-Doering oxidation furnished the desired aldehyde in good yield. Elaboration to the desired enynol **5.26** was accomplished according to the same protocol adopted in Section 5.2. Surprisingly, both

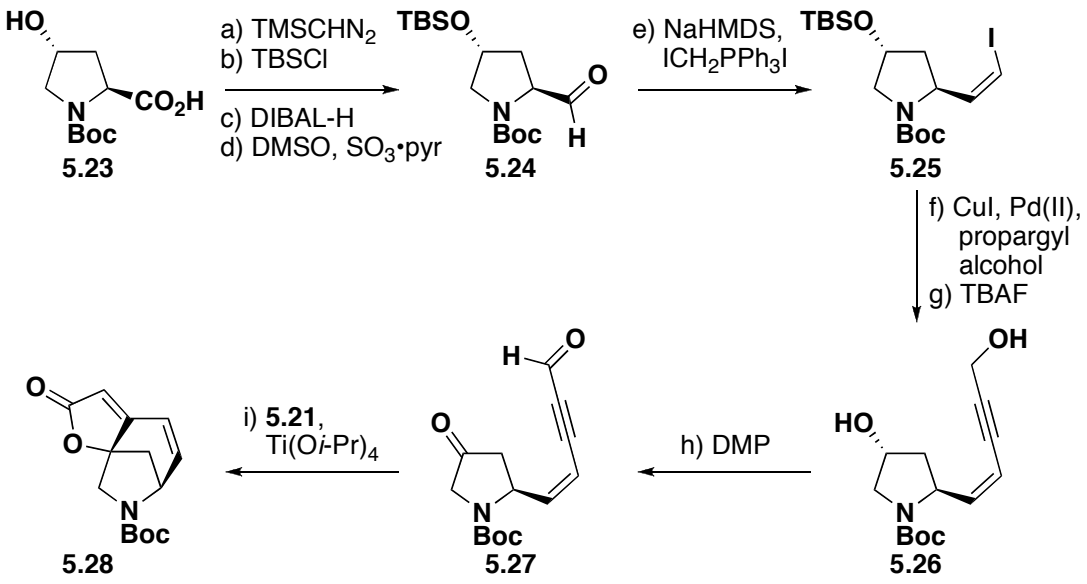

Scheme 5.5 Application of NHC-catalyzed cyclization to model substrate **5.27**. *Reagents and Conditions:* a) $TMSCHN_2$, THF/MeOH (10:1) –78 → 0 °C (99%); b) TBSCl, imidazole, CH_2Cl_2, 23 °C (98%, 2 steps); c) DIBAL-H, THF, –78 → 23 °C (98%); d) SO_3•pyr, Et_3N, DMSO/CH_2Cl_2 (2:1), 0 → 23 °C (90–97%); e) NaHMDS, ICH_2PPh_3I, THF/HMPA (10:1), –78 → –40 °C (50%); f) CuI (14 mol%), $PdCl_2(NCPh)_2$ (7 mol%), propargyl alcohol (3 equiv.) THF/piperidine (2:1), 23 °C (78%); g) TBAF, THF, 23 °C (94%); h) Dess–Martin periodinane, CH_2Cl_2, 23 °C (>95%); i) **5.21** (20 mol%), Ti(O*i*-Pr)$_4$ (2 equiv.), CH_2Cl_2, 25 °C (38%). TMS = trimethylsilyl, DIBAL-H = diisobutylaluminum hydride.

the Stork-Wittig and Sonogashira coupling were found to be poor yielding, each affording their respective product in ~30% yield when performed under conditions identical to those employed previously. While the Stork-Wittig reaction on **5.13** proved straightforward, the yield of the desired vinyl iodide **5.25** was found to be dependent upon the batch of phosphonium salt used. After some experimentation, we found that the temperature at which the phosphonium salt was prepared had a marked effect on the olefination yield, likely reflecting the quality of the prepared reagent. In particular, the use of phosphonium salt prepared at 50 °C for 3 d provided the best result, affording the desired vinyl iodide in 50% yield. Optimization of the Sonogashira reaction was also performed, and two factors proved important in improving the yield of this reaction. First, the use of high-purity vinyl iodide, which became much easier to access using the

adapted olefination protocol, provided a much cleaner reaction, and second, stirring the CuI and Pd(II) in piperidine under ambient atmosphere for 10 minutes prior to its addition to the THF solution of the vinyl iodide provided a dramatic increase to 78% yield of the coupled product. Deprotection of the secondary alcohol proved to be straightforward with TBAF, and subsequent oxidation of the ensuing diol to the corresponding keto-aldehyde with Dess–Martin proceeded without incident. Interestingly, keto-aldehyde **5.27** was found to be completely unstable to silica gel chromatography; the key finding, however, was that when this intermediate was subjected to the NHC-induced cyclization conditions delineated above, no desired product was observed, with the starting material only undergoing slow decomposition upon prolonged heating.

At this juncture, further exploration of the literature prompted us to consider the use of Lewis acid co-catalysts[9] for our reaction. In the context of this transformation (**5.27** → **5.28**), we hoped that a Lewis acid additive could potentially provide 3 beneficial effects: 1) activation of the aldehyde for attack by the carbene, 2) activation of the ketone for nucleophilic attack, and 3) coordination of both the ketone and the Breslow intermediate to organize the substrate appropriately for reaction. The examples demonstrated in the literature, however, had all been performed with some exogenous base, and thus we were concerned that our base-free conditions may not be amenable to such Lewis acid co-catalysis. We were, however, drawn to examples of NHC/Lewis acid cooperative catalysis employing $Ti(O\textit{i}Pr)_4$; this particular Lewis acid is amphoteric by virtue of its alkoxide ligands that are known to undergo rapid exchange in solution. In the context of our desired reaction, we hoped that $Ti(O\textit{i}Pr)_4$ would be both basic enough to

facilitate NHC deprotonation and Lewis acidic enough to promote the desired reaction. Ultimately, this approach proved successful, as the addition of 2 equivalents of $Ti(O\textit{i}Pr)_4$ to a CH_2Cl_2 solution of the keto-aldehyde and NHC precatalyst **5.21** (20 mol%) furnished the desired product after stirring at room temperature overnight. Furthermore, unlike the conditions employed in the absence of Lewis acid, this reaction had also reached full conversion, providing the desired product in 8% isolated yield. To the best of our knowledge, this reaction also provides the first example of NHC/Lewis acid cooperative catalysis in the absence of an exogeneous base.

5.4 Examination of Substrate Scope and Reaction Optimization

The promising leads outlined in the previous two sections prompted us to consider the possibility that the observed reaction may have some generality. Before exploring other substrates, however, we chose to return to piperidine model system **5.17** and examine the effect of Lewis-acid catalysis on the rate and yield of this reaction. Pleasingly, the use of $Ti(O\textit{i}Pr)_4$ on this model system (**5.17**) also led to full conversion and a notably higher product yield for **5.22** (37%) after reaction overnight at ambient temperature.

While we were certainly pleased with the ability of these reaction conditions to afford product on both of our model systems, the discrepancy in yield led to some consideration that the conformational equilibria of **5.17** could provide a strong biasing factor that facilitates the reaction. In particular, the presence of the carbamate protecting group on the nitrogen within the 6-membered piperidine scaffold generally leads to materials where the preferred conformation of the enynal side chain is axial (see Chapter

2 for the rationale for this conformational preference). Furthermore, the presence of the additional unsaturation in the side chain (i.e. the alkene) provided a restriction on the rotational degrees of freedom available to the system. Thus, given the conformational uniqueness of our model substrates, we set out to prepare various cyclization precursors in hopes of understanding what structural features were key contributors to the overall success of this reaction.

The first structural feature that we examined was the preferred axial orientation of the side chain. Thus, we prepared compound **5.29** (Scheme 5.6), a molecule lacking the

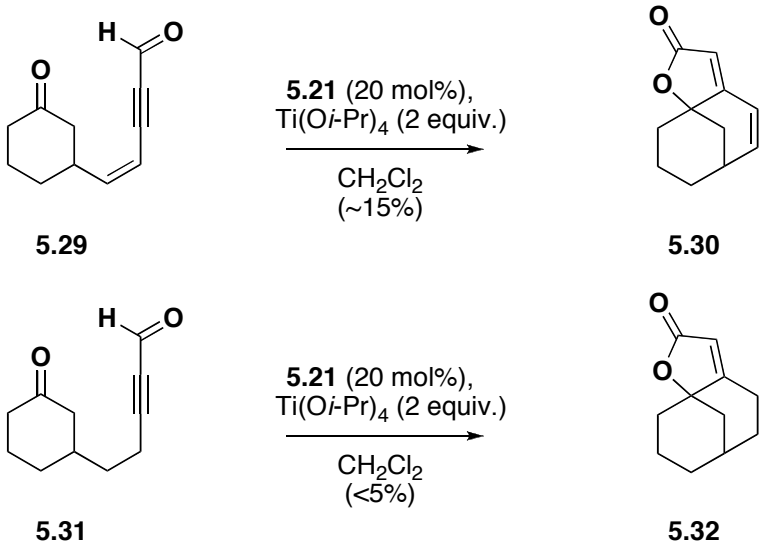

Scheme 5.6 Exploration of scope on conformationally flexible substrates **5.29** and **5.31**

N-Boc group that could bias the side chain conformation. Subjection of this intermediate to the above conditions did provide product, albeit in greatly reduced yield (~15%). Additionally, a more flexible side chain lacking the alkene further reduced the observed yield (<<5%). Although these results were not surprising given our previous analysis, these yields were disappointingly low. While we hoped that a different patterning of the reactive components in an intramolecular context could give rise to a good yielding

reaction, exploration of the generality of this reaction proved trying. Figure 5.2 shows a small selection of the compounds that could be prepared using this method. Unfortunately, in no case was product formed in greater than 10% yield, with most reactions delivering product in less than 5% yield. Having demonstrated a narrow substrate scope for efficient reaction, we chose to return to optimization of our original model systems that we felt could be applicable to the total synthesis of various *Securinega* alkaloids. In particular, we elected to perform our optimization studies with piperidine-derived substrate **5.17**.

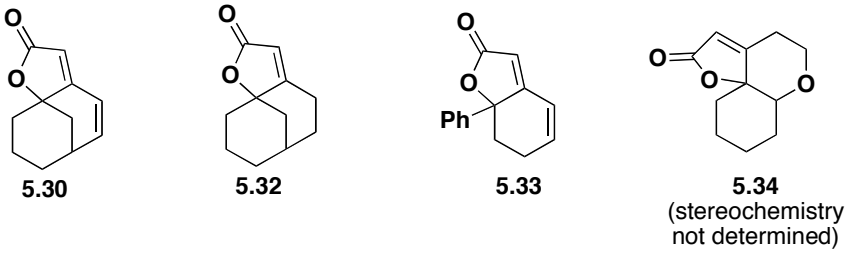

Figure 5.2 Selection of molecular scaffolds that could be prepared from our NHC-catalyzed reaction.

Our first areas of optimization were to examine the effect of catalyst structure and the inclusion of an exogeneous base in the reaction. Here, we hoped that pre-stirring the NHC precatalyst with a substoichiometric amount of base relative to catalyst could prevent any unwanted base-catalyzed reactions while providing a higher concentration of free carbene in solution. The results of these studies are presented in Table 5.1. For triazolium catalyst **5.21**, exogenous base was found to be compatible with the reaction, even though no substantial increase in yield was observed. Additionally, the identity of the amine base had only a small effect on the yield of the reaction. When imidazolium

precatalyst **5.35** was used, however, a marked effect on the identity of the base was

Table 5.1 Effect of NHC precatalyst, base, and Lewis acid loading on the cyclization of **5.17** to **5.22**.

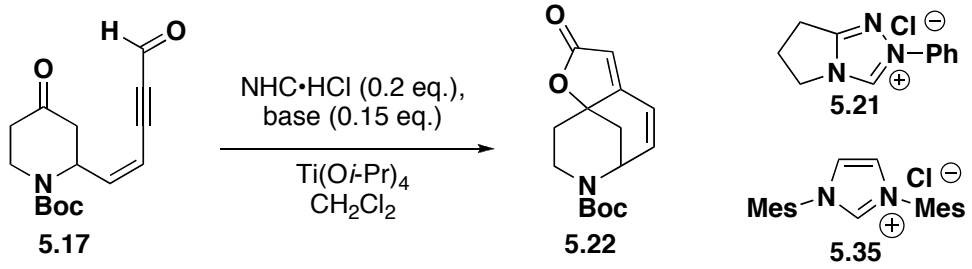

5.17 **5.22** **5.21** **5.35**

catalyst	base	Lewis acid (eq.)	solvent	yield (%)[a]
5.21	DBU	Ti(O*i*-Pr)$_4$ (2 eq.)	CH_2Cl_2	38
5.21	TMG	Ti(O*i*-Pr)$_4$ (2 eq.)	CH_2Cl_2	37
5.21	Et_3N	Ti(O*i*-Pr)$_4$ (2 eq.)	CH_2Cl_2	34
5.35	DBU	Ti(O*i*-Pr)$_4$ (2 eq.)	CH_2Cl_2	22
5.35	TMG	Ti(O*i*-Pr)$_4$ (2 eq.)	CH_2Cl_2	34
5.35	Et_3N	Ti(O*i*-Pr)$_4$ (2 eq.)	CH_2Cl_2	21
5.21	DBU	Ti(O*i*-Pr)$_4$ (2 eq.)	CH_2Cl_2	38
5.21	DBU	Ti(O*i*-Pr)$_4$ (1 eq.)	CH_2Cl_2	37
5.21	DBU	Ti(O*i*-Pr)$_4$ (0.5 eq.)	CH_2Cl_2	32
5.21	DBU	none	CH_2Cl_2	12
5.21	none	Ti(O*i*-Pr)$_4$ (1 eq.)	CH_2Cl_2	30

[a] Yields were determined by NMR analysis of the crude mixture using biphenyl as an internal standard.

demonstrated, with more basic amines giving higher yield. In particular, the combination of tetramethylguanidine (TMG) and imidazolium **5.35** gave yields (34%) that were comparable to the triazolium catalyst. Given the slightly higher yields of the triazolium/DBU system, however, we elected to proceed with these conditions in our futher studies.

Next, the effect of the Lewis acid loading was explored. These experiments demonstrated that lowering the loading from 2 equivalents to 1 equivalent was tolerated without any decrease in yield. The use of 0.5 equivalents, however, resulted in a notable decrease in yield, and furthermore, the exclusion of $Ti(O\textit{i}Pr)_4$ afforded very poor yields (12%) even though the reaction had reached near complete conversion (97%). Thus, it became clear that the Lewis acid had a beneficial effect on the reaction, consistent with our previous observations. While our original conditions employing 2 equivalents of $Ti(O\textit{i}Pr)_4$ afforded product in 38% yield in the absence of base, lowering the Lewis acid loading to 1 equivalent afforded product in 30% yield in the absence of base. Thus, the combination of base and 1 equivalent of Lewis acid appeared optimal.

Given the marked yield and rate improvement observed in the presence of a Lewis acid additive, we undertook an extensive Lewis acid screen. Interestingly, only a

Table 5.2 Effect of Lewis acid used as co-catalyst on the yield of cyclization.

catalyst	base	Lewis acid (eq.)	solvent	yield (%)[a]
5.21	DBU	$Ti(O\textit{i}\text{-}Pr)_4$ (1 eq.)	CH_2Cl_2	38
5.21	DBU	LiCl	CH_2Cl_2	0
5.21	DBU	$MgBr_2$	CH_2Cl_2	0
5.21	DBU	$Mg(OTf)_2$	THF	0
5.21	DBU	$Sc(OTf)_3$	THF	0
5.21	DBU	$Mg(O\textit{t}\text{-}Bu)_2$	THF	10
5.21	DBU	$Zr(OAc)_xOH_y$ (1 eq.)	CH_2Cl_2	29
5.21	DBU	ZrO_2	CH_2Cl_2	14
5.21	DBU	$Ti(O\textit{i}\text{-}Pr)_3Cl$ (1 eq.)	CH_2Cl_2	0
5.21	DBU	$Ti(O\textit{t}\text{-}Bu)_4$ (1 eq.)	CH_2Cl_2	16
5.21	DBU	$Ti(O\textit{t}\text{-}Bu)_4$ (0.5 eq.)	CH_2Cl_2	13

[a] Yields were determined by NMR analysis of the crude mixture using biphenyl as an internal standard.

very few number of those screened were found to afford product in any detectable yield. A variety of Lewis acids examined in this study are presented in Table 5.2. While metals other than Ti were capable of delivering the desired product, such as $Mg(O\textit{t}Bu)_4$, most Lewis acids, such as LiCl, $Mg(OTf)_2$, $MgBr_2 \bullet OEt_2$, $Sc(OTf)_3$, $La(OTf)_3$, and $Yb(OTf)_3$, were found to completely inhibit the reaction. Altering the ligand environment around the Ti(IV) was thus explored. The use of pinacol as an additive that could potentially alter the aggregation state was explored, and while tolerated, no yield improvement was observed. The use of $Ti(O\textit{t}Bu)_4$ also afforded the desired product, although the yield was substantially lower (16%). To our surprise, $Ti(O\textit{i}Pr)_3Cl$ did not provide a trace of desired product even though full consumption of the starting material had occurred. Thus, it appeared that $Ti(O\textit{i}Pr)_4$ was the optimal Lewis acid for our purposes.

Attention was then turned to the loading of the NHC precatalyst. The use of a lower catalyst loading (10 mol% precatalyst, 7.5 mol% DBU) resulted in a decreased yield (26%). Next, we opted to explore the effect of a stoichiometric amount of NHC precatalyst (1 equivalent, 0.75 equivalents DBU) on the yield, and surprisingly, the reaction was found to be much less efficient, affording product in only 20% yield. We attribute the reduced yield of the stoichiometric reaction to the fact that such a reaction could increase the concentration of reactive species in solution that could undergo unproductive intermolecular reactions.

During the course of these optimization studies, an interesting observation was made with regards to the crude NMR spectra of these reactions. Under our standard conditions (1 equiv. $Ti(O\textit{i}Pr)_4$, 0.20 equiv. NHC precatalyst **5.21**, 0.15 equiv. DBU), the material obtained from simple filtration of the reaction mixture through a small pad of

silica gel provided crude product that was of high purity, and thus the crude mass recoveries were quite poor. We speculated that the low mass balance could be a result of the product somehow forming a titanium complex that did not elute when placed on silica. Control experiments, however, demonstrated that the product was not only stable to the Lewis acid and reaction conditions but also could be quantitatively recovered by filtration through silica gel. In addition, aqueous workup and extraction did not improve the overall yield of the desired product. Given the instability of the starting material to silica gel, we considered the possibility that the starting material underwent decomposition in the presence of the Lewis acid. Thus, a solution of keto-aldehyde **5.17** was dissolved in CD_2Cl_2, and 2 equivalents of $Ti(O\textit{i}Pr)_4$ were added. The mixture was monitored by NMR, and within 15 minutes, a substantial decrease in the amount of starting material present was observed. Interestingly, no new discrete signals appeared in the ^{1}H-NMR spectrum. The reaction mixture had also become somewhat opaque, and a precipitate was observed, suggesting that the material was undergoing decomposition through some sort of polymerization. These results indicated that slow addition of the starting material to a solution of the precatalyst, DBU, and $Ti(O\textit{i}Pr)_4$ could potentially prevent undesired polymerization and increase the overall yield. Pleasingly, this hypothesis proved true. Slow addition of a solution of the starting material over a period of 5 hours afforded the desired product in 49% yield; slower addition did not improve the yield of the reaction. Interestingly, the same yield was obtained in the absence of DBU using the slow addition protocol. As an alternative to slow addition, we examined the effect of the reaction concentration where we found 0.01 M to be optimal. Once again, the reaction delivered product in 49% yield.

Disappointed with our inability improve the yield beyond 49% with methylene chloride as solvent, we returned to explore a different reaction solvent that had performed more poorly in initial solvent screens. Here, we hoped that the near insolubility of precatalyst **5.21** in toluene could further reduce the concentration of reactive species in solution and deliver an improved yield of the reaction. After some initial screens, conditions were identified under batch conditions that were superior to our previously optimal conditions in CH_2Cl_2. In particular, the combination of 0.4 equiv. **5.21** and 2.0 equiv. Ti(O*i*Pr)$_4$ at 0.036 M in toluene delivered product in 56% yield. While these conditions incorporated a higher catalyst loading than that used in our previous studies (0.2 equiv. **5.21**), we note that identical conditions in CH_2Cl_2 delivered product in only 50% yield. Pleased with this imporvement, we moved on to examine the effect of slow addition of starting material to a suspension of 0.4 equiv. **5.21** and 2.0 equiv. Ti(O*i*Pr)$_4$ in toluene to reach a final concentration of 0.03 M, and a dramatic yield improvement was observed, with product being isolated in 91% yield. Indeed, this slow addition protocol was also effective in providing a dramatic yield increase when pyrrolidine substrate **5.27** was used (22%). After some consideration, we suspected the yield with substrate **5.27** could be further improved by heating the reaction mixture in hopes of increasing the population of molecules in the correct conformation to undergo the desired reaction. Pleasingly, slow addition of pyrrolidine **5.27** to a 50 °C of reactants under otherwise identical conditions increased the yield of the reaction to 31%. With our optimization studies completed, we sought to apply our developed strategy to the synthesis of various *Securinega* alkaloids as described in the next section.

5.5 Application of the NHC Cascade Toward the Total Synthesis of Norsecurinine, Allonorsecurinine, and Secu'amamine A

Having developed an optimized protocol, we began efforts to prepare fully functionalized materials towards the total synthesis of several *Securinega* alkaloids. Our first targets were norsecurinine and the non-natural isomer allonorsecurinine, both of which we anticipated could be accessed from an appropriately functionalized common intermediate epoxide **5.38**[10] as outlined in Figure 5.3.

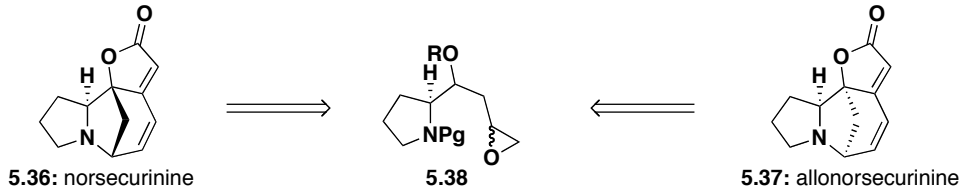

5.36: norsecurinine **5.38** **5.37:** allonorsecurinine

Figure 5.3 Retrosynthetic analysis of norsecurinine (**5.36**) and allonorsecurinine (**5.37**).

In the forward direction, *N*-Cbz proline (**5.39**, Scheme 5.7) was converted to the corresponding aldehyde by a two-step sequence involving borane-mediated reduction of the acid to the alcohol and subsequent Swern oxidation. Treatment of this aldehyde with *in situ*-generated allylindium afforded homoallylic alcohol **5.41** in high yield and diastereoselectivity. Protection of the secondary alcohol as the TBS ether and *m*-CPBA oxidation of the alkene furinished a 1:1 diastereomeric mixture of inseparable epoxides. Reductive removal of the Cbz group afforded aminoalcohols **5.43** and **5.44** that could be separated by silica gel chromatography. Our next synthetic operation required oxidation of the primary alcohol to the corresponding aldehyde. Despite several attempts with various procedures, the desired aldehyde was never observed, and these reactions instead only afforded either recovered starting material or complete decomposition. We

suspected that the tertiary amine was inhibiting the desired transformation, and thus we

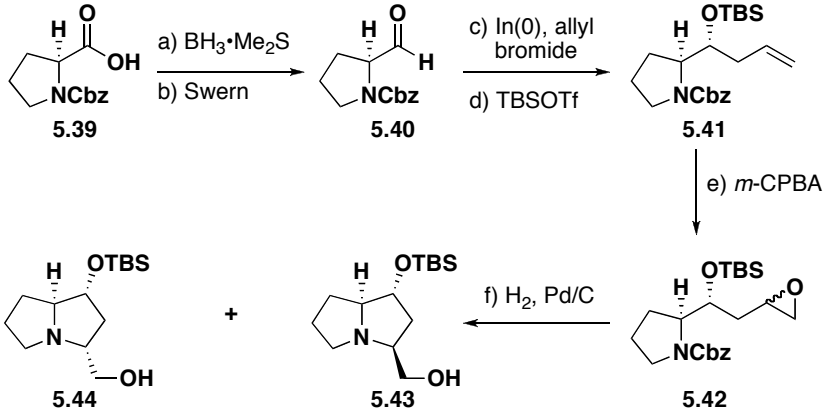

Scheme 5.7 Synthesis of amino alcohols **5.43** and **5.44**. *Reagents and Conditions:* a) BH_3•Me_2S, THF, 0 → 23 °C (99%); b) $(COCl)_2$, DMSO, Et_3N, CH_2Cl_2, –78 → 23 °C (98%); c) In(0), allylbromide, THF, 70 °C, then **5.40** –78 °C (87%); d) TBSOTf, Et_3N, CH_2Cl_2, –78 → –10 °C (92%); e) *m*-CPBA, CH_2Cl_2, 23 °C (83%); f) H_2, Pd/C, EtOAc/MeOH (1:1), 23 °C (>90%, ~1:1 **5.43**:**5.44**). OTf = trifluoromethanesulfonate, *m*-CPBA = *meta*-chloroperbenzoic acid.

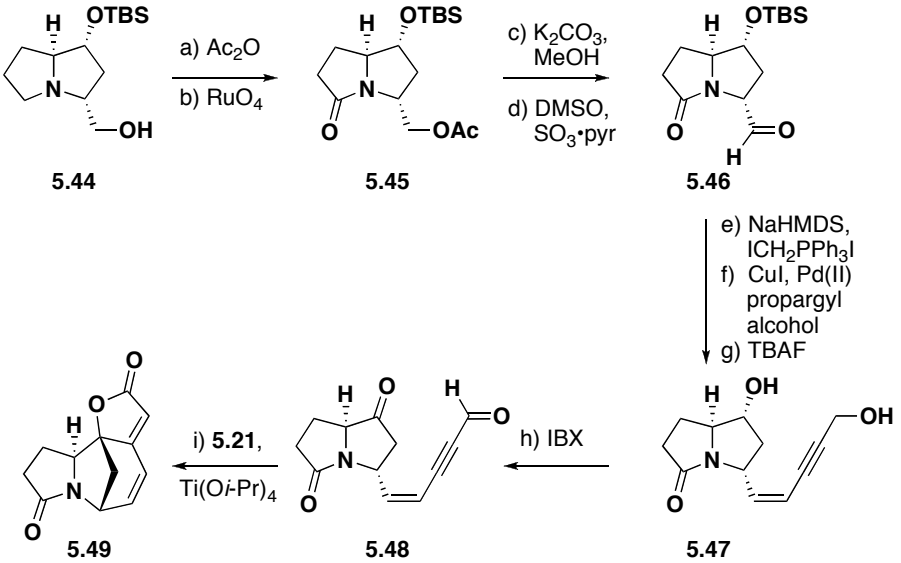

Scheme 5.8 Synthesis of oxidized norsecurinine congener **5.49**. *Reagents and Conditions:* a) Ac_2O, pyridine, 23 °C (99%); b) $RuCl_3$, $NaIO_4$, EtOAc/H_2O (1:1), 23 °C (50%); c) K_2CO_3, MeOH, 23 °C (85%); d) SO_3•pyr, Et_3N, DMSO/CH_2Cl_2 (2:1), 23 °C (85–95%); e) NaHMDS, ICH_2PPh_3I, THF/HMPA (10:1), –78 → 23 °C; f) CuI (14 mol%), $PdCl_2(NCPh)_2$ (7 mol%), propargyl alcohol (3 equiv.) THF/piperidine (2:1), 23 °C (30%, 2 steps); g) TBAF, THF, 23 °C (76%); h) IBX, MeCN, 80 °C (75–85%); i) **5.21** (20 mol%), $Ti(O\textit{i}\text{-}Pr)_4$ (2 equiv.), CH_2Cl_2, 23 °C (30%). IBX = 2-iodoxybenzoic acid.

required a method of tempering its reactivity. This goal was accomplished effectively as depicted in Scheme 5.8 by protection of the primary alcohol as the corresponding acetate and performing a regioselective RuO_4-mediated oxidation[11] to afford lactam **5.45** in 50% yield. Acetate deprotection then allowed for high-yielding Parikh-Doering oxidation to the aldehyde. Wittig reaction with the Stork ylide and Sonogashira coupling afforded the propargyl alcohol. Deprotection of the secondary alcohol and oxidation to the keto-aldehyde was accomplished with IBX in MeCN at 80 °C for 45 min, setting the stage for the key transformation. Pleasingly, treatment of key intermediate **5.48** with triazolium catalyst **5.21** and $Ti(O\textit{i}Pr)_4$ at ambient temperature overnight delivered oxidized norsecurinine in 30% yield. Here, CH_2Cl_2 had to be used as solvent due to the complete insolubility of the starting material in toluene. Additionally, the use of the other hydroxymethyl diastereomer **5.43** provided access to oxidized allonorsecurinine **5.50** (see Figure 5.4).

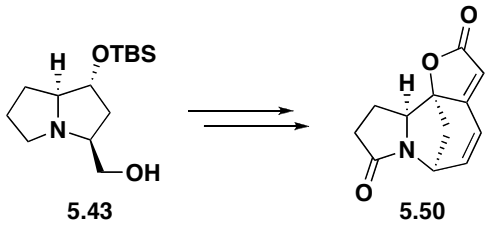

Figure 5.4 Elaboration of aminoalcohol **5.43** to oxidized allonorsecurinine congener **5.50**.

Attention now turned to secu'amamine A. Retrosynthetically, we envisioned that its [3.3.1] bicycle could be accessed from an appropriately functionalized intermediate **5.51** as depicted in Figure 5.5, and thus, the major challenge became stereoselective installation of the 3 chiral centers within the needed piperidine scaffold. In particular, accessing the 2,6-*trans* relationship between the side chains was anticipated to be challenging. Indeed, conjugate addition of metallated species to a vinylogous amide, such

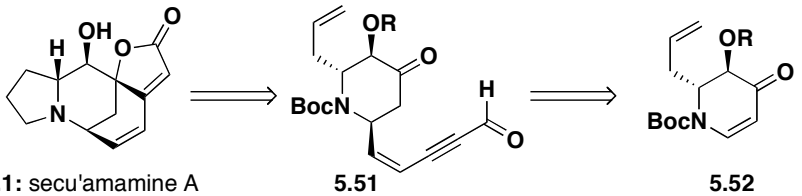

5.1: secu'amamine A **5.51** **5.52**

Figure 5.5 Retrosynthetic analysis of secu'amamine A.

as **5.52**, has been shown to give rise to the corresponding 2,6-*cis* diastereomer with high diastereoselectivities[12] as a result of the overwhelming electronic preference to undergo axial attack. We hoped, however, that the use of a very bulky Lewis acid to activate the carbonyl of the vinylogous amide would either block the less hindered face and force attack from the less electronically favored face or induce a conformational change that would place the hydroxyl and allyl groups equatorial and allow subsequent axial attack to deliver the requisite 2,6-*trans* material.

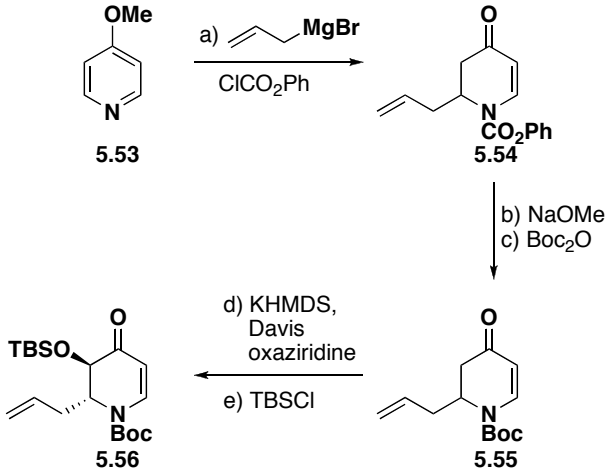

5.53 **5.54** **5.56** **5.55**

Scheme 5.9 Synthesis of vinylogous amide **5.56**. *Reagents and Conditions:* a) allylmagnesium bromide, $ClCO_2Ph$, THF, 0 °C, then 10% aq. HCl (65%); b) NaOMe, MeOH, 23 °C (94%); c) Boc_2O, DMAP, DMF, 23 °C (95%); d) KHMDS, Davis oxaziridine, THF, –78 → –40 °C (68%); e) TBSCl, imidazole, DMF, 23 °C (75%). DMAP = 4-(dimethylamino)pyridine.

Access to a conjugate addition precursor was achieved over 5 steps as outlined in Scheme 5.9. Dearomatization of 4-methoxypyridine with allylmagnesium bromide upon

activation with phenyl chloroformate delivered **5.54** after hydrolysis of the methyl enol ether. Deprotection of the nitrogen and reprotection as the corresponding Boc carbamate[13] delivered vinylogous amide **5.55**. Stereoselective hydroxylation was accomplished with KHMDS and the Davis oxaziridine at –78 °C, and the resultant alcohol was protected as the corresponding TBS ether **5.56**.

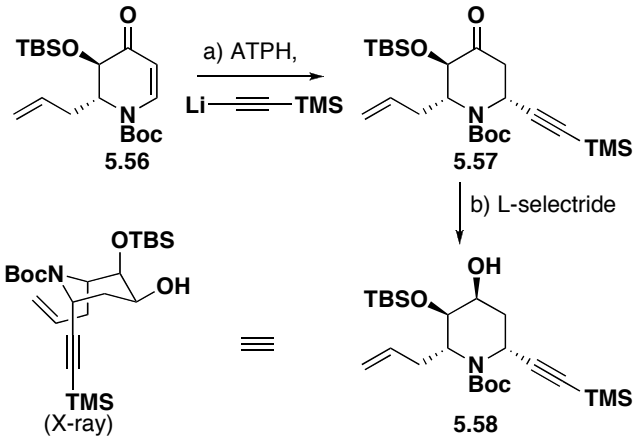

Scheme 5.10 ATPH-mediated conjugate addition to vinylogous amide **5.56**. *Reagents and Conditions:* a) $AlMe_3$, 2,6-diphenylphenol, **5.56**, CH_2Cl_2, –78 °C, then LiCCTMS, THF, –78 °C (83%, 94% brsm); b) L-selectride, THF, –78 °C (99%).

We were now in a position to attempt the proposed conjugate addition, the details of which are depicted in Scheme 5.10. Here, we chose to use Yamamoto's ATPH complex[14] (the Lewis acid resulting from a 3:1 mixture of 2,6-diphenylphenol and $AlMe_3$) as our bulky Lewis acid source; this complex has been previously shown to deliver stereochemistires opposite to that typically observed in standard cuprate addition reactions.[14] In the event, addition of a THF solution of lithium trimethylsilylacetylide to a CH_2Cl_2 solution of vinologous amide **5.56** and ATPH at –78 °C afforded a conjugate addition product in high yield (83%, 94% brsm) as a single diastereomer. 2D-NOESY studies were inconclusive in providing a structural assignment, and thus we sought to derivatize the product in hopes of providing a crystalline compound for X-ray analysis.

Thus, ketone **5.57** was subjected to reduction with L-selectride at –78 °C, delivering crystalline secondary alcohol **5.58** as a single diastereomer whose structure was confirmed by X-ray analysis. Unfortunately, this product is the result of undesired *cis* alkylation, and the 2,6-*cis*-diaxial conformation provides the rationale for the inability to conclusively determine the stereochemistry of the conjugate addition adduct using NOESY.

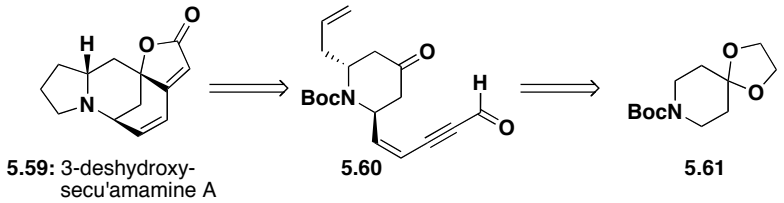

Figure 5.6 Retrosynthetic analysis of 3-deshydroxy-secu'amamine A (**5.59**).

Returning to the drawing board, we elected to target 3-deshydroxy-secu'amamine A as we anticipated that the desired 2,6-*trans*-disubstituted piperidine **5.60** (Figure 5.6) could arise from sequential *s*-BuLi alkylation reactions. Pressing forward as shown in

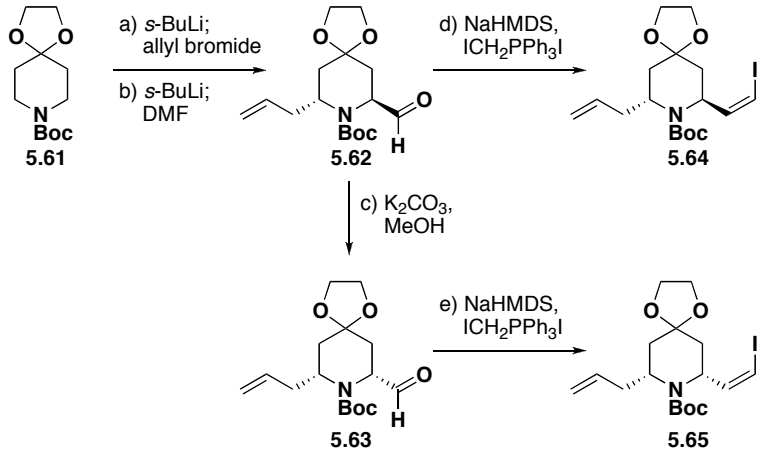

Scheme 5.11 Synthesis of *Z*-vinyl iodide **5.64**. *Reagents and Conditions:* a) *s*-BuLi, TMEDA, Et_2O, –78 → –40 °C; CuCN•2LiCl, THF, –78 °C, then allyl bromide, –78 → 23 °C (65%, unoptimized); b) *s*-BuLi, TMEDA, Et_2O, –78 → –40, then DMF –78 → –40 °C (60%); c) K_2CO_3, MeOH, 23 °C (77%); d) NaHMDS, ICH_2PPh_3I, THF/HMPA (10:1), –78 °C (80%); e) NaHMDS, ICH_2PPh_3I, THF/HMPA (10:1), –78 °C (yield not determined).

Scheme 5.11, protected ketone **5.61** was lithiated with *s*-BuLi/TMEDA, transmetallated to CuCN, treated with allyl bromide, and warmed to 23 °C overnight, affording the desired allylated product in an unoptimized yield of 65%. A second round of lithiation was then quenched with DMF afforded aldehyde **5.62** in 60% yield with good diastereoselectivity (>8:1). Our next transformation, namely conversion of the aldehyde to the corresponding vinyl iodide, provided some concern that the aldehyde could undergo facile epimerization under the strength of the basic conditions used during the olefination, and thus a portion of aldehyde **5.62** was subjected to epimerization with K_2CO_3 in MeOH at room temperature. Both aldehydes **5.62** and **5.63** were taken forward separately and treated with the Stork ylide, and after purification, NMR analysis indicated that the resultant vinyl iodides were distinct compounds, implying that epimerization in the course of the Wittig reaction did not occur and that the desired 2,6-*trans* stereochemical relationship was intact.

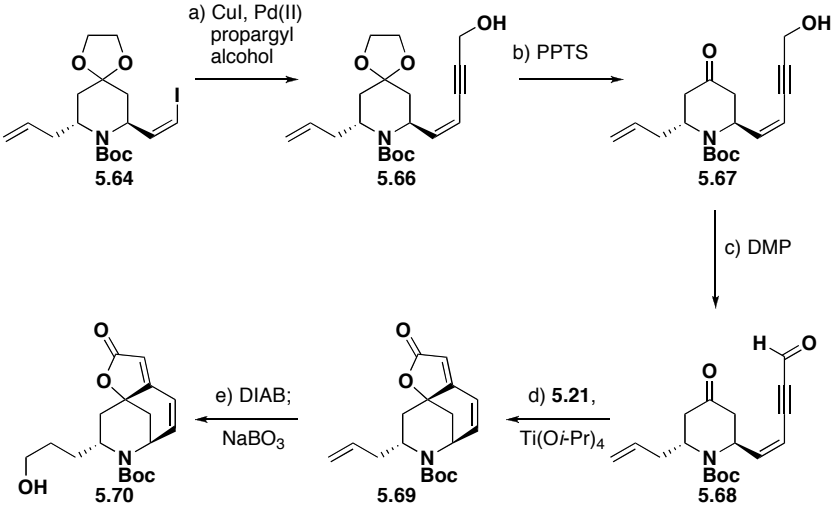

Scheme 5.12 Synthesis of tricyclic alcohol **5.70**. *Reagents and Conditions:* a) CuI (14 mol%), $PdCl_2(NCPh)_2$ (7 mol%), propargyl alcohol (3 equiv.) THF/piperidine (2:1), 23 °C (86%); b) PPTS, *t*-BuOH/H_2O (5:1), 75 °C (78%); c) Dess–Martin periodinane, CH_2Cl_2, 23 °C (>98%); d) **5.21** (40 mol%), Ti(O*i*-Pr)$_4$ (2 equiv.), toluene, 50 °C, slow addition (47%); e) DIAB, THF, –25 → 0 °C; aq. $NaBO_3$, 23 °C (72%). PPTS = pyridinium *p*-toluenesulfonat, DBU = 1,8-Diazabicyclo[5.4.0]undec-7-ene, DIAB = disiamylborane.

Sonogashira coupling (Scheme 5.12) afforded enynol **5.66** in good yield. A short screen of conditions to remove the ketal in the presence of the Boc protecting group quickly revealed that PPTS (1.5 equiv.) in *t*-BuOH/H_2O (5:1) at 75 °C for 12 h afforded the desired deprotected material in good yield (78%). Oxidation of the primary alcohol with Dess–Martin periodinane proceeded without incident, delivering cyclization precursor **5.68** in near quantitative yield (98%). Cyclization with triazolium **5.21**, DBU, and Ti(O*i*Pr)$_4$ in CH_2Cl_2 without slow addition of the starting material provided the desired product, albeit in poor yield (12%). Turning to the optimized slow addition protocol in toluene at 0.03 M afforded a dramatic improvement, with isolation of the desired product in 28% yield. Further dilution to 0.02 M further improved the yield to 35%. Finally, slow addition of **5.68** to a 50 °C suspension of reactants in toluene at a final concentration of 0.02 M delivered an optimized yield of 47% for this key transformation. The inefficiency of this reaction compared to model system **5.17** may reflect a conformational equilibrium preventing the enynal side chain from remaining fixed in the axial position. Nonetheless, this material was taken forward and subjected to hydroboration/oxidation with disiamylborane,[15] and alcohol **5.70** was obtained in 72% isolated yield. Efforts in our laboratory are currently directed toward elaborating this alcohol to 3-deshydroxy-secu'amamine A.

5.6 Conclusions

Herein, we have demonstrated that NHC/Lewis acid cooperative catalysis can be employed in a novel intramolecular cyclization using ynals as nucleophilic homoenolate equivalents and unactivated ketones as electrophiles. These studies have also provided

access to the complex bridging butenolide framework of the *Securinega* alkaloids. We anticipate that this precedent will provide opportunities for the development of new NHC-catalyzed reactions using ynals as substrates.

5.7 References

1. A. Ohsaki, H. Ishiyama, K. yoneda, J. Kobayashi, *Tetrahedron Lett.* **2003**, *44*, 3097–3099.

2. P. Liu, S. Hong, S. M. Weinreb, *J. Am. Chem. Soc.* **2008**, *130*, 7562–7563.

3. a) K. Zeitler, *Org. Lett.* **2006**, *8*, 637–640; b) K. Zeitler, I. Mager, *Adv. Synth. Catal.* **2007**, *349*, 1851–1857; c) J. Kaeobamrun, J. Mahatthananchai, P. Zheng, J. W. Bode, *J. Am. Chem. Soc.* **2010**, *132*, 8810–8812; d) Z. Q. Zhu, J. C. Xiao, *Adv. Synth. Catal.* **2010**, *352*, 2455–2458; e) Z. Q. Zhu, X.-L. Feng, N.-F. Jiang, X. Wan, J.-C. Xiao, *Chem. Commun*. **2011**, *47*, 8670–8672; f) Y.-M. Zhao, Y. Tam, Y.-J. Wang, Z. Li, J. Sun, *Org. Lett.* **2012**, *14*, 1398–1401; g) D. Du, Z. Hu, J. Jin, Y. Lu, W. Tang, B. Wang, T. Lu, *Org. Lett.* **2012**, *14*, 1274–1277.

4. J. Struble, J. W. Bode, *Tetrahedron* **2009**, *65*, 4957–4967.

5. J. Adrio, J. C. Carretero, *J. Am. Chem. Soc.* **2007**, *129*, 778–779.

6. P. Beak, W. K. Lee, *J. Org. Chem.* **1993**, *58*, 1109–1117.

7. G. Stork, K. Zhao, *Tetrahedron Lett.* **1989**, *30*, 2173–2174.

8. M. S. Kerr, J. R. de Alaniz, T. Rovis, *J. Org. Chem.* **2005**, *70*, 5725–5728.

9. For a review of NHC/Lewis acid co-operative catalysis, see: D. T. Cohen, K. A. Scheidt, *Chem. Sci.* **2012**, *3*, 53–57.

10. I. Izquierdo, M. T. Plaza, V. Yáñez, *Tetrahedron: Asym.* **2005**, *16*, 3887–3891.

11. S. Yoshifuji, K. Tanaka, Y. Nitta, *Chem. Pharm. Bull.* **1988**, *36*, 3125–3129.

12. For a representative example, see: D. L. Comins, A. Dehghani, *J. Org. Chem.* **1995**, *60*, 794–795.

13. P. S. Watson, B. Jiang, B. Scott, *Org. Lett.* **2000**, *2*, 3679–3681.

14. K. Maruoka, I. Shimada, H. Imoto, H. Yamamoto, *Synlett* **1994**, 519–520.

15. This procedure has been used for hydroboration of a related substrate: P. Magnus, J. Ródriguez-López, K. Mulholland, I. Matthews, *Tetrahedron* **1993**, *49*, 8059–8072.

5.8 Experimental Section

General Procedures. All reactions were carried out under an argon atmosphere with dry solvents under anhydrous conditions, unless otherwise noted. Dry tetrahydrofuran (THF), toluene, benzene, diethyl ether (Et_2O) and methylene chloride (CH_2Cl_2) were obtained by passing commercially available pre-dried, oxygen-free formulations through activated alumina columns. Acetonitrile (MeCN) was dried and stored over 3 Å molecular sieves. Yields refer to chromatographically and spectroscopically (^1H and ^{13}C NMR) homogeneous materials, unless otherwise stated. Reagents were purchased at the highest commercial quality and used without further purification, unless otherwise stated. Reactions were magnetically stirred and monitored by thin-layer chromatography (TLC) carried out on 0.25 mm E. Merck silica gel plates (60F-254) using UV light as visualizing agent and cerium sulfate (CAM) or aqueous $KMnO_4$, and heat as developing agents. SiliCycle silica gel (60, academic grade, particle size 0.040–0.063 mm) was used for flash column chromatography. NMR spectra were recorded on Bruker DPX 300, Avance II 400, Avance III 400 and DMX 500 instruments and calibrated using residual undeuterated solvent as an internal reference ($CDCl_3$: 7.26 ppm for ^1H, 77.0 ppm for ^{13}C; CD_3OD: 3.31 ppm for ^1H). The following abbreviations were used to explain the multiplicities: s = singlet, d = doublet, t = triplet, q = quartet, br = broad, app = apparent. IR spectra were recorded on a Perkin-Elmer 1000 series FT-IR spectrometer. High-resolution mass spectra (HRMS) were recorded in the Columbia University Mass Spectral Core facility on a JOEL HX110 mass spectrometer.

Abbreviations. Ac = acetyl, Boc = *tert*-butyloxycarbonyl, Cbz = carboxybenzyl, DIBAL-H = diisobutylaluminum hydride, DMF = *N,N*-dimethylformamide, DMSO = dimethylsulfoxide, DMP = Dess–Martin periodinane, HMPA = hexamethyphosphoramide, HMDS = bis(trimethylsilyl)amide, IBX = 2-iodoxybenzoic acid, *m*-CPBA = *meta*-chloroperbenzoic acid, TBAF = tetrabutylammonium fluoride,

TBS = *tert*-butyldimethylsilyl, THF = tetrahydrofuran, TMEDA = *N,N,N',N'*-tetramethylethylenediamine, TMS = trimethylsilyl.

Aldehyde 5.13. Ketone **5.12** (500 mg, 2.50 mmol, 1 equiv.) was dissolved in MeOH (5 mL) and cooled to 0 °C with an ice water bath. $NaBH_4$ (125 mg, 3.30 mmol, 1.32 equiv) was added in one portion. The ice bath was removed, and stirring was continued for 15 minutes. The reaction was carefully quenched by the addition of saturated aqueous NH_4Cl, and the contents were transferred to a separatory funnel. The mixture was extracted with EtOAc (3 × 10 mL), and the combined organic extracts were washed sequentially with saturated aqueous $NaHCO_3$ and brine, dried over $MgSO_4$, filtered, and concentrated. The crude alcohol was then dissolved in CH_2Cl_2 (10 mL), and solid imidazole (340 mg, 5.0 mmol, 2.0 equiv.) and TBSCl (490 mg, 3.25 mmol, 1.3 equiv.) were sequentially added at 23 °C. The reaction mixture was allowed to stir at this temperature for 12 h. The reaction contents were quenched by the addition of a saturated aqueous solution of $NaHCO_3$. The aqueous layer was extracted twice more with 10 mL portions of CH_2Cl_2, and the combined organics were dried over $MgSO_4$, filtered, and concentrated. Purification by flash chromatography (silical gel, hexanes/EtOAc, 97:3) afforded the protected alcohol (790 mg, 99%) as a clear, colorless oil. This material was then dissolved in dry Et_2O (20 mL), and TMEDA (639 mg, 825 μL, 5.5 mmol, 2.2 equiv.) was added. The solution was then cooled to –78 °C, and a solution of *s*-BuLi (1.4 M in cyclohexane, 3.2 mL, 4.5 mmol, 1.8 equiv) was added dropwise. The reaction was allowed to slowly warm to –40 °C and kept at that temperature for 1 h before being cooled again to –78 °C. DMF (1.83 g, 1.9 mL, 25.0 mmol, 10 equiv) was added, and the reaction was allowed to slowly warm to –40 °C where it was kept for an additional 1.5 h

before quenching with a saturated aqueous solution of NH_4Cl. The aqueous layer was extracted with Et_2O (3 × 20 mL), and the combined organics were dried over $MgSO_4$. Filtration, concentration, and purification by flash chromatography (silica gel, hexanes/EtOAc, 97:3 → 95:5) gives the two diastereomers of the aldehyde as a pure compound (728 mg, 85%) as a clear oil. **5.13**: ^{1}H NMR (400 MHz, $CDCl_3$, 1.04:1 mixture of rotamers) δ 9.55 (s, 1 H), 4.59 and 4.39 (rotamers, d, J = 2.0 Hz, 1 H), 4.11 (s, 1 H), 3.91 and 3.78 (rotamers, d, J = 12.8 Hz, 1 H), 3.26 (m, 1 H), 2.23 (br t, J = 14.8 Hz, 1 H), 1.90 (ddd, J = 14.0, 7.2, 2.0 Hz, 1 H), 1.47 and 1.42 (rotamers, s, 9 H), 0.844 (s, 9 H), 0.036 (s, 3 H), 0.021 (s, 3 H).

Vinyl iodide 5.14. Iodomethyltriphenylphosphonium iodide (10.2 g, 19.25 mmol, 1.25 equiv.) was suspended in 45 mL of THF at 23 °C. A solution of NaHMDS (1.0 M, 18.5 mL, 18.5 mmol, 1.2 equiv.) was added, and the resultant deep orange/brown solution was cooled to –60 °C. HMPA (6 mL) was introduced, and the reaction was cooled to –78 °C. A solution of aldehyde **5.13** (5.3 g, 15.4 mmol, 1.0 equiv.) was added as a solution in THF (15 mL) dropwise. The reaction was stirred for 60 min at –78 °C, and the cooling bath was removed. The reaction was stirred for an additional 30 min, diluted with CH_2Cl_2 (60 mL), and quenched by the addition of a saturated aqueous solution of NH_4Cl. The layers were separated, and the aqueous layer was extracted twice more with CH_2Cl_2. The combined organics were dried over $MgSO_4$, filtered, and concentrated. The crude product was purified by flash chromatography (silica gel, hexanes/EtOAc, 97:3), affording 6.1 g (85%) of product as a clear oil. **5.14**: ^{1}H NMR (400 MHz, $CDCl_3$) δ 6.71 (t, J = 7.6 Hz, 1 H), 6.11 (d, J = 7.2 Hz), 4.87 (br t, J = 6.0 Hz, 1 H), 4.11 (app t, J = 3.2 Hz, 1 H), 3.92

(br d, 12.8 Hz, 1 H), 3.28–3.19 (m, 1 H), 1.85–1.70 (m, 2 H), 1.68–1.60 (m, 2 H), 1.46 (s, 9 H), 0.87 (s, 9 H), 0.031 (s, 3 H), 0.013 (s, 3 H).

Enynol 5.15. CuI (360 mg, 1.89 mmol, 0.144 equiv) and $PdCl_2(NCPh)_2$ (360 mg, 0.939 mmol, 0.072 equiv.) were placed in a flash under ambient atmosphere. Piperidine (32 mL) was added, and the mixture was stirred at ambient temperature for 10 minutes. During this stirring, a solution of vinyl iodide **5.14** (6.1 g, 13.05 mmol, 1.0 equiv.) was dissolved in 65 mL of THF. The now green suspension of CuI/Pd(II) was then transferred to the solution of the vinyl iodide, and the resultant green solution was stirred at 23 °C for 5 minutes before propargyl alcohol (2.19 g, 2.25 mL, 39.15 mmol, 3.0 equiv.) was added by syringe. Over a period of 30 min, the solution turned from green to tan and then from tan to dark brown. Stirring was continued for 24 h at which time the reaction was concentrated under reduced pressure. The crude material was directly purified by flash chromatography (silica gel, hexanes/EtOAc, 95:5 → 88:12) gives 4.58 g (89%) of the desired product as a light yellow oil. **5.15**: ^{1}H NMR (400 MHz, $CDCl_3$) δ 6.16 (br s, 1 H), 5.42 (dd, *J* = 11.2, 1.6 Hz, 1 H), 5.09 (br s, 1 H), 4.31 (d, *J* = 5.2 Hz, 2 H), 4.11 (app t, *J* = 2.8 Hz, 1 H), 3.84 (br d, *J* = 13.6 Hz), 3.35–3.23 (m, 1 H), 3.20 (br t, *J* = 6.0 Hz, 1 H), 1.85 (ddd, *J* = 14.0, 6.8, 2.8 Hz, 1 H), 1.74 (br d, *J* = 14.0 Hz, 1 H), 1.15–1.05 (m, 2 H), 1.46 (s, 9 H), 0.87 (s, 9 H), 0.024 (s, 6 H).

Diol 5.16. TBAF (1.0 M in THF, 15 mL, 15 mmol, 1.3 equiv.) was added dropwise to a solution of silyl ether **5.15** (4.58 g, 11.58 mmol, 1.0 equiv.) in THF (55 mL) at 23 °C. The reaction was stirred at this temperature for 2 d. The reaction was quenched by the

addition of half-saturated brine and EtOAc. The layers were separated, and the aqueous layer was extracted with EtOAc (3 × 30 mL). The combined organic extracts were dried over $MgSO_4$, filtered, and concentrated. Purification by flash chromatography on silica gel (hexanes/EtOAc, 90:10 → 20:80 gives diol **5.16** as pale yellow oil (2.76 g, 85%). **5.16**: ^{1}H NMR (400 MHz, $CDCl_3$) δ 6.17 (dd, *J* = 10.8, 5.6 Hz, 1 H), 5.52 (dq, *J* = 11.2, 2.0 Hz, 1 H), 5.09 (br s, 1 H), 4.31 (d, *J* = 4.4 Hz, 1 H), 4.19 (d, *J* = 2.0 Hz, 1 H), 3.88 (dt, *J* = 14.0, 3.6 Hz, 1 H), 3.26–3.38 (m, 2 H), 1.97–1.87 (m, 2 H), 1.68–1.77 (m, 3 H), 1.61–1.66 (br s, 1 H), 1.46 (s, 9 H); ^{13}C NMR (100 MHz, $CDCl_3$) δ 155.4, 143.2, 107.4, 93.4, 82.2, 80.2, 64.4, 51.2, 49.9, 36.5, 34.7, 31.8, 28.5.

Keto-aldehyde 5.17. Diol **5.16** (113 mg, 0.40 mmol, 1.0 equiv.) was dissolved in CH_2Cl_2 (5 mL), and DMP (424 mg, 1.0 mmol, 2.5 equiv.) was added in one portion at 23 °C. The reaction was stirred for 1.5 h or until complete consumption of starting material was observed by TLC. A saturated solution of $NaHCO_3$ (5 mL) was added, and the reaction was diluted with 7 mL EtOAc. $Na_2S_2O_3$ (2 g) was added as a solid, and the reaction mixture was stirred vigorously until both layers became clear (~5–10 min). The reaction contents were transferred to a separatory funnel, and the aqueous layer was extracted with CH_2Cl_2 (3 × 7 mL). The organic extracts were then washed twice with saturated aqueous $NaHCO_3$ (5 mL each), dried over $MgSO_4$, filtered, and concentrated, affording pure keto-aldehyde **5.17** (112 mg, 99%) as a light yellow oil that turns light orange over a period of 5 min. This color change does not appear to affect the purity of the product. **5.17**: R_f = 0.43 (silica gel, hexanes/EtOAc, 1:1, UV and CAM stain; streaks slightly); IR (film) ν_{max} 2981, 2174, 1722, 1689, 1660, 1393, 1366, 1244, 1163 cm^{-1}; ^{1}H NMR (400 MHz,

$CDCl_3$) δ 9.35 (s, 1 H), 6.23 (dd, *J* = 11.2, 7.6 Hz, 1 H), 5.78 (d, *J* = 11.2 Hz, 1 H), 5.43–5.28 (br m, 1 H), 4.17 (dt, *J* = 14.0, 5.2 Hz, 1 H), 3.50 (ddd, *J* = 14.0, 9.6, 4.4 Hz, 1 H), 2.81 (dd, *J* = 15.2, 6.8 Hz, 1 H), 2.60–2.38 (m, 3 H), 1.47 (s, 9 H); ^{13}C NMR (125 MHz, $CDCl_3$) δ 206.6, 176.2, 154.3, 148.2, 108.1, 94.0, 89.3, 81.1, 52.3 44.3, 40.2, 39.4, 28.3; HRMS (FAB) calc. for $C_{15}H_{20}NO_4^+$ [M+H$^+$] 278.1392, found 278.1400.

Butenolide 5.22. Ti(O*i*Pr)$_4$ (113 mg, 117 μL, 0.396 mmol, 2.0 equiv.) was added to a suspension of precatalyst **5.21** (17.5 mg, 0.0792 mmol, 0.4 equiv.) in 4 mL of toluene at ambient temperature under Ar atmosphere. The mixture was stirred at this temperature for 10 minutes. A solution of **5.22** (55 mg, 0.198 mmol, 1.0 equiv.) in 4.0 mL of toluene was added slowly over a period of 4 h. During the addition process, the reaction color changes from clear to light orange to deep red to dark red/brown. The reaction was allowed to stir at room temperature overnight at which point the reaction mixture was concentrated to 1/3 volume. This crude mixture was purified directly by silica gel chromatography (hexanes/EtOAc, 95:5 → 75:25) afforded 50 mg (91%) of butenolide **5.22** as a white solid. Crystallization of this compound from slow evaporation of a mixture of CH_2Cl_2 and hexanes afforded X-ray quality crystals that confirmed the structure. **5.22**: R_f = 0.43 (silica gel, hexanes/EtOAc, 1:1, UV only; does not stain in common staining solutions); IR (film) ν_{max} 2975, 2934, 1760, 1692, 1406, 1165, 1096 cm^{-1}; ^{1}H NMR (400 MHz, $CDCl_3$) δ 6.78 (d, *J* = 9.2 Hz, 1 H), 6.09 (br m, 1 H), 5.77 (s, 1 H), 5.16 (br m, 1 H), 4.04 (br m, 1 H), 3.13 (br s, 1 H), 2.29–2.17 (m, 2 H), 2.02 (d, *J* = 7.6 Hz, 1 H), 1.57 (d, *J* = 11.2 Hz, 1 H), 1.47 (s, 9 H); ^{13}C NMR (100 MHz, $CDCl_3$) δ

171.6, 165.3, 154.1, 133.8, 124.2, 112.5, 83.0, 80.7, 48.3, 38.8, 37.4, 35.5, 28.3; HRMS (FAB) calc. for $C_{15}H_{20}NO_4^+$ [M+H$^+$] 278.1392, found 278.1390.

Aldehyde 5.24. To a –78 °C solution of *N*-Boc-*trans*-4-hydroxy-L-proline **5.23** (500 mg, 2.16 mmol, 1.0 equiv.) in 10 mL of THF/MeOH (9:1) was added a solution of $TMSCHN_2$ (2.0 M in toluene, 1.2 mL, 2.34 mmol, 1.1 equiv.). The bath was removed and the reaction was allowed to come to ambient temperature. After 10 minutes, 1 mL of AcOH was added, and the reaction mixture was directly concentrated and co-evaporated with DCM/hexanes mixtures to remove the remaining AcOH and toluene. This crude material was dissolved in CH_2Cl_2 (8 mL), and imidazole (264 mg, 3.88 mmol, 1.8 equiv.) and TBSCl (423 mg, 2.81 mmol, 1.3 equiv.) were added sequentially. The reaction was stirred at 23 °C for 12 h. The reaction was quenched by the addition of a saturated aqueous solution of $NaHCO_3$, and the aqueous layer was extracted with CH_2Cl_2 (3 × 10 mL). The combined organics were dried over $MgSO_4$, filtered, and concentrated. The crude material was purified by flash chromatography on silica gel (hexanes/EtOAc, 95:5 → 90:10) afforded the pure silyl ether product (766 mg, 98% over 2 steps) as a clear oil. This material was then dissolved in THF (8 mL) and cooled to –78 °C. DIBAL-H (1.0 M in toluene, 5.4 mL, 5.4 mmol, 2.5 equiv.) was added to this solution dropwise, and after 45 min at –78 °C, the cold bath was removed, and the mixture was allowed to reach ambient temperature. The reaction was quenched by the addition of 10 mL of a 1 M aqueous $KHSO_4$ solution and 2 mL of 1 M HCl. The reaction was diluted with water and Et_2O, and the mixture was stirred vigorously for 5 min. The layers were separated, and the aqueous layer was extracted twice more with Et_2O. The combined organics were

dried ($MgSO_4$), filtered, and concentrated, affording 700 mg (98%) of the primary alcohol as a clear oil. A portion of this material (80 mg, 0.24 mmol, 1.0 equiv.) was then dissolved in CH_2Cl_2 (0.4 mL) and Et_3N (97 mg, 130 μL, 0.94 mmol, 4.0 equiv.) was added. The solution was then cooled to 0 °C. In a separate flask, SO_3•pyr (115 mg, 0.72 mmol, 3.0 equiv.) was dissolved in 0.8 mL of DMSO. The resultant solution was then added dropwise to the CH_2Cl_2 solution of starting material, and the reaction was stirred at 0 °C for 10 minutes at which time the cold bath was removed. After 45 minutes, TLC analysis showed complete consumption of the starting material, and the reaction mixture was poured into a separatory funnel containing a 2:1 mixture of saturated aqueous NH_4Cl and H_2O. The aqueous was extracted with Et_2O (3 × 5 mL). The combined organics were washed once with H_2O, dried over $MgSO_4$, filtered, and concentrated to afford aldehyde **5.24** (80 mg, 99%). **5.24**: ^{1}H NMR (400 MHz, $CDCl_3$, ~2:1 mixture of rotamers) δ 9.56 (d, J = 2.4 Hz, 0.33 H), 9.44 (d, J = 3.6 Hz, 0.66 H), 4.40–4.15 (m, 2 H), 3.58–3.30 (m, 2 H), 2.09–1.87 (m, 2 H), 1.47 and 1.43 (rotamers, s, 9 H), 0.87 (s, 9 H), 0.066 (s, 6 H).

Vinyl iodide 5.25. This compound was prepared by the same procedure described for compound **5.14**. 65 mg of aldehyde **5.24** delivered 44 mg of vinyl iodide (50%) after purification by silica gel chromatography (hexanes/EtOAc, 97:3 → 94:6) as a clear, light yellow oil. **5.25**: ^{1}H NMR (400 MHz, $CDCl_3$) δ 6.50–6.30 (br m, 1 H), 6.30–6.10 (br m, 1 H), 4.40–4.21 (m, 2 H), 3.48–3.26 (m, 2 H), 2.05–1.95 (br m, 1 H), 1.80 (ddd, J = 12.4, 6.4, 4.8 Hz, 1 H), 1.44 (s, 9 H), 0.860 (s, 9 H), 0.054 (s, 3 H), 0.051 (s, 3 H).

Diol 5.26. Sonogashira coupling was accomplished as described in the preparation of compound **5.15**. 153 mg of vinyl iodide **5.25** afforded 100 mg of coupled product (78%) after purification by silica gel chromatography (hexanes/EtOAc, 95:5 → 85:15). A portion of this material (14.4 mg, 0.0377 mmol, 1.0 equiv.) was dissolved in THF (0.5 mL), and a solution of TBAF (1.0 M in THF, 57 μL, 0.057 mmol, 1.5 equiv.) was added. The reaction was stirred at 23 °C for 14 h, diluted with CH_2Cl_2, and poured into a 1:1 mixture of water and brine. The aqueous layer was extracted with CH_2Cl_2 (3 × 5 mL), and the combined organic extracts were dried over $MgSO_4$, filtered, and concentrated. Purification by flash chromatography on silica gel (hexanes/EtOAc, 4:1 → 0:1) afforded diol **5.26** (9.5 mg, 94%) as a clear oil. **5.26**: ^{1}H NMR (400 MHz, $CDCl_3$) δ 5.82 (dd, *J* = 10.8, 6.8 Hz, 1 H), 5.51 (d, *J* = 10.4 Hz), 4.79 (br s, 1 H), 4.43 (m, 1 H), 4.35 (d, *J* = 1.2 Hz, 2 H), 3.63–3.55 (br m, 1 H), 3.51 (d, *J* = 11.6 Hz), 2.31–2.21 (m, 1 H), 2.35–1.93 (br s, 2 H), 1.82 (ddd, *J* = 12.8, 7.2, 5.2 Hz, 1 H), 1.45 (s, 9 H); ^{13}C NMR (100 MHz, $CDCl_3$) δ 155.3, 144.5, 107.5, 93.5, 81.5, 80.2, 69.0, 55.9, 54.9, 51.1, 40.5, 28.4.

Keto-aldehyde 5.27. 25 mg of diol **5.26** was subjected to Dess–Martin oxidation following the procedure outlined in the synthesis of compound **5.17**, affording 23 mg of keto-aldehyde **5.27** (95%). **5.26**: R_f not determined (decomposes on silica gel); IR (film) ν_{max} 2979, 2929, 2174, 1763, 1694, 1662, 1397, 1368, 1158, 1129 cm^{-1}; ^{1}H NMR (500 MHz, $CDCl_3$) δ 9.34 (d, *J* = 0.8 Hz, 1 H), 6.29 (br t, *J* = 5.6 Hz), 5.76 (d, *J* = 11.2 Hz, 1 H), 5.21 (td, *J* = 8.8, 4.8 Hz, 1 H), 3.14 (d, *J* = 19.6 Hz, 1 H), 3.78 (d, *J* = 19.6 Hz, 1 H) 3.01 (dd, *J* = 18.8, 10.0 Hz, 1 H), 2.36 (dd, *J* = 18.8, 3.6 Hz, 1 H), 1.46 (s, 9 H); ^{13}C

NMR (125 MHz, $CDCl_3$) δ 208.7, 176.2, 153.8, 149.8, 107.2, 93.6, 89.5, 81.2, 54.0, 52.7, 43.1, 28.3; HRMS (FAB) calc. for $C_{14}H_{18}NO_4^+$ [M+H$^+$] 264.1263, found 264.1259.

Butenolide 5.28. Ti(O*i*Pr)$_4$ (43 mg, 45 μL, 0.152 mmol, 2.0 equiv.) was added to a suspension of precatalyst **5.21** (6.7 mg, 0.030 mmol, 0.4 equiv.) in 2.0 mL of toluene at ambient temperature under Ar atmosphere. The reaction mixture was transferred to a 50 °C oil bath and allowed to thermally equilibrate for 5 minutes. A solution of **5.27** (20 mg, 0.076 mmol, 1.0 equiv.) in 1.8 mL of toluene was added slowly over a period of 4 h. During the addition process, the reaction color changes from clear to light orange to deep red to dark red/brown. The reaction was allowed to stir at room temperature overnight at which point the reaction mixture was concentrated to 1/3 volume. This crude mixture was purified directly by silica gel chromatography (hexanes/EtOAc, 95:5 → 75:25) afforded 6.2 mg (31%) of butenolide **5.28** as a white solid. **5.28**: R_f = 0.42 (hexanes/EtOAc, 1:1, UV only; does not stain in common staining solutions); ^{1}H NMR (500 MHz, $CDCl_3$) δ 6.93 and 6.80 (rotamers, dd, *J* = 8.8, 6.0 Hz, 1 H), 6.57 (d, *J* = 13.2 Hz, 1 H), 5.75 (s, 1 H), 4.72 and 4.59 (rotamers, app t, *J* = 5.2 Hz, 1 H), 3.79 (d, *J* = 10.0 Hz, 1 H), 3.37 and 3.29 (rotamers, d, *J* = 10.4 Hz, 1 H), 2.66 and 2.59 (rotamers, dd, *J* = 10 Hz, 5.2 Hz, 1 H), 1.97 (d, *J* = 10.0 Hz, 1 H), 1.47 and 1.44 (rotamers, s, 9 H); ^{13}C NMR (125 MHz, $CDCl_3$) δ 171.9, 167.7, 167.3, 153.9, 153.5, 143.8, 143.0, 121.9, 121.7, 108.9, 108.6, 87.4, 86.8, 80.7, 80.6, 54.2, 53.3, 50.2, 49.8, 42.7, 42.3, 28.4; HRMS (FAB) calc. for $C_{14}H_{18}NO_4^+$ [M+H$^+$] 264.1236, found 264.1226.

Keto-aldehyde 5.29. 5.29: ^{1}H NMR (400 MHz, $CDCl_3$) δ 9.30 (d, *J* = 0.8 Hz, 1 H), 6.15 (dd, *J* = 10.8 Hz, 1 H), 5.63 (d, *J* = 10.8 Hz, 1 H), 3.18–3.05 (m, 1 H), 2.45–2.33 (m, 2 H), 2.33–2.23 (m, 1 H), 2.23–2.12 (m, 1 H), 2.12–2.01 (m, 1 H), 1.96–1.86 (m, 1 H), 1.84–1.70 (m, 1 H), 1.60–1.49 (m, 1 H); ^{13}C NMR (100 MHz, $CDCl_3$) δ 209.3, 176.5, 152.9, 106.6, 92.8, 90.5, 46.1, 41.0, 40.6, 30.5, 24.9.

Butenolide 5.30. 5.30: ^{1}H NMR (400 MHz, $CDCl_3$) δ 6.65 (d, *J* = 9.6 Hz, 1 H), 6.19 (dd, *J* = 9.2, 6 Hz, 1 H), 5.64 (s, 1 H), 2.97 (m, 1 H), 2.10 (d, *J* = 2.8 Hz), 2.01 (td, *J* = 13.2, 6.4 Hz, 1 H), 1.88–1.67 (m, 2 H), 1.62–1.48 (m, 3 H).

Aldehyde 5.31. 5.31: ^{1}H NMR (500 MHz, $CDCl_3$) δ 9.17 (s, 1 H), 2.48–2.43 (m, 2 H), 2.42–2.37 (m, 1 H), 2.31–2.23 (m, 1 H), 2.10–1.90 (m, 4 H), 1.74–1.58 (m, 3 H), 1.42–1.33 (m, 1 H); ^{13}C NMR (125 MHz, $CDCl_3$) δ 210.6, 176.9, 97.8, 81.7, 47.2, 41.1, 37.7, 33.8, 30.5, 24.8, 16.4.

Butenolide 5.33. 5.33: ^{1}H NMR (400 MHz, $CDCl_3$) δ 7.41–7.31 (m, 5 H), 6.74 (dd, *J* = 9.6 3.2 Hz, 1 H), 6.24 (ddd, *J* = 9.6, 5.6, 2.4 Hz, 1 H), 5.87 (s, 1 H), 2.76 (ddt, *J* = 12.4, 4.8, 0.8 Hz, 1 H), 2.42 (dtt, *J* = 19.6, 5.2, 1.2 Hz, 1 H), 2.14 (td, 12.0, 5.2 Hz, 1 H), 1.99–1.88 (m, 1 H); ^{13}C NMR (100 MHz, $CDCl_3$) δ 171.9, 165.4, 139.6, 137.9, 128.8, 128.4, 126.4, 121.5, 112.4, 86.9, 34.6, 25.2.

Butenolide 5.34. 5.34: ^{1}H NMR (400 MHz, $CDCl_3$) δ 5.75 (s, 1 H), 4.30 (ddd, *J* = 11.2, 5.6, 2.4 Hz, 1 H), 3.38–3.31 (m, 1 H), 3.18–3.13 (m, 1 H), 2.75–2.69 (m, 2 H), 2.10–2.01

(m, 1 H), 1.93–1.80 (m, 2 H), 1.72–1.68 (m 2H), 1.60–1.52 (m, 2 H), 1.44 (br d, J = 9.6 Hz).

Aldehyde 5.40. *N*-Cbz-proline (2.50 g, 10 mmol, 1.0 equiv.) was dissolved in THF (13 mL) and cooled to 0 °C. BH_3•Me_2S (~10 M, 2 mL, 20 mmol, 2 equiv.) was added dropwise, and the reaction was allowed to warm to ambient temperature where it was kept overnight. The reaction mixture was then carefully quenched by the addition of a saturated solution of $NaHCO_3$, and the aqueous layer was extracted with EtOAc (3 × 30 mL). The combined organics were dried over $MgSO_4$, filtered, and concentrated to give the pure primary alcohol (2.36 g, 99%) as a clear oil. This material was then taken forward without any further purification. To a –78 °C solution of oxalyl chloride (1.06 mL, 11.06 mmol, 1.11 equiv.) in CH_2Cl_2 (20 mL) was added a solution of DMSO (1.71 mL, 24.09 mmol, 2.41 equiv) in CH_2Cl_2 (15 mL) slowly via an addition funnel. After the addition was complete (~25 min), the reaction was stirred for an additional 15 min. A solution of the above primary alcohol in CH_2Cl_2 (20 mL) was then introduced dropwise by addition funnel, and the reaction mixture was stirred for 1 h at –78 °C. Et_3N was then added quickly through the addition funnel, and the reaction was stirred for 20 min before the cold bath was removed. The reaction was allowed to come to ambient temperature and was quenched with 25 mL of H_2O. The reaction mixture was transferred to a separatory funnel and extracted twice more with CH_2Cl_2 (50 mL each). The combined organic extracts were washed once with saturated aqueous $NaHCO_3$, dried over Na_2SO_4, filtered, and concentrated to afford pure aldehyde **5.40** (2.33 g, 98%) as a clear, colorless oil. **5.40**: ^{1}H NMR (500 MHz, $CDCl_3$, 1:1 mixture of rotamers) δ 9.60 (s, 0.5 H), 9.49 (d,

J = 2.0 Hz, 0.5 H), 7.40–7.30 (m, 5 H), 5.20–5.10 (m, 2 H), 4.30 (t, *J* = 6.0 Hz, 0.5 H), 4.20 (d, *J* = 6.0 Hz, 0.5 H), 3.62–3.49 (m, 2 H), 2.22–1.80 (m, 4 H).

TBS ether 5.41. Indium powder (1.24 g, 10.82 mmol, 2.0 equiv.) was suspended in THF (7 mL) at 23 °C, and allyl bromide (1.96 g, 1.4 mL, 16.23 mmol, 3.0 equiv.) was added. This mixture was heated to 70 °C for 40 min at which time the majority of the indium powder had reacted. The greyish tan mixture was allowed to cool to ambient temperature and then was cooled to –78 °C. A solution of aldehyde **5.40** (1.26 g, 5.41 mmol, 1.0 equiv.) was added dropwise as a solution in THF (3 mL). The reaction was stirred at –78 °C for 35 minutes and the cooling bath was removed. After 30 additional min, 25 mL of 1 M HCl was added, and the mixture was stirred vigorously for 5 min. The aqueous was extracted with EtOAc (3 × 25 mL). The organic extracts were dried over $MgSO_4$, filtered and concentrated. Careful purification of the crude material by flash chromatography on silica gel (hexanes/EtOAc, 95:5 → 75:25) afforded the major diastereomer (1.28 g, 87%) as a pure compound. This alcohol was subsequently dissolved in CH_2Cl_2 (30 mL) and cooled to –78 °C. Et_3N (1.41 g, 1.94 mL, 13.9 mmol, 3.0 equiv.) and TBSOTf (1.84 g, 1.60 mL, 6.98 mmol, 1.5 equiv.) were added sequentially. The reaction was allowed to warm to –10 °C before being poured into a separatory funnel containing saturated aqueous $NaHCO_3$. The aqueous was extracted with CH_2Cl_2 (3 × 20 mL). The combined organic extracts were dried over $MgSO_4$, filtered, and concentrated under reduced pressure. Purification by flash chromatography (silica gel, hexanes/EtOAc, 97:3 → 93:7) gives **5.41** (1.67 g, 92%) as a clear, colorless oil. **5.41**: ^{1}H NMR (400 MHz, $CDCl_3$, ~1.5:1 mixture of rotamers) δ 7.40–7.28 (m, 5 H), 5.80–5.60 (m, 1 H), 5.29–4.99 (m, 4

H), 4.42 (br t, J = 7.2 Hz, 0.6 H), 4.20–4.15 (m, 0.4 H), 3.91–3.74 (m, 1 H), 3.69–3.54 (m, 1 H), 3.35–3.25 (m, 1 H), 2.30–1.62 (m, 6 H), 0.89 (s, 9 H), 0.01– –0.20 (overlapping s, 6 H).

Epoxide 5.42. Silyl ether **5.41** (1.23 g, 3.16 mmol, 1.0 equiv.) was dissolved in 23 mL of CH_2Cl_2, and *m*-CPBA (77%, 1.34 g, 1.9 equiv.) was added in a single portion. The reaction was stirred at 23 °C for 24 h. The reaction was diluted with EtOAc, and transferred to a separatory funnel containing a saturated aqueous solution of Na_2SO_3. The aqueous layer was extracted twice more with EtOAc, and the combined extracts were washed sequentially with a 10% aqueous solution of Na_2CO_3 and brine. The organic layer was then dried over $MgSO_4$, filtered, and concentrated. Purificaion by silica gel flash chromatography (hexanes/EtOAc, 85:15 → 70:30) afforded a ~1:1 diastereomeric mixture of epoxide **5.42** (1.06 g, 83%) as a clear, colorless syrup. **5.42**: ^{1}H NMR (400 MHz, $CDCl_3$, ~1.5:1 mixture of rotamers) δ 7.45–7.26 (m, 5 H), 5.31–5.08 (m, 2H), 4.60–4.52 (m, 0.6 H), 4.35–4.25 (m, 0.4 H), 4.00–3.82 (m, 1 H), 3.70–3.52 (m, 1 H), 3.40–3.29 (m, 1 H), 3.10–2.85 (m, 1 H), 2.84–2.77 (m, 1 H), 2.72–2.67 (m, 0.4 H), 2.55–2.50 (br m, 0.6 H), 2.45–2.38 (m, 0.4 H), 2.20–1.6 (5.8 H), 1.52–1.39 (m, 1 H), 0.90–0.78 (overlapping s, 9 H), 0.05– –0.15 (overlapping s, 6 H).

Amino alcohols 5.43 and 5.44. Epoxide **5.42** (1.06 g, 2.62 mmol, 1.0 equiv.) was dissolved in 40 mL of EtOAc/MeOH (1:1). The reaction flask was flushed with argon, and Pd/C (10 wt%, 103 mg, 3.7 mol%) was added in one portion. The headspace of the reaction vessel was purged 3 times with H_2 (1 atm), and the flask was left under hydrogen

atmosphere at 23 °C for 12 h at which point no starting material remained. The reaction was filtered through a pad of celite, eluting with EtOAc. Concentration afforded a crude mixture of amino alcohols (700 mg, 99%) that could be separated by silica gel chromatography [DCM, MeOH/NH_4OH (5:1), 95:5 → 75:25] afforded amino alcohols **5.43** and **5.44** as pure compounds that solidified upon standing in the freezer. **5.43**: ^{1}H NMR (500 MHz, CD_3OD) δ 4.05 (d, *J* = 5.5 Hz, 1 H), 3.78 (dd, *J* = 11.5, 7.0 Hz, 1 H), 3.69 (dd, *J* = 11.5, 7.0 Hz, 1 H), 3.55–3.50 (m, 1 H), 3.36 (td, 8.0, 1.5 Hz, 1 H), 2. 80 (app t, *J* = 8.0 Hz, 1 H), 2.65–2.59 (m, 1 H), 2.28–2.25 (m, 1 H), 1.90–1.78 (m, 2 H), 1.73–1.64 (m, 2 H), 1.44–1.39 (m, 1 H). **5.44**: ^{1}H NMR (400 MHz, CD_3OD) δ 4.01 (app q, *J* = 6.0 Hz, 1 H), 3.59 (dd, *J* = 10.8, 6.4 Hz), 3.52 (dd, *J* = 10.8, 6.4 Hz, 1 H), 3.34–3.25 (m, 1 H), 2.97–2.82 (m, 2 H), 2.77–2.71 (m, 1 H), 2.22 (dt, 12.0, 6.0 Hz, 1 H), 1.96–1.87 (m, 1 H), 1.86–1.69 (m, 2 H), 1.65–1.57 (m, 1 H).

Lactam 5.45. Amino alcohol **5.44** (100 mg, 0.37 mmol, 1.0 equiv.) was dissolved in Ac_2O/pyridine (1:1) and stirred at 23 °C overnight. The reaction mixture was concentrated directly and co-evaporated with toluene 3 times to remove excess pyridine and Ac_2O. This material was then dissolved in 4 mL of EtOAc, and an aqueous solution of $NaIO_4$ (274 mg in 4 mL) was added. Finally, $RuCl_3$ (~1 mg) was added and the reaction mixture was stirred vigorously until the starting material had been consumed. The reaction was transferred to a separatory funnel and diluted with EtOAc and brine. The organic layer was then filtered through a pad of celite, dried over Na_2SO_4, filtered, and concentrated. Flash chromatography on silica gel (99:1 → 97:3) delivered lactam **5.45** (60 mg, 50% over 2 steps) as a colorless oil. **5.45**: ^{1}H NMR (400 MHz, CD_3OD) δ

4.15–4.05 (m, 3 H), 3.97 (app q, *J* = 7.2 Hz), 3.82 (app q, *J* = 7.2 Hz), 2.73–2.64 (m, 1 H), 2.47 (dt, *J* = 13.2, 7.6 Hz, 1 H), 2.42–2.30 (m, 2 H), 2.05 (s, 3 H), 1.92–1.81 (m, 1 H), 1.76 (dt, J = 13.2, 7.6 Hz, 1 H), 0.910 (s, 9 H), 0.010 (s, 6 H).

Aldehyde 5.46. Lactam **5.45** (50 mg, 0.153 mmol, 1 equiv.) was dissolved in 4 mL of MeOH, and excess K_2CO_3 was added. The reaction was stirred at ambient temperature for 1 h. The reaction was concentrated to near dryness, and the reaction contents were transferred with CH_2Cl_2 to a separatory funnel containing a half-brined aqueous solution. The aqueous layer was extracted with EtOAc (2 × 7 mL). The organic extracts were dried over Na_2SO_4, filtered, and concentrated, affording the primary alcohol (43 mg, 99%) as a crystalline solid that was used directly for the next step. Dissolution of this alcohol in CH_2Cl_2 (1 mL) was followed by addition of Et_3N (46 mg, 63 µL, 0.45 mmol, 3 equiv). In a separate flask, SO_3•pyr (71 mg, 0.45 mmol, 3 equiv.) was dissolved in DMSO (2 mL), and this solution was added to the aforementioned solution of primary alcohol dropwise at 23 °C. The reaction was stirred at 23 °C for 2 h and poured into H_2O. The aqueous layer was extracted with CH_2Cl_2 (3 × 5 mL), and the combined organics were dried over Na_2SO_4. Filtration and concentration afforded the desired aldehyde (42 mg, 98%) as a thick oil. [Note: This aldehyde was found to undergo facile hydration in the presence of alcohols or silica gel. Extraction with CH_2Cl_2 during the workup was required since the trace amounts of EtOH in bulk Et_2O readily formed the hemiacetal with this aldehyde. Furthermore, purification on silica gel delivers the hydrated aldehyde exclusively.] **5.46**: ^{1}H NMR (400 MHz, $CDCl_3$) δ 9.61 (s, 1 H), 4.39 (t, *J* = 7.6 Hz, 1 H), 3.89 (app q, *J* = 6.4

Hz, 1 H), 3.77 (app q, J = 6.4 Hz, 1 H), 2.80–2.71 (m, 1 H), 2.46–2.37 (m, 3 H), 2.09 (dt, J = 13.6, 7.2 Hz, 1 H), 1.87–1.76 (m, 1 H), 0.87 (s, 9 H), 0.071 (s, 6 H).

Diol 5.47. Aldehyde **5.46** (50 mg, 0.176 mmol, 1 equiv.) was olefinated using the same procedure to prepare **5.14**, affording 30 mg (42%) of the vinyl iodide. Sonogashira coupling was then performed as described in the preparation of **5.15**, delivering the corresponding enynol (16 mg, 65%). This material was then dissolved in THF (0.5 mL), and TBAF (1.0 M, 71 μL, 0.071 mmol, 1.5 equiv.) was added. The reaction was stirred at room temperature until complete disappearance of the starting material was observed by TLC (1 h). The reaction was diluted with H_2O and EtOAc and poured into brine. The aqueous layer was extracted with 15% *i*-PrOH in $CHCl_3$ (2 × 5 mL). These extracts were dried over Na_2SO_4, filtered, and concentrated. Purification by PTLC afforded diol **5.47** (8.0 mg, 76%). [Note: This amido-diol is exceedingly polar, and saturation of the aqueous layer with brine and extraction with 15% *i*-PrOH in $CHCl_3$ is required to obtain good mass recoveries from the aqueous layer.] **5.47**: ^{1}H NMR (500 MHz, $CDCl_3$) δ 5.96 (dd, J = 10.5, 8.0 Hz, 1 H), 5.61 (dq, J = 10.5, 2.0 Hz), 4.92 (app q, J = 7.5 Hz), 4.39 (d, J = 1.5 Hz, 2 H), 3.97 (app q, J = 7.0 Hz, 1 H), 3.88 (app q, J = 7.0 Hz), 2.70–2.50 (m, 2 H), 2.42–26 (m, 2 H), 1.90–1.75 (m, 2 H).

Keto-aldehyde 5.48. Diol **5.47** (2 mg, 0.0090 mmol, 1 equiv.) was dissolved in 1 mL of MeCN, and IBX (20 mg, 0.072 mmol, 8 equiv.) was added in one portion. The reaction was transferred to an oil bath that was pre-heated to 80 °C. The reaction was stirred at this temperature for 45 min and cooled to ambient temperature. The reaction contents

were then concentrated and filtered through celite. Concentration afforded 1.4 mg (70%) of the keto-aldehyde. **5.48**: ^{1}H NMR (400 MHz, $CDCl_3$) δ 9.34 (d, *J* = 1.2 Hz), 6.29 (dd, *J* = 11.2, 6.8 Hz, 1 H), 5.83 (d, *J* = 11.2 Hz), 5.42–5.32 (m, 1 H), 4.16 (t, *J* = 8.0 Hz, 1 H), 2.97 (dd, *J* = 19.2, 9.6 Hz, 1 H), 2.80–2.70 (m, 2 H), 2.53–2.40 (m, 3 H).

Oxidized norsecurinine 5.49. A solution of NHC precatalyst **5.21** (0.28 mg, 0.0013 mmol, 0.2 equiv.) and Ti(O*i*-Pr)$_4$ (3.6 mg, 0.013 mmol, 2 equiv.) in CH_2Cl_2 (300 μL) was added to keto-aldehyde **5.48** (1.4 mg, 0.0063 mmol, 1 equiv.), and the reaction mixture was stirred at 23 °C overnight. The reaction was filtered through a small pad of silica gel, eluting with 10% MeOH in CH_2Cl_2 and concentrated. The crude material was purified by PTLC (10% MeOH in CH_2Cl_2), affording 0.4 mg of compound **5.49** (30% yield). **5.49**: ^{1}H NMR (500 MHz, $CDCl_3$) δ 6.63–6.60 (m, 2 H), 5.79 (s, 1 H), 4.93 (t, *J* = 5 Hz), 3.73 (dd, 9.5, 6.5 Hz, 1 H), 2.63–2.57 (m, 2 H), 2.33–2.21 (m, 3 H), 2.13–2.08 (m, 1 H).

Oxidized allonorsecurinine 5.50. This compound was prepared analogously to **5.49** (30% yield). **5.50**: ^{1}H NMR (500 MHz, $CDCl_3$) δ 7.22 (dd, *J* = 9.0, 3.5 Hz, 1 H), 6.58 (dd, *J* = 9.0, 1.0 Hz, 1 H), 5.93 (s, 1 H), 4.57 (dd, *J* = 9.5, 6.0 Hz, 1 H), 4.49 (t, *J* = 5.0 Hz, 1 H), 3.49 (br s, 2 H), 2.91 (dd, *J* = 10.5, 5.0 Hz, 1 H), 2.77 (ddd, *J* = 16.5, 13.5, 8.0 Hz, 1 H), 2.30 (dd, *J* = 16.5, 9.0 Hz, 1 H), 2.20 (d, *J* = 10.5 Hz), 2.16–2.09 (m, 1 H).

Phenyl carbamate 5.54. 4-methoxypyridine (215 mg, 1.97 mmol, 1.0 equiv.) was dissolved in THF (5 mL) and cooled to –78 °C. Phenyl chloroformate (369 mg, 297 μL, 2.36 mmol, 1.2 equiv.) and allylmagnesium bromide (1.0 M in THF, 2.56 mL, 2.56

mmol, 1.3 equiv.) were added sequentially. The reaction was allowed to come to 0 °C, and 10% aqueous HCl (5 mL) was added. Stirring was continued until the hydrolysis was complete by TLC. The aqueous layer was extracted with Et_2O (3 × 10 mL), and the combined organic extracts were dried over $MgSO_4$, filtered, and concentrated. Purification on silica gel (hexanes/EtOAc, 95:5 → 75:25) afforded 327 mg (64%) of pure product. **5.54**: ^{1}H NMR (500 MHz, $CDCl_3$) δ 7.90 (dd, *J* = 9.0, 1.0 Hz, 1 H), 7.42 (t, *J* = 7.5 Hz, 2 H), 7.29 (t, *J* = 7.5 Hz, 1 H), 7.15 (d, *J* = 7.5 Hz), 5.86–5.75 (m, 1 H), 5.15 (d, *J* = 9.5 Hz, 1 H), 5.12 (d, *J* = 16.0 Hz, 1 H), 4.82–4.76 (m, 1 H), 2.90 (dd, *J* = 16.5, 5.5 Hz, 1 H), 2.57 (d, *J* = 16.5 Hz), 2.43 (dt, *J* = 14.0, 7.0 Hz, 1 H).

Boc-carbamate 5.55. Phenyl carbamate **5.54** (600 mg, 2.33 mmol, 1.0 equiv.) was dissolved in MeOH (8 mL), and NaOMe (208 mg, 3.85 mmol, 1.65 equiv) was added as a solid. The reaction was stirred at 23 °C overnight. AcOH (260 µL) was added, and the reaction was concentrated and purified directly (silica gel, hexanes/EtOAc, 1:1 → 0:1 then 10% MeOH in CH_2Cl_2) gives 301 mg (94%) of vinylogous amide. This material was dissolved in DMF (5 mL). Boc_2O (718 mg, 3.29 mmol, 1.5 equiv.) and DMAP (134 mg, 1.10 mmol, 0.5 equiv.) were added sequentially, and the reaction was stirred at 23 °C overnight. The reaction contents were poured into 50 mL of H_2O, and the aqueous layer was extracted with Et_2O (3 × 10 mL). The combined organic extracts were washed with brine, dried over $MgSO_4$, filtered, and concentrated. Purification by flash chromatography (hexanes/EtOAc, 95:5 → 80:20) afforded 494 mg (95%) of Boc carbamate **5.55** as a clear, colorless oil. **5.55**: ^{1}H NMR (500 MHz, $CDCl_3$) δ 7.74 (br s, 1 H), 5.73 (ddt, *J* = 17.5, 10.0, 7.5 Hz, 1 H), 5.29 (d, *J* = 8.0 Hz, 1 H), 5.10–5.04 (m, 2 H),

4.58 (br s, 1 H), 2.77 (dd, J = 16.5, 6.5 Hz, 1 H), 2.46 (d, J = 16.5 Hz, 1 H), 2.42 (dt, J = 14.0, 7.0 Hz, 1 H), 2.33 (dt, J = 14.0, 7.0 Hz, 1 H), 1.54 (s, 9 H).

TBS ether 5.56. KHMDS (0.5 M in toluene, 1.64 mL, 0.822 mmol, 1.3 equiv) was added to a flask containing 3 mL of THF, and the resultant solution was cooled to –78 °C. To this solution was added a solution of Boc-carbamate **5.55** (150 mg, 0.632 mmol, 1.0 equiv.) in THF (3 mL) dropwise. A solution of Davis oxaziridine (214 mg, 0.822 mmol, 1.3 equiv.) in THF (3 mL) was added dropwise. The reaction was stirred at –78 °C for 10 min and warmed to –40 °C over 1 h. The reaction was quenched at –40 °C with 3 mL of half-saturated NH_4Cl. The reaction was warmed to 23 °C with vigorous stirring, and the aqueous layer was extracted with Et_2O (3 × 10 mL). The combined organics were washed with brine, dried over $MgSO_4$, filtered, and concentrated. The crude material was purified by flash chromatography on silica gel (CH_2Cl_2/Et_2O, 97:3 → 70:30) gives hydroxylated product (109 mg, 68%). This alcohol was dissolved in DMF (2 mL), and imidazole (58 mg, 0.852 mmol, 2.0 equiv.) and TBSCl (76 mg, 0.512 mmol, 1.2 equiv.) were added sequentially. The reaction was stirred at ambient temperature overnight, poured into water, and extracted with Et_2O (3 × 7 mL). The combined organic extracts were dried over $MgSO_4$, filtered, concentrated, and purified by flash chromatography on silica gel (hexanes/EtOAc, 98:2 → 96:4). The product was isolated as a clear, colorless oil (118 mg, 75%). **5.56**: ^{1}H NMR (400 MHz, $CDCl_3$) δ 7.72 (br s, 1 H), 5.74 (ddt, J = 17.2, 10.0, 7.2 Hz, 1 H), 5.23 (br s, 1 H), 5.08 (d, J = 9.6 Hz, 1 H), 5.06 (d, J = 17.2 Hz, 1 H), 4.43 (br s, 1 H), 3.73 (br s, 1 H), 2.30 (dt, J = 14.4, 7.2 Hz, 1H), 2.20 (dt, J = 14.4, 7.2 Hz, 1 H), 1.52 (s, 9 H), 0.84 (s, 9 H), 0.11 (s, 3 H), 0.041 (s, 3 H).

Alkyne 5.57. 2,6-diphenylphenol (253 mg, 1.03 mmol, 4.5 equiv.) was dissolved in CH_2Cl_2 (2 mL) at 23 °C, and a solution of $AlMe_3$ (2.0 M in hexane, 0.171 mL, 0.343 mmol, 1.5 equiv.) was added dropwise. Bubbling ensued immediately. The mixture was stirred at 23 °C for 30 min to give ATPH. In a separate flask, *n*-BuLi (1.6 M in hexanes, 286 μL, 0.458 mmol (2.0 equiv.) was added to a solution of TMS-acetylene (49 mg, 71 μL, 0.504 mmol, 2.2 equiv.) in THF (1.25 mL) at 0 °C. The deprotonation was continued for 20 min at this temperature. The ATPH solution was cooled to –78 °C, and a solution of vinylogous amide **5.56** (84 mg, 0.229 mmol, 1.0 equiv.) in CH_2Cl_2 (1 mL) was added dropwise. During the addition of the vinylogous amide, the solution became yellow-orange. The solution of lithium TMS-acetylide was then introduced dropwise, and the reaction was stirred at –78 °C for 45 minutes before quenching by the addition of 5 mL of 1 M HCl. The aqueous layer was extracted with CH_2Cl_2, and the combined organics were dried over Na_2SO_4. Filtration and concentration provided crude material that was purified by flash chromatography on silica gel (hexanes/CH_2Cl_2, 90:10 → 60:40 until 2,6-diphenylphenol has eluted, then hexanes/EtOAc, 95:5) afforded 88 mg (83%) of product and 10 mg of starting material (12%). **5.57**: ^{1}H NMR (500 MHz, $CDCl_3$) δ 5.81 (ddt, *J* = 17.0, 10.0, 7.0 Hz, 1 H), 5.13 (dd, *J* = 17.0, 1.0 Hz, 1 H), 5.08 (d, *J* = 10.0 Hz, 1 H), 4.37 (br s, 1 H), 4.04 (d, *J* = 3.0 Hz, 1 H), 3.24 (dd, *J* = 14.0, 8.0 Hz), 2.65 (br s, 1 H), 2.41 (dt, *J* = 15.0, 7.5 Hz), 2.33 (d, *J* = 14.0 Hz, 1 H), 1.48 (s, 9 H), 0.88 (s, 9 H), 0.13 (s, 9 H), 0.075 (s, 3 H), 0.048 (s, 3 H).

Alcohol 5.58. L-selectride (1.0 M in THF, 180 μL, 0.180 mmol, 1.9 equiv.) was added dropwise to a –78 °C solution of alkyne **5.57** (44 mg, 0.0944 mmol, 1.0 equiv.) in THF (1 mL). The reaction was stirred at –78 °C for 2 h and quenched at that temperature with a saturated solution of NH_4Cl. The aqueous layer was extracted with CH_2Cl_2 (3 × 5 mL), and the combined extracts were dried over $MgSO_4$, filtered, and concentrated. Purification by column chromatography on silica gel (hexanes/EtOAc, 97:3 → 95:5) gives the product (45 mg, 99%) as a single diastereomer. Upon standing, the product crystallizes, an X-ray quality crystals could be obtained from slow evaporation from pentane. **5.58**: ^{1}H NMR (500 MHz, $CDCl_3$) δ 5.79 (app dq, *J* = 17.0, 8.5 Hz, 1 H), 5.24 (br s, 1 H), 5.13 (d, *J* = 17.0 Hz, 1 H), 5.07 (d, *J* = 10.5 Hz), 4.40–4.15 (br m, 2 H), 3.95–3.80 (br m, 1 H), 2.72–235 (br m, 2 H), 1.99 (td, *J* = 12.0, 6.0 Hz, 1 H), 1.92-78 (br m, 2 H), 1.45 (s, 9 H), 0.89 (s, 9 H), 0.13 (s, 9 H), 0.11 (s, 3 H), 0.094 (s, 3 H).

Aldehyde 5.62. A solution of *N*-Boc-piperidine **5.61** (5.09 g, 20.95 mmol, 1.0 equiv.) and TMEDA (3.90 g, 5.03 mL, 33.52 mmol, 1.6 equiv.) in Et_2O (140 mL) was cooled to –78 °C. *s*-BuLi (1.4 M in cyclohexane, 22.5 mL, 31.43 mmol, 1.5 equiv.) was added dropwise, and the reaction was slowly warmed to –50 °C, and the reaction was kept between –50 °C and –40 °C for 1 h. The reaction was cooled to –78 °C. In a separate flask, a solution of CuCN•2LiCl was prepared from dry LiCl (2.73 g, 62.86 mmol, 3.0 equiv.) and CuCN (2.81 g, 31.43 mmol, 1.5 equiv) in THF (55 mL) with stirring at 23 °C. The resultant pale green solution was transferred by canula to the lithiated starting material. The reaction mixture immediately turns bright red and fades to a tea color. This was stirred at –78 °C for 45 min before allyl bromide (12.67 g, 8.6 mL, 104.75 mmol, 5

equiv.) was added dropwise. The reaction was allowed to slowly warm to ambient temperature overnight, and the reaction was quenched by the addition of 90 mL of a 1:1 mixture of saturated aqueous NH_4Cl and concentrated NH_4OH. Stirring was continued for 20 minutes, and the resultant deep blue aqueous layer was extracted with Et_2O twice more. The combined organic extracts were dried over $MgSO_4$, filtered, and concentrated. Purification by flash chromatography on silica gel (hexanes/EtOAc, 95:5 → 85:15) affords 3.83 g (65%) of pure product. A portion of this material (3.18g, 11.22 mmol, 1.0 equiv.) was subjected to formylation under the conditions described in the synthesis of **5.13** affording 2.10 g (60%) of aldehyde **5.62** as a clear, colorless oil. **5.62**: R_f = 0.43 (hexanes/EtOAc, 7:3, CAM stain); IR (film) ν_{max} 2976, 1730, 1683, 1393, 1368, 1251, 1134 cm^{-1}; ^1H NMR (500 MHz, $CDCl_3$) δ 9.46 (d, *J* = 1.5 Hz, 1 H), 5.74 (ddt, *J* = 17.5, 10.5, 7.0 Hz, 1 H), 5.08 (app d, *J* = 17.5 Hz, 1 H), 5.05 (app d, *J* = 10.5 Hz, 1 H), 4.27 (br s, 1 H), 3.99–3.84 (m, 4 H), 3.81 (ddd, *J* = 10.0, 5.5, 2.0 Hz, 1 H), 2.51–2.40 (m, 2 H), 1.99 (br d, *J* =12.0 Hz, 1 H), 1.43 (s, 9 H); ^{13}C NMR (125 MHz, $CDCl_3$) δ 195.5, 155.5, 135.1, 117.5, 106.6, 81.7, 64.7, 63.8, 58.9, 52.0, 36.5, 35.6, 47.0, 28.1; HRMS (FAB) calc. for $C_{16}H_{26}NO_5^+$ [M+H^+] 312.1811, found 312.1824.

Aldehyde 5.63. Aldehyde **5.62** (120 mg) was dissolved in 5 mL of methanol, and excess K_2CO_3 was added. After 3.5 h, the reaction was poured into half-saturated aqueous NH_4Cl, and the aqueous layer was extracted with CH_2Cl_2 (4 × 12 mL). The combined organic extracts were dried over $MgSO_4$, filtered, and concentrated. Purification on silica gel (hexanes/EtOAc, 95:5 → 80:20) gave 92 mg (77%) of aldehyde **5.63**. **5.63**: ^1H NMR (400 MHz, $CDCl_3$) δ 9.63 (d, *J* = 0.8 Hz), 5.83–5.72 (m, 1 H), 5.11–5.04 (m, 2 H), 4.70

(br d, *J* = 6.0 Hz, 1 H), 4.42–4.34 (m, 1 H), 3.98–3.91 (m, 4 H), 3.78–3.70 (m, 1 H), 2.52–2.35 (m, 3 H), 1.85–1.76 (m, 3 H). 1.48 (s, 3 H).

Vinyl iodide 5.64. Aldehyde **5.62** (2.1 g) was subjected to Stork–Wittig olefination as described in the preparation of compound **5.14**, affording 2.35 g (80%) of vinyl iodide **5.64**. **5.64**: ^{1}H NMR (400 MHz, $CDCl_3$) δ 6.40 (t, *J* = 7.6 Hz, 1 H), 6.26 (dd, *J* = 7.6, 1.2 Hz, 1 H), 5.78 (ddt, *J* = 16.8, 10.4, 6.4 Hz, 1 H), 5.12 (dd, *J* = 16.8, 1.6 Hz, 1 H), 5.05 (dt, 10.4, 1.2 Hz, 1 H), 4.56 (dtd, *J* = 7.6, 4.8, 0.8 Hz, 1 H), 4.10–4.02 (m, 1 H), 4.00–3.80 (m, 4 H), 2.54–2.40 (m, 2 H), 2.11 (dd, *J* = 14.4, 5.2 Hz), 2.05 (dd, *J* = 14.8, 3.2 Hz, 1 H), 2.01 (dd, *J* = 14.4, 4.8 Hz, 1 H), 1.92 (dd, *J* = 14.8, 5.6 Hz, 1 H), 1.46 (s, 9 H).

Vinyl iodide 5.65. Aldehyde **5.63** (90 mg) was subjected to Stork–Wittig olefination as described in the preparation of compound **5.14**. The yield of this reaction was not determined. **5.65**: ^{1}H NMR (400 MHz, $CDCl_3$, 2.3:1 mixture of diastereomers) δ 6.70 (rotamer, dd, *J* = 8.4, 0.8 Hz, 0.26 H), 6.58 (rotamer, t, *J* = 7.6 Hz, 0.62 H), 6.34 (rotamer, d, *J* = 8.4 Hz, 0.26 H), 6.21 (rotamer, dd, *J* = 7.6, 1.6 Hz, 0.61 H), 5.83–5.70 (m, 1 H), 5.15–5.0 (m, 2 H), 4.55–4.35 (rotamers, m, 1 H), 4.09–4.88 (m, 4 H), 2.70–2.61 (rotamer, m, 0.66 H), 2.59–2.41 (rotamers, m, 1 H), 2.24 (rotamer, dd, *J* = 14.4, 5.2 Hz, 0.30 H), 2.04 (rotamer, dt, *J* = 14.4, 2.0 Hz, 0.38 H), 1.93 (rotamer, dd, *J* = 13.6, 7.2 Hz, 0.66 H), 1.91–1.83 (rotamers, m, 1.3 H), 1.80 (rotamer, dd, *J* = 13.6, 7.2 Hz, 0.66 H), 1.47 (rotamer, s, 6 H), 1.45 (rotamer, s, 3 H).

Enynol 5.66. Vinyl iodide **5.64** (2.35 g) was subjected to Sonogashira coupling conditions as described in the preparation of compound **5.15**, affording 1.68 g (86%) of the coupled product. **5.66**: R_f = 0.24 (silica gel, hexanes/EtOAc, 7:3, UV and CAM stain); IR (film) ν_{max} 3414, 2975, 1667, 1393, 1369, 1123, 1014, 731 cm^{-1}; ^1H NMR (500 MHz, $CDCl_3$) δ 5.84 (dd, *J* = 11.5, 4.0 Hz, 1 H), 5.83–5.70 (m, 1 H), 5.55 (dd, *J* = 11.5, 2.0 Hz), 5.08 (d, *J* = 16.5 Hz, 1 H), 5.02 (d, *J* = 10 Hz, 1 H), 4.76 (br s, 1 H), 4.28 (br s, 2 H), 3.94–3.78 (m, 5 H), 3.52 (br s, 1 H), 2.53–2.49 (m, 1 H), 2.40–2.30 (m, 1 H), 2.22 (dd, *J* = 15.0, 6.0 Hz, 1 H), 2.10–1.95 (m, 3 H), 1.43 (s, 9 H); ^{13}C NMR (125 MHz, $CDCl_3$) δ 155.3, 143.6, 135.3, 117.4, 107.7, 106.0, 94.3, 81.6, 80.2, 63.8, 63.7, 51.4, 51.1, 51.0, 39.2, 38.0, 34.1, 28.4; HRMS (FAB) calc. for $C_{20}H_{30}NO_5^+$ [M+H^+] 364.2124, found 364.2134.

Ketone 5.67. PPTS (92 mg, 0.368 mmol, 1.5 equiv.) was added to a solution of compound **5.66** (89 mg, 0.245 mmol, 1.0 equiv.) in *t*-BuOH/H_2O (5:1, 3 mL). The mixture was stirred at 75 °C for 15 h, cooled to ambient temperature, and concentrated under reduced pressure. The crude material was purified by flash chromatography (silica gel, hexanes/EtOAc, 90:10 → 75:25) to give 61 mg (78%) of ketone **5.67**. **5.67**: ^1H NMR (400 MHz, $CDCl_3$) δ 5.80–5.60 (m, 3 H), 5.10–5.0 (m, 3 H), 4.36–4.18 (m, 3 H), 3.69 (br s, 1 H), 2.84 (dd, *J* = 18.0, 6.8 Hz, 1 H), 2.73 (ddd, *J* = 17.6, 6.4, 1.2 Hz, 1 H), 2.72–2.63 (m, 1 H), 2.57 (dd, *J* = 17.2, 2.0 Hz, 1 H), 2.63–2.52 (br s, 1 H), 2.09–1.99 (m, 1 H), 1.49 (s, 9 H).

Keto-aldehyde 5.68. A solution of alcohol **5.67** (207 mg, 0.648 mmol, 1.0 equiv.) in 2 mL of CH_2Cl_2 was treated with DMP (343 mg, 0.810 mmol, 1.25 equiv.), and the reaction was stirred for 1.5 h at 23 °C. The reaction was quenched by the addition of 8 mL of saturated aqueous $NaHCO_3$ and 8 mL of EtOAc with vigorous stirring. $Na_2S_2O_3$ (1.50 g) was added as a solid, and vigorous stirring was continued until both layers became clear. The reaction mixture was then transferred to a separatory funnel where the aqueous layer was extracted twice more with CH_2Cl_2. The combined organic extracts were washed twice with saturated aqueous $NaHCO_3$, dried over $MgSO_4$, filtered, and concentrated to afford 202 mg (98%) of pure keto-aldehyde **5.68**. **5.68**: R_f = 0.52 (silica gel, hexanes/EtOAc, 1:1, UV and CAM stain); IR (film) ν_{max} 2976, 2174, 1729, 1691, 1665, 1530, 1391, 1367, 1168, 1119 cm^{-1}; ^1H NMR (500 MHz, $CDCl_3$) δ 9.32 (s, 1 H), 6.20 (dd, *J* = 11.5, 6.0 Hz, 1 H), 5.71 (d, *J* = 11.5 Hz, 1 H), 5.75–5.65 (m, 1 H), 5.20–5.10 (br s, 1 H), 5.10–5.0 (m, 2 H), 4.21 (br s), 2.88 (dd, *J* = 18.0, 7.0 Hz, 1 H), 2.68–2.52 (m, 4 H), 2.12–2.01 (m, 1 H), 1.43 (s, 9 H); ^{13}C NMR (125 MHz, $CDCl_3$) δ 205.6, 176.2, 154.2, 151.2, 118.6, 107.0, 94.3, 89.3, 80.8, 51.7, 51.1, 42.9, 41.0, 40.9, 28.2; HRMS (FAB) calc. for $C_{18}H_{24}NO_4^+$ [M+H$^+$] 318.1705, found 318.1694.

Butenolide 5.69. $Ti(OiPr)_4$ (170 mg, 177 μL, 0.598 mmol, 2.0 equiv.) was added to a suspension of precatalyst **5.21** (26.4 mg, 0.120 mmol, 0.4 equiv.) in 8 mL of toluene at ambient temperature under Ar atmosphere. The reaction mixture was transferred to a 50 °C oil bath and allowed to thermally equilibrate for 10 minutes. A solution of **5.68** (95 mg, 0.299 mmol, 1.0 equiv.) in 7 mL of toluene was added slowly over a period of 8 h. During the addition process, the reaction color changes from clear to light orange to deep

red to dark red/brown. The reaction was allowed to stir at room temperature overnight at which point the reaction mixture was concentrated to 1/3 volume. This crude mixture was purified directly by silica gel chromatography (hexanes/EtOAc, 95:5 → 75:25) afforded 45 mg (47%) of butenolide **5.69** as a clear, colorless oil. **5.69**: R_f = 0.52 (silica gel, hexanes/EtOAc, 1:1, UV); IR (film) ν_{max} 2928, 1761, 1690, 1392, 1368, 1170, 1105, 918 cm^{-1}; ^1H NMR (500 MHz, $CDCl_3$) δ 6.59 (d, *J* = 9.5 Hz, 1 H), 6.33 (dd, *J* = 9.5, 6.0 Hz, 1 H), 5.75 (ddt, *J* = 18.0, 10.5, 7.5 Hz, 1 H), 5.71 (s, 1 H), 5.14–5.08 (m, 2 H), 4.97 (dtd, *J* = 7.0, 3.5, 0.5 Hz, 1 H), 3.74 (dtd, *J* = 10.5, 6.5, 4.0 Hz, 1 H), 2.68–2.54 (m, 2 H), 2.50 (dd, *J* = 12.0, 2.5 Hz, 1 H) 2.21 (dd, *J* = 14.5, 6.5 Hz, 1 H), 1.99 (ddd, *J* = 12.0, 4.0, 1.5 Hz, 1 H), 1.93 (ddd, *J* = 14.5, 6.5, 1.5 Hz, 1 H), 1.63–1.55 (m, 1 H), 1.49 (s, 9 H); ^{13}C NMR (125 MHz, $CDCl_3$) δ 171.9, 166.3, 155.2, 136.9, 134.2, 121.9, 118.4, 110.8, 81.8, 80.8, 50.3, 50.2, 41.1, 37.0, 36.2, 28.4; HRMS (FAB) calc. for $C_{18}H_{24}NO_4^+$ [M+H^+] 318.1705, found 318.1694.

Alcohol 5.70. To a –25 °C solution of butenolide **5.69** (71 mg, 0.224 mmol, 1.0 equiv.) in THF (2.0 mL) was added a solution of DIAB (0.5 M in THF, 2.24 mL, 1.12 mmol, 5.0 equiv.) dropwise. The reaction was kept at this temperature for 2 h then slowly warmed to 10 °C over 2 h at which point the reaction was quenched by the addition of a few drops of water to quench the excess borane reagent. An aqueous solution of $NaBO_3$•H_2O (450 mg in 3 mL) was then introduced, and the reaction was stirred under argon with vigorous stirring for 4.5 h at ambient temperature. Et_2O (7 mL) and water (5 mL) were added, and the reaction mixture was transferred to a separatory funnel where the layers were separated. The aqueous layer was extracted with Et_2O (2 × 5 mL), and the combined

organic extracts were dried over $MgSO_4$. Filtration and concentration afforded crude material that was purified by silica gel column chromatography (hexanes/EtOAc, 90:10 → 25:75) afforded 54 mg (72%) of the desired primary alcohol **5.70** as a clear, colorless oil. **5.70**: R_f = 0.14 (silica gel, hexanes/EtOAc, 1:1, UV); IR (film) ν_{max} 3465, 2978, 2941, 2871, 1755, 1685, 1645, 1394, 1168, 1105 cm^{-1}; ^1H NMR (500 MHz, $CDCl_3$) δ 5.78 (d, *J* = 9.5 Hz, 1 H), 3.63 (dd, *J* = 9.5, 5.5 Hz, 1 H), 5.72 (s, 1 H), 4.90–4.85 (m, 1 H), 3.75–3.68 (m, 1 H), 3.70–3.60 (m, 2 H), 2.56 (dd, *J* = 12.5, 3.0 Hz, 1 H), 2.16 (dd, *J* = 14.5, 5.5 Hz, 1 H), 2.07 (dd, *J* = 14.5, 6.5 Hz, 1 H), 1.98 (dd, *J* = 12.5, 4.0 Hz, 1 H), 1.98–1.88 (m, 2 H), 1.70–1.60 (m, 2 H), 1.49 (s, 9 H); HRMS (FAB) calc. for $C_{18}H_{26}NO_5^+$ [M+H^+] 336.1811, found 336.1817.

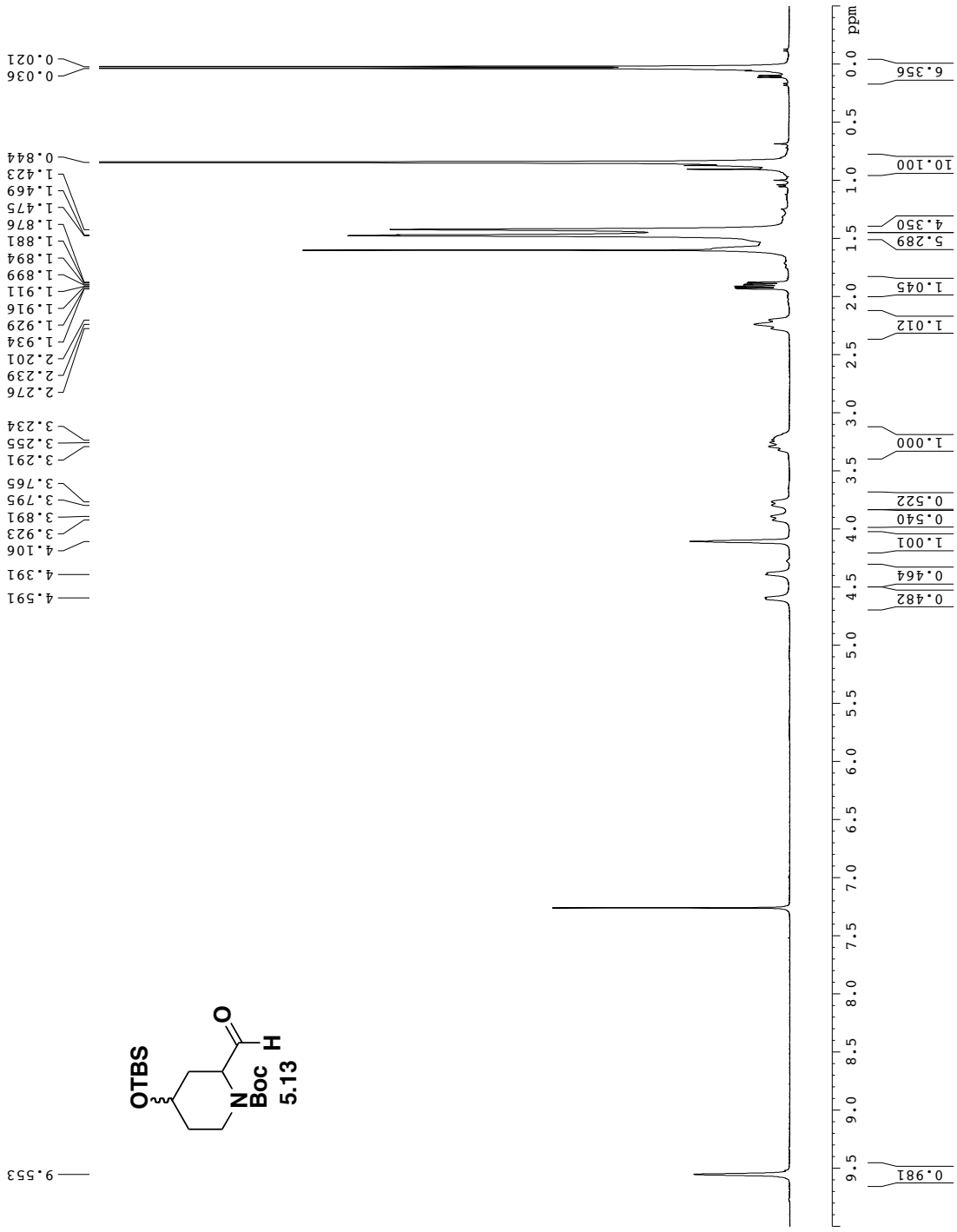
OTBS
N
Boc
H
O
5.13
ppm
0.0
0.5
1.0
1.5
2.0
2.5
3.0
3.5
4.0
4.5
5.0
5.5
6.0
6.5
7.0
7.5
8.0
8.5
9.0
9.5
6.356
10.100
4.350
5.289
1.045
1.012
1.000
0.522
0.540
1.001
0.464
0.482
0.981
0.021
0.036
0.844
1.423
1.469
1.475
1.876
1.881
1.894
1.899
1.911
1.916
1.929
1.934
2.201
2.239
2.276
3.234
3.255
3.291
3.765
3.795
3.891
3.923
4.106
4.391
4.591
9.553

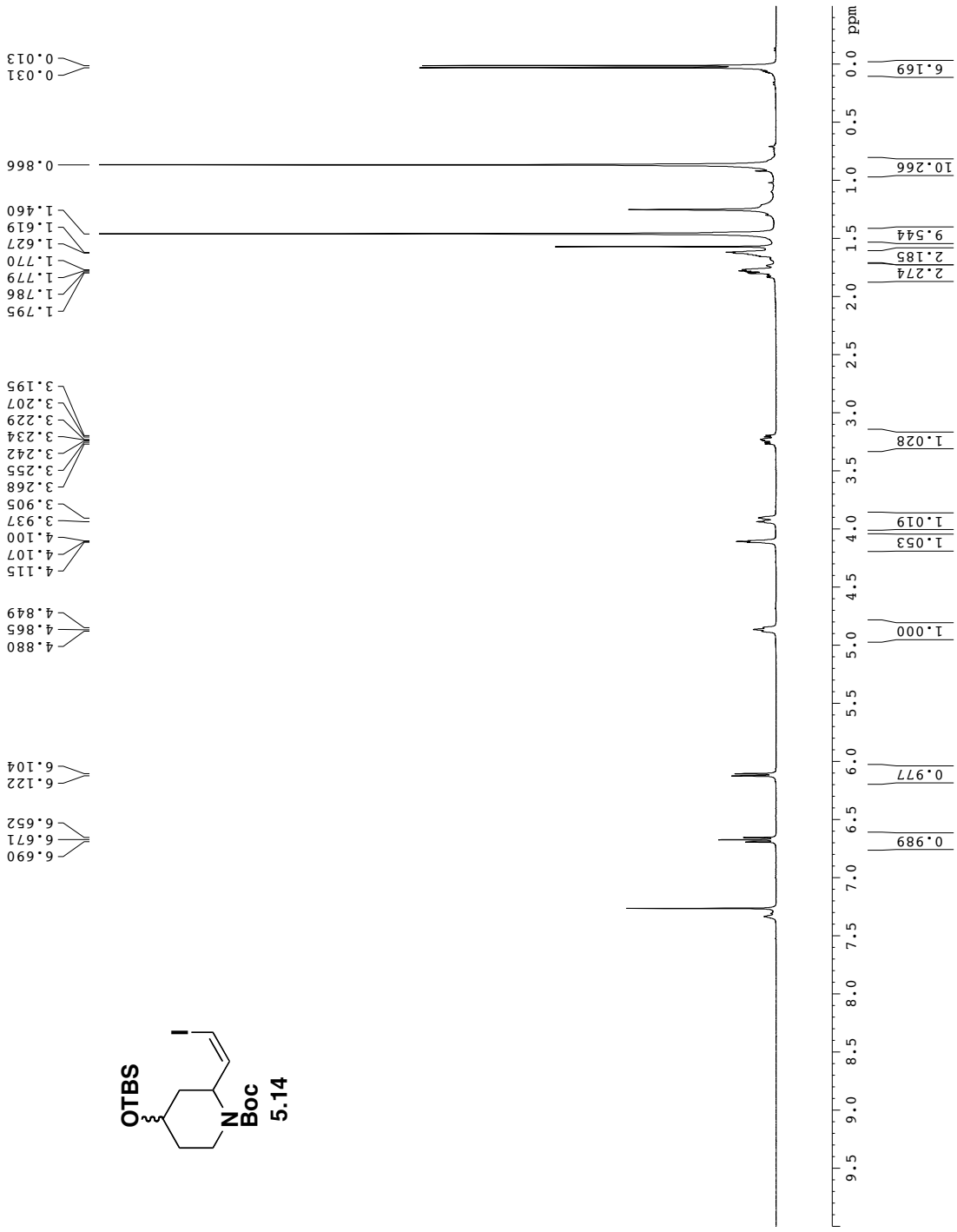
OTBS
N
Boc
I
5.14
ppm
0.0
0.5
1.0
1.5
2.0
2.5
3.0
3.5
4.0
4.5
5.0
5.5
6.0
6.5
7.0
7.5
8.0
8.5
9.0
9.5
6.169
10.266
9.544
2.185
2.274
1.028
1.019
1.053
1.000
0.977
0.989
0.013
0.031
0.866
1.460
1.619
1.627
1.770
1.779
1.786
1.795
3.195
3.207
3.229
3.234
3.242
3.255
3.268
3.905
3.937
4.100
4.107
4.115
4.849
4.865
4.880
6.104
6.122
6.652
6.671
6.690

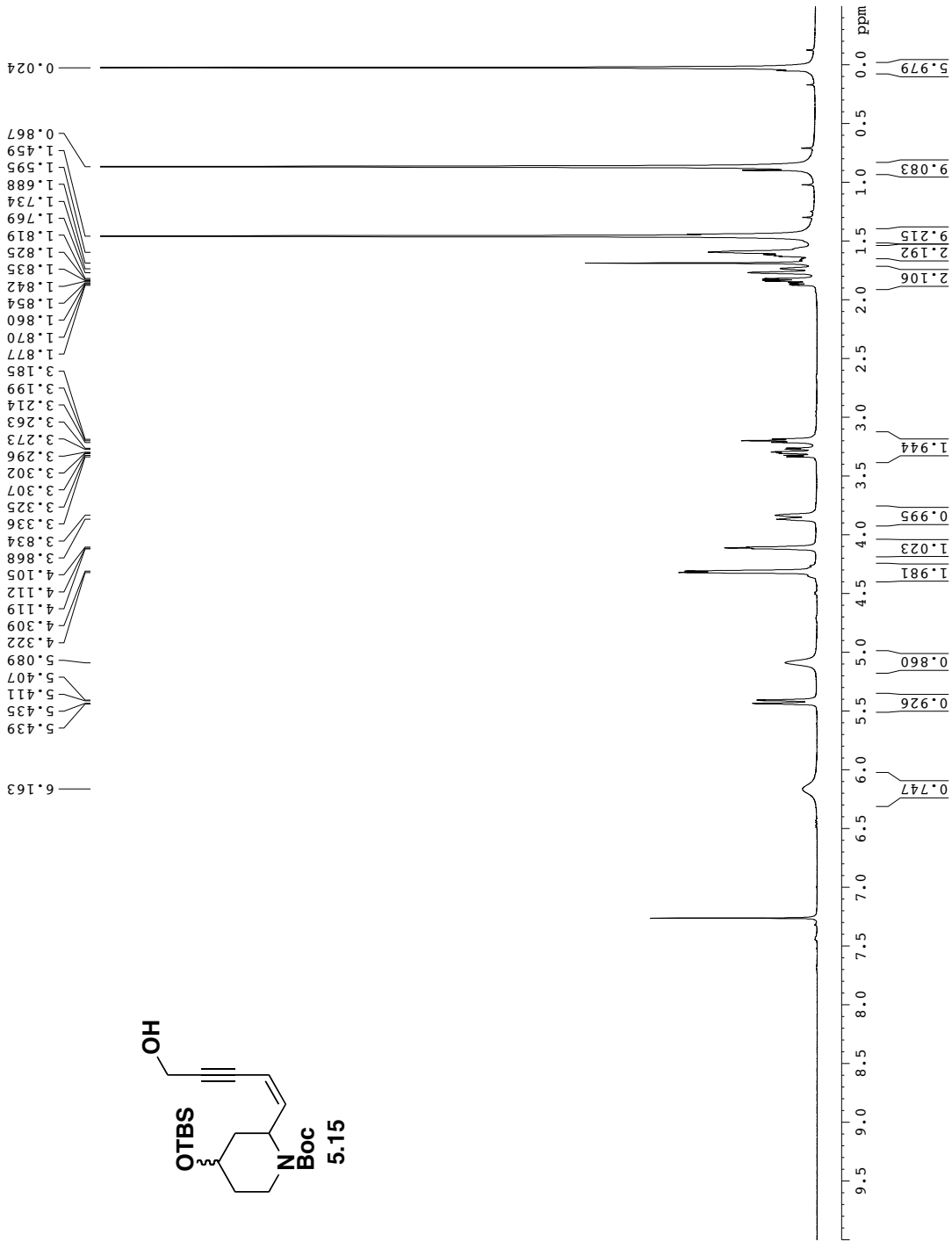
OH
OTBS
N
Boc
5.15
ppm
5.979
9.083
9.215
2.192
2.106
1.944
0.995
1.023
1.981
0.860
0.926
0.747
0.024
0.867
1.459
1.595
1.688
1.734
1.769
1.819
1.825
1.835
1.842
1.854
1.860
1.870
1.877
3.185
3.199
3.214
3.263
3.273
3.296
3.302
3.307
3.325
3.336
3.834
3.868
4.105
4.112
4.119
4.309
4.322
5.089
5.407
5.411
5.435
5.439
6.163

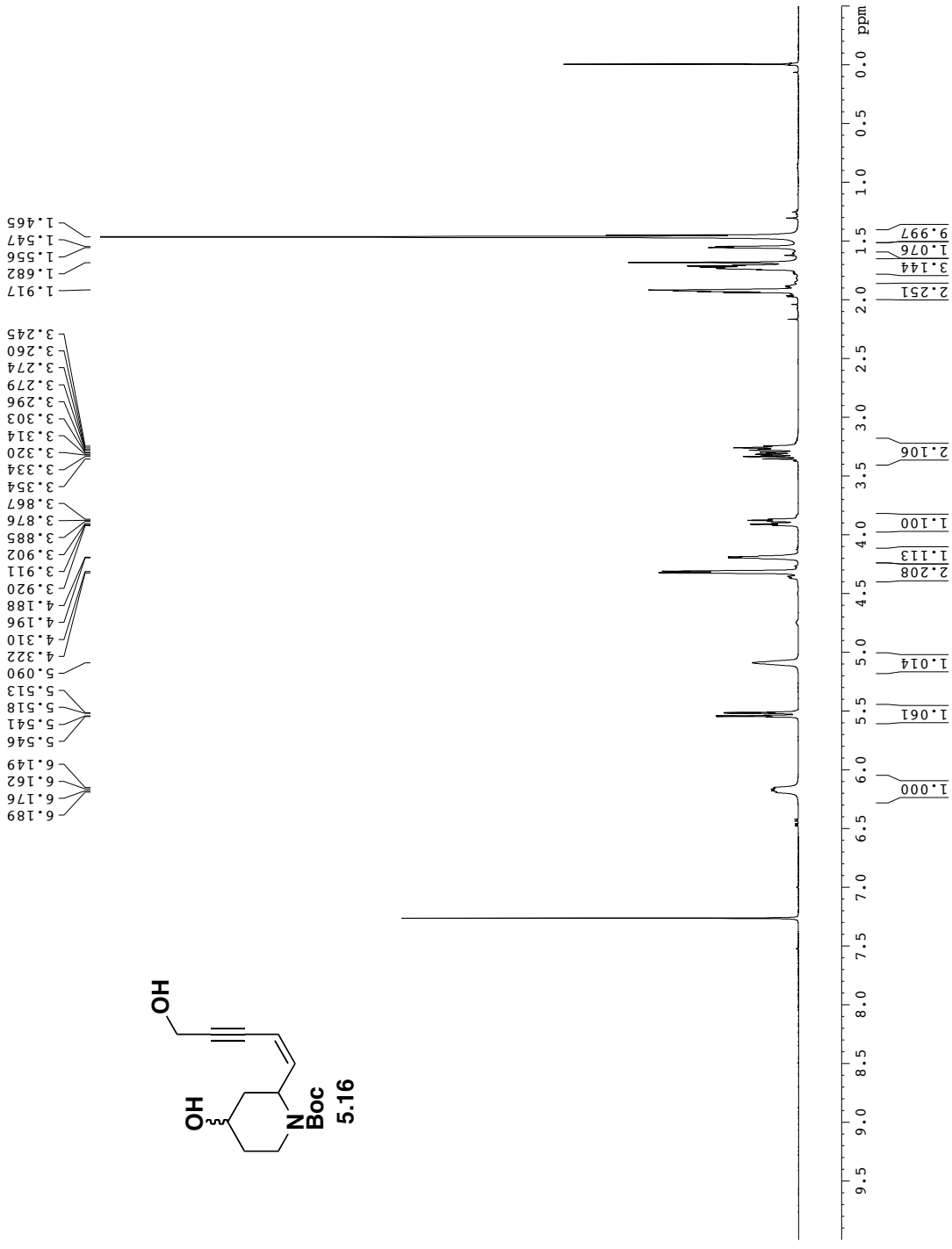
OH
OH
N
Boc
5.16
ppm
0.0
0.5
1.0
1.5
2.0
2.5
3.0
3.5
4.0
4.5
5.0
5.5
6.0
6.5
7.0
7.5
8.0
8.5
9.0
9.5
1.000
1.061
1.014
2.208
1.113
1.100
2.106
9.997
1.076
3.144
2.251
1.917
1.682
1.556
1.547
1.465
3.245
3.260
3.274
3.279
3.296
3.303
3.314
3.320
3.334
3.354
3.867
3.876
3.885
3.902
3.911
3.920
4.188
4.196
4.310
4.322
5.090
5.513
5.518
5.541
5.546
6.149
6.162
6.176
6.189

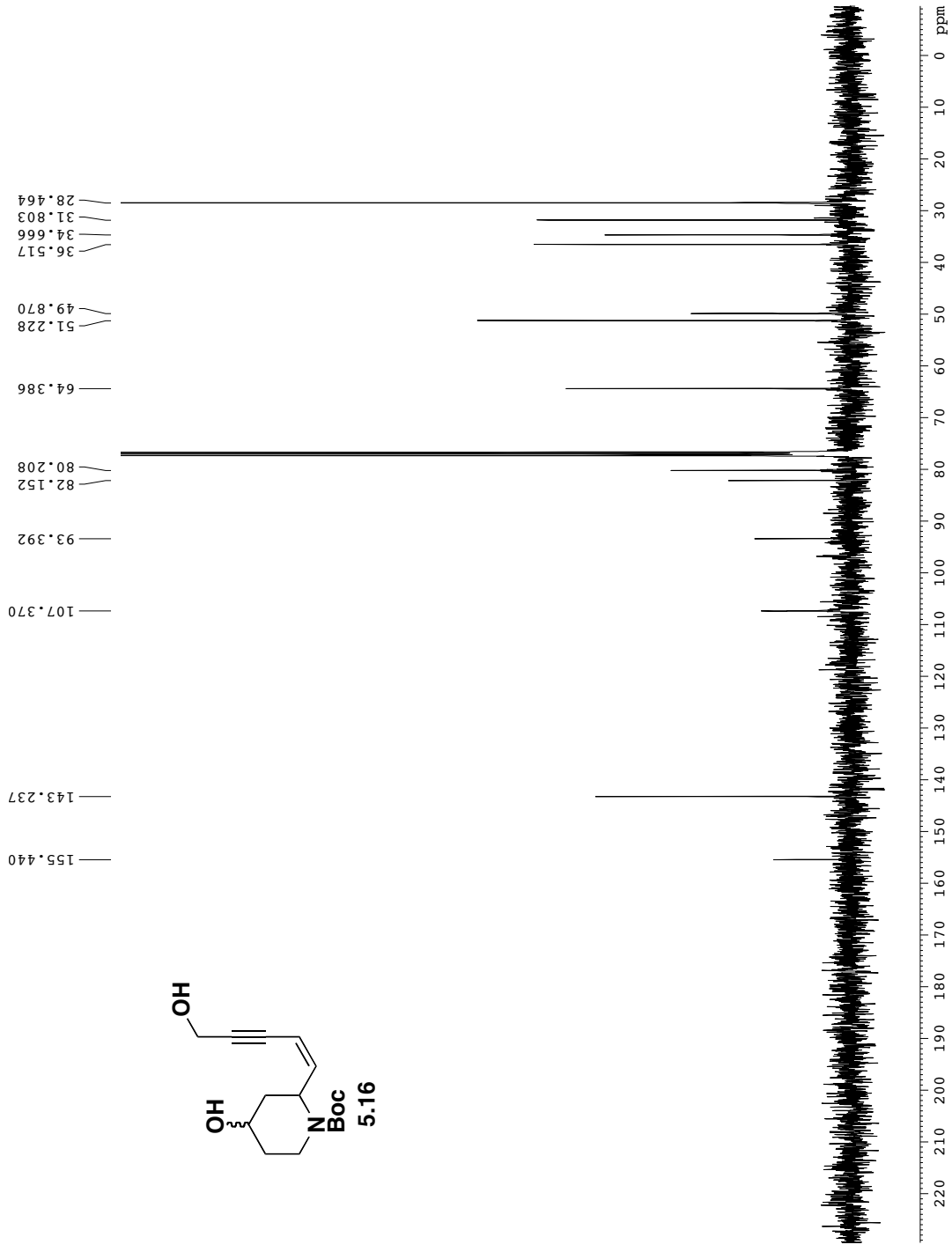
155.440
143.237
107.370
93.392
82.152
80.208
64.386
51.228
49.870
36.517
34.666
31.803
28.464
ppm
OH
OH
N
Boc
5.16

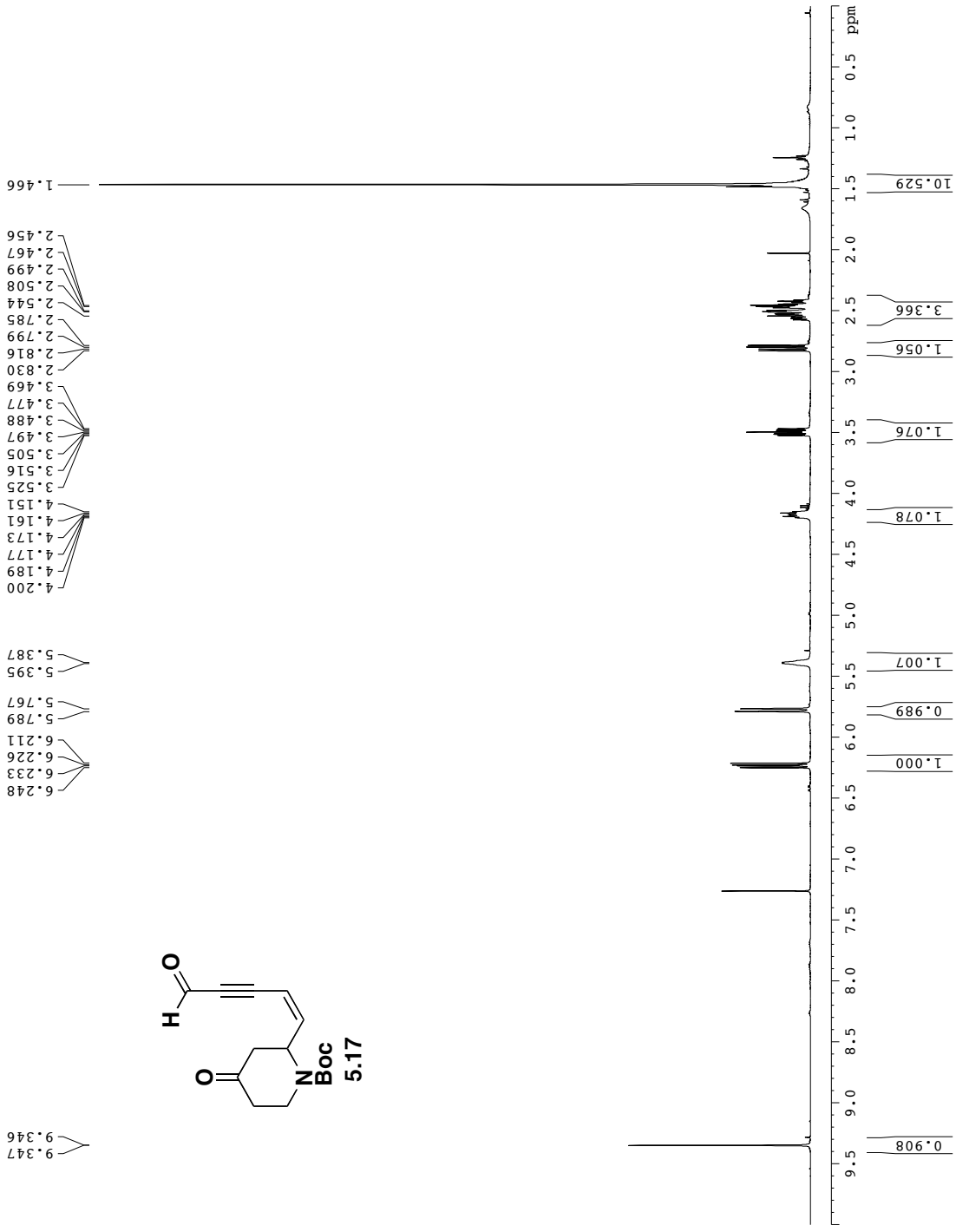
ppm
0.5
1.0
1.5
2.0
2.5
3.0
3.5
4.0
4.5
5.0
5.5
6.0
6.5
7.0
7.5
8.0
8.5
9.0
9.5
10.529
3.366
1.056
1.076
1.078
1.007
0.989
1.000
0.908
1.466
2.456
2.467
2.499
2.508
2.544
2.785
2.799
2.816
2.830
3.469
3.477
3.488
3.497
3.505
3.516
3.525
4.151
4.161
4.173
4.177
4.189
4.200
5.387
5.395
5.767
5.789
6.211
6.226
6.233
6.248
9.346
9.347
O
H
O
N
Boc
5.17

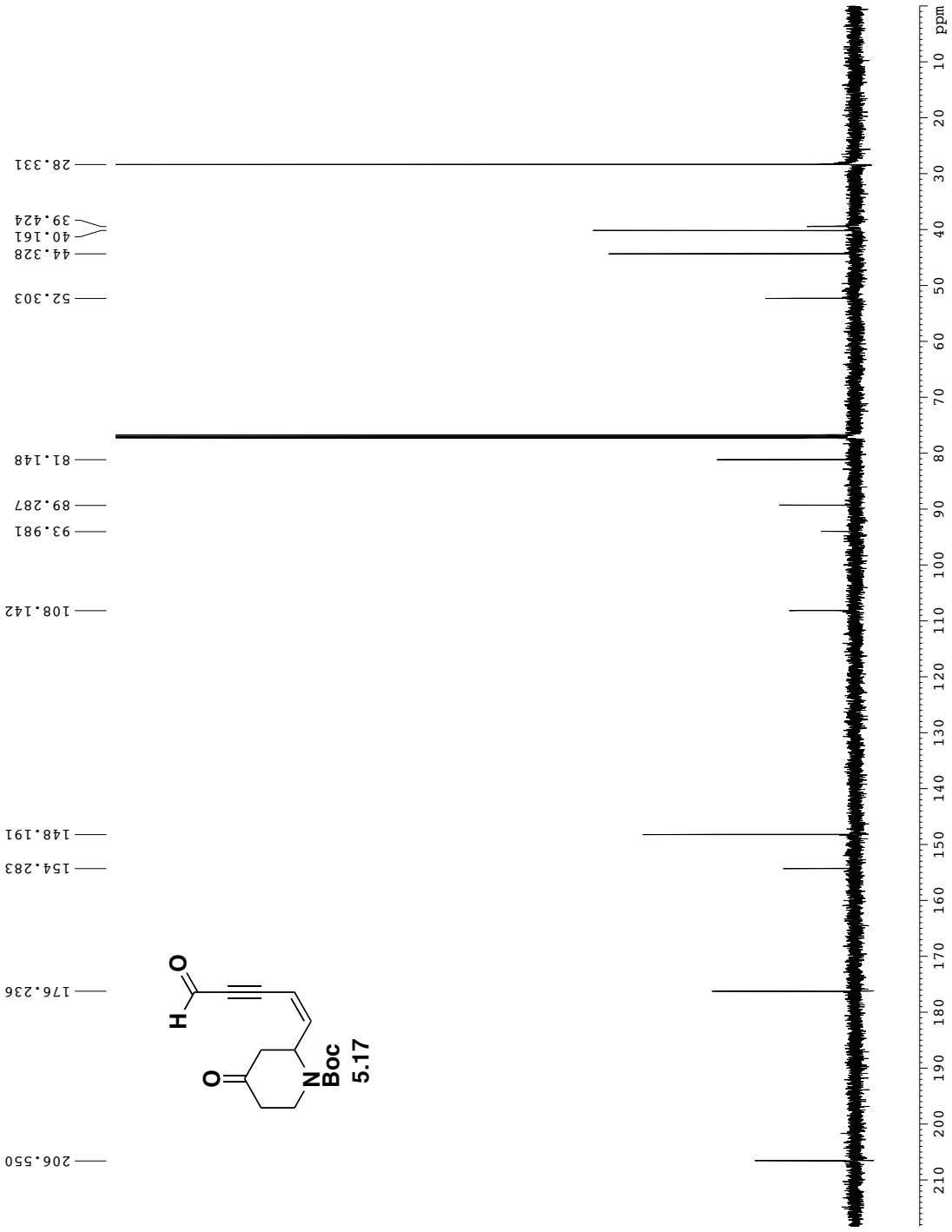
28.331
39.424
40.161
44.328
52.303
81.148
89.287
93.981
108.142
148.191
154.283
176.236
206.550
O
H
O
N
Boc
5.17
ppm

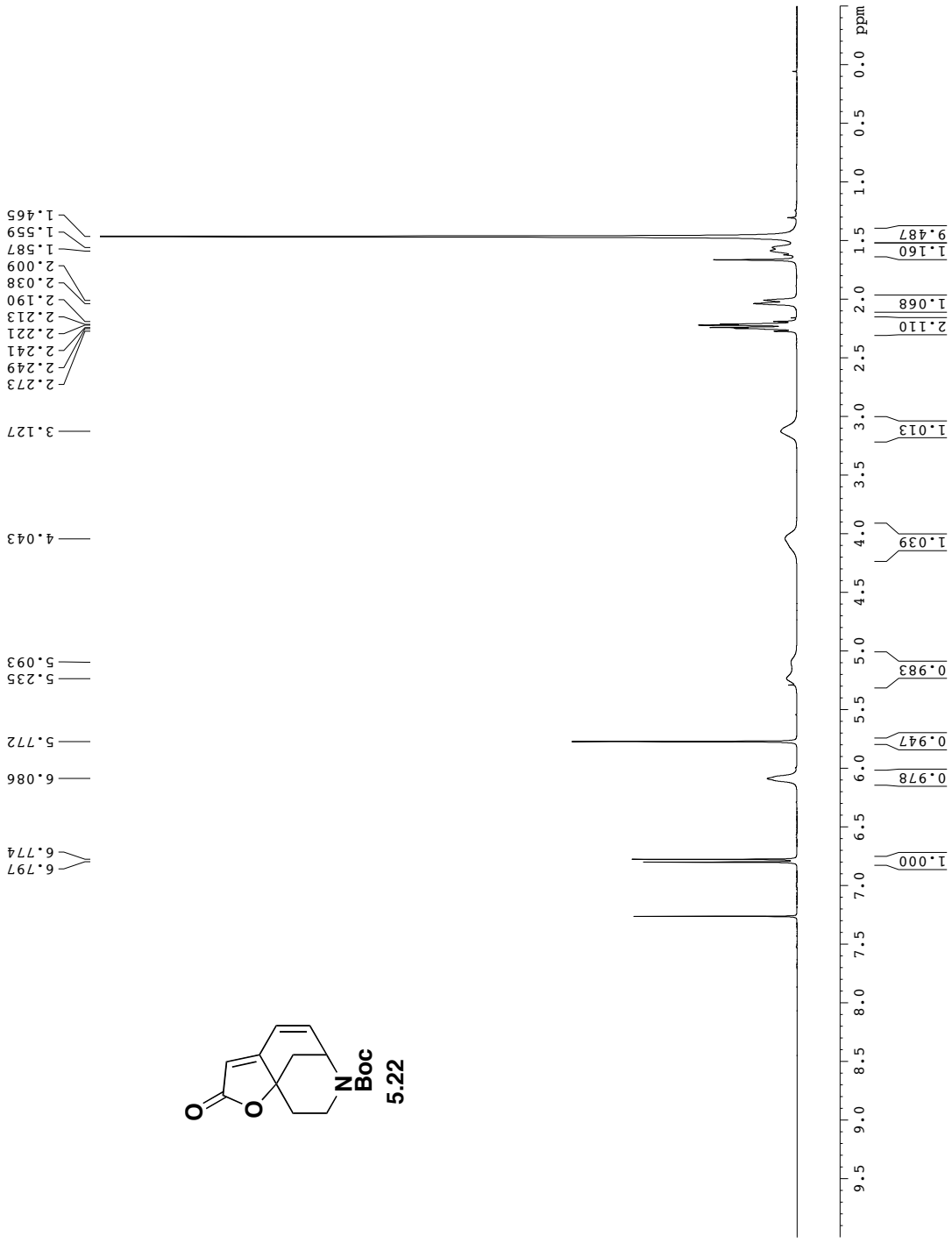
ppm
0.0
0.5
1.0
1.5
2.0
2.5
3.0
3.5
4.0
4.5
5.0
5.5
6.0
6.5
7.0
7.5
8.0
8.5
9.0
9.5
1.000
0.978
0.947
0.983
1.039
1.013
2.110
1.068
1.160
9.487
6.797
6.774
6.086
5.772
5.235
5.093
4.043
3.127
2.273
2.249
2.241
2.221
2.213
2.190
2.038
2.009
1.587
1.559
1.465
O
O
N
Boc
5.22

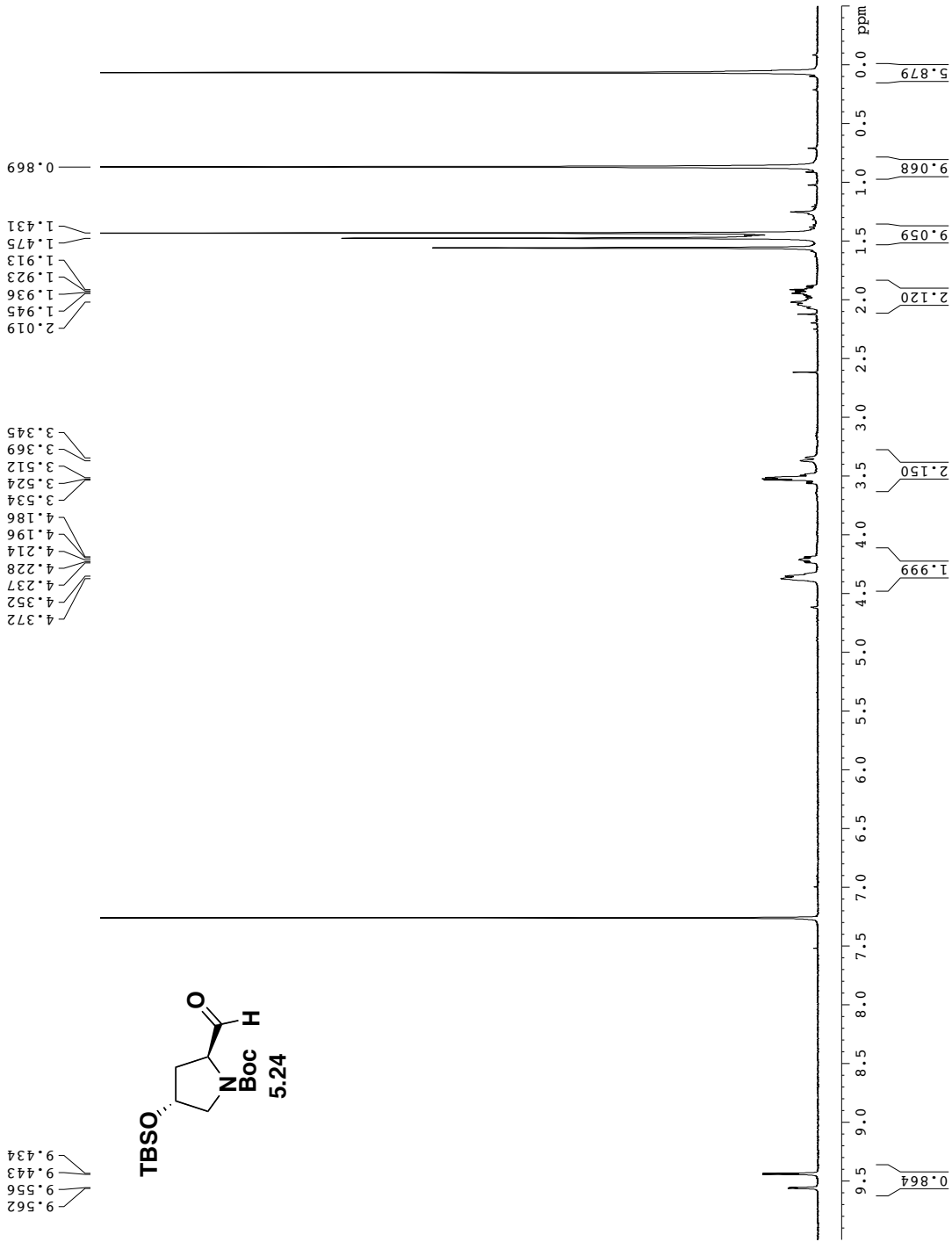
TBSO
N
Boc
O
H
5.24
9.562
9.556
9.443
9.434
4.372
4.352
4.237
4.228
4.214
4.196
4.186
3.534
3.524
3.512
3.369
3.345
2.019
1.945
1.936
1.923
1.913
1.475
1.431
0.869
0.864
1.999
2.150
2.120
9.059
9.068
5.879
ppm

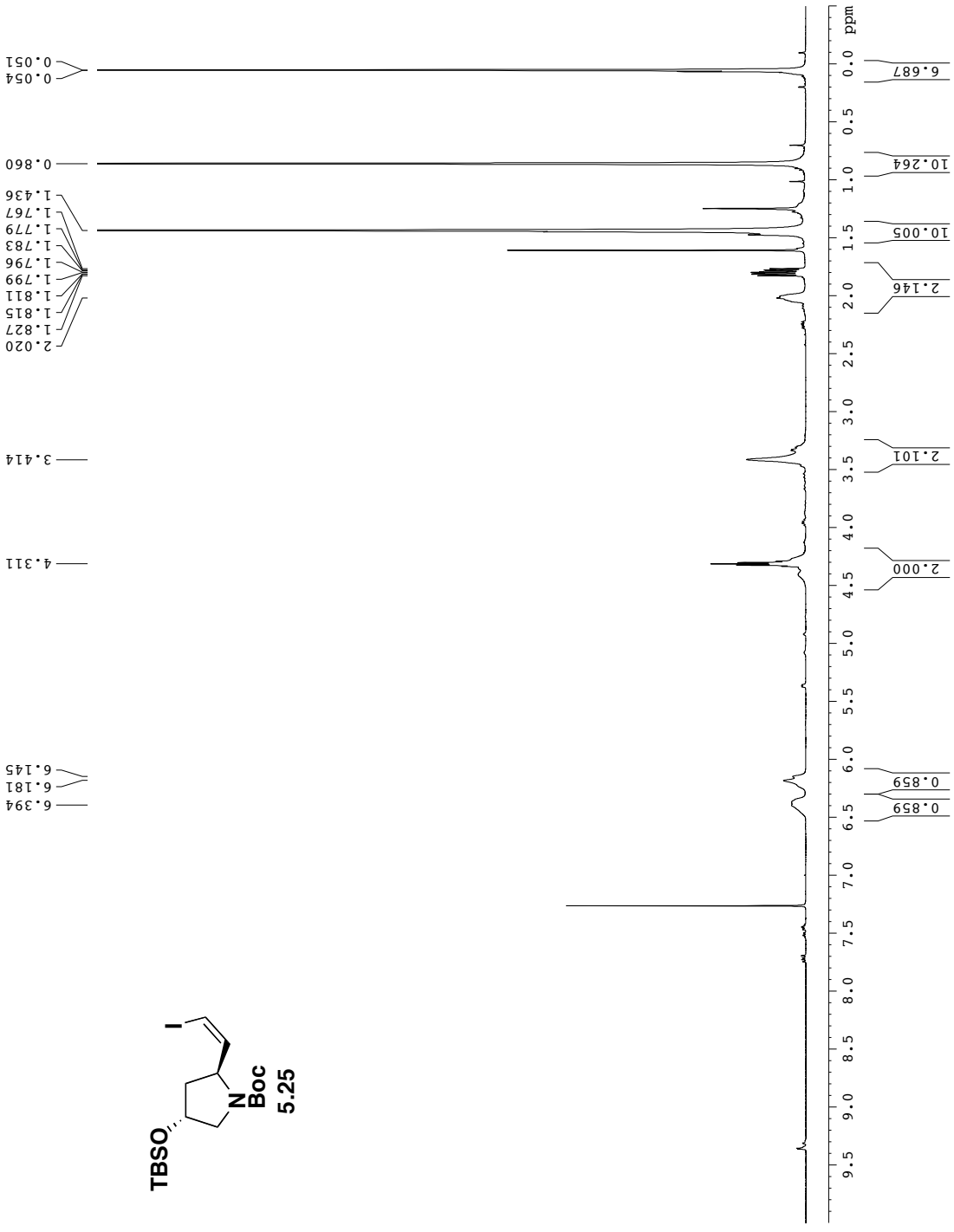
TBSO
N
Boc
I
5.25
ppm
0.0
0.5
1.0
1.5
2.0
2.5
3.0
3.5
4.0
4.5
5.0
5.5
6.0
6.5
7.0
7.5
8.0
8.5
9.0
9.5
6.687
10.264
10.005
2.146
2.101
2.000
0.859
0.859
6.145
6.181
6.394
4.311
3.414
2.020
1.827
1.815
1.811
1.799
1.796
1.783
1.779
1.767
1.436
0.860
0.054
0.051

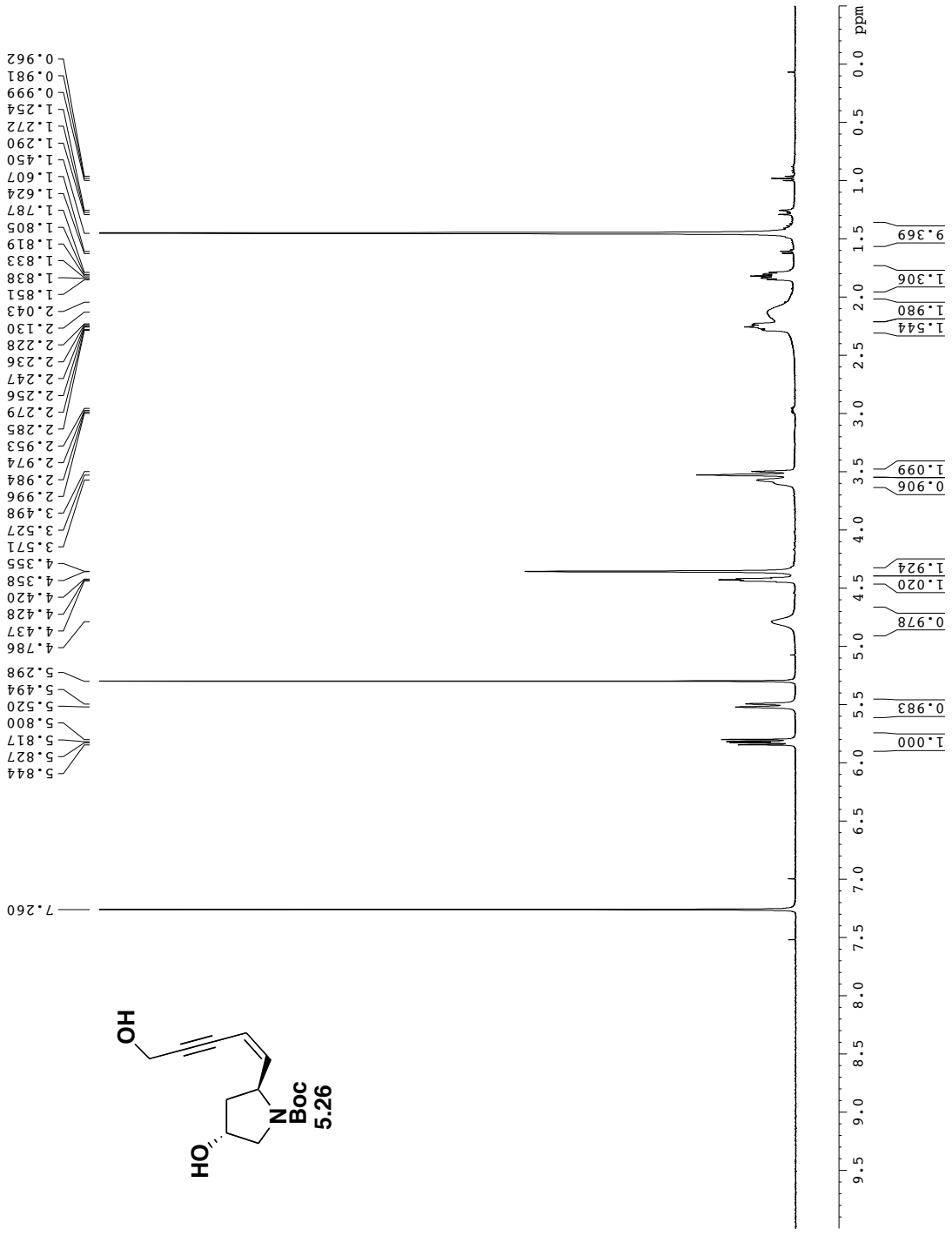
OH
HO
N
Boc
5.26
ppm
9.369
1.306
1.980
1.544
1.099
0.906
1.924
1.020
0.978
0.983
1.000
7.260
5.844
5.827
5.817
5.800
5.520
5.494
5.298
4.786
4.437
4.428
4.420
4.358
4.355
3.571
3.527
3.498
2.996
2.984
2.974
2.953
2.885
2.879
2.256
2.247
2.236
2.228
2.130
2.043
1.851
1.838
1.833
1.819
1.805
1.787
1.624
1.607
1.450
1.290
1.272
1.254
0.999
0.981
0.962

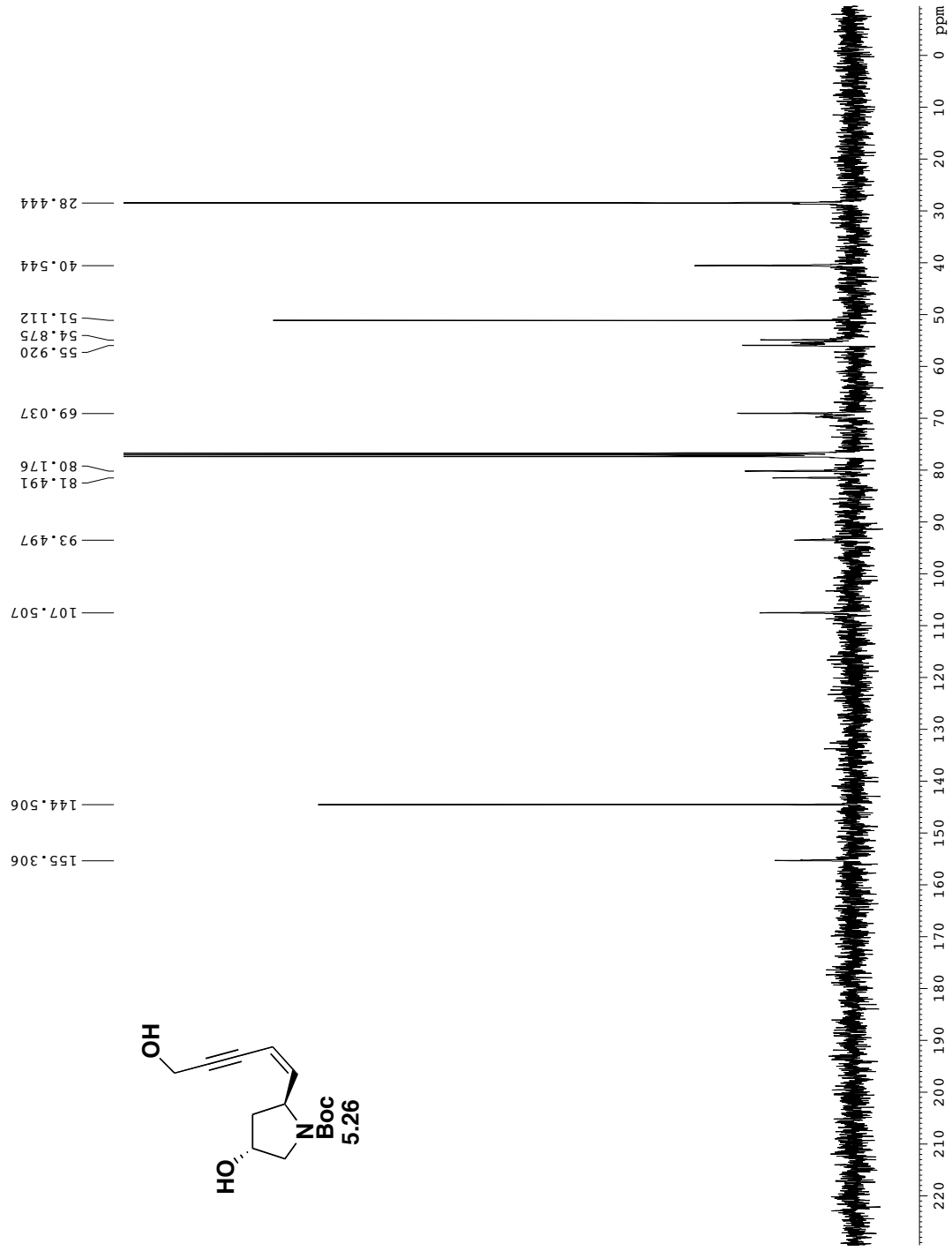
28.444
40.544
51.112
54.875
55.920
69.037
80.176
81.491
93.497
107.507
144.506
155.306
OH
HO
N
Boc
5.26
ppm

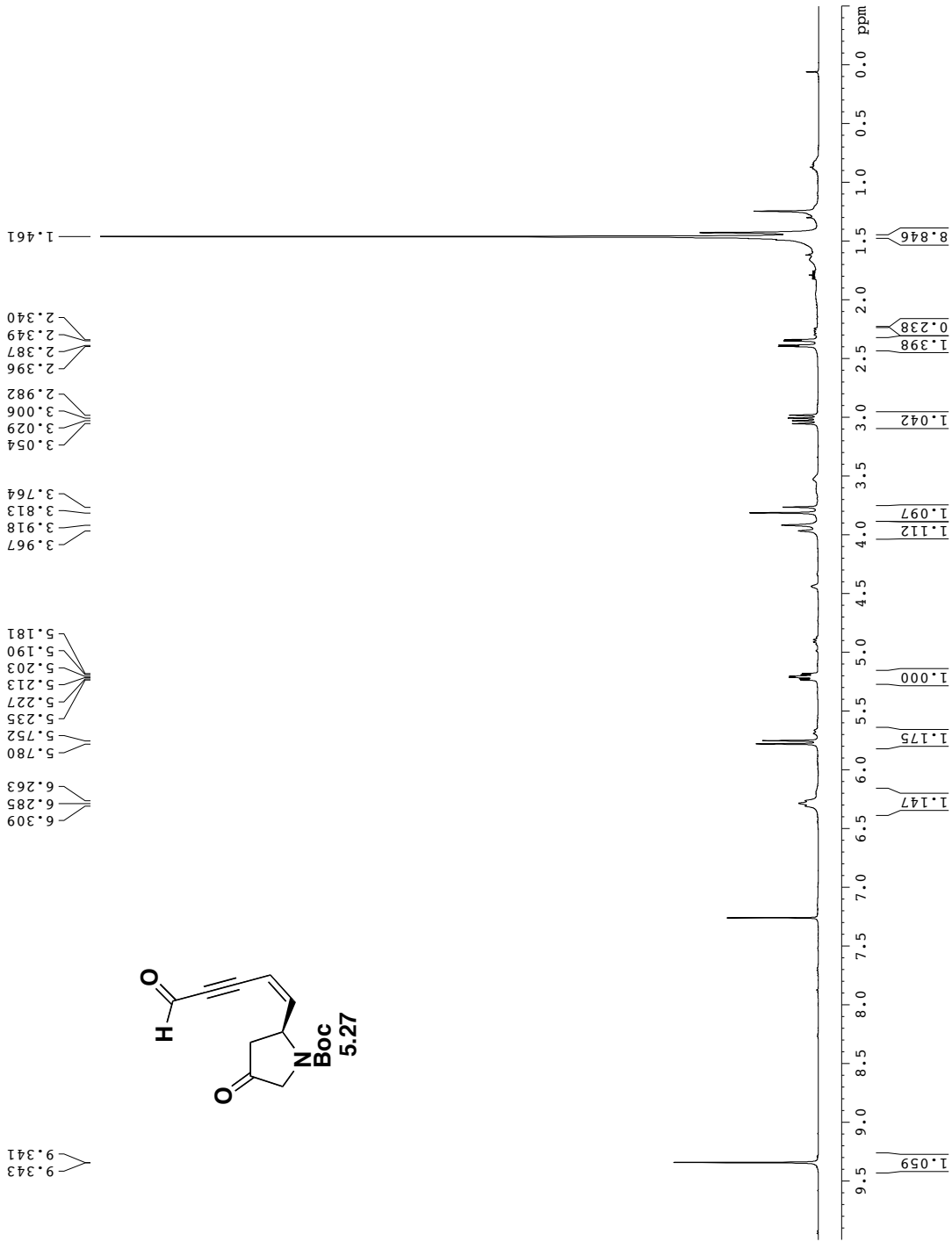
ppm
0.0
0.5
1.0
1.5
2.0
2.5
3.0
3.5
4.0
4.5
5.0
5.5
6.0
6.5
7.0
7.5
8.0
8.5
9.0
9.5
1.059
8.846
0.238
1.398
1.042
1.097
1.112
1.000
1.175
1.147
1.461
2.340
2.349
2.387
2.396
2.982
3.006
3.029
3.054
3.764
3.813
3.918
3.967
5.181
5.190
5.203
5.213
5.227
5.235
5.752
5.780
6.263
6.285
6.309
9.341
9.343
O
H
O
N
Boc
5.27

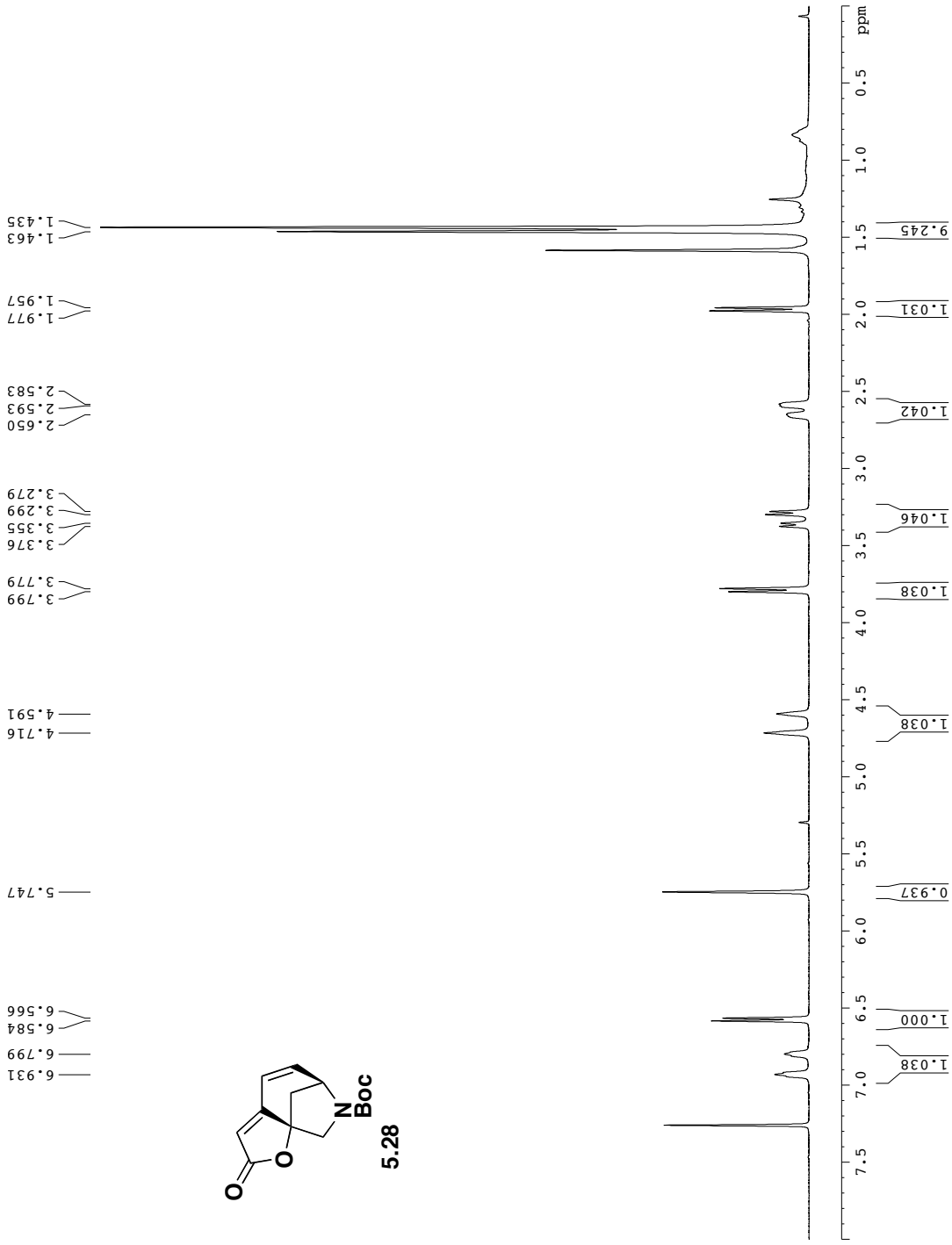
1.435
1.463
1.957
1.977
2.583
2.593
2.650
3.279
3.299
3.355
3.376
3.779
3.799
4.591
4.716
5.747
6.566
6.584
6.799
6.931
9.245
1.031
1.042
1.046
1.038
1.038
0.937
1.000
1.038
ppm
0.5
1.0
1.5
2.0
2.5
3.0
3.5
4.0
4.5
5.0
5.5
6.0
6.5
7.0
7.5
O
O
N
Boc
5.28

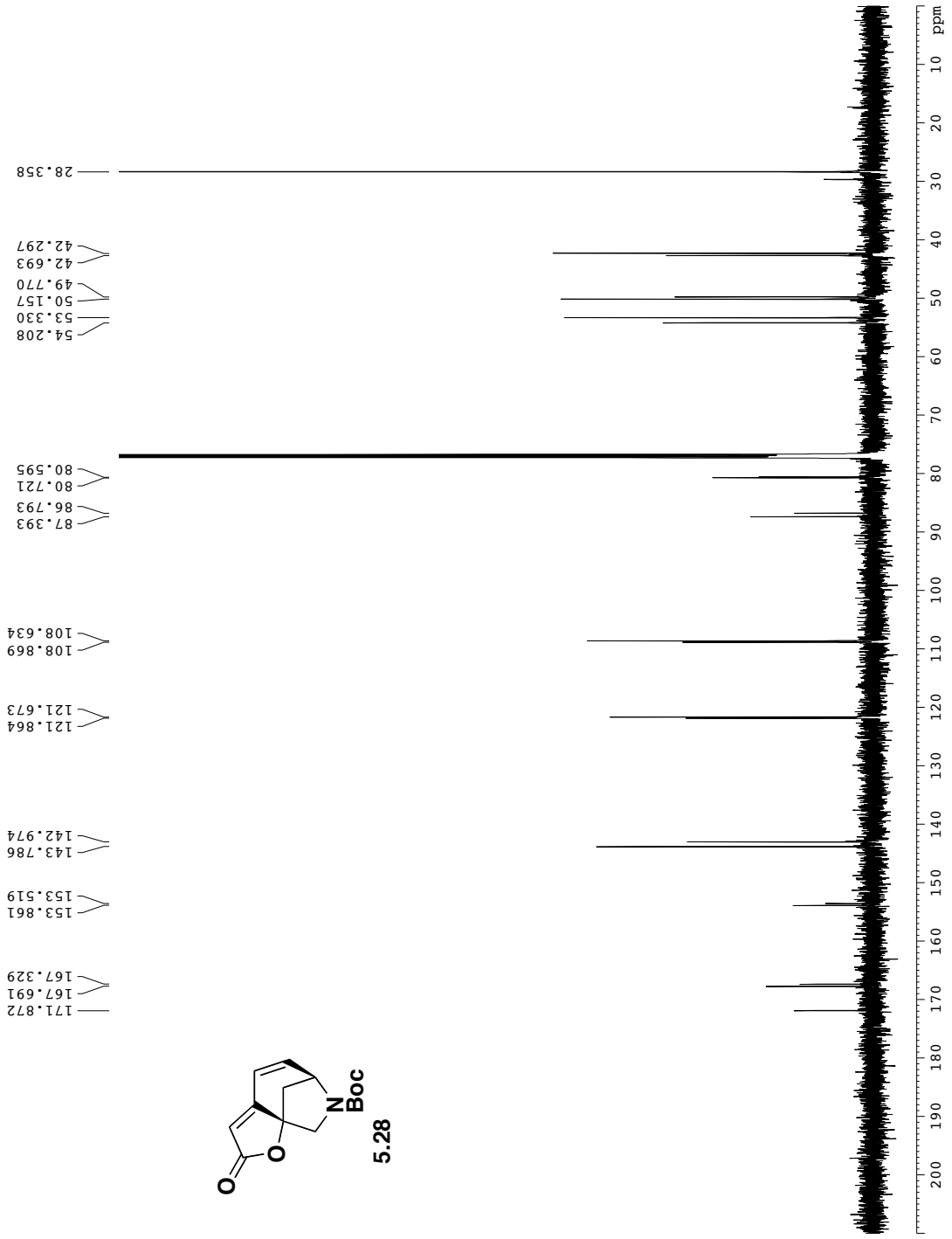
28.358
42.297
42.693
49.770
50.157
53.330
54.208
80.595
80.721
86.793
87.393
108.634
108.869
121.673
121.864
142.974
143.786
153.519
153.861
167.329
167.691
171.872
ppm
10
20
30
40
50
60
70
80
90
100
110
120
130
140
150
160
170
180
190
200
N
Boc
O
O
5.28

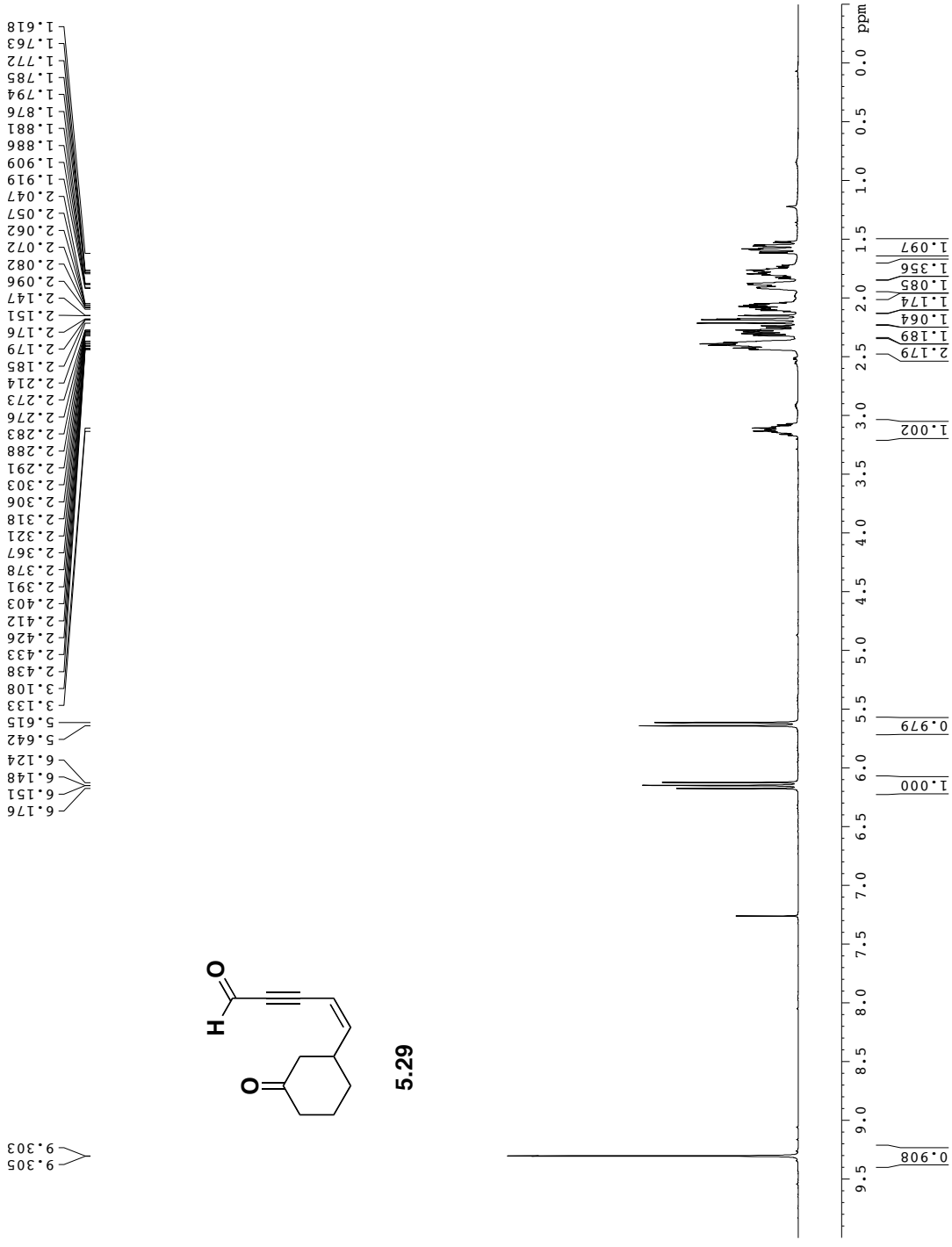
9.303
9.305
6.176
6.151
6.148
6.124
5.642
5.615
3.133
3.108
2.438
2.433
2.426
2.412
2.403
2.391
2.378
2.367
2.321
2.318
2.306
2.303
2.291
2.288
2.283
2.276
2.273
2.214
2.185
2.179
2.176
2.151
2.147
2.096
2.082
2.072
2.062
2.057
2.047
1.919
1.909
1.886
1.881
1.876
1.794
1.785
1.772
1.763
1.618
O
H
O
5.29
0.908
1.002
0.979
1.000
2.179
1.189
1.064
1.174
1.085
1.356
1.097
ppm

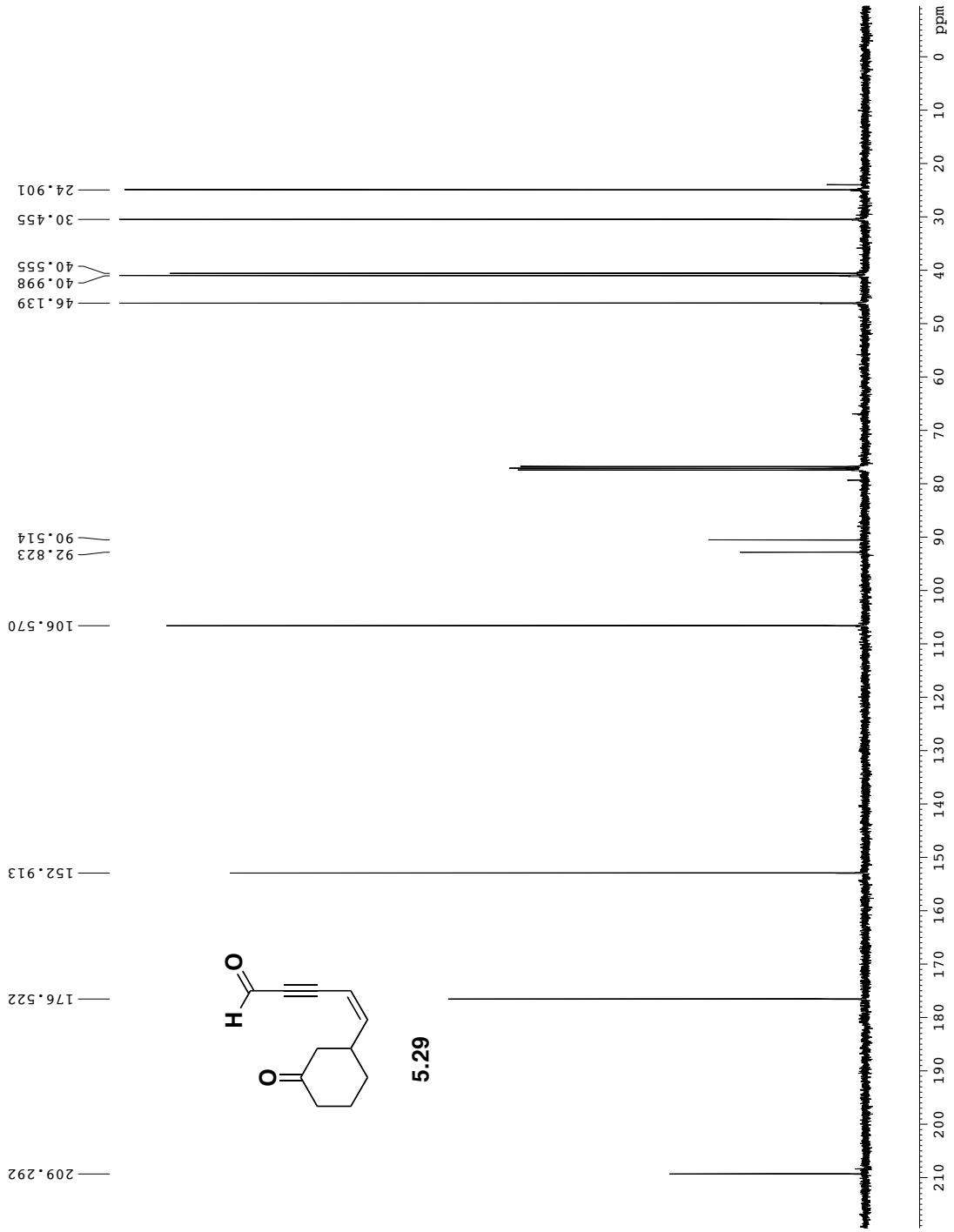
209.292
176.522
152.913
106.570
92.823
90.514
46.139
40.998
40.555
30.455
24.901
5.29
O
H
O
0 10 20 30 40 50 60 70 80 90 100 110 120 130 140 150 160 170 180 190 200 210 ppm

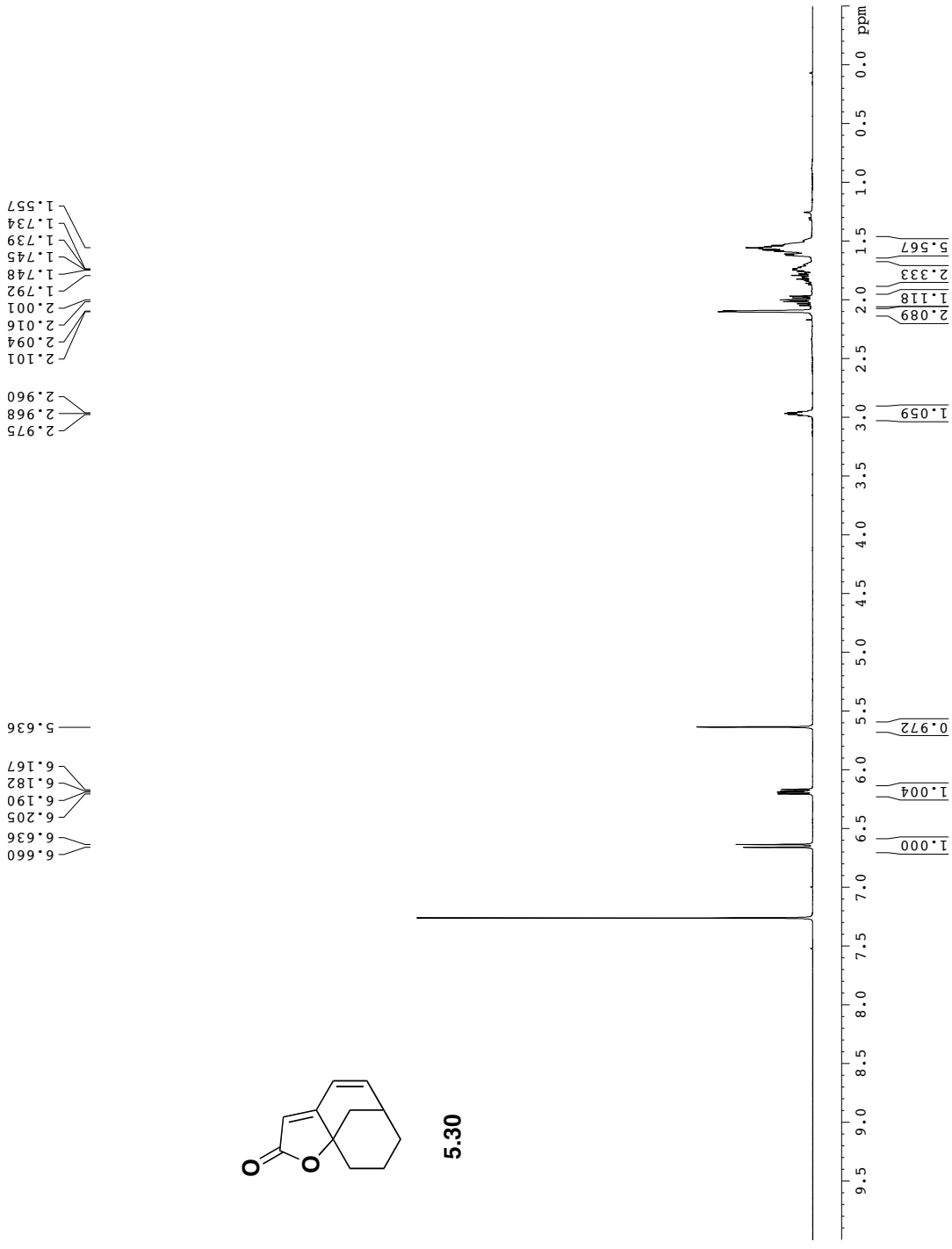
5.30
O
O
6.660
6.636
6.205
6.190
6.182
6.167
5.636
2.975
2.968
2.960
2.101
2.094
2.016
2.001
1.792
1.748
1.745
1.739
1.734
1.557
1.000
1.004
0.972
1.059
2.089
1.118
2.333
5.567
ppm

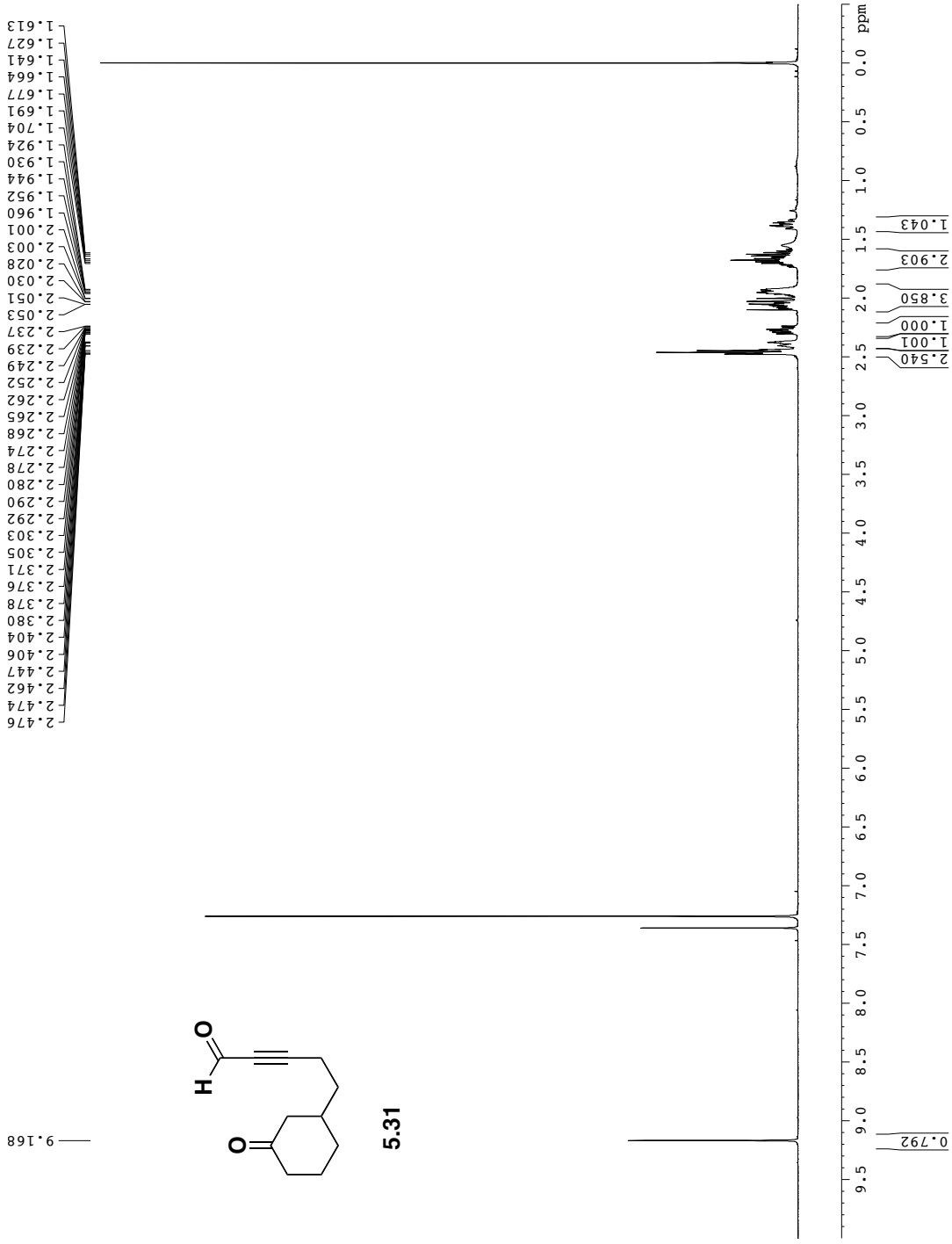
9.168
2.476
2.474
2.462
2.447
2.406
2.404
2.380
2.378
2.376
2.371
2.305
2.303
2.292
2.290
2.280
2.278
2.274
2.268
2.265
2.262
2.252
2.249
2.239
2.237
2.053
2.051
2.030
2.028
2.003
2.001
1.960
1.952
1.944
1.930
1.924
1.704
1.691
1.677
1.664
1.641
1.627
1.613
0.792
1.043
2.903
3.850
1.000
1.001
2.540
ppm
0.0
0.5
1.0
1.5
2.0
2.5
3.0
3.5
4.0
4.5
5.0
5.5
6.0
6.5
7.0
7.5
8.0
8.5
9.0
9.5
O
H
O
5.31

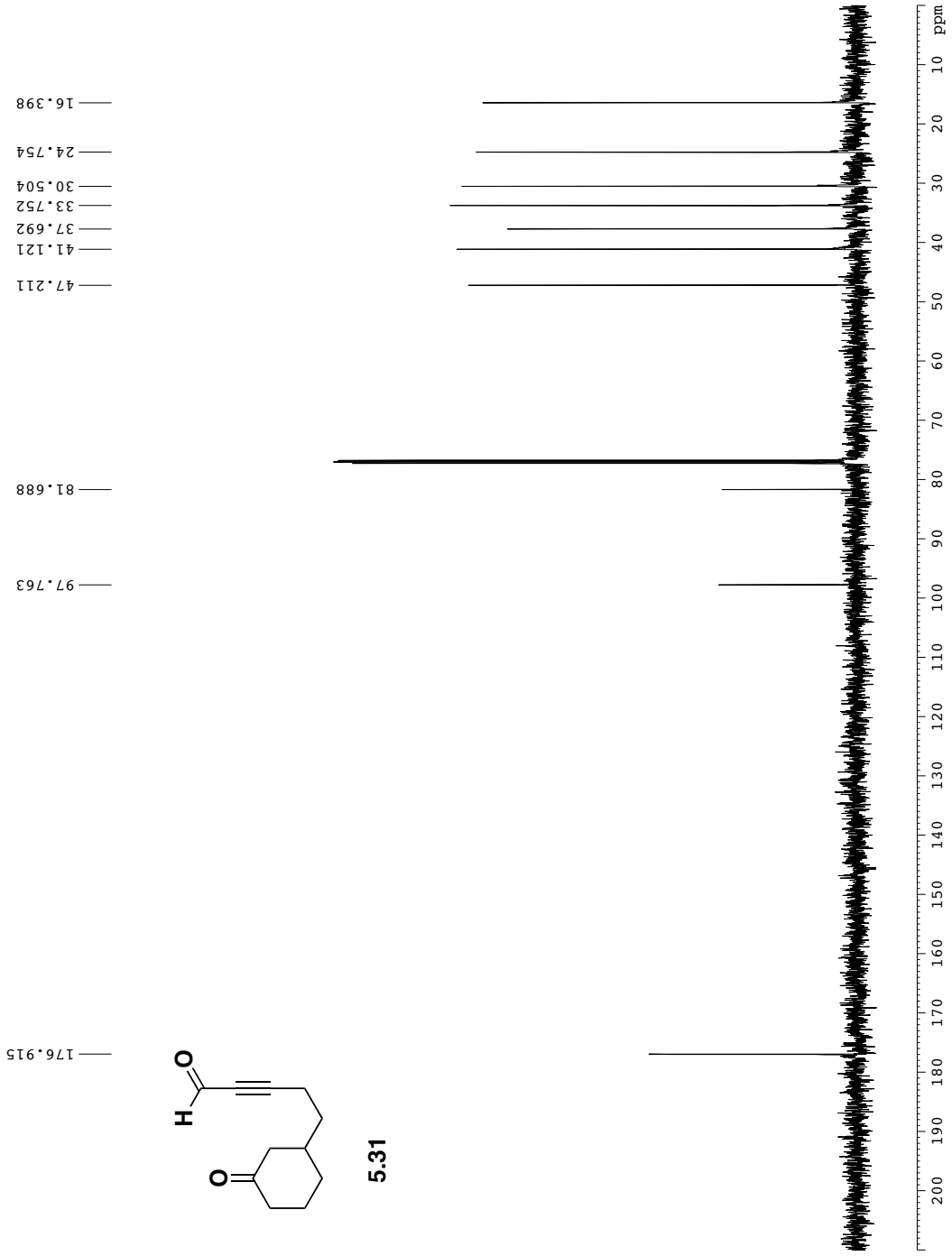
176.915
97.763
81.688
47.211
41.121
37.692
33.752
30.504
24.754
16.398
ppm
10
20
30
40
50
60
70
80
90
100
110
120
130
140
150
160
170
180
190
200
O
H
O
5.31

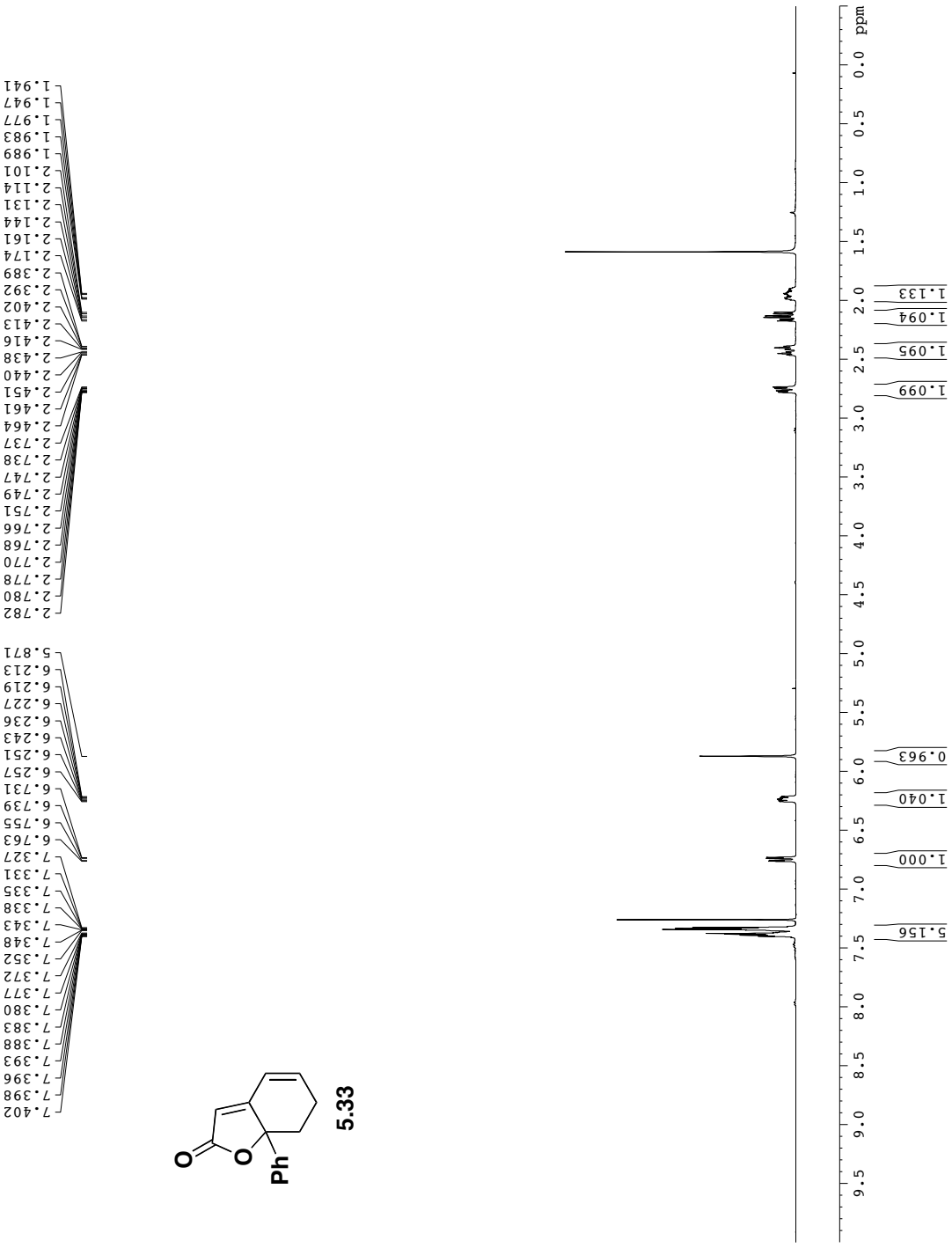
7.402
7.398
7.396
7.393
7.388
7.383
7.380
7.377
7.372
7.352
7.348
7.343
7.338
7.335
7.331
7.327
6.763
6.755
6.739
6.731
6.257
6.251
6.243
6.236
6.227
6.219
6.213
5.871
2.782
2.780
2.778
2.770
2.768
2.766
2.751
2.749
2.747
2.738
2.737
2.464
2.461
2.451
2.440
2.438
2.416
2.413
2.402
2.392
2.389
2.174
2.161
2.144
2.131
2.114
2.101
1.989
1.983
1.977
1.947
1.941
O
O
Ph
5.33
ppm
9.5
9.0
8.5
8.0
7.5
7.0
6.5
6.0
5.5
5.0
4.5
4.0
3.5
3.0
2.5
2.0
1.5
1.0
0.5
0.0
5.156
1.000
1.040
0.963
1.099
1.095
1.094
1.133

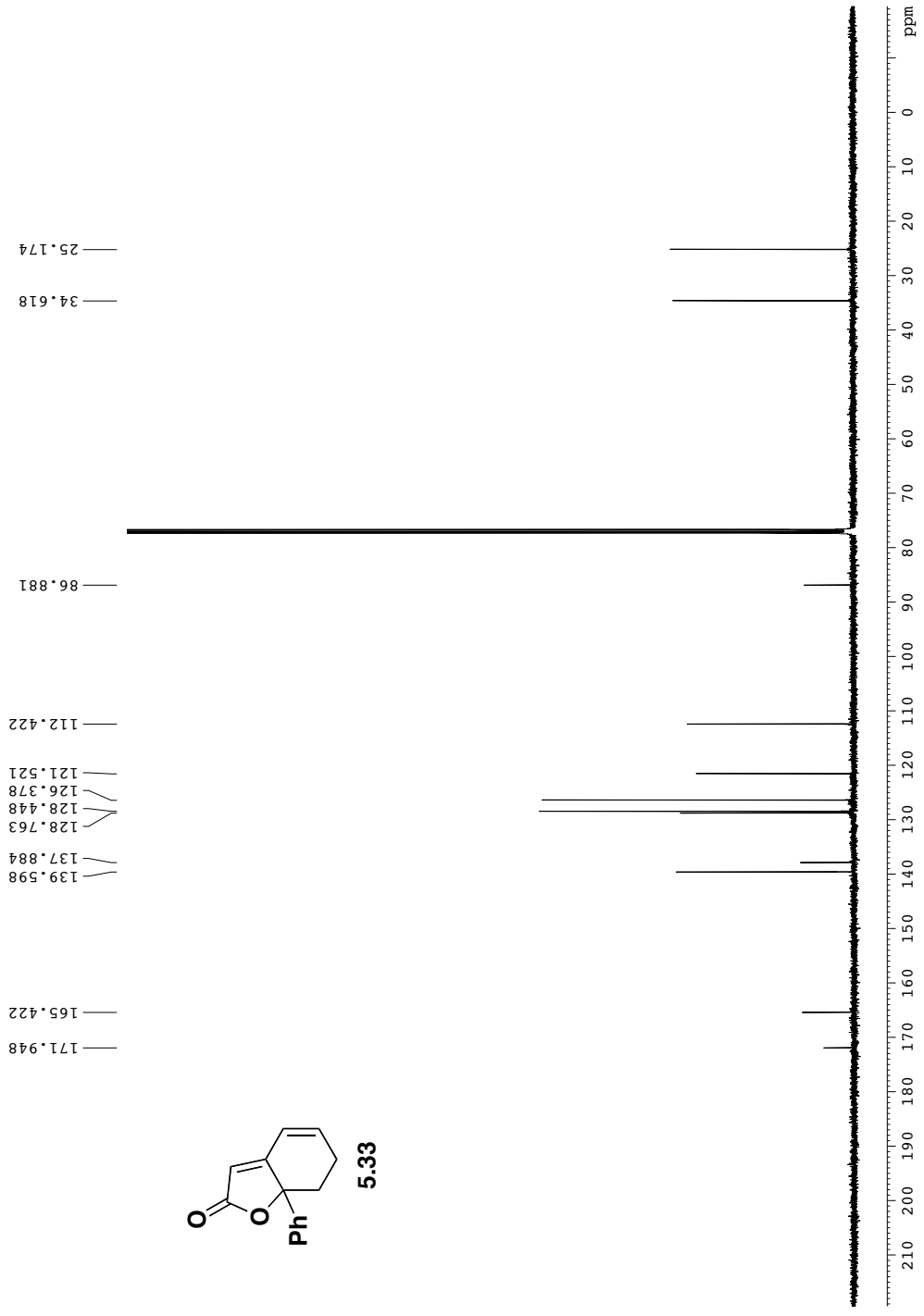
25.174
34.618
86.881
112.422
121.521
126.378
128.448
128.763
137.884
139.598
165.422
171.948
ppm
0
10
20
30
40
50
60
70
80
90
100
110
120
130
140
150
160
170
180
190
200
210
O
O
Ph
5.33

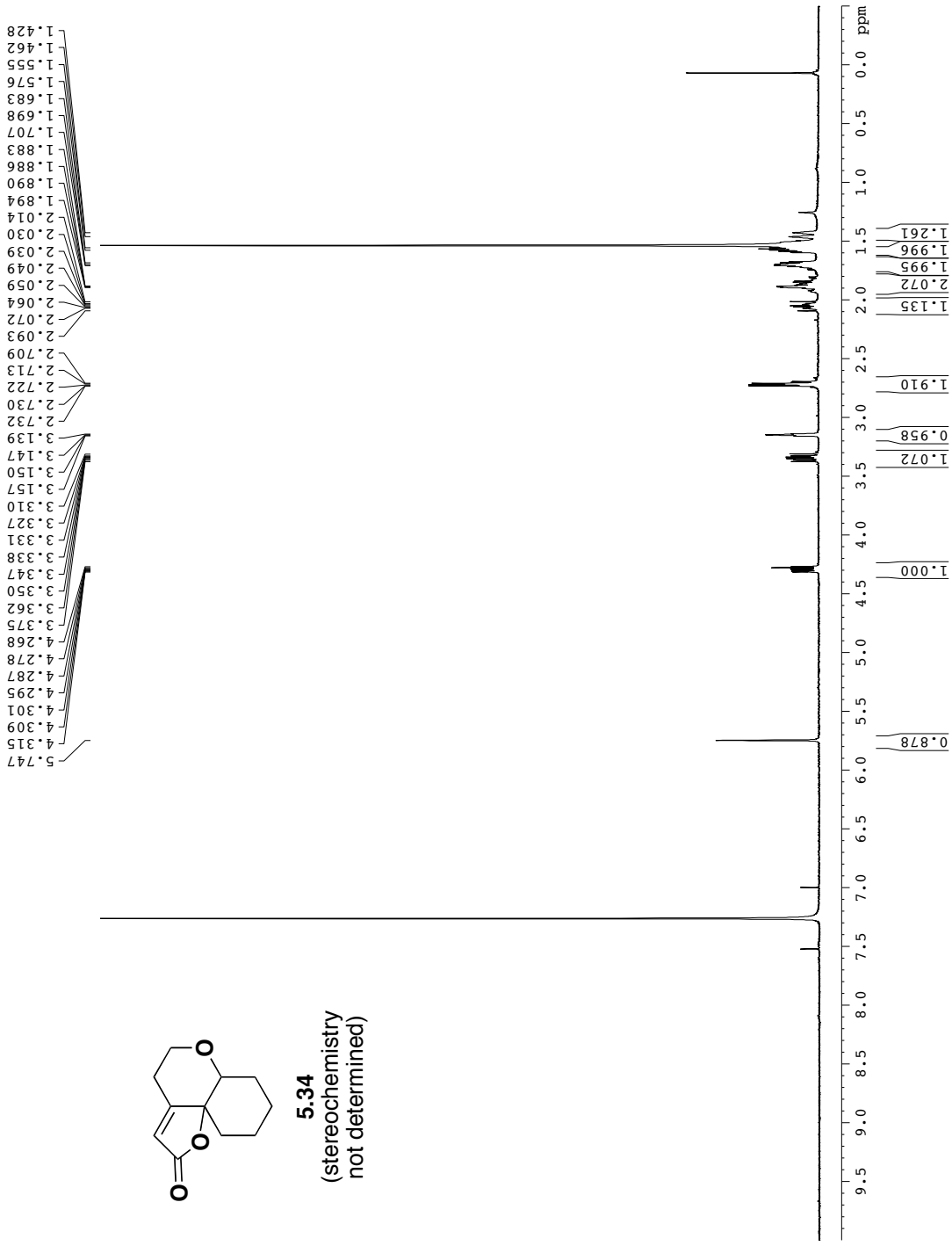

5.34
(stereochemistry not determined)

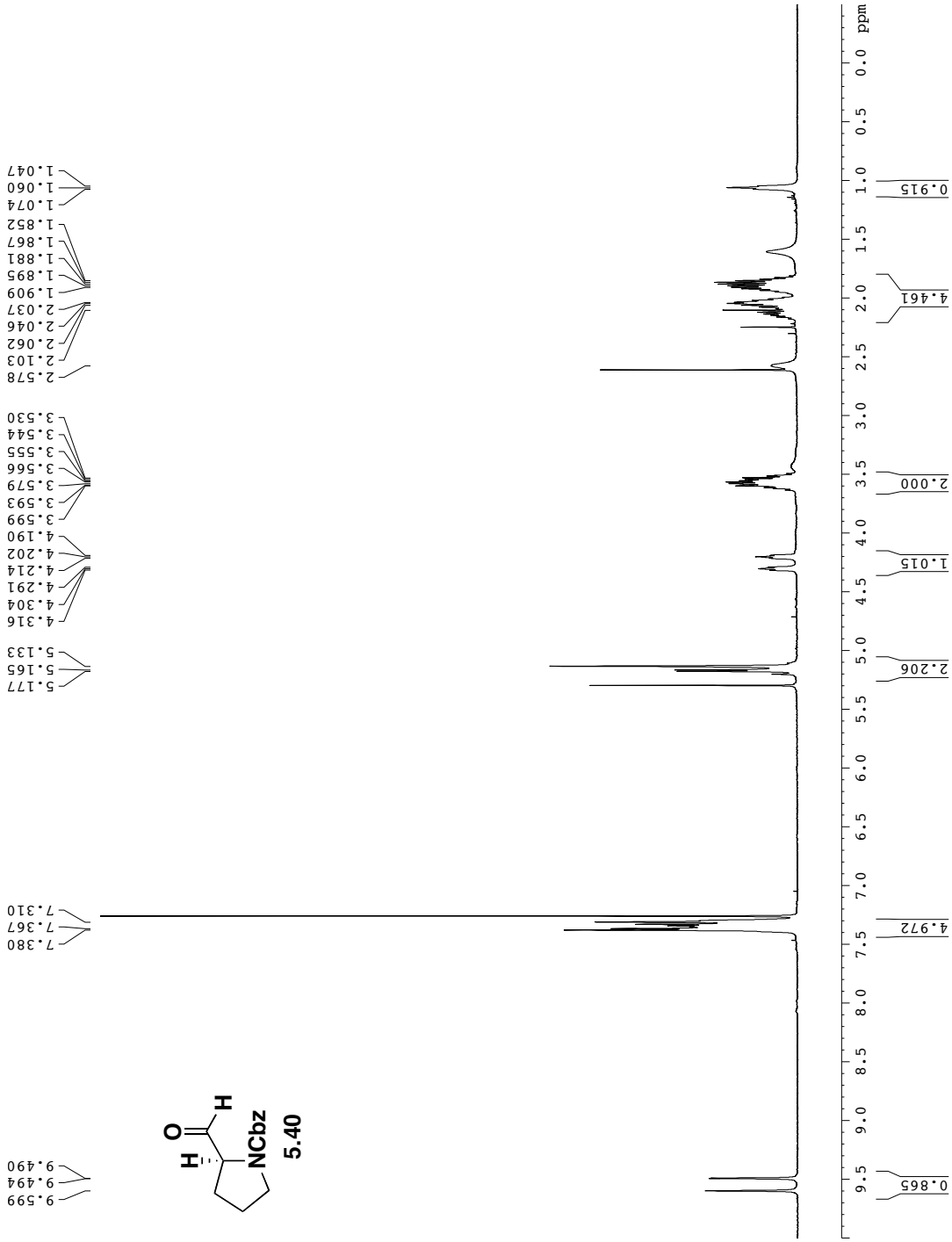
9.599
9.494
9.490
7.380
7.367
7.310
5.177
5.165
5.133
4.316
4.304
4.291
4.214
4.202
4.190
3.599
3.593
3.579
3.566
3.555
3.544
3.530
2.578
2.103
2.062
2.046
2.037
1.909
1.895
1.881
1.867
1.852
1.074
1.060
1.047
O
H
H
NCbz
5.40
0.865
4.972
2.206
1.015
2.000
4.461
0.915
ppm

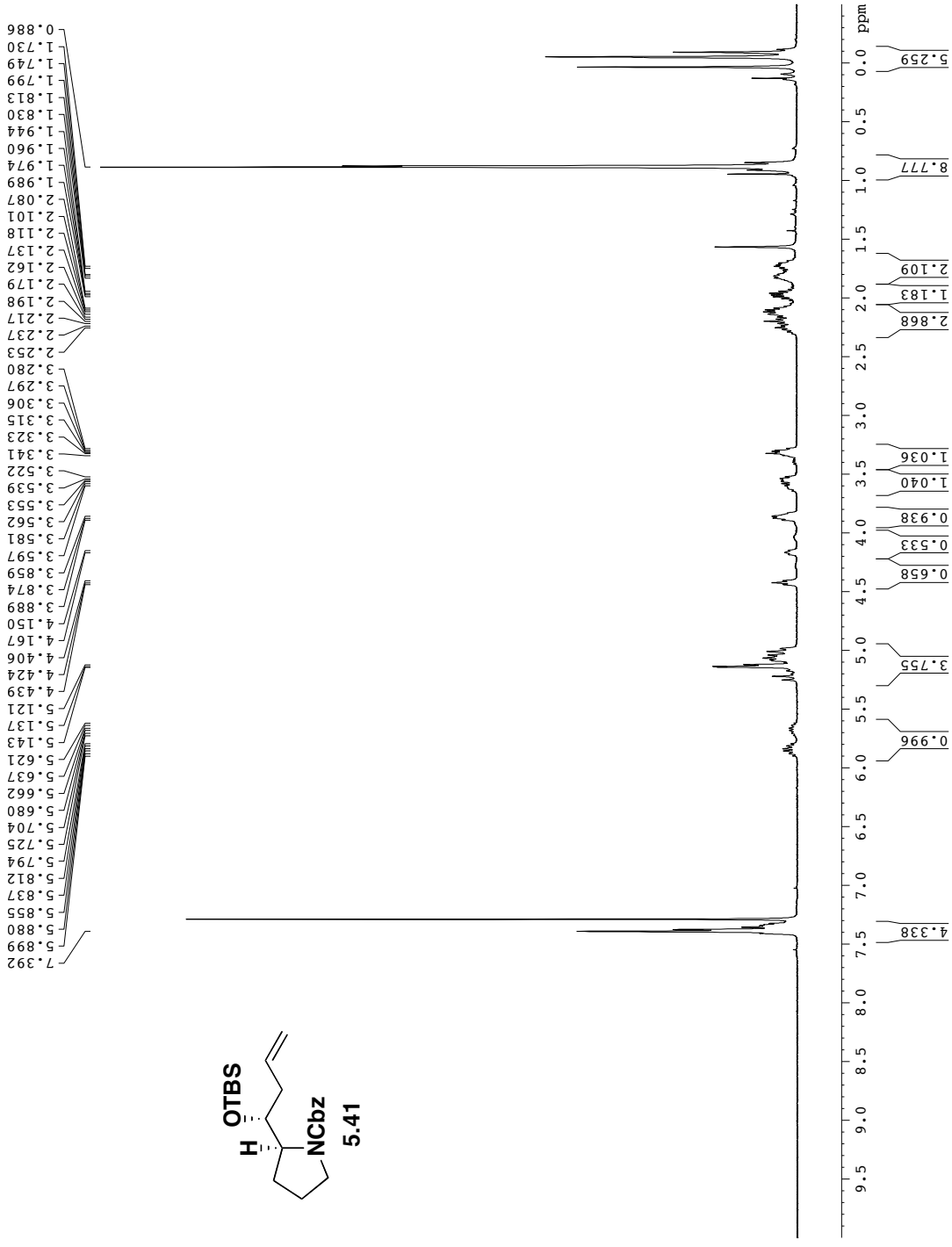
OTBS
H
NCbz
5.41
ppm
5.259
8.777
2.868
1.183
2.109
1.036
1.040
0.938
0.533
0.658
3.755
0.996
4.338

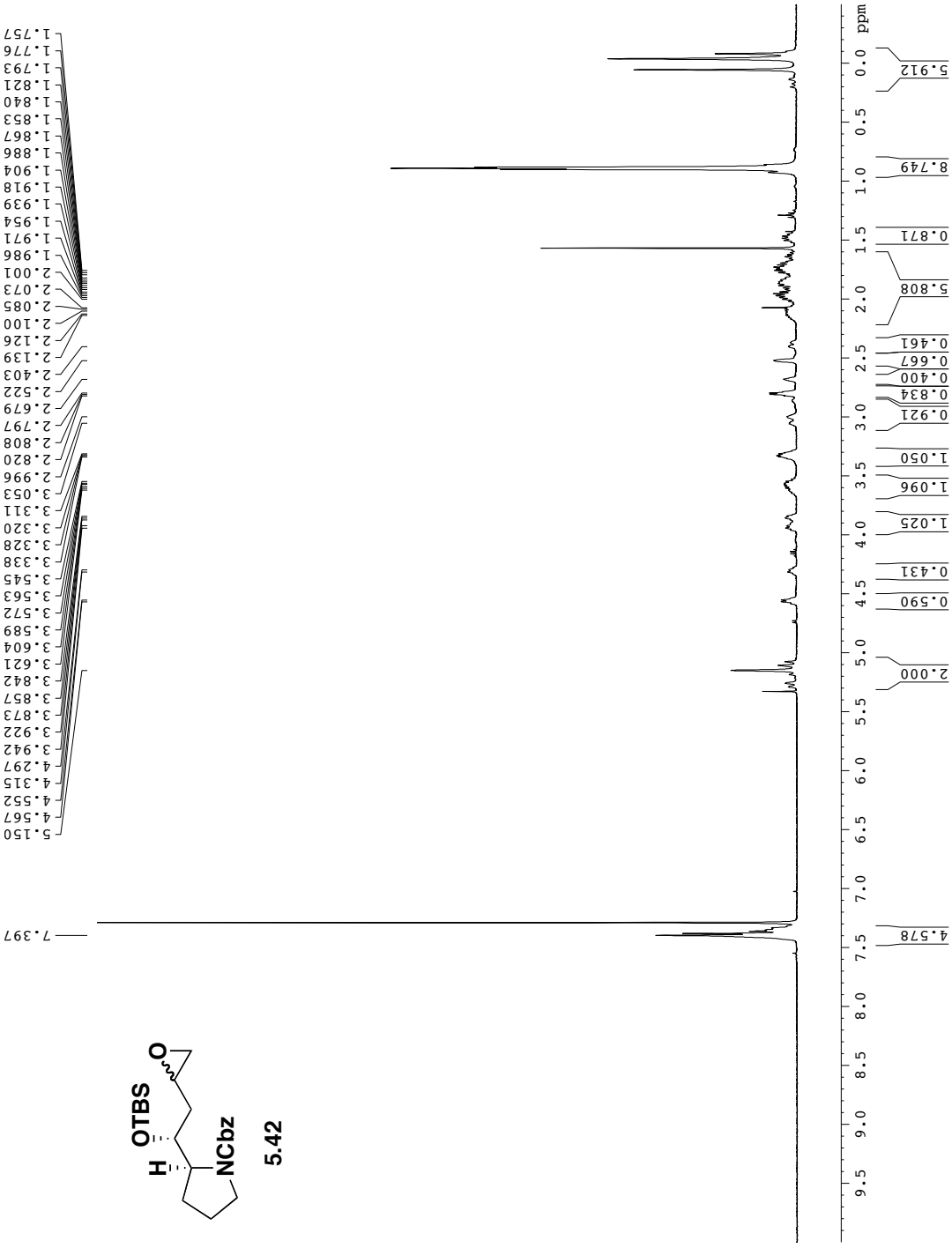
OTBS
H
O
NCbz
5.42
ppm
4.578
2.000
0.590
0.431
1.025
1.096
1.050
0.921
0.834
0.400
0.667
0.461
5.808
0.871
8.749
5.912
7.397

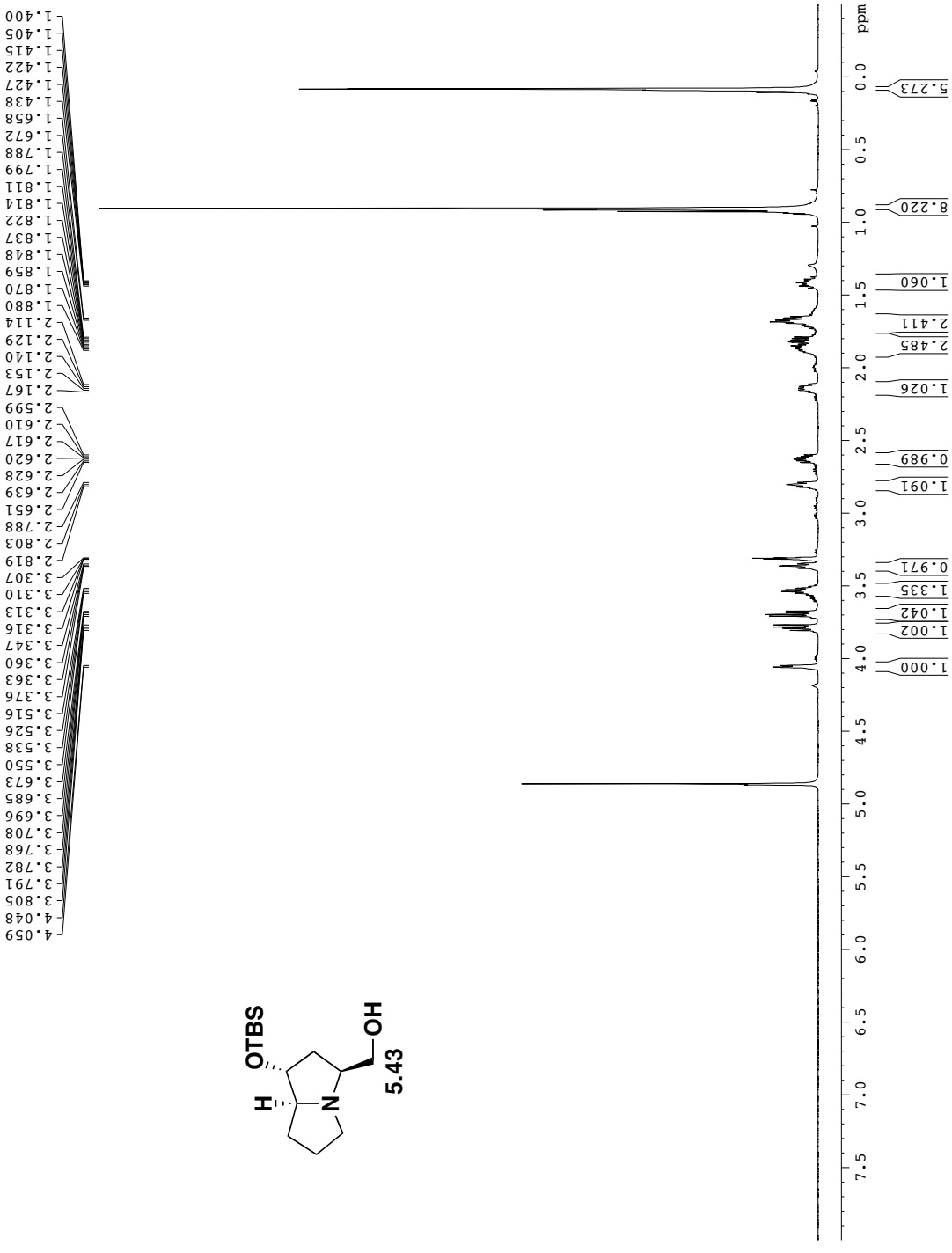
OTBS
H
N
OH
5.43
ppm
0.0
0.5
1.0
1.5
2.0
2.5
3.0
3.5
4.0
4.5
5.0
5.5
6.0
6.5
7.0
7.5
5.273
8.220
1.060
2.411
2.485
1.026
0.989
1.091
0.971
1.335
1.042
1.002
1.000
4.059
4.048
3.805
3.791
3.782
3.768
3.708
3.696
3.685
3.673
3.550
3.538
3.526
3.516
3.376
3.363
3.360
3.347
3.316
3.313
3.310
3.307
2.819
2.803
2.788
2.651
2.639
2.628
2.620
2.617
2.610
2.599
2.167
2.153
2.140
2.129
2.114
1.880
1.870
1.859
1.848
1.837
1.822
1.814
1.811
1.799
1.788
1.672
1.658
1.438
1.427
1.422
1.415
1.405
1.400

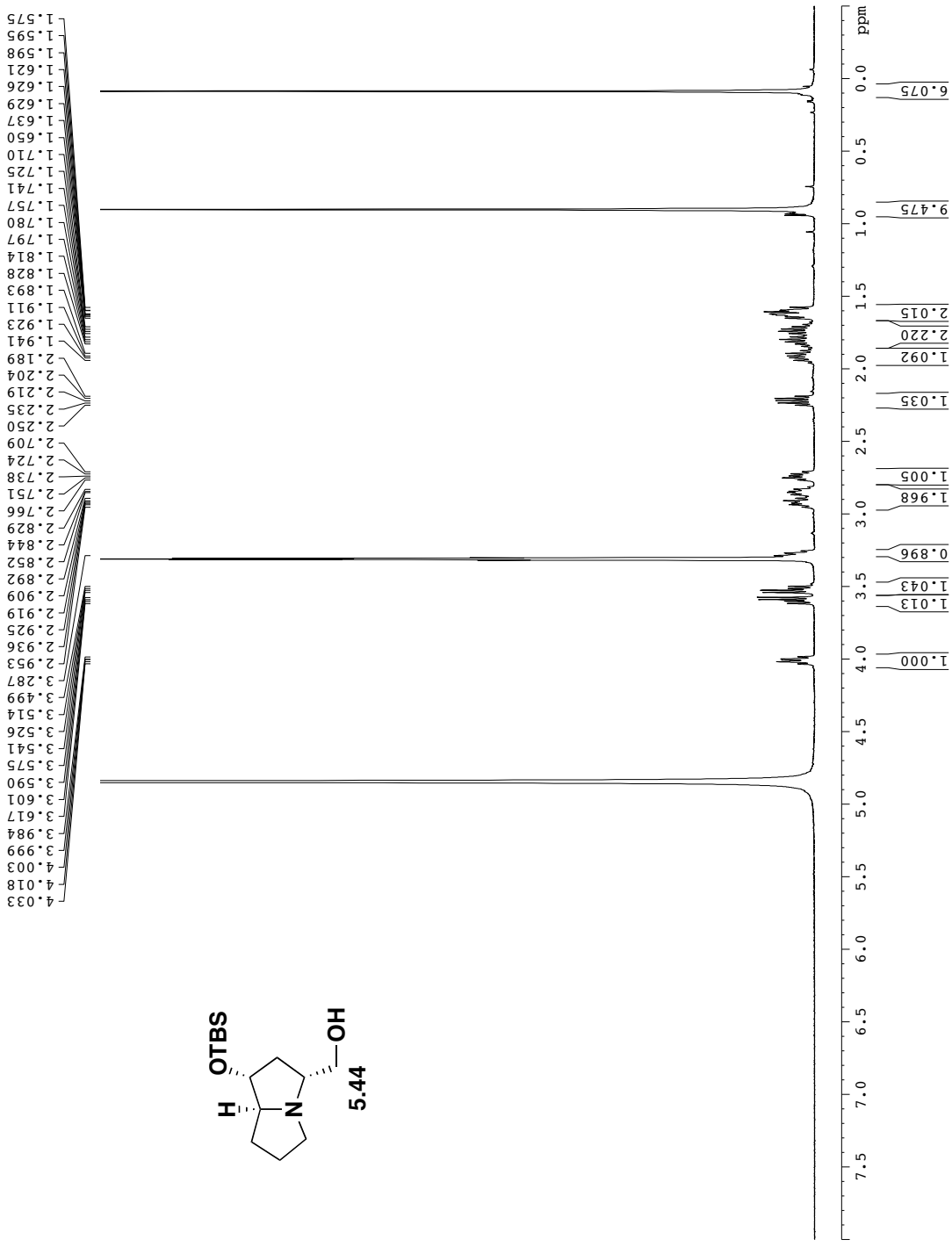
OTBS
H
N
OH
5.44
ppm
6.075
9.475
2.015
2.220
1.092
1.035
1.005
1.968
0.896
1.043
1.013
1.000

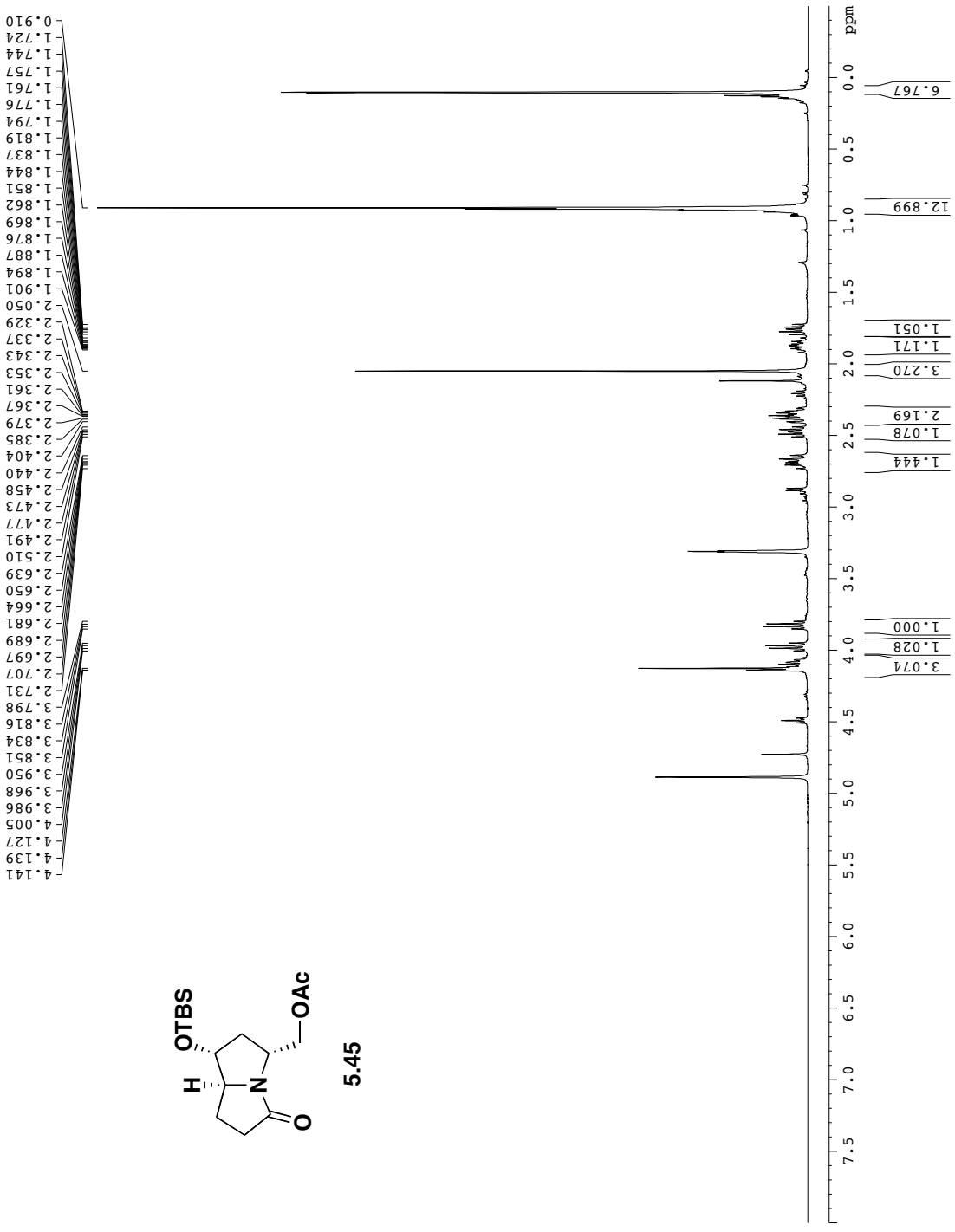
OTBS
OAc
H
N
O
5.45
ppm
6.767
12.899
1.051
1.171
3.270
2.169
1.078
1.444
1.000
1.028
3.074

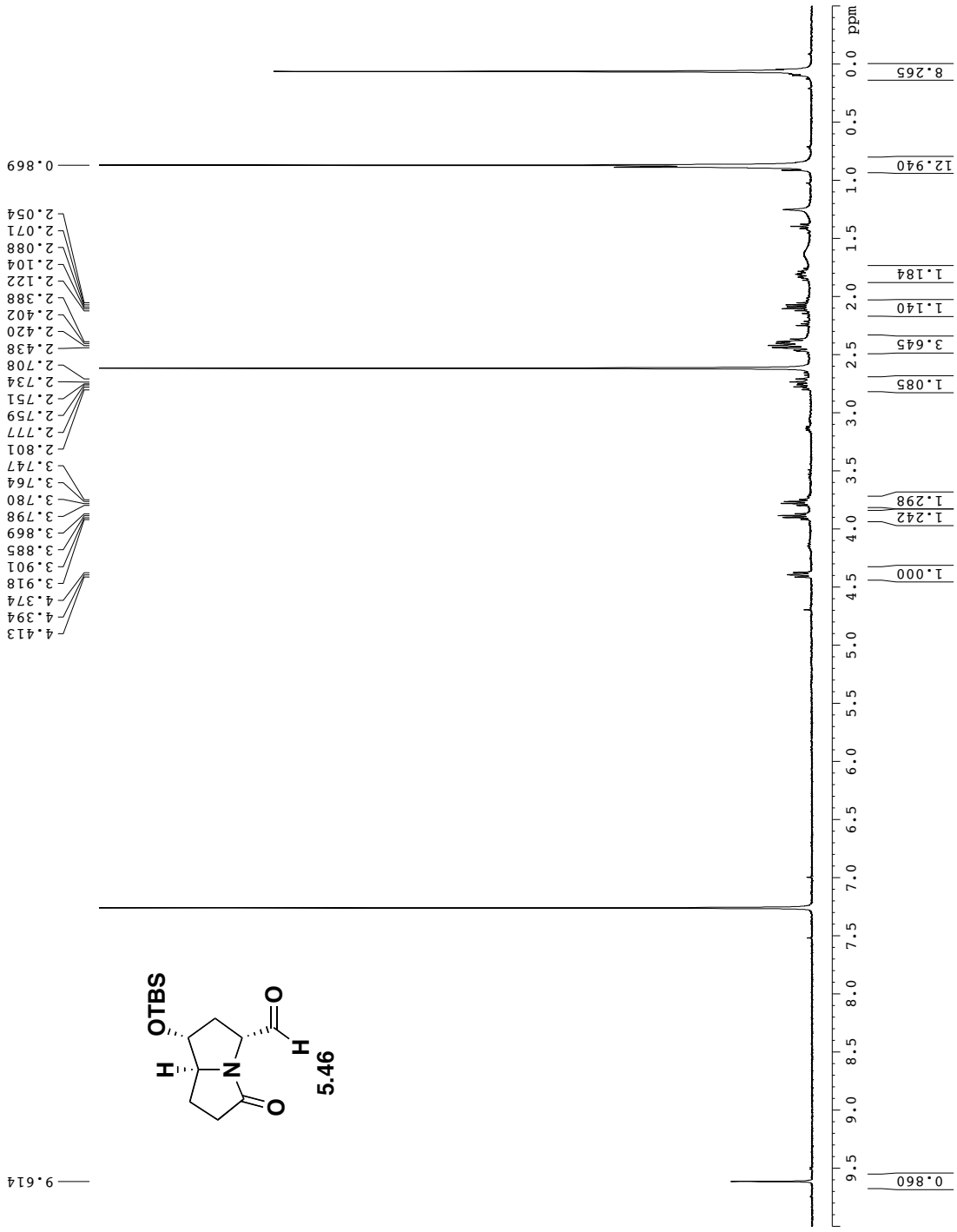
OTBS
H
N
O
O
H
5.46
ppm
0.0
0.5
1.0
1.5
2.0
2.5
3.0
3.5
4.0
4.5
5.0
5.5
6.0
6.5
7.0
7.5
8.0
8.5
9.0
9.5
8.265
12.940
1.184
1.140
3.645
1.085
1.298
1.242
1.000
0.860
0.869
2.054
2.071
2.088
2.104
2.122
2.388
2.402
2.420
2.438
2.708
2.734
2.751
2.759
2.777
2.801
3.747
3.764
3.780
3.798
3.869
3.885
3.901
3.918
4.374
4.394
4.413
9.614

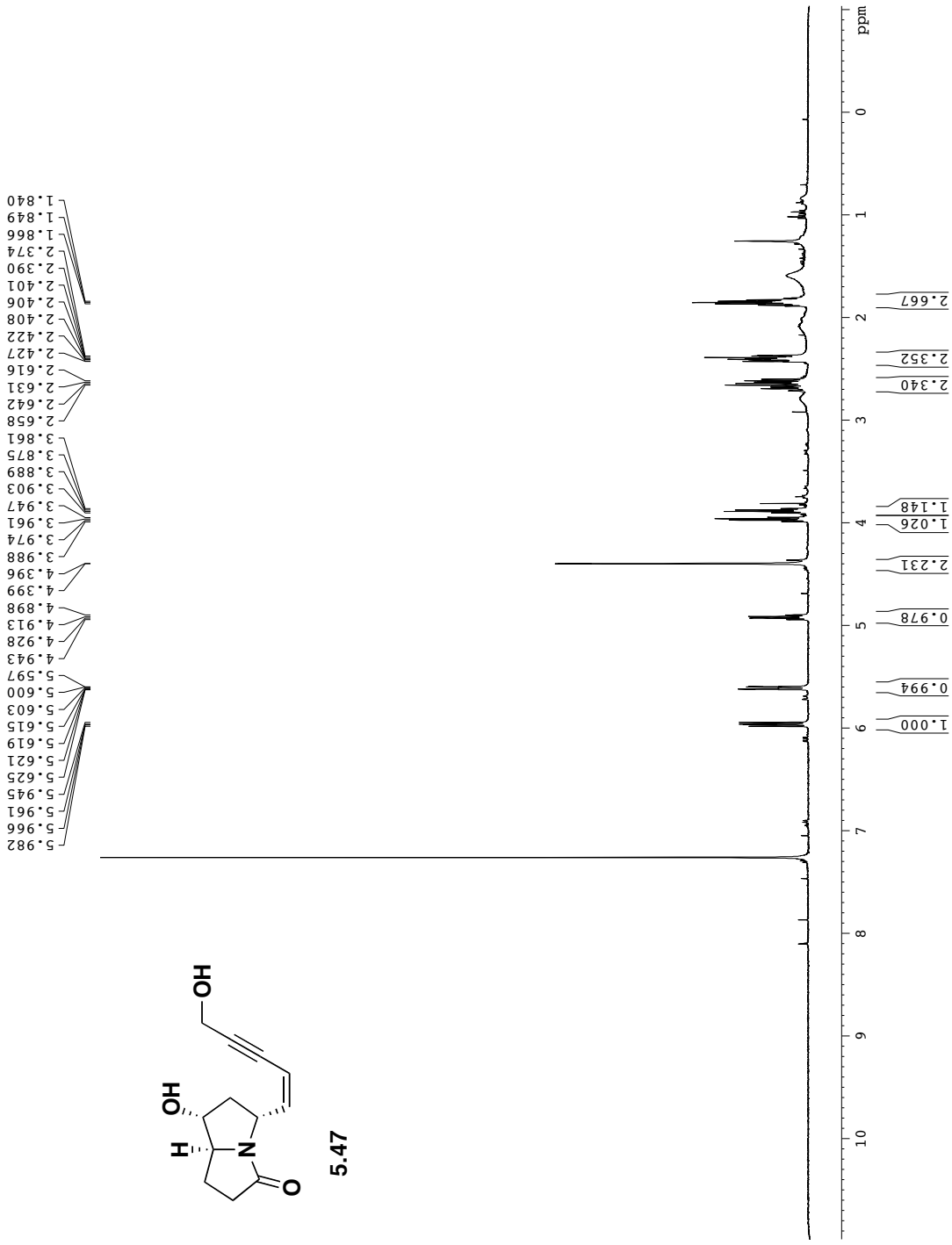
OH
OH
H
N
O
5.47
5.982
5.966
5.961
5.945
5.625
5.621
5.619
5.615
5.603
5.600
5.597
4.943
4.928
4.913
4.898
4.399
4.396
3.988
3.974
3.961
3.947
3.903
3.889
3.875
3.861
2.658
2.642
2.631
2.616
2.427
2.422
2.408
2.406
2.401
2.390
2.374
1.866
1.849
1.840
2.667
2.352
2.340
1.148
1.026
2.231
0.978
0.994
1.000
ppm

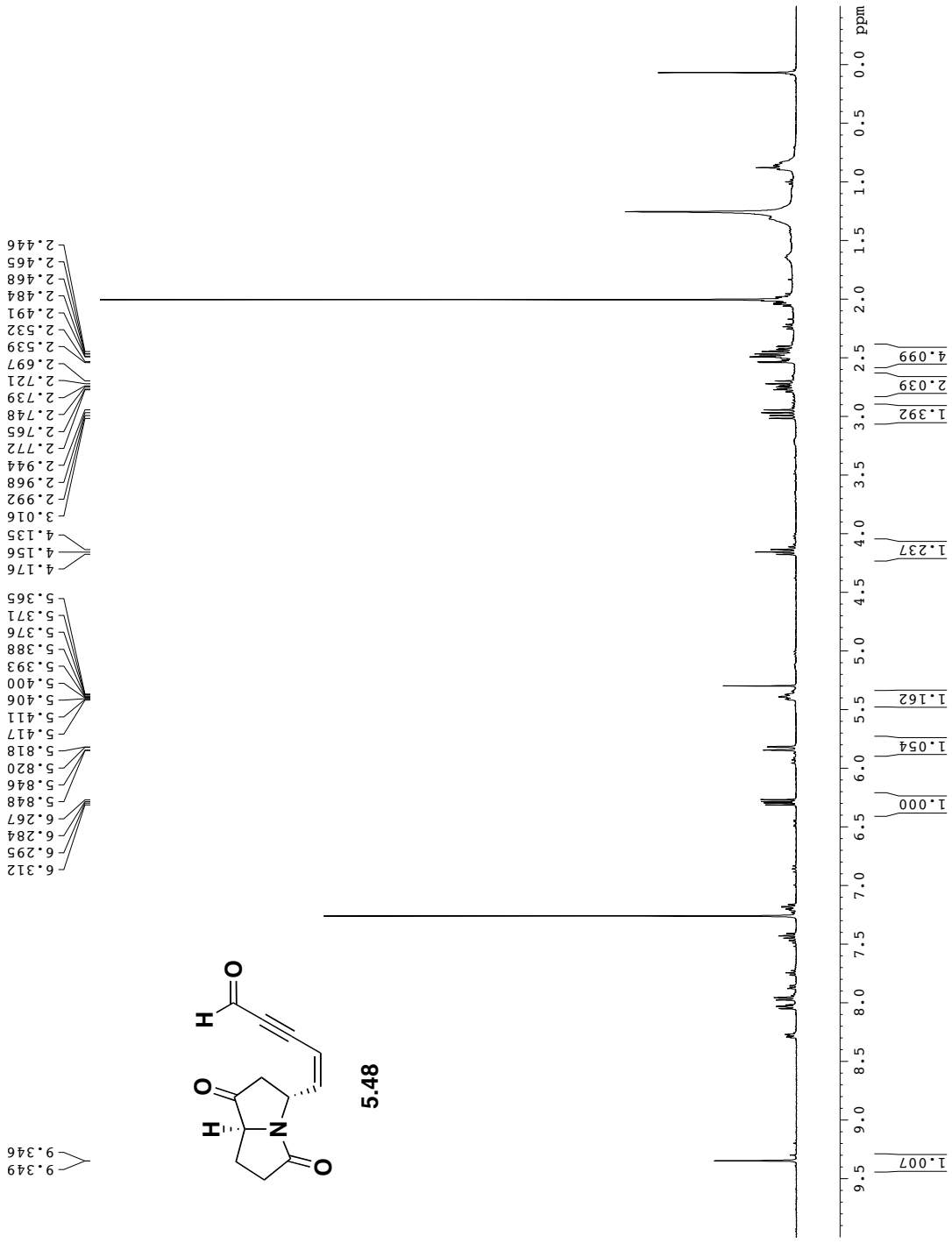
9.349
9.346
6.312
6.295
6.284
6.267
5.848
5.846
5.820
5.818
5.417
5.411
5.406
5.400
5.393
5.388
5.376
5.371
5.365
4.176
4.156
4.135
3.016
2.992
2.968
2.944
2.772
2.765
2.748
2.739
2.721
2.697
2.539
2.532
2.491
2.484
2.468
2.465
2.446
5.48
1.007
1.000
1.054
1.162
1.237
1.392
2.039
4.099
ppm

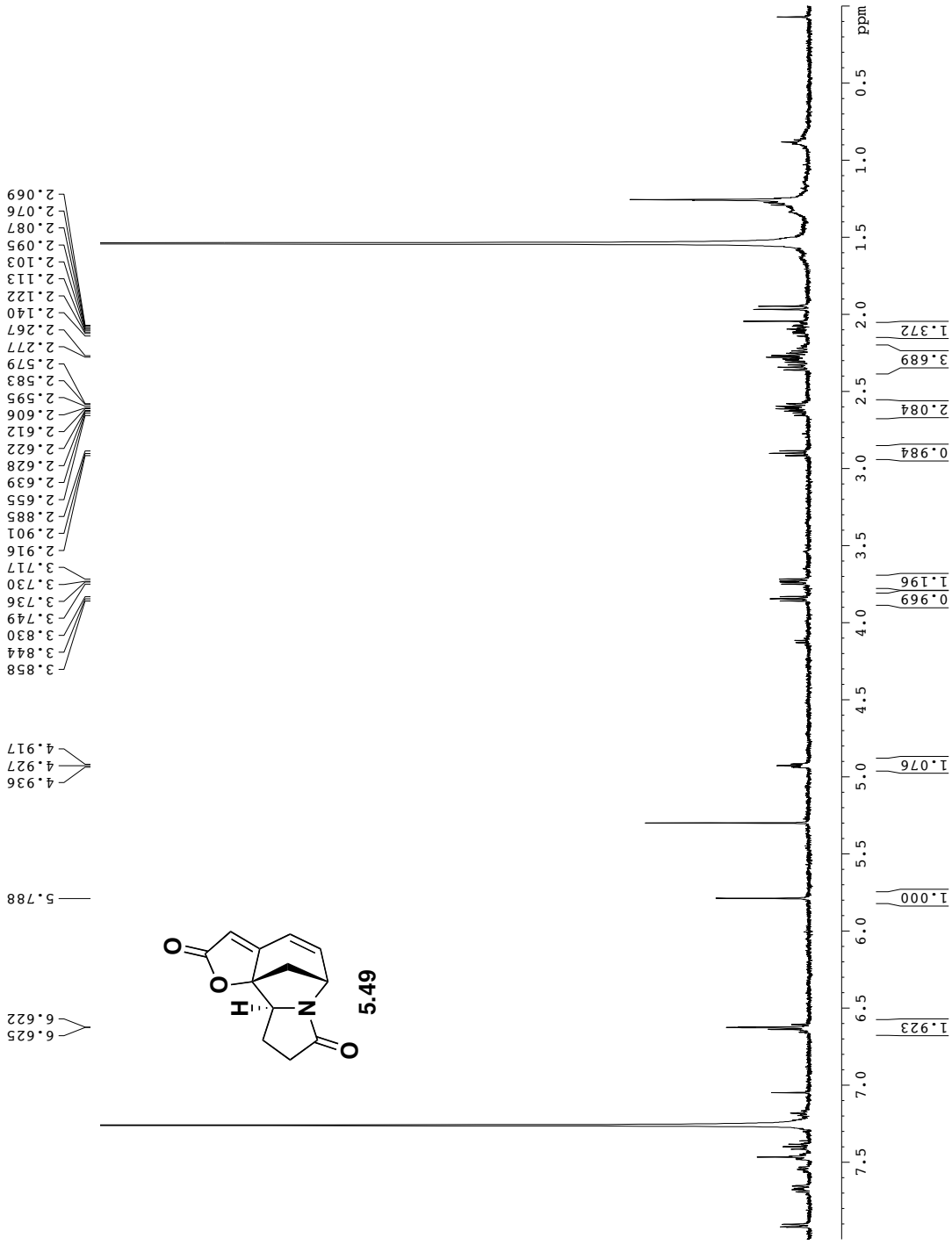
5.49
ppm
0.5
1.0
1.5
2.0
2.5
3.0
3.5
4.0
4.5
5.0
5.5
6.0
6.5
7.0
7.5
1.923
1.000
1.076
0.969
1.196
0.984
2.084
3.689
1.372
6.625
6.622
5.788
4.936
4.927
4.917
3.858
3.844
3.830
3.749
3.736
3.730
3.717
2.916
2.901
2.885
2.655
2.639
2.628
2.622
2.612
2.606
2.595
2.583
2.579
2.277
2.267
2.140
2.122
2.113
2.103
2.095
2.087
2.076
2.069

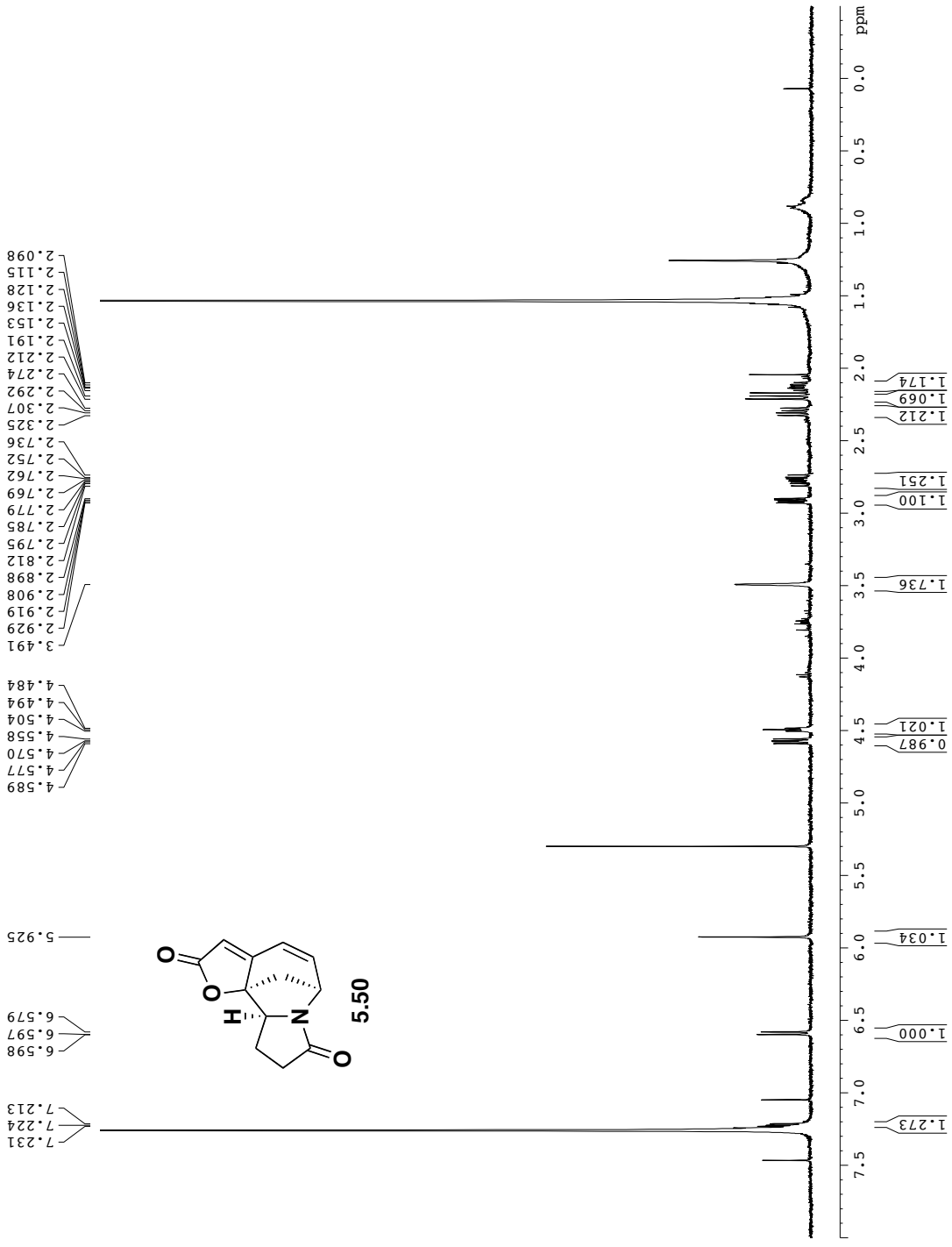
7.231
7.224
7.213
6.598
6.597
6.579
5.925
4.589
4.577
4.570
4.558
4.504
4.494
4.484
3.491
2.929
2.919
2.908
2.898
2.812
2.795
2.785
2.779
2.769
2.762
2.752
2.736
2.325
2.307
2.292
2.274
2.212
2.191
2.153
2.136
2.128
2.115
2.098
5.50
1.273
1.000
1.034
0.987
1.021
1.736
1.100
1.251
1.212
1.069
1.174
ppm

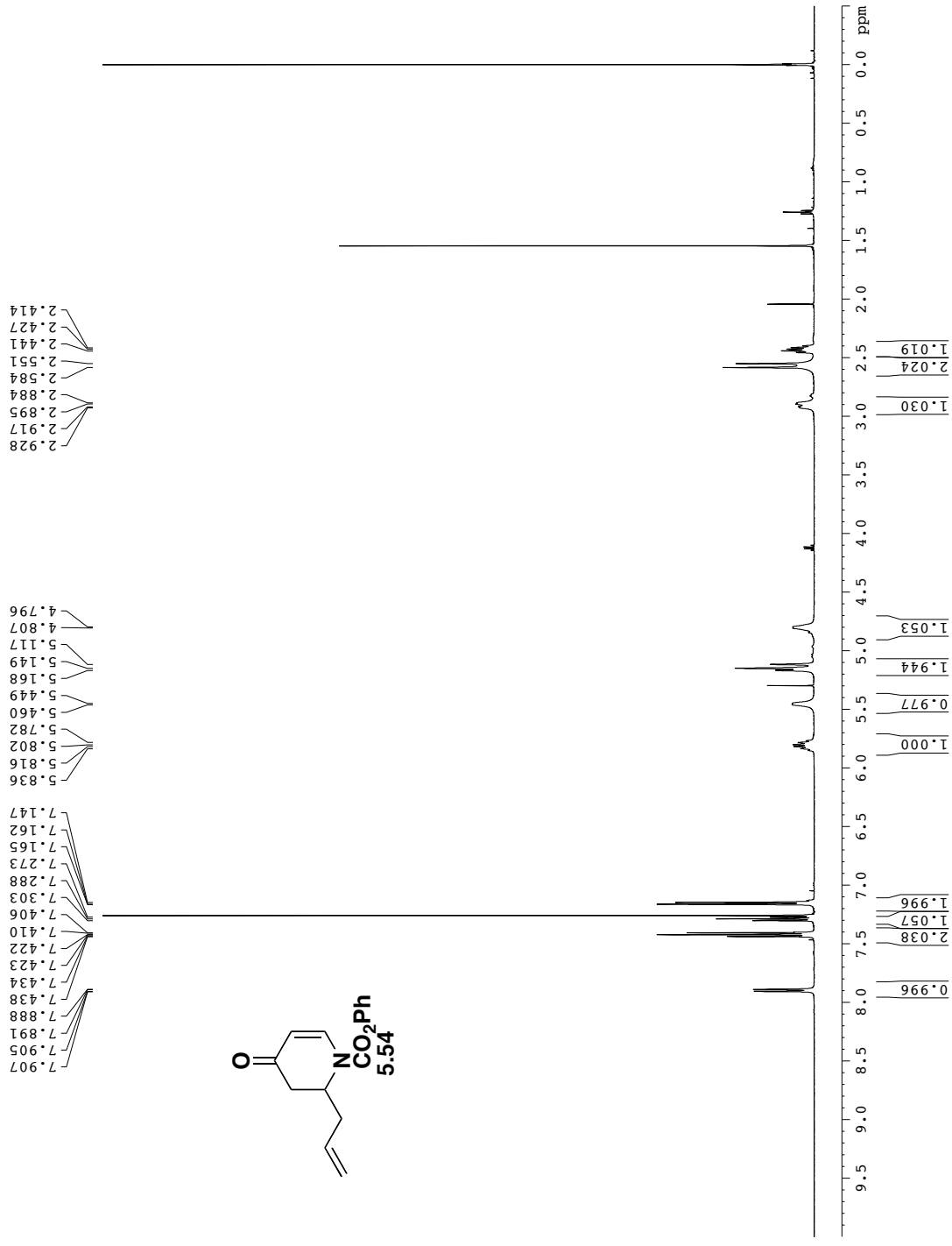
O
N
CO2Ph
5.54
ppm
0.0
0.5
1.0
1.5
2.0
2.5
3.0
3.5
4.0
4.5
5.0
5.5
6.0
6.5
7.0
7.5
8.0
8.5
9.0
9.5
0.996
2.038
1.057
1.996
1.000
0.977
1.944
1.053
1.030
2.024
1.019
7.907
7.905
7.891
7.888
7.438
7.434
7.423
7.422
7.410
7.406
7.303
7.288
7.273
7.165
7.162
7.147
5.836
5.816
5.802
5.782
5.460
5.449
5.168
5.149
5.117
4.807
4.796
2.928
2.917
2.895
2.884
2.584
2.551
2.441
2.427
2.414

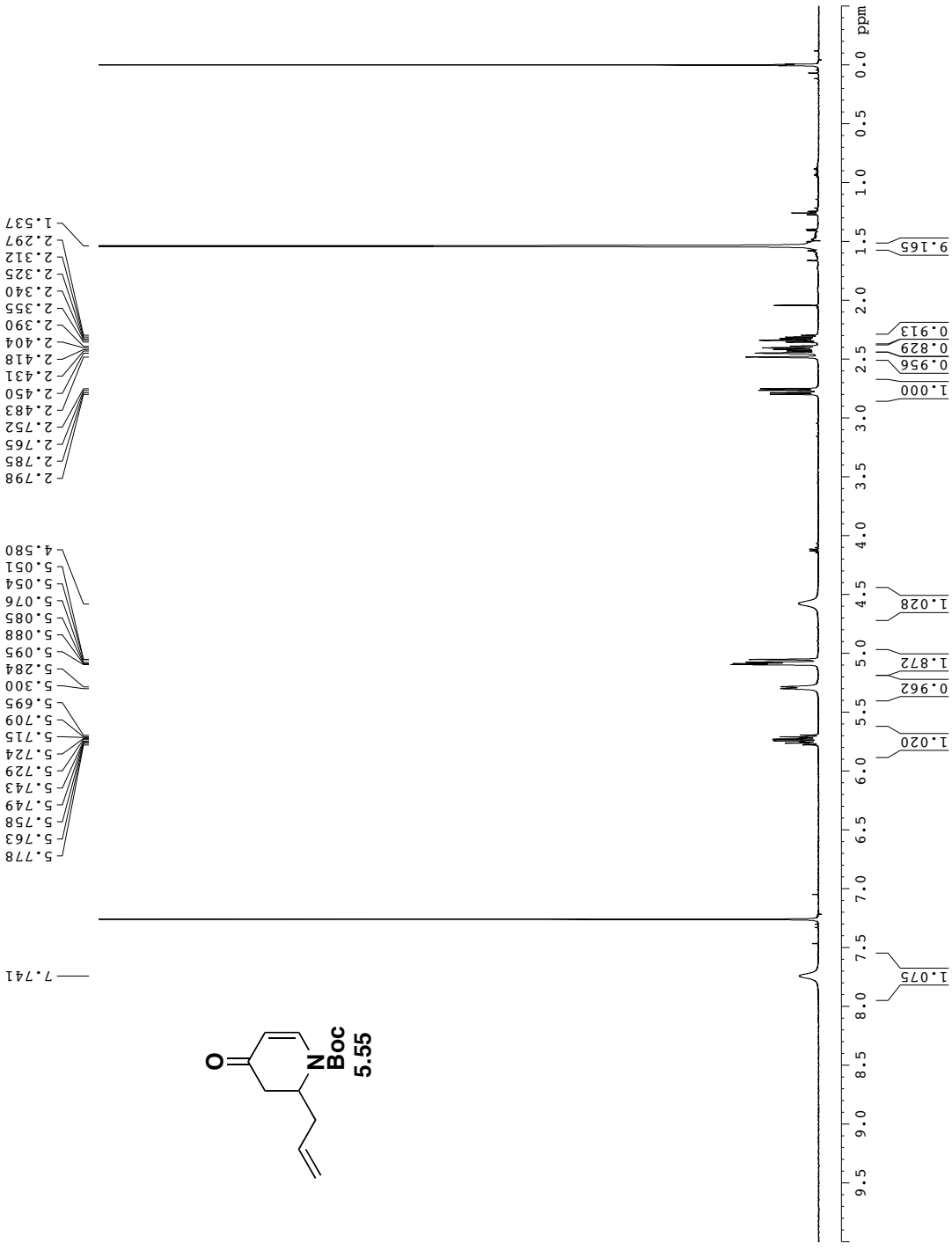
O
N
Boc
5.55
ppm
9.165
0.913
0.829
0.956
1.000
1.028
1.872
0.962
1.020
1.075
1.537
2.297
2.312
2.325
2.340
2.355
2.390
2.404
2.418
2.431
2.450
2.483
2.752
2.765
2.785
2.798
4.580
5.051
5.054
5.076
5.085
5.088
5.095
5.284
5.300
5.695
5.709
5.715
5.724
5.729
5.743
5.749
5.758
5.763
5.778
7.741

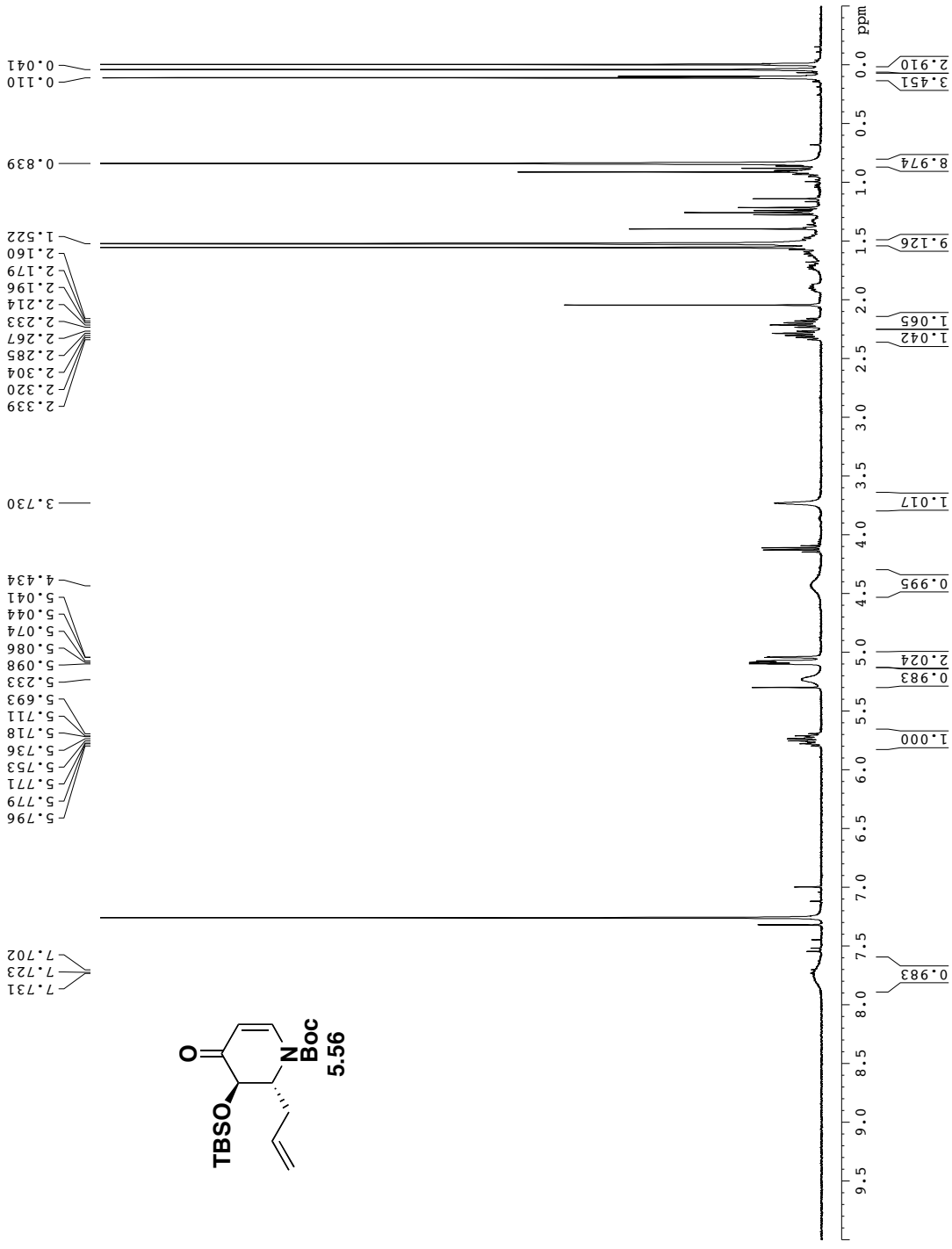
0.041
0.110
0.839
1.522
2.160
2.179
2.196
2.214
2.233
2.267
2.285
2.304
2.320
2.339
3.730
4.434
5.041
5.044
5.074
5.086
5.098
5.233
5.693
5.711
5.718
5.736
5.753
5.771
5.779
5.796
7.702
7.723
7.731
ppm
0.0
0.5
1.0
1.5
2.0
2.5
3.0
3.5
4.0
4.5
5.0
5.5
6.0
6.5
7.0
7.5
8.0
8.5
9.0
9.5
2.910
3.451
8.974
9.126
1.065
1.042
1.017
0.995
0.983
2.024
1.000
0.983
O
N
Boc
TBSO
5.56

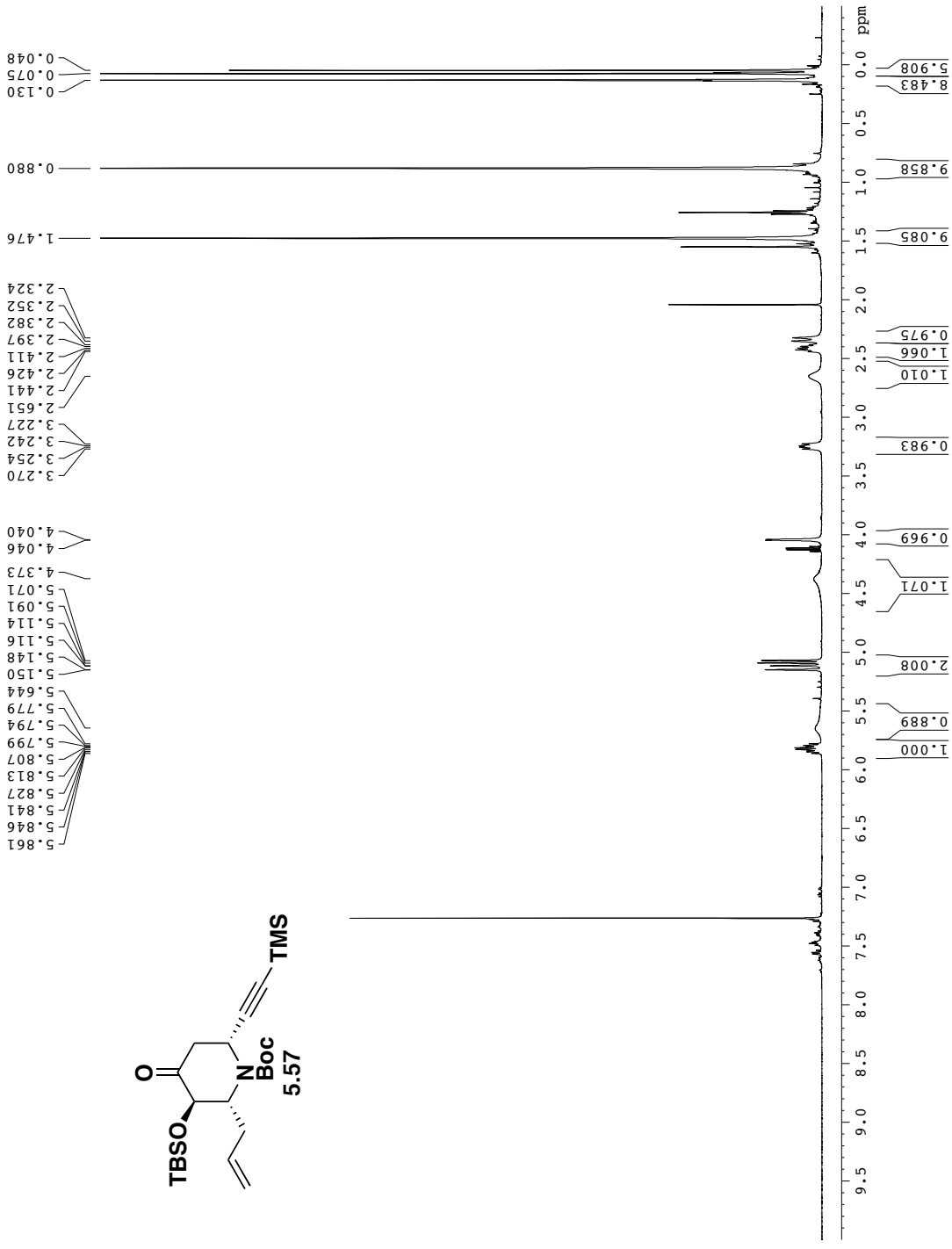
TMS
N
Boc
O
TBSO
5.57
ppm

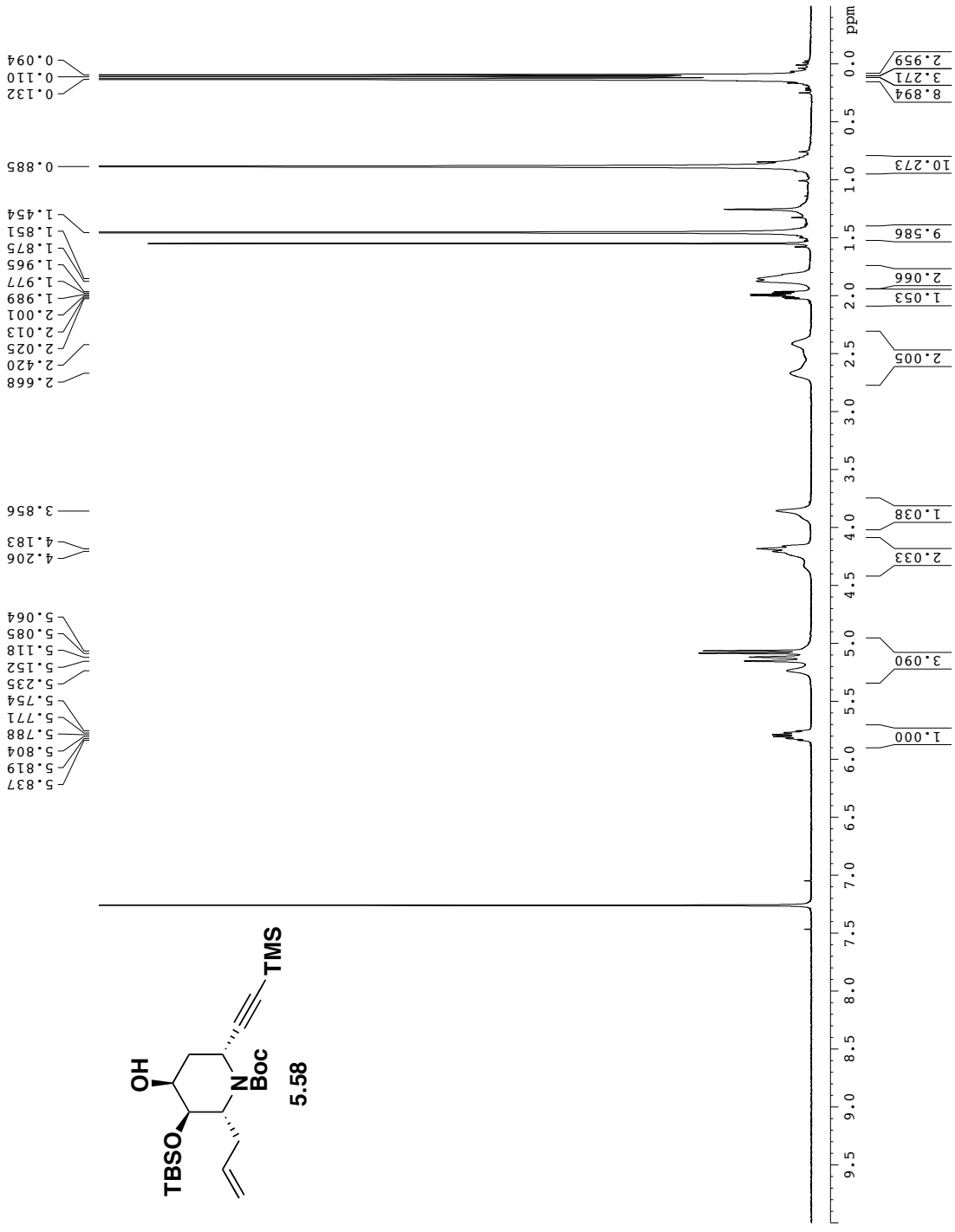
TMS
OH
N
Boc
TBSO
5.58
ppm
0.0
0.5
1.0
1.5
2.0
2.5
3.0
3.5
4.0
4.5
5.0
5.5
6.0
6.5
7.0
7.5
8.0
8.5
9.0
9.5
2.959
3.271
8.894
10.273
9.586
2.066
1.053
2.005
1.038
2.033
3.090
1.000
0.094
0.110
0.132
0.885
1.454
1.851
1.875
1.965
1.977
1.989
2.001
2.013
2.025
2.420
2.668
3.856
4.183
4.206
5.064
5.085
5.118
5.152
5.235
5.754
5.771
5.788
5.804
5.819
5.837

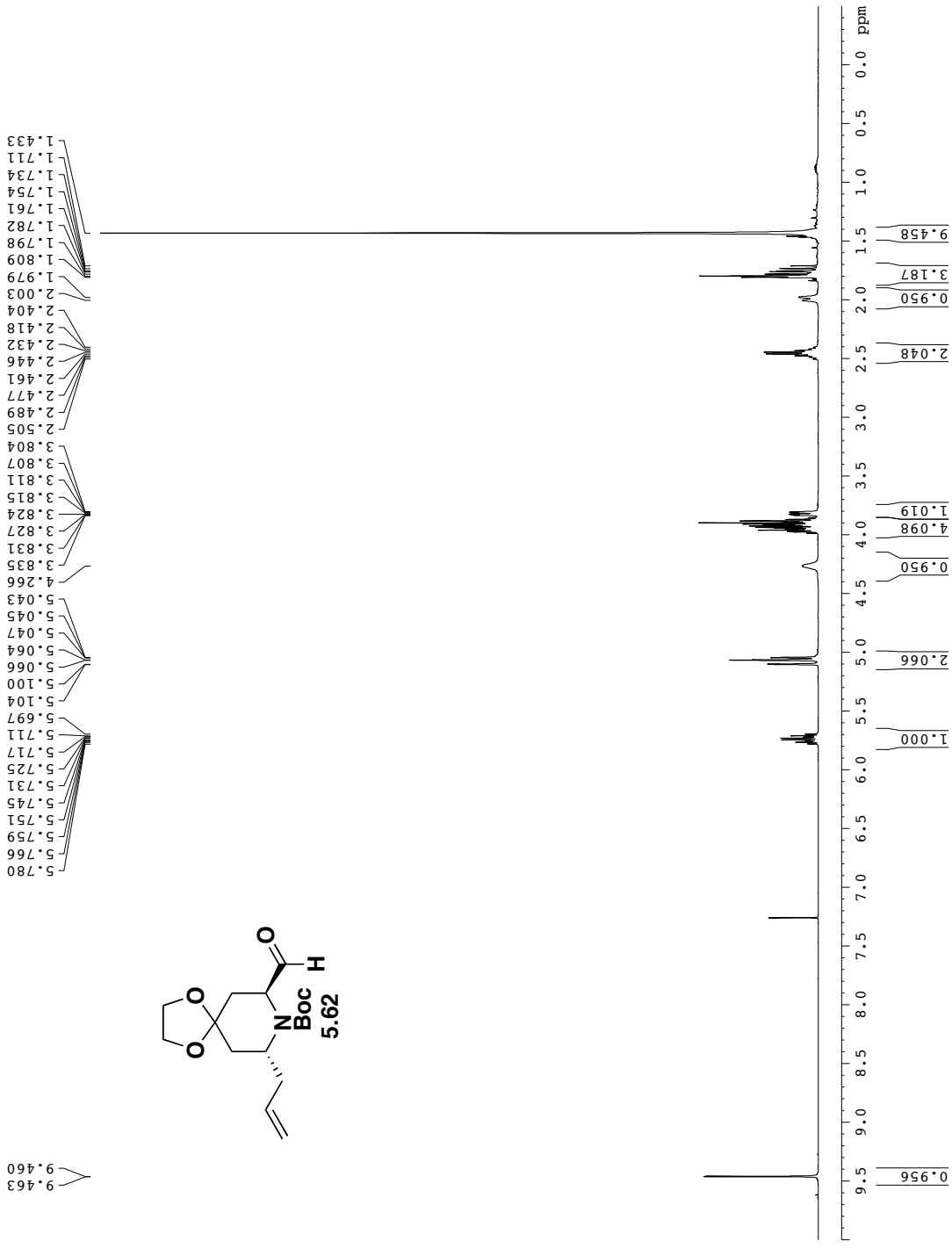
9.463
9.460
5.780
5.766
5.759
5.751
5.745
5.731
5.725
5.717
5.711
5.697
5.104
5.100
5.066
5.064
5.047
5.045
5.043
4.266
3.835
3.831
3.827
3.824
3.815
3.811
3.807
3.804
2.505
2.489
2.477
2.461
2.446
2.432
2.418
2.404
2.003
1.979
1.809
1.798
1.782
1.761
1.754
1.734
1.711
1.433
O
H
N
Boc
O
O
5.62
0.956
9.458
3.187
0.950
2.048
1.019
4.098
0.950
2.066
1.000
ppm

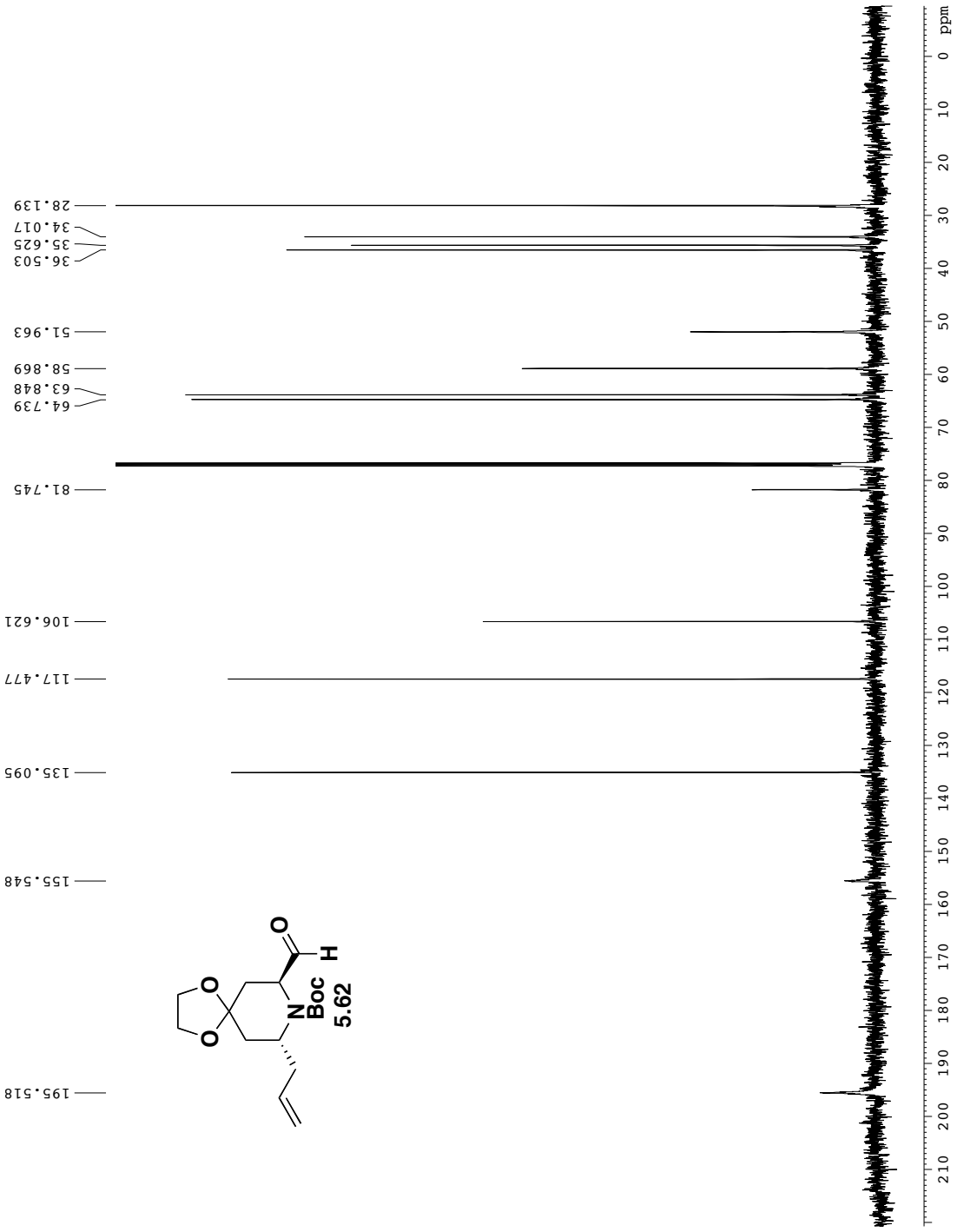
28.139
34.017
35.625
36.503
51.963
58.869
63.848
64.739
81.745
106.621
117.477
135.095
155.548
195.518
O
H
N
Boc
5.62
O
O
ppm

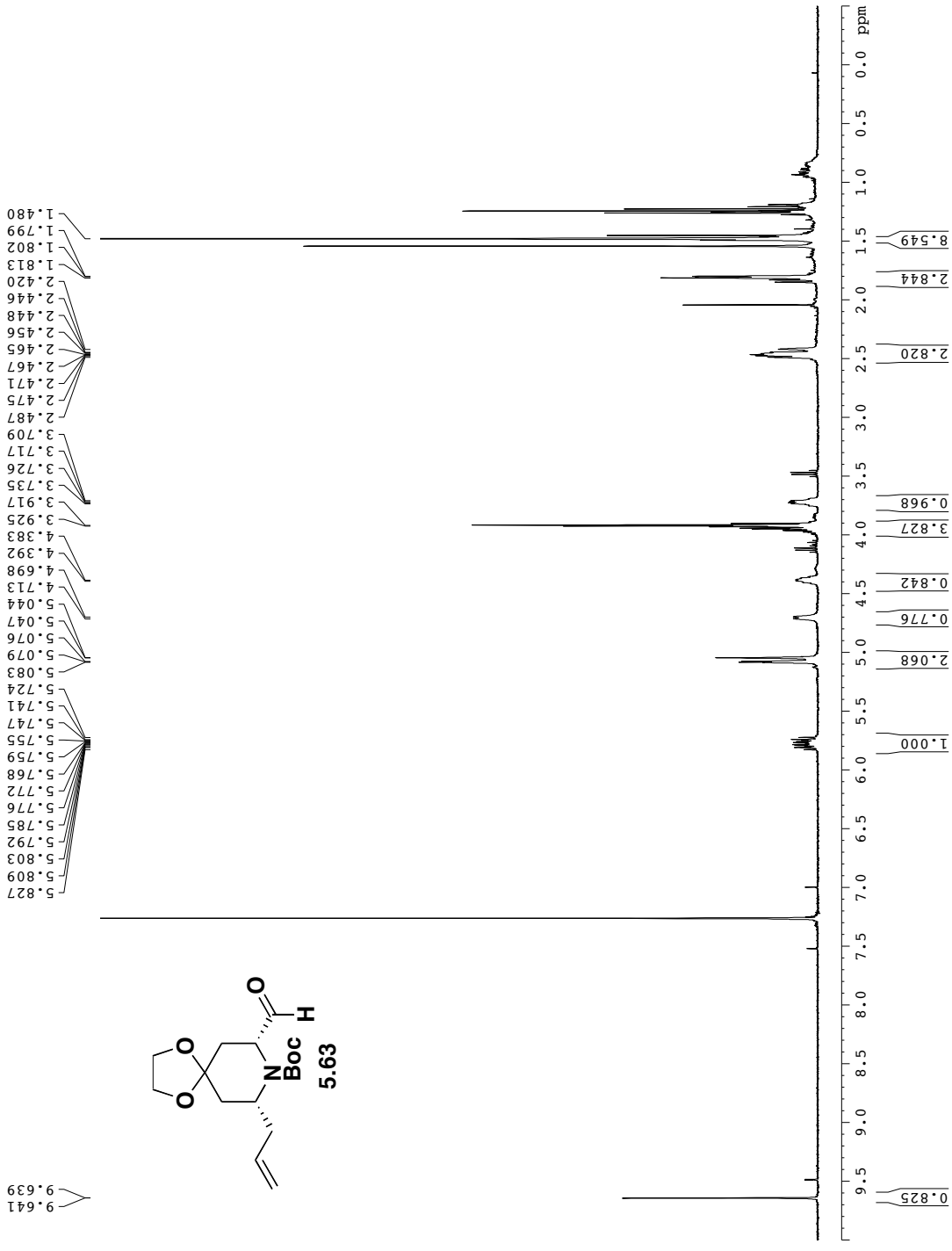
9.641
9.639
5.827
5.809
5.803
5.792
5.785
5.776
5.772
5.768
5.759
5.755
5.747
5.741
5.724
5.083
5.079
5.076
5.047
5.044
4.713
4.698
4.392
4.383
3.925
3.917
3.735
3.726
3.717
3.709
2.487
2.475
2.471
2.467
2.465
2.456
2.448
2.446
2.420
1.813
1.802
1.799
1.480
O
H
N
Boc
O
O
5.63
0.825
8.549
2.844
2.820
0.968
3.827
0.842
0.776
2.068
1.000
ppm

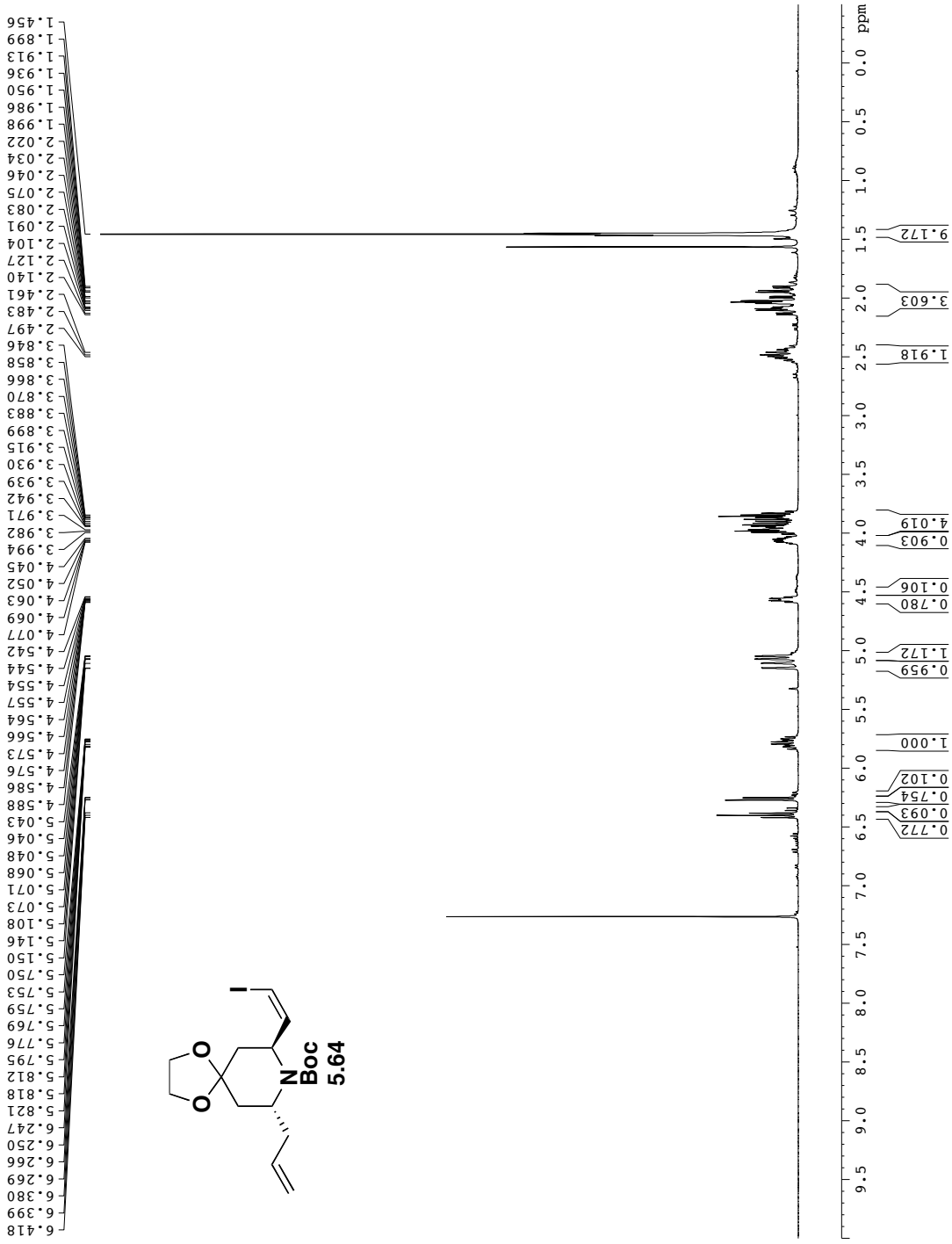
I
O
O
N
Boc
5.64
ppm
9.172
3.603
1.918
4.019
0.903
0.106
0.780
1.172
0.959
1.000
0.102
0.754
0.093
0.772

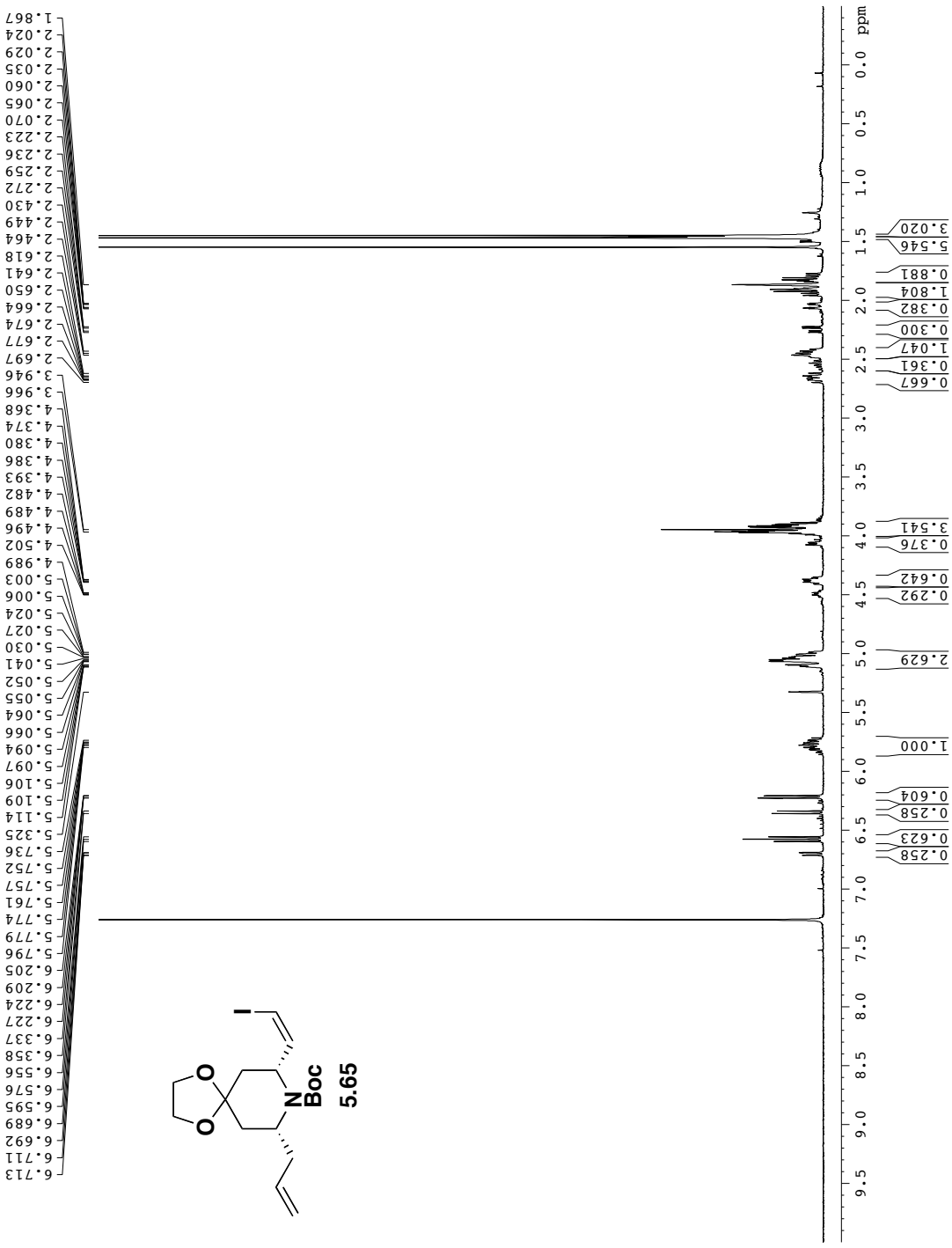
5.65
ppm
0.0
0.5
1.0
1.5
2.0
2.5
3.0
3.5
4.0
4.5
5.0
5.5
6.0
6.5
7.0
7.5
8.0
8.5
9.0
9.5
3.020
5.546
0.881
1.804
0.382
0.300
1.047
0.361
0.667
3.541
0.376
0.642
0.292
2.629
1.000
0.604
0.258
0.623
0.258

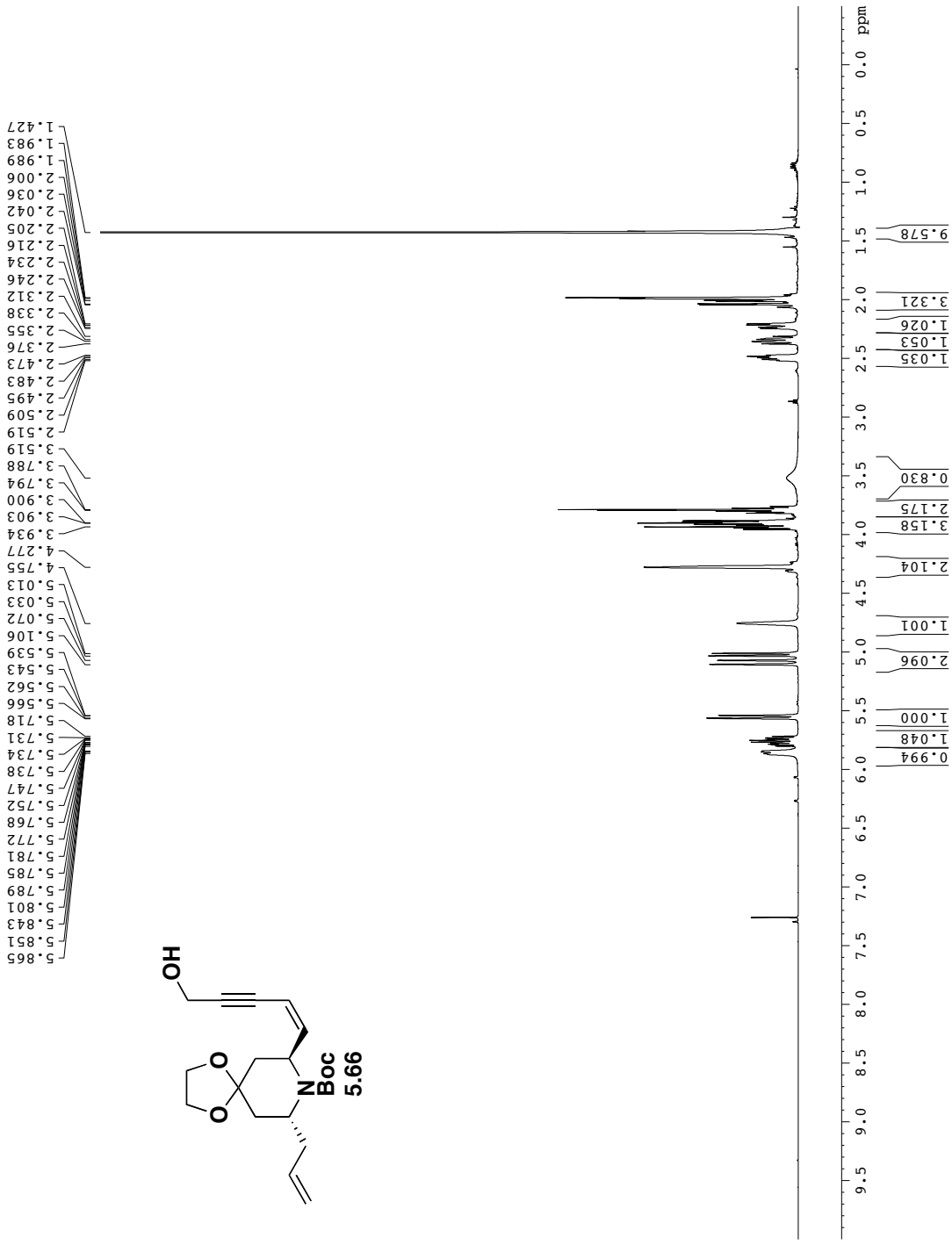
OH
O
O
N
Boc
5.66
ppm
0.0
0.5
1.0
1.5
2.0
2.5
3.0
3.5
4.0
4.5
5.0
5.5
6.0
6.5
7.0
7.5
8.0
8.5
9.0
9.5
9.578
3.321
1.026
1.053
1.035
0.830
2.175
3.158
2.104
1.001
2.096
1.000
1.048
0.994
1.427
1.983
1.989
2.006
2.036
2.042
2.205
2.216
2.234
2.246
2.312
2.338
2.355
2.376
2.473
2.483
2.495
2.509
2.519
3.519
3.788
3.794
3.900
3.903
3.934
4.277
4.755
5.013
5.033
5.072
5.106
5.539
5.543
5.562
5.566
5.718
5.731
5.734
5.738
5.747
5.752
5.768
5.772
5.781
5.785
5.789
5.801
5.843
5.851
5.865

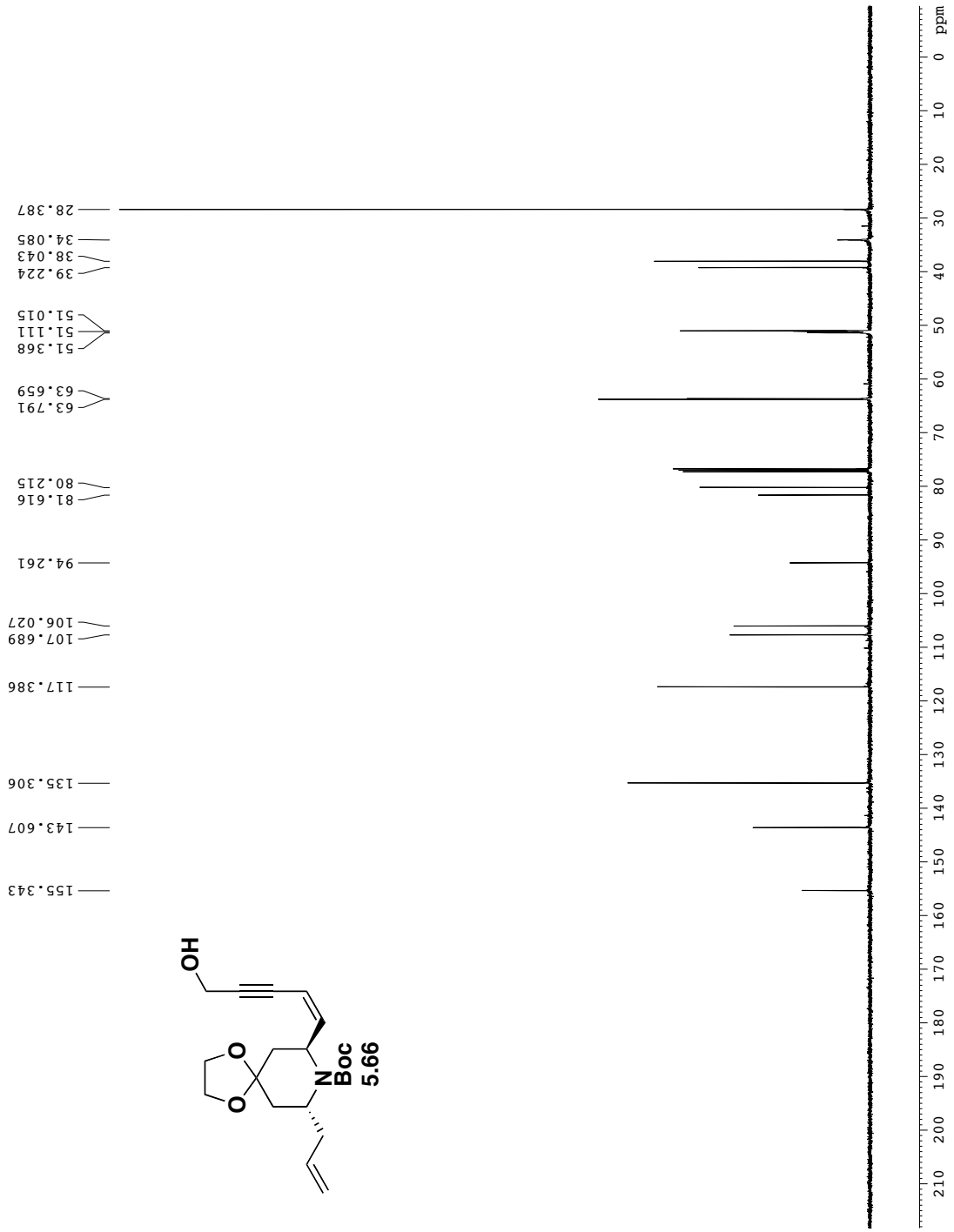
155.343
143.607
135.306
117.386
107.689
106.027
94.261
81.616
80.215
63.791
63.659
51.368
51.111
51.015
39.224
38.043
34.085
28.387
OH
O
O
N
Boc
5.66
0 ppm
10
20
30
40
50
60
70
80
90
100
110
120
130
140
150
160
170
180
190
200
210

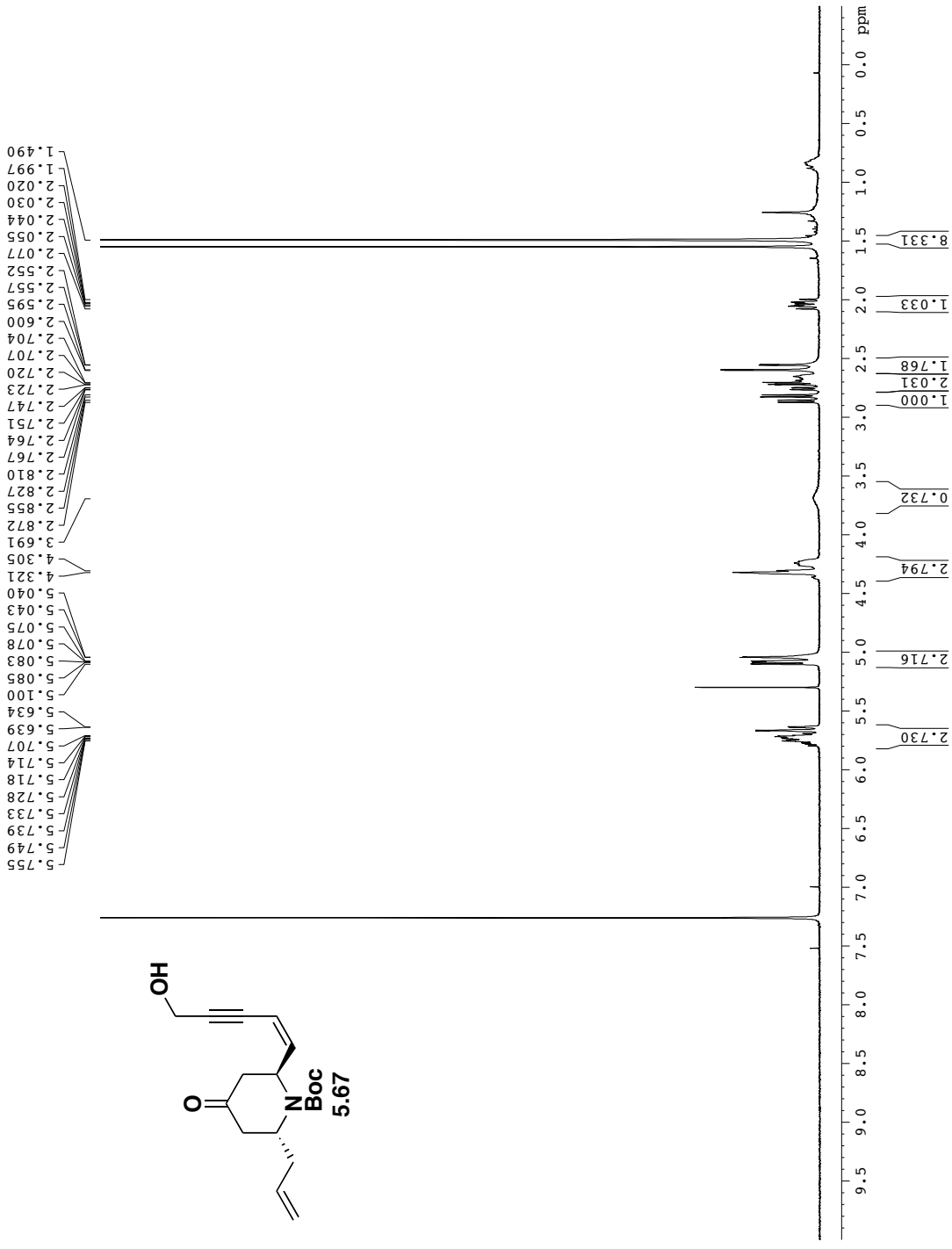
OH
O
N
Boc
5.67
ppm
0.0
0.5
1.0
1.5
2.0
2.5
3.0
3.5
4.0
4.5
5.0
5.5
6.0
6.5
7.0
7.5
8.0
8.5
9.0
9.5
8.331
1.033
1.768
2.031
1.000
0.732
2.794
2.716
2.730
1.490
1.997
2.020
2.030
2.044
2.055
2.077
2.552
2.557
2.595
2.600
2.704
2.707
2.720
2.723
2.747
2.751
2.764
2.767
2.810
2.827
2.855
2.872
3.691
4.305
4.321
5.040
5.043
5.075
5.078
5.083
5.085
5.100
5.634
5.639
5.707
5.714
5.718
5.728
5.733
5.739
5.749
5.755

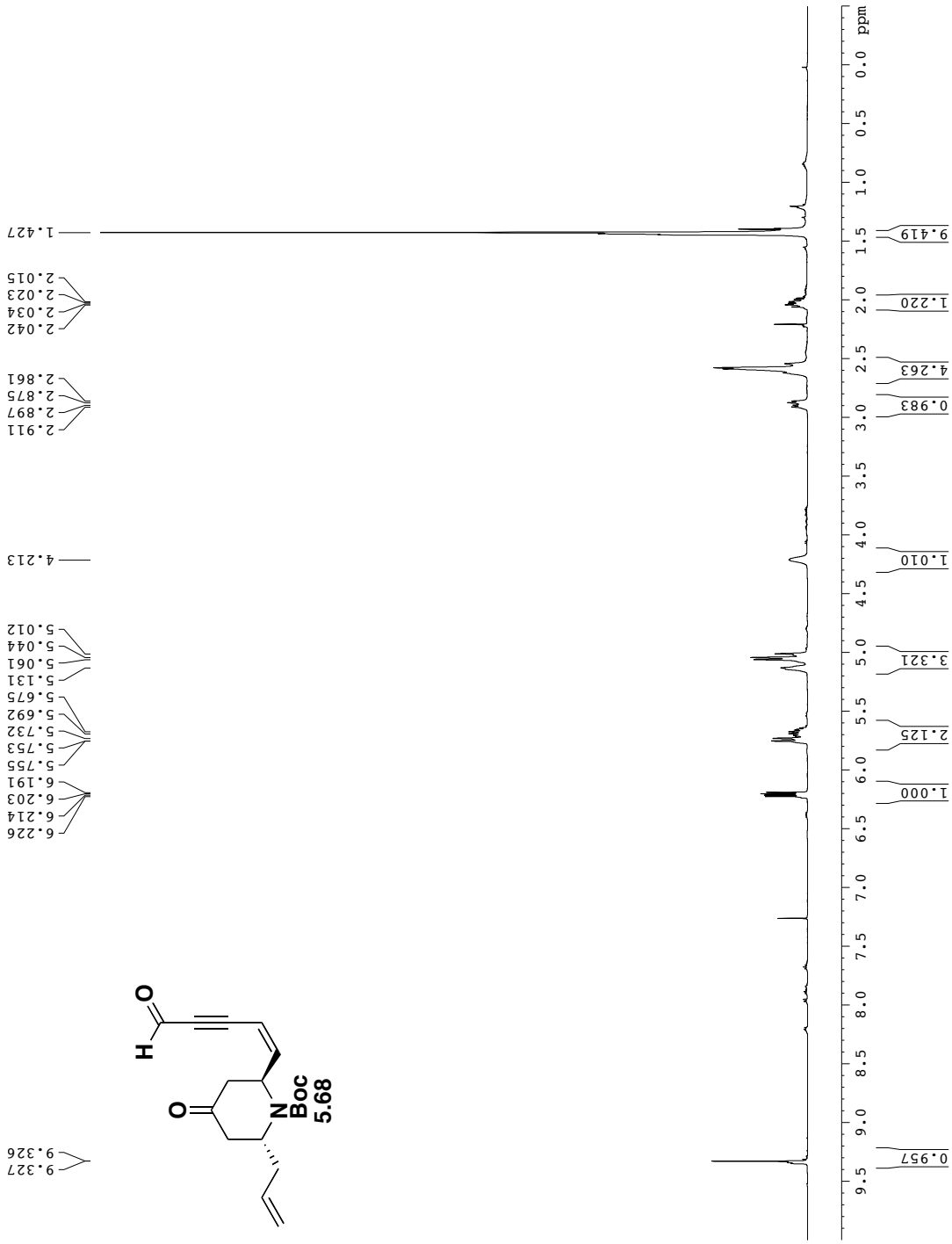
ppm
0.0
0.5
1.0
1.5
2.0
2.5
3.0
3.5
4.0
4.5
5.0
5.5
6.0
6.5
7.0
7.5
8.0
8.5
9.0
9.5
0.957
9.419
1.220
4.263
0.983
1.010
3.321
2.125
1.000
1.427
2.042
2.034
2.023
2.015
2.911
2.897
2.875
2.861
4.213
5.012
5.044
5.061
5.131
5.675
5.692
5.732
5.753
5.755
6.191
6.203
6.214
6.226
9.326
9.327
O
H
O
N
Boc
5.68

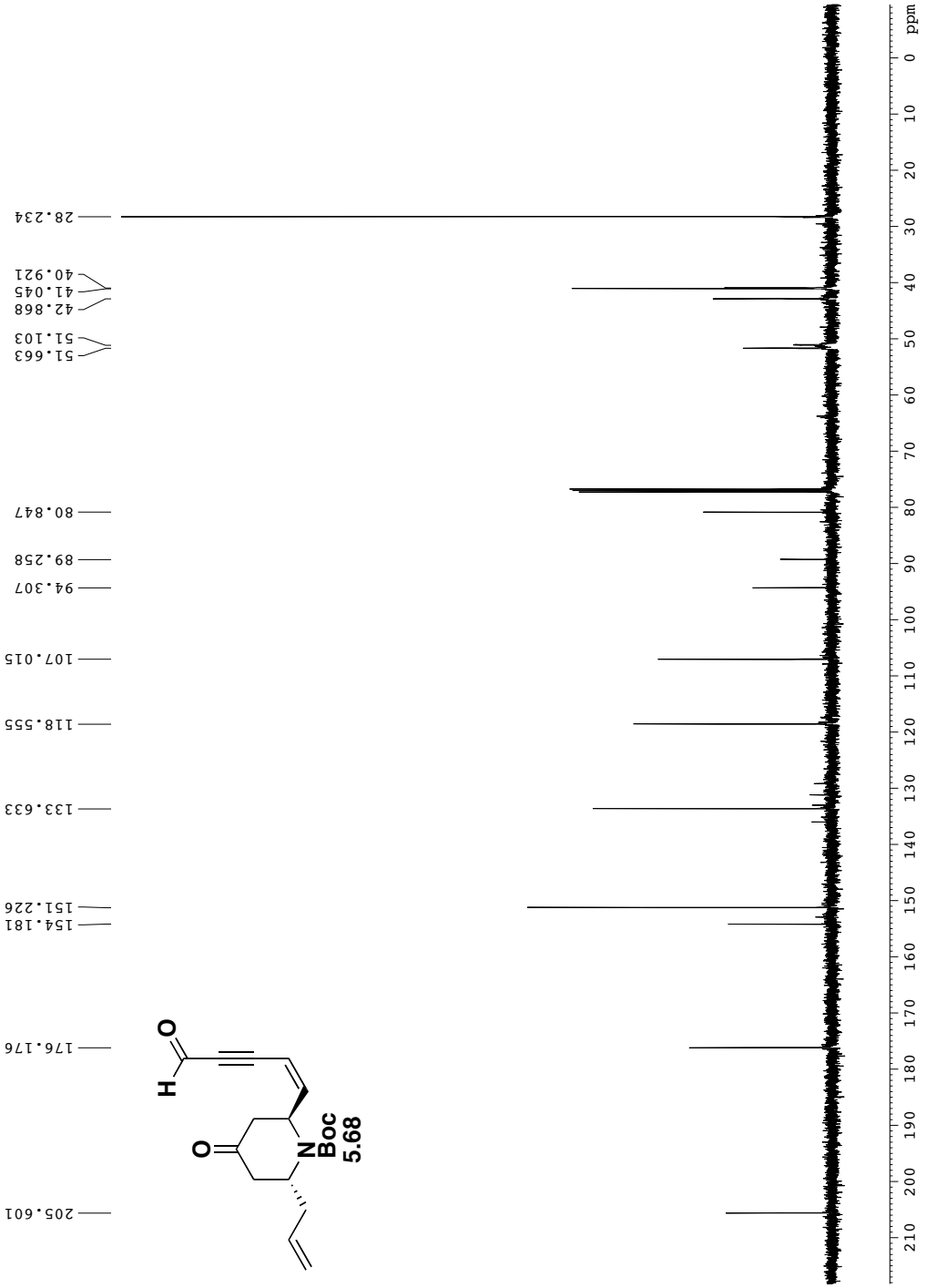
28.234
40.921
41.045
42.868
51.103
51.663
80.847
89.258
94.307
107.015
118.555
133.633
151.226
154.181
176.176
205.601
O
H
O
N
Boc
5.68
ppm

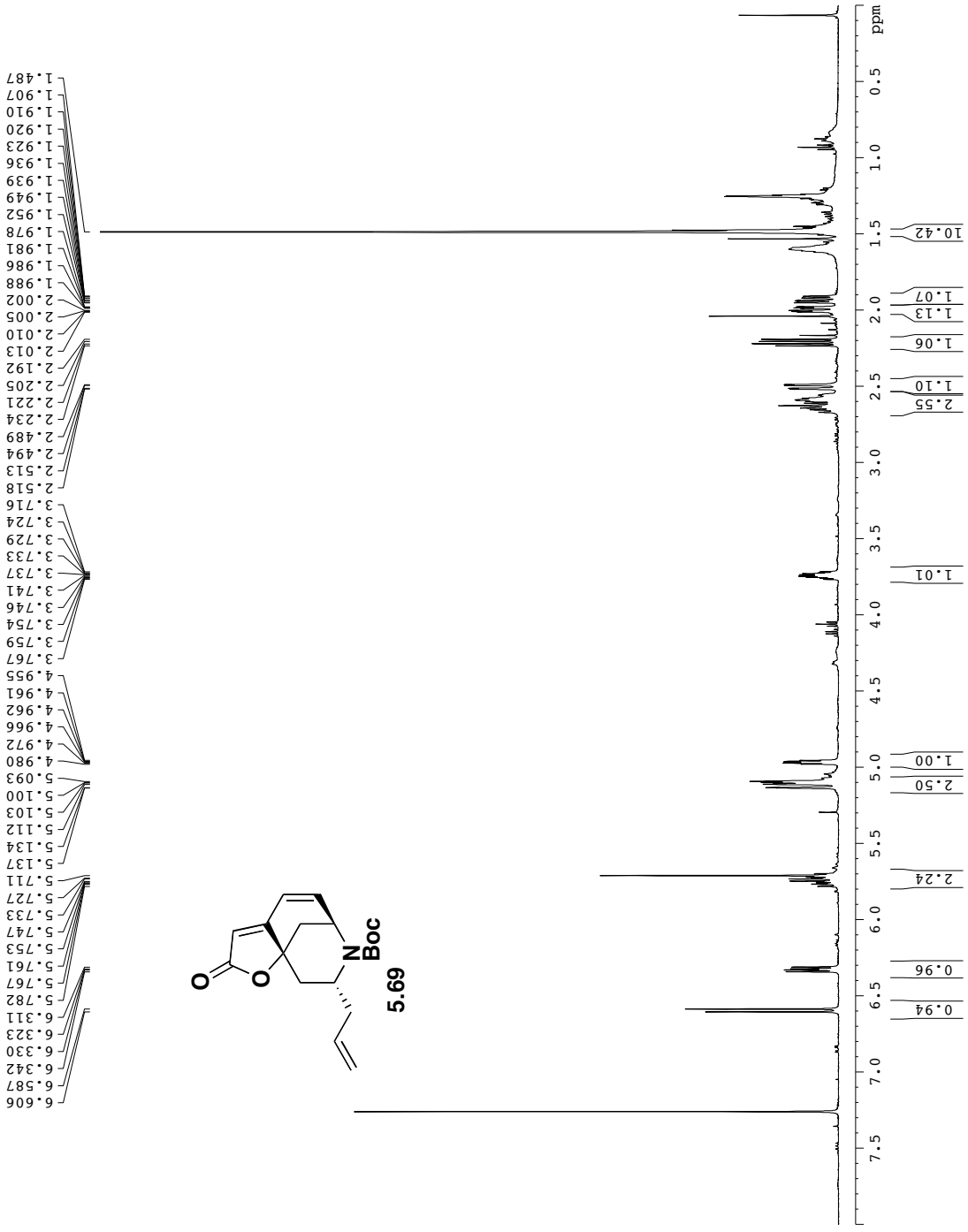
ppm
0.5
1.0
1.5
2.0
2.5
3.0
3.5
4.0
4.5
5.0
5.5
6.0
6.5
7.0
7.5
10.42
1.07
1.13
1.06
1.10
2.55
1.01
1.00
2.50
2.24
0.96
0.94
1.487
1.907
1.910
1.920
1.923
1.936
1.939
1.949
1.952
1.978
1.981
1.986
1.988
2.002
2.005
2.010
2.013
2.192
2.205
2.221
2.234
2.489
2.494
2.513
2.518
3.716
3.724
3.729
3.733
3.737
3.741
3.746
3.754
3.759
3.767
4.955
4.961
4.962
4.966
4.972
4.980
5.093
5.100
5.103
5.112
5.134
5.137
5.711
5.727
5.733
5.747
5.753
5.761
5.767
5.782
6.311
6.323
6.330
6.342
6.587
6.606
O
O
N
Boc
5.69

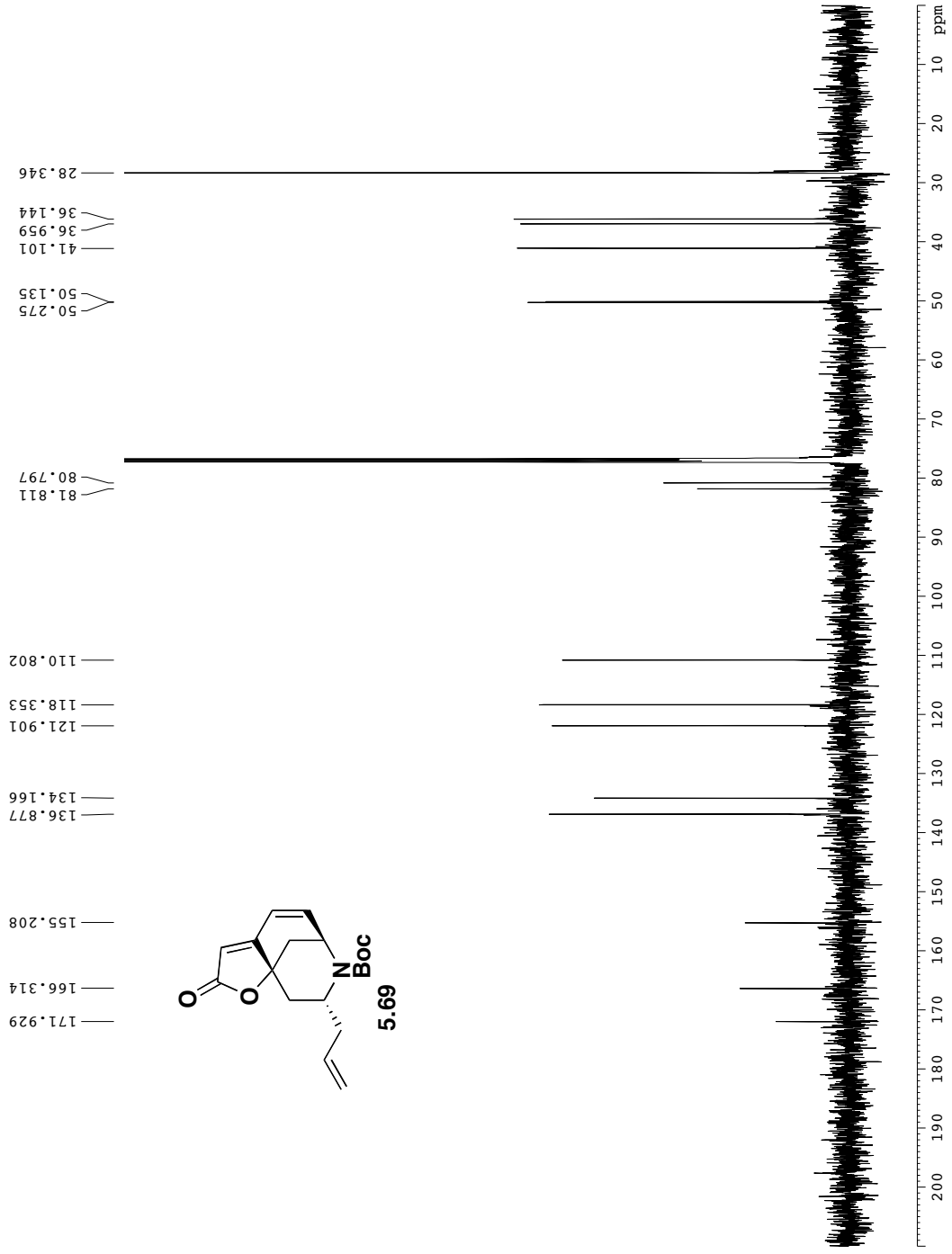
28.346
36.144
36.959
41.101
50.135
50.275
80.797
81.811
110.802
118.353
121.901
134.166
136.877
155.208
166.314
171.929
O
O
N
Boc
5.69
ppm

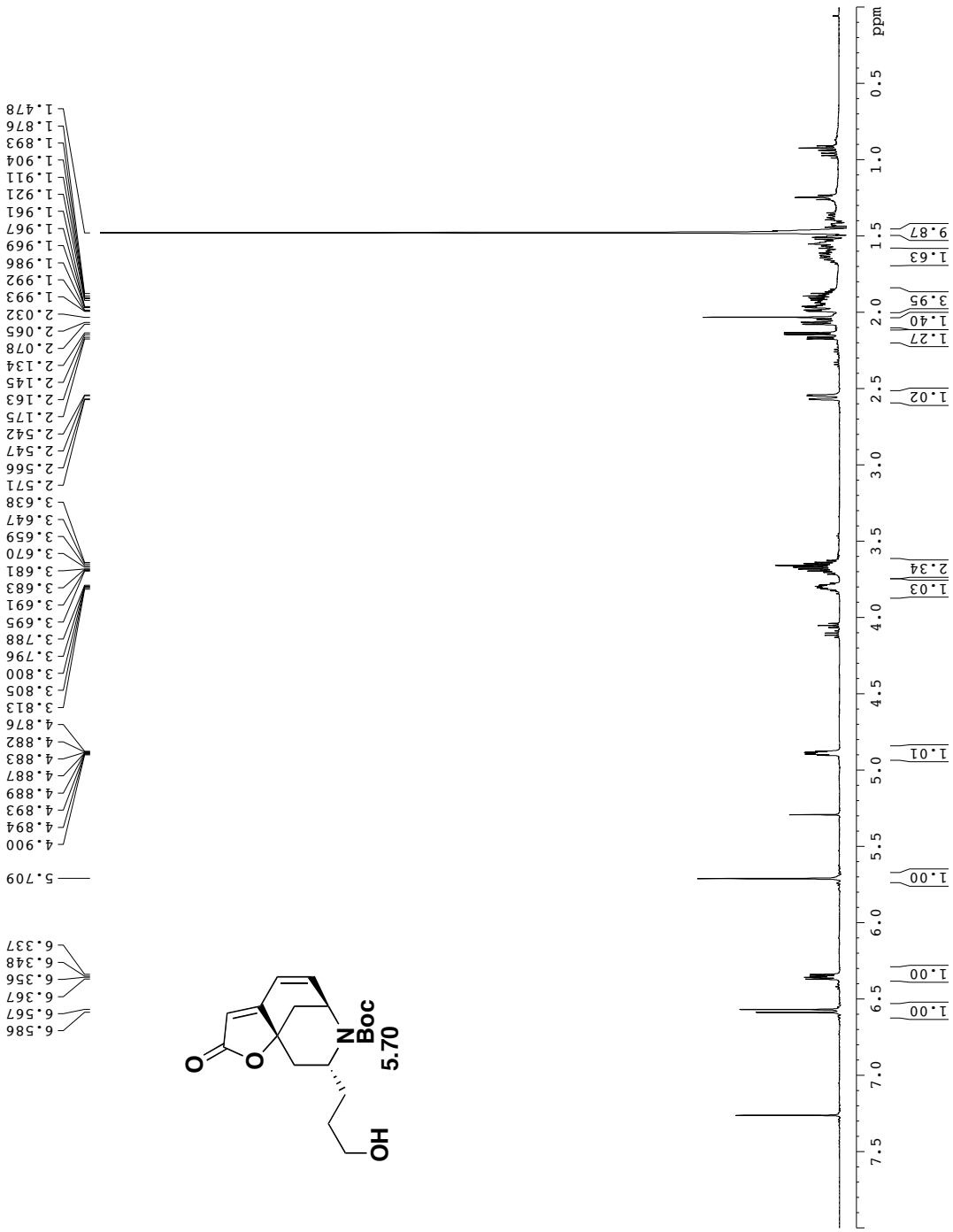
1.478
1.876
1.893
1.904
1.911
1.921
1.961
1.967
1.969
1.986
1.992
1.993
2.032
2.065
2.078
2.134
2.145
2.163
2.175
2.542
2.547
2.566
2.571
3.638
3.647
3.659
3.670
3.681
3.683
3.691
3.695
3.788
3.796
3.800
3.805
3.813
4.876
4.882
4.883
4.887
4.889
4.893
4.894
4.900
5.709
6.337
6.348
6.356
6.367
6.567
6.586
O
O
N
Boc
5.70
OH
ppm
0.5
1.0
1.5
2.0
2.5
3.0
3.5
4.0
4.5
5.0
5.5
6.0
6.5
7.0
7.5
9.87
1.63
3.95
1.40
1.27
1.02
2.34
1.03
1.01
1.00
1.00
1.00

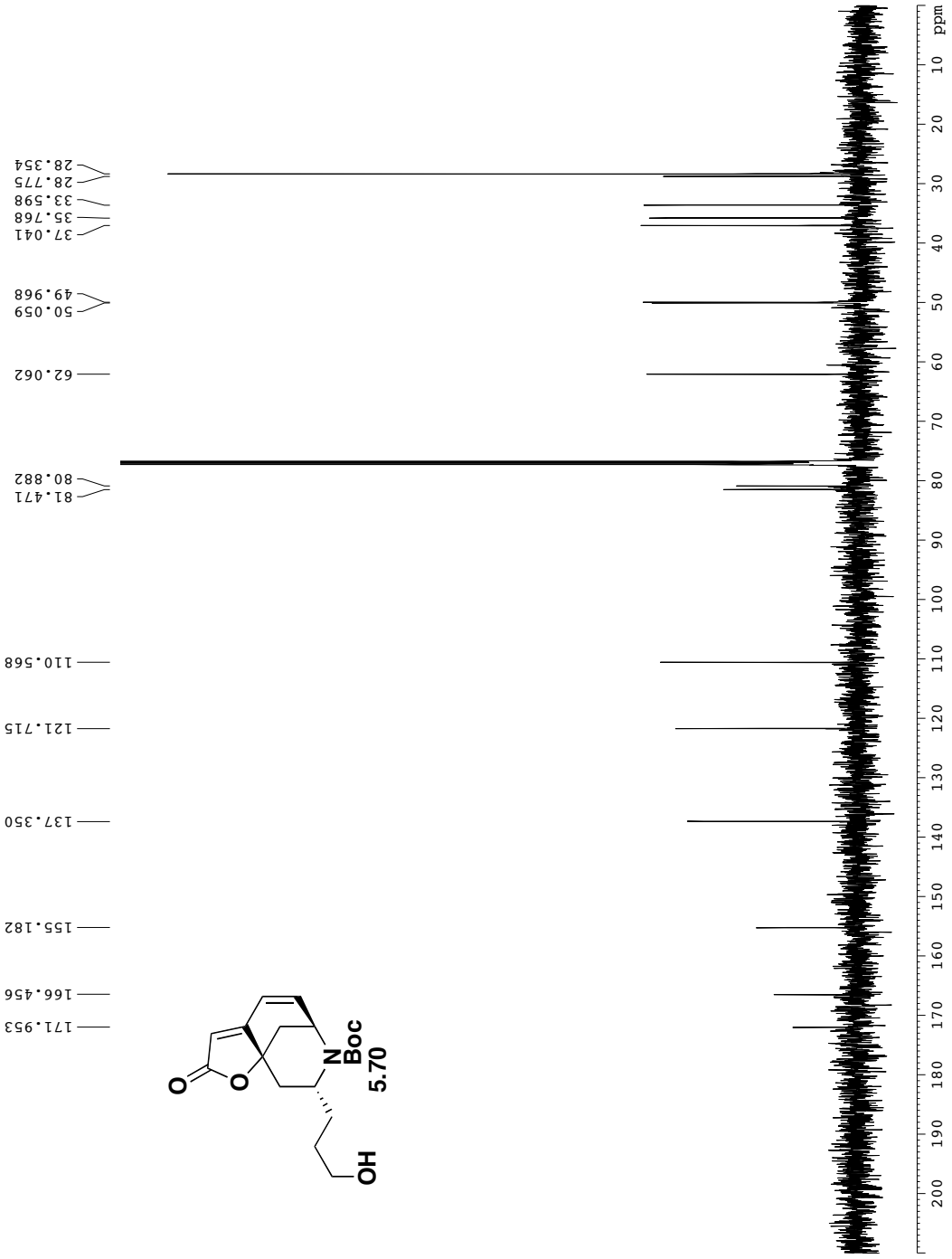
28.354
28.775
33.598
35.768
37.041
49.968
50.059
62.062
80.882
81.471
110.568
121.715
137.350
155.182
166.456
171.953
ppm
10
20
30
40
50
60
70
80
90
100
110
120
130
140
150
160
170
180
190
200
O
O
N
Boc
5.70
OH